The Chemistry of Cyclopentadienyliron Complexes of Arenes with Sulfur, Oxygen and Nitrogen Bridges

by

Karen Margaret Epp

A Thesis

Submitted to the Faculty of Graduate Studies

in Partial Fulfillment of the Requirements

for the Degree of

Doctor of Philosophy

in Chemistry

Department of Chemistry

The University of Manitoba

Winnipeg, Manitoba

THE UNIVERSITY OF MANITOBA

FACULTY OF GRADUATE STUDIES

*****

COPYRIGHT PERMISSION PAGE

The Chemistry of Cyclopentadienyliron Complexes of Arenes with Sulfur, Oxygen and Nitrogen Bridges

BY

Karen Margaret Epp

A Thesis/Practicum submitted to the Faculty of Graduate Studies of The University of Manitoba in partial fulfillment of the requirements of the degree of

Doctor of Philosophy

Dedicated to my parents

Abstract

This study illustrates the versatility of $CpFe^+$ activated S_NAr in the synthesis of oligomeric, polymeric and macrocyclic systems. Initially, the efficiency of this synthetic strategy was demonstrated by the use of chloro- and nitro- (arene)$CpFe^+$ complexes in the design of a variety of species with aliphatic or aromatic oxygen, sulfur or nitrogen bridges. Interest in the chemical behavior of these complexes led to the electrochemical investigation of selected species. Specifically, it was found that the iron centers of etheric complexes behaved as isolated redox centers whereas a small degree of interaction between metal centers was measured with respect to similar thioetheric analogues. An extension of these studies focused on the investigation of the rate of the reaction of the first reduction species of these complexes with the solvent in addition to the determination of several activation parameters. It was found that the nature of the bridging ligand as well as temperature affected the behavior of these species. Cyclopentadienyliron activated nucleophilic aromatic substitution was further investigated with respect to several polymerization techniques. Monomeric design was achieved by the preparation of the complex followed by isolation of the organic counterpart using photolytic demetallation. This two step process allowed for the synthesis of monomeric units which were polymerized using Scholl reaction conditions or ring-opening metathesis polymerization techniques. The synthesis of polyaromatic ether and thioethers with pendent $CpFe^+$ moieties by the reaction of the appropriate complex and dinucleophile in a one-step process is presented for the first time. Several nitrogen containing macrocyclic complexes were prepared via a two-step process in which the design of a species as desired was achieved by the reaction of a bimetallic complex with a variety of dinucleophiles in the ring closure step.

Acknowledgements

First and foremost, I would like to express my deepest thanks to my supervisor, Dr. Alaa S. Abd-El-Aziz for his guidance and support throughout the duration of my studies.

I would also like to take this opportunity to acknowledge Manitoba Hydro for their gracious financial support throughout the duration of my Ph.D. studies with special thanks to Mr. J. Carneiro.

The Faculty of Graduate Studies and Department of Chemistry at the University of Manitoba is thanked for accepting me as a graduate student.

I would like to acknowledge the University of Winnipeg for providing me with the facilities necessary to reach this goal. I would also like to thank Dr. H. Hutton for his help in solving some complex NMR spectra. Dr. J. Peeling and Dr. B. Pettitt are thanked for their insightful discussions.

I would like to extend my heartfelt appreciation and gratitude to a number of individuals whom I have had the pleasure of working with as group members. Shelly Bernardin, Andrea Edel, Leslie May, Erin Todd, Nicole Gavel and Jonathan Fine must be thanked for the time they took out of their schedules to proofread my thesis. Special thanks goes to Leslie May for her help in the synthesis of the macrocyclic materials.

I can't say enough about all the people who have helped me in so many ways throughout the course of my studies. There are two people I can't begin to thank enough. I would like to thank Laine Friesen for her friendship and faith that will never be forgotten. Also, I would like to say to Christine de Denus what I have not said enough. Thank you. When it's all said and done, I can't imagine having done this without you. Your knowledge and input have been invaluable and your enthusiasm for success, contagious.

Finally, I would like to thank my friends and family for their prayers and support throughout my academic career. Mom and Dad, no one has inspired, encouraged and believed in me as much as you. You inspire me every day of my life to be the best I can be. You have given me words of wisdom and advice exactly when I needed them; and with your abundant love and support, you have encouraged me to become the woman I am today.

Contents

List of Figures

List of Tables

Abbreviations

A	Frequency factor
APT	Attached Proton Test
$(Bu)_4N^+I^-$	Tetrabutylammonium iodide
CF_3COOH	Trifluoroacetic acid
Cp	Cyclopentadienyl
Cp^*	Pentamethylcyclodienyl
$Cr(CO)_3$	Chromium tricarbonyl
CV	Cyclic voltammetry or cyclic voltammogram
Cy	Cyclohexyl
DMAc	Dimethyl acetamide
DMF	Dimethyl formamide
DMSO	Dimethyl sulfoxide
e^-	electron
Ea	Activation energy
EtOH	Ethanol
E_{pa}	Anodic peak potential
E_{pc}	Cathodic peak potential
$E_{1/2}$	Half-wave potential
E_λ	Switching potential
E°	Formal redox potential
Fc/Fc^+	Ferrocene/ferrocenium redox couple
Fe^+Cp	Ironcyclopentadienyl

$FeCp_2$	Ferrocene
FID	Free induction decay
$\Delta G^{\ddagger}$	Gibb's free energy of activation
GPC	Gel Permeation Chromatography
h	Planck's constant
$\Delta H^{\ddagger}$	Enthalpy of activation
^1H-^1H COSY	Homonuclear Correlated Spectroscopy
^1H-^{13}C COSY	Heteronuclear Correlated Spectroscopy
HMPA	Hexamethylphosphoric acid
H_2O_2	Hydrogen peroxide
hν	photolysis
I_λ	Switching current
$(i_{pa})_o$	Anodic peak current at time zero
i_{pc}	Cathodic peak current
IR	Infrared
K	Degree Kelvin
$K^{\ddagger}$	Activated complex equilibrium constant
k_B	Boltzmann's constant
k_f	The rate of the following chemical reaction
m-CPBA	3-chloroperbenzoic acid
MeCN	Acetonitrile
Me_2CO	Acetone
$Mn^+(CO)_3$	Manganese tricarbonyl

Mn	Number average molecular weight
MS	Mass Spectrometry
Mw	Weight Average molecular weight
NH_4PF_6	Ammonium hexafluorophosphate
NMP	N-methyl pyrollidine
NMR	Nuclear Magnetic Resonance
1D-NMR	One-dimensional Nuclear Magnetic Resonance
2D-NMR	Two-dimensional Nuclear Magnetic Resonance
Nu^-	Nucleophile
$PhNO_2$	Nitrobenzene
ROP	Ring-opening polymerization
ROMP	Ring-opening metathesis polymerization
Ru^+Cp	Rutheniumcyclopentadienyl
Ru^+Cp^*	Rutheniumpentamethylcyclopentadienyl
S	Solvent molecule
$\Delta S^‡$	Entropy of activation
S_NAr	Nucleophilic aromatic substitution
T	Tau
TBAP	Tetrabutylammonium perchlorate
$TBAPF_6$	Tetrabutylammonium hexafluorophosphate
TGA	Thermal gravimetric analysis
Tg	Glass transition temperature
THF	Tetrahydrofuran

tos	p-toluenesulfonate
UV	Ultraviolet
V	Volt(s)
V/s	Volts per second
ν	scan rate

1.0 Chemistry of Organometallic Arene Complexes

1.1 Introduction

The temporary complexation of metallic moieties to the π-electron system of an aromatic compound has had a substantial impact on the development of transition metal chemistry.[1-3] It has been well established in organic chemistry that aromatic compounds readily undergo electrophilic aromatic substitution reactions.[4] It has also been demonstrated that, under certain circumstances, an aryl halide will undergo nucleophilic aromatic substitution reactions. However, for this reaction to occur, there must be electron-withdrawing substituents on the ring.[5] The electron-withdrawing capabilities of the transition metal moieties when complexed to aromatic compounds will be one of the central themes of this work.

The activation of aryl halides toward nucleophilic reactions has been investigated with respect to a number of metal moieties such as cyclopentadienyliron ($CpFe^+$), cyclopentadienylruthenium ($CpRu^+$), pentamethylcyclopentadienylruthenium (Cp^*Ru^+), chromium tricarbonyl ($Cr(CO)_3$), and manganese tricarbonyl ($Mn(CO)_3^+$). Mechanistic investigations involving the reactivity of a number of halobenzene metal complexes toward nucleophilic aromatic substitution with the methoxide ion allowed for a comparison of the electron-withdrawing capability of the metal moieties with respect to one another.[6,7] Figure 1.1 summarizes the relative electron-withdrawing power of some of the metal moieties mentioned above.[8] A one-dimensional examination of these

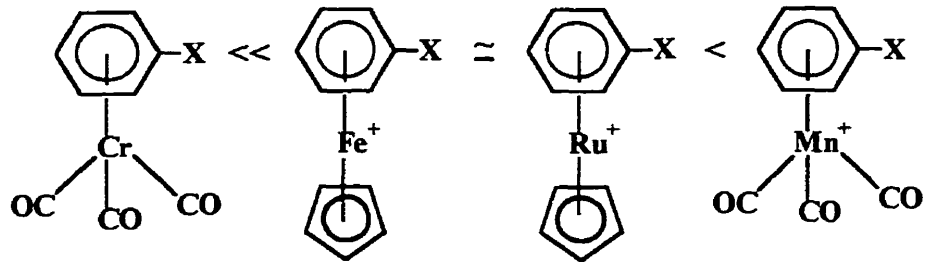

numeric estimation of the reactivity	**<< 1 very small**	**1**	**1**	**10^3**

Figure 1.1: Relative electron-withdrawing ability of metallic moieties upon π-complexation to an aryl halide

metal moieties based on their capacity to activate aromatic compounds toward nucleophilic reactions suggests $Mn(CO)_3^+$ as the metal moiety of choice. All of the aforementioned metal moieties have been applied to some degree to the activation of aromatic compounds.[9-19] In spite of the activating ability of some of these metal moieties, the extent of their application is often hampered by factors such as high cost, toxicity and limitation with respect to the number of aromatics to which they may be complexed. The moderate electron-withdrawing ability of $CpFe^+$ in association with its low cost, ease of complexation and decomplexation and low toxicity enhances its practical synthetic utility.

Although it has been demonstrated that under the appropriate reaction conditions the complexation of a metal moiety to aromatic compounds may be employed in the promotion of a variety of chemical reactions, the use of $CpFe^+$ in the activation of aromatic compounds toward nucleophilic aromatic substitution reactions is the primary focus of this study and will be considered in further detail.[8]

1.2 Synthesis and Reactivity of η^6-Arene-η^5-Cyclopentadienyliron Complexes

1.2.1 Synthesis

Although Coffield and coworkers are noted for the preparation of the first η^6-arene-η^5-cyclopentadienyliron complex in 1957, the low yield of their procedure limited its extensive application.[20] Nesmeyanov and coworkers are highly regarded in the field of aromatic organoiron chemistry for their contribution of an alternative preparation of these mixed sandwich complexes.[21-24] Nesmeyanov described the successful replacement of one of the cyclopentadienyl ligands of ferrocene with an appropriate arene in the presence of $AlCl_3$ and Al. The advantage of this methodology was the isolation of the desired complexes in yields of up to 40%, a marked improvement over the methodology reported by Coffield. Further work in this area produced dramatic increases in yield, as high as 90% in select cases, upon the addition of a stoichiometric amount of H_2O or concentrated HCl.[25] Figure 1.2 represents the general scheme of the ligand exchange reaction that allows for the isolation of the cationic complexes as their hexafluorophosphate or tetrafluoroborate salts following an appropriate workup procedure.

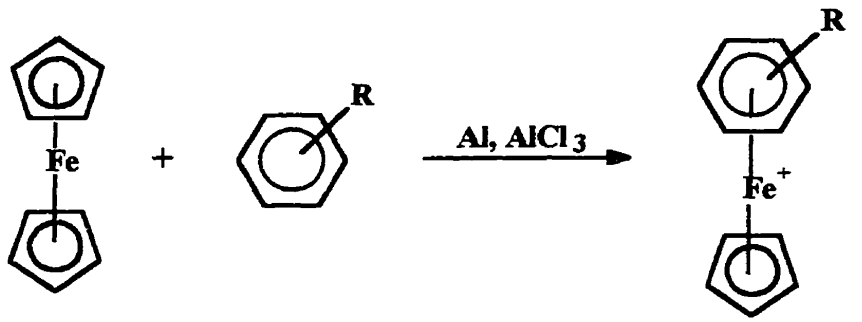

Figure 1.2: The preparation of mixed sandwich complexes of iron via the ligand exchange reaction

Typically, excess arene is added to ferrocene in the presence of $AlCl_3$ and Al for 3 to 24 hours at a temperature ranging between 80-165°C.[25-36] Although the addition of a solvent is not usually necessary since the arene itself may serve as the solvent, one of two options may be considered in the use of solid arenes. The solid arene may simply be melted and serve as the reaction solvent, or an inert solvent such as decalin may be added to the reaction mixture.

The ligand exchange reaction has resulted in variable success when the aromatic ring to be complexed is altered. Thorough investigation of a variety of aromatic compounds revealed that ring substitution takes place more readily in the presence of an arene ring or cyclopentadienyl ring with electron donating groups but is hampered by the presence of electron withdrawing substituents.[37] These observations are rationalized by the electrophilic mechanism which has been suggested for this reaction (Figure 1.3).[38-39] A key step in the proposed mechanism is the formation of a complex involving $AlCl_3$ and an electron rich cyclopentadienyl rings of ferrocene. This results in a weakening of the iron-ring bond to form the free CpFe+ unit which undergoes further reaction with an

aromatic substrate to yield the desired η^6-arene-η^5-cyclopentadienyliron cation. It is this species which is then subject to an exchange with the desired arene ligand.

The hindered reaction of the cyclopentadienyl ring substituted with electron withdrawing groups is then justified by the decreased electron density of the ring. This limits attack by $AlCl_3$ which makes the substituted cyclopentadienyl ring less susceptible to cleavage. It is important to note that regardless of the features of the cyclopentadienyl and arene rings, the aluminum powder is an essential component of the reaction mixture as it prevents the oxidation of ferrocene to the ferrocinium cation.[25-28, 35-37, 39]

In 1993, a communication appeared which describes the preparation of η^6-arene-η^5-cyclopentadienyliron complexes in higher yields and employing reaction times of 4 minutes.[40] This attempted improvement of the ligand exchange reaction utilizes the same reagent mixture as previously reported but makes use of a conventional microwave oven for the purpose of carrying out the reaction.

The synthesis of a large number of monocationic species of simple arenes has dominated the application of the ligand exchange reaction. However, this methodology has also received considerable attention as a route to complexed heterocyclic mono- and di-cationic derivatives and until recently the reaction of polyaromatic compounds in the presence of excess ferrocene was reported as the exclusive synthetic route to the preparation of bis(cyclopentadienyliron) complexes.[30, 32-34, 41-45]

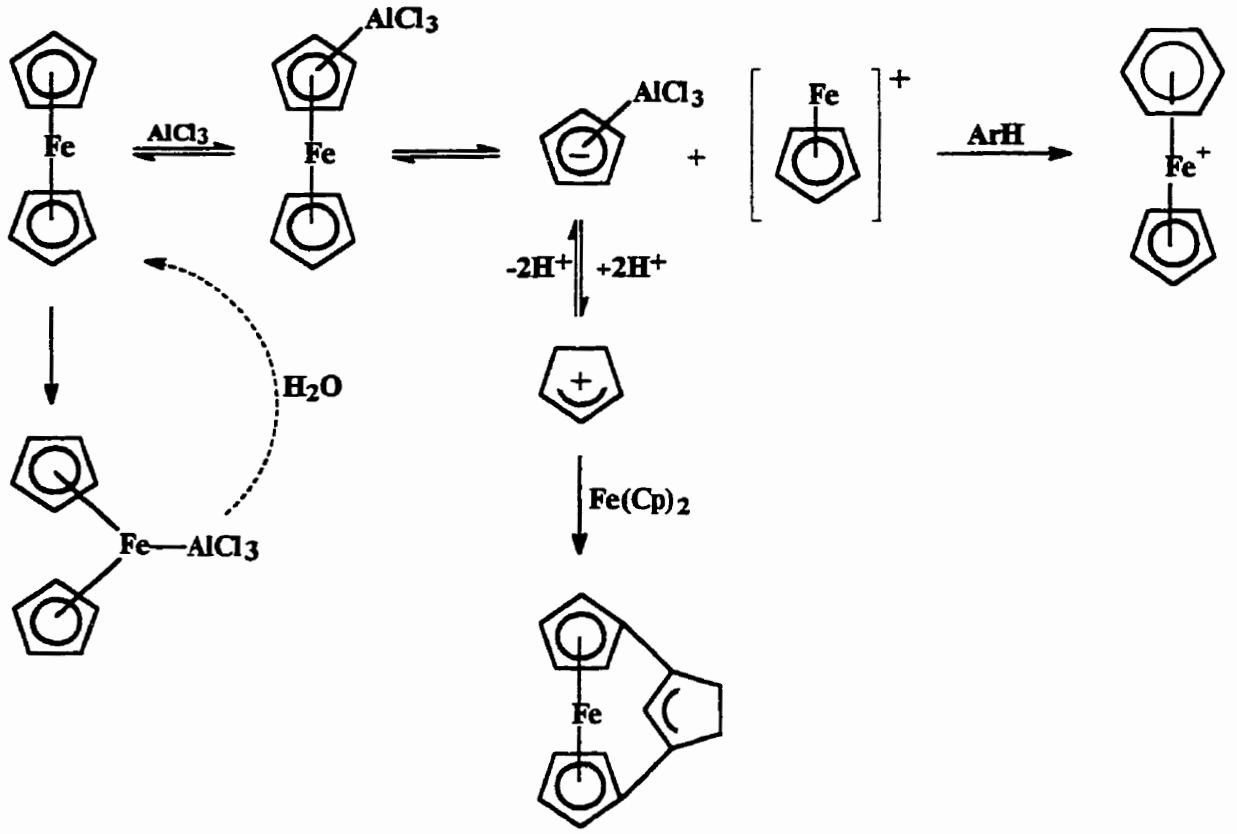

Figure 1.3: The mechanism of the ligand exchange reaction

1.2.2 Nucleophilic Aromatic Substitution Reactions

The wide variety of chemical reactions that η^6-arene-η^5-cyclopentadienyliron complexes can undergo, including reactions with either of the complexed rings, their substituents or the iron itself, thoroughly demonstrates their remarkable reactivity.[46-47] These complexes are susceptible to photolytic cleavage, oxidation and reduction reactions and nucleophilic addition and substitution modifications. The reactivity of

these complexes toward nucleophilic aromatic substitution reactions is the basis for this work and will therefore be the essence of the following discussion.

According to traditional organic chemistry, aromatic compounds are readily susceptible to electrophilic attack and, in the presence of one or more electron-withdrawing substituents, are equally inclined to act as electron acceptors and undergo reaction in the presence of a nucleophile.[5] The ability for an organometallic species such as $CpFe^+$ to act as a strong electron-withdrawing group and activate a complexed arene toward nucleophilic attack was initially investigated and reported by Nesmeyanov and his coworkers in 1967.[48] They determined the activation of this metallic moiety to be equivalent to that of two nitro groups. It was also demonstrated that chloroarenes when complexed to $CpFe^+$ will undergo nucleophilic aromatic substitution in the presence of a variety of carbon, oxygen, sulfur and nitrogen nucleophiles under fairly mild reaction conditions.[49] Subsequent consideration of η^6-arene-η^5-cyclopentadienyliron complexes has established the nucleophilic substitution of nitro substituted arenes in the presence of a nucleophile, a suitable base and an appropriate reaction solvent. Figure 1.4 presents a general scheme outlining the nucleophilic aromatic substitution reaction of nucleophiles with η^6-arene-η^5-cyclopentadienyliron complexes.

The use of this methodology for the preparation of important organic precursors as well as species with biological or industrial potential demonstrates its synthetic utility. Specifically, both mono- and disubstituted chlorobenzene $CpFe^+$ complexes have successfully undergone S_NAr reactions in the presence of a number of carbanion nucleophiles and are recognized as a viable route to carbon-carbon bond formation (Figure 1.5).[50-57] A notable advantage of this synthetic strategy is the option of preparing

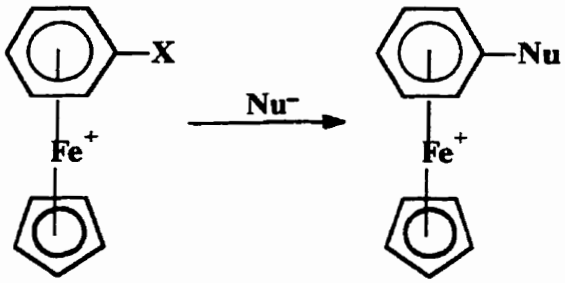

X = Cl, NO_2

Figure 1.4: Nucleophilic substitution of cyclopentadienyliron activated chloro- and nitro-substituted arenes

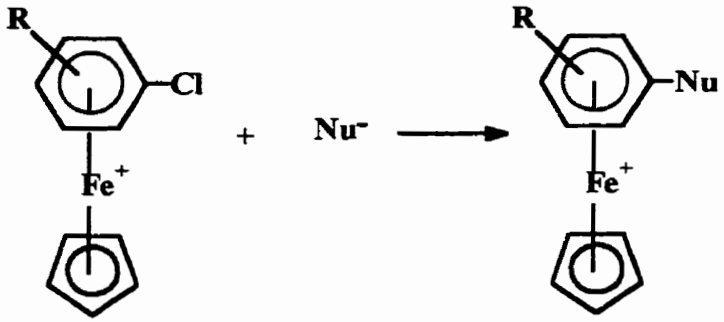

R = H, CH_3, Cl

Nu⁻ = (CN)CH(SO_2Ph)
(CN)CH(CO_2Et)
(CN)C(Et)(CO_2Ph)
MeCH(CO_2Et)
EtCH(CO_2Et)

Figure 1.5: Reaction of various carbanion nucleophiles with η^6-(chloroarene)-η^5-cyclopentadienyliron complexes

either symmetric or asymmetric derivatives by the successive substitution of dichlorobenzene complexes with nucleophiles which may be the same or different.

Nucleophilic aromatic substitution of η^6-dichloroarene-η^5-cyclopentadienyliron complexes with nitrogen nucleophiles has been investigated in some detail by Helling and Hendrickson who reported exclusive monosubstitution in the presence of primary amines.[58-59] The rationale suggested for this observation was the formation of a zwitterionic cyclohexadienyliron complex possessing an exocyclic double bond. The formation of this electron rich complex results from the deprotonation of an α-XH group (X = C, N, O, S) bonded to the complexed aromatic ring of a $CpFe^+$ complex under basic reaction conditions and renders the complex inactive toward further nucleophilic substitution (Figure 1.6).

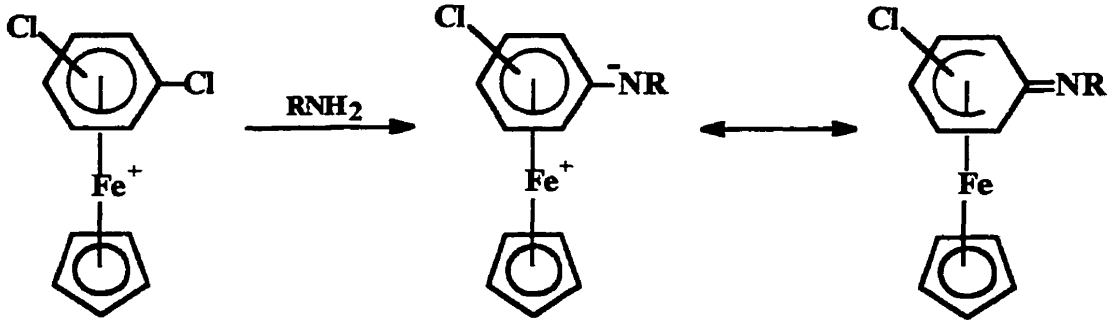

Figure 1.6: Zwitterion formation

A similar scenario results from the reaction of η^6-dichloroarene-η^5-cyclopentadienyliron complexes with carbon nucleophiles possessing a methine proton.[36,50] The lack of reactivity of the second chloro substituent on the complexed arene ring has been overcome in the case of primary amines upon the addition of an appropriate amount of

acetic acid to the reaction mixture.[58] Selective substitution of dichloroarene complexes may be achieved in the presence of secondary amine nucleophiles. The nitro group is known to be a better leaving group than chlorine and as a result (nitroarene)$CpFe^+$ derivatives have been employed in nucleophilic aromatic substitution reactions with amines.[60]

In addition to the above mentioned carbon and nitrogen nucleophiles which have been demonstrated to readily undergo substitution with (chloroarene)Fe^+Cp complexes, the formation of etheric and thioetheric linkages also occurs in the presence of oxygen and sulfur nucleophiles.[61-63] The double nucleophilic substitution reaction of a variety of oxygen, sulfur, and/or nitrogen containing 1,2-dinucleophiles with 1,2-substituted dichloroarenes represents a unique approach to heterocyclic systems (Figure 1.7).[64-66]

The reaction of (chloroarene)Fe^+Cp complexes with a variety of aliphatic and aromatic oxygen dinucleophiles has been studied extensively resulting in the preparation of mono-, bi- and polymetallic species.[67-70]

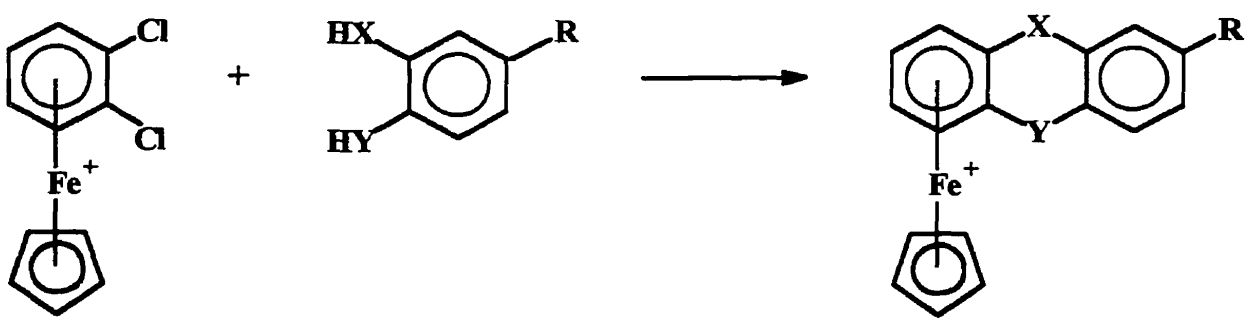

Figure 1.7: Reaction of 1,2-dinucleophiles with η^6-o-dichloroarene-η^5-cyclopentadienyliron complexes in heterocycle formation

1.2.3 Demetallation

Recently, the importance of organometallic reagents in organic synthesis has become increasingly apparent.[71-73] The influence that the $CpFe^+$ moiety has had on the modification of chemical species as an exclusive route to some organic compounds is no exception. It is the ease with which the metallic moiety may be removed from the backbone of the modified organic ligand which is often recognized as an important feature of organoiron chemistry.

Pyrolytic sublimation, electrolysis, and photolysis all represent techniques which may be applied in the cleavage of the metallic moiety from the organic ligand. Pyrolytic sublimation is frequently used in the case of thermally stable η^6-arene-η^5-cyclopentadienyliron complexes and involves heating the complex to high temperature under partial vacuum.[45, 74] Electrolytic reduction has been used to remove some heterocyclic ligands from their parent metallated complexes.[75] Despite the success demonstrated with these methods, photolytic demetallation represents the most convenient method and as a result dominates the various routes which have been employed for the liberation of the metal moiety from the attached organic ligand.

Photolytic demetallation involves the irradiation of a cyclopentadienyliron complex dissolved in a suitable solvent using visible or ultraviolet light and allows for the isolation of the desired organic species in yields ranging from 50-100%.[45, 76-77] In addition to the removal of the modified organic species, ferrocene and an iron(II) salt are generated in the process (Figure 1.8).[78]

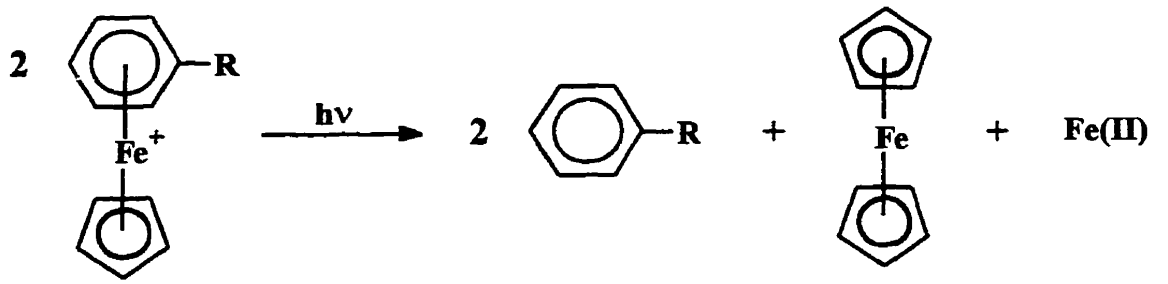

Figure 1.8: Liberation of the arene by photolytic demetallation

It has been shown that the mechanism of this reaction is a photodisproportionation reaction as a result of a photoinduced electron transfer from the solvent to the complex.[79] In the case of (arene)cyclopentadienyliron complexes, liberation of the modified arene ligand is a result of arene replacement which may take place by a six electron ligand or by three two-electron ligands. The solvent dependency of this reaction was suggested by a study carried out by Gill and Mann who concluded that CH_3CN was one of the most efficient solvents.[80-82]

1.2.4 NMR Studies of η^6-Arene-η^5-Cyclopentadienyliron Complexes

Nuclear magnetic resonance spectroscopy (NMR) has become a primary tool in the identification of η^6-arene-η^5-cyclopentadienyliron complexes. It has been suggested that due to bonding interactions with the metal d orbitals, hybridization of the arene electrons takes place upon the complexation of the $CpFe^+$ metal moiety to uncomplexed arenes resulting in distinguishing spectroscopic features.[33, 83-84] The most distinctive feature of the ^1H NMR spectra of $CpFe^+$ complexed arenes is the 0.8 to 1.1 ppm

downfield shift of the Cp resonances in comparison to those representative of ferrocene.[64] A similar downfield shift of methyl and methylene protons was also noted. Diagnostic features of the ^{13}C NMR include the downfield shift of 6.0 to 9.0 ppm representative of the Cp carbons as compared to ferrocene in addition to a 40 ppm upfield shift of the complexed arene carbon resonances relative to the free arene.[65]

1.3 Organometallic Polymers

1.3.1 Introduction

The heightened interest in inorganic and organometallic polymers stems from the need for new specialty materials that meet the rigorous demands of our technologically advanced society.[85] Due to the emphasis on preparing materials with specific properties for well-defined applications within an economical and environmentally conscious context, polymer chemistry has developed into a highly interdisciplinary field composed of organic, polymer, physical, inorganic chemistry and chemical engineering.[85-90]

One of the most direct approaches to controlling the chemical behavior of the desired material is by the incorporation of different monomer unit structures into the architecture of the polymer chain. The incorporation of metallic species into the polymer structure allows for the inclusion of a large number of elements in the periodic table, in almost limitless combinations. In fact, it may be said that the array of potential materials is limited only by the chemists own intent and imagination. A case in point is the variety of materials prepared by traditional polymer chemists whose repertoire of materials is

composed of a few typical elements such as C, H, N, S, P, Cl, Br, O, and F.[89-90] On the other hand, the scope of materials imaginable when combining these elements with the 44 metals available is staggering. In addition, many of the metals available for possible use in polymer preparation can also be present in several oxidation states.[89-90]

Several unique features contribute to the wealth of potential applications that exist for transition metal-containing polymers.[90] The ability to regulate the oxidation state of the metal by changing the metal ligand is just one characteristic which contributes to their value. Changing the ligands also allows control of these highly colored species with respect to their absorption of visible or UV light. The ability of the heavy nuclei to absorb neutrons, X-rays and other types of radiation suggests the potential that the resulting material may provide protection from radiation, or its presence promote selective cleavage and degradation of the polymer. Hence, this field has witnessed the systematic and intelligent design of a wide variety of materials with a diversity of applications including polymeric conductors and semiconductors, preceramic materials, polymer bound catalysts, shields for UV and other high energy radiation, biosensors, polymers with high stability, and flame retardency.[90]

Regardless of the diversity of the synthetic methods, the combination of several side-group variations and the possible incorporation of a large number of elements presents limitless opportunities for the nature of the resulting metal-containing materials. Consequently, a distinction may be made between organometallic polymers: (i) which contain the metal atom in the polymeric backbone or (ii) where the metal moiety is pendent to the backbone of the polymer chain. Although a review of all the recent developments in this diverse field is beyond the scope of this discussion, each

classification will be mentioned briefly with emphasis on macromolecules with pendent metal moieties.

1.3.2 Polymers Containing Metals in the Backbone

One of the main objectives of organometallic chemists is to prepare stable, processable, and high molecular weight polymers containing metals as a regular structural unit of the polymer. They hope to modify the polymeric properties of purely organic systems by the incorporation of various metal moieties into the polymer structure.[85-90] Coordination and metallocene polymers represent two examples of polymers that incorporate transition metals into the backbone of the polymer chain.

Until recently, one of the main routes to the preparation of metallocene containing polymers was the use of condensation polymerization techniques. The syntheses of titanium-containing polyesters, polyethers, polythioethers and polyamines from the reaction of dicyclopentadienyltitanium dichloride (Cp_2TiCl_2) with diacid salts, diols, dithiols and diamines are examples.[88] Similar types of ferrocene-containing polymers as well as poly 1,1'-ferrocenylenes have been prepared by a variety of coupling reactions.[91-95] However, these methods have generally led to the isolation of low molecular weight polymeric species.

The incorporation of ferrocene into polymeric structures has experienced a resurgence due to the work of Ian Manners and his coworkers who have developed the use of ring-opening polymerization (ROP) as a new route to polymers containing skeletal ferrocene units. Ring-opening polymerization generally occurs via chain-growth processes

and represents a unique route to the preparation of metal-containing polymers. The restrictive stoichiometric and conversion requirements, which often result in low molecular weight species via condensation techniques do not play a role here.[85] Manners has taken advantage of previously published investigations of [1]ferrocenophanes which showed that these compounds possess strained, ring-tilted structures in which the planes of the cyclopentadienyl ligands are tilted with respect to one another as compared to the parallel cyclopentadienyl ligands of ferrocene.[85, 96] Figure 1.9 illustrates the thermally induced ring-opening polymerization of both [1] and [2] ferrocenophanes developed by Manners for the preparation of ferrocene-containing high molecular weight polymers.[96-103] More recently, greater control over the chain length of the desired species has been achieved when [1] and [2] ferrocenophanes were subjected to ROP in the presence of an anionic initiator.[104-107]

The incorporation of ferrocene into the backbone of the polymer chain intially attracted the attention of the areospace industry in their search for polymers with high

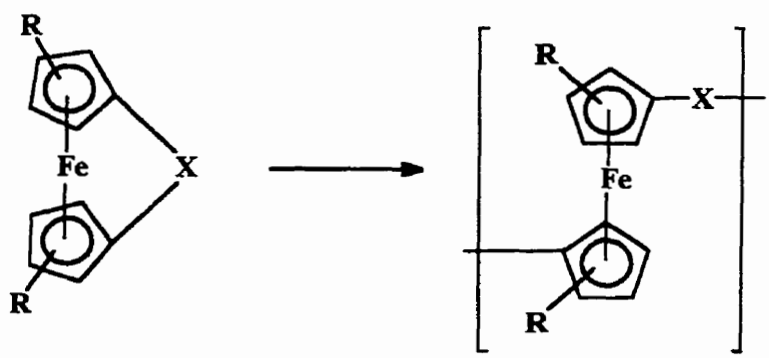

Figure 1.9: Ring-opening polymerization of [1] and [2] ferrocenophanes

thermal stability for use as lubricants and gaskets for jet engines, radiation shields and combustion regulators for solid-state rocket fuel.[90] Continued interest in these systems is maintained by their intriguing electrochemical properties which have shown evidence for through bridge interactions between the iron centers.[97-101, 103-104]

Integration of transition metals into the backbone of the polymer chain is also observed in the form of coordination polymers as a result of bridging of the metal by σ-bonded organic ligands.[90] Many transition metals, including the lanthanides and actinides, have been incorporated into these types of metal-containing polymers. The tendency of some of these materials to exhibit a high degree of non-linear optical activity or electrical conductivity has spurred extensive synthetic investigation. The majority of these polymeric species are insoluble, and in combination with their ease of degradation makes them useful for the controlled release of drugs or growth hormone.[90] Figure 1.10 illustrates one example of a coordination polymer which incorporates ruthenium into the polymer backbone.[108]

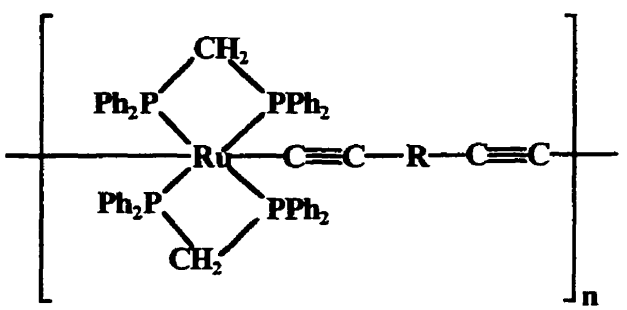

Figure 1.10: Ruthenium coordination polymer

1.3.3 Organometallic Polymers with Pendent Metal Moieties

Polymers in which the metal moieties are pendent to the backbone of a mainly organic polymer chain have been shown to have a marked effect on the physical and chemical nature of the resulting material. A universal feature of all polymeric species and one which continues to plague polymer chemists alike is the decreased solubility experienced with increased molecular weight. However, it has been demonstrated that a slight modification of the polymer structure in the form of a side group addition can increase the solubility of the polymeric material. Relative to its organic counterpart, a marked increase in polymer solubility may be observed upon π-complexation of a metal moiety.[19]

Perhaps the most readily applied route to the synthesis of metal-containing polymers originated in the 1960's with the discovery that vinyl ferrocene and other vinylic transition metal π-complexes undergo polymerization under the same conditions as conventional monomers to form the corresponding polymeric material.[109] Vinyl-organometallic polymers are formed from the addition of the vinyl units where either or both X and Y may be metal-containing moieties and result in the synthesis of homopolymers (when X=Y) and copolymers (when X≠Y) (Figure 1.11).[86]

Figure 1.11 illustrates the diversity of metals that may be appended to the backbone of the polymer chain employing just one synthetic approach. It would be futile then to attempt a comprehensive review of polymeric materials of this type in any detail here. Consequently, the following discussion will be limited to those reports in which the metallic species is pendent to polymeric chains with etheric and thioetheric linkages.

As of late, ruthenium has shown the greatest promise as the metal of choice in the synthesis of polyaromatic ethers and thioethers with pendent metallic moieties. In 1985, a noteworthy communication by Segal described the application of S_NAr reactions in the preparation of poly(ether-ether-ketone) with pendent $CpRu^+$ metal moieties.[17] The liberation of the metallic moiety via photolytic demetallation or thermal arene replacement reactions was a distinct benefit of this innovative synthetic approach to polyethers. The presence of the pendent metallic moiety also enhanced the solubility of the complexed polymer in DMSO and acetonitrile relative to the insoluble nature of the purely organic analogue.

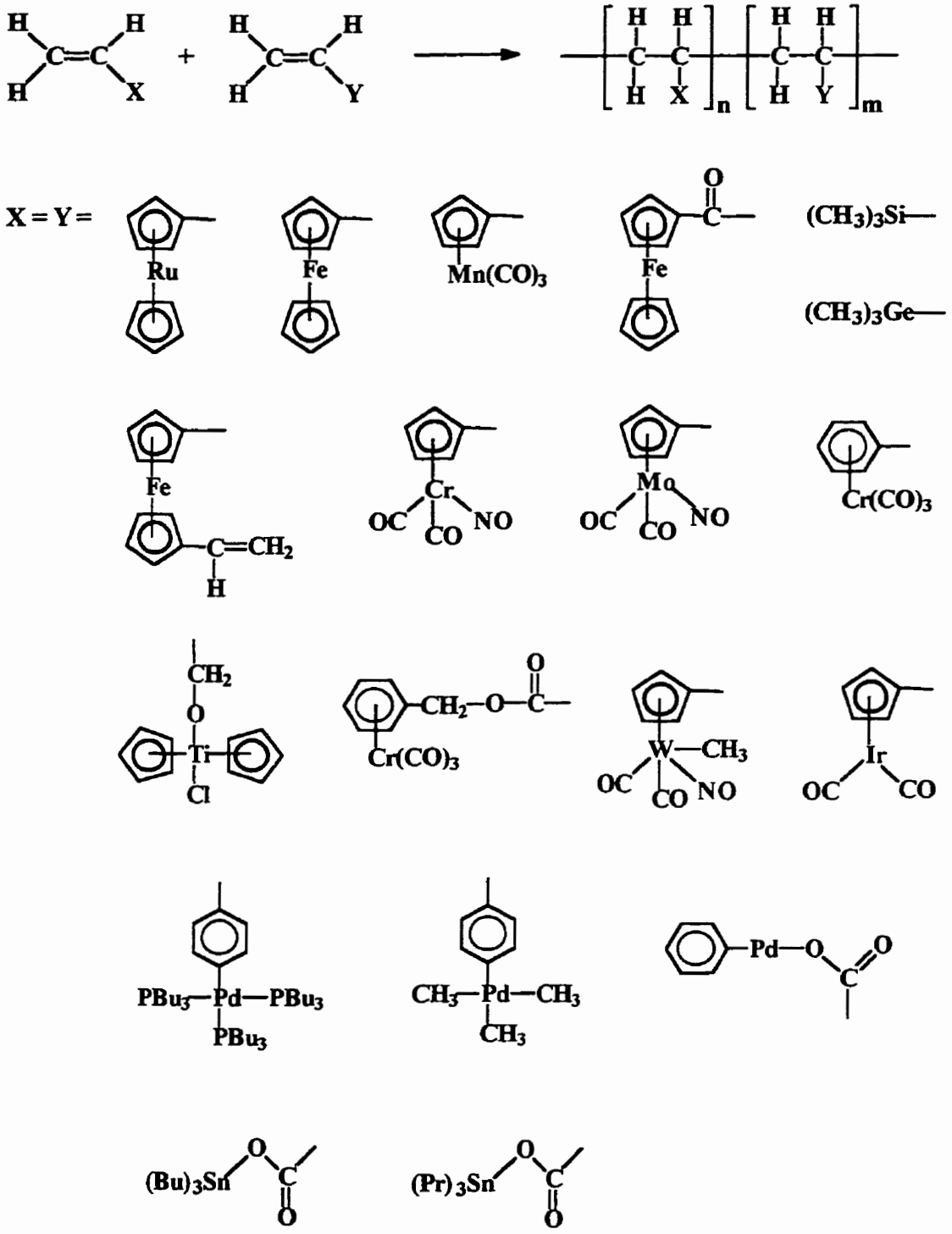

Figure 1.11: Formation of polymers with pendent metallic moieties from the addition of vinyl units

The reaction of the (1,4-dichlorobenzene)$Ru^{+}Cp^{*}$ complex with various aromatic ether and thioether dinucleophiles allows for the isolation of the corresponding metallated polymeric materials.[19, 110] Acetonitrile, DMF and DMSO soluble metallated poly(phenylene sulfide) and poly(phenylene oxide) have been prepared by Dembek and coworkers following the reaction sequence illustrated in Figure 1.12. Despite Dembek's success in the preparation of the metallated materials, attempts to isolate the free organic polymers were hindered by premature precipitation resulting in incomplete removal of the $Ru^{+}Cp^{*}$ moiety.

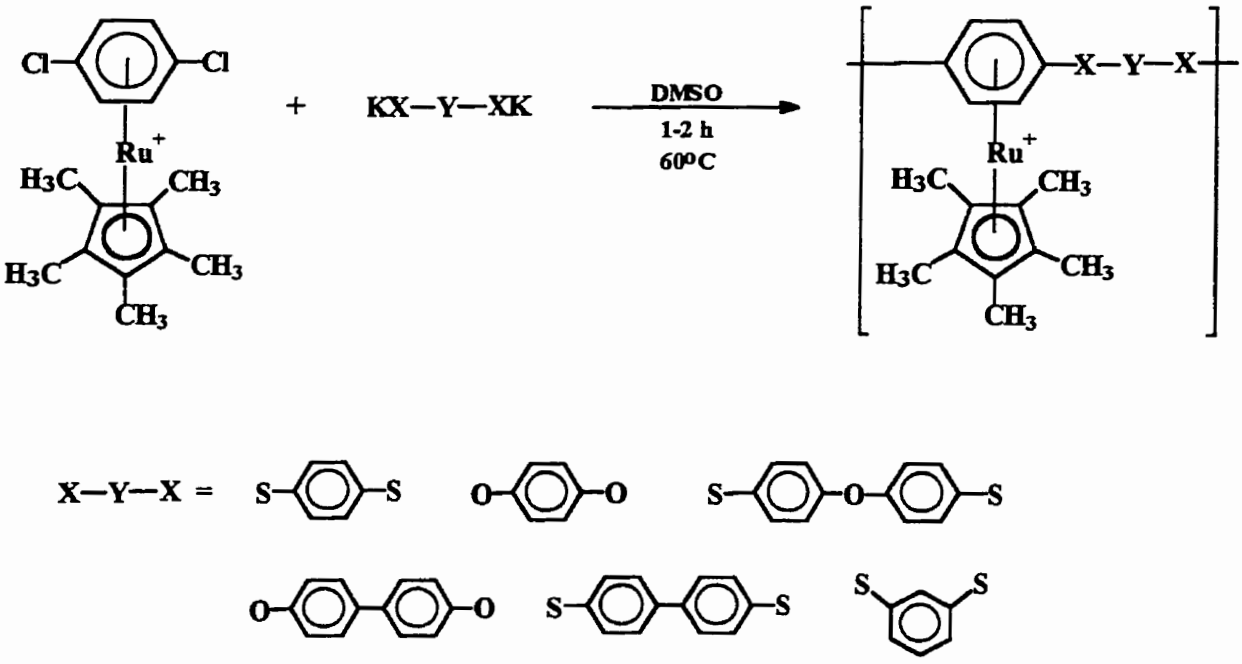

Figure 1.12: The preparation of poly(phenylene sulfide) and poly(phenylene oxide) with pendent $Cp^{*}Ru^{+}$

More recently, Abd-El-Aziz and coworkers have described the use of $CpFe^{+}$ activated chloroarenes in the stepwise preparation of oligomeric species with etheric linkages.[70] This methodology involves the successive reaction of p-dichloro- and p-dihydroxy- terminated poly(cyclopentadienyliron) cations under very mild reaction conditions that allowed for the preparation of metallated oligomeric species with up to 35 pendent metallic moieties. Furthermore, photolytic demetallation was successfully employed for the isolation of the modified organic counterpart in which the molecular weight was virtually monodisperse. The synthetic strategy described above is depicted in Figure 1.13 and summarizes the controlled design of these oligomeric systems.

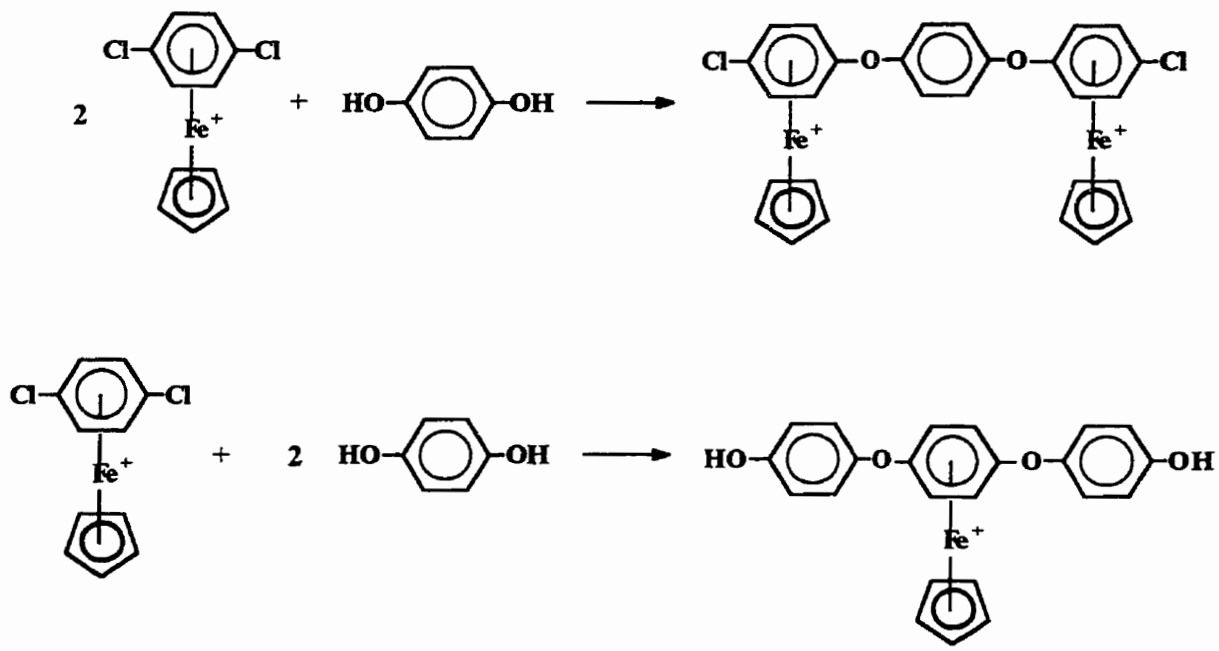

Figure 1.13a: Preparation of starting material for the stepwise synthesis of oligomeric polyethers with pendent $CpFe^{+}$ moieties[70]

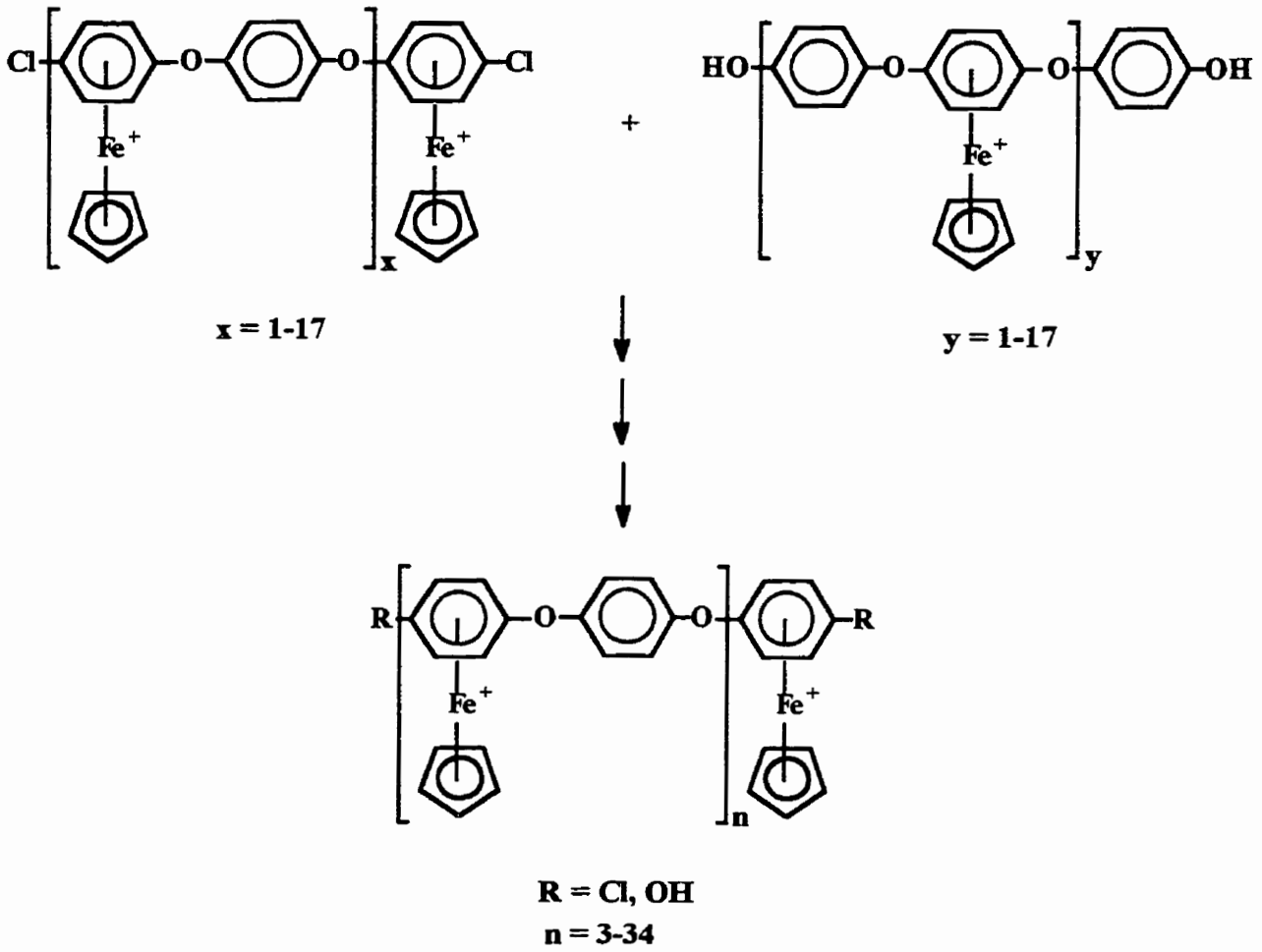

Figure 1.13b: The stepwise design of oligomeric aromatic ethers via $CpFe^{+}$ activated nucleophilic aromatic substitution reactions[70]

1.4 Polyarylethers and Polyarylthioethers

1.4.1 Engineering Thermoplastics

Thermal stability, chemical resistance, flame retardancy, high mechanical strength and potential electrical properties are some of the characteristics inherent to polymeric materials that incorporate aryl ether and thioether linkages as a fundamental component of their molecular structure.[111-119] These attributes provide the basis for a family of polymeric materials referred to as "high performance plastics" or "engineering plastics". The commercial development of these materials has given rise to a class of high-performance plastics that are recognized for their superior performance in a number of demanding applications.[111, 113, 121-123] Engineering plastics continually enter industrial markets previously dominated by metals and great potential exists for further development of these materials with far reaching consequences.

The drive for commercial development of engineering plastics stems from their attractive balance of properties in addition to their cost efficiency.[123] The value of these types of polymers is magnified by the incorporation of various chemical functionalities into the polymer structure in an attempt to design materials with specific qualities.[116-117, 120, 123-124] Several industrially significant high performance engineering thermoplastics are represented in Figure 1.14, and combine ether, thioether, carbonyl, sulfone and amine linkages within the backbone of the polymer chain.

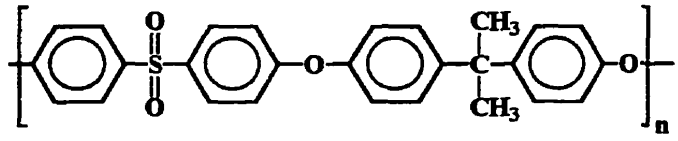

UDEL Polysulfone

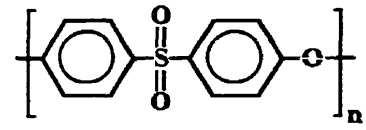

Vitrex Polyethersulfone

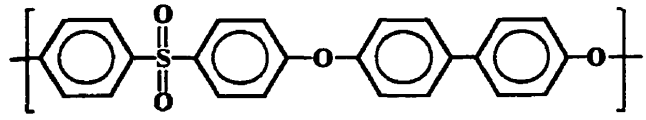

Radel Polyethersulfone

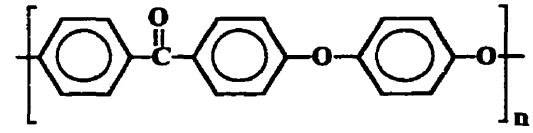

Vitrex Polyetheretherketone

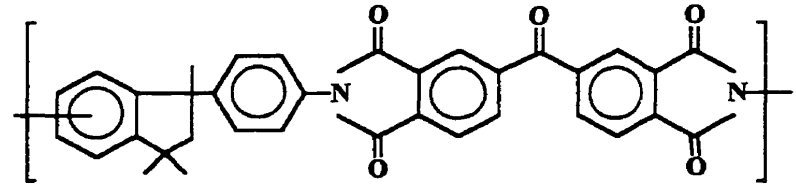

Larc-TPI Polyimide

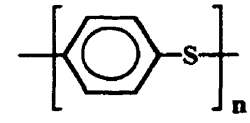

Polyphenylene Sulfide

Figure 1.14: Industrially important engineering thermoplastics

Due to the structural variations in these materials, no one synthetic approach has been developed for the preparation of the above polymers. As a result, the synthetic methodology applied for polymer preparation is selective with respect to the structural intricacies of the material itself and its intended purpose.[123-124] Several of the most commonly applied methods and recently developed methods used in the synthesis of polyarylethers and polyarylthioethers will be mentioned briefly in the following discussion.

1.4.2 Electrophilic Synthetic Methods

Electrophilic techniques used in the preparation of polyarylethers and polyarylthioethers take advantage of the electron rich nature of aromatic compounds and rely on the attack by electron deficient species to the ring. Monomer selection plays an important role in determining the success of any polymerization reaction. For instance, although other sources have been noted, electron deficient species such as sulfonium ($-SO_2^+$), acylium ($-CO^+$), and carbenium (R_3C^+) ions are predominantly generated from their corresponding acid halides or the free acid.[124] In the case of the aromatic species, it has been noted that ether activated aromatic rings are more apt to undergo electrophilic reactions than aromatic rings that incorporate electron-withdrawing groups or have neighboring rings with these types of substituents whose effect may be transmitted through the aromatic structure.

Some of the earliest publications describing the use of electrophilic techniques in the preparation of polymeric materials appeared in 1888 and 1897 by Friedel and Crafts and by Genvresse, respectively, and report the reaction of benzene and sulfur in the presence of aluminum chloride resulting in the synthesis of poly(phenylene sulfide) (Figure 1.15).[123, 125-126] However, only very low molecular weight products were isolated and the structure of these materials has been questioned as to whether they would even have the structural potential to be considered polymers.

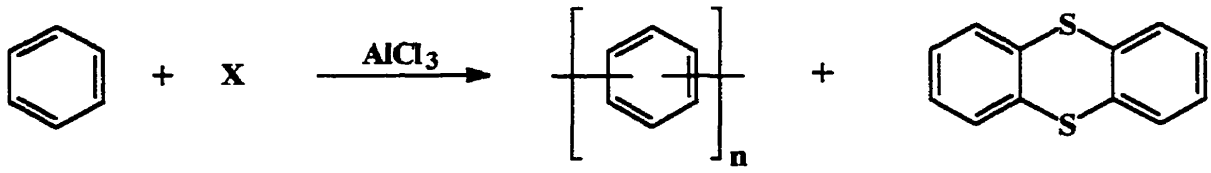

$X = S_8, S_2Cl_2, SCl_2$

Figure 1.15: Preparation of poly(phenylene sulfide) in the presence of Friedel-Crafts catalysts

Further development of electrophilic techniques acknowledged the unique catalytic nature of Friedel-Crafts catalysts. Aluminum chloride, ferric chloride, antimony pentachloride, molybdenum pentachloride, indium trichloride and trifluoromethanesulfonic acid were among the species to demonstrate particularly high activity and were subsequently found to be useful in these polymerization reactions.[123-124, 127-131] $FeCl_3$ and $AlCl_3$ are the most readily used catalysts. Although both melt and solution polymerization processes have been successfully used, solution techniques are generally the method of choice in order to avoid the use of very high reaction temperatures.[127] Nitrobenzene is generally the solvent of choice in these reactions since it allows for the solubility of the monomers and resulting polymers and was found to be compatible with the Lewis acid catalysts.

Friedel-Crafts techniques have been extensively studied with respect to the preparation of polyethersulfones because the polymers are obtained in high yield. However, stoichiometric amounts of $AlCl_3$ are required to promote the successful polymerization of polyetherketones. This poses difficulties in polymer isolation and promotes branching.[124, 127] More recent innovations in $AlCl_3$ based electrophilic

processes have employed the use of Lewis bases in conjunction with Lewis acid catalysts in an attempt to control polymerization, especially with regard to possible side reactions (Figure 1.16).[124]

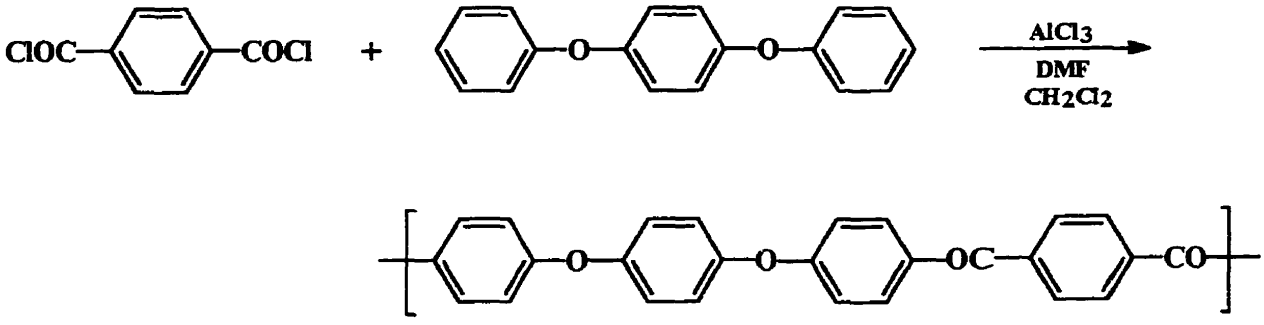

Figure 1.16: Polymerization using Lewis acid catalysts in the presence of Lewis bases

Structural studies of polymeric species have determined a definite relationship between polymer structure and the melt and mechanical processibility of the corresponding materials. Essentially, linear polymers yield the toughest polymers.[128, 130-131] The formation of ortho structures during chain growth and/or chain branches by post reaction on polymer repeat units represent some of the most common defects generated as a result of electrophilic processes and tend to change a tough polymer into brittle material. The preparation of linear polymers is inherent via electrophilic reaction where a single monomer such as 1,4-phenoxybenzenesulfonyl chloride is employed (Figure 1.17).[128, 130] Polymerization is moderated by the presence of the sulfonyl group which promotes sulfonylation of the rings entirely in the para position. In contrast, utilizing two monomeric species, one of which is composed solely of etheric linkages, introduces a

higher potential for structural defects. This stems from the fact that the sulfonylation of diphenyl ether directly allows for the possibility of a substantial amount of ortho-substituted products to be formed as a result of the absence of the directionally moderating sulfone groups (Figure 1.17).[128, 130] As the reaction proceeds, branching occurs causing a decrease in the concentration of the phenoxy end groups. Although electrophilic methods may be used effectively for polymer synthesis, these routes generally result in more structural flaws as compared to nucleophilic routes.

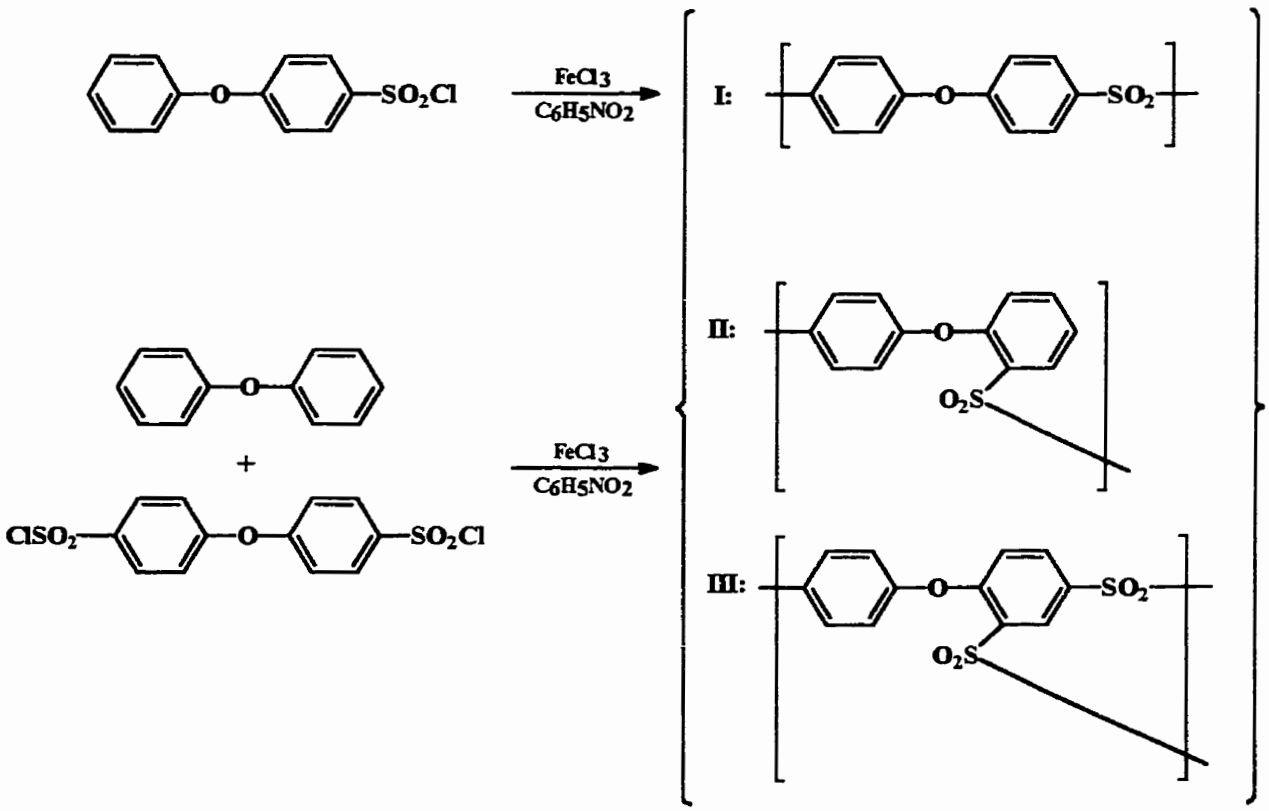

Figure 1.17: Structural characteristics of polymeric species resulting from one and two monomer processes

1.4.3 Nucleophilic Methods

In the past few decades, nucleophilic displacement techniques have been exploited as a viable route to the preparation of commercially important engineering thermoplastics. This is ironic because the electron-rich nature of an aromatic ring imposes certain restrictions on their reaction toward nucleophiles. Be that as it may, aromatic nucleophilic displacement reactions have been studied using both activated and unactivated nitro- or haloarenes with alkali metal phenolates and thiophenolates.[132] Nucleophilic displacement of a leaving group on an activated system generally proceeds by a two-step addition-elimination mechanism which involves the formation of a highly energetic Meisenheimer complex followed by loss of the leaving group. When the aromatic ring bears strong electron-withdrawing substituents in addition to a good leaving group, nucleophilic displacements take place under mild reaction conditions.[132]

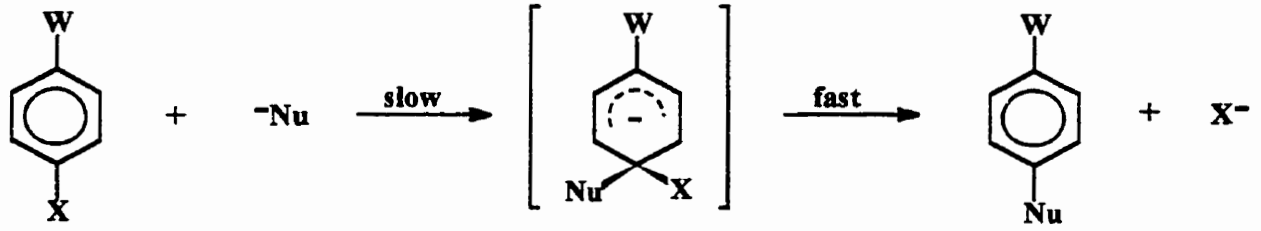

Figure 1.18: Two-step nucleophilic substitution mechanism via the highly reactive Meisenheimer complex

The reaction of a number of di- and poly- haloaromatics with various metal sulfides, which were either added unreacted or formed in situ from sulfur and the metal oxide or carbonate, was investigated by Macallum in the formation of poly(phenylene sulfide).[125, 133-138] In particular, he focused on the reaction of 1,4-dichlorobenzene with sodium carbonate and sulfur in a sealed container at 275-360°C as illustrated in Figure 1.19. The commercial utilization of this process was hindered by its highly exothermic nature which made it difficult to control. Additionally, the composition and physical properties of the polymers were highly sensitive to the reactant ratios employed.[136] About a decade later, Edmonds and Hill reported the procedure which is presently used for the preparation of a variety of arylene sulfide polymers from readily available starting materials.[123, 134] Poly(phenylene sulfide) is industrially produced by the reaction of 1,4-dichlorobenzene and sodium sulfide in a polar solvent (Figure 1.20).

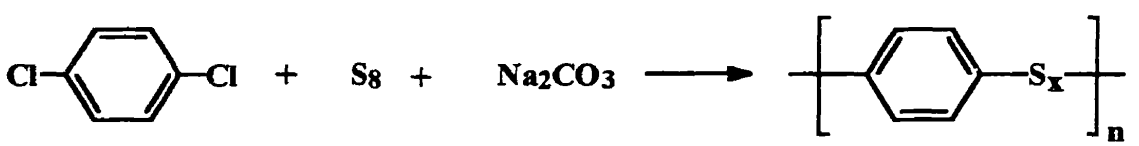

Figure 1.19: Preparation of poly(phenylene sulfide) by the Macallum polymerization process

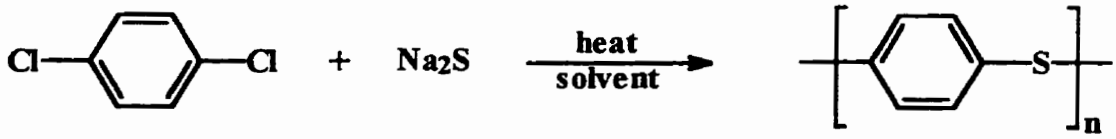

Figure 1.20: Industrial process used for the preparation of poly(phenylene sulfide)

Generally, the preparation of high molecular weight polymers via nucleophilic substitution results from the reaction of bisphenates or bisthiophenates with aromatic dihalides and is a prime representative of step-growth or condensation polymerization.[124] For the most part, nucleophilic routes are dominated by the use of either sodium hydroxide or alkali metal carbonates as bases for the formation of the desired bisphenates or bisthiophenoxides (Figures 1.21 and 1.22).[123-124, 139-145]

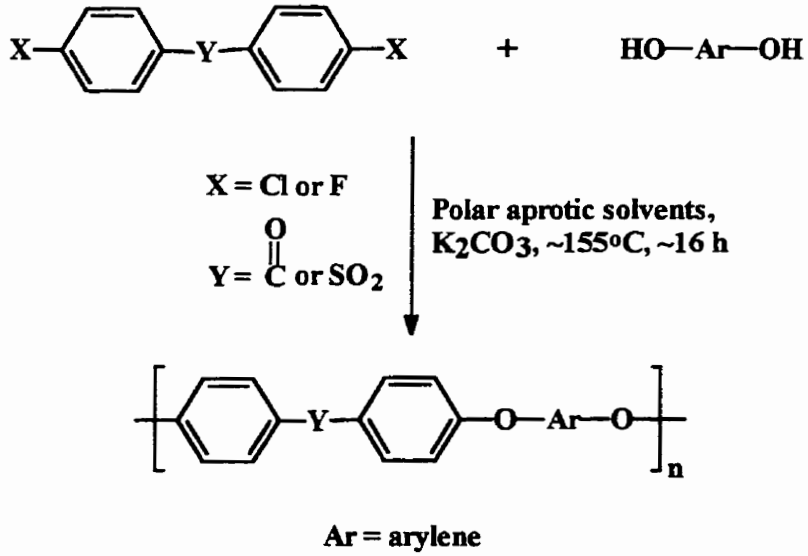

Figure 1.21: Nucleophilic substitution reaction using the carbonate process

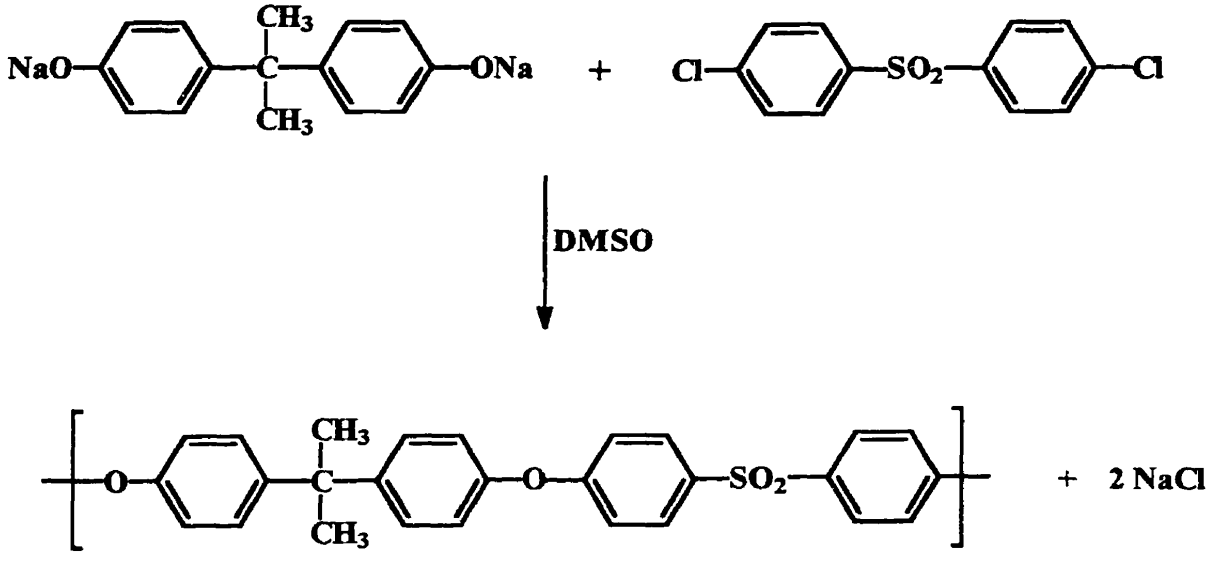

Figure 1.22: Nucleophilic substitution using the caustic process

Regardless of the methodology applied, several factors play a crucial role in the production of polymers with useful properties. The reactivity of the aromatic dihalide is dependent upon both the activating groups and the halide to be displaced. The reported order of ease of displacement in activated aromatic halides is usually F>>Cl>Br>I.[124, 139-140] Consideration of the nucleophilicity and thermal stability of the bisphenate during polymerization is another issue which must be explored. Although the presence of an electron-withdrawing substituent is essential for the nucleophilic activation of the haloaromatic monomer, its presence is found to be detrimental to the phenate monomer.[125, 140] Whereas electron-donating substituents para to the phenate group enhance its nucleophilicity; the electron-withdrawing capability of certain chemical functionalities render the bisphenol more acidic and its corresponding phenoxide less reactive.

The stepwise nature of these routes also implies the need of a 1:1 stoichiometric ratio of the bisphenate to the dihalide in the preparation of high molecular weight species.[124-125, 139-145] As a result, it is crucial to attain high purity monomers and avoid any side reactions that may disrupt these ideal conditions. A potential disturbance in ideal stoichiometry when sodium hydroxide is used as a base is the hydrolysis of the halo substituents of the dihalide monomer (Figure 1.23).[125, 139, 142]

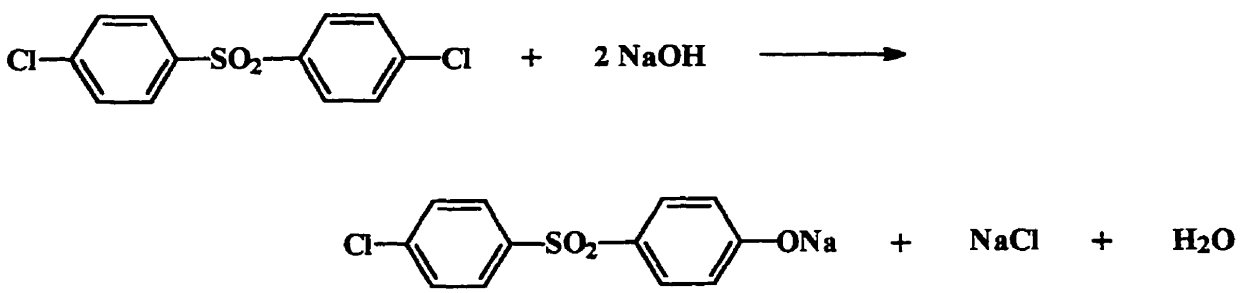

Figure 1.23: Potential stoichiometric disturbance due to the presence of excess sodium hydroxide

For, instance, sodium hydroxide is formed by the hydrolysis of the bisphenol salt due to the presence of water and reacts with the polymer end groups or dichlorophenyl sulfone according to Figure 1.23. Consequently, the stoichiometry of the reaction is disrupted since the sodium salt that is produced is not nucleophilic enough to react and results in termination of the polymerization process. It is important to note then that in this case, the use of stoichiometric amounts of sodium hydroxide are crucial to avoid side reactions. This is one of the fundamental reasons why alkali metal carbonate processes have been

favored in nucleophilic substitution reactions. It has been observed that small excesses of inorganic carbonate can be tolerated in the reaction and is not detrimental to the resulting molecular weight of the isolated polymeric material.[144] Furthermore, whereas the caustic process requires the generation of the bisphenate salt from the reaction of the bisphenol and sodium hydroxide prior to nucleophilic reaction, the carbonate process allows the formation of the desired nucleophile in situ.

A recent investigation conducted by Riffe and coworkers presents the use of nucleophilic substitution routes for the synthesis of poly(arylene ether ether sulfides).[146] The first step in this methodology involves the nucleophilic reaction of difluorodiphenyl sulfoxide with hydroquinone or 4,4'-diphenol in the presence of K_2CO_3 using a mixture of NMP/toluene as the solvent. Further reduction of the sulfoxide in the presence of a stoichiometric amount of oxalyl chloride and two molar equivalents of tetrabutylammonium iodide allowed for the preparation of the corresponding sulfide containing polymer (Figure 1.24).

The use of anhydrous sodium sulfide in the incorporation of sulfide linkages has recently witnessed a rejuvenation in the preparation of poly(sulfide sulfone). Maita and Dutta demonstrated the use of the activated nucleophilic displacement reaction of bis(4-nitrophenyl)sulfone and Na_2S at 200°C in NMP in the preparation of the corresponding sulfide containing polymer as illustrated in Figure 1.25.

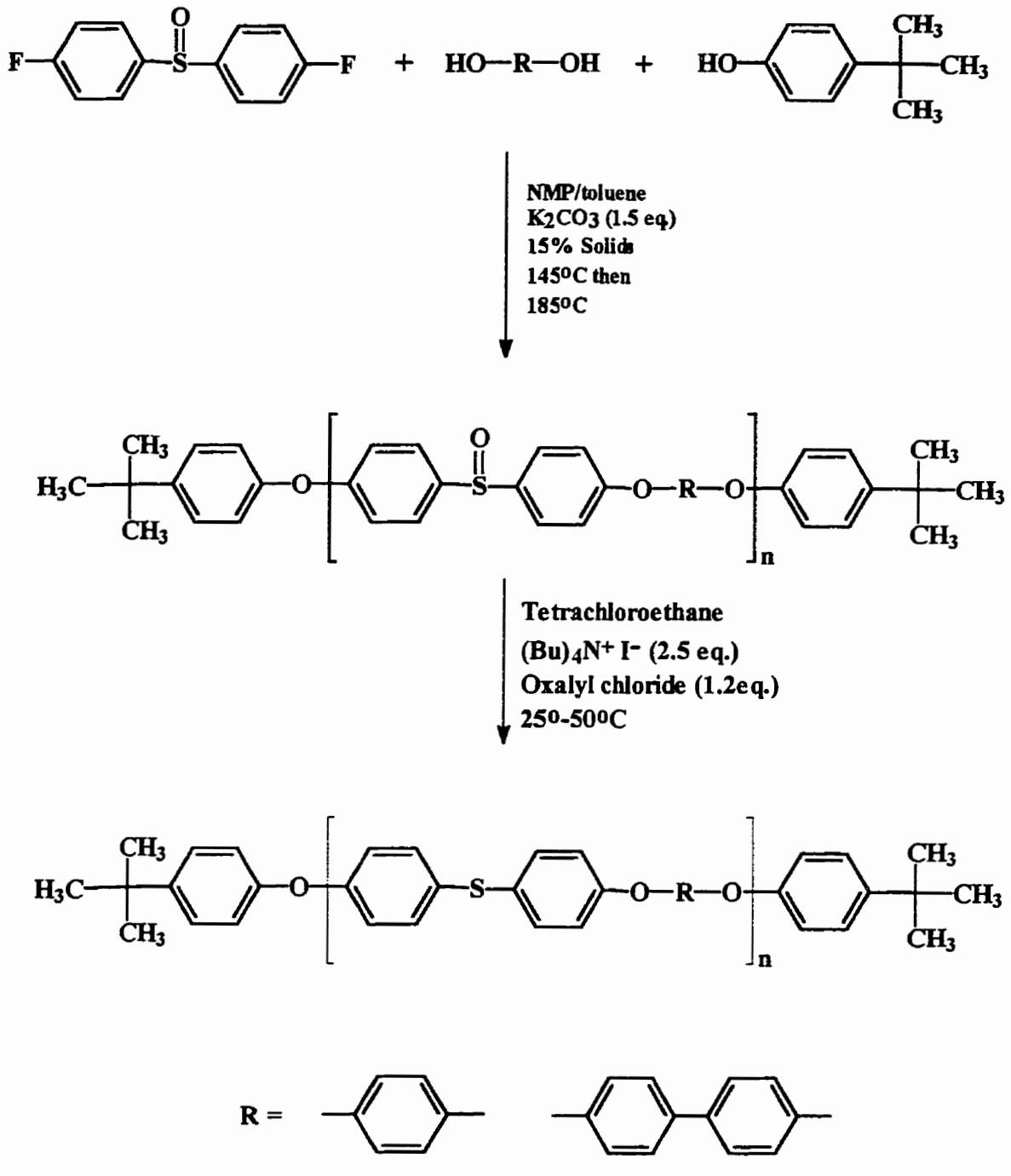

Figure 1.24: Synthesis of poly(arylene ether ether sulfides)

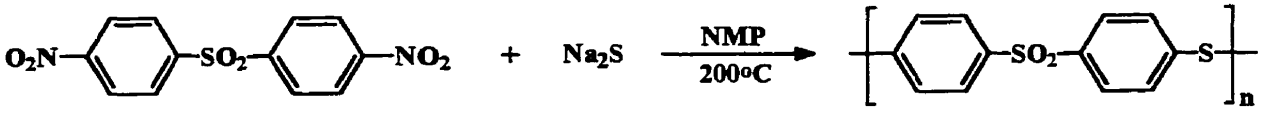

Figure 1.25: Preparation of poly(sulfide sulfone) by the reaction of activated nitro monomers with anhydrous sodium sulfide

1.4.4 Scholl Polymerization

In the past decade, Percec and coworkers have demonstrated the utility of the Scholl reaction in the preparation of various polyarylethers. Essentially, the Scholl reaction involves the elimination of two aryl hydrogen atoms resulting in the formation of an aryl-aryl bond in the presence of Friedel-Crafts catalysts.[148-157] Extensive investigation has shown that the reaction proceeds most successfully when dinaphthoxy containing monomers are subjected to polymerization in the presence of ferric chloride as the catalyst. The polymerizations can be run in nitrobenzene at room temperature. Figure 1.26 shows an example of the Scholl reaction for the preparation of an aromatic polyethersulfone.

The reaction is believed to proceed via a cation-radical mechanism where a radical-cation is generated at one of the naphthoxy groups due to the one electron oxidation of the monomer by $FeCl_3$.[151-152, 155, 157] It is the ease of oxidizability of the napthoxy groups in this initial step that makes these monomers most appropriate for Scholl polymerization. Chain growth then continues as a result of either electrophilic or radical propagation steps

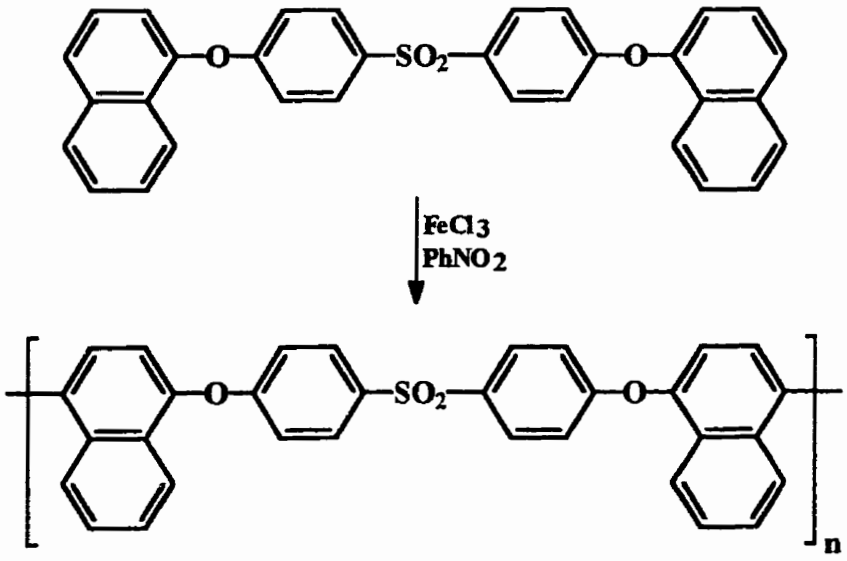

Figure 1.26: Preparation of a polyethersulfone via the Scholl reaction

with termination taking place due to the combination of the cation-radical with the counter-anion or with a fragment of it. Although several attempts have been made in the preparation of some commercial polyarylethers by the reaction of diphenyl terminated monomers as exemplified in Figure 1.27, only low molecular weight materials were isolated.[149, 154-155, 157] Details of the Scholl reaction will be considered more extensively in Section 4.1 of this work.

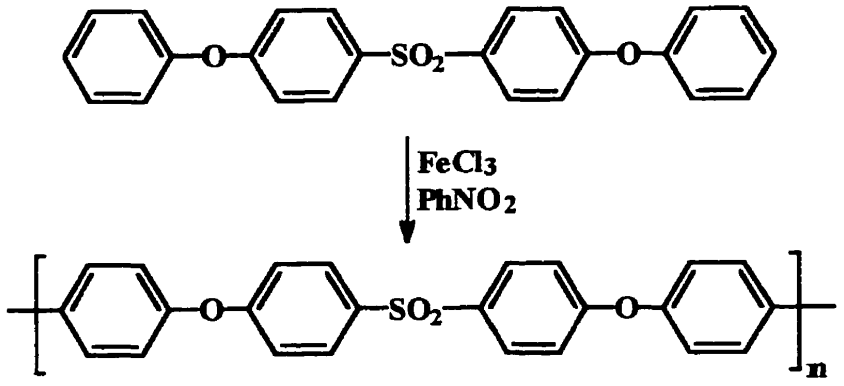

Figure 1.27: Low molecular weight polyethers with diphenyl terminated monomers

1.4.5 Ullmann Polymerization

It has been stated that the studies of Ullmann in the early 1900's with regard to the preparation of diarylethers precipitated the development of the well known nucleophilic and electrophilic processes which have been employed commercially in the synthesis of many engineering thermoplastics. The Ullmann reaction is best recognized as a method for the preparation of polyaromatic ethers involving the reaction of alkali metal phenoxides with aryl halides where the halogen containing monomer is not activated by an electron-withdrawing group.[158-160] Figure 1.28 illustrates the reaction of the sodium salt of Bisphenol A with a dibromo momomer under Ullmann reaction conditions. Copper based species such as copper halides, copper oxides and metallic copper are used to catalyze the reaction. Copper oxides demonstrated the greatest reactivity.[161] Mechanistic studies concluded that the cuprous ion is the active species which coordinates with the pi system of the aromatic halide making the resulting complex more susceptible to carbon halogen

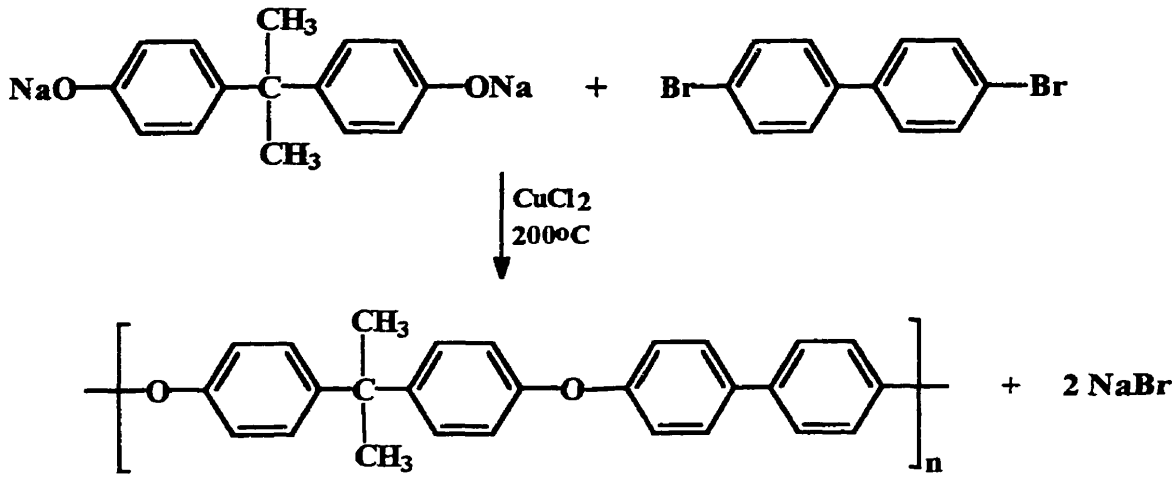

Figure 1.28: Preparation of poly(1,4-phenylene oxide)

using Ullmann reaction conditions

cleavage.[162-165] The proposed mechanism for the Ullmann reaction is illustrated in Figure 1.29.

Several aspects of the reaction conditions have been identified as playing influential roles in determining the success of this process. For instance, the phenols are generally reacted in the form of their corresponding alkali metal salts where the greater reactivity of the potassium phenoxide is favored over the sodium counterparts.[159] An interesting observation of this reaction is the order of ease of halide replacement with respect to the haloaromatic monomer. The activity of the aryl halide is the reverse of that seen for polyether formation from activated halides or in short decreases in the order I>Br>Cl>>F.[161-165] The effect of the haloaromatic is most obviously illustrated by the dramatic decrease in yield, from 70% to 10%, experienced in utilizing iodobenzene or chlorobenzene, respectively, under identical reaction conditions. Despite the high yields of

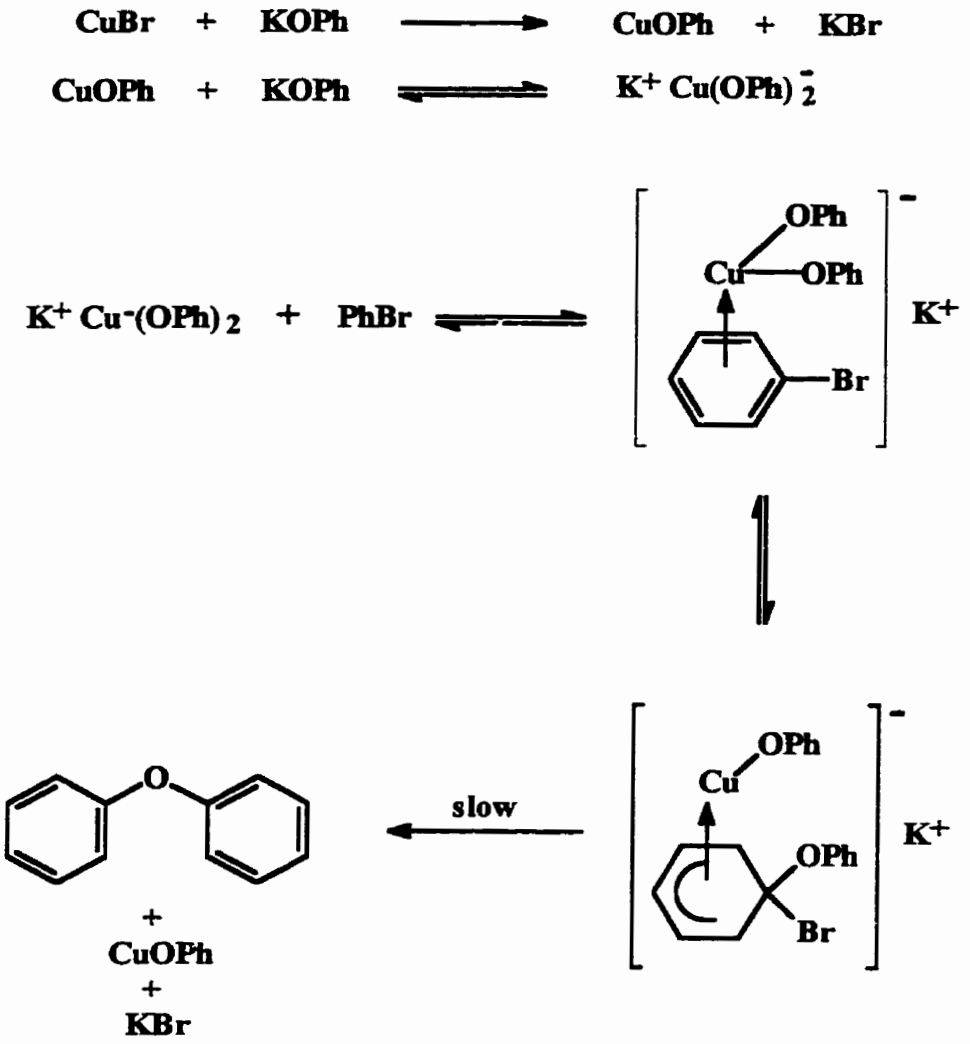

Figure 1.29: Mechanism of the Ullmann reaction

product isolated with the use of iodobenzene starting materials, the expense of these compounds often encourages the use of their brominated derivatives with a slight decrease in yield. In addition to these considerations of the haloaromatic starting materials, the activity of the phenolic unit was completely hindered by the presence of methyl groups in both ortho positions to the hydroxy group. However, the presence of one ring substituent ortho to the hydroxy group was not found to greatly affect the outcome of the reaction.[166]

Another aspect of the reaction conditions which has been demonstrated as influential in determining the success of product formation is the choice of the solvent. Although a variety of solvents including DMF, HMPA, DMSO, collidine, pyridine and nitrobenzene have been investigated as potential solvents for the Ullmann reaction, cuprous chloride in pyridine has been determined to be the preferred catalyst/solvent system.[167] Figure 1.30 illustrates the reaction of the potassium salt of 1,3-dihydroxybenzene with bromobenzene resulting in the isolation of two products, 1,3-diphenoxybenzene and 1,3-phenoxyphenol. With regard to the reported solvent studies, of particular interest is the dramatic effect that water and acidic solvents had on the efficiency of the reaction.[159] Although the above reaction carried out in pyridine alone resulted in the isolation of 1,3-diphenoxybenzene and 1,3-phenylphenol in 72 and 15% yields, respectively, the addition of only a minute amount of water (2%) caused a decrease in the yields to 22 and 4%. Although the Ullmann ether synthesis has been demonstrated as a viable route to the preparation of polyarylethers, its potential for industrial application is hindered by the low to moderate product yields resulting from possible side reactions such as the Ullmann coupling process, reductive dehalogenation and halogen exchange between the catalyst and aryl halide

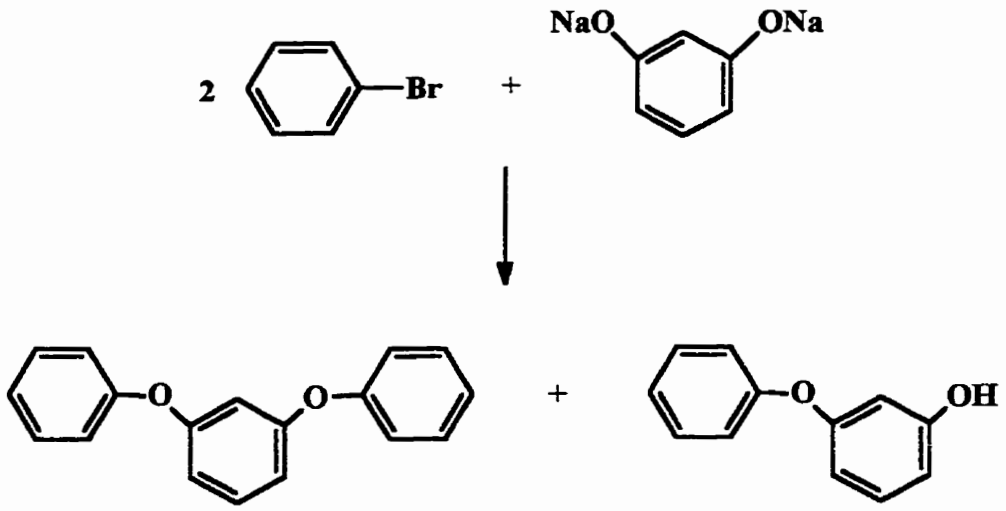

Figure 1.30: Two products resulting from the Ullmann reaction in the presence of acidic solvents

1.4.6 Nickel-Catalyzed Coupling Reaction

Nickel-catalyzed coupling represents one of the more novel routes to the preparation of polyarylethers. Aryl dihalides are reacted in the presence of zero valent nickel which promotes the formation of an aryl-aryl bond by the elimination of the two aryl halides (Figure 1.31).[168-169] The polymerization takes place most effectively under an inert atmosphere in a dry aprotic solvent in which zero valent nickel is generated from a three component mixture of a nickel salt, triphenylphosphine and a reducing metal such as Mg, Mn, or Zn.[168]

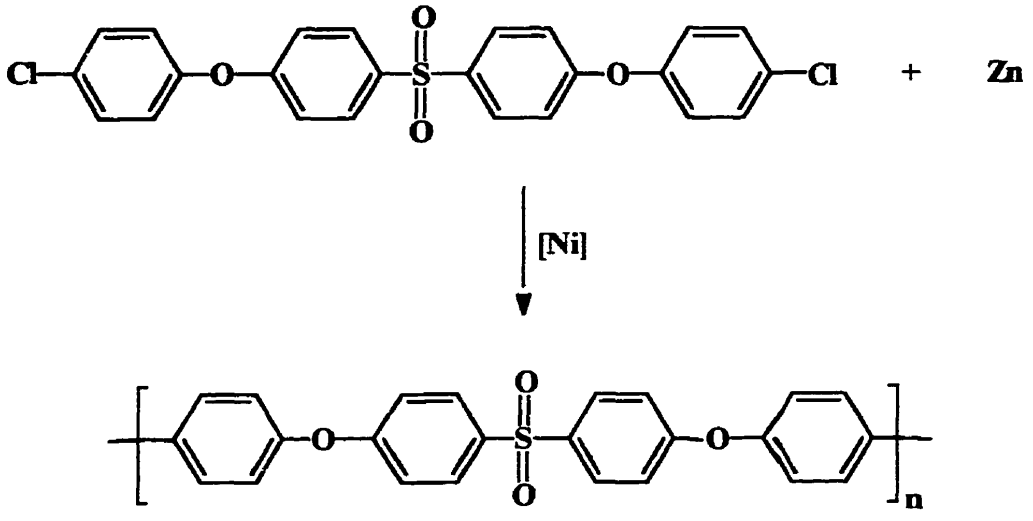

Figure 1.31: Nickel catalyzed preparation of a polyethersulfone

More specifically, optimal reagent mixtures are composed of a less than 2% mole ratio of nickel based on the amount of aryl dichloride, high triphenylphosphine/nickel ratios and an excess of zinc which are subjected to moderate reaction temperatures.[169-171] Monomer units must be chosen carefully to ensure that any functional groups present are inert toward the zinc/nickel catalyst system. It has been observed that electron-withdrawing substituents allow for the isolation of the products in the greatest yield with the exception of nitro and protic groups which are not tolerated at all.[169] Side reactions are a concern when the starting reagents include electron-donating groups as part of their structure.[168-169] In an attempt to prepare high molecular weight materials, the solubility of the monomer and its corresponding polymer in the reaction medium must be considered.

Figure 1.32 outlines the proposed mechanism of the nickel-catalyzed polymerization process.[168] It is postulated that the initial step in the process involves the

generation of the active zero valent Ni complex by the reduction of the nickel halide from Ni(II) to Ni(0). The subsequent oxidative addition of the aryl chloride results in the preparation of the corresponding Ni(II) intermediate which, following reduction in the presence of Zn, undergoes a second oxidative addition of aryl chloride in the formation of a diaryl Ni(III) complex. Liberation of the biaryl product involves a rapid reductive elimination process yielding a Ni(I) complex which is reduced further and may re-enter the cycle. At the same time, the Ni(I) species may react with arylchloride by oxidative addition to yield an arylnickel(III) intermediate which is reduced to arylnickel(I) and may re-enter the cycle in this form.

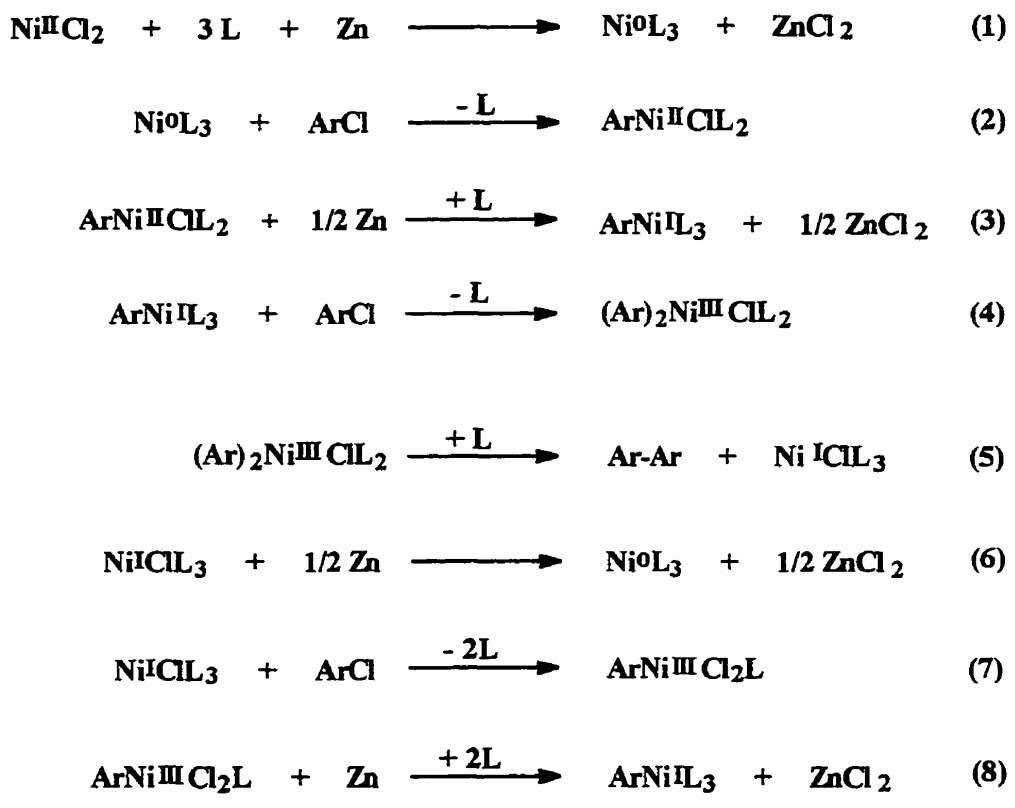

Figure 1.32: The nickel catalyzed mechanism

1.4.7 Palladium-catalyzed Cross-Coupling of Tin Reagents

The coupling reaction of bifunctional tin reagents with dihalides in the presence of a palladium catalyst has proven to be an effective route to polyarylethers.[172-173] Figure 1.33 is an example of the polymerization of 4,4'-bis(tri-n-butylstannyl)diphenyl ether with 4,4-dibromodiphenyl sulfone to yield moderately high molecular weight polysulfones.

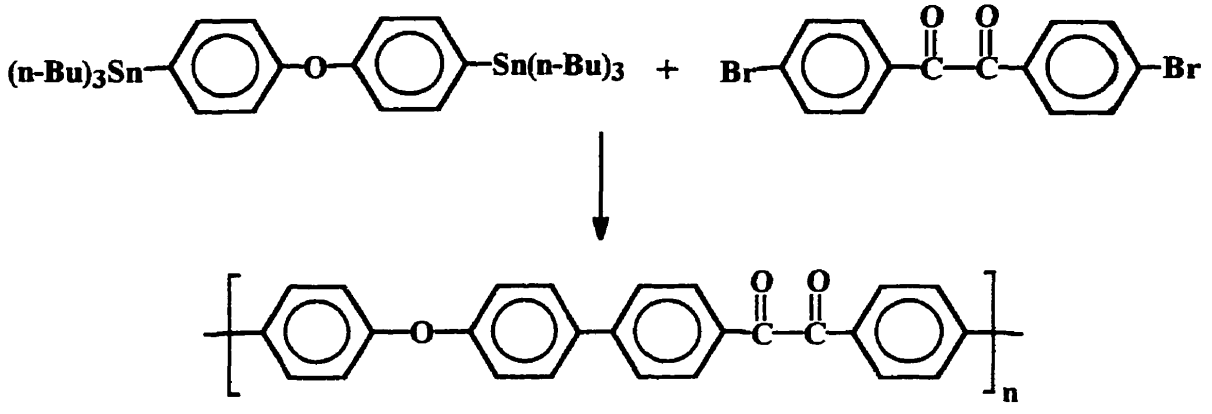

Figure 1.33: Palladium catalyzed polymerization of 4,4'-bis(tri-n-butylstannyl)diphenyl ether with 4,4'-dibromodiphenyl sulfone

A 2:1 triphenylphosphine:palladium chloride catalyst system in DMAc at 165°C has been determined as the ideal conditions for the reaction. However, as is the case with most synthetic techniques, there are both advantages and disadvantages to the use of this method. This method benefits from the tolerance of pendent functional groups which may be included on the monomer unit yet suffers from low reaction yields.[172-173]

1.4.8 Temporary Complexation to a Metal Moiety

The activation of chloroarenes toward nucleophilic aromatic substitution reactions upon complexation to a metal moiety has been studied as a potential alternative for the synthesis of polyarylethers and thioethers.

Based on the superior reactivity of $(CO)_3Mn^+$ complexed chloroarenes toward reactivity with various nucleophiles, it is no surprise that these complexes have been investigated as a possible route to ether synthesis.[9-11] Figure 1.34 illustrates the reaction of a $(CO)_3Mn^+$ complex with the sodium salt of phenol in the preparation of the corresponding diphenyl ether. Pearson employed this methodology in the preparation of various diaryl ether and triaryl diethers which may be used further as precursors in natural product syntheses. Despite the success experienced in using the complexation of this metallic moiety for the incorporation of etheric linkages, the inability to prepare 1,2, 1,3, and 1,4-dichloroarene complexes restricts further use of this process for this polymer synthesis.[10]

It was mentioned previously that in comparison to other metal moieties that have been used to activate haloarenes toward nucleophilic aromatic substitution, the $Cr(CO)_3$ complexes have been shown to be the least reactive. The reaction of (1,4-dichlorobenzene)-$Cr(CO)_3$ with mono- or diphenoxides has resulted in the preparation of aryl ethers.[16, 175] The disadvantage of this reaction was the inability to obtain the desired disubstituted product without having to separate it from the mixture of products that results from the reaction (Figure 1.35).[16]

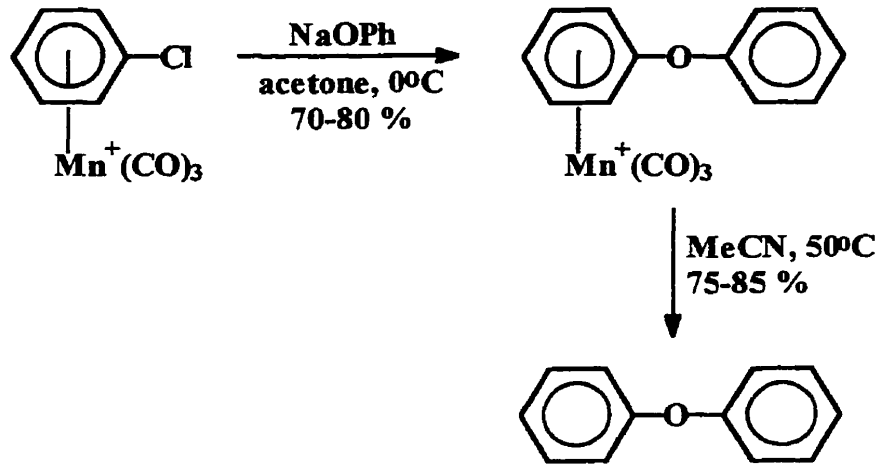

Figure 1.34: Complexation of the $(CO)_3Mn^+$ in the promotion of chloroarene toward S_NAr reactions in the preparation of ether linkages

Double nucleophilic substitution of (1,4-dichlorobenzene)-$Cr(CO)_3$ with the potassium salt of bisphenol A was also successfully attained and presents the potential for the production of high molecular weight species via further nucleophilic substitution. The efficiency of this reaction in the presence of 18-crown-6 with a reaction time of 2 hours is demonstrated by the isolation of the desired product in 73% yield (Figure 1.36). The reduced reactivity of $Cr(CO)_3$ complexes requires the use of polar aprotic solvents, high temperatures, prolonged reaction times, and phase transfer catalysts such as 18-crown-6.

More recently, ruthenium and iron based metal moieties have attracted considerable attention as possible routes to ether and thioether containing compounds.

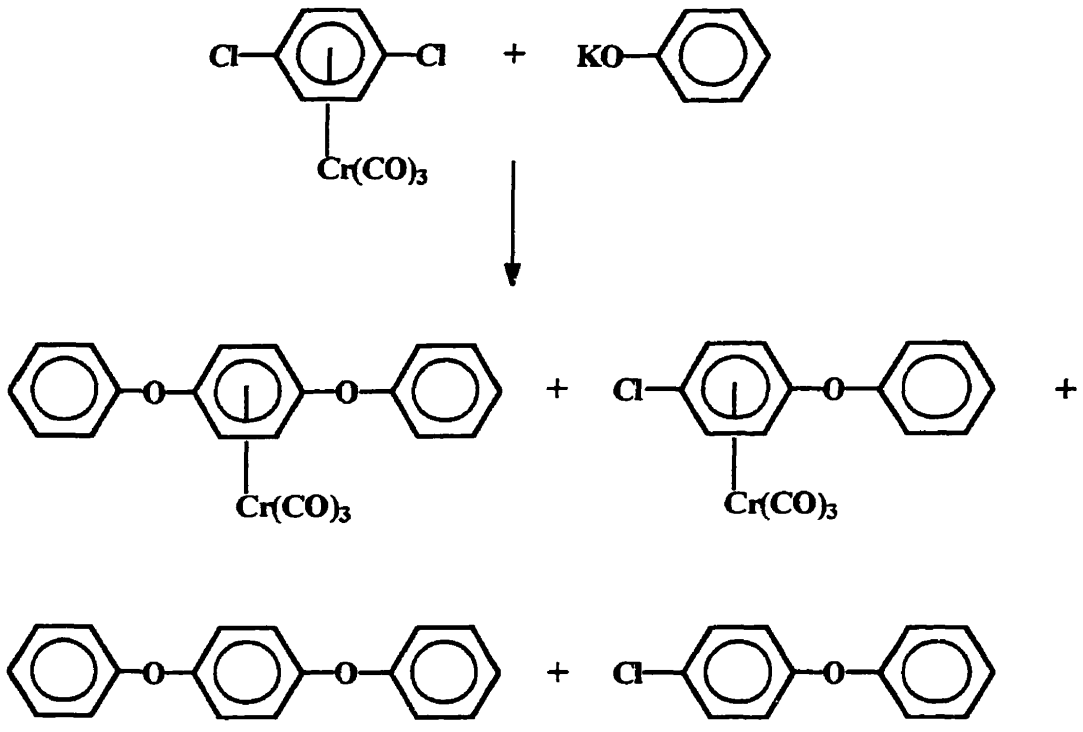

Figure 1.35: Nucleophilic aromatic substitution of (1,4-dichlorobenzene)$Cr(CO)_3$ with the potassium salt of phenol

The moderate activation capabilities in comparison with the chromium and manganese metal moieties in addition to the number of chloroarenes to which they can be complexed, the ease of liberation of their modified ligands from the complex, and their environmentally safe co-ligands epitomize the appealing qualities of iron and ruthenium complexes. Several reports have appeared which outline the use of $CpRu^+$, Cp^*Ru^+ and $CpFe^+$ (chloroarene) metal complexes for the incorporation of aliphatic and/or aromatic ether and thioether linkages in a variety of compounds.[17-19, 67-70, 110, 176-178]

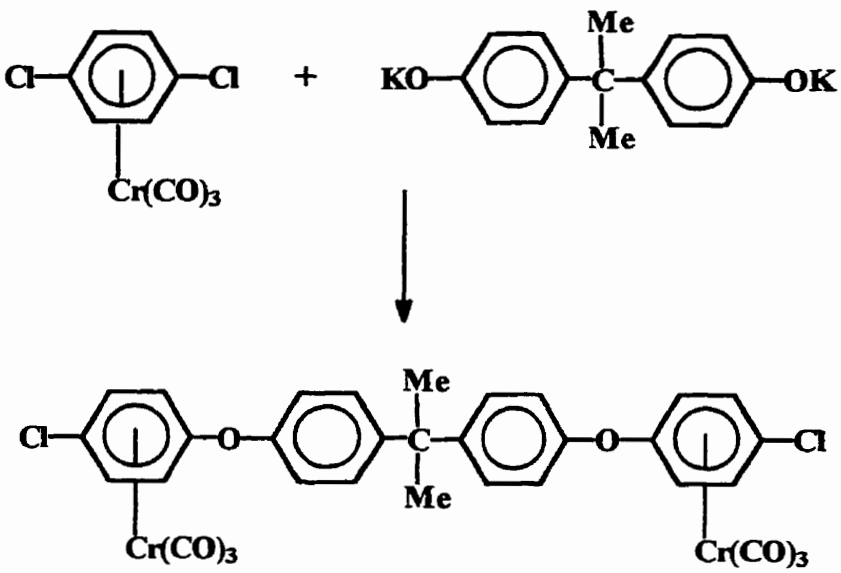

Figure 1.36: Double nucleophilic substitution reaction resulting in the preparation of bimetallic $Cr(CO)_3$ complexes

In particular, two different approaches have been investigated in the use of $CpFe^+$ and $CpRu^+$ complexes as an alternative route to the preparation of thermally stable engineering plastics. The first method takes advantage of the ease with which modified organic ligands may be removed from their corresponding organometallic counterparts. This has allowed for the preparation of unique organic monomeric units which are suitable for polyesterification or the Scholl reaction in the synthesis of polymers. For example, Pearson and coworkers have used the polyesterification of monomers generated using this organometallic route to produce poly(ether-esters).[176-177]

Segal reported the preliminary research concerning the nucleophilic aromatic substitution capabilities of pendent metallic moieties in the preparation of organometallic polymers. He succeeded in preparing high molecular weight poly(ether-ether-ketone)

with pendent $CpRu^+$ moieties (Figure 1.37).[17] Furthermore, Segal was able to isolate the organic polymer species simply by photochemical or thermal arene displacement. Unfortunately, the organometallic poly(phenylene oxide) and poly(phenylene sulfide) materials produced by Dembek and coworkers by the reaction of (1,4-dichlorobenzene)Cp^*Ru^+ with various dihydroxy- and dithioxy- aromatic nucleophiles were not successfully isolated as their organic counterparts (Figure 1.12) .[18-19, 110] Nonetheless, the preparation of these acetonitrile, DMF, and DMSO soluble organometallic polymers exemplifies the synthetic utility of this technique.

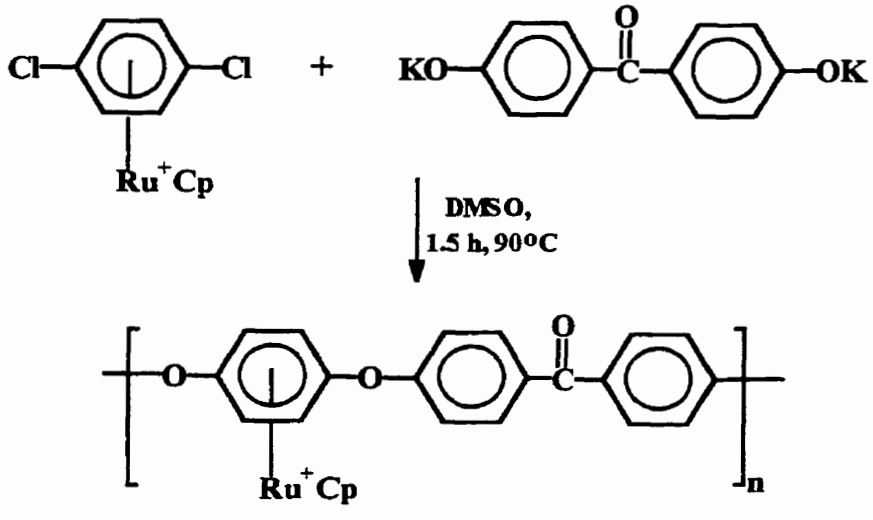

Figure 1.37: Preparation of poly(ether-ether-ketone) with pendent $CpRu^+$ metal moieties

Until recently, the use of the ligand exchange reaction of a polyaromatic compound with excess ferrocene was the primary route for obtaining high molecular weight species with pendent $CpFe^+$ moieties.[41-45] The nucleophilic aromatic substitution of a 2:1 molar ratio of mono- or dichloroarene $CpFe^+$ complexes with aliphatic or aromatic diols has allowed the isolation of a variety of diiron complexes.[67-69] Detailed investigation of this technique utilizing aromatic diols has demonstrated that employing either a one- or two- step reaction strategy offers the opportunity to synthesize symmetric and asymmetric species, respectively. An extension of this methodology has been used in the preparation of oligomeric aromatic ethers containing up to 35 metals.[70] The general reaction scheme for this synthetic strategy is based on the structure of monomers generated from the reaction of (1,4-dichlorobenzene)Fe^+Cp hexafluorophosphate and hydroquinone and is schematically represented in Figure 1.13.

Essentially, the chain length of the oligomeric species increases via successive nucleophilic aromatic substitution reactions of chloro- and hydroxy- terminated metallic species. The utilization of a 2:1 molar ratio of a complex containing two terminal hydroxy substituents with (1,4-dichlorobenzene)Fe^+Cp allowed for disubstitution of the chlorine substituents and resulted in the isolation of a higher molecular weight species with terminal hydroxy groups. Alternatively, the reaction of a dichloro-terminated oligomeric species with hydroquinone in a 2:1 ratio generated the corresponding dichloro-terminated complex with the appropriate number of metallic moieties. Successive reaction of the terminal dihydroxy or dichloro substituents of the resulting oligomeric polymetallic complexes allowed for control over the nature and molecular weight of the resultant product. This methodology presents a unique strategy in the

preparation of polyaromatic ethers.

This synthetic strategy presents an efficient alternative to aromatic ether synthesis under very mild reaction conditions. Photolytic demetallation of the organometallic oligomers also allowed for the isolation of the purely organic analogues in good yield.[67-69] One drawback of this synthetic strategy is the numerous reaction steps which must be employed to achieve higher molecular weight species. An obvious advantage of this methodology over traditional methods is the ability to control the molecular weight of the resulting species precisely.

2.0 Synthesis of Bis(cyclopentadienyliron) Arene Complexes with Sulfur and Nitrogen Bridges

2.1 Synthetic Routes to the Preparation of Thioether Linkages

Interest in the preparation of sulfide containing compounds originates from their importance as intermediates in organic synthesis as well as their potential use as pharmaceutical agents.[179-183] Their high thermal stability and their potential as conducting materials further warrants an investigation of these compounds.[180] Although there are limited publications describing the synthesis of aryl aryl bis-sulfides,[184-187] numerous studies report successful efforts in the preparation of alkyl alkyl and alkyl aryl mono- and bis-sulfides.[188-198] Routes for the synthesis of aryl aryl sulfides, in particular, often suffer from harsh and/or complicated reaction conditions, the need for activated starting materials and even contamination. Consequently, exploration of new synthetic methodologies to these compounds continues to attract the attention of chemists worldwide.

The most widely recognized synthetic method of alkyl aryl and aryl aryl sulfides is the reaction of alkyl and aryl halides with the sodium and potassium salt of thiols (Figure 2.1).[199]

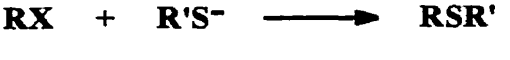

Figure 2.1: Preparation of sulfide linkages by displacement reactions

Analogous to the Williamson reaction, the most common method used for the preparation of a variety of symmetric and asymmetric diethers, alkyl halides are generally used as the reagent of choice due to the availability of these species and the fact that halides are relatively good leaving groups. However, sulfuric and sulfonic esters may be used in place of halides.[199] It has been demonstrated that the mobility of the halide in these displacement reactions is greatly affected by the nature of the starting material. It has been determined that the reaction is especially favorable with primary halides, with secondary halides resulting in much lower yields, and tertiary halides causing the reaction to fail completely. If the desired leaving group is attached to an aromatic ring, the presence of a strong electron-withdrawing group or appropriate catalyst is necessary to promote the reaction. However, it has been observed that if a polar aprotic solvent such as DMF, DMSO, tetraglyme, 1-methyl-2-pyrrolidinone or HMPA is employed, then even unactivated aryl halides react in the presence of an aryl thioxide anion albeit in low yields and under harsh reaction conditions.[199]

The use of phase transfer techniques may strongly accelerate anionic substitution reactions and has been utilized in the formation of both aliphatic and aromatic thioether linkages with varying success. The use of phase transfer catalysts is often applied in anticipation of higher yields, better selectivity, shorter reaction times, milder conditions, cheaper reagents and greater convenience. Herriott and Picker reported the syntheses of sulfides and dithioacetals according to Figure 2.2a and 2.2b, respectively.[200]

$X = Br, I$

$R^1 = C_6H_5, n\text{-}C_4H_9, i\text{-}C_3H_7—CH_2$

$R^2 = CH_3, C_2H_5, i\text{-}C_3H_7, n\text{-}C_8H_{17}$

Figure 2.2a: The use of a phase transfer catalyst in the synthesis of alkyl-alkyl and alkyl-aryl sulfides

$R^1 = i\text{-}C_4H_9, n\text{-}C_4H_9, C_6H_5$

Figure 2.2b: The preparation of dithioacetals via phase transfer catalyzed anionic substitution reactions

Several asymmetrical sulfides were isolated in yields of greater than 90% from the reaction of the desired thiol with an alkyl bromide or iodide in the presence of tricaprylmethylammonium chloride with 15 minute reaction times at room temperature (Figure 2.2a). In an attempt to use dichloromethane as a co-solvent, it was observed that double displacement of the chloride ions from dichloromethane took place resulting in the generation of the corresponding symmetrical thioacetals (Figure 2.2b).[200] As in the previous reaction, the symmetrical thioacetals were isolated in excellent yield following stirring of the appropriate reagents for 15 minutes at room temperature. Although several

symmetrical and asymmetrical sulfides were successfully prepared by this method, the synthesis of bis-sulfides was limited to the halogen displacement of dichloromethane.

Phase transfer catalysts have also been used in the activation of S_NAr reactions of aromatic substrates. Rolla and coworkers described the use of S_NAr reactions of 1,2- and 1,3-dichlorobenzene with thiolates under liquid-liquid phase transfer catalyst conditions.[201] A heterogeneous mixture of the substrate, dicyclohexano-18-crown-6 as a catalyst, and solution of the thiol in aqueous concentrated KOH were stirred at 110°C under a nitrogen atmosphere according to Figure 2.3.

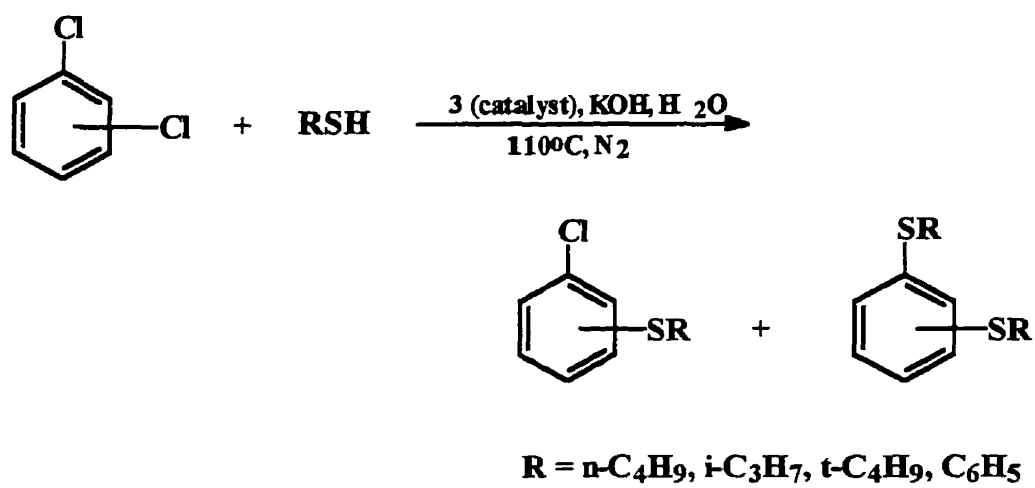

Figure 2.3: Dicyclohexano-18-crown-6 as a phase transfer catalyst in the preparation of aryl-aryl sulfides

It was observed that numerous variables determined the relative success of the reaction and the ratio of products formed. The most prominent effect was the dramatic impact that varying amounts of KOH in the aqueous phase had on the reaction rate. Specifically, significantly reduced reaction times were required with increasing concentrations of KOH solution. This was attributed to the fact that anionic nucleophiles are transferred as nonhydrated species from the aqueous to the organic phase in the presence of concentrated alkaline solutions. The product distribution of the reaction depended on both the nature of the substrates and the thiols.[201] The mobility of the first chlorine in the displacement proceeded as expected and followed the order 1,2- > 1,3- > 1,4-dichlorobenzene with the thiolates reacting according to primary alkyl > secondary alkyl > tertiary alkyl >> aryl. The relative reduced reactivity of aryl thiolates in comparison to their aliphatic counterparts is clearly demonstrated by the study of thiophenol. Only a 21% conversion of the corresponding aromatic products was observed which emphasizes the use of this technique in the preparation of alkyl aryl thioethers rather than wholly aromatic thioether linkages.

Campbell reported the reaction of an aliphatic or aromatic metal halide and thiol in an amide solvent which demonstrates the role of the solvent in many reaction processes (Figure 2.4).[184-185]

$$\mathbf{ArSK} + \mathbf{Ar'X} \xrightarrow[\text{solvent}]{\text{amide}} \mathbf{ArSAr'} + \mathbf{KX}$$

Figure 2.4: The Preparation of Bis-Sulfides in the Presence of an Amide Solvent

Initial investigations applied Ullmann-like conditions in the presence of copper salts, resulting in no reaction. Further examination of the reaction illustrated the dependency of this methodology on amide solvents presumably due to their high boiling points and consequent ability to solubilize the otherwise insoluble potassium thiolate. Although the exact function of the amide solvent had not been determined, it seemed to have a significant impact on the bimolecular nucleophilic substitution reaction.[184-185] Several factors which hinder the generality of this reaction include the use of a weak thiolate nucleophile made unreactive through electron-withdrawing groups or, alternatively, an unreactive halide containing strong electron donors which cause nucleophile repulsion. Additionally, both expected and unexpected by-products resulted in many of these reactions. Although various mono-, bis- and tris-sulfides and mono- and bis-phenylmercapto heterocyclics were prepared via this technique, Figure 2.5 illustrates some of the alkyl-aryl and aryl-aryl bis-sulfides that were isolated.

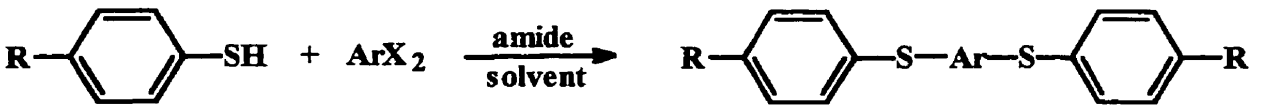

R = H, p-$(CH_3)_3C$

X = o-, m-, or p-Cl, p-Br

Ar = C_6H_4, -$C_6H_4OC_6H_4$-, -$C_6H_4C_6H_4$-

Figure 2.5: Bimolecular nucleophilic substitution in the preparation of various alkyl-aryl and aryl-aryl bis-sulfides

Modified displacement reactions have also been applied successfully in the preparation of aromatic mono- and di-sulfides. Bunnett and Creary report the synthesis of diaryl sulfides via the photochemical stimulation of an aryl halide and an arenethiolate ion in refluxing liquid ammonia under a nitrogen atmosphere (Figure 2.6).[185-186] In spite of the low solubility of many aryl iodides in liquid ammonia, the reaction was observed to proceed accordingly with the desired arenethiolate ion.

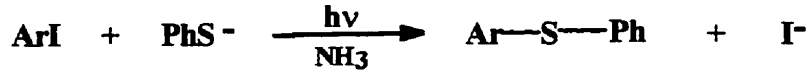

Figure 2.6: The photochemically induced synthesis of diaryl sulfides

The obvious advantage of this synthetic strategy is the successful preparation of aryl sulfides in relatively high yields. However, the reaction suffers from the fact that in many cases the desired products could be isolated only in the presence of a small amount of starting material or impurities. The flexibility of this methodology is exemplified by the reaction of dihalobenzenes under the same reaction conditions to yield the corresponding disubstituted products. A representative reaction of 1,3-chloroiodobenzene with thiophenoxide ion to form the bis-sulfide, 1,3-di(thiophenoxy)benzene in 91% yield accompanied by a mere trace of 1,3-chlorophenyl phenyl sulfide is shown in Figure 2.7.

It is suggested in Figure 2.7 that the monosubstitution product is not an intermediate in the formation of the bis-sulfide. This was determined by several kinetic studies which showed that 1,3-chloroiodobenzene was 17.4 times more reactive than the corresponding monosubstitution product.[185-186] These relative reactivity measurements support the notion that the monosubstitution product is too unreactive to participate as a major reaction intermediate. Table 2.1 summarizes the specific reaction conditions applied in the production of some of the bis-sulfides. Generally, chloroiodobenzene substrates yielded the best results while fluoro-containing starting materials allowed for substitution of the iodine substituent exclusively and resulted in the isolation of the corresponding monosubstituted product.

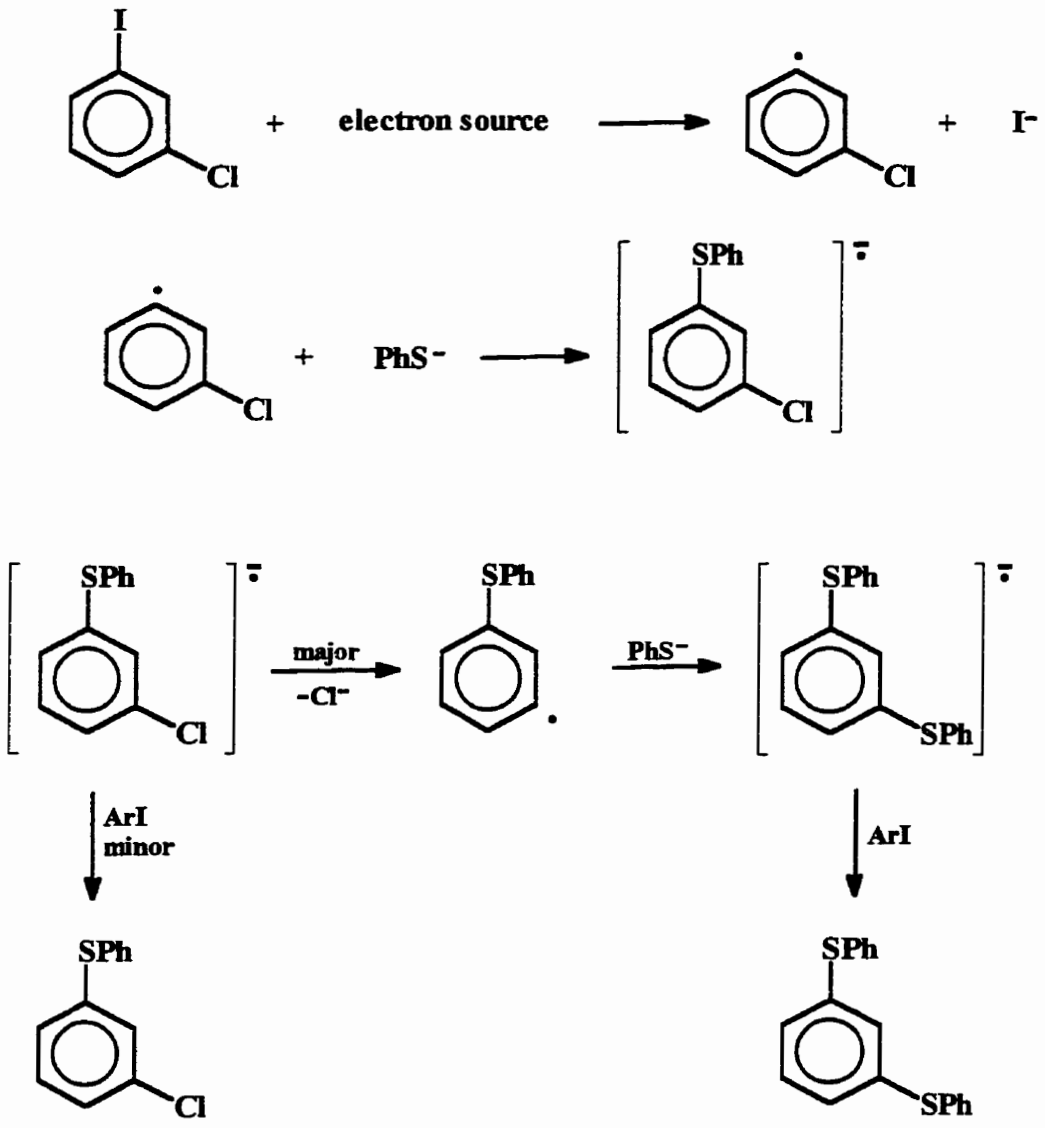

Figure 2.7: Reaction of 1,3-chloroiodobenzene with thiophenoxide in liquid ammonia

Table 2.1: Reaction Conditions and Resulting Products in the Production of Aryl Aryl Disulfides

Substrate	Reaction time (min.)	Sulfide Product	% Yield
1,3-ClC_6H_4I	150	1,3-$PhSC_6H_4SPh$	91
1,4-ClC_6H_4I	120	1,4-$PhSC_6H_4SPh$	89
1,3-BrC_6H_4Br	190	1,3-$PhSC_6H_4SPh$	92
1,3-ClC_6H_4Br	180	1,3-$PhSC_6H_4SPh$	55
1,4-BrC_6H_4Br	300	1,4-$PhSC_6H_4SPh$	64
1,2-ClC_6H_4I	90	1,2-$PhSC_6H_4SPh$	77
1,3-FC_6H_4I	100	1,3-FC_6H_4SPh	96

Although displacement reactions represent the most readily applied routes to the preparation of sulfur containing compounds, reductive techniques have also been successfully employed. The reduction of sulfoxides, sulfones and thiol esters in the presence of a variety of reagents has been achieved with varying success.

The reduction of sulfoxides by $LiAlH_4$ is the most extensively investigated reagent in the formation of the corresponding sulfides. However, several other reagents have been studied.[199] One method which has been studied and allows for the deoxygenation of both aliphatic and aromatic sulfoxides to the corresponding sulfides takes place in the presence of trichloromethylsilane/sodium iodide in acetonitrile solution.[202] Detailed exploration of this methodology indicated that one equivalent of trichloromethylsilane and two equivalents of sodium iodide per equivalent of sulfoxide was the optimum ratio to complete the reaction. Mechanistic investigations determined that only two out of three chlorine atoms in trichloromethylsilane were important in the conversion of the sulfoxide

to the sulfide according to Figure 2.8.[202] The attraction of this methodology stems from the mild reaction conditions and the instantaneous nature of the reaction.

The conversion of sulfones to sulfides is widely recognized as a difficult operation due to the general stability of sulfones in the presence of reducing agents. Lithium aluminum hydride and diisobutylaluminum hydride (Dibal-H) have been used with some success in the reduction of sulfones to their corresponding sulfides.[199] However, for the most part, there is no general method for the reduction of sulfones and sulfoxides.

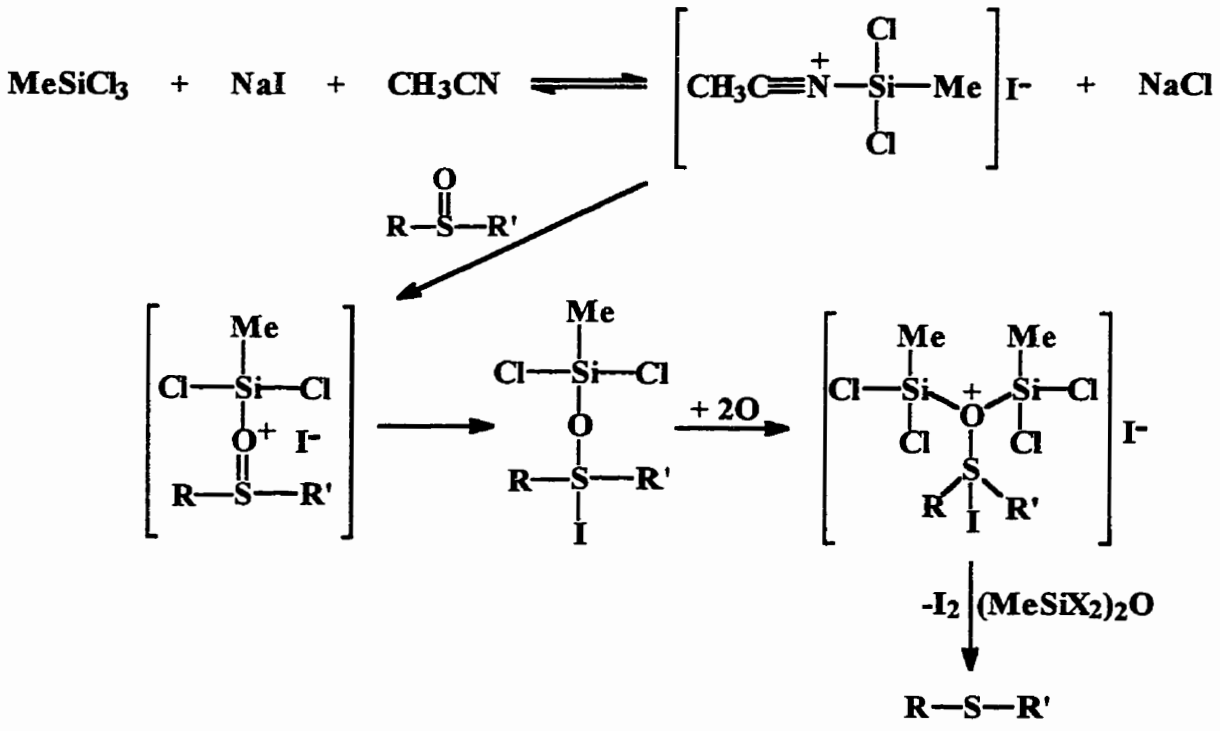

Figure 2.8: Mechanistic investigations of the reduction of sulfoxides to sulfides in the presence of trichloromethylsilane/sodium iodide in acetonitrile

2.2 Results and Discussion

2.2.1 Synthesis of Diaryl Alkyl and Diaryl Aryl Disulfides

Section 2.1 described a variety of methods which have been reported for the preparation of diaryl disulfides with either aliphatic or aromatic linkages.[184-202] However, harsh reaction conditions, complicated procedures, low yields and a limited variety of compounds which may be prepared by one technique represent several drawbacks of these methods. Since the development of the chemistry of η^6-arene-η^5-cyclopentadienyliron complexes, much attention has been given to the reactivities of halogenated arene complexes. In particular, cyclopentadienyliron activated S_NAr reactions have proven to be a viable method for the formation of ether and thioether linkages under mild reaction conditions and in good yield. This methodology has been thoroughly investigated in the preparation of a variety of symmetric and asymmetric mono-, bis- and poly-(cyclopentadienyliron) complexes with aliphatic and aromatic ether bridges.[67-70] The flexibility of this technique is further exemplified by the ability to prepare bis(cyclopentadienyliron) complexes with aliphatic or aromatic thioether or amine linkages as desired. Interest in the wide variety of bimetallic complexes prepared by this strategy not only demonstrates the generality of this methodology but generates model compounds which will aid in the formation and identification of similar species of high molecular weight.

2.2.2.1 Reactions of η^6-Chloroarene-η^5-Cyclopentadienyliron Hexafluorophosphate Complexes with Aliphatic Disulfides

Several reports have appeared which describe the reaction of η^6-(chloroarene)-η^5-cyclopentadienyliron complexes with a variety of oxygen dinucleophiles in the preparation of the corresponding bimetallic complexes with etheric linkages.[67-70] The synthetic versatility of this methodology was observed in the highly controlled design of aromatic ethers with up to 35 pendent metallic moieties.[70] One obvious advantage of this technique is the capability of preparing macromolecular species of a particular molecular weight.

Typically, η^6-chloroarene-η^5-cyclopentadienyliron complexes are reacted with a dihydroxy aliphatic or aromatic compound in the presence of an appropriate base and stirred in a polar aprotic solvent system. Figure 2.9 illustrates the reaction of the η^6-chlorobenzene complex with hydroquinone under very mild conditions, leading to the formation of the corresponding dicationic complex. Generally, a 2:1 molar ratio of a chloroarene complex with the desired dihydroxy nucleophile and K_2CO_3 are stirred for 17 hours at room temperature in a mixture of THF/DMF under a nitrogen atmosphere.[67-68, 70] However, attempts to incorporate aliphatic ether linkages using the same reaction conditions resulted in the isolation of the starting complex exclusively. The rationale behind this observation was the lower acidity and nucleophilicity of aliphatic diols in comparison to their aromatic counterparts as indicated by their higher pKa values.[69] Consequently, a slight modification involving the use of potassium tert-butoxide, a

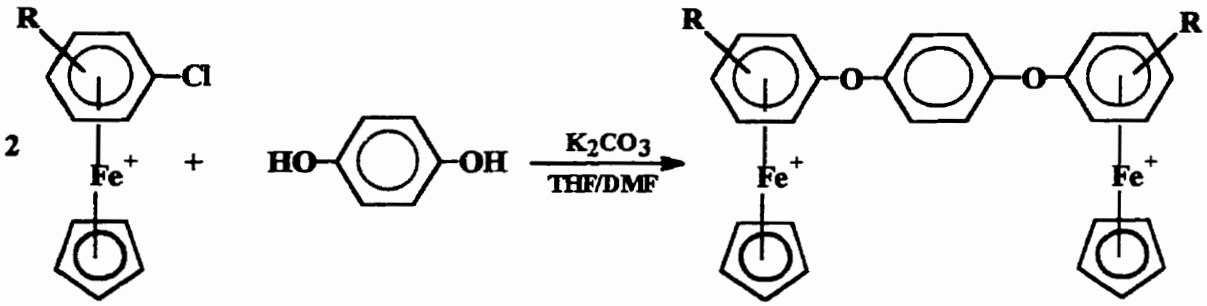

R = H, 2-Cl, 3-Cl, 4-Cl,
2-CH_3, 3-CH_3, 4-CH_3,
2,5-CH_3, 2,6-CH_3

Figure 2.9: Reaction of η^6-chlorobenzene-η^5-cyclopentadienyliron hexafluorophosphate with hydroquinone

stronger base, was ideal for generating aliphatic dioxide ions $^-O(CH_2)_xO^-$ and allowed for the preparation of the desired bimetallic complexes.

In an extension of this synthetic strategy, chloroarene complexes **2.1-2.8** were investigated in the reaction with aliphatic dithiols **2.9-2.12** utilizing reaction conditions similar to those employed in the generation of bimetallic complexes with aromatic ether linkages. Bis(cyclopentadienyliron) arene complexes containing aliphatic sulfide bridges were prepared by the reaction of a 2:1 molar ratio of an η^6-(chloroarene)-η^5-(cyclopentadienyliron) hexafluorophosphate complex **2.1-2.8** with the desired aliphatic dithiol **2.9-2.12** in the presence of an excess of K_2CO_3. These reagents were stirred in a mixture of THF/DMF (4:1) at room temperature for 16 hours under a nitrogen atmosphere (Scheme 2.1). All reactions proceeded smoothly and allowed for the isolation of the desired diiron complexes with thioether linkages as yellow solids in yields ranging from 60-93% as summarized in Table 2.3.

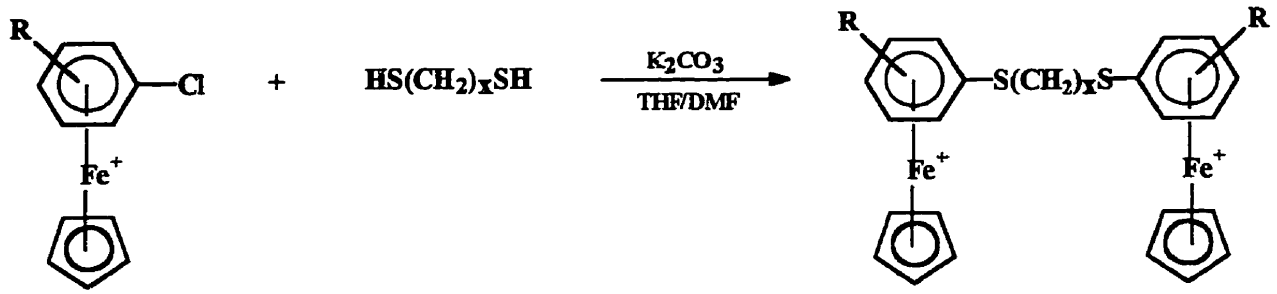

2.1 R = H
2.2 R = 2-CH_3
2.3 R = 3-CH_3
2.4 R = 4-CH_3
2.5 R = 2-Cl
2.5 R = 3-Cl
2.6 R = 4-Cl
2.7 R = 2,5-CH_3
2.8 R = 2,6-CH_3

2.9 x = 2
2.10 x = 4
2.11 x = 6
2.12 x = 8

2.13 R = H; x = 2
2.14 R = H; x = 4
2.15 R = H; x = 6
2.16 R = H; x = 8
2.17 R = 2-CH_3; x = 2
2.18 R = 2-CH_3; x = 4
2.19 R = 2-CH_3; x = 6
2.20 R = 3-CH_3; x = 2
2.21 R = 3-CH_3; x = 4
2.22 R = 3-CH_3; x = 6
2.23 R = 4-CH_3; x = 2
2.24 R = 4-CH_3; x = 4
2.25 R = 4-CH_3; x = 6
2.26 R = 2-Cl; x = 6
2.27 R = 3-Cl; x = 4
2.28 R = 4-Cl; x = 2
2.29 R = 4-Cl; x = 4
2.30 R = 4-Cl; x = 6
2.31 R = 4-Cl: x = 8
2.32 R = 2,6-CH_3; x = 2
2.33 R = 2,6-CH_3; x = 6

Scheme 2.1

The ^{1}H and ^{13}C NMR data of complexes **2.13-2.33** showed all the expected peaks, as reported in Tables 2.2 and 2.3 (pages 76-79). It is important to note that unless otherwise noted, all NMR spectra of the $CpFe^{+}$ complexes were obtained using acetone-d_6 as the solvent with chemicals shifts being referenced with respect to the quintet at 2.04 ppm and septet at 29.8 ppm appearing in the ^{1}H and ^{13}C NMR spectra, respectively. As a result of the symmetrical nature of these complexes, the NMR spectra are quite simple and the cyclopentadienyl (Cp) groups are represented by a single peak in the range of 5.07-5.30 ppm and 78.65-81.89 ppm in the ^{1}H and ^{13}C NMR spectra, respectively. Figure 2.10 depicts the ^{1}H NMR spectrum for complex **2.15** and outlines the expected chemical shift regions for the aliphatic and complexed aromatic protons. The Cp resonance appears as a singlet at 5.16 ppm while the complexed aromatic protons appear as a group of peaks at 6.44-6.56 ppm. The aliphatic protons are upfield from the aromatic protons and are located at 3.29, 1.81 and 1.61 ppm representative of the α-, β- and γ- protons, respectively. The ^{13}C NMR spectrum is shown in Figure 2.11 and was run as an Attached Proton Test (APT) in which those carbon atoms attached to an odd number of protons will appear below the baseline and those attached to an even number of protons appear above the baseline.[203] The resonance that is attributed to the ten protons of the two cyclopentadienyl rings appears below the baseline at 78.67 ppm. Due to the symmetrical nature of the species, three resonances representative of the complexed aromatic protons are expected. The peaks are in a similar region of the spectrum as the Cp resonance at 85.12, 86.16 and 87.98 ppm. Analogous to the signals of the aliphatic resonances in the ^{1}H NMR spectra, the aliphatic carbon resonances also appear upfield in the carbon spectra at 32.02, 29.42, and 28.47 ppm for the α-, β- and γ- carbon resonances, respectively. A

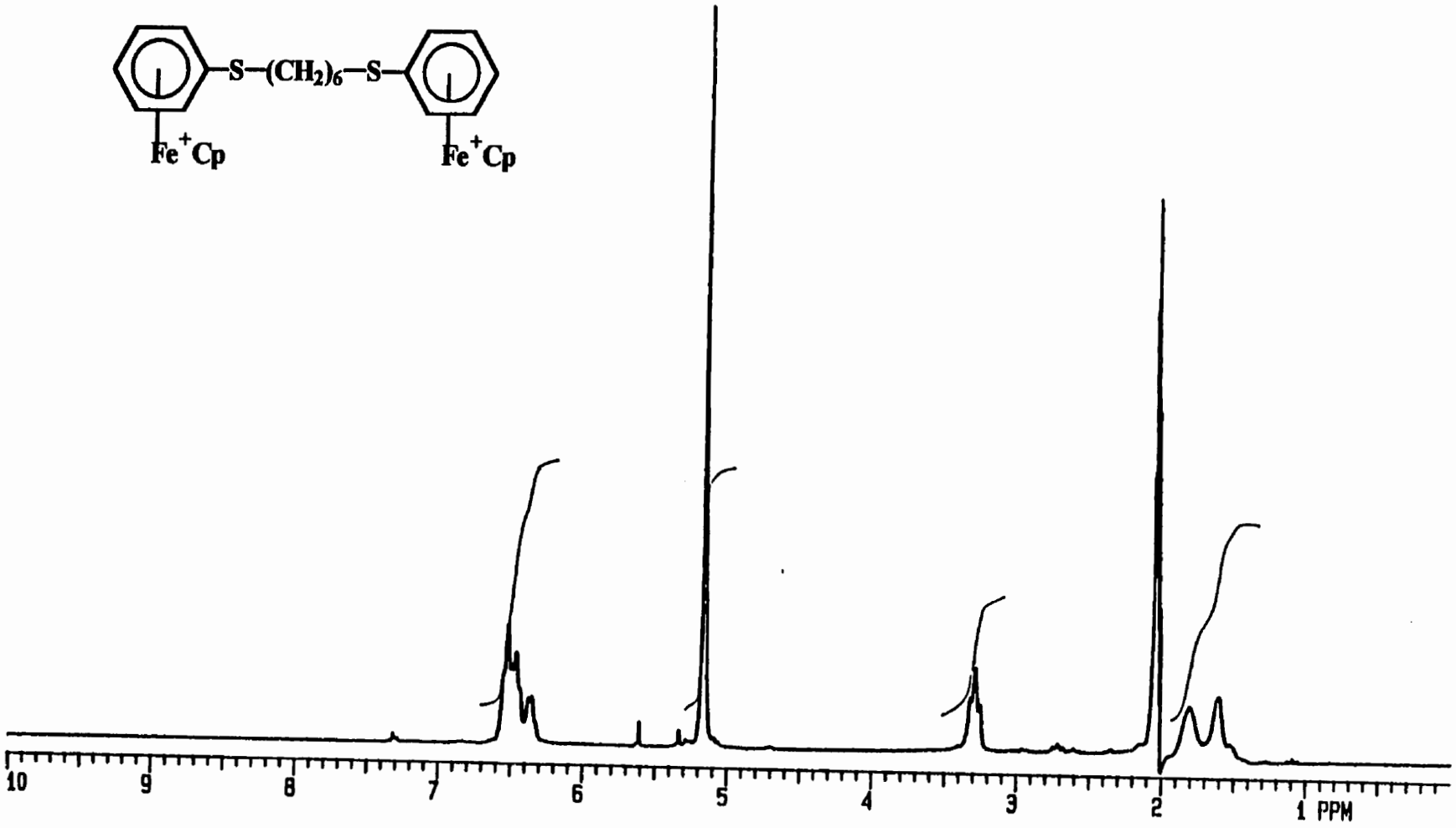

Figure 2.10: ^{1}H NMR spectrum of complex **2.15** in acetone-d_6.

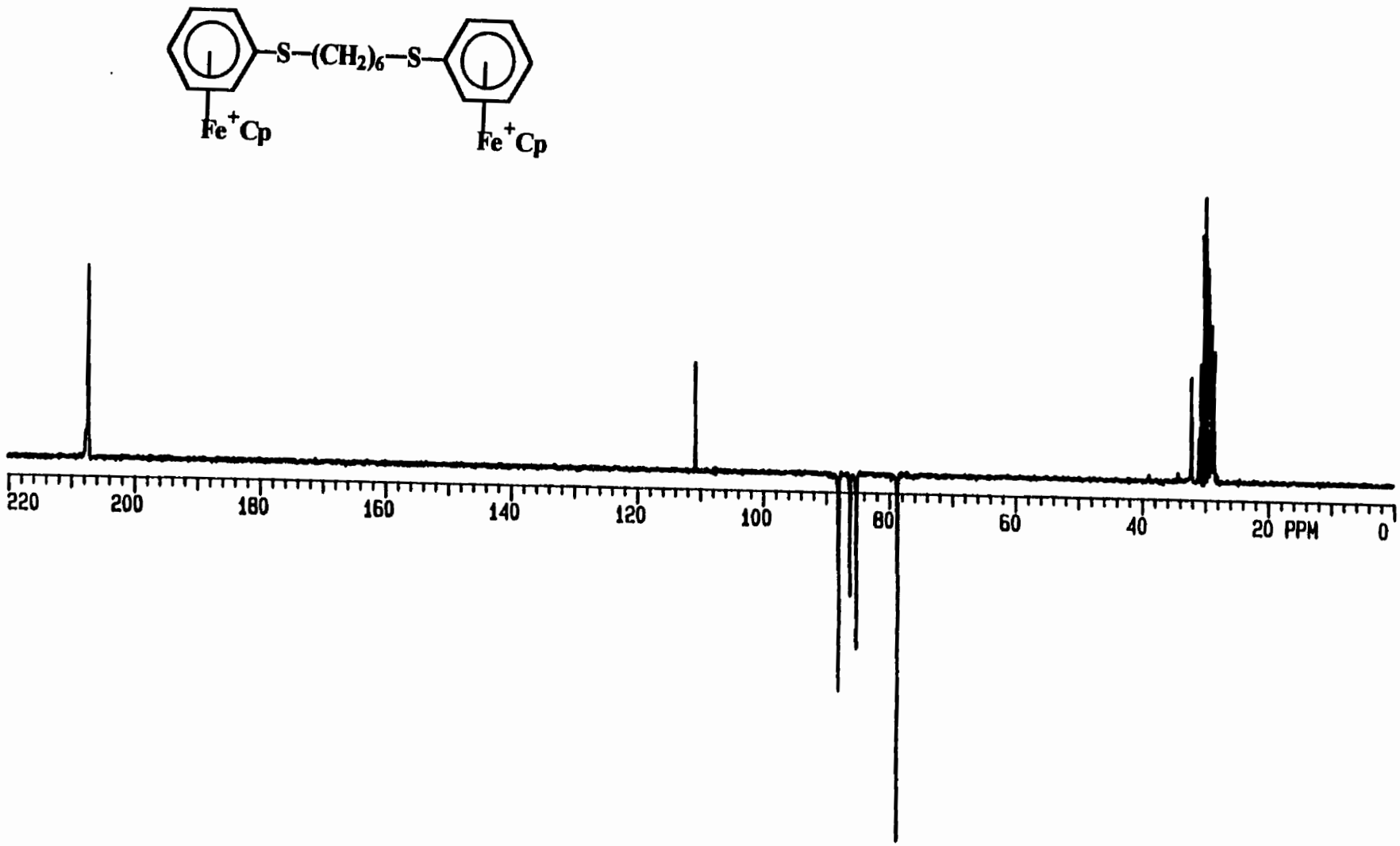

Figure 2.11: ^{13}C NMR spectrum of complex **2.15** in acetone-d_6.

single peak representative of the quaternary carbon appears above the baseline in the spectrum at 110.77 ppm.

In the case of complex **2.17**, the presence of diastereomers was indicated in the ^{1}H NMR spectrum by the presence of two cyclopentadienyl resonances at 5.09 and 5.10 ppm. The chirality induced in this complex is a result of the ortho substituted methyl group and the complexation of the iron moieties. Figure 2.12 illustrates two possible diastereomers of complex **2.17**. These complexes can be designated as R,R or S,S (enantiomeric pairs) for one diastereomer and R,S and S,R (enantiomeric pairs) for the other diastereomer. The observation of two methyl resonances at 2.60 and 2.62 ppm further supports the identification of the diastereomers of this compound. The ratios of these two isomers were measured from the ^{1}H NMR spectrum and appeared to be approximately equal. The ^{1}H NMR spectrum for complex **2.17** is shown in Figure 2.13.

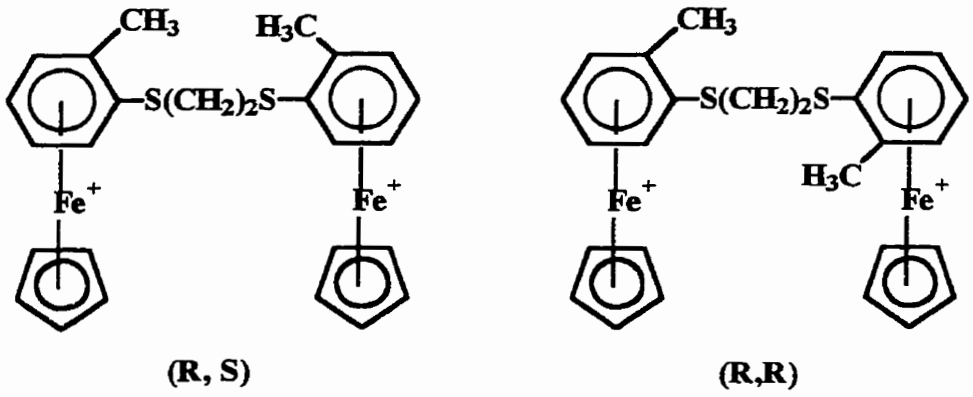

Figure 2.12: Two possible diastereomers of complex **2.17**

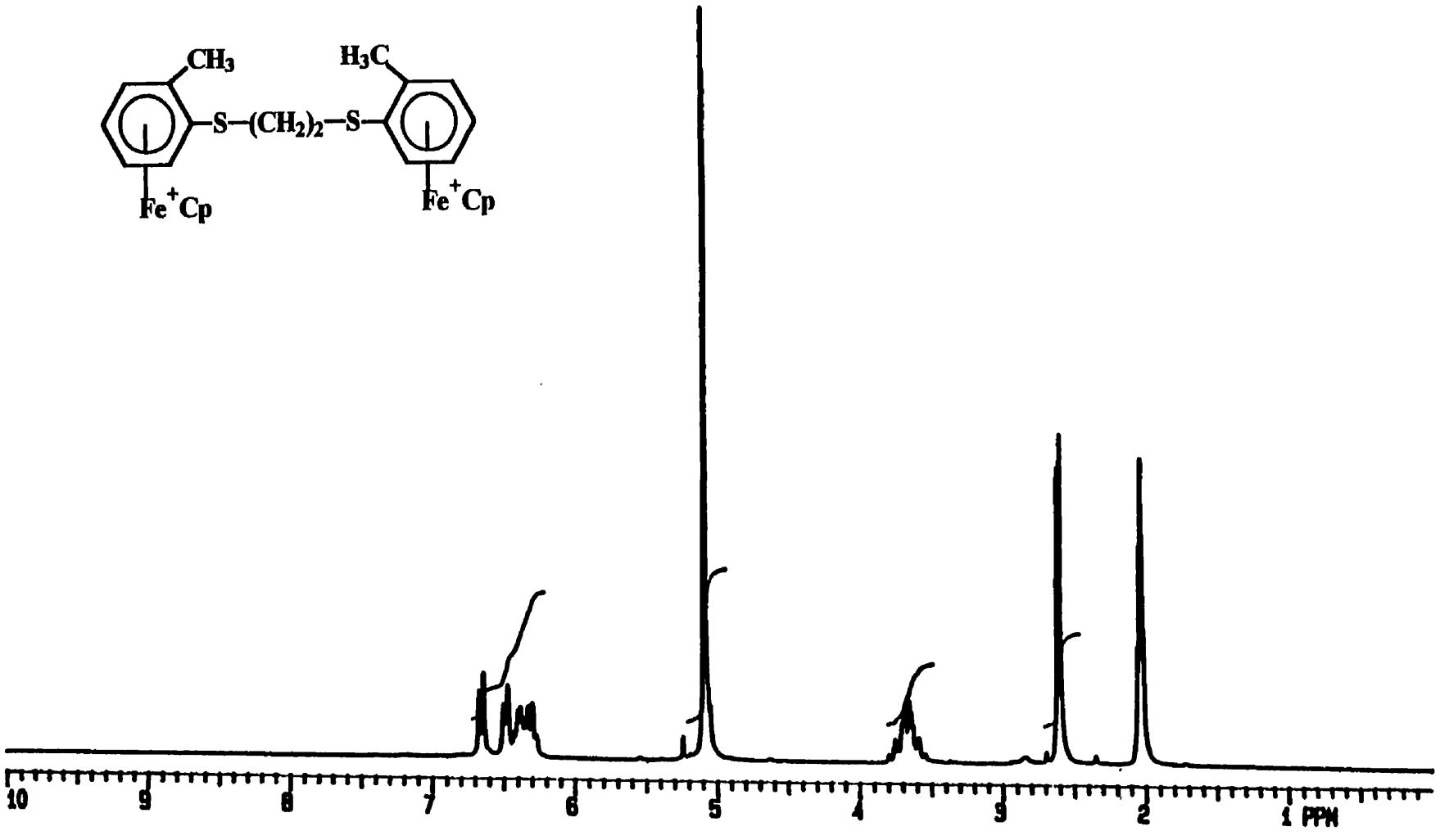

Figure 2.13: ^{1}H NMR spectrum of complex **2.17** in acetone-d_6.

The preparation of bimetallic complexes with linkages of varying chain length was explored as a result of their potential use as monomeric units in the synthesis of polymeric materials. This is especially important in those cases where the complexed aromatic component of the complex possesses a chlorine substituent which may undergo further nucleophilic aromatic substitution reaction.[70] Changing the chain length offers the potential for varying the properties of the resulting materials in terms of solubility and/or size/charge relationships. It is important to point out that neither the progress of the reaction nor the yields of the products were hindered by the use of the series of dinucleophiles incorporating from two to eight methylene groups.

Table 2.2: ^{1}H NMR Data of Alkyl-Alkyl Disulfide Complexes **2.13-2.33**.

δ (acetone-d_6), ppm			
Complex	**Cp (s, 10H)**	**Complexed Aromatic[a]**	**Others[a]**
2.13	5.21	6.36-6.64 (m, 10H)	3.69 (s, 2H, CH_2)
2.14	5.17	6.34-6.59 (m, 10H)	2.02 (m, 4H, β-CH_2)[b] 3.37 (t, 4H, J = 7.2, α-CH_2)
2.15	5.16	6.44-6.56 (m, 10H)	1.61 (m, 4H, γ-CH_2) 1.81 (m, 4H, β-CH_2) 3.29 (t, 4H, J = 6.9, α-CH_2)
2.16	5.16	6.35-6.56 (m, 10H)	1.27-1.48 (m, 4H, δ-CH_2) 1.64-1.78 (m, 4H, γ-CH_2) 2.67-2.71 (m, 4H, β-CH_2) 3.27 (t, 4H, J = 7.2, α-CH_2)
2.17[c]	5.09 5.10	6.30-6.40 (m, 4H) 6.49 (d, 2H, J = 5.9) 6.65 (d, 2H, J = 6.2)	2.60 (s, 3H, CH_3) 2.62 (s, 3H, CH_3) 3.66 (m, 4H, CH_2)
2.18	5.09	6.29 (t, 2H, J = 5.9) 6.40 (t, 2H, J = 6.0) 6.48 (d, 2H, J = 5.9) 6.62 (d, 2H, J = 6.3)	2.03 (m, 4H, β-CH_2)[b] 2.59 (s, 6H, CH_3) 3.38 (m, 4H, α-CH_2)
2.19	5.07	6.27 (t, 2H, J = 6.0) 6.38 (t, 2H, J = 6.2) 6.47 (d, 2H, J = 6.2) 6.57 (d, 2H, J = 6.2)	1.64 (m, 4H, γ-CH_2) 1.84 (m, 4H, β-CH_2) 2.58 (m, 6H, CH_3) 3.30 (t, 4H, J = 6.4, α-CH_2)
2.20	5.12	6.30 (d, 2H, J = 6.1) 6.40 (t, 2H, J = 6.2) 6.51 (d, 2H, J = 6.6) 6.56 (s, 2H)	2.55 (s, 6H, CH_3) 3.66 (s, 4H, CH_2)
2.21	5.11	6.28 (d, 2H, J = 6.0) 6.40 (t, 2H, J = 6.0) 6.43-6.49 (m, 2H) 6.52 (s, 2H)	2.20 (m, 4H,β-CH_2) 2.56 (s, 6H, CH_3) 3.30-3.41 (m, 4H, α-CH_2)
2.22	5.10	6.27 (d, 2H, J = 5.9) 6.35-6.45 (m, 4H) 6.49 (s, 2H)	1.52 (m, 4H, γ-CH_2) 1.78 (m, 4H, β-CH_2) 2.56 (s, 6H, CH_3) 3.28 (t, 4H, J = 7.3, α-CH_2)
2.23	5.13	6.41 (d, 4H, J = 6.4) 6.54 (d, 4H, J = 6.4)	2.49 (s, 6H, CH_3) 3.63 (s, 4H, CH_2)

2.24	5.12	6.40 (d, 4H, J = 6.7) 6.49 (d, 4H, J = 6.7)	1.98 (m, 4H, β-CH_2) 2.50 (s, 6H, CH_3) 3.38 (t, 4H, J = 7.2, α-CH_2)
2.25	5.10	6.44 (m, 8H)	1.60 (m, 4H, γ-CH_2) 1.79 (m, 4H, β-CH_2) 2.48 (s, 6H, CH_3) 3.26 (m, 4H, α-CH_2)
2.26	5.20	6.44-6.48 (m, 4H) 6.75-6.79 (m, 2H) 6.88-6.92 (m, 2H)	1.68 (m, 4H, γ-CH_2) 1.88 (m, 4H, β-CH_2) 3.37 (t, 4H, J = 6.6, α-CH_2)
2.27	5.27	6.50-6.57 (m, 4H) 6.59 (d,2H, J = 5.8) 6.96 (s, 2H)	1.98 (m, 4H, β-CH_2) 3.44 (m, 4H, α-CH_2)
2.28	5.30	6.74 (d, 4H, J = 6.8) 6.85 (d, 4H, J = 6.8)	3.69 (s, 4H, CH_2)
2.29	5.28	6.65 (d, 4H, J = 6.8) 6.83 (d, 4H, J = 6.8)	1.97-2.02 (m, 4H, β-CH_2) 3.34 (m, 4H, α-CH_2)
2.30	5.27	6.64 (d, 4H, J = 6.8) 6.82 (d, 4H, J = 6.8)	1.58 (m, 4H, γ-CH_2) 1.78 (m, 4H, β-CH_2) 3.28 (t, 4H, J = 7.3, α-CH_2)
2.31	5.27	6.61 (d, 4H, J = 6.8) 6.83 (d, 4H, J = 7.0)	1.29 (m, 8H, δ & γ-CH_2) 165-1.80 (m, 4H, β-CH_2) 3.26 (t, 4H, α-CH_2)
2.32	5.07	6.37 (t, 2H, J = 6.9) 6.48 (d, 4H, J = 5.8)	2.78 (s, 12H, CH_3) 3.18 (s, 4H, CH_2)
2.33	5.09	6.30-6.41 (m, 4H) 6.48-6.52 (m, 2H)	1.40 (m, 4H, γ-CH_2) 1.64 (m, 4H, β-CH_2) 2.83 (s, 12H, CH_3) 2.87 (t, 4H, J = 7.4, α-CH_2)

[a] J values in Hertz. [b] Signal obscured by solvent peak. [c] Diastereoisomers present.

Table 2.3: ^{13}C NMR Data of Alkyl-Aryl Disulfide Complexes **2.13-2.33**.

δ (acetone-d_6), ppm				
Complex	**Yield (%)**	**Cp (10H)**	**Complexed Aromatic**	**Others**
2.13	82	79.06	87.10, 87.20, 88.60, 108.36*	32.62 (CH_2)
2.14	82	78.65	85.37, 86.28, 88.01, 110.25*	28.16 (β-CH_2), 31.81 (α-CH_2)
2.15	81	78.67	85.14, 86.16, 87.98, 110.77*	28.47 (γ-CH_2), 29.42 (β-CH_2) 32.02 (α-CH_2)
2.16	78	78.48	84.92, 86.03, 87.82, 110.78*	28.80 (δ-CH_2), 29.81 (γ-CH_2), 30.99 (β-CH_2) 38.83 (α-CH_2)
2.17	70	79.15	86.63, 87.21, 89.70, 101.55*, 107.84*	19.95 (CH_3), 32.52 (CH_2)
2.18	75	79.05	84.60, 85.99, 86.83, 89.51, 100.38*, 110.21*	19.82 (CH_3), 28.00 (β-CH_2), 31.87 (α-CH_2)
2.19	85	78.98	84.26, 85.85, 86.73, 89.45, 100.50*, 110.76*	19.45 (CH_3), 28.89 (γ-CH_2), 29.14 (β-CH_2), 32.28 (α-CH_2)
2.20	80	79.31	85.40, 87.46, 87.86, 87.95, 104.36*, 107.60*	20.54 (CH_3), 32.68 (CH_2)
2.21	93	79.16	83.88, 86.53, 86.93, 87.56, 104.11*, 109.90*	20.56 (CH_3), 28.47 (β-CH_2), 31.82 (α-CH_2)
2.22	78	78.98	83.47, 86.04, 86.67, 87.37, 103.78*, 110.26*	20.42 (CH_3), 28.60 (γ-CH_2), 29.43 (β-CH_2) 32.07 (α-CH_2)
2.23	79	79.37	86.63, 88.87, 102.96*, 106.36*	20.07 (CH_3), 32.73 (CH_2)
2.24	60	79.32	85.14, 88.65, 102.51*, 108.78*	20.10 (CH_3), 28.55 (β-CH_2), 31.93 (α-CH_2)

2.25	80	79.30	84.95, 88.64, 102.27*, 109.23*	20.12 (CH_3), 28.67 (γ-CH_2), 29.05 (β-CH_2), 32.40 (α-CH_2)
2.26	82	80.67	83.71, 85.92, 86.90, 88.56, 103.82*, 111.89*	28.53 (γ-CH_2), 31.91 (β-CH_2), 28.80 (α-CH_2)
2.27	78	81.21	84.25, 85.80, 86.90, 87.93, 107.67*, 111.55*	28.25 (β-CH_2), 31.90 (α-CH_2)
2.28	87	81.42	86.41, 88.72, 106.45*, 108.17*	32.50 (CH_2)
2.29	74	81.89	84.46, 88.21, 106.05*, 109.50*	28.29 (β-CH_2), 31.82 (α-CH_2)
2.30	81	81.25	84.57, 88.40, 105.94*, 111.19*	28.74 (γ-CH_2), 29.41 (β-CH_2), 32.31 (α-CH_2)
2.31	94	81.25	84.64, 88.44, 105.97*, 108.60*	29.09 (δ-CH_2) 29.50 (γ-CH_2) 32.54 (β-CH_2) 38.95 (α-CH_2)
2.32	77	79.15	87.93, 89.27, 101.22*, 108.04*	21.59 (CH_3), 38.14 (CH_2)
2.33	72	79.22	87.90, 89.37, 101.52*, 108.24*	21.65 (CH_3), 24.65 (γ-CH_2), 34.53 (β-CH_2) 36.36 (α-CH_2)

* Quaternary carbon.

2.2.1.2 Reactions of η^6-Chloroarene-η^5-cyclopentadienyliron Hexafluorophosphate Complexes with Aromatic Disulfides

In the course of investigations involving the preparation of bis(cyclopentadienyliron) arene complexes with etheric and thioetheric linkages, the synthesis of isomeric (η^6-phenylenedithiobis(benzene))bis(η^5-cyclopentadienyliron) hexafluorophosphates was also achieved. These complexes were prepared by the combination of chloroarene complexes **2.1-2.8**, isomeric dithiols **2.34-2.36**, and potassium carbonate in a THF/DMF (4:1) mixture for 16 hours at room temperature under a nitrogen atmosphere (Scheme 2.2). All the reactions proceeded in an efficient manner with the corresponding diiron complexes being isolated as yellow solids in yields ranging from 70-95%. Due to the activation of the chloroarene ring toward nucleophilic aromatic substitution by the complexation of the $CpFe^+$ moiety, the experimental conditions applied in the synthesis of this class of bimetallic complexes with thioether linkages were very mild compared to those used in the traditional synthesis of uncomplexed aromatic thioethers.[186, 191-192, 195]

The successful preparation of complexes **2.37-2.47** were verified using ^1H and ^{13}C NMR and the data summarized in Tables 2.4 and 2.5. In the same way that the diiron complexes with aliphatic sulfur linkages exhibit one peak in the proton and carbon NMR for the cyclopentadienyl (Cp) protons, a strong singlet representative of the Cp protons is also observed in the case when aromatic sulfur linkages are incorporated. As was mentioned previously, this is a consequence of the symmetrical nature of these complexes.

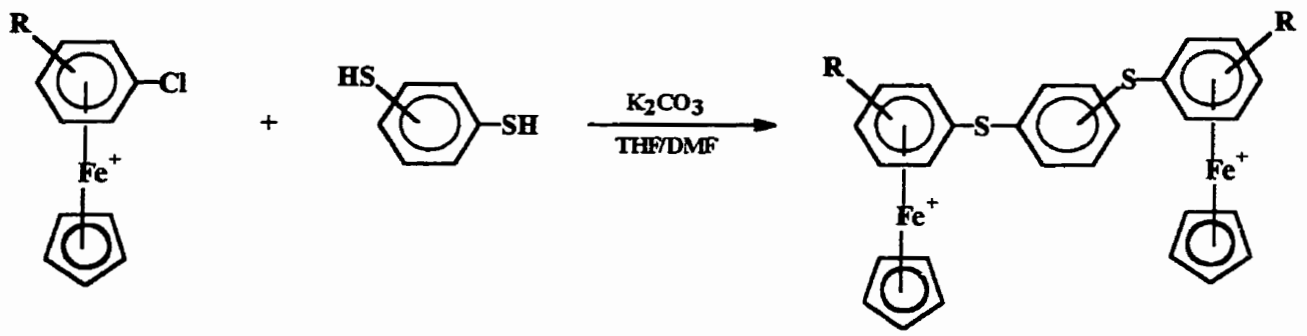

2.1 - 2.8

2.34 1,2
2.35 1,3
2.36 1,4

2.37 R = H; 1,2
2.38 R = H; 1,3
2.39 R = H; 1,4
2.40 R = 3-CH_3; 1,3
2.41 R = 4-CH_3; 1,2
2.42 R = 4-CH_3; 1,3
2.43 R = 2-Cl; 1,3
2.44 R = 2,5-CH_3; 1,4
2.45 R = 2,6-CH_3; 1,2
2.46 R = 2,6-CH_3; 1,3
2.47 R = 2,6-CH_3; 1,4

Scheme 2.2

Figures 2.14 and 2.15 show the ^{1}H and ^{13}C NMR spectra representative of complex **2.47**, respectively. It is important to note that in the case of those complexes resulting from the reaction of chloroarene complexes with isomeric dithiols, a group of peaks representing the uncomplexed aromatic protons will be observed downfield from the complexed aromatic resonances. The spectral separation of these two groups of peaks due to shielding effects is extremely valuable in confirming the structures of these complexes.[203] The symmetry of these complexes is clearly exemplified by the ^{1}H NMR of this particular example in which the Cp, methyl and uncomplexed aromatic protons found at 5.18, 2.65 and 7.14 ppm, respectively, are all singlets. The complexed protons are found upfield

from the uncomplexed aromatic protons in the form of a triplet at 6.48 ppm and a doublet at 6.56 ppm as expected. The symmetry of this complex is further verified by the simplicity of the ^{13}C NMR spectrum where the Cp, methyl and uncomplexed aromatic protons are represented by single resonances below the baseline at 79.56, 21.28, and 129.81 ppm, respectively. Two resonances appear for the complexed aromatic carbons; a strong peak at 89.84 ppm represents the four equivalent carbon atoms adjacent to the carbons with methyl substituents attached, and a less intense peak representative of the other two complexed aromatic carbon atoms. The analysis is completed by the identification of three peaks found above the baseline at 99.53, 108.28 and 134.25 ppm for the quaternary carbon atoms with the resonance of the uncomplexed quaternary carbon atom appearing furthest downfield.

The synthetic value of this methodology in the preparation of complexes containing thioetheric linkages has been thoroughly demonstrated. An important feature which has been alluded to in the discussion of the previous example is the ability to prepare sterically crowded species in good yield, using the same mild reaction conditions. The preparation of complex **2.47** proceeded as expected in 78% yield. Another illustration of the versatility of this methodology is the isolation of complex **2.45** as a yellow solid in 77% yield. Surprisingly, the site of nucleophilic substitution was not at all affected by its sterically crowded environment. The ^{1}H and ^{13}C NMR spectra of complex **2.45** are shown in Figures 2.16 and 2.17, respectively, with the chemical shifts appearing in the expected regions as mentioned above for complex **2.47**.

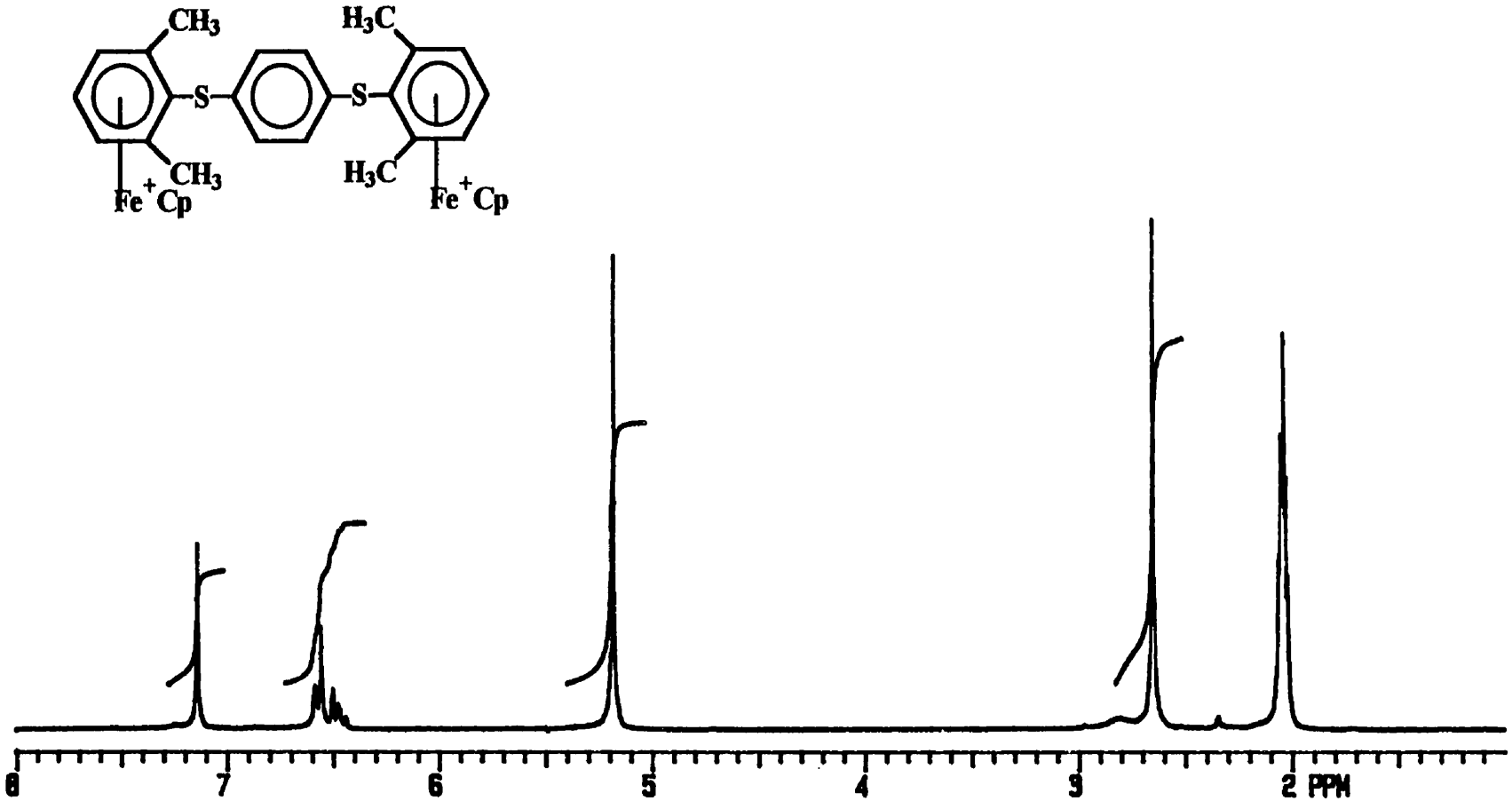

Figure 2.14: ^{1}H NMR spectrum of complex **2.47** in acetone-d_6.

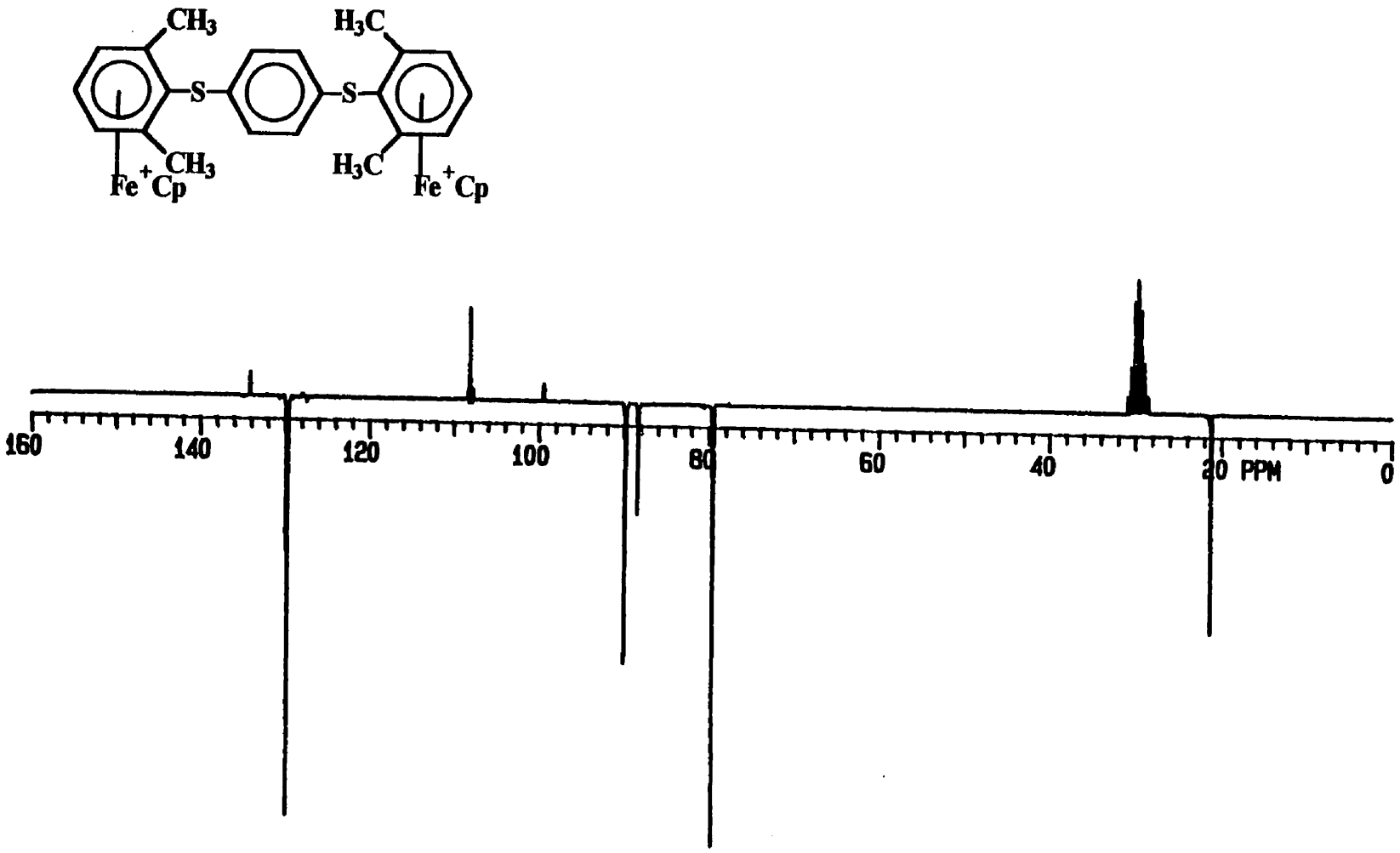

Figure 2.15: ^{13}C NMR spectrum of complex **2.47** in acetone-d_6.

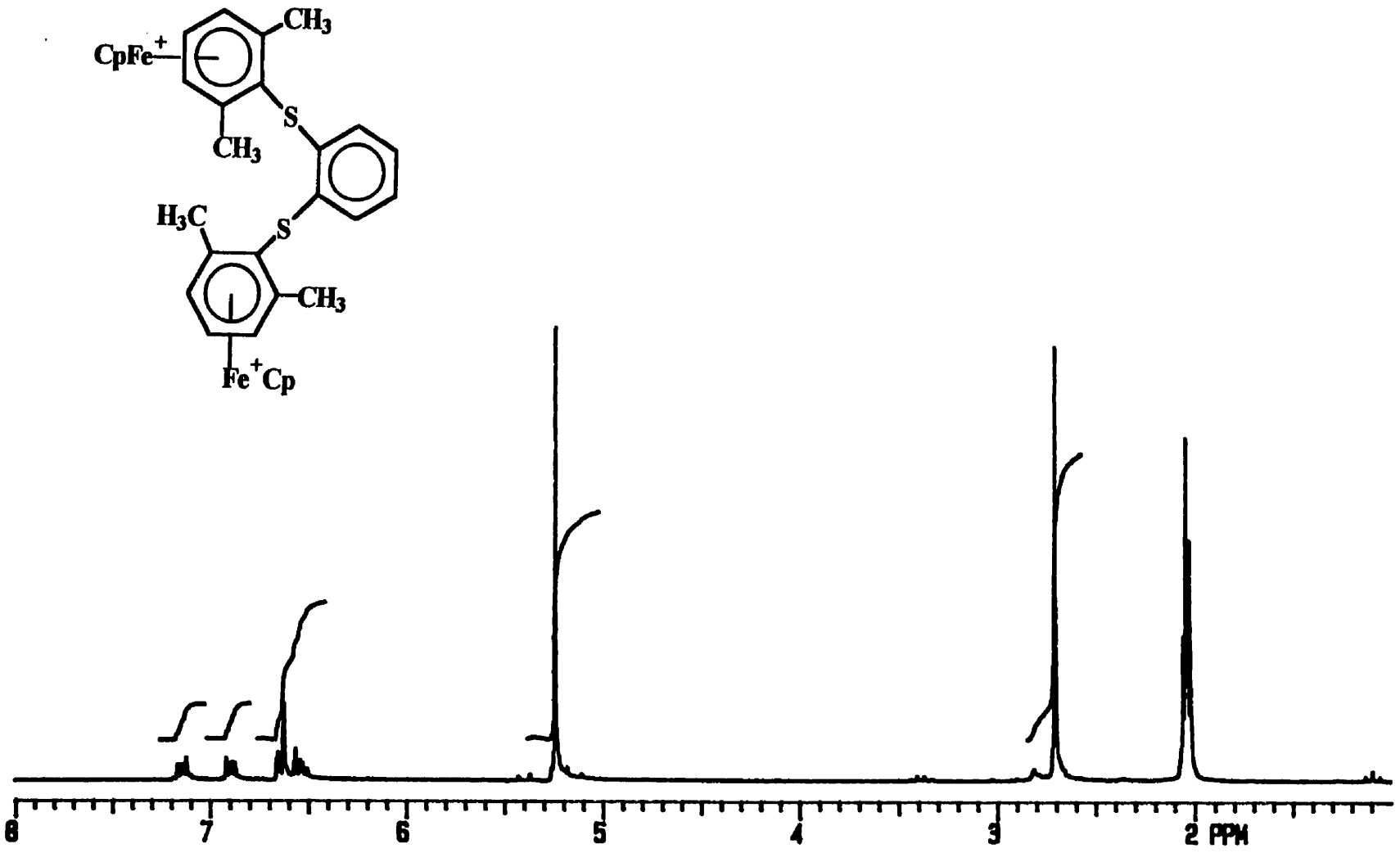

Figure 2.16: ^{1}H NMR spectrum of complex **2.45** in acetone-d_6.

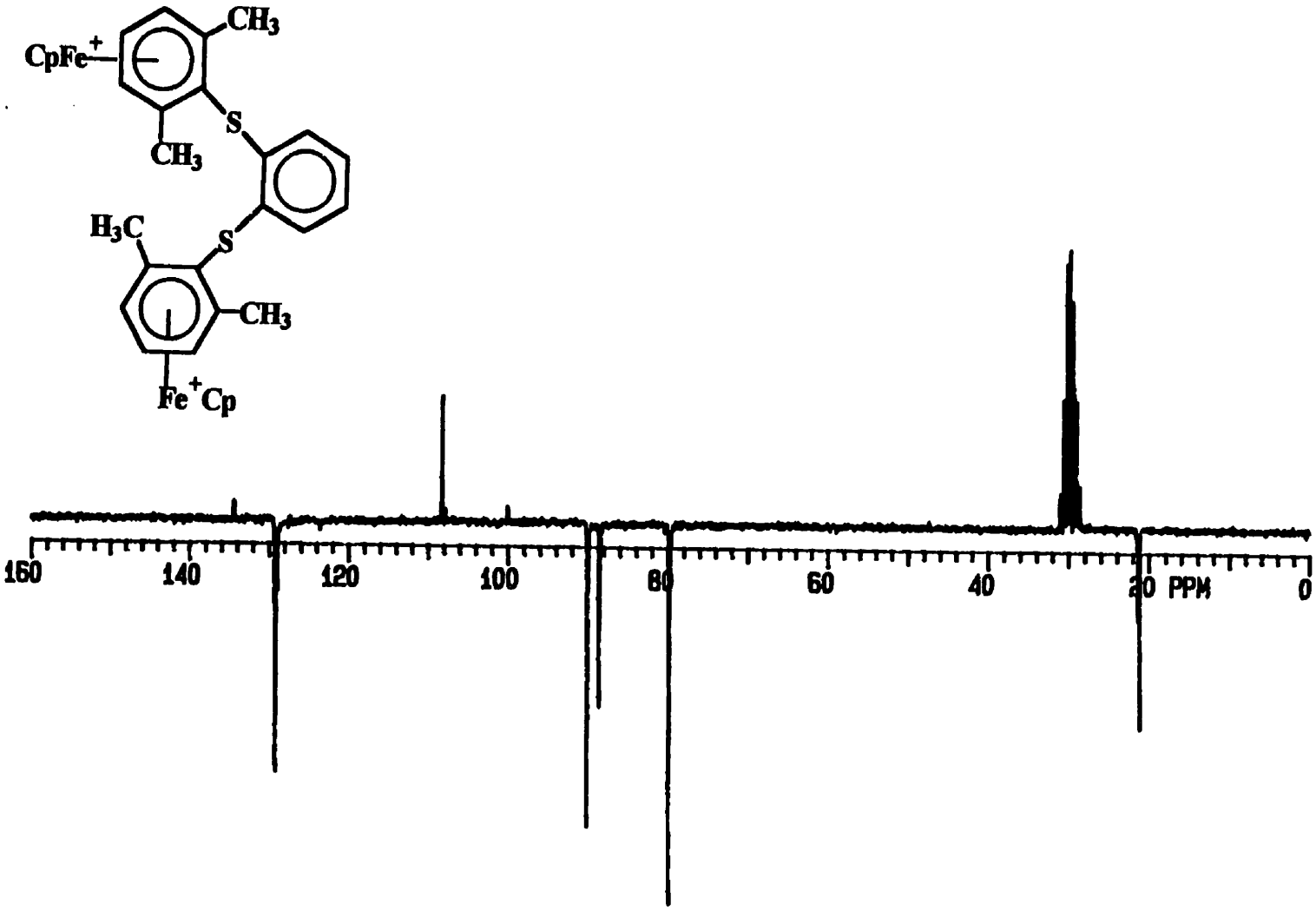

Figures 2.17: ^{13}C NMR spectrum of complex **2.45** in acetone-d_6.

Table 2.4: ^{1}H NMR Data of Aryl-Aryl Disulfide Complexes **2.37-2.47**.

δ (acetone-d_6), ppm				
Complex	**Cp (s, 10H)**	**Complexed Aromatic[a]**	**Uncomplexed Aromatic[a]**	**Others**
2.37	5.24	6.51 (br.s.,10H)	7.59-7.57 (m, 2H) 7.72-7.79 (m, 2H)	
2.38	5.22	6.42-6.51 (m, 10H)	7.73-8.05 (m, 4H)	
2.39	5.24	6.40-6.52 (m, 10H)	7.82 (s, 4H)	
2.40	5.17	6.32-6.46 (m, 6H) 6.50 (s, 2H)	7.68-7.75 (m 2H) 7.82-7.87 (m, 4H) 7.92-7.93 (m, 2H)	2.54 (s, 6H, CH_3)
2.41	5.20	6.45 (br.s., 8H)	7.48-7.69 (m, 3H) 7.85 (d, 1H, J = 7.3)	2.53 (s, 6H, CH_3)
2.42	5.18	6.40-6.47 (m, 8H)	7.73-7.94 (m, 4H)	2.50 (s, 6H, CH_3)
2.43[b]	5.26 5.29	6.26-6.55 (m,8H)	7.96-8.23 (m, 4H)	
2.44	5.15	6.31 (s, 2H) 6.39 (d, 4H, J = 5.9) 6.53 (d, 4H, J = 6.1)	7.62 (s, 4H)	2.47 (s, 6H, CH_3) 2.64 (s, 6H, CH_3)
2.45	5.25	6.55 (m, 2H) 6.64 (m, 4H)	6.88-6.92 (m, 2H) 7.12-7.17 (m, 2H)	2.71 (s, 12H, CH_3)
2.46	5.17	6.50-6.60 (m, 6H)	7.07-7.30 (m, 4H)	2.57 (s, 12H. CH_3)
2.47	5.18	6.48 (t, 2H, J = 6.0) 6.56 (d, 2H, J = 6.0)	7.14 (s, 4H)	2.65 (s, 12H CH_3)

[a] J values in Hertz. [b] Diastereoisomers present.

Table 2.5: ^{13}C NMR Data and Yields of Aryl-Aryl Disulfide Complexes **2.37-2.47**

δ (acetone-d_6), ppm					
Complex	**Yield (%)**	**Cp (10H)**	**Complexed Aromatic**	**Uncomplexed Aromatic**	**Others**
2.37	95	79.25	87.81, 89.12, 106.41*	132.24, 135.35*, 135.98	
2.38	90	79.19	87.39, 87.54, 88.81, 109.01*	133.10*, 133.20, 136.95, 140.17	
2.39	70	79.27	87.52, 87.95, 88.96, 108.33*	132.89*, 136.30	
2.40	95	78.58	85.41, 85.53, 87.00, 87.26, 87.84, 87.93, 103.71*, 106.49*, 106.61*	132.17*, 132.28*, 132.25*, 135.41, 135.48, 138.44, 138.52	19.64 (CH_3)
2.41	76	79.55	88.78, 89.41, 103.86*, 104.42*	132.06, 135.57* 135.70	20.16 (CH_3)
2.42	71	79.54	87.29, 89.16, 103.42*, 106.72*	133.05, 133.19*, 136.39, 139.51	20.16 (CH_3)
2.43[a]	81	81.12 81.17	86.11, 86.20, 87.21, 87.25, 87.57, 89.11, 89.15, 110.99*, 111.08*	131.40*, 133.97, 138.70, 141.79, 142.17, 142.98*	
2.44	85	79.76	87.99, 88.09, 89.56, 89.63, 90.25, 90.31, 101.75*, 103.74*, 104.67*, 105.09*	133.43*, 134.64, 134.84	19.54 (CH_3), 20.06, 20.10 (CH_3)
2.45	77	79.80	88.57, 90.02, 100.02*, 108.25	129.02, 129.19, 134.49*	21.27 (CH_3)
2.46	90	79.75	88.73, 89.98, 99.12*, 108.29	125.18, 126.59, 131.74, 137.42*	21.16 (CH_3)
2.47	78	79.56	88.36, 89.84, 99.53*, 108.28*	129.81, 134.25*	21.28 (CH_3)

[a] Diastereoisomers present. * Quaternary carbons.

2.2.1.3 Reaction of η^6-Chloroarene-η^5-Cyclopentadienyliron Hexafluorophosphate Complexes with 4-Hydroxythiophenol

With the success achieved in the design of diiron complexes with etheric and thioetheric linkages, a natural extension of this synthetic route involved the application of this strategy in the preparation of bis(cyclopentadienyliron) complexes of arenes with mixed ether/thioether bridges. The reactions of chloroarene complexes **2.1, 2.4-2.5** and **2.6-2.8** with 4-hydroxythiophenol were investigated under the same mild reaction conditions as used in the preparation of diiron complexes with aliphatic and aromatic thioether bridges and resulted in the isolation of complexes **2.49-2.54**. The synthetic details are represented in Scheme 2.3.

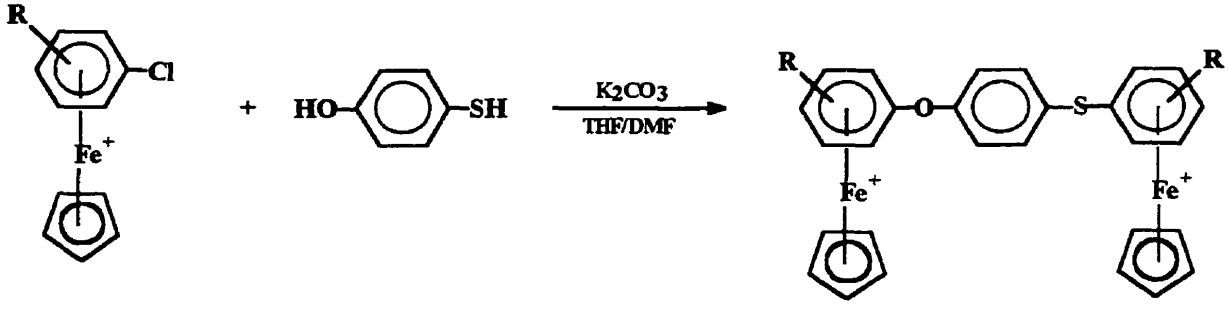

2.1 - 2.8 **2.48**

2.49 R = H
2.50 R = 4-CH_3
2.51 R = 2-Cl
2.52 R = 4-Cl
2.53 R = 2,5-CH_3
2.54 R = 2,6-CH_3

Scheme 2.3

The NMR data and yields of complexes **2.49-2.54** are presented in Tables 2.6 and 2.7. The peaks of the NMR spectra were assigned on the basis of the prior analysis of the symmetric complexes described in Section 2.2.3. The asymmetry of the resulting complexes is clearly demonstrated by a more detailed NMR investigation of complex **2.50** which shows the presence of two strong singlets at 5.17 and 5.24 ppm representing the protons of the two inequivalent Cp rings as shown in Figure 2.18. The para structure of the diiron complex induces the appearance of doublets for both the complexed and uncomplexed aromatic protons. Four sets of doublets at 6.33, 6.39, 6.41 and 6.47 ppm are identified for the complexed aromatic protons as a result of the asymmetric design of complex **2.50**. This same rationale is used to explain the doublets at 7.52 and 7.89 ppm representative of the inequivalent uncomplexed aromatic protons. The methyl substituents appear as two singlets at 2.50 and 2.52 ppm. The asymmetric nature of complex **2.50** is further verified by the ^{13}C NMR with two resonances appearing at 78.49 and 79.17 ppm for the Cp protons and two resonances representative of the methyl substituents at 19.67 and 19.89 ppm (Figure 2.19). Six resonances representative of the complexed and uncomplexed aromatic protons appear. The complexed aromatic resonances are found in the same region of the spectrum as the Cp resonances at 77.86, 85.19, 87.67 and 88.52 ppm with the uncomplexed aromatic resonances appearing further downfield at 122.91 and 138.46 ppm. The quaternary carbon resonances are easily identified as the only six resonances that appear above the baseline in the spectrum.

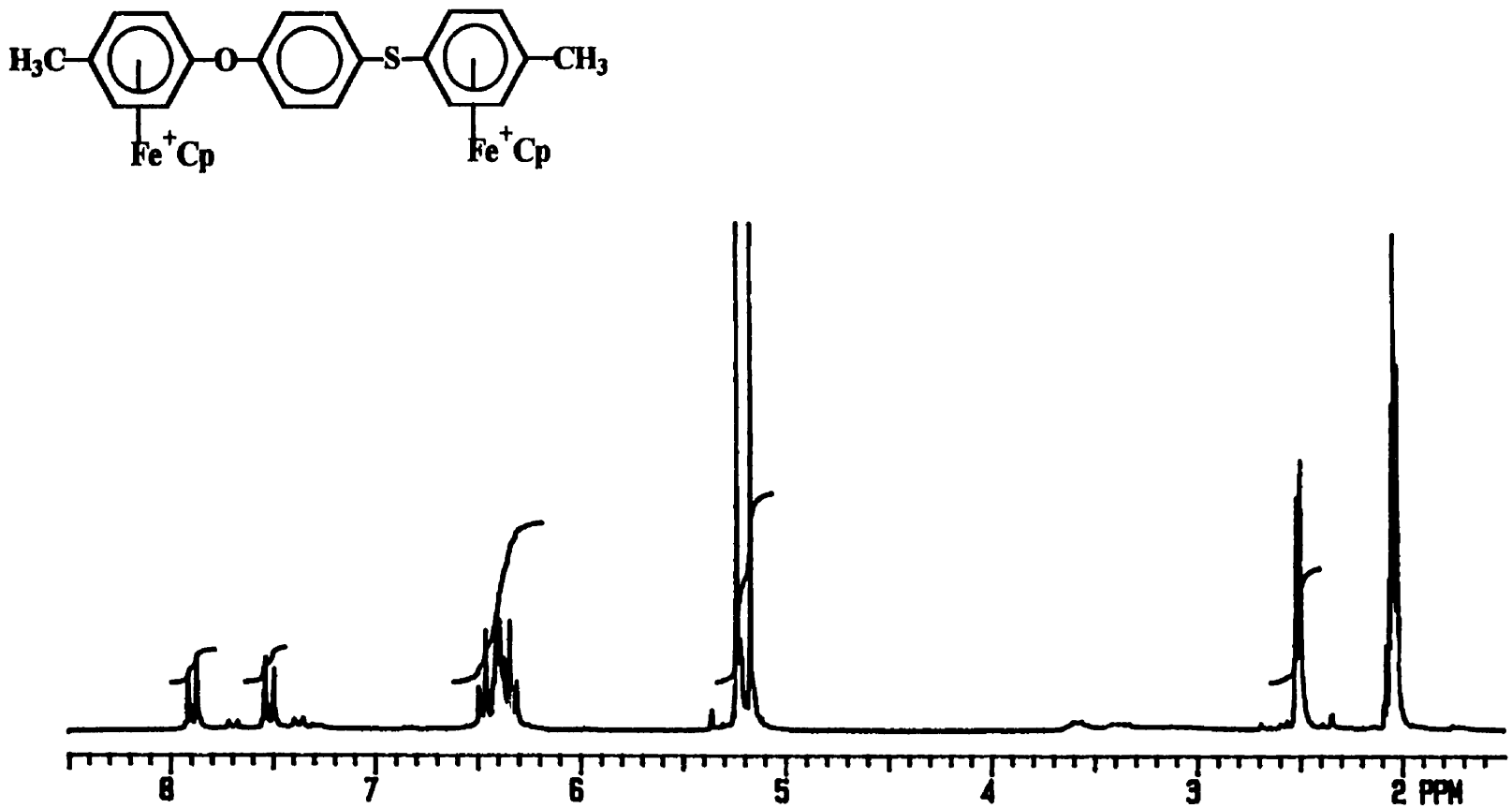

Figure 2.18: ^{1}H NMR spectrum of complex **2.50** in acetone-d_6.

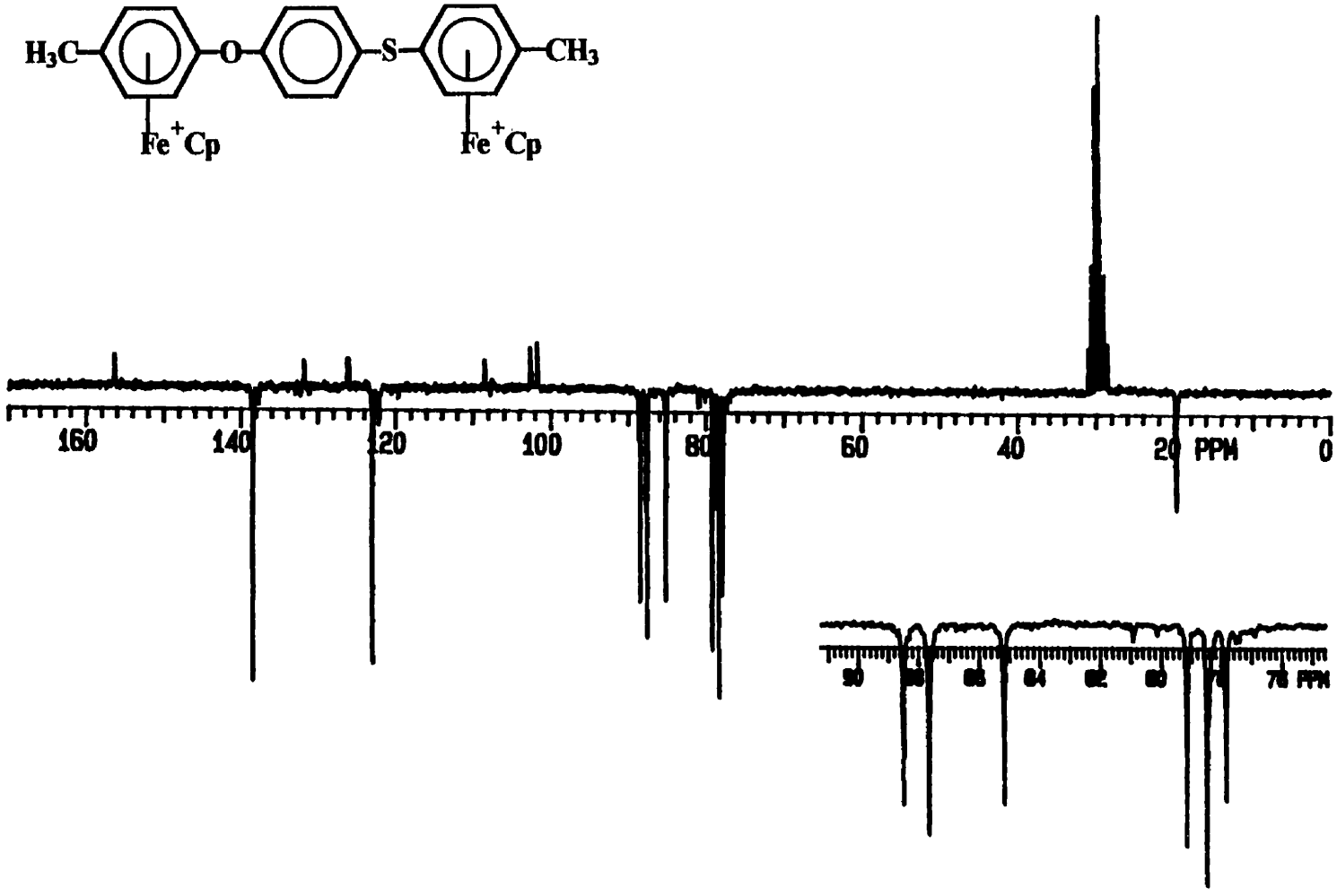

Figure 2.19: ^{13}C NMR spectrum of complex **2.50** in acetone-d_6.

The NMR spectra of complex **2.53** clearly exhibited the presence of two diastereomers. Figures 2.20a and 2.20b show the ^{1}H and ^{13}C NMR spectra of complex **2.53**. The region of the ^{1}H NMR spectrum ranging from 5.00-5.20 ppm is one of the most important regions of the spectrum for the identification of diastereomers. The presence of diastereomers is indicated by the appearance of two strong singlets and two smaller peaks for the protons of the Cp rings. The region of the ^{13}C NMR representative of the Cp carbon atoms verified the presence of diastereomers for complex **2.53** due to the observation of four different peaks in the range of 77.0-81.0 ppm.

The flexibility of this synthetic strategy has been clearly illustrated by the variety of symmetric and asymmetric etheric and thioetheric containing complexes that were prepared. The application of this synthetic strategy demonstrates an innovative approach to the synthesis of bis-sulfides and provides one of the most general, inexpensive and least toxic routes to this class of compounds.

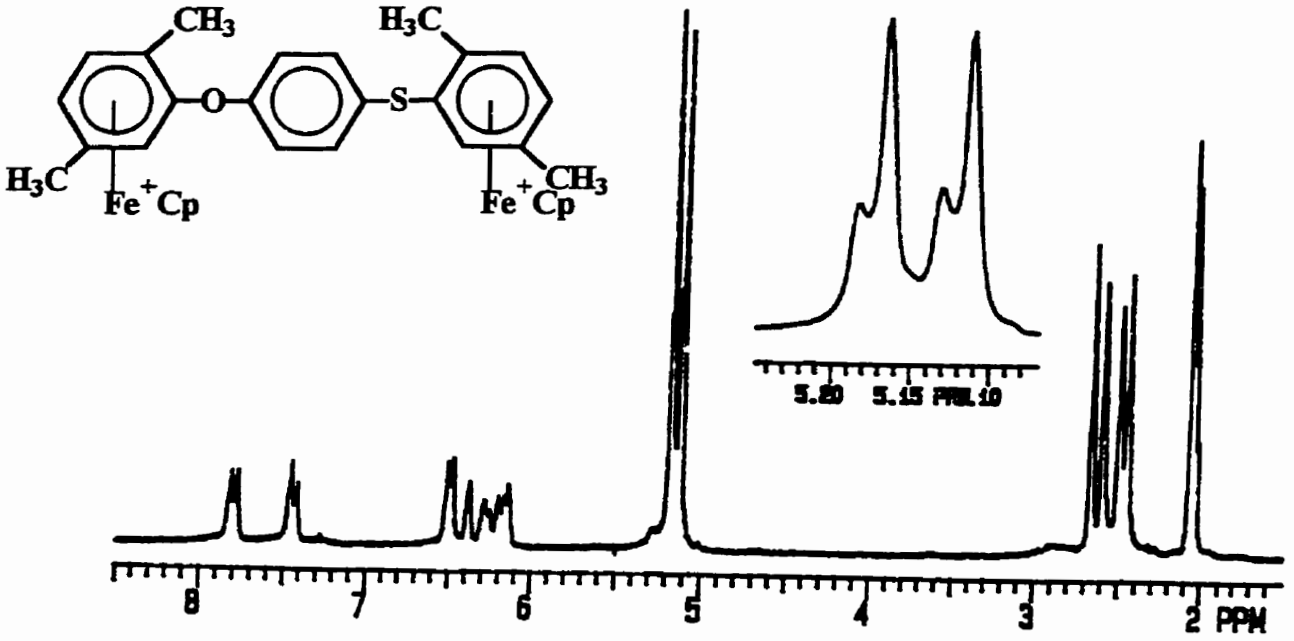

Figure 2.20a: ^{1}H NMR spectrum of complex **2.53** in acetone-d_6.

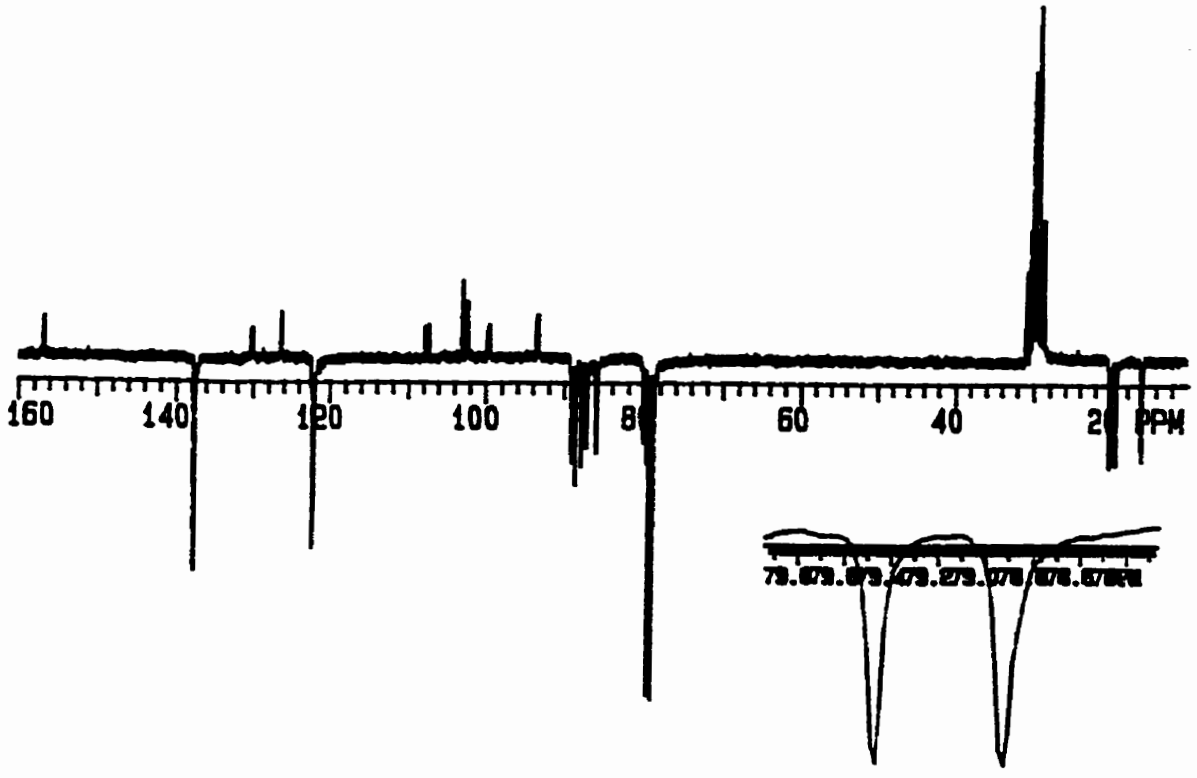

Figure 2.20b: ^{13}C NMR spectrum of complex **2.53** in acetone-d_6.

Table 2.6: ^{1}H NMR Data of Mixed Etheric/Thioetheric Bridged Complexes **2.49-2.54**.

δ (acetone-d_6), ppm				
Complex	**Cp (s, 10H)**	**Complexed Aromatic[a]**	**Uncomplexed Aromatic[a]**	**Others**
2.49	5.21 5.28	6.36-6.52 (m, 10H)	7.57 (d, 2H, J = 8.7) 7.94 (d, 2H, J = 8.7)	
2.50	5.17 5.24	6.33 (d, 2H, J = 6.8) 6.39 (d, 2H, J = 7.0) 6.41 (d, 2H, J = 6.7) 6.47 (d, 2H, J = 7.0)	7.52 (d, 2H, J = 8.7) 7.89 (d, 2H, J = 8.7)	2.50 (s, 3H, CH_3) 2.52 (s, 3H, CH_3)
2.51[b]	5.27 5.28 5.36 5.37	6.15-6.65 (m, 6H) 7.00 (t, 2H, J = 7.2)	7.71 (d, 2H, J = 8.8) 8.04 (d, 2H, J = 8.7)	
2.52	5.31 5.39	6.37-6.47 (m,4H) 6.64 (d, 2H, J = 6.8) 6.81 (d, 2H, J = 5.9)	7.57 (d, 2H, J = 8.5) 7.93 (d, 2H, J = 8.5)	
2.53[b]	5.11 5.12 5.17 5.18	6.14-6.28 (m, 2H) 6.38 (br.s., 2H) 6.49 (d, 2H, J = 5.6)	7.43 (d, 2H, J = 8.4) 7.79 (d, 2H, J = 8.1)	2.44 (s, 3H, CH_3) 2.49 (s, 3H, CH_3) 2.58 (s, 3H, CH_3) 2.65 (s. 3H, CH_3)
2.54	5.14 5.17	6.30-6.42 (m, 4H) 6.53 (t, 2H, J = 6.6)	6.80 (d, 2H, J = 8.7) 7.18 (d, 2H, J = 8.7)	2.70 (s, 6H, CH_3) 2.71 (s, 6H, CH_3)

[a] J values in Hertz. [b] Diastereoisomers present.

Table 2.7: ^{13}C NMR Data and Yields of Mixed Etheric/Thioetheric Bridged Complexes **2.49-2.54**.

δ (acetone-d_6), ppm					
Complex	**Yield (%)**	**Cp (10H)**	**Complexed Aromatic**	**Uncomplexed Aromatic**	**Others**
2.49	83	78.85 79.04	78.35, 85.77, 86.25, 86.92, 87.96, 88.49, 111.08*, 126.12*	123.41, 133.39*, 139.05, 156.56*	
2.50	73	78.49 79.17	77.86, 85.19, 87.67, 88.52, 101.74*, 102.56*, 108.61*, 126.12*	122.91, 131.94*, 138.47, 156.34*	19.67 (CH_3), 19.89 (CH_3)
2.51[a]	84	80.94 81.00 81.50 81.55	79.64, 79.72, 85.30, 85.41, 86.72, 86.77, 87.34, 87.50, 87.53, 87.85, 87.87, 89.43, 89.46, 89.58, 89.62, 99.20*, 103.96, 104.04*, 112.73, 112.94*, 125.60, 125.72*	123.66, 123.81, 130.41, 130.63*, 140.10, 140.13, 157.57, 157.63*	
2.52	82	80.53 81.22	77.98, 84.70, 87.71, 88.38, 105.06*, 106.10*, 110.87*, 125.70*	123.33, 132.54*, 139.05, 156.33*	
2.53[a]	91	78.92 29.47	80.01, 80.02, 85.99, 86.04, 87.07, 87.14, 87.70, 88.66, 89.05, 89.10, 93.35, 93.54*, 99.57, 99.83*, 102.42*, 102.97*, 107.50, 107.83*, 126.46*	122.06, 122.21, 130.09*, 130.33*, 137.51, 137.57, 156.81*, 156.90*	19.28 (CH_3), 19.84 (CH_3), 19.91 (CH_3), 19.97 (CH_3)
2.54	62	79.19 79.82	87.74, 88.47, 89.43, 102.24*, 102.54*, 107.44*, 109.28*	117.42, 123.48*, 132.84, 158.16*	20.01 (CH_3), 21.54 (CH_3)

[a] Diastereomers present. * Quaternary carbons.

2.2.1.4 Photolytic Demetallation of Thioether Containing Diiron Complexes

There are three main routes that have been applied for the removal of the modified organic ligand from their $CpFe^+$ counterparts: pyrolytic sublimation, electroreductive techniques and photolytic demetallation.[45, 57, 75-77] It has been established that photolytic demetallation is the most popular method applied in the degradation of cyclopentadienyliron complexes to yield their free organic counterparts. Nesmeyanov and coworkers established that in a variety of solvents, photolysis liberated the free arene, ferrocene, and an iron (II) salt.[79] It was found that solvents with σ-donor ligands were the most effective for this degradation process. Gill and Mann have made similar studies on the photolytic behavior of complexed ligands.[80-81]

This is a crucial step in the preparation of monomeric and oligomeric species for further use in the synthesis of polymeric materials. The preparation of the cyclopentadienyliron complexes was carried out as described in the previous sections of this chapter and the complexes then dissolved in an acetonitrile/dichloromethane mixture and irradiated with a xenon lamp for 4 hours under a nitrogen atmosphere. Schemes 2.4, 2.5 and 2.6 summarize the various thioetheric compounds successfully isolated via the photolytic demetallation of their corresponding cyclopentadienyliron complexes.

The desired thioetheric compounds **2.55-2.85** were isolated by column chromatography as white or pale yellow solids or clear oils in yields ranging from 70-96%. The identities of these disulfides were confirmed by ^1H and ^{13}C NMR, elemental analysis,

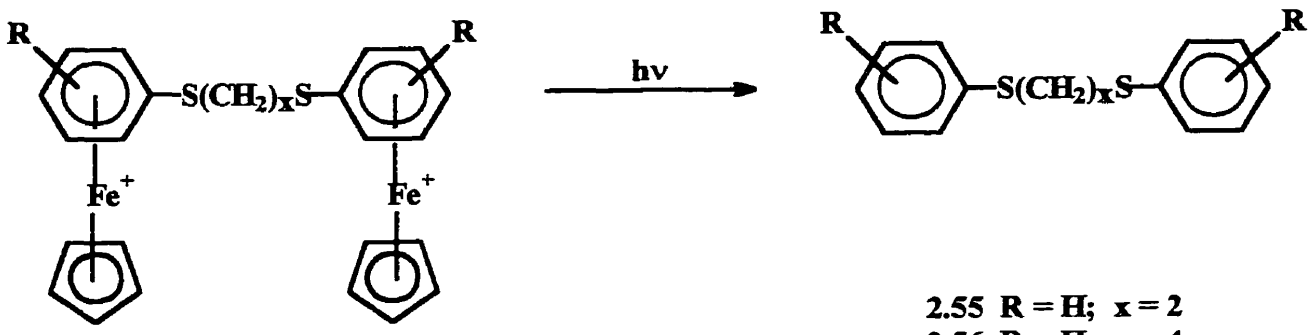

2.55 R = H; x = 2
2.56 R = H; x = 4
2.57 R = H; x = 6
2.58 R = 2-CH_3; x = 2
2.59 R = 2-CH_3; x = 4
2.60 R = 2-CH_3; x = 6
2.61 R = 3-CH_3; x = 2
2.62 R = 3-CH_3; x = 4
2.63 R = 3-CH_3; x = 6
2.64 R = 4-CH_3; x = 2
2.65 R = 4-CH_3; x = 4
2.66 R = 4-CH_3; x = 6
2.67 R = 2-Cl; x = 6
2.68 R = 3-Cl; x = 4
2.69 R = 4-Cl; x = 2
2.70 R = 4-Cl; x = 4
2.71 R = 4-Cl; x = 6
2.72 R = 4-Cl; x = 8
2.73 R = 2,6-CH_3; x = 2

Scheme 2.4

mass spectrometry (MS) and melting point, with the data summarized in Tables 2.8-2.13.

The most distinctive features of the ^1H and ^{13}C NMR spectra which verify the liberation of the compound from its corresponding complex are the absence of the cyclopentadienyliron peak and the downfield shift of the arene resonances. The ^1H NMR spectra of complex **2.21** and its organic counterpart compound **2.62** are shown in Figure 2.21 illustrate the

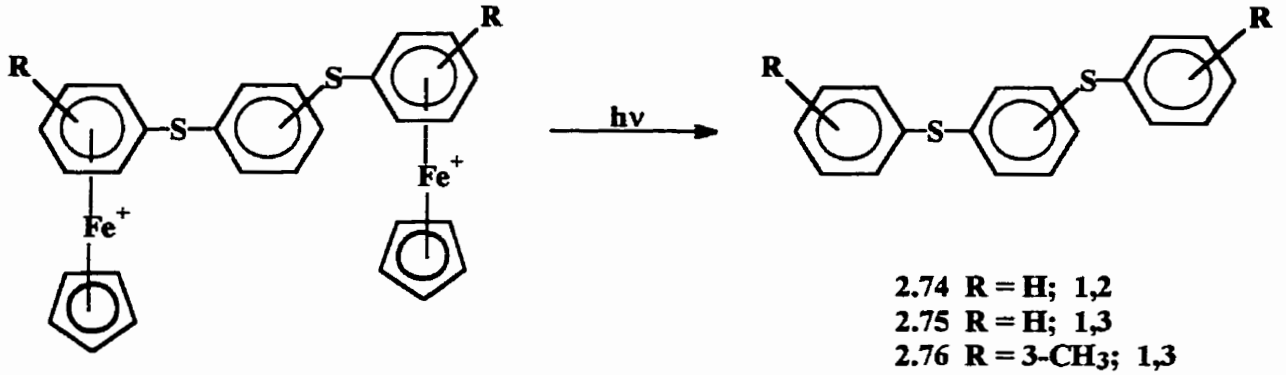

2.74 R = H; 1,2
2.75 R = H; 1,3
2.76 R = 3-CH_3; 1,3
2.77 R = 4-CH_3; 1,2
2.78 R = 4-CH_3; 1,3
2.79 R = 2-Cl; 1,3
2.80 R = 2,5-CH_3; 1,4
2.81 R = 2,6-CH_3; 1,2
2.82 R = 2,6-CH_3; 1,3

Scheme 2.5

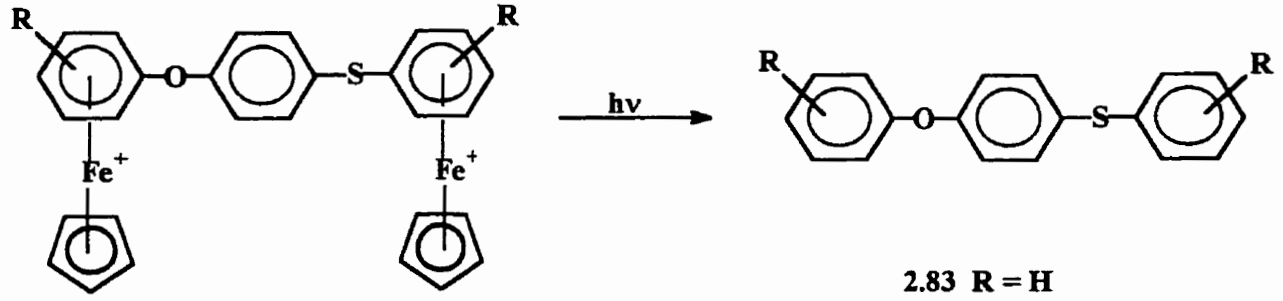

2.83 R = H
2.84 R = 4-CH_3
2.85 R = 2,5-CH_3

Scheme 2.6

dramatic changes observed upon the removal of the pendent cyclopentadienyliron metal moieties. It is important to note that the NMR spectra of all organic compounds were obtained using $CDCl_3$ as the solvent with chemicals shifts referenced with respect to the sharp singlet at 7.24 ppm and three resonances centered at 77.0 ppm in the ^1H and ^{13}C NMR spectra, respectively. In the ^1H NMR spectra of Figure 2.21, verification of the successful isolation of the pure organic compound is found in the disappearance of the resonance at 5.11 ppm in Figure 2.21a which represents the Cp protons of the metallic moiety. Additionally, there is a notable downfield shift of the arene protons upon decomplexation. Figure 2.21b shows the ^1H NMR spectrum of compound **2.62** in which the arene protons appear in the range of 6.94-7.15 ppm; in Figure 2.21b these are dramatically shifted downfield appearing as a series of doublets and triplets, as expected, in the range of 6.28-6.52 ppm. Similar observations are made in the case of the ^{13}C NMR spectrum of these compounds. For instance, Figures 2.22a and 2.22b show the ^{13}C NMR spectra of complex **2.21** and compound **2.62,** respectively, in which the disappearance of the cyclopentadienyl resonance at 79.16 ppm and the downfield shift of the four arene resonances appearing in the range of 83.88-87.56 ppm to 126.01-129.78 ppm further supports the successful isolation of compound **2.62**.

Figures 2.23a and 2.23b show the ^1H NMR spectra of complex **2.46** and compound **2.82**, respectively. These species differ slightly from the previously discussed derivatives because the thioether linkage is aromatic rather than aliphatic in nature and therefore results in many of the peaks possessing chemical shifts in similar regions of the spectra. Nonetheless, characteristic features such as the disappearance of the Cp resonance at 5.17 ppm in Figure 2.23a indicates successful demetallation. However, in

this particular example the change of the chemical shifts of the aromatic protons can not be described as a general downfield shift of the aromatic peaks upon decomplexation. As mentioned previously, and as seen in Figure 2.23a, the complexed and uncomplexed aromatic protons are separated into two separate regions in the spectrum with the uncomplexed aromatic resonances appearing further downfield at 6.50-6.60 ppm in comparison to their complexed counterparts. Indeed a general downfield shift of a majority of the aromatic resonances is observed, with the exception of the singlet found at 6.23 ppm which has shifted upfield significantly. Following integration, this resonance was attributed to the single highlighted proton in the structure corresponding to Figure 2.23b.

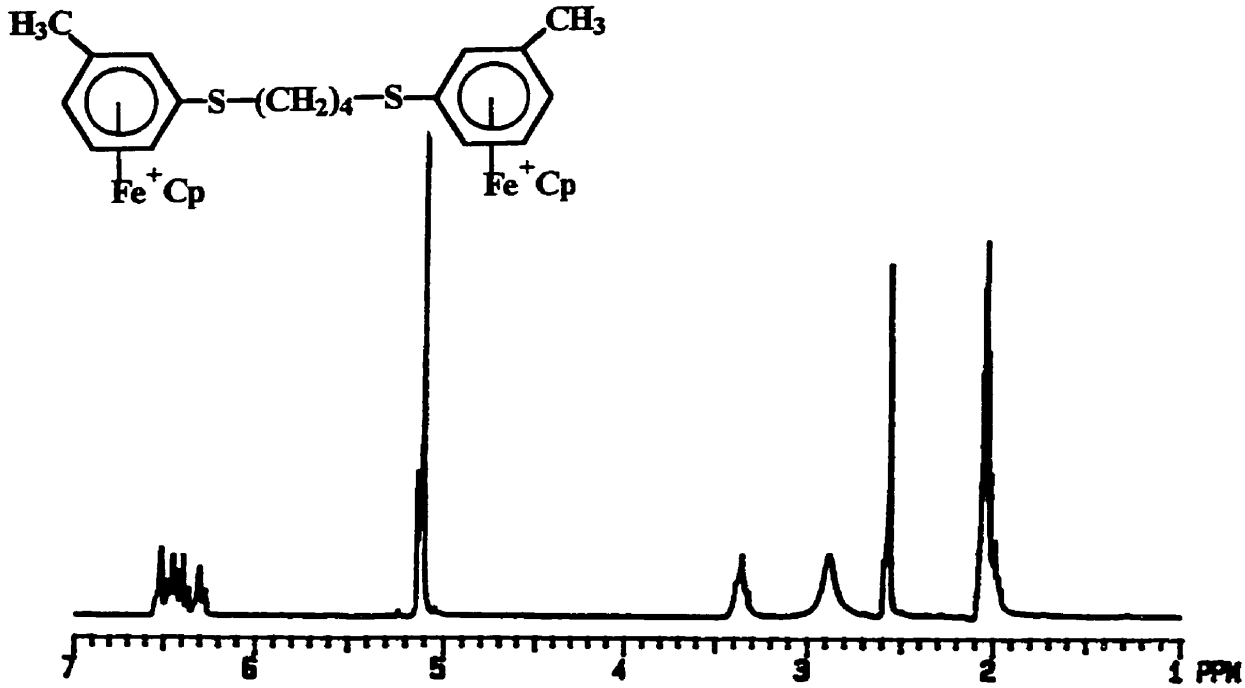

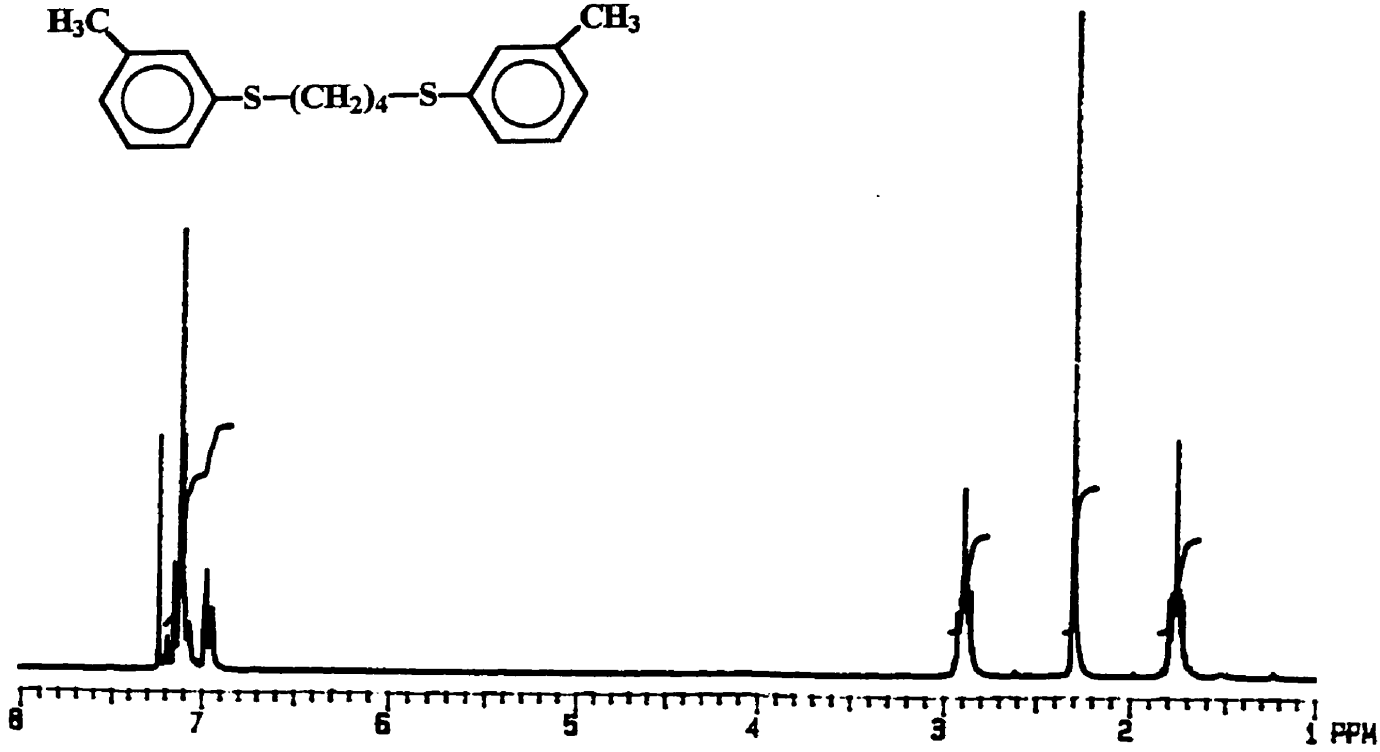

Figure 2.21a and 2.21b: ^{1}H NMR spectra of complex **2.21** in acetone-d_6 and compound **2.62** in $CDCl_3$, respectively.

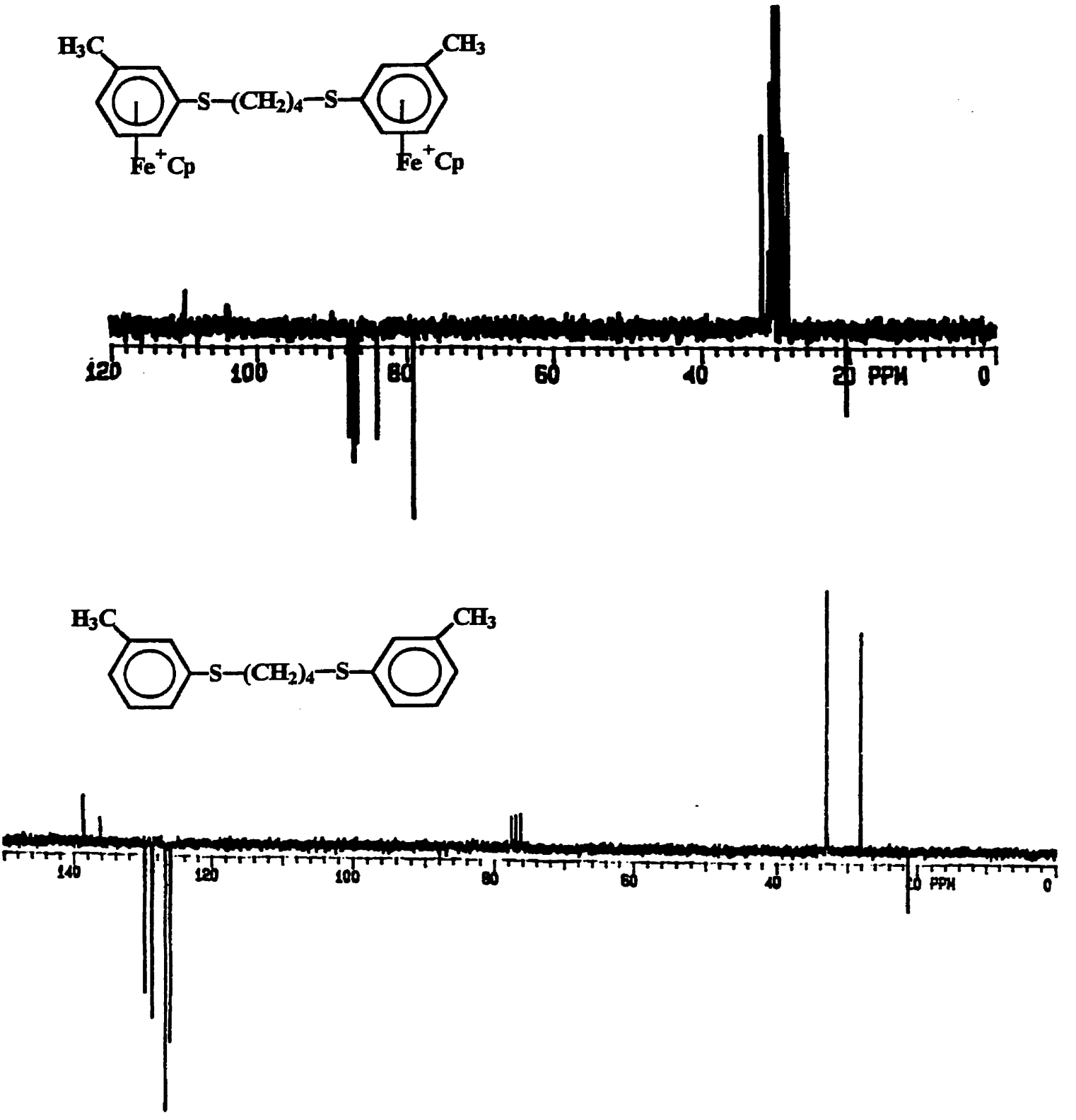

Figure 2.22a and 2.22b: ^{13}C NMR spectra of complex **2.21** in acetone-d_6 and compound **2.62** in $CDCl_3$, respectively.

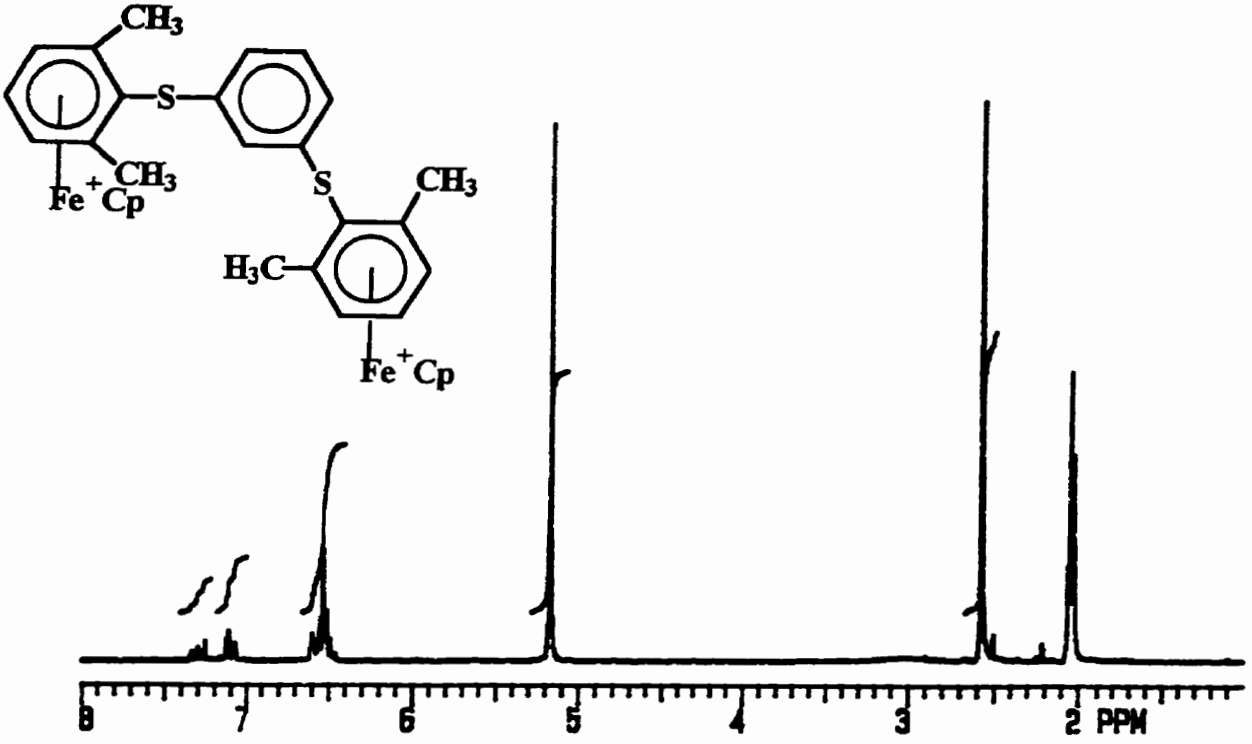

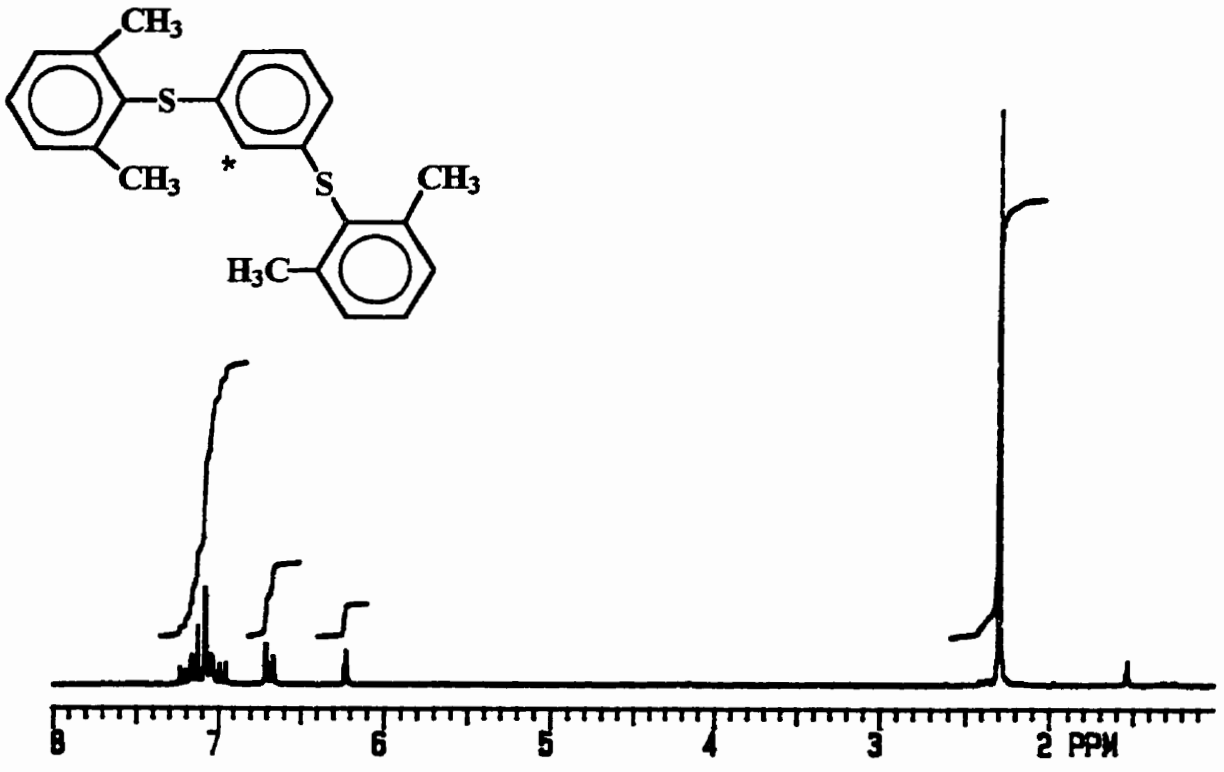

Figure 2.23a and 2.23b: ^{1}H NMR spectra of complex **2.46** in acetone-d_6 and compound **2.82** in $CDCl_3$, respectively.

Table 2.8: ^{1}H NMR Data, Yields and Melting Points of Disulfide Compounds **2.55-2.73**.

			δ ($CDCl_3$), ppm	
Complex	**Yield (%)**	**m.p. (°C)**	**Aromatic[a]**	**Others[a]**
2.55	77	61.5-62.5	7.20-7.27 (m, 10H)	3.05 (s, 4H, CH_2)
2.56	87	78	7.10-7.24 (m, 10H)	1.68-1.72 (m, 4H, β-CH_2) 2.82-2.85 (m, 4H, α-CH_2)
2.57	93	oil	7.14-7.33 (m, 10H)	1.40-1.62 (m, 8H, β & γ CH_2) 2.89 (t, 4H, J = 7.1, α-CH_2)
2.58	70	37-38	7.19-7.30 (m, 8H)	2.47 (s, 6H, CH_3) 3.16 (s, 4H, CH_2)
2.59	95	46-48	7.20-7.33 (m, 8H)	1.91 (quintet, 4H, J = 6.7, β-CH_2) 2.45 (s, 6H, CH_3) 3.00 (t, 4H, J = 6.7, α-CH_2)
2.60	86	oil	7.09-7.29 (m, 8H)	1.47-1.53 (m, 4H, γ-CH_2) 1.67-1.73 (m, 4H, β-CH_2) 2.38 (s, 6H, CH_3) 2.91 (t, 4H, J = 7.0, α-CH_2)
2.61	70	46-47	7.11-7.29 (m, 8H)	2.42 (s, 6H, CH_3) 3.19 (s, 4H, CH_2)
2.62	83	oil	6.95-6.98 (m, 6H) 7.08-7.20 (m, 2H)	1.73-1.80 (m, 4H, β-CH_2) 2.31 (s, 6H, CH_3) 2.86-2.93 (m, 4H, α-CH_2)
2.63	78	49-50.5	6.94-6.97 (m, 2H) 7.08-7.15 (m, 6H)	1.39-1.46 (m, 4H, γ-CH_2) 1.56-1.65 (m, 4H, β-CH_2) 2.30 (s, 6H, CH_3) 2.88 (t, 4H, J = 7.2, α-CH_2)
2.64	83	oil	7.07 (d, 4H, J = 8.1) 7.20 (d, 4H, J = 8.1)	2.31 (s, 6H, CH_3) 2.99 (4H, CH_2)
2.65	77	oil	7.07 (d, 4H, J = 8.0) 7.22 (d, 4H, J = 7.7)	1.72 (quintet, 4H, J = 6.5, β-CH_2) 2.30 (s, 6H, CH_3) 2.85 (t, 4H, J = 6.9, α-CH_2)
2.66	80	52.5-54.5	7.07 (d, 4H, J = 7.2) 7.22 (d, 4H, J = 7.0)	1.39-1.40 (m, 4H, γ-CH_2) 1.54-1.61 (m, 4H, β-CH_2) 2.29 (s, 6H, CH_3) 2.83 (t, 4H, J = 6.5, α-CH_2)
2.67	96	oil	7.06-7.36 (m, 8H)	1.45-1.54 (m, 4H, g-CH_2) 1.66-1.72 (m, 4H, β-CH_2) 2.91 (t, 4H, J = 7.0, α-CH_2)

2.68	73	oil	7.09-7.26 (m, 8H)	1.74-1.79 (m, 4H, β-CH_2) 2.88-2.95 (m, 4H, α-CH_2)
2.69	90	78.5-80	7.24 (br.s., 8H)	3.03 (s, 4H, CH_2)
2.70	76	oil	7.24 (br.s., 8H)	1.75 (br.s., 4H, β-CH_2) 2.89 (br.s., 4H, α-CH_2)
2.71	75	69-71	7.22 (br.s., 8H)	1.40-1.44 (m, 4H, γ-CH_2) 1.56-1.63 (m, 4H, β-CH_2) 2.86 (t, 4H, J = 7.1, α-CH_2)
2.72	93	oil	7.24 (br.s., 8H)	1.31-1.39 (m, 8H, δ & γ-CH_2) 1.56-1.66 (m, 4H, β-CH_2) 2.88 (t, 4H, J = 7.2, α-CH_2)
2.73	81	oil	7.24 (br.s., 6H)	2.60 (s, 12H, CH_3) 2.88 (s, 4H, CH_2)

[a] J values in Hertz.

Table 2.9: ^{13}C NMR and MS Data of Disulfide Compounds **2.55-2.73**.

δ ($CDCl_3$), ppm			
Complex	**M/z (M^+, %)**	**Aromatic**	**Others**
2.55	246 (24)	126.56, 128.03, 130.01, 134.98*	33.34 (CH_2)
2.56	274 (31)	127.61, 130.57, 130.93, 138.17*	29.81 (β-CH_2), 34.92 (α-CH_2)
2.57	302 (29)	125.61, 128.74, 128.83, 136.79*	28.21 (γ-CH_2), 28.89 (β-CH_2), 33.39 (α-CH_2)
2.58	274 (26)	126.34, 126.45, 128.97, 130.31, 134.23*, 138.39*	20.43 (CH_3), 32.38 (CH_2)
2.59	302 (31)	125.51, 126.32, 127.71, 130.04, 135.77*, 137.42*	20.32 (CH_3), 28.06 (β-CH_2), 32.35 (α-CH_2)
2.60	330 (100)	125.30, 126.30, 127.35, 130.00, 136.19*, 137.20*	20.32 (CH_3), 28.46 (γ-CH_2), 28.81 (β-CH_2), 32.67 (α-CH_2)
2.61	274 (29)	126.87, 127.36, 128.81, 130.52, 134.71*, 138.79*	21.27 (CH_3), 33.29 (CH_2)
2.62	302 (30)	126.01, 126.75, 128.68, 129.78, 136.16*, 138.59*	20.18 (CH_3), 28.11 (β-CH_2), 33.11 (α-CH_2)
2.63	330 (87)	125.79, 126.52, 128.61, 129.50, 136.53*, 138.47*	21.30 (CH_3), 28.25 (γ-CH_2), 28.94 (β-CH_2), 33.38 (α-CH_2)
2.64	274 (29)	129.80, 130.76, 131.25*, 136.77*	21.05 (CH_3), 33.99 (CH_2)
2.65	302 (28)	129.55, 130.13, 132.61*, 136.12*	21.00 (CH_3), 28.20 (β-CH_2), 33.99 (α-CH_2)
2.66	330 (77)	129.61, 129.86, 132.95*, 135.91*	20.99 (CH_3), 28.26 (γ-CH_2), 29.08 (β-CH_2), 34.28 (α-CH_2)
2.67	371 (17) 373 (11) 375 (2)	126.14, 127.02, 127.93, 129.60, 133.16*, 135.92*	28.38 (β-CH_2), 32.27 (α-CH_2)
2.68	343 (6) 345 (4) 347 (1)	125.88, 126.75, 128.24, 129.84, 134.63*, 137.32*	27.77 (β-CH_2), 32.79 (α-CH_2)

2.69	315 (5) 317 (3) 319 (1)	129.20, 131.52, 132.82*, 133.37*	33.63 (CH_2)
2.70	343 (8) 345 (5) 347 (1)	128.99, 130.59, 134.45*, 135.31*	27.87 (β-CH_2) 33.45 (α-CH_2)
2.71	371 (19) 373 (12) 375 (2)	128.85, 130.13, 131.54*, 135.30*	28.12 (γ-CH_2), 28.73 (β-CH_2), 33.60 (α-CH_2)
2.72		128.88, 130.15, 131.55*, 135.48*	28.61 (δ-CH_2), 28.92 (γ-CH_2), 33.77 (β-CH_2), 39.05 (α-CH_2)
2.73	302 (15)	128.12, 128.25, 132.40*, 143.02*	22.04 (CH_3), 34.44 (CH_2)

* Quaternary carbons.

Table 2.10: ^{1}H NMR Data, Yields and Melting Points of Disulfide Compounds **2.74-2.82**.

			δ ($CDCl_3$), ppm	
Complex	**Yield (%)**	**m.p. (°C)**	**Aromatic[a]**	**Others[a]**
2.74	72	oil	7.08-7.10 (m, 4H)	
2.75	90	oil	7.12-7.18 (m, 8H) 7.33-7.36 (m, 6H)	
2.76	95	oil	7.08 - 7.17 (12H)	2.30 (s, 6H, CH_3)
2.77	87	61.5-63	7.04 (s, 4H) 7.12 (d, 4H, J = 8.1) 7.30 (d, 4H, J = 8.2)	2.35 (s, 6H, CH_3)
2.78	81	71.5-73	6.94-7.05 (m, 4H) 7.08 (d, 4H, J = 8.0) 7.24 (d, 4H, J = 8.0)	2.31 (s, 6H, CH_3)
2.79	75	oil	7.09-7.19 (m, 6H) 7.30-7.40 (m, 6H)	
2.80	74	oil	7.00 (br.s., 2H) 7.05 (s, 4H) 7.12 (d, 4H, J = 7.1)	2.25 (s, 6H, CH_3) 2.30 (s, 6H, CH_3)
2.81	78	oil	6.42-6.46 (m, 2H) 6.80-6.84 (m, 2H) 7.18-7.26 (m, 6H)	2.45 (s, 12H, CH_3)
2.82	93	87-89	6.23 (br.s., 1H) 6.69 (dd, 2H, J = 7.7, J = 1.8) 6.95-7.20 (m, 7H)	2.29 (s, 12H, CH_3)

[a] J values in Hertz.

Table 2.11: ^{13}C NMR and MS Data of Disulfide Compounds **2.74-2.82**

δ ($CDCl_3$), ppm			
Complex	**m/z (M^+, %)**	**Aromatic**	**Others**
2.74	294 (100)	127.46, 129.31, 131.34, 131.75, 134.41*, 137.34*	
2.75	294 (100)	128.72, 128.87, 130.36, 130.82, 131.32, 132.74, 134.83*, 138.67*	
2.76	322 (100)	128.00, 128.49, 129.07, 129.12, 129.53, 130.90, 132.58*, 133.99*, 137.82*, 139.13*	21.28 (CH_3)
2.77	322 (100)	126.95, 128.45*, 130.15, 130.45, 132.46, 137.52*, 137.75*	21.57 (CH_3)
2.78	322 (100)	126.62, 128.60*, 128.99, 129.34*, 130.09, 132.87, 137.98*, 138.65*	21.72 (CH_3)
2.79	363 (9) 365 (6) 367 (1)	127.30, 128.13, 129.95, 130.22, 131.02, 131.60, 134.61, 134.69*, 135.17*, 145.01*	
2.80	350 (100)	129.03, 129.75, 130.50, 132.72*, 133.92, 134.41*, 136.39*, 137.10*	20.08 (CH_3), 20.79 (CH_3)
2.81	350 (100)	125.26, 125.43, 128.51, 129.19, 131.01*, 135.39*, 143.87*	21.74 (CH_3)
2.82	350 (100)	121.78, 122.09, 128.36, 129.00, 129.28, 129.88*, 138.94*, 143.65*	21.62 (CH_3)

* Quaternary carbons.

Table 2.12: ^{1}H NMR Data, Yields and Melting Points of Mixed Ether/Thioether Bridged Compounds **2.83-2.85**.

δ ($CDCl_3$), ppm				
Complex	**Yield (%)**	**m.p. (°C)**	**Aromatic[a]**	**Others[a]**
2.83	73	oil	6.94 (d, 2H, J = 7.6) 7.02 (d, 2H, J = 7.6) 7.11-7.19 (m, 2H) 7.24-7.38 (m, 8H)	
2.84	94	oil	6.89 (d, 2H, J = 8.6) 6.91 (d, 2H, J =8.5) 7.11 (m, 4H) 7.20 (d, 2H, J = 8.3) 7.29 (d, 2H, J = 8.4)	2.31 (s, 3H, CH_3) 2.32 (s, 3H, CH_3)
2.85	76	oil	6.72-6.95 (m, 6H) 7.04-7.22 (m, 6H)	2.14 (s, 3H, CH_3) 2.20 (s, 3H, CH_3) 2.25 (s, 3H, CH_3) 2.30 (s, 3H, CH_3)

[a] J values in Hertz.

Table 2.13: ^{13}C NMR and MS Data of Mixed Ether/Thioether Bridged Compounds **2.83-2.85**.

		δ ($CDCl_3$), ppm	
Complex	**m/z (M^+, %)**	**Aromatic**	**Others**
2.83	281 (100)	119.80, 124.27, 126.92, 129.00*, 129.58, 129.96, 130.36, 132.23*, 134.73, 154.20*, 157.51*	
2.84	306 (100)	118.80, 119.33, 128.54*, 128.86*, 129.90, 130.30, 130.52, 133.18, 133.33*, 136.76*, 154.16*, 157.44*	20.72 (CH_3), 21.04 (CH_3)
2.85	334 (100)	117.91, 120.61, 125.08, 126.75*, 127.59*, 127.88, 130.26, 131.22, 131.56, 132.86, 135.02*, 135.36*, 136.17*, 137.18*, 153.80*, 157.42*	15.73 (CH_3), 19.96 (CH_3), 20.88 (CH_3), 20.96 (CH_3)

* Quaternary carbons

2.2.2 Synthesis of Diaryl Alkyl and Diaryl Aryl Disulfones

2.2.2.1 Fuctionalization of Bis(cyclopentadienyliron) Arene Complexes with Sulfone Linkages

Although it has been demonstrated that one route applied in the functionalization of diiron arene complexes is the reaction of terminal chlorine substituted complexes in a second nucleophilic aromatic substitution reaction, the presence of the thioether linkages in complexes **2.13-2.33, 2.37-2.47** and **2.49-2.54** offers the potential for functionalization via the oxidation of the sulfides to their corresponding sulfoxides or sulfones based on established experimental procedures.[204-207] A 1986 report by Madesclaire has extensively reviewed most of the oxidation procedures of sulfide compounds and the oxidizing agents used in these reactions.[206] The focus of the present study was the oxidation of the sulfides to their sulfone counterparts due to the potential use of these compounds in material science, organic synthesis and the pharmaceutical industry.[179, 183, 189, 209-212] Although hydrogen peroxide in glacial acetic acid, potassium permanganate and m-chloroperbenzoic acid (m-CPBA) have been found to be very useful oxidants, sulfide containing cyclopentadienyliron arene complexes are most readily oxidized to their corresponding sulfones in the presence of hydrogen peroxide ($H_2O_2/TiCl_3$) or m-CPBA in dichloromethane.[206-213]

Schemes 2.7-2.9 illustrate the synthetic strategy undertaken in the preparation of bis(cyclopentadienyliron) arene complexes with sulfone linkages from their disulfide

precursors. The parent sulfide containing complex was reacted in the presence of a 10-fold excess of m-chloroperbenzoic acid and heated for 8 hours at 60°C in a DMF/CH_2Cl_2 solvent mixture.[31] Generally, the oxidation of the bis-sulfide diiron complexes proceeded with the corresponding sulfones being isolated as yellow solids in yields ranging from 70-96%. Even in the case of the sterically crowded complex **2.32**, oxidation to its sulfone counterpart, **2.101**, was achieved under mild reaction conditions and the complex isolated in 85% yield. However, it is believed that steric hindrance did play a role in the inability to isolate the corresponding disulfone of the parent sulfide complex **2.41**, 1,2-bis([η^6-4-methylthiophenoxy-η^5-cyclopentadienyl]iron)benzene hexafluorophosphate.

^1H, ^{13}C NMR and IR spectroscopies were used in the identification of these complexes and the results are summarized in Tables 2.14-2.19. Both the NMR and IR data possess distinctive features to verify the conversion of the sulfide to the sulfone. Two characteristic infrared absorbances in the range of 1160-1090 cm^{-1} and 1350-1275 cm^{-1} indicative of the sulfone functionality were present. Due to the lower solubility of several of the sulfones, some of the NMR studies were carried out using DMSO-d_6 as a solvent rather than acetone-d_6.

A typical ^1H NMR spectrum of complex **2.87** is shown in Figure 2.24 and should be compared to Figure 2.10 which presents the ^1H NMR spectrum of the parent sulfide complex **2.15**. It is also important to note that the electron-withdrawing nature of the sulfonyl groups resulted in the downfield shift of the cyclopentadienyl peak in the NMR spectra compared to the corresponding sulfide complexes. This is clearly evident in the downfield

2.86 R = H; x = 2
2.87 R = H; x = 6
2.88 R = 2-CH_3; x = 4
2.89 R = 3-CH_3; x = 2
2.90 R = 3-CH_3; x = 4
2.91 R = 3-CH_3; x = 6
2.92 R = 4-CH_3; x = 2
2.93 R = 4-CH_3; x = 4
2.94 R = 4-CH_3; x = 6
2.95 R = 2-Cl; x = 6
2.96 R = 3-Cl; x = 4
2.97 R = 3-Cl; x = 6
2.98 R = 4-Cl; x = 4
2.99 R = 4-Cl; x = 6
2.100 R = 4-Cl; x = 8
2.101 R = 2,6-CH_3; x = 2

Scheme 2.7

shift from 5.16 to 5.40 ppm of the singlet representative of the cyclopentadienyl protons in Figure 2.24. Additionally, the strong electron-withdrawing influence of the sulfonyl groups also affects the chemical shifts of the complexed aromatic protons which appear approximately one-half ppm downfield from their original position in the sulfide complex. The aliphatic components are affected less dramatically with the greatest influence being on the protons α to the sulfone functionalities.

The conversion of the thioether linkage to its sulfonyl counterpart is clearly evident in the case of those complexes which possess mixed thioether/ether linkages as a result of the reaction of chloroarene complexes with 4-hydroxythiophenol. For instance, Figure 2.25 shows portions of the ^{1}H NMR spectra of complex **2.52** and its sulfone containing counterpart, **2.105**. Even disregarding the dramatic chemical shifts of both the complexed and uncomplexed aromatic protons in comparing these two spectra, the increased chemical shift difference between the two strong singlets representative of the Cp protons in Figure 2.25b, following oxidation, clearly indicates the presence of the strong electron-withdrawing functionality.

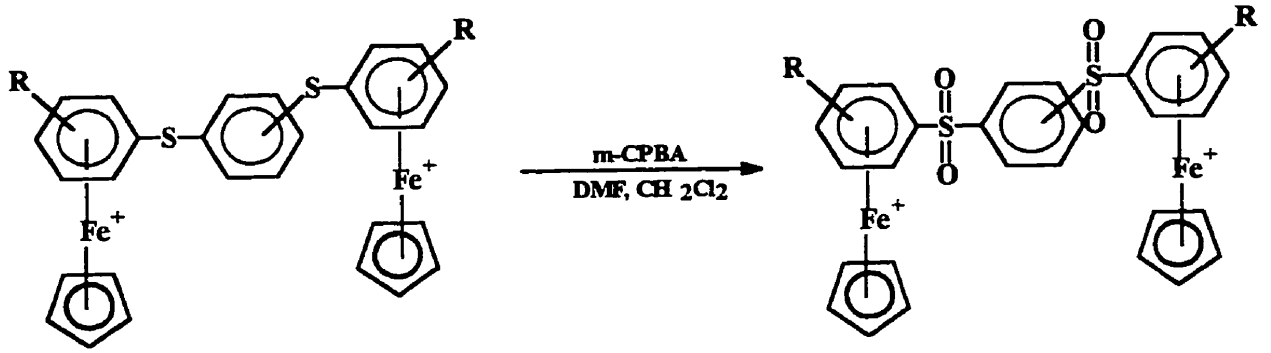

2.102 R = 3-CH_3; 1,3
2.103 R = 4-CH_3; 1,3

Scheme 2.8

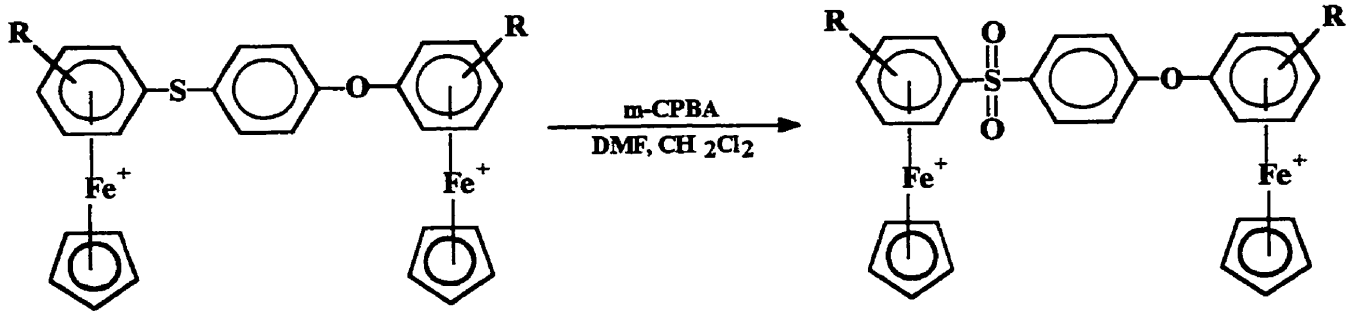

2.104 R = 3-CH_3; 1,4
2.105 R = 4-Cl; 1,4

Scheme 2.9

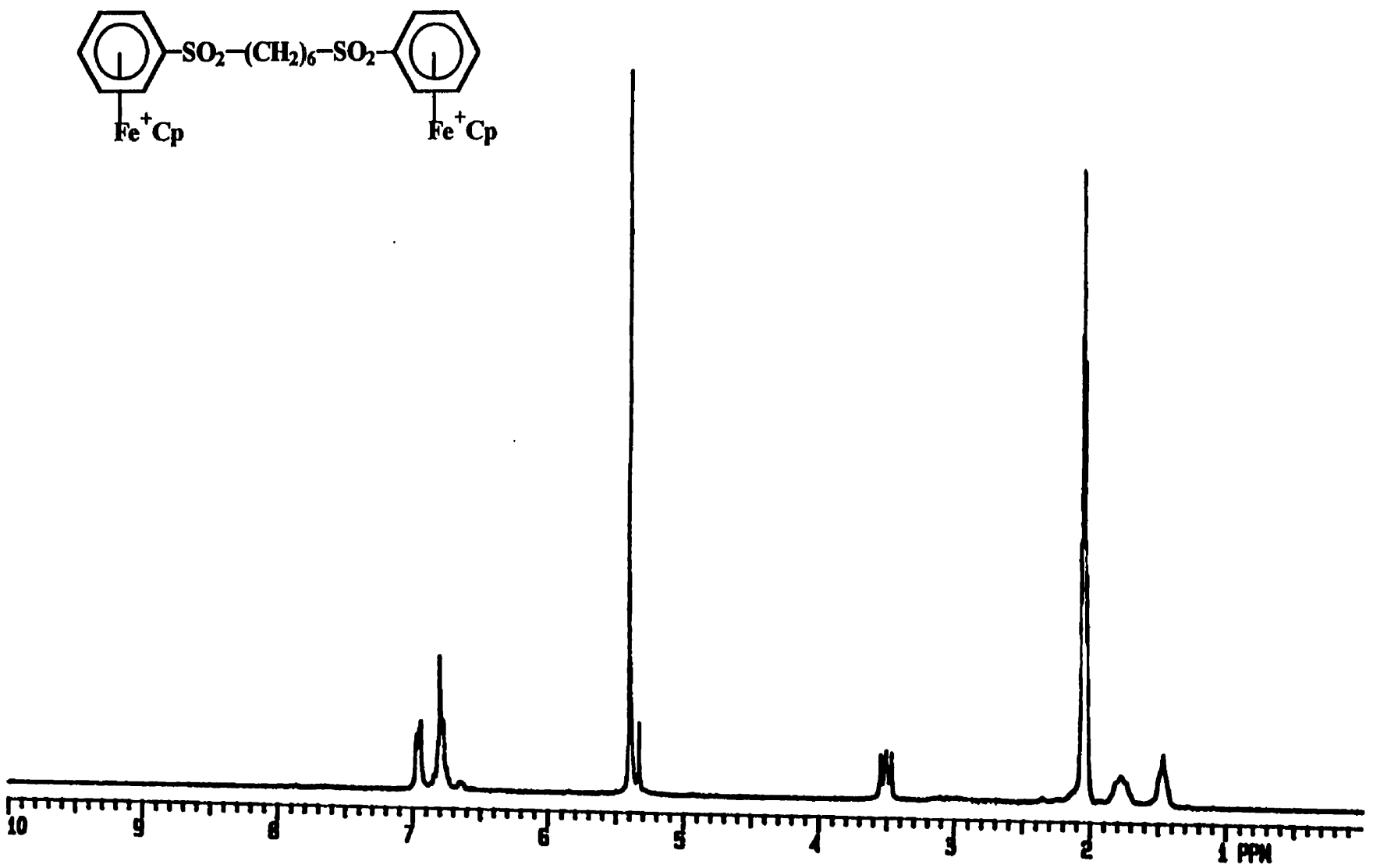

Figure 2.24: ^{1}H NMR spectrum of complex **2.87** in acetone-d_6.

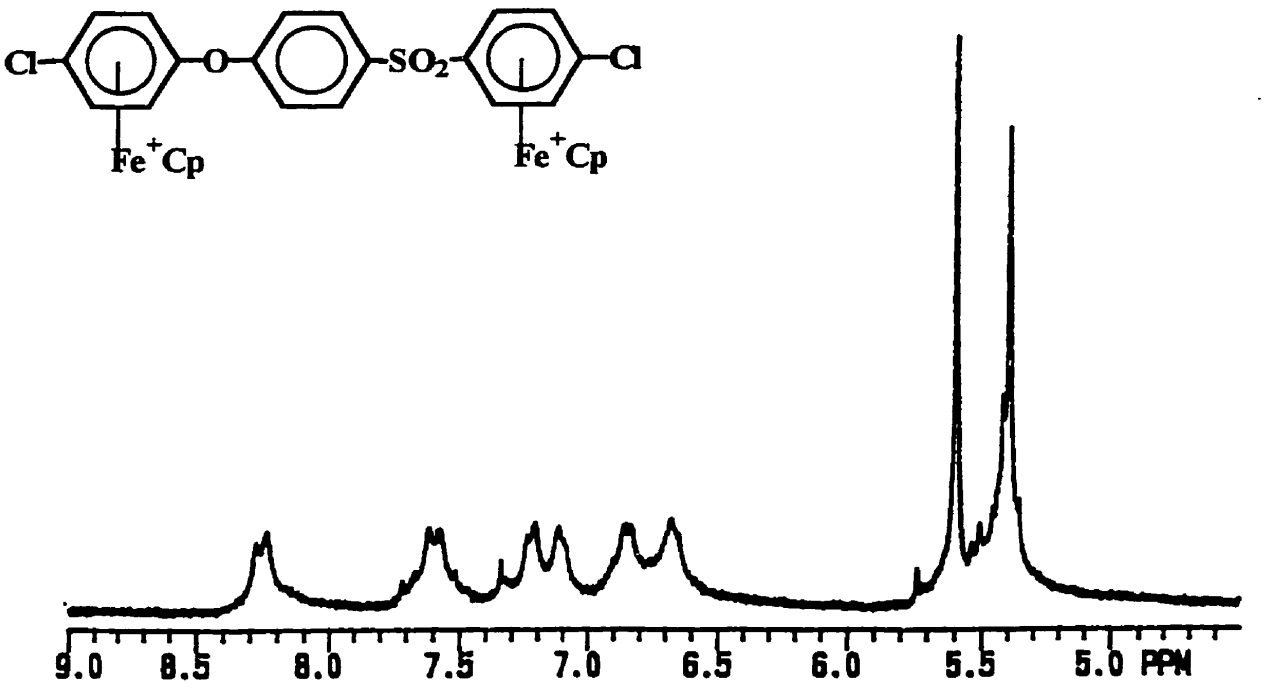

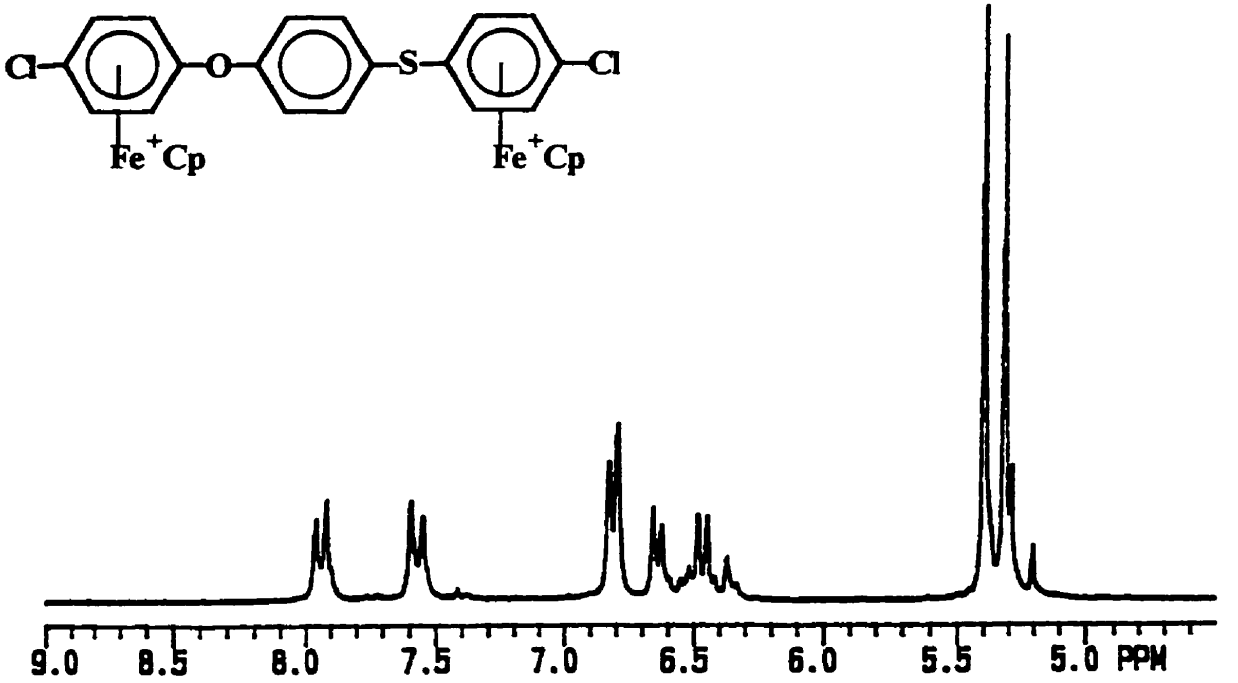

Figure 2.25a and 2.25b: ^{1}H NMR spectra of complex **2.52** and **2.105**, respectively, in acetone-d_6.

Table 2.14: ^{1}H NMR and IR Data of Diiron Sulfone Complexes **2.86-2.101**.

δ (acetone-d_6), ppm				
Complex	**Cp (s, 10H)**	**Complexed Aromatic[a]**	**Others[a]**	**ν_{max} (cm^{-1}) SO_2**
2.86	5.40	6.80-6.85 (m, 6H) 7.00-7.04 (m, 4H)	4.16 (s, 4H, CH_2)	1090 1330
2.87	5.40	6.77-6.80 (m, 6H) 6.94-6.97 (m, 4H)	1.45-1.46 (m, 4H, γ-CH_2) 1.74-1.81 (m, 4H, β-CH_2) 3.50 (t, 4H, J = 7.8, α-CH_2)	1160 1330
2.88	5.36	6.64-6.77 (m, 6H) 6.93 (m, 2H)	2.78-2.81 (m, 4H, β-CH_2) 2.83 (s, 6H, CH_3) 3.60-3.68 (m, 4H, α-CH_2)	1150 1325
2.89	5.34	6.72 (br.s., 4H) 6.90 (br.s., 4H)	2.65 (s, 6H, CH_3) 4.09 (s, 4H, CH_2)	1155 1340
2.90	5.36	6.74 (br.s., 4H) 6.86 (br.s., 4H)	1.99-2.05 (m, 4H, β-CH_2) 2.83 (s, 6H, CH_3) 3.58-3.59 (m, 4H, α-CH_2)	1155 1340
2.91	5.35	6.71 (br.s., 4H) 6.86 (br.s., 4H)	1.38-1.52 (m, 4H, γ-CH_2) 1.69-1.85 (m, 4H, β-CH_2) 2.68 (s, 6H, CH_3) 3.48 (t, 4H, J = 7.7, α-CH_2)	1155 1340
2.92	5.35	6.71 (d, 4H, J = 6.6) 6.94 (d, 4H, J = 6.6)	2.66 (s, 6H, CH_3) 4.11 (s, 4H, CH_2)	1155 1340
2.93	5.36	6.88 (d, 4H, J = 7.3) 6.70 (d, 4H, J = 7.3)	1.97 (br.s, 4H, CH_2) 2.67 (s, 6H, CH_3) 3.59 (br.s, 4H, CH_2)	1155 1324
2.94	5.35	6.70 (d, 4H, J = 6.7) 6.89 (d, 4H, J = 6.7)	1.44-1.49 (m, 4H, γ-CH_2) 1.72-1.77 (m, 4H, β-CH_2) 3.49 (t, 4H, J = 7.8, α-CH_2)	1155 1340
2.95	5.50	6.78 (t, 2H, J = 5.7) 6.95 (t, 2H, J = 5.6) 7.06 (d, 2H, J = 6.3) 7.14 (d, 2H, J = 6.2)	1.51-1.57 (m, 4H, γ-CH_2) 1.86-1.97 (m, 4H, β-CH_2) 3.67 (t, 4H, J = 7.5, α-CH_2)	1155 1325
2.96	5.52	6.90-6.96 (m, 4H) 7.14-7.26 (m, 4H)	1.95-2.06 (m, 4H, β-CH_2) 3.64-3.68 (m, 4H, α-CH_2)	1160 1330
2.97	5.52	6.91-6.98 (m, 4H) 7.16 (d, 2H, J = 6.1) 7.27 (s, 2H)	1.45-1.48 (m, 4H, γ-CH_2) 1.83-1.86 (m, 4H, β-CH_2) 3.58 (t, 4H, J = 7.8, α-CH_2)	1155 1335

2.98[b]	5.40	6.95 (d, 4H, J = 5.9) 7.11 (d, 4H, J = 6.1)	1.72 (br.s., 4H, β-CH_2) 3.63 (br.s., 4H, α-CH_2)	1160 1335
2.99	5.52	7.11 (d, 4H, J = 7.0) 7.13 (d, 4H, J = 6.3)	1.44-1.45 (m, 4H, γ-CH_2) 1.73-1.82 (m, 4H, β-CH_2) 3.53 (t, 4H, J = 7.9, α-CH_2)	1155 1335
2.100	5.52	7.11 (br.s., 8H)	1.29-1.39 (m, 8H, γ & δ-CH_2) 1.72-1.81 (m, 4H, β-CH_2) 3.45 (t, 4H, α-CH_2)	
2.101	5.36	6.62 (d, 4H, J = 5.9) 6.73-6.79 (m, 2H)	2.83 (s, 12H, CH_3) 4.25 (s, 4H, CH_2)	1160 1335

[a] J values in Hertz. [b] Solvent used was DMSO-d_6.

Table 2.15: ^{13}C NMR Data and Yields of Diiron Sulfone Complexes **2.86-2.101**.

δ (acetone-d_6), ppm				
Complex	**Yield (%)**	**Cp (10H)**	**Complexed Aromatic**	**Others**
2.86[a]	83	78.89	88.20, 88.49, 90.64, 100.91*	47.64 (CH_2)
2.87	84	80.04	89.24, 89.46, 91.47, 103.98*	22.77 (γ-CH_2), 29.04 (β, CH_2), 55.55 (α-CH_2)
2.88	80	78.92	87.14, 88.40, 90.27, 101.03*, 103.45*	18.31 (CH_3), 20.37 (β-CH_2), 53.24 (α-CH_2)
2.89	89	80.47	87.80, 88.86, 89.30, 92.12, 102.29*, 105.87*	20.57 (CH_3), 49.29 (CH_2)
2.90[a]	87	79.03	85.99, 87.52, 87.57, 90.70, 101.42*, 104.09*	19.84 (CH_3), 20.50 (β-CH_2), 53.23 (α-CH_2)
2.91	77	80.26	87.47, 88.78, 89.06, 91.80, 103.57*, 105.70*	20.62 (CH_3), 22.77 (γ-CH_2), 27.86 (β-CH_2), 55,83 (α-CH_2)
2.92[a]	93	79.12	87.81, 88.26, 99.43*, 106.62*	20.17 (CH_3), 47.74 (CH_2)
2.93	84	79.05	87.24, 88.34, 100.51*, 106.46*	20.15 (CH_3), 20.59 (β-CH_2), 53.26 (α-CH_2)
2.94	70	80.23	88.60, 89.59, 102.58*, 107.78*	20.77 (CH_3), 22.81 (γ-CH_2), 27.86 (β-CH_2), 55.59 (α-CH_2)
2.95	76	82.03	88.71, 90.44, 91.36, 91.77, 103.12*, 107.92*	22.49 (γ-CH_2), 27.96 (β-CH_2), 55.02 (α-CH_2)
2.96	72	82.38	88.38, 89.00, 89.36, 92.00, 103.94*, 108.44*	21.82 (β-CH_2), 54.98 (α-CH_2)
2.97	75	82.34	88.41, 89.03, 89.38, 91.98, 104.20*, 108.39*	22.70 (γ- CH_2), 27.92 (β-CH_2), 55.70 (α-CH_2)
2.98[a]	94	81.02	87.91, 88.34, 101.09*, 108.63*	20.42 (β-CH_2), 53.15 (α-CH_2)
2.99	77	82.23	89.26, 89.57, 103.14*, 110.09*	22.65 (g- CH_2), 27.72 (β-CH_2), 55.52 (α- CH_2)

2.100	96	82.27	89.32, 89.64, 103.24*, 110.08*	22.98 (δ-CH_2), 28.63 (γ-CH_2), 30.18 (β-CH_2), 55.79 (α-CH_2)
2.101[a]	85	79.28	89.48, 90.40, 103.97*, 107.05*	20.72 (CH_3), 47.76 (CH_2)

[a] Solvent used was DMSO-d_6. * Quaternary carbons

Table 2.16: ^{1}H NMR Data of Diiron Sulfone Complexes **2.102-2.103**.

δ (acetone-d_6), ppm				
Complex	**Cp (s, 10H)**	**Complexed Aromatic[a]**	**Uncomplexed Aromatic[a]**	**Others[a]**
2.102	5.45	6.68-6.71 (br.s., 4H) 7.04-7.11 (m, 4H)	8.00 (t, 1H, J = 7.8) 8.50 (d, 2H, J = 7.9) 8.74 (s, 1H)	2.64 (s, 6H, CH_3)
2.103	5.45	6.68 (d, 4H, J = 6.7) 7.09 (d, 4H, J = 6.6)	8.00 (t, 1H, J = 7.6) 8.51 (d, 2H, J = 7.9) 8.73 (s, 1H)	2.62 (s, 6H, CH_3)

[a] J values in Hertz.

Table 2.17: ^{13}C NMR and IR Data and Yields of Diiron Sulfone Complexes **2.102-2.103**.

δ (acetone-d_6), ppm						
Complex	**Yield (%)**	**Cp (s, 10H)**	**Complexed Aromatic**	**Uncomplexed Aromatic**	**Others**	**ν_{max} (cm^{-1}) SO_2**
2.102	95	80.66	86.92, 88.44, 89.13, 92.01, 104.87*, 106.19*	128.45, 133.53, 135.60, 141.65*	20.56 (CH_3)	1095 1350
2.103	83	80.61	88.01, 89.89, 103.86*, 108.11*	128.43, 133.53, 135.55, 141.66*	20.74 (CH_3)	1100 1345

* Quaternary carbons.

Table 2.18: ^{1}H NMR Data of Mixed Ether/Sulfone Diiron Complexes **2.104-2.105**.

δ (acetone-d_6), ppm				
Complex	**Cp (s, 10H)**	**Complexed Aromatic[a]**	**Uncomplexed Aromatic[a]**	**Others[a]**
2.104	5.21 5.41	7.02 (br.s., 2H) 6.25-6.69 (m, 6H)	7.53 (d, 2H, J = 7.5) 8.23 (d, 2H, J = 7.4)	2.55 (s, 3H, CH_3) 2.65 (s, 3H, CH_3)
2.105	5.39 5.59	6.67 (d, 2H, J = 6.8) 6.85 (d, 2H, J = 6.6) 7.11 (d, 2H, J = 6.8) 7.21 (d, 2H, J = 6.9)	7.59 (d, 2H, J = 8.0) 8.26 (d, 2H, J = 7.9)	

[a] J values in Hertz.

Table 2.19: ^{13}C NMR and IR Data and Yields of Mixed Ether/Sulfone Complexes **2.104-2.105**.

δ (acetone-d_6), ppm						
Complex	**Yield (%)**	**Cp (s, 10H)**	**Complexed Aromatic**	**Uncomplexed Aromatic**	**Others**	**ν_{max} (cm^{-1}) SO_2**
2.104	81	78.59	78.18, 80.93, 86.10, 86.81, 87.66, 88.63, 91.34, 103.91*, 105.68*, 130.82*	121.32, 131.91, 135.54*, 160.25*	19.97 (CH_3) 20.67 (CH_3)	1105 1275
2.105	83	80.97 82.45	79.54, 88.10, 88.27, 89.89, 105.43*, 105.59*, 109.94 *, 131.12*	122.13, 132.53, 135.78*, 160.14*		1100 1350

* Quaternary carbons

2.2.2.2 Photolytic Demetallation of Sulfonyl Containing Diiron Complexes

The use of photolytic demetallation for the removal of the modified organic ligand from its cyclopentadienyliron parent complex has been discussed previously in Section 2.2.5 of this work. The same experimental procedure was applied in the isolation of compounds **2.106-2.121**. The bimetallic complexes were dissolved in an acetonitrile/dichloromethane solvent mixture, subjected to intense visible light radiation for a period of 4 hours under a nitrogen atmosphere and isolated via column chromatography in yields ranging from 70-94%. Schemes 2.10-2.12 show the sulfonyl containing compounds that were isolated using this methodology.

^{1}H and ^{13}C NMR, elemental analysis, mass spectrometry (MS) and infrared spectrophotometry were used to verify the isolation of compounds **2.106-2.121** and the results summarized in Tables 2.20-2.25. The melting points of these compounds are also recorded in Tables 2.20, 2.22 and 2.24. As was observed in the isolation of the thioether containing compounds from their corresponding diiron complexes, the most notable piece of evidence indicative of successful demetallation is the disappearance of the cyclopentadienyl peak in both the ^{1}H and ^{13}C NMR spectra. This observation is accompanied by a dramatic downfield chemical shift of the complexed aromatic protons upon the removal of the pendent cyclopentadienyliron metallic moiety. Figures 2.26 and 2.27 show the ^{1}H and ^{13}C NMR spectra of compound **2.119** which was isolated as a light yellow oil in 84% yield. Verification of the identity of the desired compound was

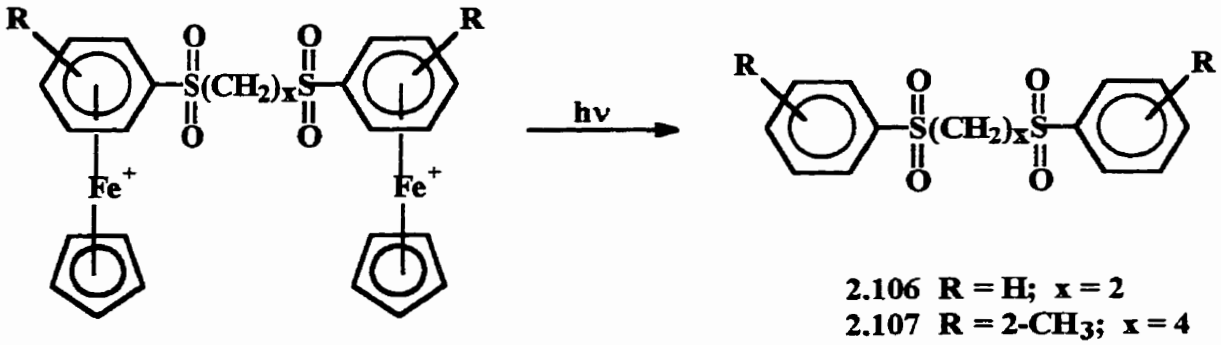

2.106 R = H; x = 2
2.107 R = 2-CH_3; x = 4
2.108 R = 3-CH_3; x = 2
2.109 R = 3-CH_3; x = 4
2.110 R = 3-CH_3; x = 6
2.111 R = 4-CH_3; x = 2
2.112 R = 4-CH_3; x = 6
2.113 R = 2-Cl; x = 6
2.114 R = 3-Cl; x = 4
2.115 R = 4-Cl; x = 4
2.116 R = 4-Cl; x = 8
2.117 R = 2,6-CH_3; x = 2

Scheme 2.10

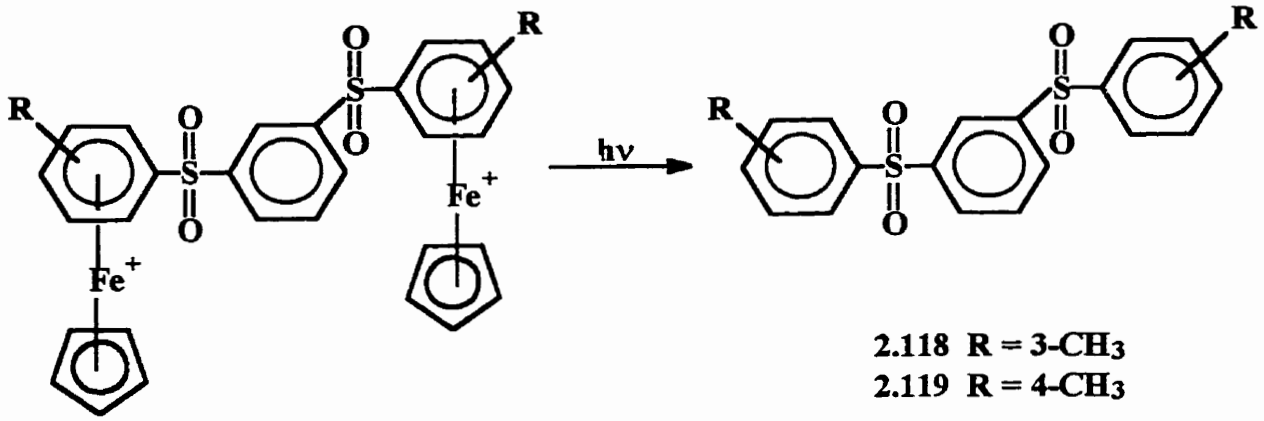

Scheme 2.11

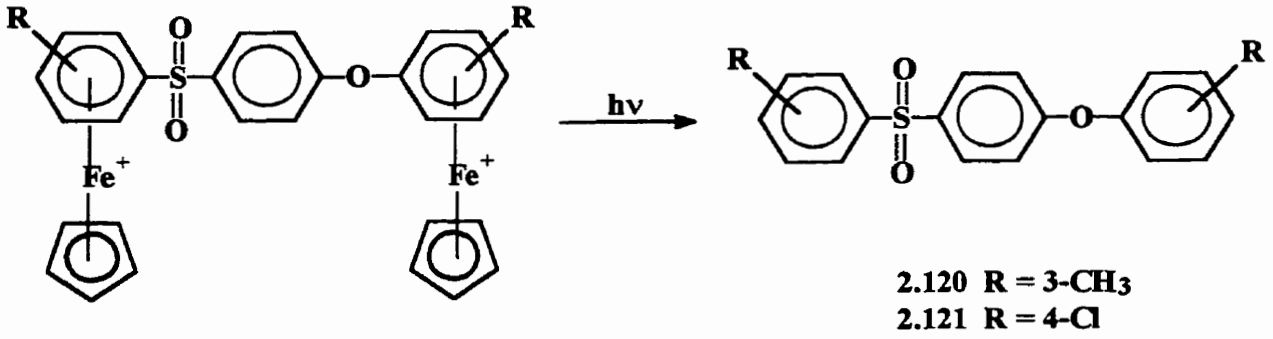

Scheme 2.12

supported by the absence of a cyclopentadienyl resonance in the range of 5.00-5.50 ppm and the appearance of the expected coupling pattern for the molecular structure of interest. The molecular structure of complex **2.119** has been labeled in Figure 2.26 to aid in the discussion of the spectral pattern observed. The doublets at 7.27 and 7.80 ppm are representative of protons 1 and 2, respectively, with the resonance appearing furthest downfield attributed to those protons adjacent to the sulfonyl functionality. Protons 4 and 6 appear at 7.59 and 8.45 ppm as a triplet and singlet, respectively, as expected. The interesting feature of this spectral pattern is the appearance of a doublet at 8.03 ppm representative of protons 3 and 5. Figure 2.27 shows the ^{13}C NMR spectrum of complex **2.119** with five resonances appearing below the baseline in the range of 126.31-131.58 ppm indicative of the aromatic carbons. Additionally, a single peak at 21.58 ppm verifies the presence of the methyl substituent with the three small peaks above the baseline at 137.26, 143.65 and 144.98 ppm attributed to the quaternary carbons.

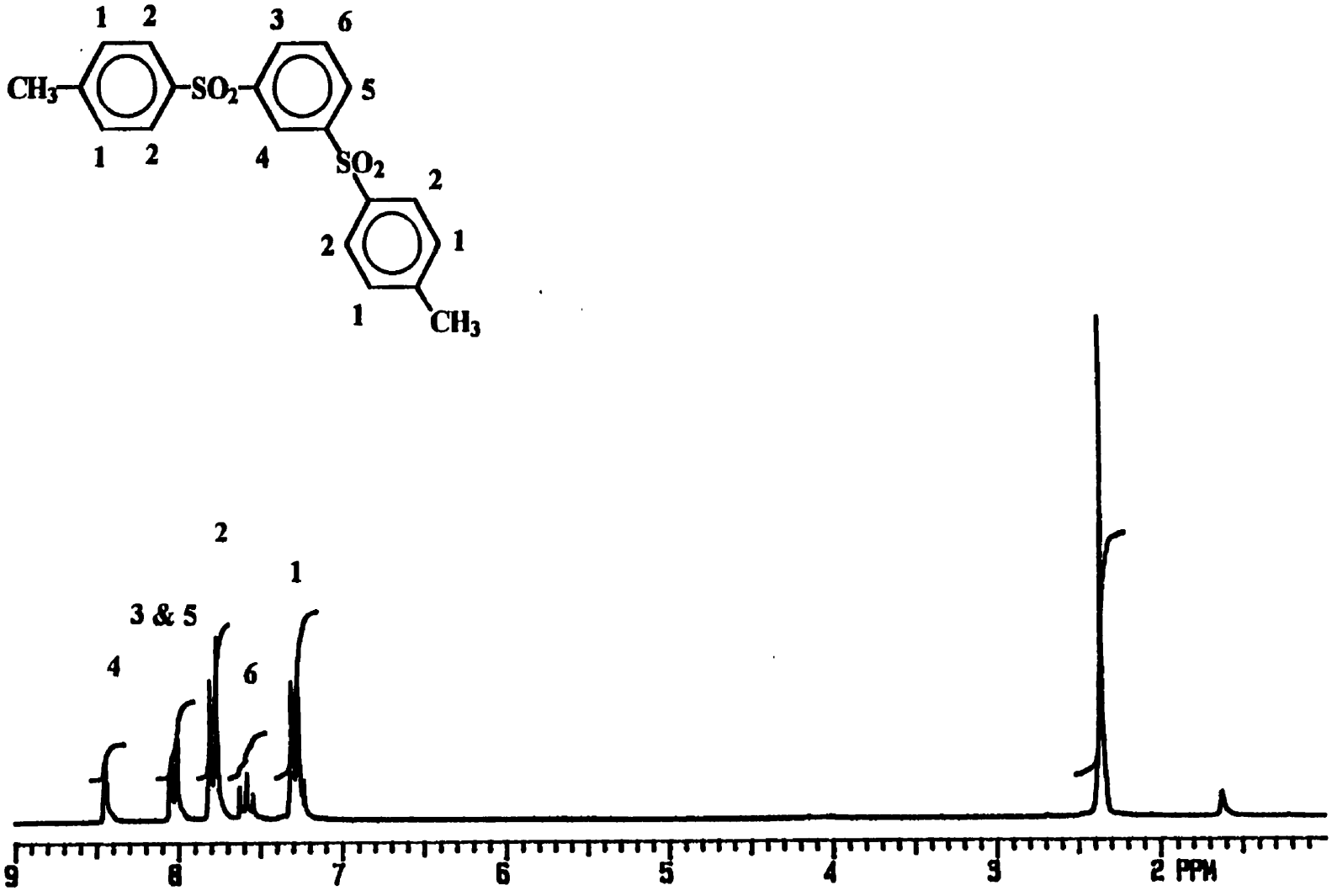

Figure 2.26: ^{1}H NMR spectrum of compound **2.119** in $CDCl_3$.

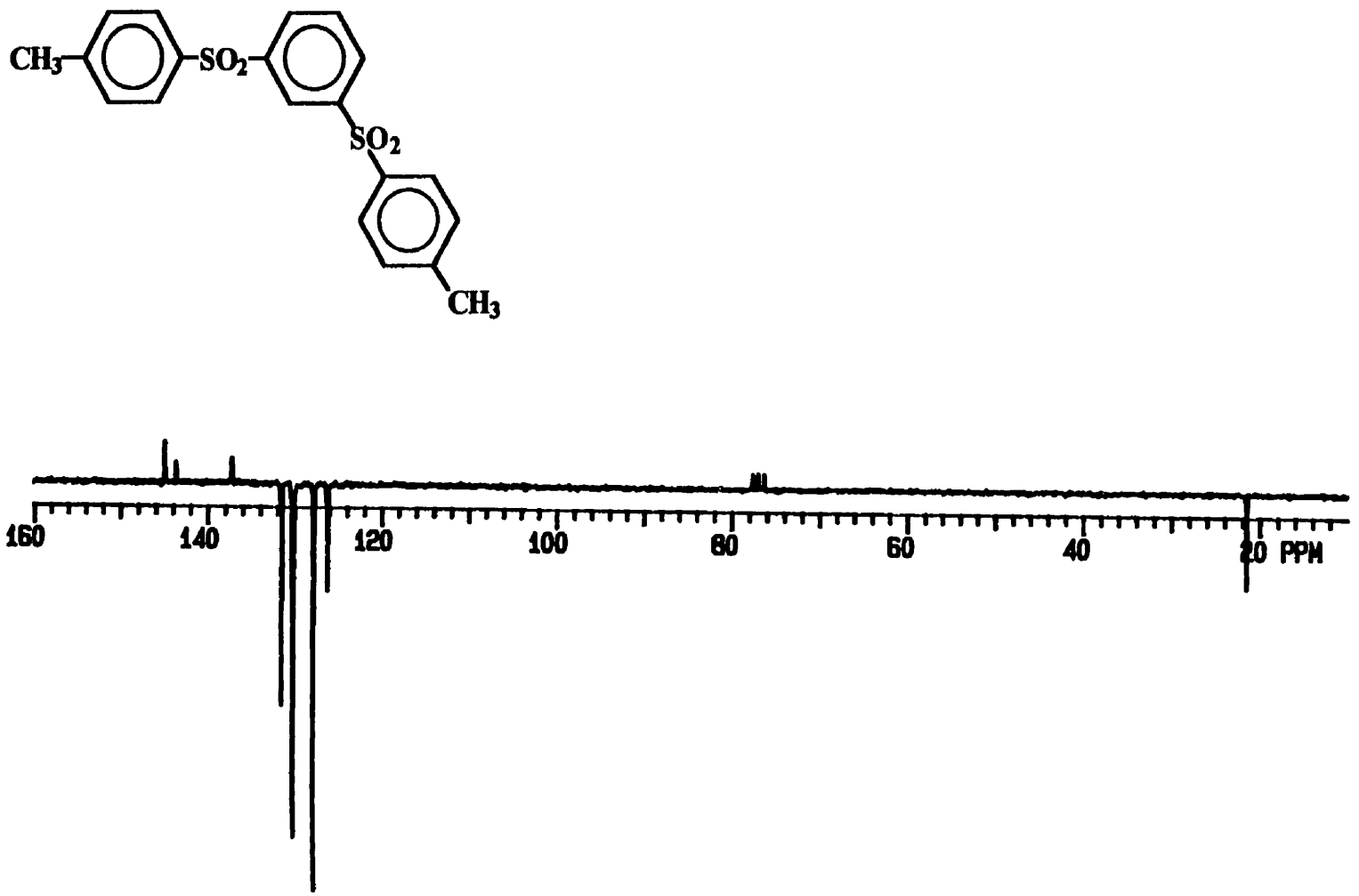

Figure 2.27: ^{13}C NMR spectrum of compound **2.119** in $CDCl_3$.

Table 2.20: ^{1}H NMR and IR Data, Yields and Melting Points of Aliphatic Bridged Sulfone Compounds **2.106-2.117**.

			δ ($CDCl_3$), ppm		
Complex	**Yield (%)**	**m.p. (°C)**	**Aromatic[a]**	**Others[a]**	**ν_{max} (cm^{-1}) SO_2**
2.106	92	173-174.5	7.53-7.71 (m, 6H) 7.84-7.88 (m, 4H)	3.43 (s, CH_2)	1150 1310
2.107	77	151-153	7.29-7.37 (m, 4H) 7.46-7.54 (m, 2H) 7.91 (d, 2H, J = 7.9)	1.77-1.85 (m, 4H, β-CH_2) 2.64 (s, 6H, CH_3) 3.05-3.08 (m, 4H, α-CH_2)	1150 1320
2.108	88	137-139	7.45-7.48 (m, 4H) 7.63-7.65 (m, 4H)	2.44 (s, 6H, CH_3) 3.40 (s, 4H, CH_2)	1140 1320
2.109	90	oil	7.23 (br.s., 4H) 7.45 (br.s., 4H)	1.60 (br.s., 4H, β-CH_2) 2.22 (s, 6H, CH_3) 2.84 (br.s., 4H, α-CH_2)	1155 1320
2.110	83	134-136.5	7.44 (br.s., 4H) 7.67 (br.s.,4H)	1.33-1.34 (m, 4H, γ-CH_2) 1.62-1.67 (m, 4H, β-CH_2) 2.43 (s, 6H, CH_3) 3.01 (t, 4H, J = 7.7, α-CH_2)	1150 1325
2.111	81	200-201.5	7.36 (d, 4H, J = 7.9) 7.72 (d, 4H, J = 8.1)	2.45 (s, 6H, CH_3) 3.38 (s, 4H, CH_2)	1150 1320
2.112	76	124-126.5	7.34 (d, 4H, J = 8.0) 7.74 (d, 4H, J = 8.2)	1.32-1.36 (m, 4H, γ-CH_2) 1.65-1.68 (m, 4H, β-CH_2) 2.43 (s, 6H, CH_3) 3.00 (t, 4H, J = 7.7, α-CH_2)	1155 1325
2.113	86	oil	7.49-7.62 (m, 4H) 7.74-7.86 (m, 4H)	1.30-1.49 (m, 4H, γ-CH_2) 1.59-1.69 (m, 4H, β-CH_2) 3.04 (t, 4H, J = 7.4, α-CH_2)	1155 1320

2.114	74	141-142.5	7.46-7.64 (m, 4H) 7.72-7.85 (m, 4H)	1.86 (m, 4H, β-CH_2) 3.08 (t, 4H, J = 7.3, α-CH_2)	1155 1330
2.115	80	183-184.5	7.53 (d, 4H, J = 8.7) 7.80 (d, 4H, J = 8.8)	1.81-1.88 (m, 4H, β-CH_2) 3.02-3.05 (m, 4H, α-CH_2)	1150 1310
2.116	77	oil	7.53 (d, 4H, J = 8.7) 7.82 (d, 4H, J = 8.7)	1.18-1.23 (m, 8H, δ & γ-CH_2) 1.55 (br.s., 4H, β-CH_2) 3.03 (t, 4H, J = 8.0, α-CH_2)	
2.117	70	231-232	7.16 (d, 4H, J = 7.4) 7.36 (d, 4H, J = 7.6)	2.63 (s, 12H, CH_3) 3.50 (s, 4H, CH_2)	1155 1315

[a] J values in Hertz.

Table 2.21: ^{13}C NMR and MS Data of Aliphatic Bridged Sulfone Compounds **2.106-2.117**.

δ ($CDCl_3$), ppm			
Complex	**m/z (M^+, %)**	**Aromatic**	**Others**
2.106	366 (100)	128.04, 129.69, 134.54, 138.00*	49.48 (CH_2)
2.107	366 (38.4)	126.65, 130.09, 132.80, 133.81, 136.83*, 137.85*	20.32 (CH_3) 21.33 (β-CH_2) 54.45 (α-CH_2)
2.108	338 (46)	125.16, 128.28, 129.50, 135.31, 137.84*, 140.14*	21.33 (CH_3) 49.53 (CH_2)
2.109	366 (51)	124.78, 127.92, 128.98, 134.42, 138.35*, 139.45*	21.05 (CH_3) 21.25 (β-CH_2) 55.07 (α-CH_2)
2.110	394 (26)	124.90, 128.04, 128.99, 134.33, 138.78*, 139.44*	21.16 (CH_3) 22.19 (γ-CH_2) 27.56 (β-CH_2) 55.76 (α-CH_2)
2.111	338 (42)	128.09, 130.30, 135.03*, 145.75*	21.71 (CH_3) 49.73 (CH_2)
2.112	394 (38)	127.88, 129.81, 136.01*, 144.59 *	21.50 (CH_3) 22.34 (γ-CH_2) 27.63 (β-CH_2) 55.93 (α-CH_2)
2.113	435 (12) 437 (7) 439 (1)	126.06, 127.97, 130.62, 133.84, 135.48*, 140.73*	22.17 (γ-CH_2) 27.58 (β-CH_2) 55.81 (α-CH_2)
2.114	407 (18) 409 (12) 411 (2)	126.11, 128.09, 130.74, 134.11, 135.73*, 140.53*	21.39 (β-CH_2) 55.34 (α-CH_2)
2.115	407 (21) 409 (14) 411 (2)	129.49, 129.76, 137.26*, 140.78*	21.48 (β-CH_2) 55.44 (α-CH_2)
2.116		129.55, 129.64, 137.66*, 140.46*	22.52 (δ-CH_2) 28.06 (γ-CH_2) 28.62 (β-CH_2) 56.57 (α-CH_2)
2.117	366 (24)	131.87, 133.42, 134.96*, 140.78*	22.93 (CH_3) 48.31 (CH_2)

* Quaternary carbons.

Table 2.22: ^{1}H NMR and IR Data, Yields and Melting Points of Aromatic Bridged Sulfone Compounds **2.118-2.119**.

			δ ($CDCl_3$), ppm		
Complex	**Yield (%)**	**m.p. (°C)**	**Aromatic[a]**	**Others[a]**	**ν_{max} (cm^{-1}) SO_2**
2.118	78	oil	7.37-7.40 (m, 4H) 7.62 (t, 1H, J = 7.9) 7.72 (br.s., 4H) 8.06 (d, 1H, J = 7.9) 8.07 (d, 1H, J = 7.9) 8.48 (s, 1H)	2.39 (s, 6H, CH_3)	1155 1335
2.119	84	oil	7.27 (d, 4H, J = 8.1) 7.59 (t, 1H, J = 7.9) 7.80 (d, 4H, J = 8.1) 8.03 (d, 1H, J = 7.9) 8.04 (d, 1H, J = 7.9) 8.45 (s, 1H)	2.38 (s, 6H, CH_3)	1160 1330

[a] J values in Hertz.

Table 2.23: ^{13}C NMR and MS Data of Aromatic Bridged Sulfone Compounds **2.118-2.119**.

		δ ($CDCl_3$), ppm	
Complex	**m/z (M^+, %)**	**Aromatic**	**Others**
2.118	386 (100)	125.56, 127.16, 128.63, 129.95, 131.04, 132.38, 135.22, 140.48*, 140.62*, 144.03*	21.83 (CH_3)
2.119	386 (100)	126.31, 127.85, 130.16, 130.44, 131.58, 137.26*, 143.65*, 144.98*	21.58 (CH_3)

* Quaternary carbons.

Table 2.24: ^{1}H NMR and IR Data, Yields and Melting Points of Mixed Ether/Sulfone Bridged Compounds **2.120-2.121**.

			δ ($CDCl_3$), ppm		
Complex	**Yield (%)**	**m.p. (°C)**	**Aromatic[a]**	**Others[a]**	**ν_{max} (cm^{-1}) SO_2**
2.120	80	oil	6.83 (br.s., 2H) 6.96-7.02 (m, 3H) 7.20-7.37 (m, 3H) 7.72 (br.s., 2H) 7.85 (d, 2H, J = 8.9)	2.32 (s, 3H, CH_3) 2.38 (s, 3H, CH_3)	1160 1335
2.121	94	oil	6.95 (d, 2H, J = 6.9) 7.00 (d, 2H, J = 7.0) 7.33 (d, 2H, J = 8.8) 7.45 (d, 2H, J = 8.5) 7.84 (d, 2H, J = 8.5) 7.85 (d, 2H, J = 8.5)		1160 1335

[a] J values in Hertz.

Table 2.25: ^{13}C NMR and MS Data of Mixed Ether/Sulfone Bridged Compounds **2.120-2.121**.

		δ ($CDCl_3$), ppm	
Complex	**m/z (M^+, %)**	**Aromatic**	**Others**
2.120	338 (100)	117.27, 117.56, 120.92, 124.56, 125.80, 127.67, 129.06, 129.80, 133.76, 134.93*, 139.45*, 140.43*, 141.81*, 154.79*, 162.10*	21.29 (CH_3)
2.121	379 (23) 381 (15) 383 (3)	117.84, 121.64, 128.32 *, 128.93, 129.60, 130.03, 130.25, 135.05*, 140.00*, 140.42*, 153,42*, 161.84*	

* Quaternary carbons

2.2.3 Synthesis of Diaryl Alkyl and Diaryl Aryl Nitrogen Containing Complexes

2.2.3.1 Preparation of Bis(cyclopentadienyliron) Arene Complexes with Aliphatic Amine Bridges

In an attempt to expand the versatility of our synthetic strategy, the use of diamines as nucleophiles in the search for bis(cyclopentadienyliron) arene complexes with amine bridges was examined. Previous investigations in the synthesis of complexes with certain amine functionalities using ligand exchange techniques resulted in the preparation of the desired complexes in very low yields.[29] A case in point was the isolation of η^6-diphenylamine-η^5-cyclopentadienyliron hexafluorophosphate in only 6% yield.[29] Interestingly, reactions of aromatic amines with η^6-(arene)-η^5-cyclopentadienyliron complexes proceeded to give the diphenylamine only if nitroarene complexes were used as a starting materials, as opposed to the chloroarene complexes.[58, 65] Nucleophilic substitution has also been employed in the synthesis of a number of complexes with amine groups, including heterocyclic complexes.[58, 60, 65]

In the present study, the reaction of the chloroarenes **2.1** and **2.6** with 1,6-hexanediamine, **2.122**, in a 2:1 molar ratio in the presence of K_2CO_3 in THF was investigated and resulted in the formation of the desired diiron species, **2.123** and **1.124**, in 28 and 17% yield, respectively (Scheme 2.13). These results reflected similar behavior observed by Sutherland and coworkers in the nucleophilic aromatic substitution reactions

of ethylenediamine with (chlorobenzene)- or isomeric (chlorotoluene)-cyclopentadienyliron complexes in which long reaction times resulted in poor yields and impure products.[213] On the other hand, adding an excess of the diamine, **1.122**, to the 1,4-dichloroarene complex, **2.6**, in the presence of glacial acetic acid led to double nucleophilic substitution as shown in Scheme 2.13. In an earlier study, it was proposed that under basic experimental conditions, the monosubstituted product with the diamine would deprotonate to give the zwitterion-cyclohexadienyl complex, as illustrated in Figure 2.28.[214] The zwitterion is electron rich and prevents further substitution of the second chlorine group. The addition of glacial acetic acid prevented the deprotonation, allowing for the second substitution to occur.

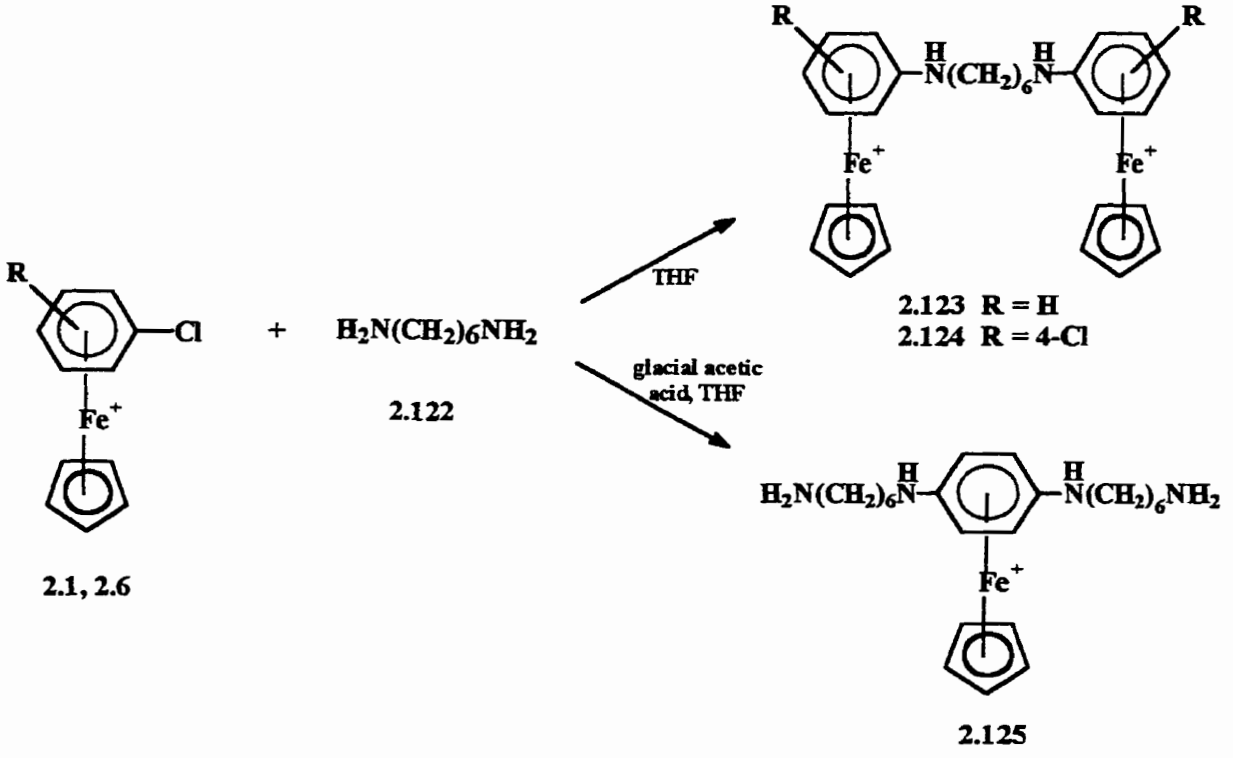

Scheme 2.13

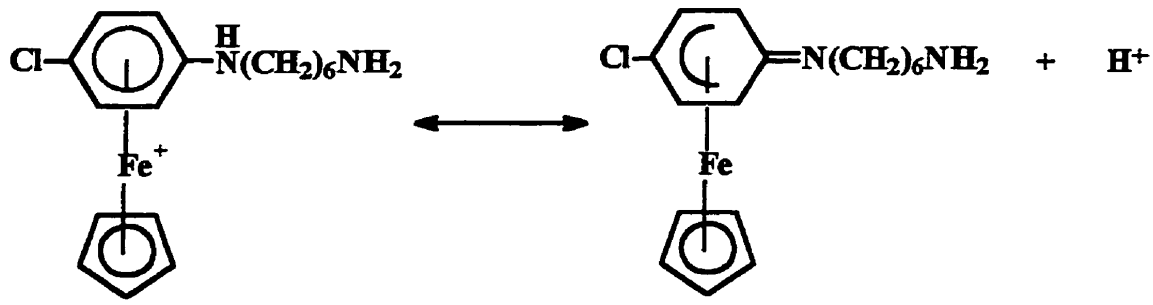

Figure 2.28: Formation of a zwitterion-cyclohexadienyl complex

As a result of the low yields obtained upon the nucleophilic aromatic substitution reaction of (chloroarene)cyclopentadienyliron complexes with diamine nucleophiles, nitroarene complexes, **2.126-2.131**, were investigated as starting materials since the nitro group is a better leaving group than chlorine. A wide variety of η^6-nitroarene-η^5-cyclopentadienyliron complexes have been prepared due to their potential use in the synthesis of compounds with biological applications or possible use in materials science.[57, 177, 214] The synthesis of a variety of starting nitroarene complexes has been thoroughly investigated and established as a two-step process.[215, 216] The general reaction of the initial step is illustrated in Figure 2.29 and involves the preparation of the desired alkylaniline complex via the ligand exchange of alkylanilines with ferrocene in the presence of $AlCl_3$ and Al and using decalin as a solvent. This reaction mixture is stirred at 160°C for 5 hours and the desired complexes isolated as their hexafluorophosphate salts in good yield. The subsequent oxidation of the alkylaniline complexes in the presence of H_2O_2 in CF_3COOH allowed for the preparation of the corresponding alkylnitrobenzene complexes according to Figure 2.30.[215]

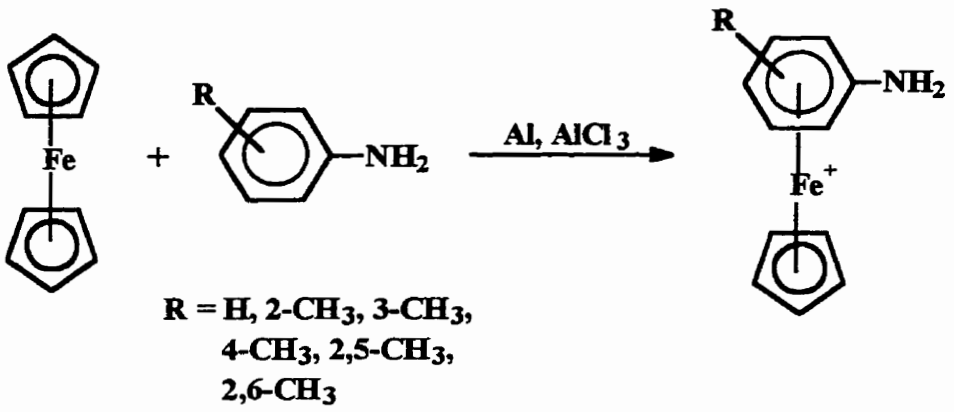

Figure 2.29: Preparation of alkylaniline $CpFe^+$ complexes via the ligand exchange reaction

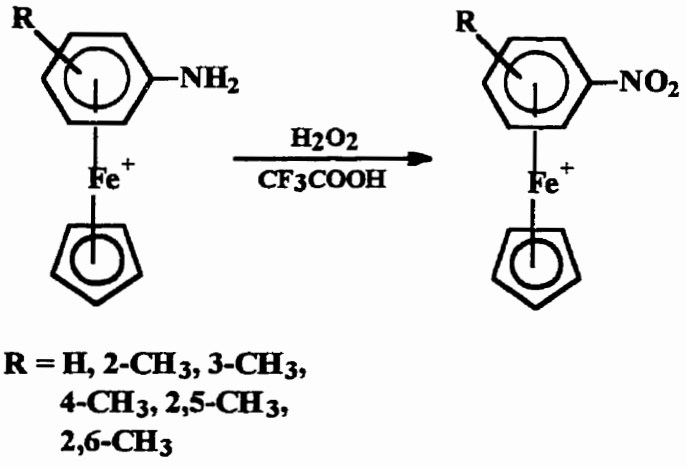

Figure 2.30: Preparation of η^6-nitro-η^5-cyclopentadienyliron complexes via oxidation of the corresponding aniline complex in the presence of H_2O_2 and trifluoroacetic acid

Scheme 2.14 outlines the synthetic methodology followed in the preparation of diiron complexes with aliphatic diamine linkages. Following similar conditions to those established in the synthesis of bimetallic cyclopentadienyliron complexes with etheric and thioetheric linkages, the appropriate η^6-nitroarene-η^5-cyclopentadienyliron hexafluorophosphate complexes were combined with the desired aliphatic diamine in a 2:1 molar ratio in the presence of K_2CO_3 in a THF/DMF solvent mixture and stirred at 60°C under a nitrogen atmosphere. Due to the enhanced reactivity of the nitroarene complexes, a shorter reaction time of 3-5 hours was employed which minimized decomposition of the starting material and the products and resulted in a dramatic increase in yield.

In the course of our investigations, nucleophilic substitution reactions of three aliphatic diamines with different methylene chains were examined. Typically, the nitroarene complexes reacted with the diamines to produce the desired complexes as expected. It is important to note that increasing the number of methylene groups in the chain from 2 to 6 resulted in an increase in the yield of the reaction (Table 2.28). However, some steric problems were experienced in the use of the 2,6-dimethylnitrobenzene complex as a starting material. The yields of these reactions dropped dramatically due to the presence of these two methyl groups ortho to the nitro group.

The yields and spectroscopic information were collected and are presented in Tables 2.26 and 2.27. Figures 2.31-2.33 show the ^1H and ^{13}C NMR spectra of complex **2.142**. Due to the symmetrical nature of the complex, the ^1H NMR spectrum is quite simple and success is established by the presence of the cyclopentadienyl resonance at 4.85 ppm. Further evidence of the synthesis of complex **2.142** is the appearance of the

doublets at 5.85 and 6.10 ppm representative of the complexed aromatic protons. One very distinctive feature of the ^{1}H NMR spectrum which indicates the presence of the amine linkage is the broad singlet at 5.94 ppm. The disappearance of this resonance upon the addition of D_2O to the sample, as shown in Figure 2.32, verifies its identity as the proton associated to the amine functionality. The expected peaks in the ^{13}C NMR spectrum further support the successful preparation of complex **2.142**.

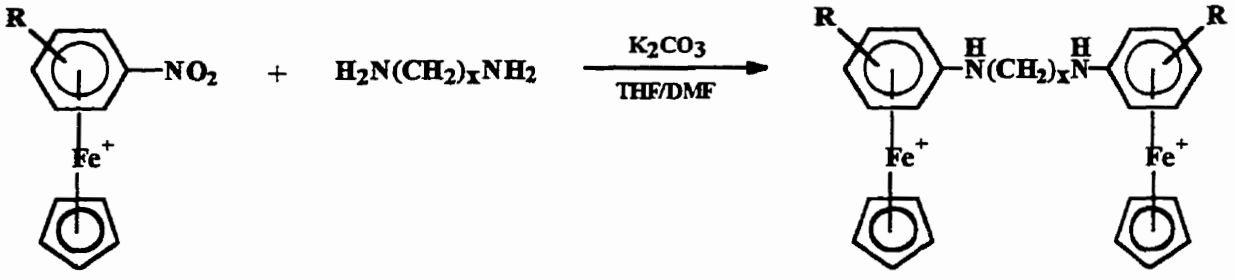

2.126 R = H
2.127 R = 2-CH_3
2.128 R = 3-CH_3
2.129 R = 4-CH_3
2.130 R = 2,5-CH_3
2.131 R = 2,6-CH_3

2.132 x = 2
2.133 x = 4
2.122 x = 6

2.134 R = H; x = 2
2.135 R = H; x = 4
2.123 R = H; x = 6
2.136 R = 2-CH_3; x = 2
2.137 R = 2-CH_3; x = 4
2.138 R = 2-CH_3; x = 6
2.139 R = 3-CH_3; x = 2
2.140 R = 3-CH_3; x = 4
2.141 R = 3-CH_3; x = 6
2.142 R = 4-CH_3; x = 2
2.143 R = 4-CH_3; x = 6
2.144 R = 2,5-CH_3; x = 6
2.145 R = 2,6-CH_3; x = 2
2.146 R = 2,6-CH_3; x = 4
2.147 R = 2,6-CH_3; x = 6

Scheme 2.14

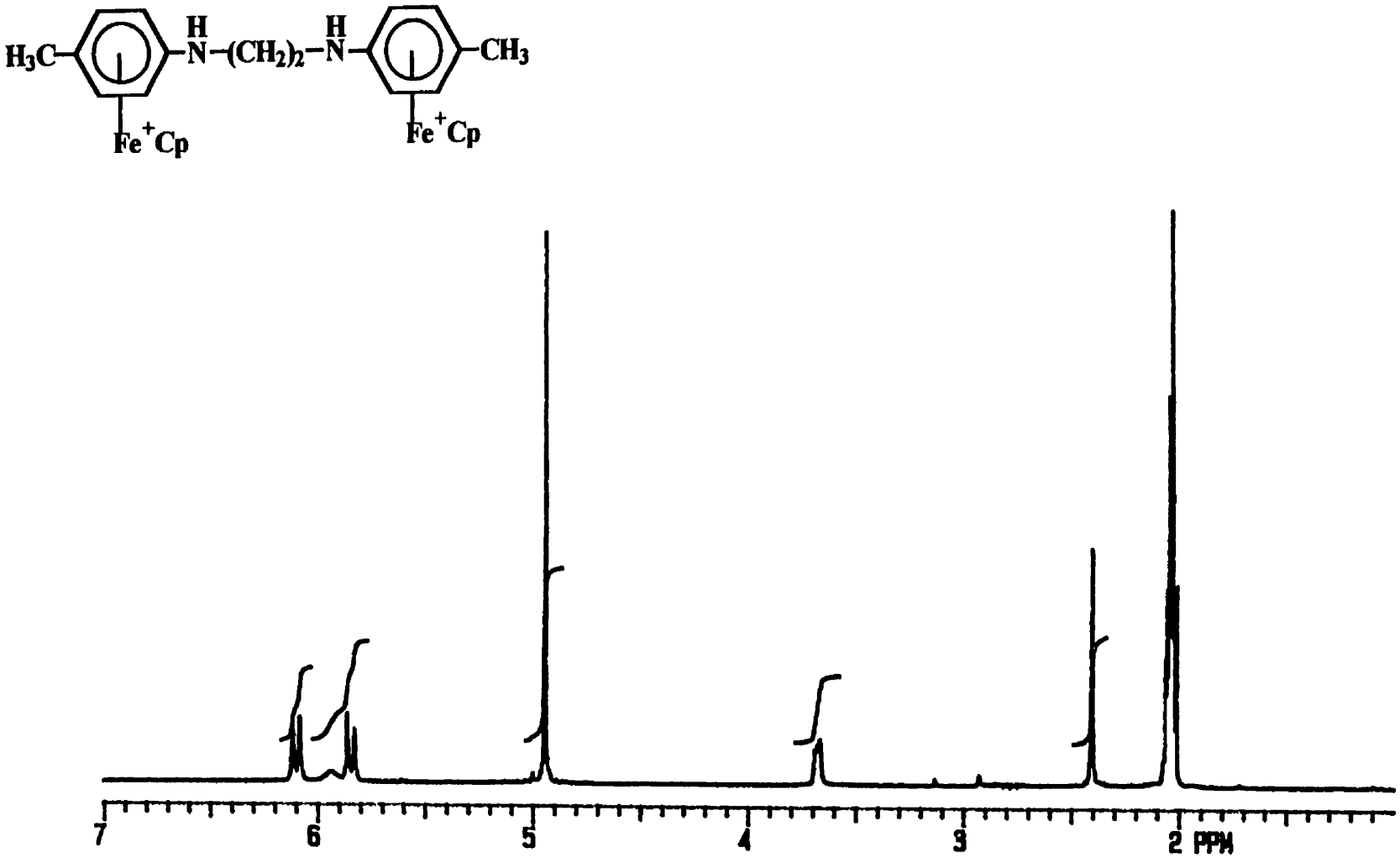

Figure 2.31: ^{1}H NMR spectrum of complex **2.142** in acetone-d_6.

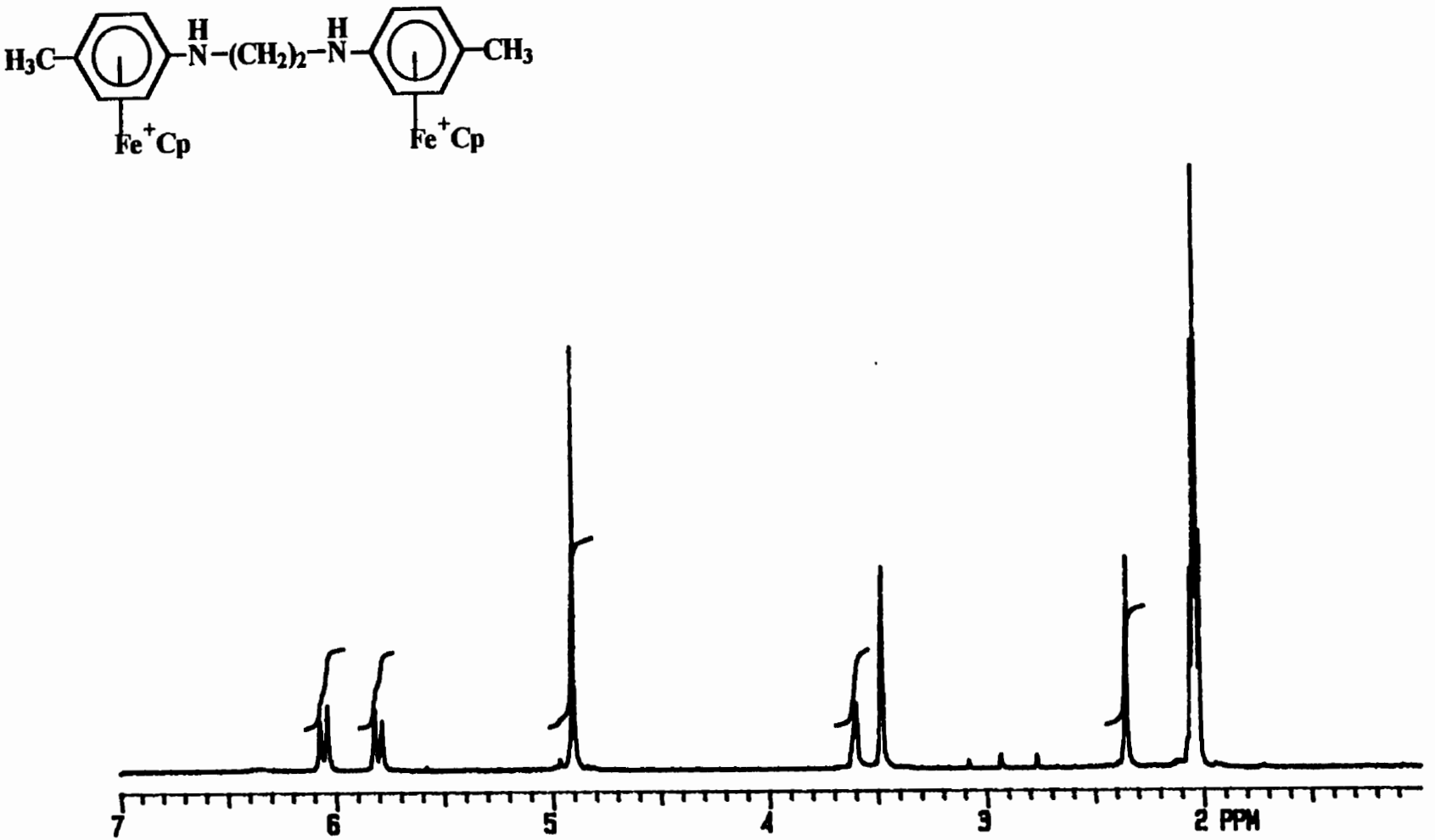

Figure 2.32: ^{1}H NMR spectrum of complex **2.142** in acetone-d_6 and D_2O.

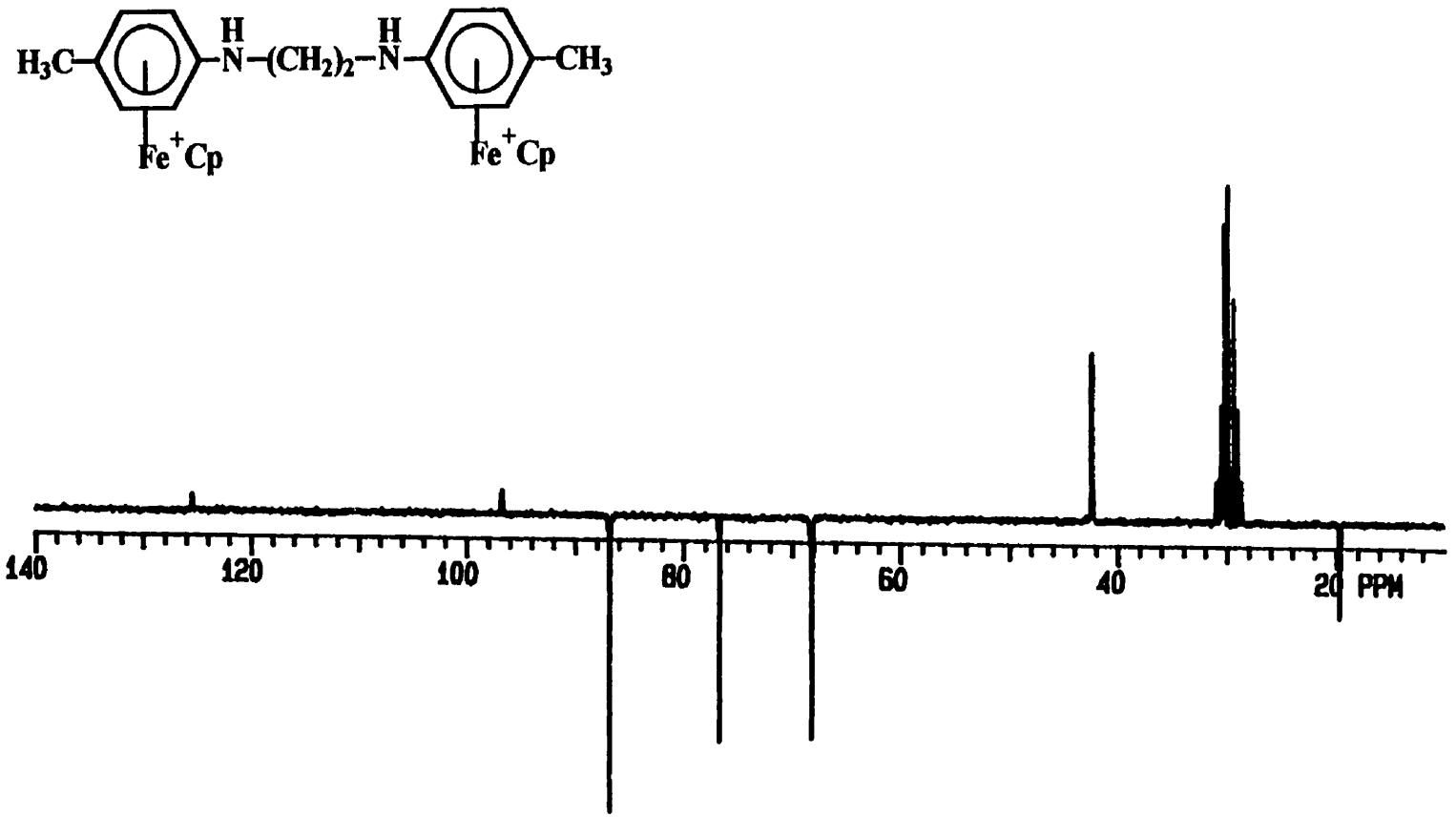

Figure 2.33: ^{13}C NMR spectrum of complex **2.142** in acetone-d_6.

Table 2.26: ^{1}H NMR Data of Diiron Amine Complexes **2.134-2.147**.

δ (acetone-d_6), ppm			
Complex	**Cp (s, 10H)**	**Complexed Aromatic[a]**	**Others[a]**
2.134	5.02	5.92 (d, 4H, J = 6.6) 6.07-6.10 (m, 4H) 6.18 (t, 2H, J = 6.4)	3.74 (d, 4H, J = 5.3, α-CH_2) 6.05 (br.s., 2H, NH)
2.135	4.98	5.85 (d, 4H, J = 6.4) 6.03 (t, 4H, J = 5.8) 6.16 (t, 2H, J = 5.5)	1.89 (m, 4H, β-CH_2) 3.41 (m, 4H, α-CH_2) 5.98 (br.s., 2H, NH)
2.123	4.96	5.81 (d, 4H, J = 6.6) 5.91-6.09 (m, 4H) 6.13-6.17 (m, 2H)	1.51 (m, 4H, γ-CH_2) 1.74 (m, 4H, β-CH_2) 3.31 (m, 4H, α-CH_2) 5.92 (br.s., 2H, NH)
2.136[b]	4.89 4.92	5.93-6.04 (m, 4H) 6.11-6.21 (m, 4H)	2.41 (s, 3H, CH_3) 2.42 (s, 3H, CH_3) 3.85 (m, 4H, CH_2) 5.70 (br.s., 2H, NH)
2.137	4.89	5.92 (t, 4H, J = 6.5) 6.10 (d, 2H, J = 6.5) 6.15 (d, 2H, J = 5.9)	1.99 (m, 4H, β-CH_2) 2.40 (s, 6H, CH_3) 3.49 (m, 4H, α-CH_2) 5.62 (br.s., 2H, NH)
2.138	4.88	5.84-5.94 (m, 4H) 6.06-6.16 (m, 4H)	1.56 (m, 4H, γ-CH_2) 1.80 (m, 4H, β-CH_2) 2.40 (s, 6H, CH_3) 3.41 (m, 4H, α-CH_2) 5.56 (br.s., 2H, NH)
2.139	4.93	5.62-6.11 (m, 8H)	2.47 (s, 6H, CH_3) 3.69 (m, 4H, CH_2) 5.95 (br.s., 2H, NH)[c]
2.140	4.90	5.73-5.81 (m, 2H) 5.94 (d, 2H, J = 5.9) 6.06 (t, 2H, J = 6.3)	1.87 (quintet, 4H, J = 6.8, β-CH_2) 2.45 (s, 6H, CH_3) 5.84 (br.s., 2H, NH)[c]
2.141	4.90	5.73-5.83 (m, 4H) 5.94 (d, 2H, J = 5.9) 6.05 (t, 2H, J = 6.1)	1.53 (m, 4H, γ-CH_2) 1.74 (m, 4H, β-CH_2) 2.45 (s, 6H, CH_3) 3.28-3.37 (m, 2H, α-CH_2) 5.83 (br.s., 2H, NH)
2.142	4.95	5.85 (d, 4H, J = 6.9) 6.10 (d, 4H, J = 6.7)	2.41 (s, 6H,CH_3) 3.66-3.69 (m, 4H, CH_2) 5.94 (br.s., 2H, NH)

2.143	4.91	5.75 (d, 4H, J = 6.9) 6.05 (d, 4H, J = 6.9)	1.50-1.56 (m, 4H, γ-CH_2) 1.70-1.79 (m, 4H, β-CH_2) 2.40 (s, 6H, CH_3) 3.61 (t, 4H, J = 7.0, α-CH_2) 5.85 (br.s., 2H, NH)
2.144[d]	4.82	5.84-5.88 (m, 4H) 6.07 (d, 2H, J = 6.0)	1.55 (m, 4H, γ-CH_2) 1.82 (m, 4H, β-CH_2) 2.36 (s, 6H, CH_3) 2.46 (s, 6H, CH_3) 3.41 (m, 4H, α-CH_2) 5.45 (br.s., 2H, NH)
2.145[d]	4.90	5.96 (t, 2H, J = 6.2) 6.20 (d, 4H, J = 6.0)	2.57 (s, 12H, CH_3) 3.66 (s, 4H, CH_2)
2.146[d]	4.87	5.91 (t, 2H, J = 6.0) 6.14 (d, 4H, J = 6.0)	1.74 (quintet, 4H, J = 7.3, β-CH_2) 2.55 (s, 12H, CH_3) 3.41 (t, 4H, J = 6.5, α-CH_2)
2.147[d]	4.88	5.90 (t, 2H, J = 5.9) 6.13 (d, 4H, J = 6.0)	1.42 (m, 4H, γ-CH_2) 1.65 (m, 4H, β-CH_2) 2.56 (s, 12H, CH_3) 3.37 (t, 4H, J = 7.0, α-CH_2)

[a] J values in Hertz. [b] Diastereoisomers present. [c] NH overlaps with aromatic. [d] NH unobserved.

Table 2.27: ^{13}C NMR and IR Data and Yields of Aliphatic Bridged Amine

Complexes **2.134-2.147**

δ (acetone-d_6), ppm					
Complex	**Yield (%)**	**Cp (10H)**	**Complexed Aromatic**	**Others**	**IR ν_{NH}, cm^{-1}**
2.134	48	76.26	68.99, 81.57, 86.61, 126.53*	42.36 (CH_2)	3435
2.135	62	76.17	68.51, 81.19, 86.62, 127.37*	26.77 (β-CH_2), 43.28 (α-CH_2)	3420
2.123	78	75.34	67.54, 80.34, 85.77, 126.55*	26.32 (γ-CH_2), 28.39 (β-CH_2), 42.61 (α-CH_2)	3405
2.136[a]	44	76.75	66.71, 66.87, 80.82, 83.01*, 85.27, 88.99, 126.13*	17.75 (CH_3), 17.80 (CH_3), 42.33 (CH_2) 42.53 (CH_2)	3440
2.137	63	76.46	66.16, 80.26, 83.27*, 85.07, 88.71, 126.03*	17.64 (CH_3), 26.66 (β-CH_2), 43.37 (α-CH_2)	3435
2.138	70	76.18	65.63, 79.90, 82.85*, 84.78, 88.47, 125.96*	17.54 (CH_3), 26.98 (γ-CH_2), 28.91 (β-CH_2), 43.31 (α-CH_2)	3440
2.139	46	76.60	67.60, 70.36, 82.03, 85.89, 102.09*, 126.18*	20.65 (CH_3), 42.46 (CH_2)	3420
2.140	89	76.33	66.90, 69.69, 81.48, 85.65, 101.84*, 126.65*	20.57 (CH_3), 26.62 (β-CH_2), 43.15 (α-CH_2)	3420
2.141	43	76.21	66.72, 69.52, 81.32, 85.55, 101.74*, 126.74*	20.52 (CH_3), 26.93 (γ-CH_2), 29.05 (β-CH_2), 43.34 (α-CH_2)	3425
2.142	30	76.73	68.22, 86.85, 96.77*, 125.51*	19.65 (CH_3), 42.20 (CH_2)	3415
2.143	71	76.65	67.71, 86.84, 96.39*, 126.37*	19.66 (CH_3), 27.17 (γ-CH_2), 29.26 (β-CH_2), 43.54 (α-CH_2)	3420

2.144	44	76.90	67.71, 80.62, 81.74*, 87.99, 100.71*, 125.74*	17.35 (CH_3), 20.51 (CH_3), 27.35 (γ-CH_2), 29.37 (β-CH_2), 43.72 (α-CH_2)	3438
2.145	17	77.77	82.78, 88.66, 97.27*, 107.78*	19.70 (CH_3), 48.45 (CH_2)	3415
2.146	22	77.97	82.59, 88.99, 89.14*, 126.09*	18.07 (CH_3), 29.29 (β-CH_2), 48.34 (α-CH_2)	3430
2.147	28	77.53	82.07, 88.58, 88.48*, 125.84*	19.76 (CH_3), 27.22 (γ-CH_2), 31.61 (β-CH_2), 48.18 (α-CH_2)	3440

[a] Diastereomers present. * Quaternary carbons.

2.2.3.2 Preparation of Bis(cyclopentadienyliron) Arene Complexes with Aromatic Amine Bridges

Following the investigation with aliphatic amines, the displacement of the nitro group using aromatic diamines as nucleophiles was examined. Scheme 2.15 shows examples of the reactions of 1,3- and 1,4-phenylenediamines, **2.148** and **2.149**, with nitroarene complexes, **2.126, 2.128** and **2.129**. Although these reactions proceeded to produce the diiron complexes with aromatic diamine bridges, the reaction with 1,2-phenylenediamine failed to give the desired product but rather yielded a mixture of products.

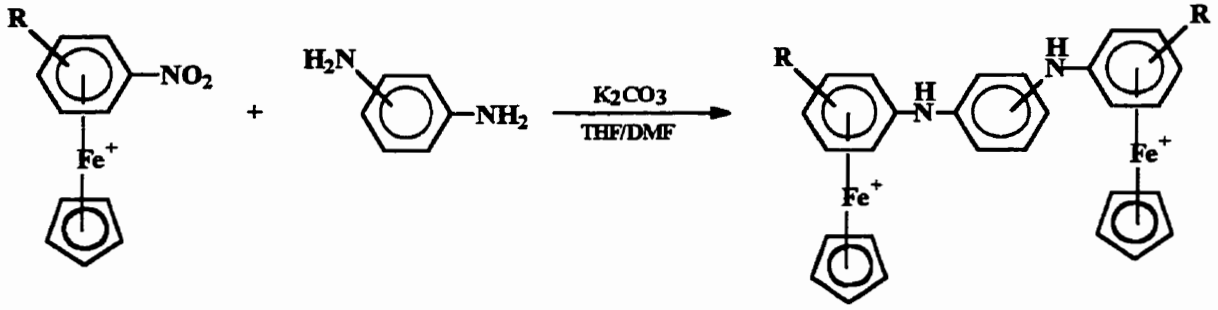

2.126, 2.128 & 2.129

2.148 1,3
2.149 1,4

2.150 R = H; 1,3
2.151 R = H; 1,4
2.152 R = 3-CH_3; 1,3
2.153 R = 3-CH_3; 1,4
2.154 R = 4-CH_3; 1,4

Scheme 2.15

^{1}H and ^{13}C NMR spectroscopy and IR spectrophotometry were used to verify the identity of the complexes and the data are summarized in Tables 2.28 and 2.29. Figures 2.34 and 2.35 show the ^{1}H and ^{13}C NMR spectra, respectively, of complex **2.150** which represent spectral features typical of these complexes. The strong Cp singlet characteristic of bimetallic cyclopentadienyliron complexes appears at 5.06 ppm. It was mentioned previously that a significant spectral chemical shift separation is characteristically observed in the case of complexes composed of both complexed and uncomplexed aromatic protons. This is indeed a spectral feature evident with complexes **2.150-2.154**. In Figure 2.34, the complexed aromatic protons appear upfield at 6.14-6.36 ppm in comparison to the uncomplexed aromatic proton resonances appearing at 7.20-7.37 and 7.59 ppm. Integration techniques which identified the singlet at 8.11 ppm as representative of two protons in addition to the disappearance of this peak upon the addition of D_2O to the ^{1}H NMR identified this resonance as that of the amine functionality. The incorporation of the amine functionality into the molecular structure of complexes **2.150-2.154** was further supported by absorbances in the region of 3395-3420 cm^{-1} of the infrared spactra.

The ^{13}C NMR spectrum run as an Attached Proton Test (APT) verified the structure of complex **2.150** with the Cp, complexed and uncomplexed aromatic carbons with an odd number of protons all appearing below the baseline in the spectrum in the expected spectral regions. The Cp and complexed aromatic carbon resonances appeared between 72.00-88.00 ppm and the three uncomplexed aromatic resonances significantly further downfield at 116.19, 119.66 and 132.24 ppm. The two peaks appearing above the baseline at 112.30 and 141.44 ppm complete the expected resonances corresponding to complex **2.150** and are attributed to the quaternary carbon atoms of the complexed and

uncomplexed arene rings, respectively. With the exception of reactions in the presence of 1,2-phenylenediamine, the desired products were obtained in yields ranging from 54-66% as summarized in Table 2.29.

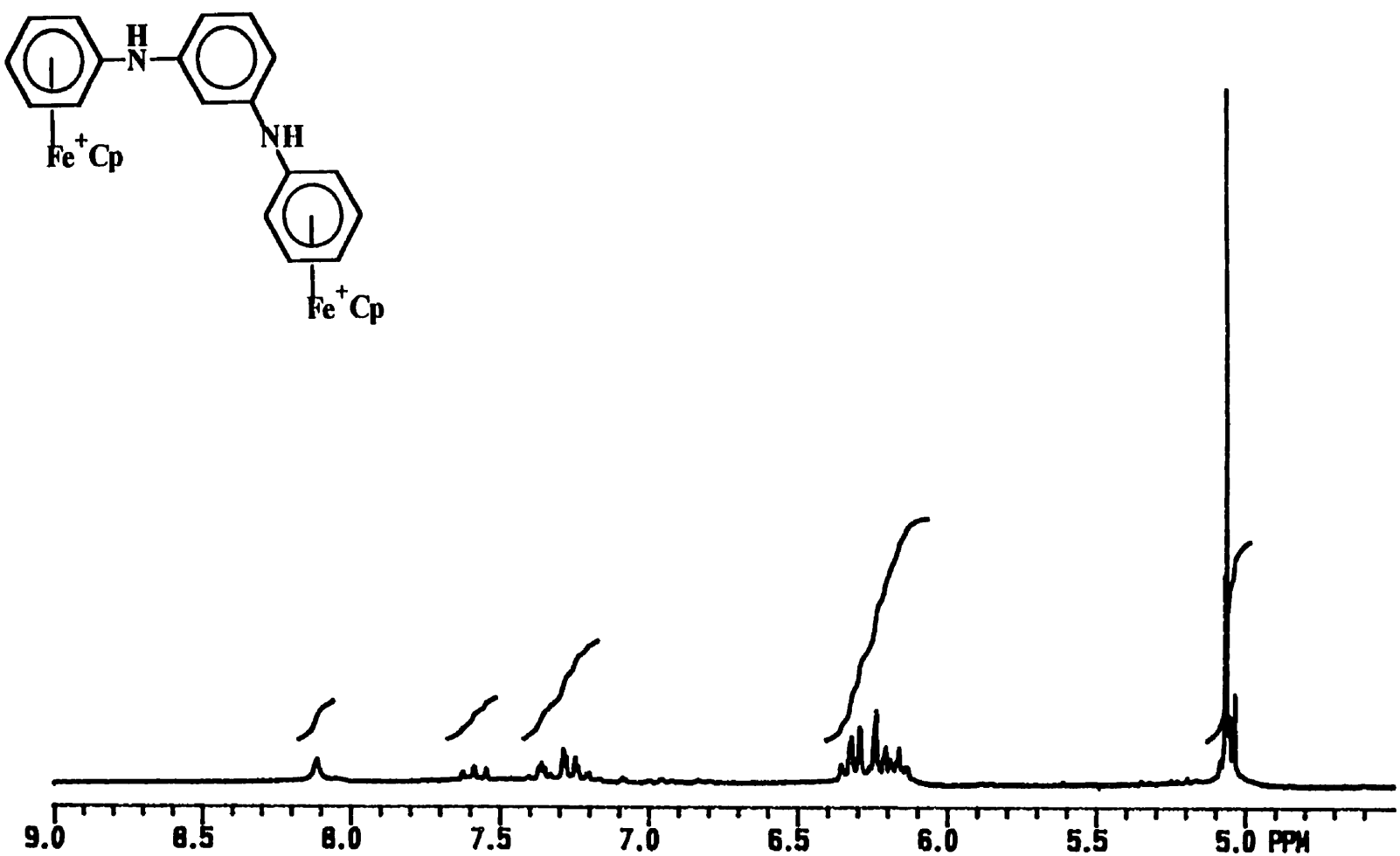

Figure 2.34: ^{1}H NMR spectrum of complex **2.150** in acetone-d_6.

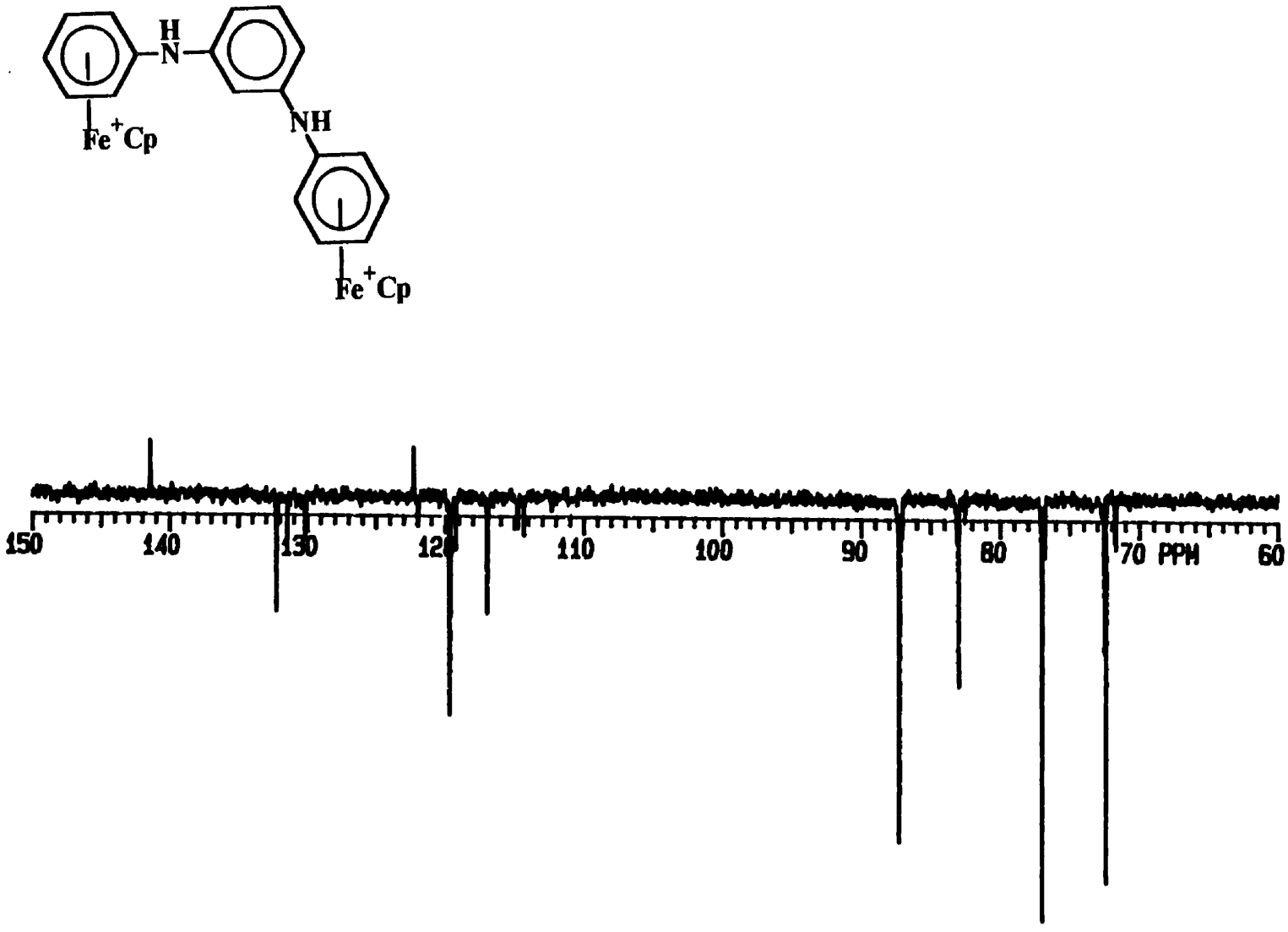

Figure 2.35: ^{13}C NMR spectrum of complex **2.150** in acetone-d_6.

Table 2.28: ^{1}H NMR Data of Aromatic Bridged Amine Complexes **2.150-2.154**.

δ (acetone-d_6), ppm				
Complex	**Cp (s, 10H)**	**Complexed Aromatic[a]**	**Aromatic[a]**	**Others[a]**
2.150	5.06	6.14-6.26 (m, 6H)	7.20-7.37 (m, 3H) 7.59 (t, 1H, J = 8.0)	8.11 (br.s., 2H, NH)
2.151	5.03	6.31-6.40 (m, 6H) 6.47-6.54 (m, 4H)	7.10 (d, 2H, J = 8.8) 7.67 (d, 2H, J = 8.8)	5.45 (br.s., 2H, NH)
2.152	5.01	6.07-6.28 (m, 8H)	7.33-7.34 (m, 2H) 7.58-7.64 (m, 2H)	2.52 (s, 6H, CH_3) 8.03 (br.s., 2H, NH)
2.153[b]	4.91	6.25 (d, 4H, J = 6.1) 6.31 (s, 2H) 6.42 (t, 2H, J = 6.1)	7.82 (d, 1H, J = 7.5) 7.90 (d, 1H, J = 7.5) 7.94 (d, H, J = 7.5) 8.06 (d, 1H, J = 7.5)	2.53 (s, 6H, CH_3)
2.154	4.95	6.26 (d, 4H, J = 6.9) 6.41 (d, 4H, J = 6.8)	7.82 (d, 1H, J= 6.7) 7.90 (d, 1H, J = 7.5) 7.93 (d, 1H, J = 7.4) 8.03 (d, 1H, J = 6.9)	2.52 (s, 6H, CH_3) 8.06 (br.s., 2H, NH)

[a] J values in Hertz. [b] NH unobserved.

Table 2.29: ^{13}C NMR and IR Data and Yields of Aromatic Bridged Amine Complexes **2.150-2.154**.

δ (acetone-d_6), ppm						
Complex	**Yield (%)**	**Cp (10H)**	**Complexed Aromatic**	**Uncomplexed Aromatic**	**Others**	**IR ν_{NH_2} cm^{-1}**
2.150	59	77.02	72.49, 83.06, 87.26, 122.30*	116.69, 119.66, 132.24, 141.44*		3420
2.151	62	77.75	79.28, 85.30, 87.34, 122.42*	116.26, 129.15*, 131.69, 151.19*		3400
2.152	54	77.34	70.84, 73.82, 83.46, 86.51, 96.93*, 107.97*	116.88, 119.48, 131.47, 132.18, 141.53*	20.83 (CH_3)	3395
2.153	61	78.18	80.50, 80.58, 88.03, 88.81, 103.65*, 121.03*	131.27, 132.23, 141.53*, 141.63*	20.54 (CH_3)	3410
2.154	66	78.22	78.75, 87.55, 101.52*, 107.81*	120.15*, 131.08, 132.22	19.80 (CH_3)	3415

[a] Quaternary carbons.

3.0 Kinetic and Thermodynamic Investigations of η^6-Arene-η^5-$CpFe^+$ Complexes

3.1 Introduction

Interest in the properties of novel organometallic species has prompted the investigation of several unique features of these complexes. It is the oxidation/reduction properties of numerous organometallic arene species which has led to interest in an improved understanding of the electron transfer reactions of these systems.[99, 103, 217-220] In particular, many of these species are noted for their ability or their potential to act as electron-reservoirs[1, 8, 221-225] and to exhibit mixed-valency[32, 223, 226-230] and conductivity.[231] As a result, the electrochemical behavior of redox systems of this type has been investigated with respect to a variety of potential applications.[232-238]

3.1.1 η^6-Arene-η^5-$CpFe^+$ Complexes

A variety of voltammetric methods have been exploited by inorganic, physical, and biological chemists for studies such as the examination of oxidation and reduction processes in various media, adsorption processes on surfaces, and electron-transfer mechanisms at chemically modified electrode surfaces. In particular, both polarographic and cyclic voltammetric investigations have been conducted in an attempt to gain a better understanding of the oxidation/reduction properties of η^6-arene-η^5-cyclopentadienyliron

systems.[25, 221, 232-234, 239-242] Preliminary studies suggested that the reduction of the 18-electron $CpFe^+$ complexes was achieved by two distinct 1-electron reduction steps. It has been established that, regardless of the complex of interest, the initial electron transfer results in the generation of the neutral and chemically reversible 19-electron complex. However, the electrochemical behavior of the highly reactive 20-electron complex formed by means of the subsequent electron transfer depends on the nature of the complex of interest and on the experimental conditions employed (Figure 3.1).[221, 233-234, 242] The half-wave potentials of a variety of (arene)$CpFe^+$ complexes bearing a substituent on the arene or cyclopentadienyl ring have been recorded in several solvents. Experiments in solvents such as DMF, DMF/THF (1:2), MeCN, H_2O, or H_2O/EtOH (1:1) demonstrated a definite solvent dependence on the corresponding half-wave potentials.[242-246]

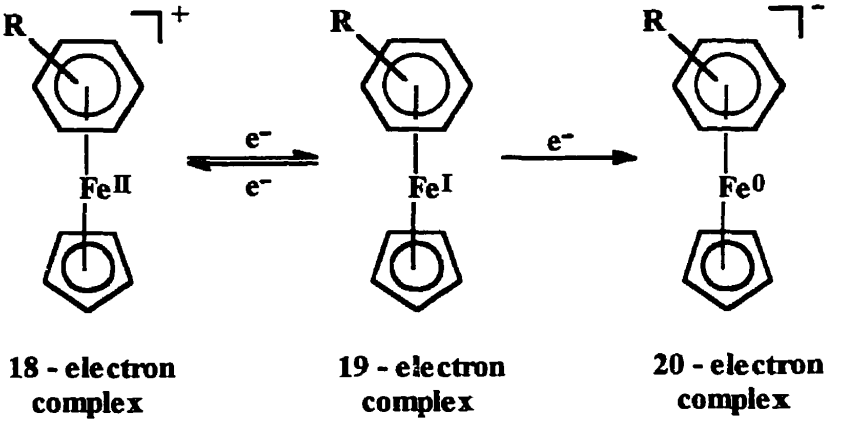

Figure 3.1: 18 - 19 - 20 electron complexes prepared by the electrochemical reduction of η^6-(arene)-η^5-(cyclopentadienyl)iron complexes

Specifically, the electrochemical behavior of complexes composed of arene or cyclopentadienyl ligands may be predicted on the basis of the structural aspects of these ligands. In two studies, the use identical reaction conditions demonstrated more negative half-wave potentials in compounds with electron-donating substituents on the benzene ring compared to compounds with electron-withdrawing substituents.[224, 242, 247] Studies involving (substituted arene)$CpFe^+$ and (arene)(substituted Cp)Fe^+ complexes have also shown a correlation between the $E_{1/2}$ potentials and Hammett's σ_p parameter.[242] Furthermore, the ability of the substituent's polar effect to influence both the magnitude of the reduction potential and the chemical reactivity of the complex was demonstrated in a study involving a wide range of monosubstituted and 1,2-disubstituted benzene cyclopentadienyliron complexes.[234] The reduction potentials of several complexed polycyclic arenes were compared with their corresponding hydrogenated counterparts and, in accordance with the previously observed trends, a decrease in reduction potentials was noted upon hydrogenation.

The effect of the substituent on the reduction potentials of cyclopentadienyliron complexes was further demonstrated with respect to 2- and 3- ring polycyclic species.[234] Figure 3.2 shows the derivatives of indane, fluorene and anthracene, along with their respective reduction potentials, which were used as part of this study. For derivatives of indane and fluorene, which involve variation of one substituent, the reduction potentials increased with the substituent in the order $NH < CH_2 < O < S < CO$. A similar trend was observed in the case of complexes such as anthracene which involve two ring substituents, X and Y. It was observed that if one of these substituents was the same in each of the derivatives, then it was changes in the second group which affected the

reduction potential. An increase in the reduction potential was observed in the order NH < CR_2 < direct bond < O < S < SO_2. It is important to note that the observations mentioned above apply to the $E_{1/2}$ of the first one-electron reduction, with the reduction potentials corresponding to the second reduction process being more negative by 0.5 to 0.8 V.

The stepwise reduction of these complexes is of interest to investigators due to the ability of the species generated to act as electron-reservoirs. The notion of reservoirs in terms of electrons, protons and radicals has been demonstrated to be of importance in many chemical processes including biological redox reactions and cycles, catalysis for radical transfer reactions, transport of metal ions across membranes, and transport of oxygen by hemoglobin.[54] Electron-reservoirs are potentially useful in homogeneous charge transfer reactions and therefore present intriguing catalytic properties in the reduction of other species in solution. It is the stepwise generation of the neutral $19e^-$ species which arouses particular interest for this purpose.[241-242] One report appeared which describes the generation of an extremely unstable $21e^-$ dianionic system based on the (naphthalene)FeCp system.[248]

Electrolysis is one of several techniques which has been investigated for the removal of the pendent metal moiety from its ligands. It has been observed that the cathodic reduction of the $[(arene)CpFe^{II}]^+$ 18-electron complexes results in the decomplexation of the metal moiety to yield quantitative amounts of Fe^{2+}, cyclopentadiene, and benzene.[225] The efficiency of this process was found to be highly dependent on the nature of the ligand, where arene ligands bearing less than three

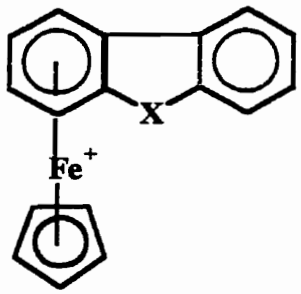

	$E_{1/2}$ (V)
a X = O;	-1.82
b X = CH_2;	-1.84
c X = NH;	-1.97

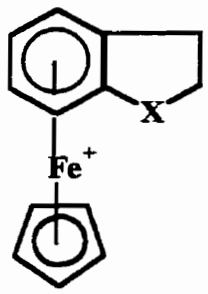

	$E_{1/2}$ (V)
d X = CO;	-1.21
e X = S;	-1.63
f X = O;	-1.70
g X = CH_2;	-1.74
h X = NH;	-1.78

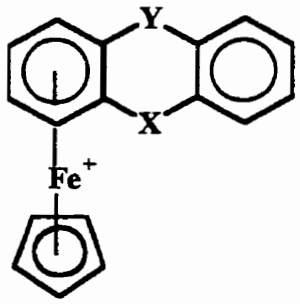

Y = S	$E_{1/2}$ (V)
i X = S;	-1.54
j X = O;	-1.62
k X = direct bond;	-1.63
l X = CH_2;	-1.69

Y = O	$E_{1/2}$ (V)
m X = SO_2;	-1.39
n X = S;	-1.62
o X = O;	-1.68
p X = direct bond;	-1.70
q X = CMe_2;	-1.75

Figure 3.2: Half-wave potentials for the first reduction step of $CpFe^+$ complexes of derivatives of indane, fluorene and anthracene.

methyl groups were the most readily susceptible to reaction.[224] Figure 3.3 illustrates the electrocatalytic cycle which was proposed to account for the above observations, where the exchange of the arene ligand for solvent ligands in complex A results in the generation of the corresponding Fe^{I} species, B.[225] It is this species that effectively reduces the cationic Fe^{II} starting complex and liberates the other ligands. It has been suggested that donor ligands promote liberation of the metal moiety by polyhapto ligand exchange.[247] A distinct solvent effect has been observed with the rate of decoordination increasing in the order $Me_2CO < CH_2Cl_2 < DMF < MeCN$. Regardless of the chosen solvent, individual hapticity changes remain unidentified.

Due to the interesting electrochemical behavior exhibited by the monometallic complexes, Manners and Bard[99, 103, 218, 232, 249] extended the investigation of these species to their bi- and polymetallic counterparts. It has been established that in the case of polymetallic complexes there is potential for interaction between metal centers where the probability and degree of interaction is highly dependent on the nature of the metal of interest and the bridging ligands. Figure 3.4 shows the cyclic voltammogram of a bis(cyclopentadienyliron) phenanthroline complex which showed that there is electrochemical communication between the two metals via the backbone of the coordinating ligand.[218] A measurement of the separation of the formal potentials (ΔE°) by cyclic voltammetry allows one to gauge the degree of interaction between the metal centers. That is, a species with multiple isolated redox centers of the same type would appear identical to one with one redox center.[251] It has been determined that the interaction or lack of interaction between metal centers is highly influenced by the identity of the metal and the bridging ligands. Controlled potential coulometry is often

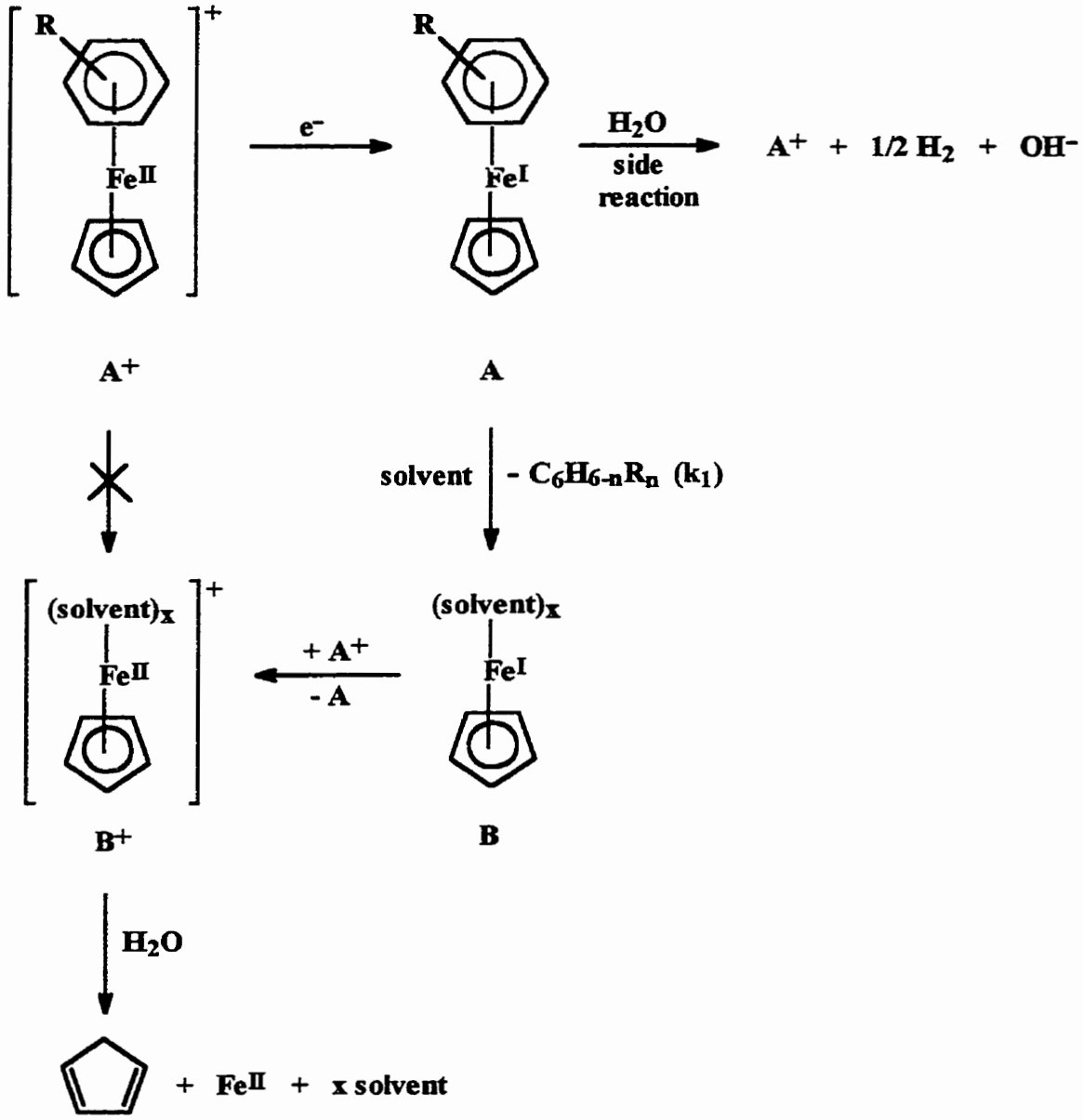

Figure 3.3: Electrocatalytic decomplexation of 18-electron complexes

applied as a means of establishing the number of isolated redox centers in a polymetallic system by measuring the number of electrons involved in the electron transfer process.[252-254] During his investigation of the bimetallic phenanthroline complex, Bard not only demonstrated the potential for interaction between the two metals in bimetallic complexes but also showed that the chemical reversibility noted in these systems may be dependent on the scan rate.[218] In this case, low scan rates showed evidence for an irreversible electrochemical system which became completely reversible at high scan rates.

The focus of this study is the effect of temperature and bridging ligand on the electrochemical behavior of some mono- and bi-(cyclopentadienyliron) complexes with oxygen and sulfur linkages using cyclic voltammetry as a means of determining some thermodynamic and kinetic characteristics of selected complexes.

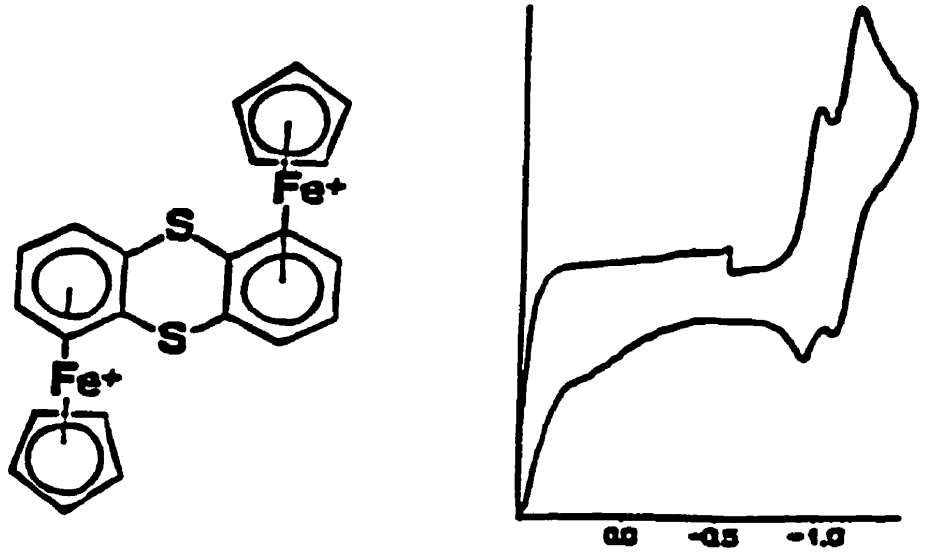

Figure 3.4: Cyclic Voltammogram of a bimetallic $CpFe^{+}$ phenanthroline complex showing electrochemical communication between the two metal centers[218]

3.2 Results and Discussion

3.2.1 Electrochemical Behavior of Cyclopentadienyliron Complexes

In this study, the chemical reversibility and the heterogeneous electron transfer rate constants of selected complexes were examined using cyclic voltammetry. Initial studies of the monoiron cyclopentadienyliron complexes have established that the reduction process of this class of compounds proceeds in two successive reduction steps.[233-234] With a hanging mercury drop electrode (HMDE) as a working electrode, it was generally observed that the first reduction was chemically reversible at all temperatures studied. In the case of complexes containing sulfides as substituents on the benzene, it was typically noted that the difference in potential between the anodic and cathodic peaks for the second reduction was greater than that for the first. This observation was attributed to a slower rate of electron transfer in the second reduction step than in the first.[234] The present study focuses on a variety of mono- and bimetallic arene complexes with ether and thioether bridges (Figure 3.5) in DMF using platinum disk or glassy carbon working electrode at temperatures ranging from 233 to 293K in the presence of TBAP as the supporting electrolyte.

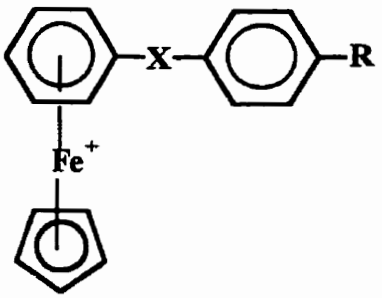

[3.1]$^{+}$: X = O, R = H
[3.2]$^{+}$: X = S, R = CH_3

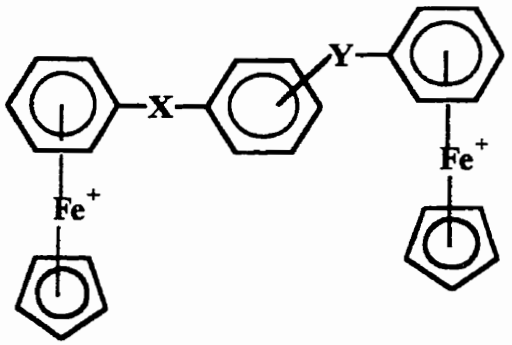

[3.3]$^{2+}$: 1,4; X = Y = O
[3.4]$^{2+}$: 1,2; X = Y = S
[3.5]$^{2+}$: 1,3; X = Y = S
[3.6]$^{2+}$: 1,4; X = Y = S
[3.7]$^{2+}$: 1,4; X = O; Y = SO_2
[3.8]$^{2+}$: 1,4; X = Y = SO_2

Figure 3.5: Complexes studied by cyclic voltammetry and controlled potential electrolysis

3.2.2.1 Cyclic Voltammetric Investigations of Monometallic Complexes with Oxygen and Sulfur Substitutents

The monometallic complexes examined here were observed to exhibit electrochemical behavior which was consistent with analogous complexes studied previously.[234] The chemical reversibility of the first reduction step of the monometallic complexes, $[\mathbf{3.1}]^+$ and $[\mathbf{3.2}]^+$, resulting in the generation of the neutral $19e^-$ complex, was found to be highly dependent on the temperature and on the substituent on the complexed arene. In the case of the platinum working electrode, the $18e^-/19e^-$ couple was determined to be chemically reversible at 253 K for both monometallic complexes, $[\mathbf{3.1}]^+$ and $[\mathbf{3.2}]^+$ (Table 3.1). However, the effect of the substituent on the electrochemical behavior of the complexed arene species was evident upon the transfer of the second electron at room temperature. It was observed that the thioether complex, $[\mathbf{3.2}]^0$, was considerably more stable than its ether counterpart, $[\mathbf{3.1}]^0$, which decomposed rapidly. Although a wave corresponding to the $19e^-/20e^-$ couple was evident for both complexes when using a glassy carbon working electrode, the second reduction process of complex $[\mathbf{3.2}]^{0/-}$ was found to be chemically reversible ($E_{1/2}$ = -2.48 V vs Fc/Fc^+) at room temperature.

Table 3.1: CV Parameters for Complexes $[3.1]^+$ - $[3.8]^{2+}$ at T = 253 K, v = 0.2 V/s, Pt working electrode, in DMF with $E_{1/2}$ vs $FeCp_2$.

Complex Number	E_{pa}, V	E_{pc}, V	$E_{1/2}$, V
$[3.1]^+$	-1.69	-1.84	-1.77
$[3.2]^+$	-1.62	-1.76	-1.69
$[3.3]^{2+}$	-1.70	-1.87	-1.79
$[3.4]^{2+}$	-1.64	-1.86	-1.75
$[3.5]^{2+}$	-1.58	-1.81	-1.70
$[3.6]^{2+}$	-1.61	-1.75	-1.68
$[3.7]^{2+}$	-1.47 -1.74	-1.60 -1.89	-1.54 -1.82
$[3.8]^{2+}$	-1.48	-1.69	-1.59

3.2.2.2 Cyclic Voltammetric Investigations of Bimetallic Complexes with Oxygen and Sulfur Bridges

The electrochemical behavior of cyclopentadienyliron complexes was further extended to the cyclic voltammetric investigation of isomeric sulfur-bridged aromatic bimetallic $CpFe^+$ complexes, $[3.3]^{2+}$ - $[3.8]^{2+}$. Interest in this series of complexes stems from earlier work of Bard and coworkers[232, 251] who showed that, in the case of similar complexes, one metal moiety undergoes a reduction which is closely followed by the reduction of the second metal moiety at a more negative potential. It has been proposed that electrochemical behavior of this type indicates some measurable degree of interaction between the iron centers. Upon the transfer of the first electron, the presence of the sulfur bridge allows the increased electron density of the first iron moiety to be dispersed across to the second metal moiety, making reduction more difficult. Two closely spaced, yet distinguishable, waves were observed for the $36e^-/38e^-$ reduction

process for the 1,2- and 1,4-substituted disulfide complexes $[\mathbf{3.4}]^{2+}$ and $[\mathbf{3.6}]^{2+}$. The explanation for the observed cyclic voltammograms corresponding to $[\mathbf{3.4}]^{2+}$ and $[\mathbf{3.6}]^{2+}$ is that, due to the presence of the sulfur bridge, a small degree of electronic interaction between the two metals is detected. In the case of complexes $[\mathbf{3.4}]^{2+}$ and $[\mathbf{3.6}]^{2+}$, severe overlap of the individual $36e^-/37e^-$ and $37e^-/38e^-$ reductions prompted the use of digital simulation of the CV wave shapes to extract the ΔE° values. Figure 3.6 shows the experimental cyclic voltammogram and corresponding digital simulation, obtained as outlined in the experimental section of this work using the Digisim simulation program version 2.0 from Bioanalytical Systems Incorporated, for complex $[\mathbf{3.6}]^{2+}$. It was found that the 1,2- and 1,4-substituted complexes both demonstrated a limited degree of interaction through the sulfur-arene bridge as indicated by a formal potential separation of ca 70-80 mV. By contrast, the CV of the 1,3-substituted analogue $[\mathbf{3.5}]^{2+}$ showed no measurable difference between formal potentials of its $36e^-/37e^-$ and $37e^-/38e^-$ couples, probably due to electronic effects, and this complex therefore behaved as if the iron centers were electronically isolated.

In an attempt to gain a better understanding of the electrochemical behavior of bis(cyclopentadienyl)iron complexes, several bimetallic complexes containing oxygen, sulfur and sulfone bridges were investigated with various working electrodes and at several temperatures. Complex $[\mathbf{3.3}]^{2+}$ allowed the comparison of the CV of a bimetallic complex with that of its previously mentioned monometallic counterpart $[\mathbf{3.1}]^{+}$. The chemical reversibility of both reduction steps of complex $[\mathbf{3.3}]^{2+}$ was discovered to be highly dependent on temperature. For instance, the generation of the $38e^-$ complex

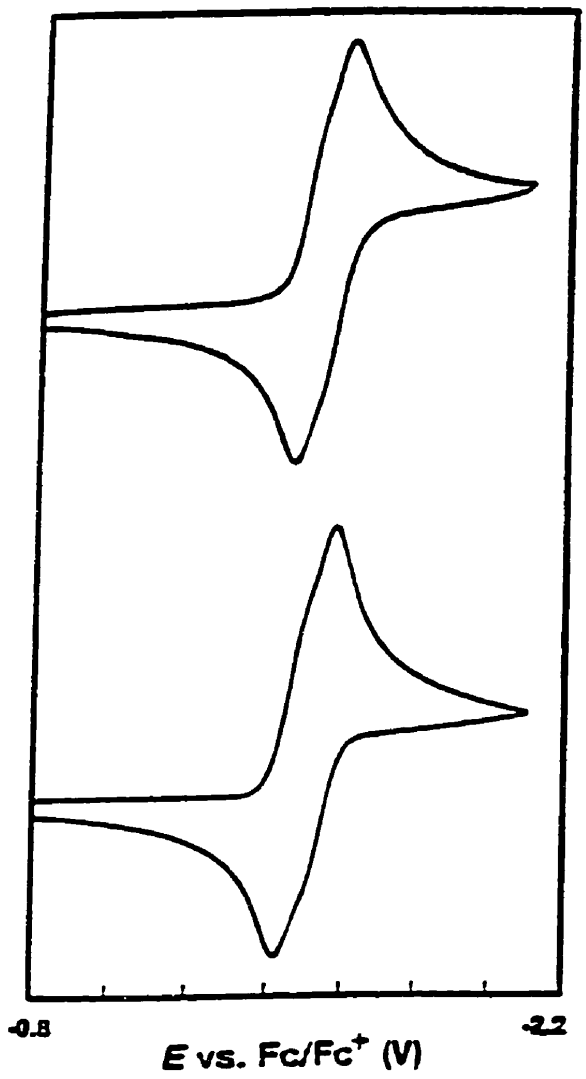

Figure 3.6: Cyclic Voltammograms at Pt of 2 mM complex $[\mathbf{3.6}]^{2+}$ in DMF containing 0.1 M TBAP; $\nu = 0.1$ V/s at 253 K. Simulated (bottom) and experimental.

was found to be partially chemically reversible at 293 K with the second reduction process being chemically irreversible. Comparison of the CV at 293 K with that at 233 K demonstrated a change in the electrochemical behavior of the complex at the lower temperature, with the first electron transfer process being represented as a single

chemically reversible wave at $E_{1/2}$ = -1.75 V vs. Fc/Fc^+ (Figure 3.7). Following the first reduction step, the chemical stability of the $38e^-$ complex was proposed to increase with a decrease in temperature. Comparatively, the $40e^-$ complex was observed to be unstable regardless of the temperature (293-233 K) and time frames (0.05 - 1.0 V/s) studied. Based on the similarities of the cyclic voltammograms of complexes $\mathbf{[3.1]^+}$ and $\mathbf{[3.3]^{2+}}$, it is proposed that the iron centers of the bimetallic complex are isolated. Electron transfer processes similar to those pertaining to the reduction of complexes $\mathbf{[3.4]^{2+}}$ and $\mathbf{[3.6]^{2+}}$ and involving a two step process are also believed to hold for complexes such as $\mathbf{[3.3]^{2+}}$. In the case of complexes $\mathbf{[3.4]^{2+}}$ and $\mathbf{[3.6]^{2+}}$, which contain sulfur bridges, it was demonstrated that it was possible to distinguish between the generation of the $37e^-$ and $38e^-$ products. However, it is proposed that the noninteracting metal centers of the oxygen bridged complex $\mathbf{[3.3]^{2+}}$ are reduced by two rapid and successive one-electron transfer steps at each iron site. That is, two electron transfer waves representative of the $36e^-/38e^-$ and $38e^-/40e^-$ processes are observed in the cyclic voltammogram. The mechanism proposed here is in accordance with previous studies of complexes with noninteracting centers (Figure 3.8).[251, 258-259]

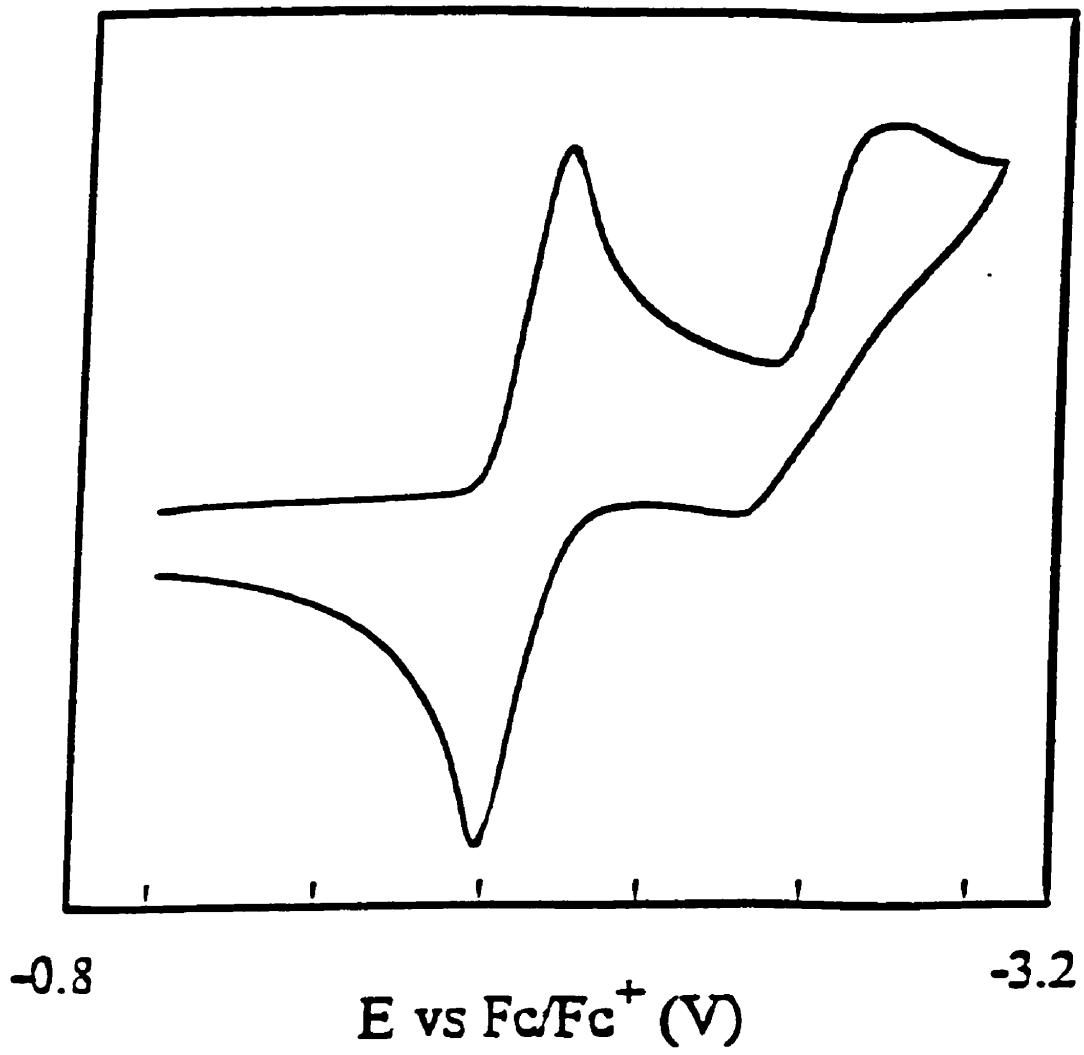

Figure 3.7: Cyclic Voltammogram at glassy carbon of 2.0 mM complex $[\mathbf{3.3}]^{2+}$ in DMF containing 0.1 TBAP at 233 K: $\nu = 0.2$ V/s.

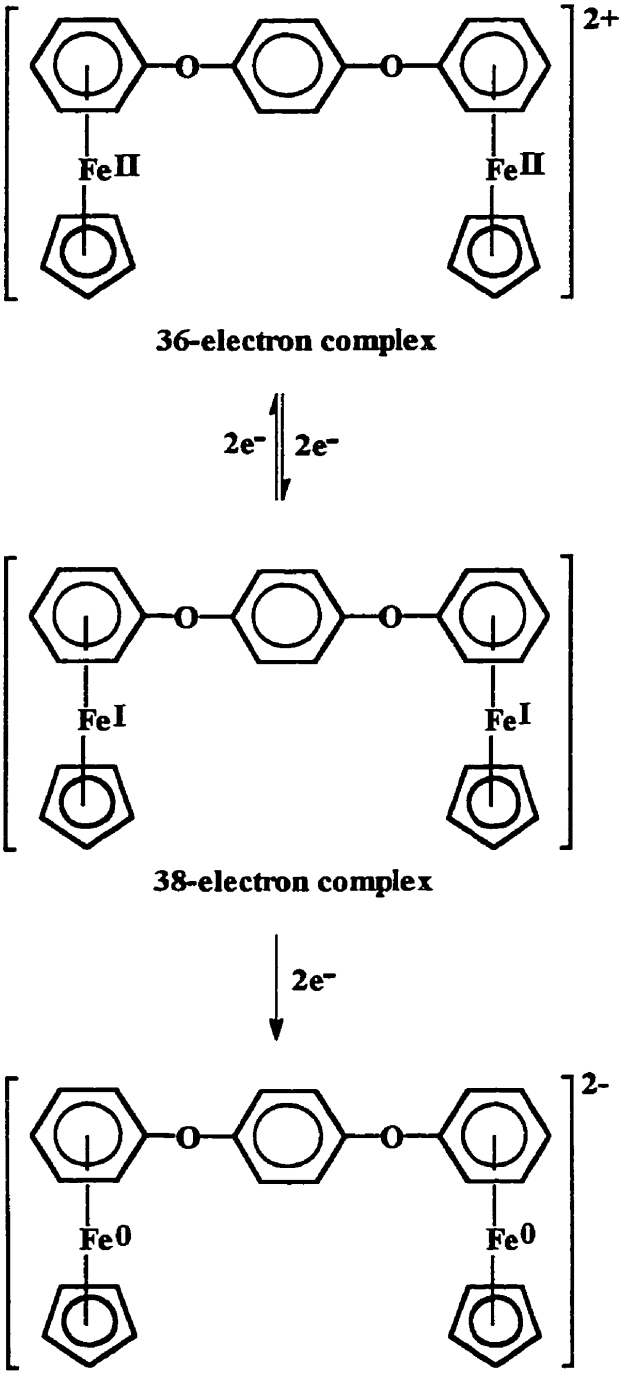

Figure 3.8: Formation of neutral and anionic species of complex **[3.3]**$^{2+}$ in two steps with the addition of two electrons in each step

3.2.2 Controlled Potential Coulometric Studies

In the case of complex $[\mathbf{3.3}]^{2+}$, controlled potential coulometry of a solution containing 0.149 mmol of complex at a large platinum mesh electrode was employed to provide indisputable evidence for the transfer of two electrons in the first reduction step. Plateau currents measured from stirred solution voltammograms recorded before and after a partial electrolysis at an applied voltage of -1.93 V vs. Fc/Fc^{+} demonstrated that 18.1% of the complex was reduced without noticeable decomposition. From the 5.05 C of charge passed during electrolysis, an apparent n-value of 1.94 equiv./mol was determined (Figure 3.9). Electrolysis experiments that were extended to greater conversions demonstrated noticeable decomposition of the reduced complex, even at the lowest temperature of 228 K. Coulometric determinations with higher conversions were hindered by the formation of decomposition products which irreversibly adsorbed and passivated all electrode surfaces. This was especially evident in the case of glassy carbon electrode surfaces.

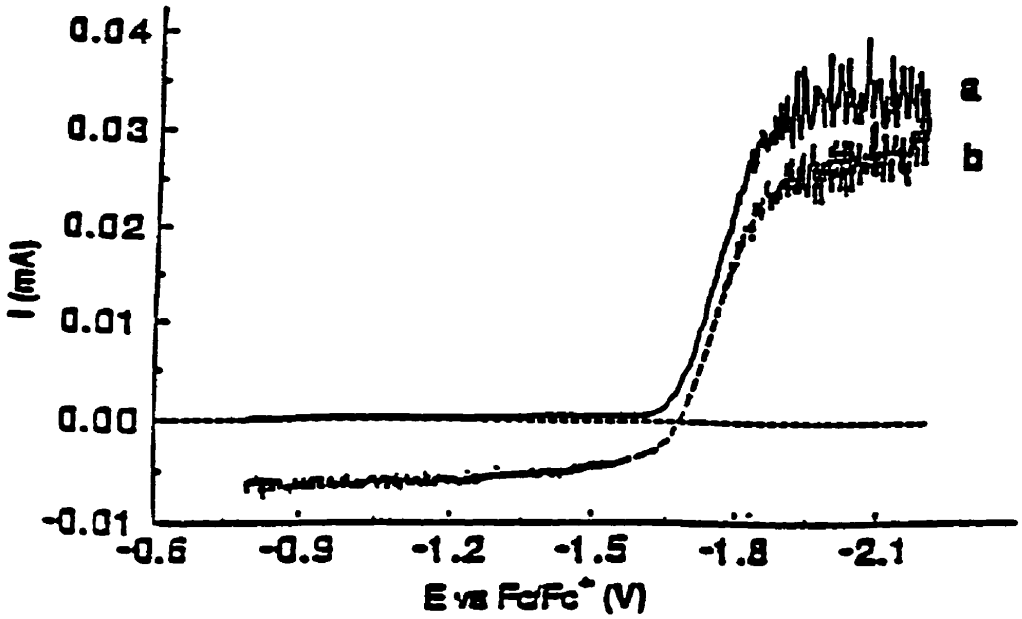

Figure 3.9: Stirred solution voltammograms of 3.0 mM of complex $[\mathbf{3.3}]^{2+}$ at 243 K in DMF/0.1 M $TBAPF_6$ recorded (a) before and (b) after partial electrolysis (Q = 5.05 C) at an applied potential of -1.93 V vs Fc/Fc^+.

3.2.3 Comparison of the Stability of Oxygen and Sulfur Containing Complexes

The electrochemical processes described previously were investigated using DMF as the solvent at various temperatures. Although the first reduction step of complex $[\mathbf{3.3}]^{2+}$ was observed to be partially chemically reversible at 293 K at various CV scan rates (0.05-1.0 V/s), a substantial increase in the chemical reversibility was evident with a decrease in temperature to 253 K due to an increase in the stability of the complex. This follows from the fate of the $38e^-$ complex involving either a second reduction or a decomposition process with the solvent. Employing the method of Nicholson and

Shain,[260] the pseudo first-order rate constant for the reaction of the $38e^-$ complex with the solvent was determined at a variety of scan rates (0.05-1.0 V/s) with the average rate being reported with a standard deviation between 10 and 30%. Using this method for the calculation of the rate constant for an irreversible following chemical reaction of an electrochemical process involves the determination of the ratio of the anodic and cathodic peak currents according to equation 3.1.[260]

$$\frac{i_{pa}}{i_{pc}} = \frac{(i_{pa})_o}{i_{pc}} + \frac{0.485\,(i_\lambda)}{i_{pc}} + 0.086 \qquad \text{Equation 3.1}$$

where: $(i_{pa})_o$ is the uncorrected anodic peak current, (i_{pc}) is the cathodic peak current, and (i_λ) is the current at the switching current. Tau (τ), a variable which is a measure of the time spent between the switching potential (E_λ) and $E_{1/2}$, is calculated using equation 3.2 and is crucial in the determination of the rate constant.

$$\tau = \frac{E_\lambda - E_{1/2}}{\nu} \qquad \text{Equation 3.2}$$

The theoretical relationship between i_{pa}/i_{pc} and $(k_f\,\tau)$, as determined by Nicholson and Shain, is illustrated in Figure 3.10 where the calculated value of i_{pa}/i_{pc} may be used to obtain the value of $\log(k_f\,\tau)$ from the graph. The value of the rate constant may then be obtained following manipulation of the log $(k_f\,\tau)$ equation with respect to τ.

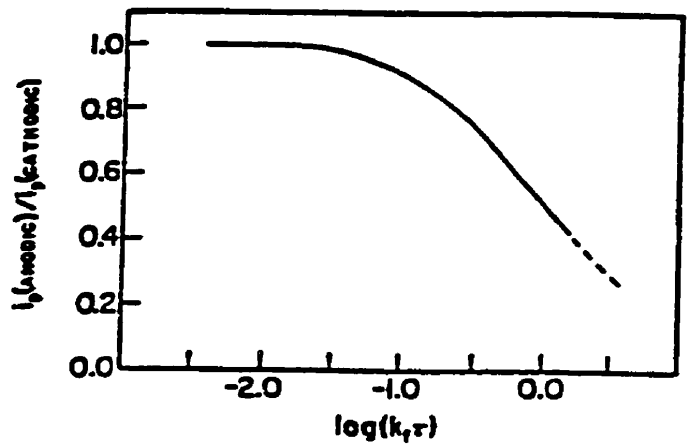

Figure 3.10: Theoretically determined relationship between the current ratio and ($k_f \tau$) according to the method of Nicholson and Shain

In the systems studied in this work, the rate constant determined using the method of Nicholson and Shain refers to the reaction of the $38e^-$ complex with the solvent. This following chemical reaction results in decomposition to yield neutral ferrocene and a decomplexed iron species.[233-234] Figure 3.11 illustrates the proposed decomposition process with respect to the $[3.3]^{2+/0}$ couple where the identity of these products has been determined using ^1H and ^{13}C NMR.

$$[\{(C_6H_5O)Fe^{II}Cp)\}_2C_6H_4]^{2+} + 2e \rightleftharpoons [\{(C_6H_5O)Fe^{I}Cp)\}_2C_6H_4]$$

$$[\{(C_6H_5O)Fe^{I}Cp)\}_2C_6H_4] + nS \xrightarrow{k} 2\,[S_n(Fe^{I}Cp)] + [(C_6H_5O)_2C_6H_4]$$

$$2\,[S_n(Fe^{I}Cp)]_2 \xrightarrow{fast} Fe^{II}(Cp)_2 + Fe^0 + 2nS$$

Figure 3.11: Decomposition process with respect to $[3.3]^{2+/0}$

The thioether bridged complexes $[\mathbf{3.4}]^{2+}$-$[\mathbf{3.6}]^{2+}$ exhibited instability as a result of solvent substitution in the same manner as that observed for the $38e^-$ species of the oxygen bridged complex $[\mathbf{3.3}]^{2+}$, albeit to a much smaller degree. As illustrated in Figure 3.12, comparison of the rate constants for complexes $[\mathbf{3.3}]^0$ and $[\mathbf{3.5}]^0$ shows enhanced stability of the sulfur containing complex, $[\mathbf{3.5}]^0$ at all temperatures studied. The difference between the oxygen and sulfur bridged species is especially prominent at room temperature where the latter complex survives approximately five times longer than the former species.

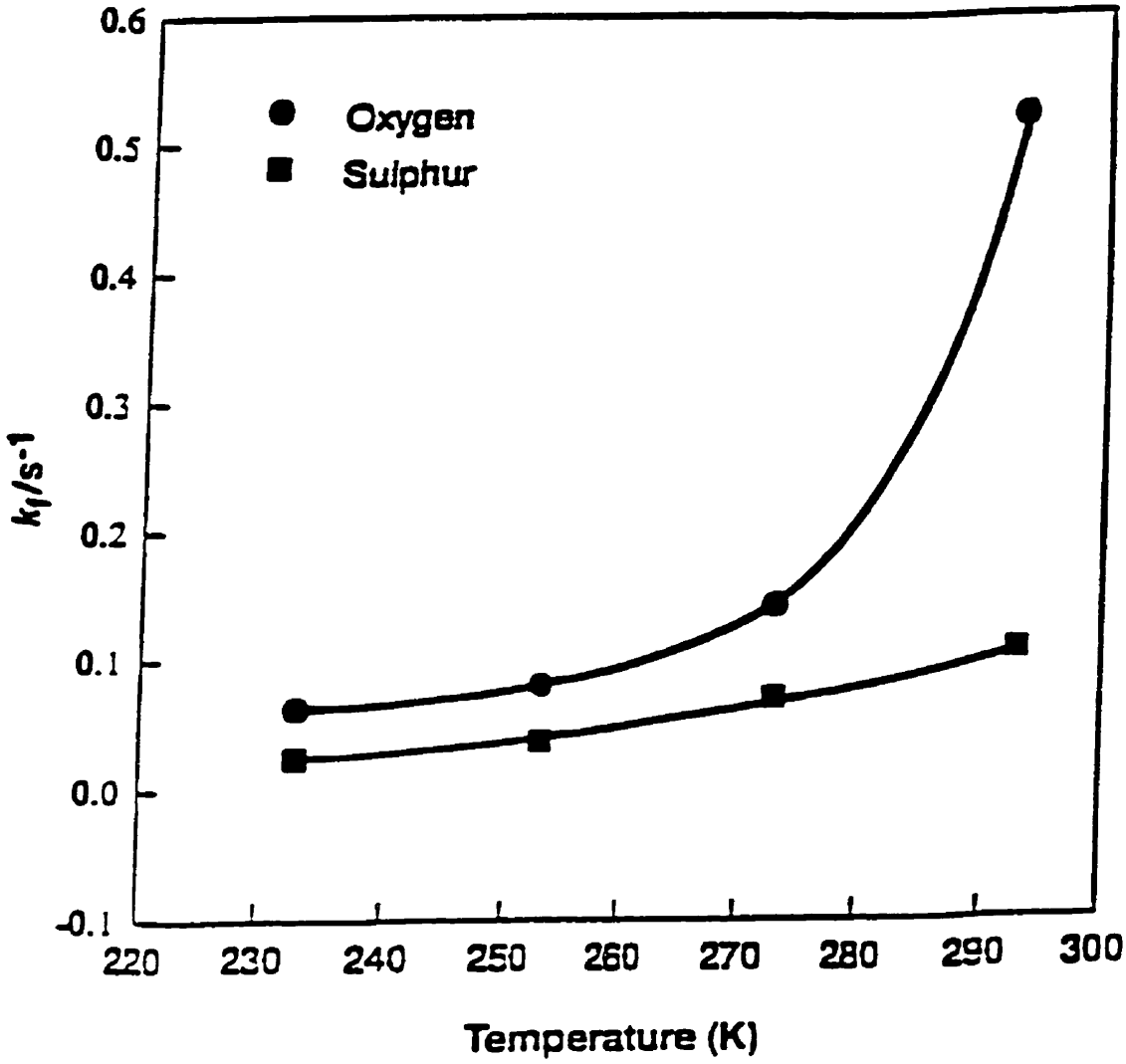

Figure 3.12: Plot of temperature vs. the rate constant of the reaction of the electrochemically generated $38e^-$ complexes, $[3.3]^0$ and $[3.5]^{2+}$, with the solvent (DMF)

3.2.4 Electrochemical Behavior of Bimetallic Sulfone Complexes

In addition to the ether and thioether bridged bimetallic complexes, a series of sulfone containing complexes, $[\mathbf{3.7}]^{2+}$ and $[\mathbf{3.8}]^{2+}$ was examined. The representative voltammograms of complexes $[\mathbf{3.3}]^{2+}$, $[\mathbf{3.7}]^{2+}$ and $[\mathbf{3.8}]^{2+}$ recorded in DMF at 233 K are shown in Figure 3.13. As expected, based on previous studies of monoiron sulfones, the reduction process takes place at more positive potentials than in the ether bridged analogues.[234] A limited degree of interaction between the iron centers of $[\mathbf{3.8}]^{2+}$ was indicated by a small separation between the $36e^-/37e^-$ and $37e^-/38e^-$ processes. Complex $[\mathbf{3.7}]^{2+}$ differs in a fundamental way from complexes $[\mathbf{3.3}]^{2+}$ and $[\mathbf{3.8}]^{2+}$ in that it incorporates a mixed oxygen/sulfone aromatic bridge into its molecular structure. In considering the cyclic voltammogram of complex $[\mathbf{3.7}]^{2+}$, a large formal separation, nearly 200 mV, between the $36e^-/37e^-$ and $37e^-/38e^-$ couples was determined. However, it is important to note that this phenomenon is not the result of a significant degree of interaction between the iron centers, but rather is attributed to the chemically different environments of the two metal centers. The evidence presented here of two one-electron reductions in the mixed oxygen/sulfur complex supports the suggested mechanism for the aforementioned bimetallic complexes in which reduction was proposed to take place via an overall two-electron process in the generation of the corresponding $38e^-$ complex.

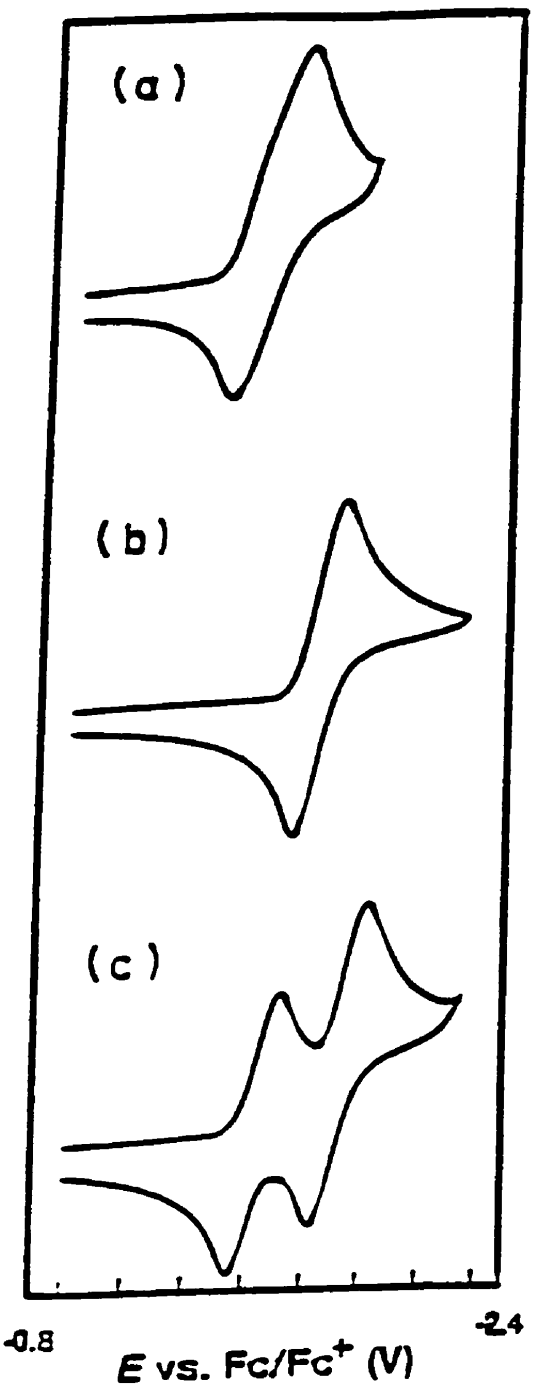

Figure 3.13: Cyclic voltammogram at Pt; $\nu = 0.2$ V/s; 233 K: (a) complex $[\mathbf{3.8}]^{2+}$ in DMF containing 0.1 M TBAP; (b) complex $[\mathbf{3.3}]^{2+}$ in DMF containing 0.1 M TBAP; (c) complex $[\mathbf{3.7}]^{2+}$ in DMF containing 0.1 M TBAP.

3.2.5 Thermodynamic Studies

3.2.5.1 Thermodynamic Investigations of Sulfur Complexes $[3.9]^{2+}$-$[3.12]^{2+}$

The method of Nicholson and Shain[260] is a useful technique for the determination of the pseudo-first order rate constant for the reaction of the $38e^-$ complex, generated in the electrochemical reduction of a bis(cyclopentadienyliron) complex, with the solvent (Figure 3.11). Figure 3.14 shows a series of sulfur-bridged bis(cyclopentadienyliron) complexes for which these rate constants have been determined at various temperatures. Tables 3.2 - 3.5 (pages 195-196) summarize the determined rate constants of complexes $[3.9]^{2+}$ - $[3.12]^{2+}$ at temperatures ranging from 233-273 K.

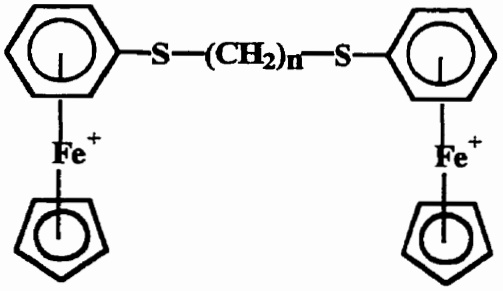

$[3.9]^{2+}$: n = 2
$[3.10]^{2+}$: n = 4
$[3.11]^{2+}$: n = 6
$[3.12]^{2+}$: n = 8

Figure 3.14: Series of sulfur-containing complexes investigated with respect to their activation parameters

The electrochemical determination of the rate constant pertaining to the reaction of an electrochemically generated species with the solvent is related to the properties of the molecules involved in the reaction. Activated complex theory offers a theoretical description of chemical kinetics and attempts to identify the principal features governing the size of the rate constant in terms of a model of events that take place during the reaction.[255, 256] The most important feature of this theory is the formation of the "activated complex" which corresponds to the transition state of the reaction and represents the maximum potential energy of the system (Figure 3.15).[255]

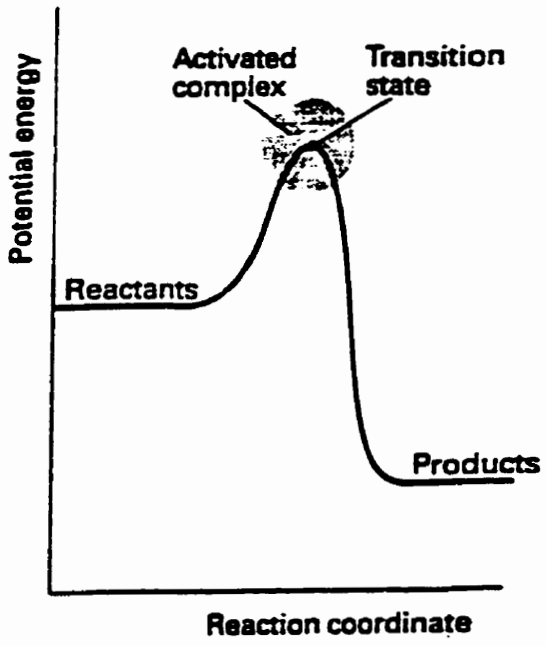

Figure 3.15: A reaction profile indicative of the formation of the activated complex[255]

In the investigation of chemical kinetics, the temperature at which the reaction is conducted has been observed to be particularly influential on the rate of reaction. Empirically, most reaction rates vary with temperature according to the Arrhenius equation,[255]

$$k = Ae^{-E_a/RT} \qquad \text{Equation 3.3}$$

where A is the frequency factor and E_a is the activation energy. This relationship provides a useful procedure for the comparison of systems in which the observed rate constants on a logarithmic scale are linear versus 1/T.[257] The plots of ln k versus 1/T used for the determination of E_a for complexes $\mathbf{[3.9]^{2+}}$ - $\mathbf{[3.12]^{2+}}$ are shown in Figures 3.16 - 3.19. This type of analysis allows for the generation of a line with a slope corresponding to $-E_a/R$ where the activation energy may be interpreted as a general measure of the relative ease with which thermally activated processes pass over an energy barrier.[255, 256]

One of the fundamental assumptions of activated complex theory is the establishment of an equilibrium between the reactants and the activated complex according to equation 3.4[256]

$$A + B \rightleftharpoons (AB)^{\ddagger} \longrightarrow \text{products} \qquad \text{Equation 3.4}$$

where the equilibrium constant is given by

$$K^{\ddagger} = \frac{[(AB)^{\ddagger}]}{[A][B]}. \qquad \text{Equation 3.5}$$

The rate constant of the forward reaction may be related to the equilibrium constant of the activated complex such that[256]

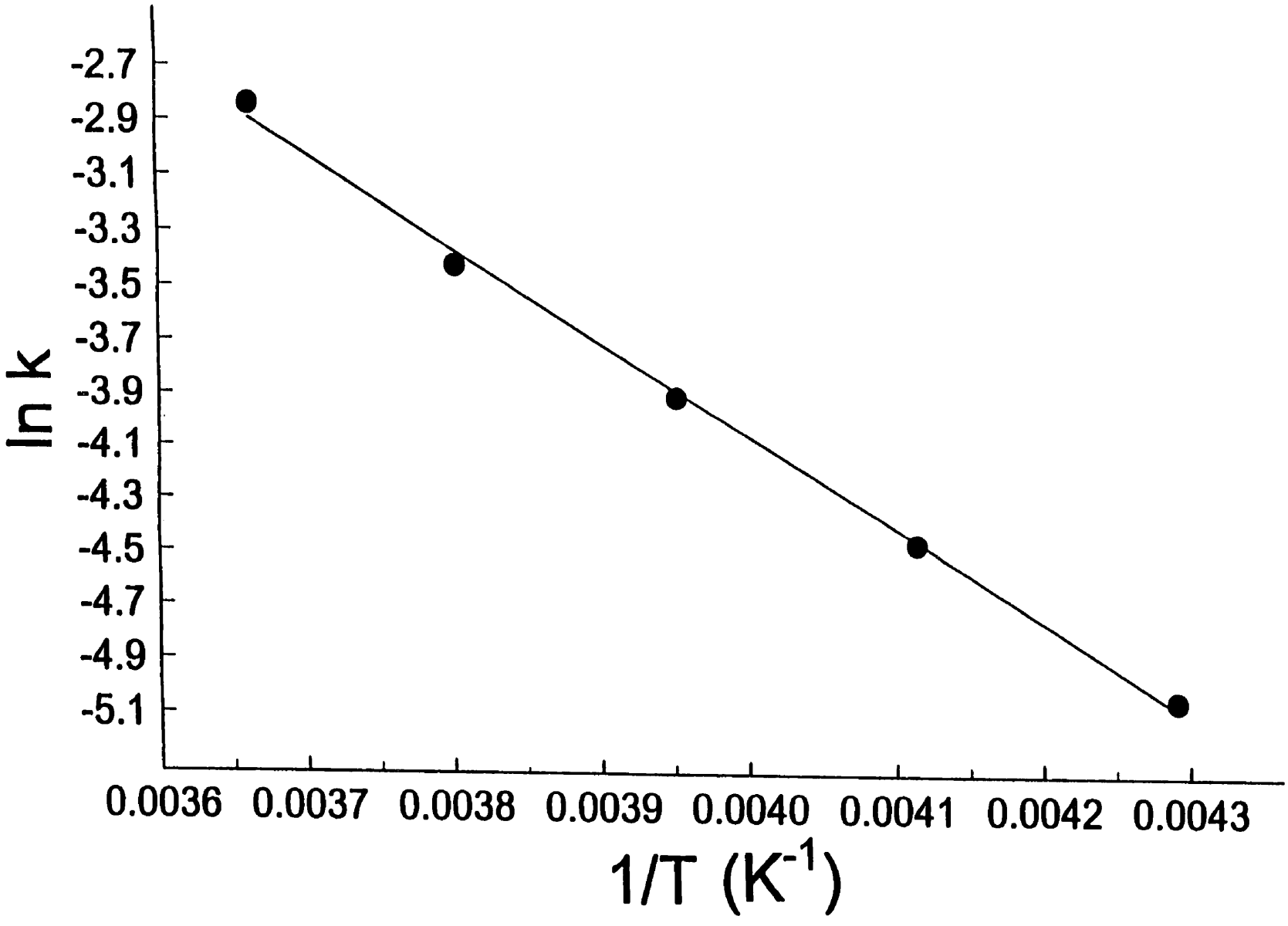

Figure 3.16: Plot of ln k versus 1/T for the determination of E_a for complex $[3.9]^{2+}$

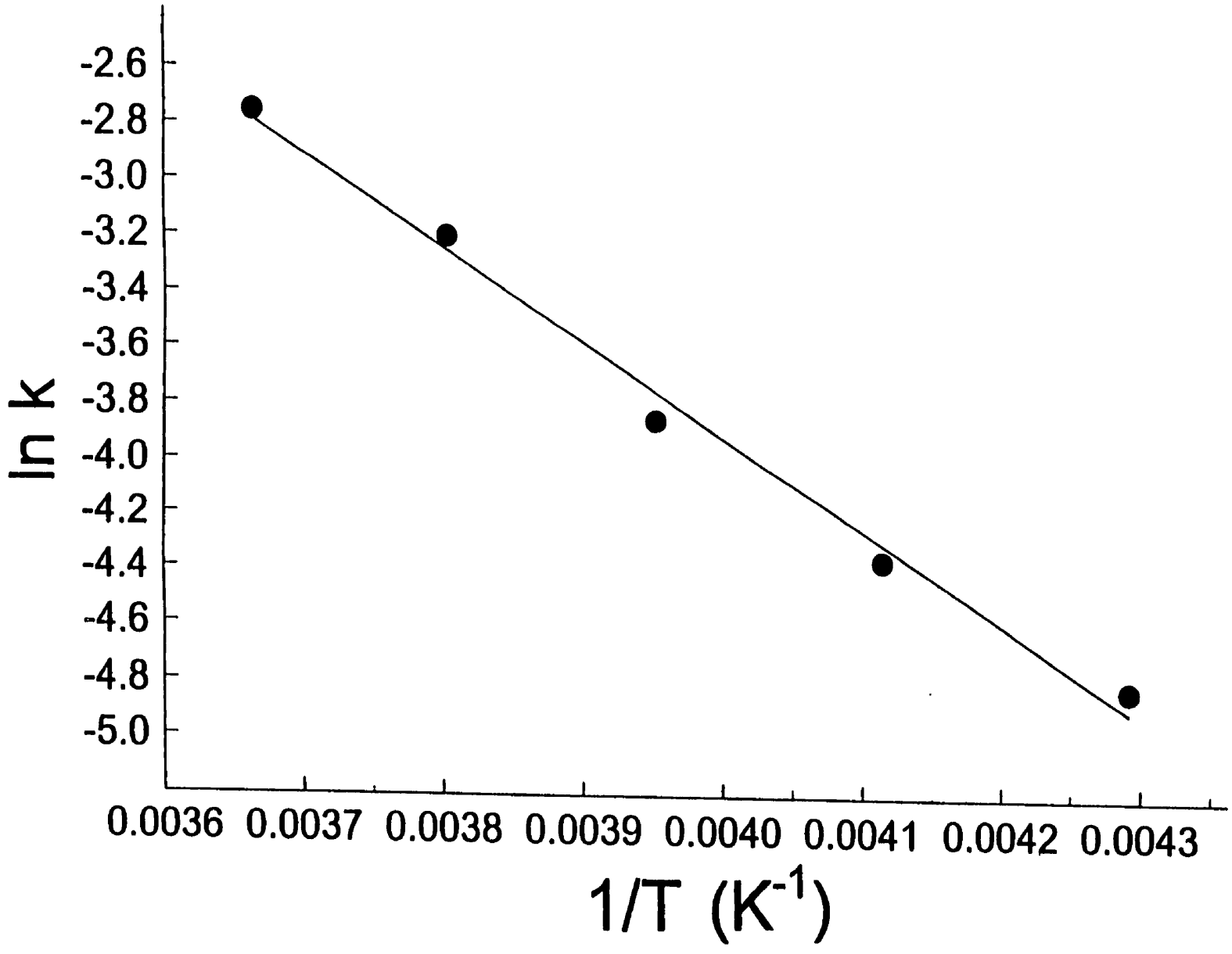

Figure 3.17: Plot of ln k versus 1/T for the determination of E_a for complex $[\mathbf{3.10}]^{2+}$

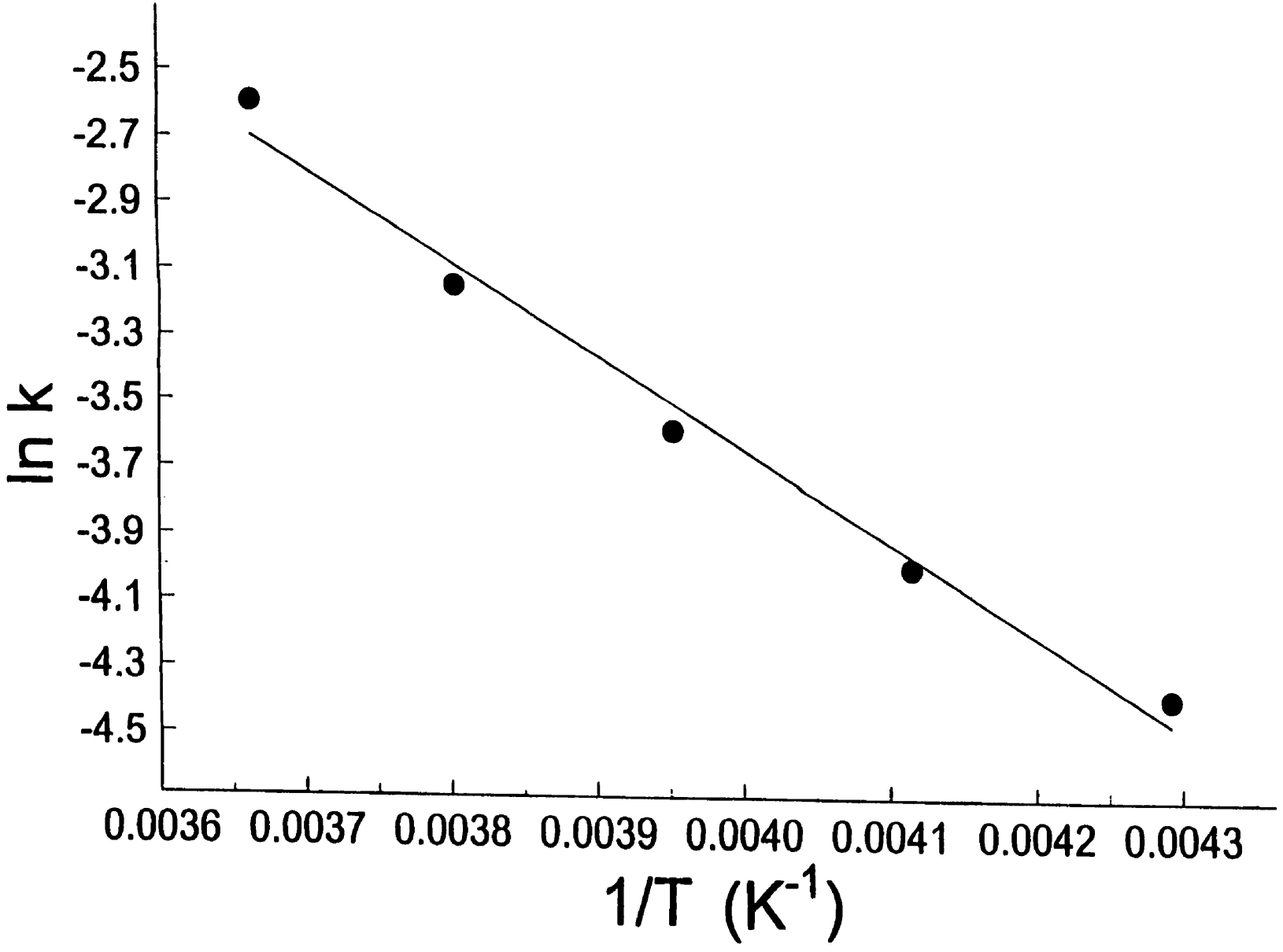

Figure 3.18: Plot of ln k versus 1/T for the determination of E_a for complex $[3.11]^{2+}$

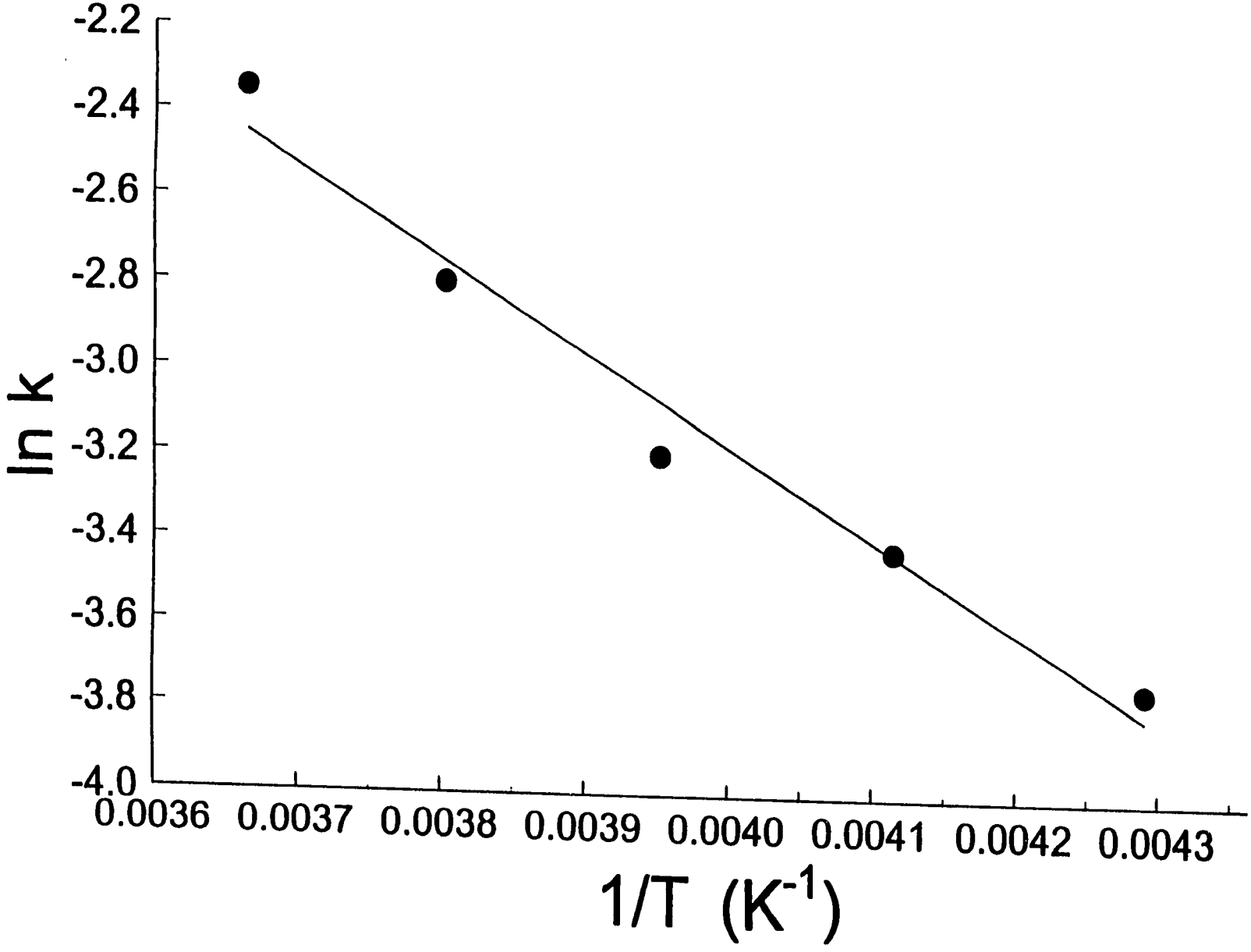

Figure 3.19: Plot of ln k versus 1/T for the determination of E_a for complex $[3.12]^{2+}$

$$k = \frac{k_B T}{h} K \qquad \text{Equation 3.6}$$

where k_B is Boltzmann's constant and h is Planck's constant. It is the equilibrium conditions which permit the consideration of the temperature dependence of the rate constant in terms of the quantities $\Delta G^{\ddagger}$, $\Delta H^{\ddagger}$ and $\Delta S^{\ddagger}$ as the standard free energy of activation, enthalpy of activation and entropy of activation. In terms of thermodynamics, it may be written that[257]

$$\Delta G^{\ddagger} = -RT\ln K^{\ddagger} \qquad \text{Equation 3.7}$$

$$\Delta G^{\ddagger} = \Delta H^{\ddagger} - T\Delta S^{\ddagger}. \qquad \text{Equation 3.8}$$

Finally, the rate constant of the forward reaction can be expressed in the same form as equation 3.3 such that[257]

$$k = \frac{k_B T}{h} e^{-\Delta G^{\ddagger}/RT} = \frac{k_B T}{h} e^{-\Delta H^{\ddagger}/RT} e^{\Delta S^{\ddagger}/R}. \qquad \text{Equation 3.9}$$

Evaluation of the activation parameters follows from a plot of ln (k/T) versus 1/T resulting in the generation of a line whose slope is $-\Delta H^{\ddagger}/R$. Figures 3.20 - 3.23 show the plots of ln (k/T) versus 1/T for the determination of the enthalpy of activation for complexes **[3.9]**$^{2+}$ - **[3.12]**$^{2+}$. Calculation of the entropy of activation follows from equation 3.10[257]

$$\Delta S^{\ddagger} = R \ln\left(\frac{hk}{k_B T}\right) + \frac{\Delta H^{\ddagger}}{T} \qquad \text{Equation 3.10}$$

where the rate constant corresponding to 253 K was used. The values of k and T were selected in the middle of the experimental range since the experimental uncertainty

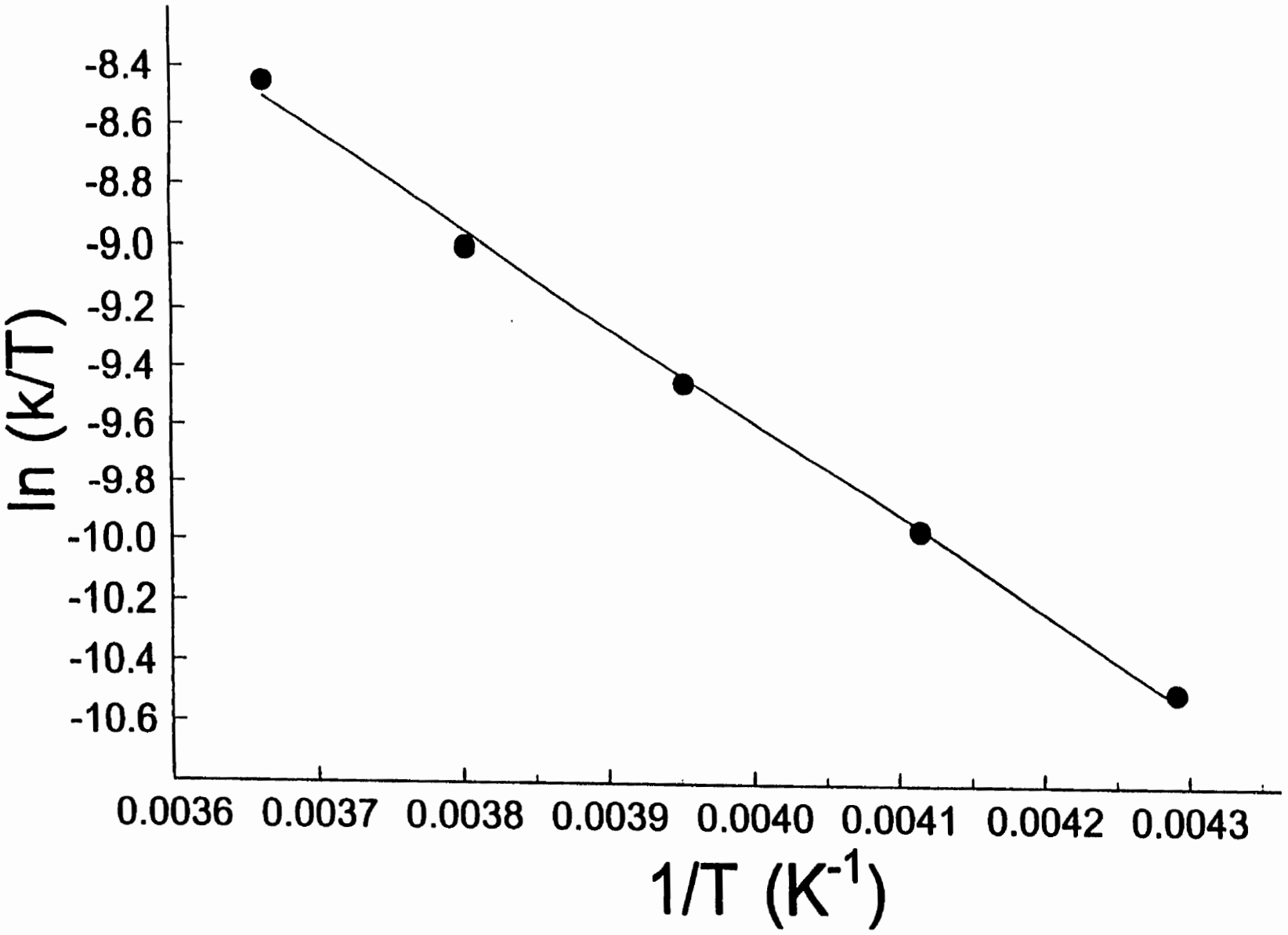

Figure 3.20: Plot of ln (k/T) versus 1/T for the determination of $\Delta H^{\ddagger}$ for complex **[3.9]**$^{2+}$

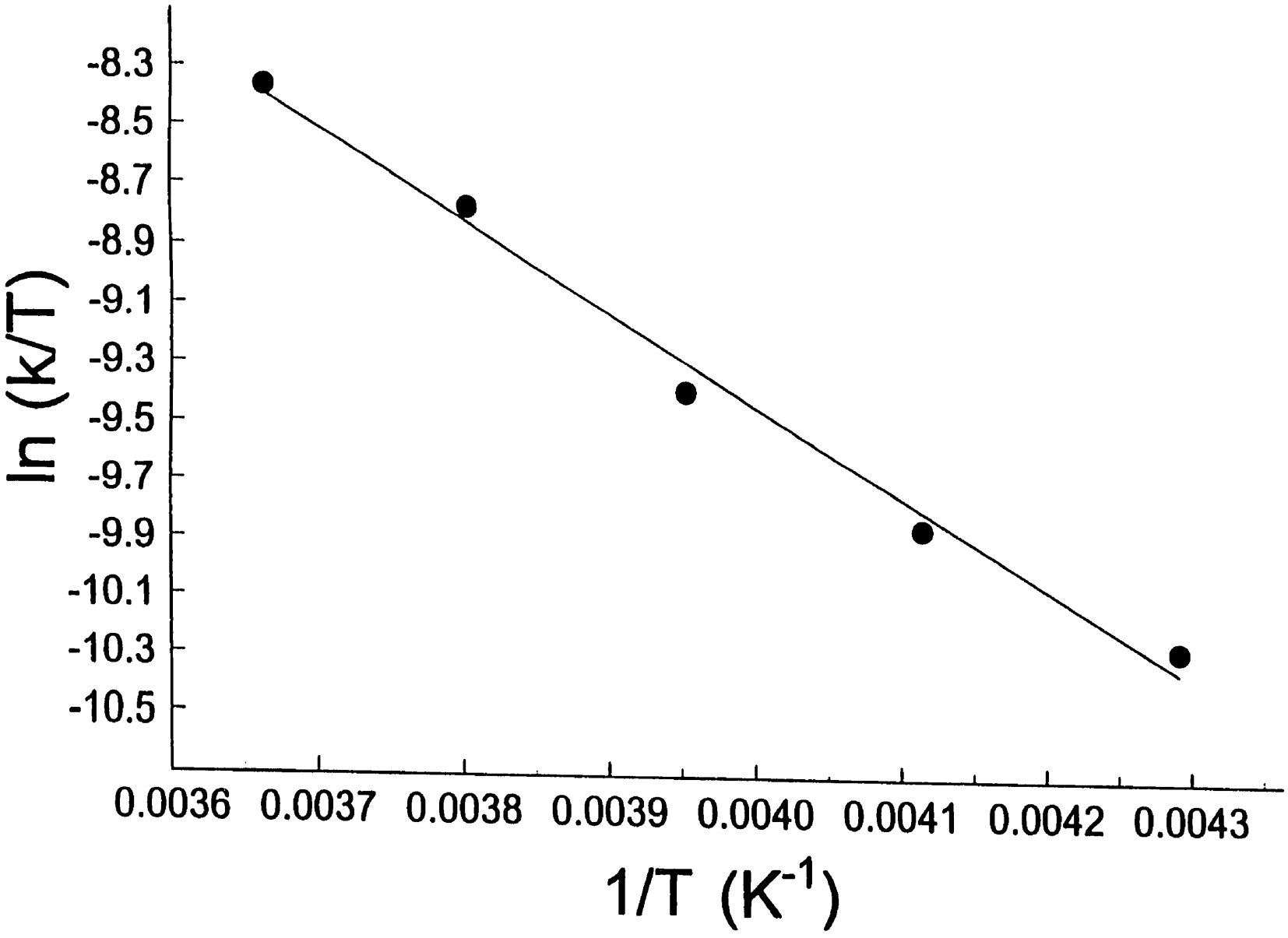

Figure 3.21: Plot of ln (k/T) versus 1/T for the determination of $\Delta H^{\ddagger}$ for complex **[3.10]**$^{2+}$

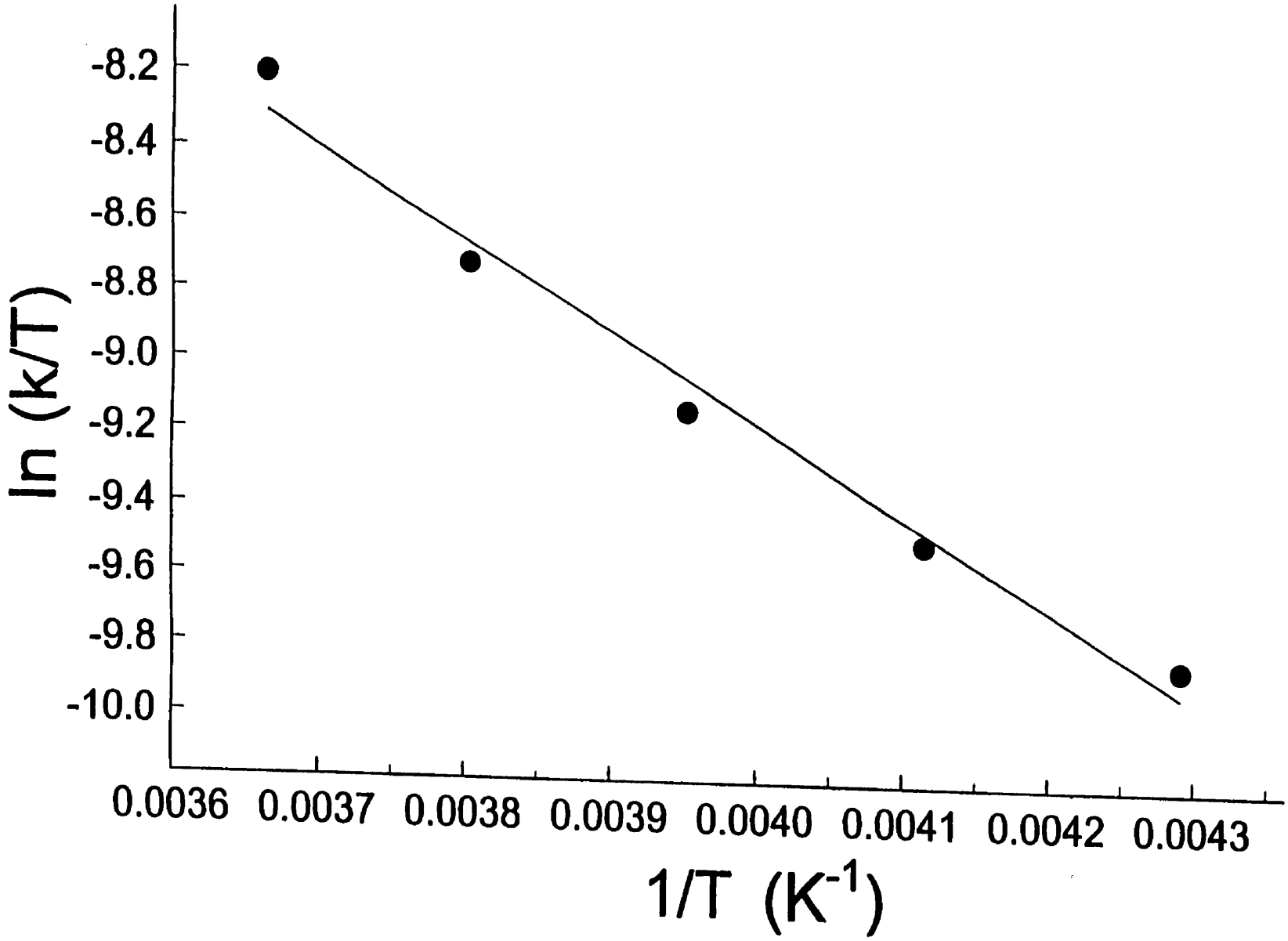

Figure 3.22: Plot of ln (k/T) versus 1/T for the determination of $\Delta H^{\ddagger}$ for complex **[3.11]**$^{2+}$

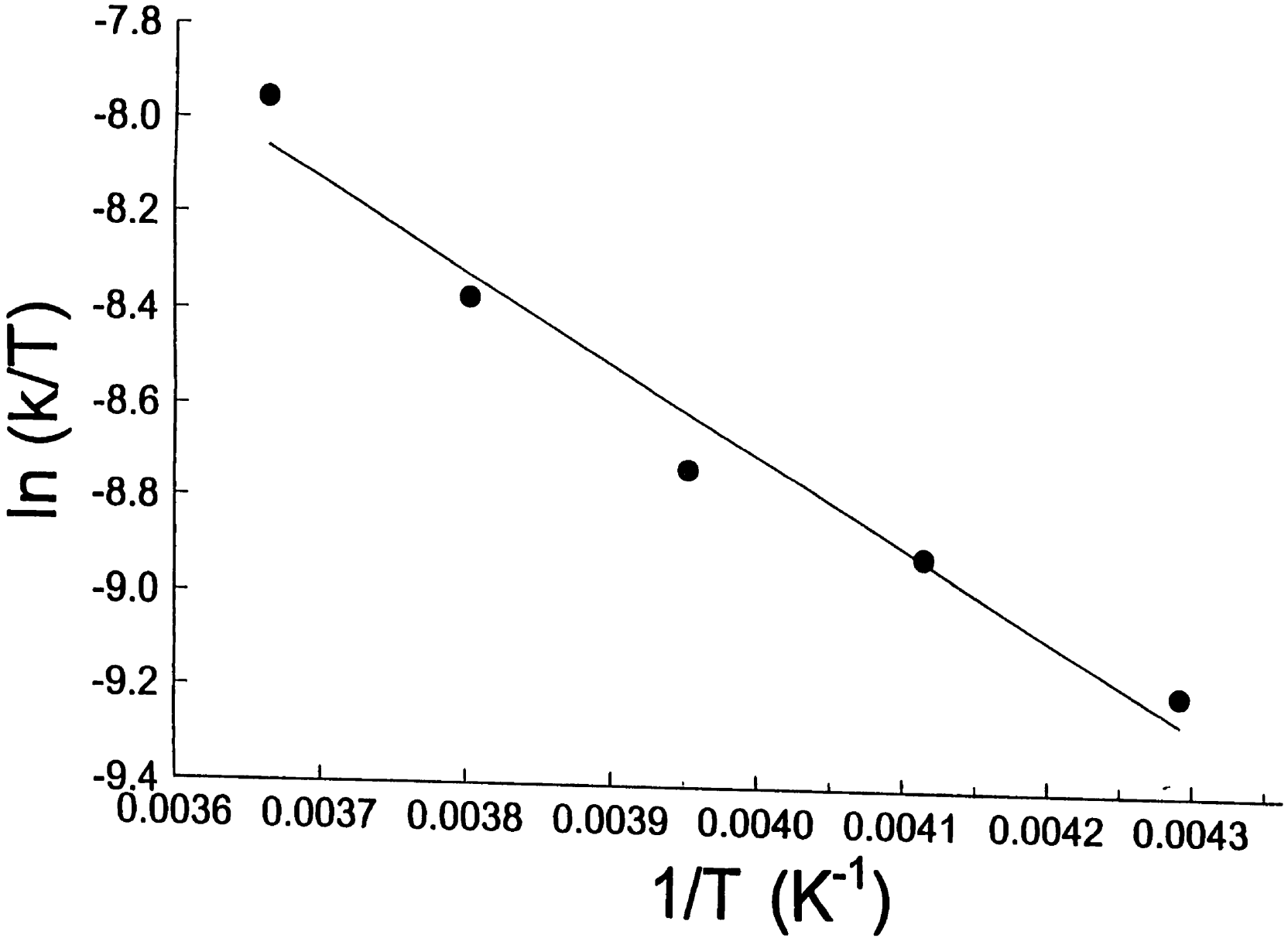

Figure 3.23: Plot of ln (k/T) versus 1/T for the determination of $\Delta H^{\ddagger}$ for complex $[3.12]^{2+}$

in Ea is the order of RT.[257] Finally, $\Delta G^{\ddagger}$ may be calculated from equation 3.8 at 253 K for comparison. Tables 3.2 - 3.5 summarize the activation parameters corresponding to complexes $[\mathbf{3.9}]^{2+}$ - $[\mathbf{3.12}]^{2+}$.

In this investigation, the rate constants which have been obtained from the cyclic voltammetric studies pertain to the reaction of the electrochemically generated $38e^{-}$ complex with the solvent and is the rate determining step for the process being considered. With respect to activated-complex theory, E_a may be loosely referred to as the minimum energy required by the reactants to form the corresponding products. Considering complexes $[\mathbf{3.9}]^{2+}$ - $[\mathbf{3.12}]^{2+}$, E_a and $\Delta H^{\ddagger}$ were observed to decrease with an increase in the chain length of the bridging aliphatic sulfur ligand. This observation may be attributed to the fact that as the chain length increases, the iron metal moieties are separated by a greater distance making their interaction with the solvent more viable. It is interesting to note that only a slight decrease in E_a and $\Delta H^{\ddagger}$ was observed when the chain length increased from two to four methylene units. However, a more significant decrease in these two variables was noted when the sulfur bridging chain length increased beyond four methylene units. If the observed decrease in E_a and $\Delta H^{\ddagger}$ is indeed due to the separation of the metal moieties, then perhaps a minimum separation deters reaction whereas a noticeable increase in the efficiency of the reaction process is evident as the distance between the metal moieties increases.

Table 3.2: Kinetic Data and Activation Parameters of Complex **[3.9]**$^{2+}$

Temperature (K)	ln k_f	k_f (s^{-1})	Ea ($kJmol^{-1}$)	$\Delta G^{\ddagger}$ ($kJmol^{-1}$)	$\Delta H^{\ddagger}$ ($kJmol^{-1}$)	$\Delta S^{\ddagger}$ ($Jmol^{-1}K^{-1}$)
233	-5.0360	0.0065	28.7	69.9	26.6	-171.0
243	-4.4654	0.0115				
253	-3.9170	0.0199				
263	-3.4265	0.0325				
273	-2.8404	0.0584				

Table 3.3: Kinetic Data and Activation Parameters of Complex **[3.10]**$^{2+}$

Temperature (K)	ln k_f	k_f (s^{-1})	Ea ($kJmol^{-1}$)	$\Delta G^{\ddagger}$ ($kJmol^{-1}$)	$\Delta H^{\ddagger}$ ($kJmol^{-1}$)	$\Delta S^{\ddagger}$ ($Jmol^{-1}K^{-1}$)
233	-4.8159	0.0081	27.9	69.7	25.8	-173.7
243	-4.3662	0.0127				
253	-3.8585	0.0211				
263	-3.2040	0.0406				
273	-2.7551	0.0636				

Table 3.4: Kinetic Data and Activation Parameters of Complex **[3.11]**$^{2+}$

Temperature (K)	ln k_f	k_f (s^{-1})	Ea ($kJmol^{-1}$)	$\Delta G^{\ddagger}$ ($kJmol^{-1}$)	$\Delta H^{\ddagger}$ ($kJmol^{-1}$)	$\Delta S^{\ddagger}$ ($Jmol^{-1}K^{-1}$)
233	-4.3820	0.0125	23.3	69.2	21.2	-189.6
243	-4.0001	0.0183				
253	-3.5899	0.0276				
263	-3.1489	0.0429				
273	-2.5943	0.0747				

Table 3.5: Kinetic Data and Activation Parameters of Complex **[3.12]**$^{2+}$

Temperature (K)	ln k_f	k_f (s^{-1})	Ea ($kJmol^{-1}$)	$\Delta G^{\ddagger}$ ($kJmol^{-1}$)	$\Delta H^{\ddagger}$ ($kJmol^{-1}$)	$\Delta S^{\ddagger}$ ($Jmol^{-1}K^{-1}$)
233	-3.7381	0.0238	17.9	68.3	15.8	-207.8
243	-3.4143	0.0329				
253	-3.1942	0.041				
263	-2.7969	0.061				
273	-2.3465	0.0957				

In some cases, interpretation of the kinetic data in terms of the thermodynamic parameters allows a great deal of insight to be gained into the nature of the activated complex. From Tables 3.2 - 3.5, a definite increasing negative value of the entropy of activation is evident with increasing chain length of the sulfur bridge. Again, the more negative entropy of activation of complex $[\mathbf{3.12}]^{2+}$ as compared to $[\mathbf{3.9}]^{2+}$ may be attributed to the chain length of the sulfur bridge with the transition state of the complex of shorter chain length being more constrained. The increased negative $\Delta S^{\ddagger}$ value with increasing chain length may also due to the nature of the reactants themselves whose entropy would increase in an increased chain length.

3.2.5.2 Thermodynamic Investigation of Oxygen Complexes $[3.13]^{2+}$ - $[3.15]^{2+}$

In this investigation, the reduction of a series of oxygen bridged mono- and bimetallic cyclopentadienyliron complexes, $[3.13]^{+}$, $[3.14]^{+}$ and $[3.15]^{2+}$, resulted in the generation of the corresponding $19e^{-}$ ($[3.13]^{+}$ and $[3.14]^{+}$) and $38e^{-}$ ($[3.15]^{2+}$) species (Figure 3.24 - 3.26). The cyclic voltammetric study of these complexes was used to determine the rate constants corresponding to the reaction of the $19e^{-}$ and $38e^{-}$ species with the solvent in a manner similar to that outlined in Figure 3.11. The rate constant for this reaction, in addition to several thermodynamic parameters, was determined following the same procedure as described in Section 3.2.5.1 for a series of aliphatic sulfur bridged bimetallic complexes, $[3.9]^{2+}$ - $[3.12]^{2+}$. The kinetic data and activation parameters corresponding to complexes $[3.13]^{+}$, $[3.14]^{+}$ and $[3.15]^{2+}$ are summarized in Tables 3.6 - 3.8.

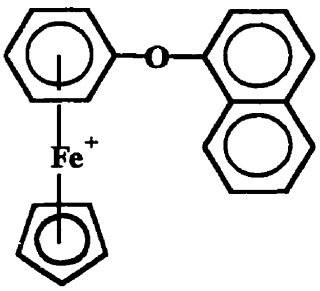

[3.13]+

Figure 3.24: Naphthol-capped oxygen-containing monometallic complex investigated with respect to its activation parameters

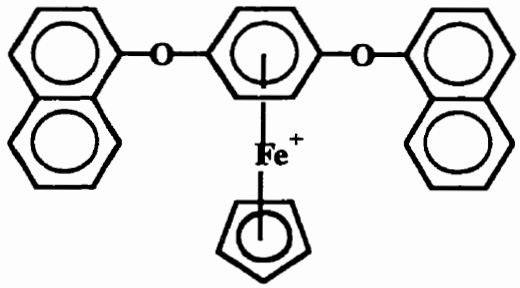

[3.14]+

Figure 3.25: Symmetrical naphthol-capped oxygen-containing monometallic complex investigated with respect to its activation parameters

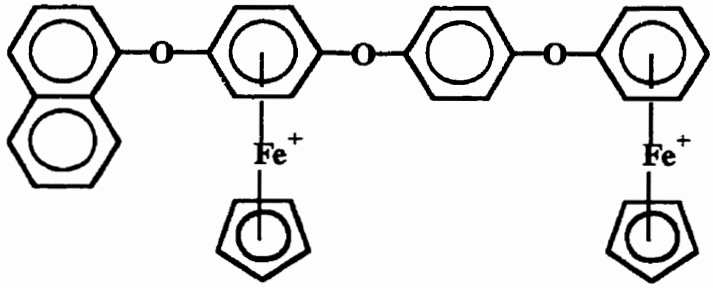

[3.15]2+

Figure 3.26: Naphthol-capped oxygen-containing bimetallic complex investigated with respect to its activation parameters

Table 3.6: Kinetic Data and Activation Parameters of Complex **[3.13]**$^{+}$

Temperature (K)	ln k_f	k_f (s^{-1})	Ea ($kJmol^{-1}$)	$\Delta G^{\ddagger}$ ($kJmol^{-1}$)	$\Delta H^{\ddagger}$ ($kJmol^{-1}$)	$\Delta S^{\ddagger}$ ($Jmol^{-1}K^{-1}$)
233	-0.7369	0.4786	8.2	61.2	6.1	-217.7
243	-0.3091	0.7341				
253	0.1913	1.2108				
263	-0.3941	0.6743				

Table 3.7: Kinetic Data and Activation Parameters of Complex **[3.14]**$^{+}$

Temperature (K)	ln k_f	k_f (s^{-1})	Ea ($kJmol^{-1}$)	$\Delta G^{\ddagger}$ ($kJmol^{-1}$)	$\Delta H^{\ddagger}$ ($kJmol^{-1}$)	$\Delta S^{\ddagger}$ ($Jmol^{-1}K^{-1}$)
233	-0.6234	0.5361	23.3	60.8	21.2	-156.4
243	0.0688	1.0712				
253	0.3966	1.4868				
263	0.7825	2.1870				

Table 3.8: Kinetic Data and Activation Parameters of Complex **[3.15]**$^{2+}$

Temperature (K)	ln k_f	k_f (s^{-1})	Ea ($kJmol^{-1}$)	$\Delta G^{\ddagger}$ ($kJmol^{-1}$)	$\Delta H^{\ddagger}$ ($kJmol^{-1}$)	$\Delta S^{\ddagger}$ ($Jmol^{-1}K^{-1}$)
233	-2.2377	0.1067	25.0	64.9	22.9	-165.9
243	-2.0303	0.1313				
253	-1.5502	0.2122				
263	-1.4275	0.2399				
273	-0.5221	0.5933				
283	0.0730	1.0757				

A significant increase in E_a and $\Delta H^{\ddagger}$ in the order $[\mathbf{3.13}]^{2+} < [\mathbf{3.14}]^{2+} < [\mathbf{3.15}]^{2+}$ is evident from Tables 3.6 - 3.8. Based on these observations, it may be generally stated that combination of the reactants in the formation of the corresponding activated complex takes place more efficiently in the case of the monometallic species. However, the most significant change in E_a and $\Delta H^{\ddagger}$ is observed with respect to monometallic complexes $[\mathbf{3.13}]^{+}$ and $[\mathbf{3.14}]^{+}$. Perhaps the $19e^{-}$ complex generated from $[\mathbf{3.14}]^{+}$ does not react as readily with the solvent as a result of the bulky naphthol substituents on either side of the metal moiety. In contrast, the structure of $[\mathbf{3.13}]^{+}$ would not be subject to any steric interference.

In comparing oxygen containing complexes, $[\mathbf{3.13}]^{+}$, $[\mathbf{3.14}]^{+}$, and $[\mathbf{3.15}]^{2+}$ with respect to the entropy of activation, it is observed that $\Delta S^{\ddagger}$ becomes more negative in the order $[\mathbf{3.13}]^{2+} < [\mathbf{3.15}]^{2+} < [\mathbf{3.14}]^{2+}$. This trend may be explained by the increased rigidity of the systems with an increased number of aromatic rings. It appears as though the bulky naphthol substituent has a significant impact on the nature of the transition state. It is observed that the greater the number of bulky naphthol substituents incorporated into the molecular structure, the more constrained the activated complex as compared to the reactants.

4.0 Scholl Polymerization

4.1 The Scholl Reaction

Section 1.4 of this work describes some methods that have been used in the past and others that are presently being developed for the preparation of polyethers and polythioethers. In particular, the Scholl reaction has demonstrated great promise in the preparation of both polyethers and polythioethers via the incorparation of oxygen and sulfur linkages as an integral part of the monomeric molecular structure.[148-156] The Scholl reaction involves the formation of an aryl-aryl bond as a result of the coupling between two aromatic groups in the presence of a Friedel-Crafts catalyst. A generic representation of the reaction is illustrated in Figure 4.1 and highlights the elimination of two aromatic hydrogens during the course of the reaction.

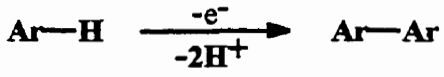

Figure 4.1: Aryl-Aryl bond formation by the Scholl Reaction

The Scholl reaction has been established as a general route to a wide variety of high molecular weight aromatic polyethers. The driving force behind the development of this synthetic strategy follows from the initial isolation of low molecular weight

poly(p-phenylene).[261] Subsequent synthetic investigations of this methodology have allowed for the preparation of higher molecular weight species from a variety of monomeric units. Terminal bis(1-naphthyloxy), bis(2-naphthyloxy), bis(phenoxy), and bis(phenylthio) monomers containing alkane, diethylene oxide and nonnucleophilic aromatic central units have all resulted in polymer formation to some degree.[148-156] The most thoroughly investigated and successful polymerizations were observed in the case of bis(1-naphthyloxy) monomers. This was explained with respect to the presence of the bulky binaphthyl group which increased the solubility of the growing polymer chain thereby reducing the likelihood of premature precipitation during polymerization. Many functional groups including ketones, sulfones, sulfones with fluorocarbons, and methylene groups have been successfully incorporated into the polymers resulting from the Scholl reaction of bis(1-naphthyloxy) monomers (Figure 4.2).[157] Additionally, high molecular weight polymers have been obtained from bis(1-naphthyloxy) monomers with totally aromatic central units.[157]

The reaction is typically conducted under oxidative reaction conditions via a cation-radical mechanism. Although a variety of oxidizing agents including Bronsted acids, oxidative Lewis acids, halogens, metal salts, electron-donor-acceptor complexes, irradiations, zeolite surfaces and anodic electrochemical oxidation have allowed for the coupling reaction to proceed, a stoichiometric amount of $FeCl_3$ in dry nitrobenzene remains the most commonly applied reaction condition.[157] The choice of solvent has also been shown to play an important role in the success of polymerization, since nucleophilic solvents such as THF and pyridine inhibit the reaction.

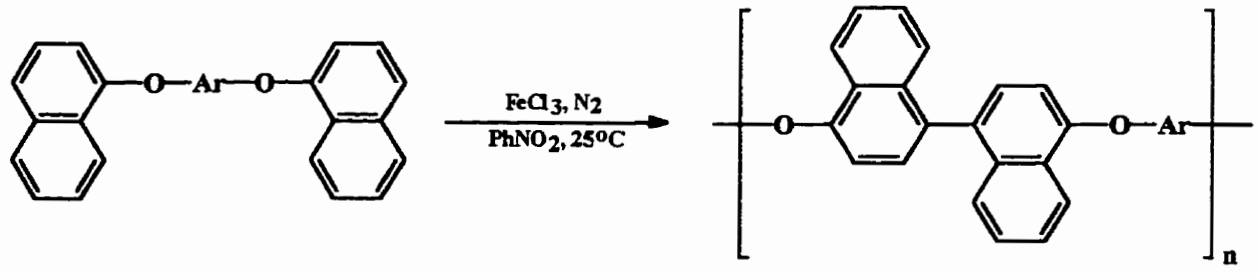

The following have been used as Ar Groups:

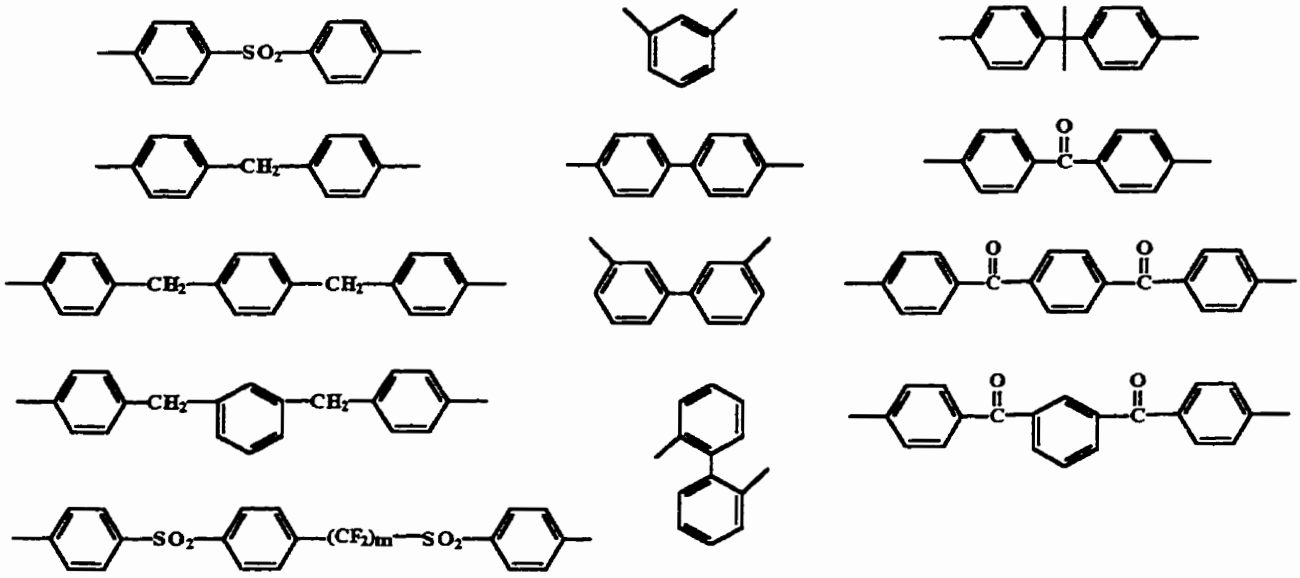

Figure 4.2: Bis(1,1'-binaphthoxy) monomers polymerized by the Scholl reaction

The polymerization of bis(1-naphthyloxy) monomers takes place with coupling at the C4 position of the 1-naphthyloxy group via a cation-radical mechanism as outlined in Figure 4.3.[152-153, 155, 157] The initial step of the reaction involves a single-electron transfer reaction of the aromatic species resulting in the formation of a cation-radical, **4.3c**. The

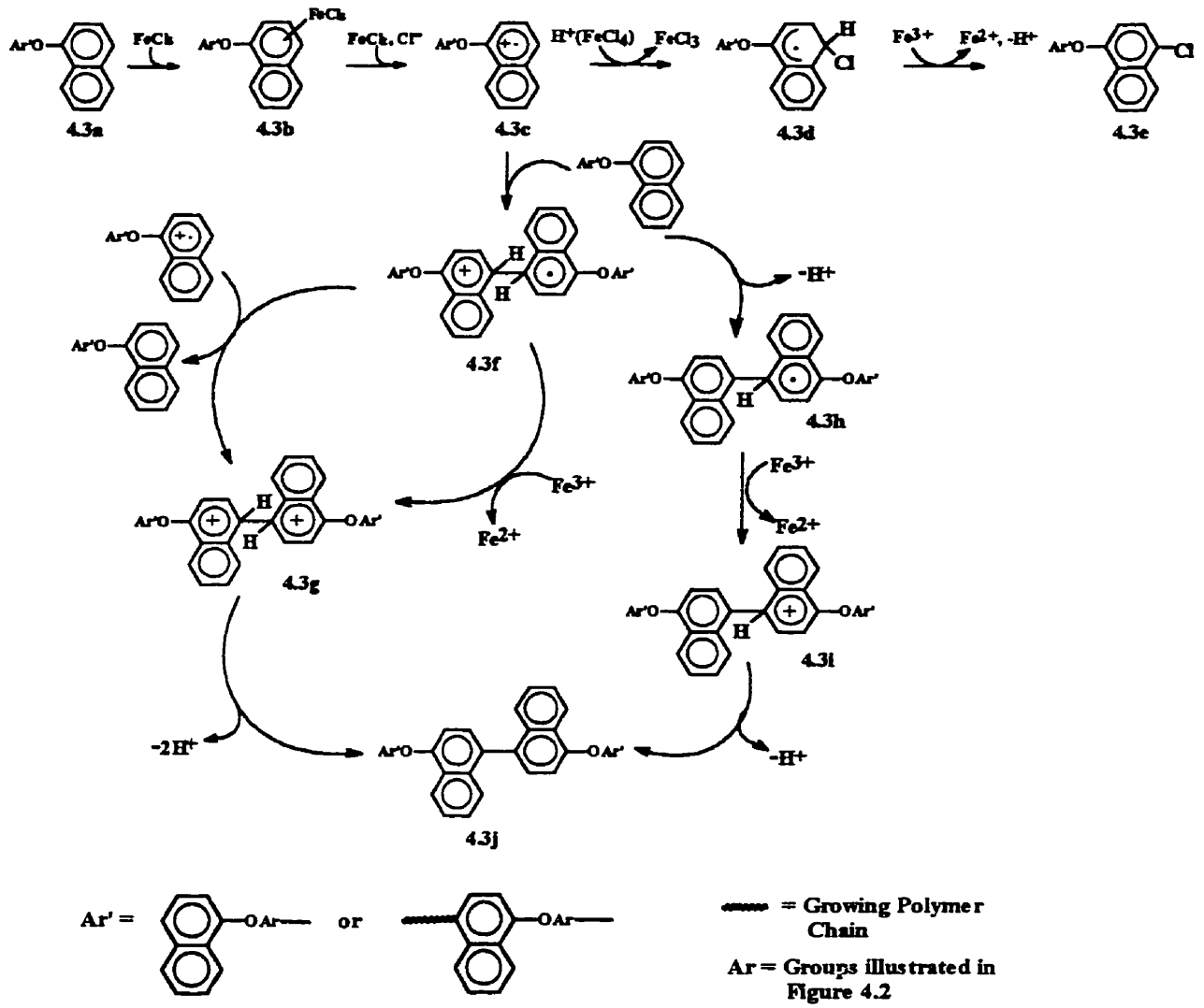

Figure 4.3: Mechanism of the Scholl Reaction

reaction proceeds via the dimerization of this species to the corresponding cation-radical dimer, **4.3f**. The eventual formation of dimer **4.3j** may now be a result by two distinct pathways. In one case, **4.3c** or $FeCl_3$ may act as oxidants in the formation of an intermediate dimeric species, **4.3g**. The subsequent elimination of two protons allows for

the generation of **4.3j**. Another route involves the loss of a proton from **4.3f** to give the corresponding dimeric radical, **4.3h**. This species may undergo an oxidation process yielding **4.3i** which, following the elimination of a second proton, gives the desired dimer **4.3j**. Subsequent reaction of the larger species following the same process is the essence of polymer propagation. Abstraction of Cl^- from $FeCl_4^-$ by cation-radical **4.3c** followed by oxidation of **4.3d** and the loss of a proton results in the generation of a chain end and termination of the polymerization process.

4.2 Results and Discussion

Based on the discussion in Section 1.4, it is evident that numerous synthetic methods exist for the preparation of polyethers and polythioethers. However, in many respects the Scholl reaction represents one of the most attractive routes due to its versatility with respect to the monomers which may be employed, the availability of those monomeric units as well as its relatively mild reaction conditions.[148-157] The monomers utilized in the present study were selected with the intention of investigating the impact that the incorporation of various functional groups would have on polymerization. Functionalities incorporated in the monomeric structure included para- linked aromatic spacers, bulky naphthyl groups or aliphatic bridges. Several reaction conditions including monomer concentration, monomer:catalyst ratio and time were examined with respect to individual monomers.

4.2.1 Monomer Synthesis

4.2.1.1 Preparation of Bimetallic Complexes with Terminal Chlorines

The preparation of five different monomeric units was achieved by a three step process which exploited the activation of (chloroarene)$CpFe^+$ complexes toward nucleophilic aromatic substitution reactions with various dinucleophiles. The production of monomers suitable for polymerization using typical Scholl reaction conditions began with the preparation of bimetallic $CpFe^+$ complexes with terminal chlorine substituents in the para position. Reaction of these complexes in the presence of an excess of 1-naphthol followed by photolytic demetallation resulted in the isolation of monomers with terminal naphthyl groups which, as mentioned previously, are ideal for polymerization via the Scholl reaction. Scheme 4.1 outlines the experimental details utilized in the preparation of the initial bimetallic complexes and shows the variety of functional groups which were incorporated into the monomeric units. Preparation of the chlorine terminated bimetallic $CpFe^+$ complexes followed a strategy similar to that used in the preparation of the sulfur containing bimetallic complexes as outlined in Sections 2.2.2 and 2.2.3 of this work. A 2:1 molar ratio of η^6-(1,4-dichlorobenzene)-η^5-(cyclopentadienyliron) hexafluorophosphate and the desired nucleophile are reacted in the presence of an excess of K_2CO_3 in a THF/DMF solvent mixture under a nitrogen atmosphere resulting in the generation of the corresponding bimetallic complex, **2.29** and **4.1-4.4** (Scheme 4.1). The ^1H and ^{13}C NMR spectra of complex **4.3** are shown in Figures 4.4 and 4.5, respectively.

The symmetrical nature of bimetallic $CpFe^{+}$ complexes prepared in the above mentioned procedure have been discussed previously. It is well recognized then that a strong resonance representative of the cyclopentadienyl component of these complexes is a characteristic feature of the NMR spectra. Figure 4.4 illustrates the ^{1}H NMR spectrum of complex **4.3** and shows the intense peak arising from the Cp protons at 5.13 ppm. The complexed aromatic protons appear clearly as two doublets at 6.03 and 6.50 ppm, as would be expected for para substitution of the aromatic ring. The remainder of the resonances representative of this complex appear further upfield as a result of their aliphatic character. It is important to note that, in the case of complexes **4.1, 4.2** and **4.4**, ^{1}H NMR spectra would differ significantly from that of complex **4.3** due to the aromatic constituents of their bridges. The spectral features of these complexes are dominated by resonances downfield from the Cp resonance. Specifically, two distinct aromatic regions are evident with the peaks of the complexed aromatic protons appearing upfield in comparison to their uncomplexed counterparts. The ^{13}C NMR spectrum of complex **4.3** is shown in Figure 4.5. The spectral separation of the peaks into two distinct regions of the spectrum characterizes the structural features of complex **4.3**. In short, the spectrum is separated into the aliphatic components of its structure, whose peaks appear between 24.11 to 47.56 ppm. Those resonances representative of the aromatic constituents of complex **4.3** appear further downfield with the Cp carbons resonating at 77.93 ppm and the complexed aromatic carbons appearing at 102.17 and 127.33 ppm. The spectral features of complexes **4.1, 4.2** and **4.4** again differ slightly from those of complex **4.3** due to the aromatic nature of their linkages. The NMR, IR data and yields of complexes **2.29**

and **4.1-4.4** are summarized in Tables 2.2, 2.3, 4.1 and 4.2 and support the identification of the respective complexes.

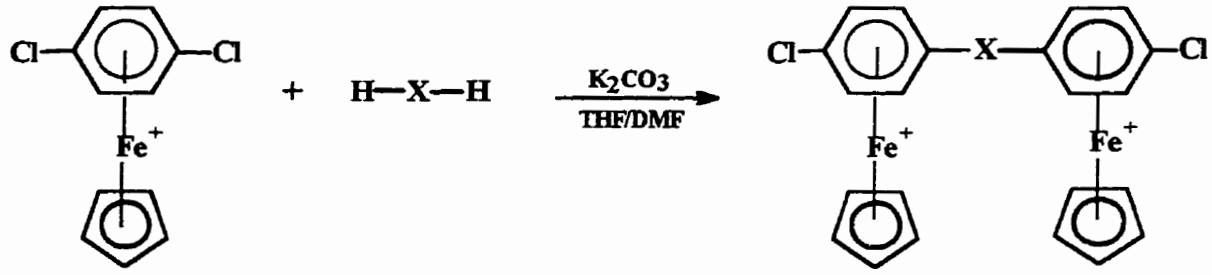

X = **4.1**

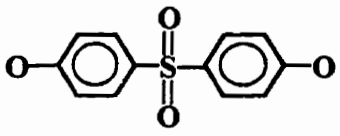

4.2

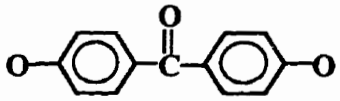

2.29 S—$(CH_2)_4$—S

4.3

4.4

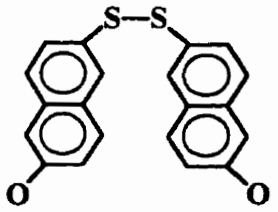

Scheme 4.1

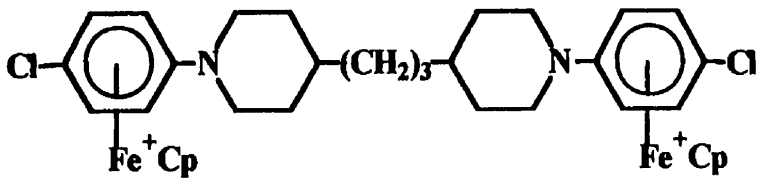

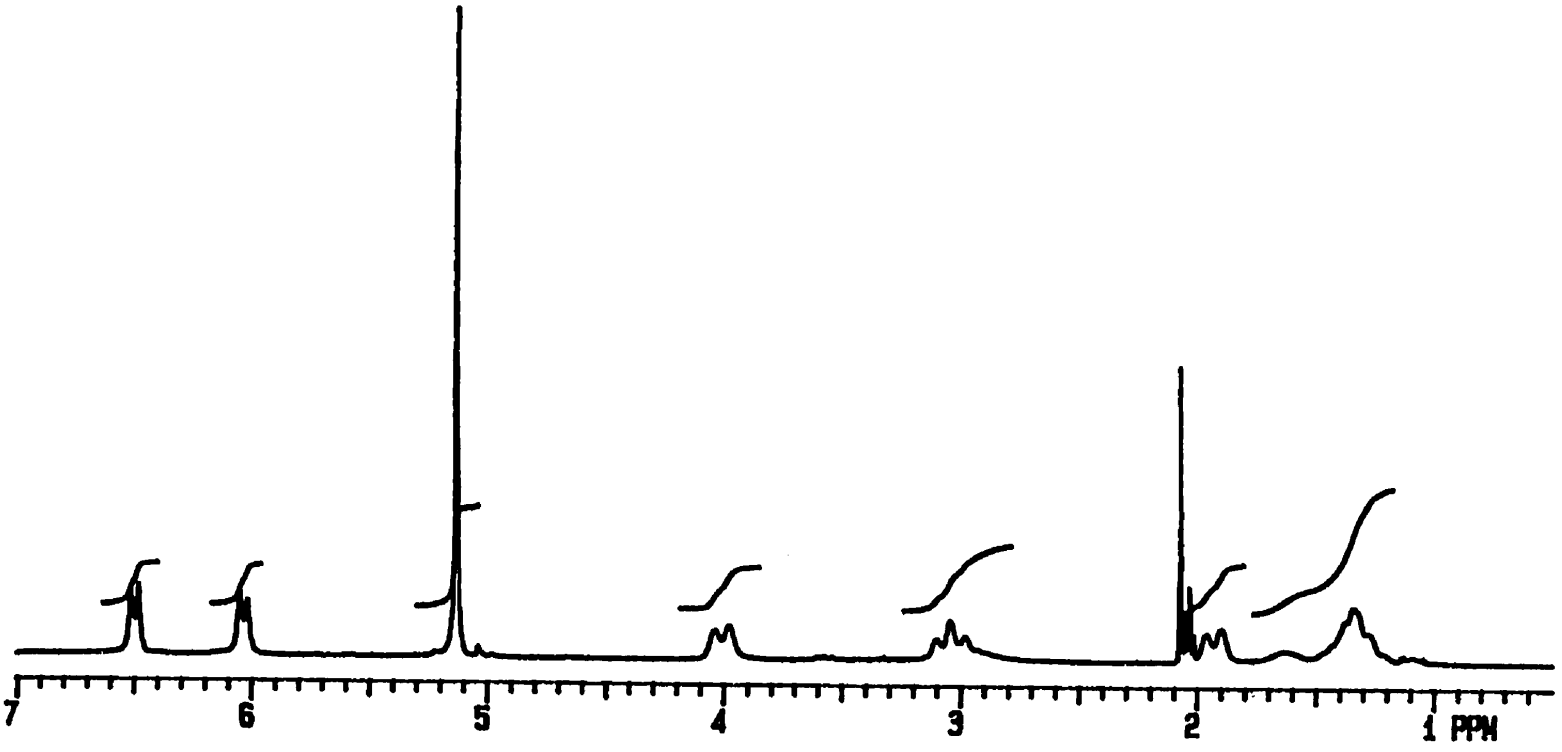

Figure 4.4: ^{1}H NMR spectrum of complex **4.3** in acetone-d_6.

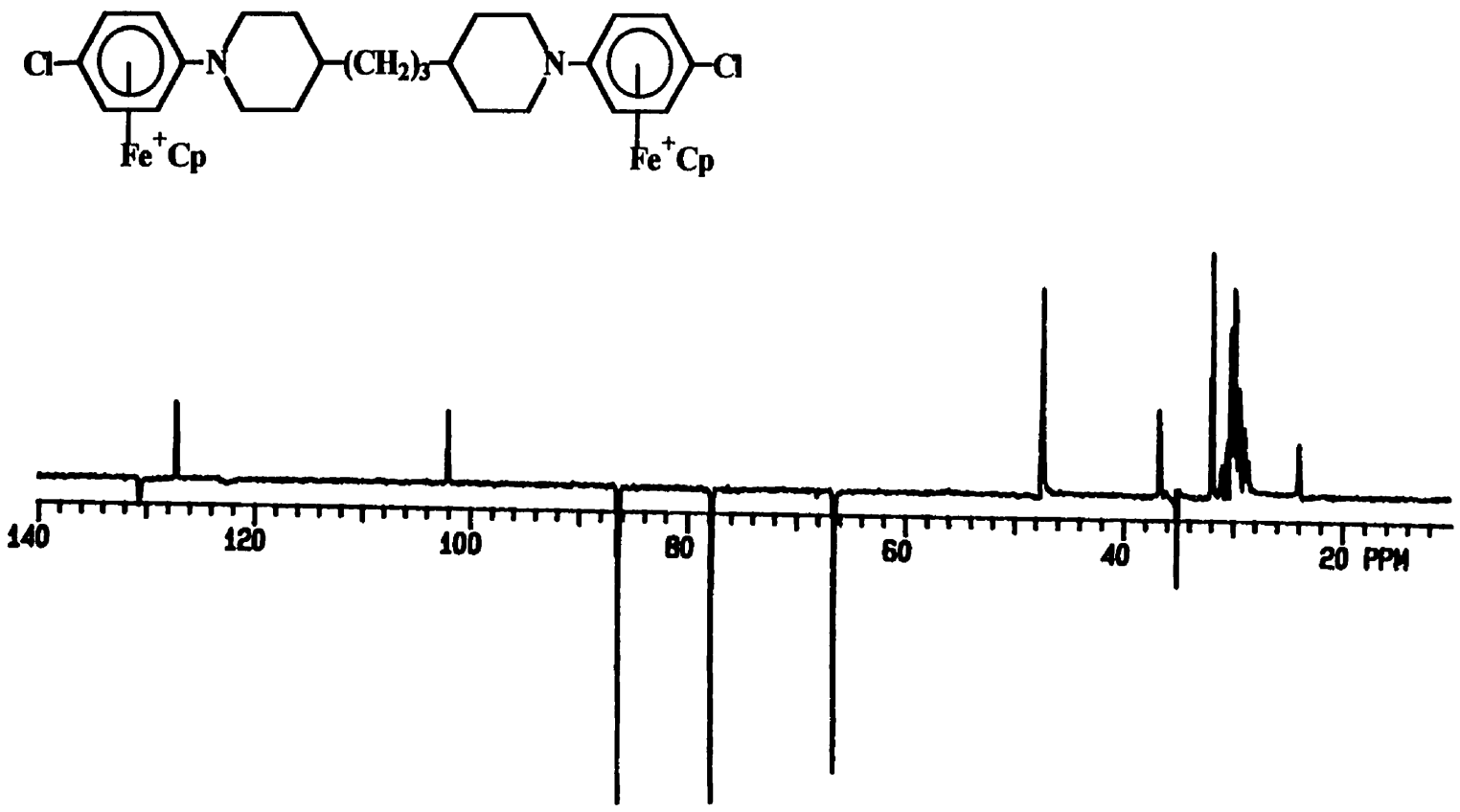

Figure 4.5: ^{13}C NMR spectrum of complex **4.3** in acetone-d_6.

Table 4.1: ^{1}H NMR Data of Diiron Complexes **4.1-4.4**

δ (acetone-d_6), ppm				
Complex	**Cp (s, 10H)**	**Complexed Aromatic[a]**	**Uncomplexed Aromatic[a]**	**Others[a]**
4.1	5.42	6.68 (d, 4H, J = 6.9) 6.87 (d, 4H, J = 6.8)	7.56 (d, 4H, J = 8.9) 8.15 (d, 4H, J = 8.8)	
4.2	5.42	6.65 (d, 4H, J = 6.2) 6.87 (d, 4H, J = 6.3)	7.51 (d, 4H, J = 8.4) 7.95 (d, 4H, J = 8.4)	
4.3	5.13	6.03 (d, 4H, J = 7.2) 6.50 (d, 4H, J = 7.2)		1.26-1.38 (m, 10H, CH_2) 1.61-1.63 (m, 2H, CH) 1.91-1.97 (m, 4H, CH_2) 3.05 (t, 4H, J = 12.5, CH_2) 4.01 (d, 4H, J = 11.9, CH_2)
4.4	5.40	6.58 (d, 4H, J = 6.9) 6.83 (d, 4H, J = 6.8)	7.53 (dd, 2H, J = 2.4, 8.8) 7.78-7.83 (m, 2H) 7.89-7.90 (m, 2H) 8.00 (d, 2H, J = 8.7) 8.11 (d, 2H, J = 8.9) 8.29 (br.s., 2H)	

[a] J values in Hertz.

Table 4.2: ^{13}C NMR and IR Data and Yields of Diiron Complexes **4.1-4.4**

δ (acetone-d_6), ppm						
Complex	**Yield (%)**	**Cp (s, 10H)**	**Complexed Aromatic**	**Uncomplexed Aromatic**	**Others**	**ν_{max} (cm^{-1})**
4.1	93.6	80.56	78.81, 87.69, 105.23*, 131.59	121.46, 131.21, 139.22*, 158.42*		1153 1266 (SO_2)
4.2	91.4	80.83	78.43, 88.10, 105.35*, 132.67*	121.28, 133.55, 136.17*, 157.63*	194.16 (CO)	1655 (CO)
4.3	73.5	77.93	66.67, 86.54, 102.17*, 127.33*		24.11 (CH_2) 32.04 (CH_2) 35.24 (CH) 36.82 (CH_2) 47.56 (CH_2)	1255 (CN)
4.4	88.6	81.04	78.10, 88.31, 105.50*, 133.00*	119.00, 122.30, 127.70, 127.90, 130.63, 132.12, 133.82*, 134.71*, 135.46*, 152.67*		

* Quaternary carbon.

4.2.1.2 1-Naphthol Capped Bimetallic Complexes

The presence of the terminal chlorine substituents in complexes **2.29** and **4.1-4.4** makes them reactive toward further nucleophilic aromatic substitution with excess 1-naphthol, giving the corresponding capped 1-naphthoxy bimetallic $CpFe^{+}$ complexes. The reaction of complexes **2.29** and **4.1-4.4** with 1-naphthol in the presence of K_2CO_3 as the base in a THF/DMF solvent mixture allowed for the preparation of the desired capped bimetallic complexes according to Scheme 4.2.

Complexes **4.5-4.9** were isolated as yellow solids in 77.0 - 81.3 % yield via filtration following their precipitation in 10% HCl. The identity of complexes **4.5-4.9** was determined using NMR and IR techniques as summarized in Tables 4.3 and 4.4. In comparing the spectra of complexes **2.29** and **4.1-4.4** with their capped 1-naphthoxy counterparts, **4.5-4.9**, the appearance of an abundance of resonances in the region of the spectrum characteristic of uncomplexed aromatic peaks is the most outstanding feature. The ^{1}H NMR spectra of complexes **4.3** and **4.8** are shown in Figures 4.4 and 4.6, respectively. The obvious change in the spectral pattern is the appearance of several peaks between 7.3-8.2 ppm attributed to the presence of the uncomplexed aromatic structure of the terminal naphthyl groups. Considering complex **4.8** specifically, the presence of the naphthyl groups is easily identified by comparing the spectrum with the spectral features of complex **4.3**. Similar changes in the ^{13}C NMR spectra verified the success of the 1-naphthol capping reaction with a series of peaks appearing above and below the baseline between 116.15-135.95 ppm.

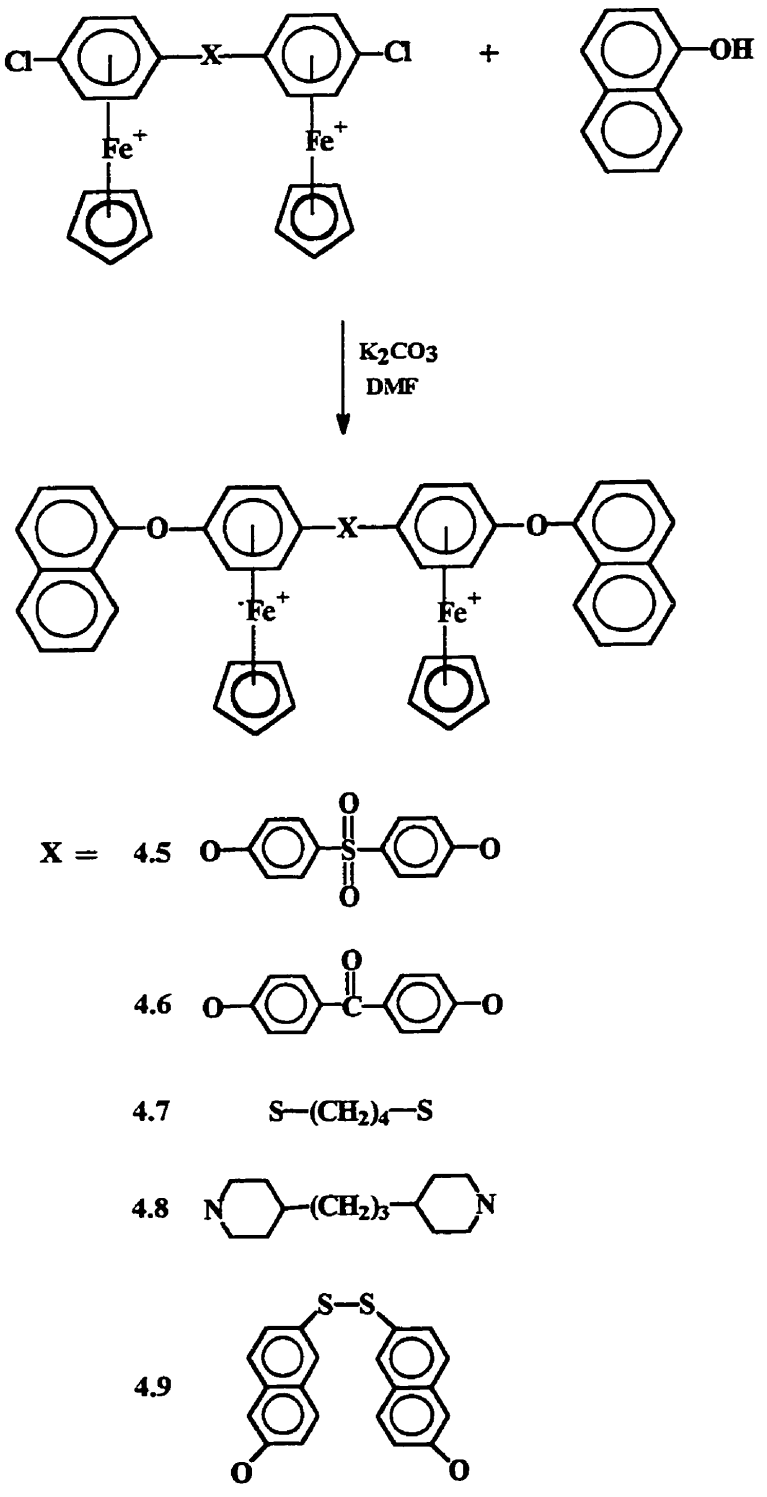
Cl
X
Cl
Fe+
Fe+
+
OH
K2CO3
DMF
O
X
O
Fe+
Fe+
X =
4.5
O
S
O
O
O
4.6
O
C
O
O
4.7
S—(CH2)4—S
4.8
N
(CH2)3
N
4.9
S—S
O
O

Scheme 4.2

In the case of complexes **4.5, 4.6** and **4.9**, the presence of the terminal naphthyl groups is evident by an increase of resonances in the uncomplexed aromatic region of the spectra. It is important to note that, for these complexes, the identification of the peaks representative of individual naphthyl protons is complicated by the overlapping of the uncomplexed aromatic peaks of the bridging ligand.

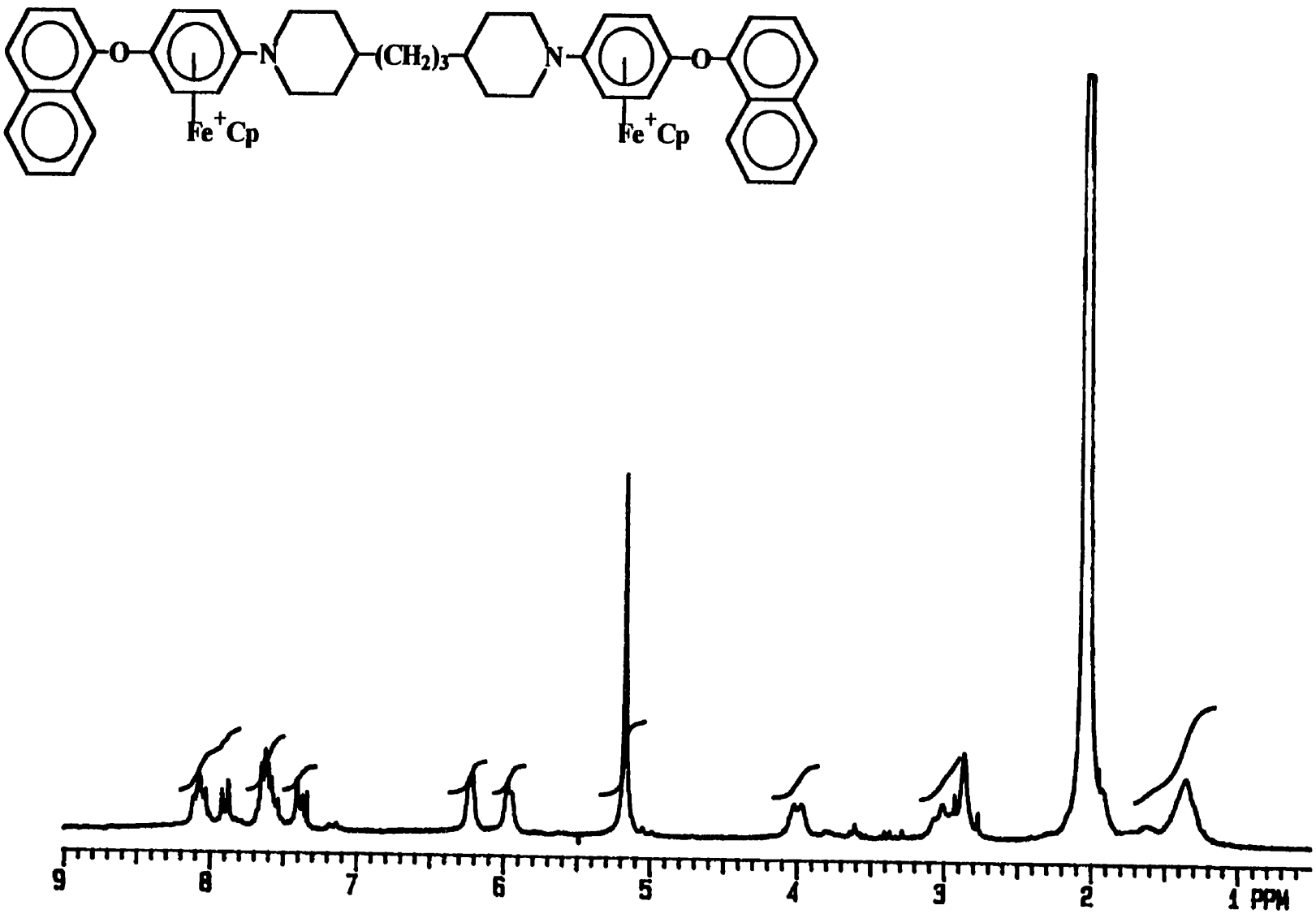

Figure 4.6: ^{1}H NMR spectrum of complex **4.8** in acetone-d_6.

Table 4.3: ^{1}H NMR Data of Capped 1-Naphthol Diiron Complexes **4.5-4.9**.

δ (acetone-d_6), ppm				
Complex	**Cp (s, 10H)**	**Complexed Aromatic[a]**	**Uncomplexed Aromatic[a]**	**Others[a]**
4.5	5.37	6.47-6.54 (m, 8H)	7.44-7.47 (m, 6H) 7.62-7.65 (m, 6H) 7.93 (d, 2H, J = 7.7) 8.02-8.08 (m, 8H)	
4.6	5.41	6.55 (s, 8H)	7.46-7.65 (m, 12H) 7.93-8.09 (m, 10H)	
4.7	5.42	6.46-6.55 (m, 8H)	7.44-7.48 (m, 2H) 7.58-7.64 (m, 6H) 7.92-8.09 (m, 6H)	1.88-2.00 (m, 4H, β-CH_2) 3.34-3.37 (m, 4H, α-CH_2)
4.8	5.17	5.96 (d, 4H, J = 5.9) 6.23 (d, 4H, J = 5.8)	7.34-7.41 (m, 2H) 7.54-7.65 (m, 6H) 7.90 (d, 2H, J = 7.9) 8.03-8.12 (m, 4H)	1.29-1.50 (m, 10H, CH_2) 1.62-1.66 (m, 2H, CH) 1.91-1.98 (m, 4H, CH_2) 2.95-3.09 (m, 4H, CH_2) 3.95-4.00 (m, 4H, CH_2)
4.9	5.38	6.47 (s, 8H)	7.42-7.66 (m, 10H) 7.75-8.09 (m, 14H) 8.23 (br.s., 2H)	

[a] J values in Hertz.

Table 4.4: ^{13}C NMR and IR Data and Yields of Capped 1-Naphthol Diiron Complexes **4.5-4.9**.

δ (acetone-d_6), ppm						
Complex	**Yield (%)**	**Cp (s, 10H)**	**Complexed Aromatic**	**Uncomplexed Aromatic**	**Others**	**ν_{max} (cm^{-1})**
4.5	81.3	79.54	76.56, 78.38, 126.60*, 135.93*	116.52, 121.25, 121.71, 126.85, 127.07, 128.05, 129.12, 129.26*, 131.40, 132.49*, 139.06*, 150.33*, 159.36*		1106 1266 (SO_2)
4.6	78.3	78.29	75.57, 76.57, 125.40*, 134.08*	115.99, 119.74, 120.82, 126.18, 127.31, 128.33, 128.67*, 130.79*, 132.40, 134.73*, 149.42*, 157.47*,	193.34 (CO)	1650 (CO)
4.7	78.3	78.29	75.61, 82.32, 105.23*, 131.09*	115.96, 120.38, 125.03*, 125.78, 126.85, 127.94, 134.31*, 148.53*	26.81 (CH_2) 30.64 (CH_2)	
4.8	77.0	76.96	65.72, 75.96, 129.62*, 135.95*	116.15, 121.89, 125.62*, 126.42, 126.84, 127.71, 127.96, 129.07, 135.95*, 151.24*	24.20 (CH_2) 32.30 (CH_2) 35.32 (CH) 36.96 (CH_2) 47.97 (CH_2)	1265 (CN)
4.9	79.2	79.21	76.46, 96.54*, 131.98*	116.80, 118.13, 121.70, 121.79, 126.65*, 126.82, 126.90, 127.23, 127.39, 127.94, 128.04, 129.12, 129.29, 132.29*, 134.17*, 134.75*, 135.97*, 150.50*, 152.66*		

* Quaternary carbon.

4.2.1.3 Preparation of Scholl Monomers by Photolytic Demetallation

It was mentioned previously that one of the most favorable techniques for the liberation of modified ligands from their corresponding complexes is photolytic demetallation. The dissolution of the desired complex in an CH_3CN/CH_2Cl_2 solvent mixture followed by irradiation under a xenon lamp for 4 hours allowed the isolation of the free organic ligand.[45, 76-77] Purification by column chromatography or extraction techniques gave the desired compound as a white or pale yellow solid or oil in good yield. The structures of the monomers investigated are outlined in Scheme 4.3. Several techniques including ^1H and ^{13}C NMR, IR, MS and melting points were utilized in the characterization of the monomeric units (Tables 4.5 and 4.6).

The preparation of the desired organic species is most clearly indicated by the ^1H and ^{13}C NMR spectra. Complexes **4.13** and **4.14** will be discussed in some detail in an attempt to discern the features of these compounds. The aromatic region of the NMR spectra is less complicated then the aliphatic component of complex **4.13**, and as a result has been selected to exemplify the distinguishing features of the photolytic process with respect to 1-naphthol capped monomers. The ^1H and ^{13}C NMR spectra of compound **4.13** are shown in Figures 4.7 and 4.8, respectively. In comparing the ^1H NMR spectra of complexes **4.8** and **4.13** in Figures 4.6 and 4.7, the most significant spectral change is the disappearance of the resonance at 5.17 ppm, representative of the cyclopentadienyl ring. A similar observation is made in the case of the ^{13}C NMR where the cyclopentadienyl carbon resonance is originally seen at 79.96 ppm in the complexed species but is absent in

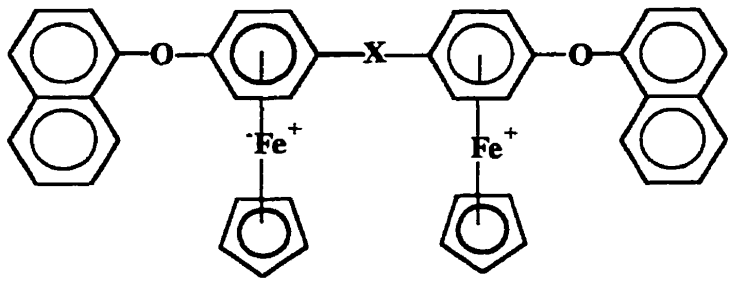

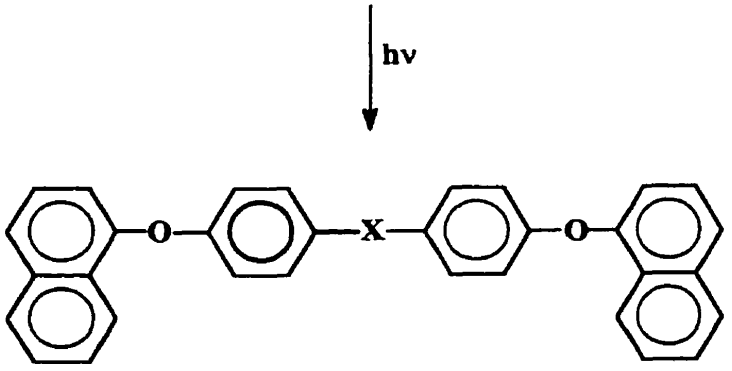

X =

4.10 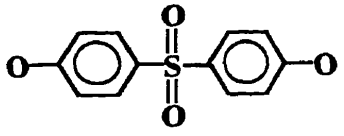

4.11 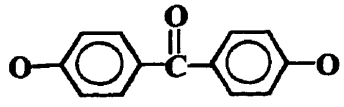

4.12 

4.13 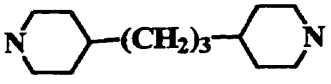

4.14 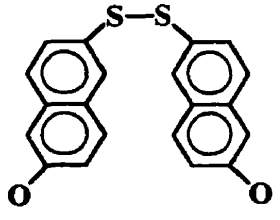

Scheme 4.3

the spectrum shown in Figure 4.8. A more subtle spectral change which is observed upon the photolytic cleavage of the pendent metal moiety is the downfield shift of the aromatic peaks. Figure 4.6 shows the ^{1}H NMR spectrum of complex, **4.8**. It is important to note that the benzenoid protons of this complex appear as two doublets at 5.95 and 6.25 ppm. Following the exposure of this complex to photolytic demetallation, the resonance representative of these protons collapsed to a strong singlet located at 6.98 ppm. The remainder of the peaks in this region are attributed to the presence of the 1-naphthyl constituents and have been assigned in accordance with previous studies conducted by Percec.[152] The structure of compound **4.13** is labeled in Figure 4.7 to simplify the discussion of peak identity. As illustrated in the figure, the protons labeled H2 in the figure appear as a doublet and are shifted furthest upfield of all the aromatic protons. The strong singlet at 6.98 ppm corresponds to those aromatic protons (A and B) which are not included in the 1-naphthoxy unit of the monomer. The peak representing the H3 protons typically appears as a triplet, and in the case of compound **4.13,** is found at 7.31 ppm. Finally, a series of multiplets in the regions of 7.47-7.55, 7.82-7.86 and 8.27-8.31 ppm are attributed to protons H4, H6 and H7, H5 and H8, respectively. It is important to take particular interest in the peaks of protons H5 and H8, since these resonances are the most distinguishing resonances following polymerization.

Figure 4.8 shows the ^{13}C NMR spectrum of compound **4.13** and helps to verify the isolation of the pure organic compound as a result of the disappearance of the Cp resonance at 76.96 ppm, as well as a significant downfield shift of the complexed aromatic carbons from 65.72 and 75.96 ppm to 118.13 and 120.26 ppm, respectively, upon removal of the pendent metallic moiety. Although the 1-napthoxy rings typically appear as a series

of seven resonances,[148-156] in the case of compound **4.13**, only six peaks are observed. An intense peak appears at 122.10 ppm and is attributed to two carbons. On the other hand, Figure 4.9 shows the carbon spectrum of compound **4.12** in which the resonances signifying the presence of the 1-naphthoxy rings are clearly observed as 7 resonances appearing below the baseline at 113.61, 121.89, 123.54, 125.67, 125.93, 136.55, and 126.68 ppm. The identity of these peaks is further supported by their small intensity as compared to the only other aromatic rings within this structure which would be expected to be of greater intensity and appear at 118.87 and 132.19 ppm.

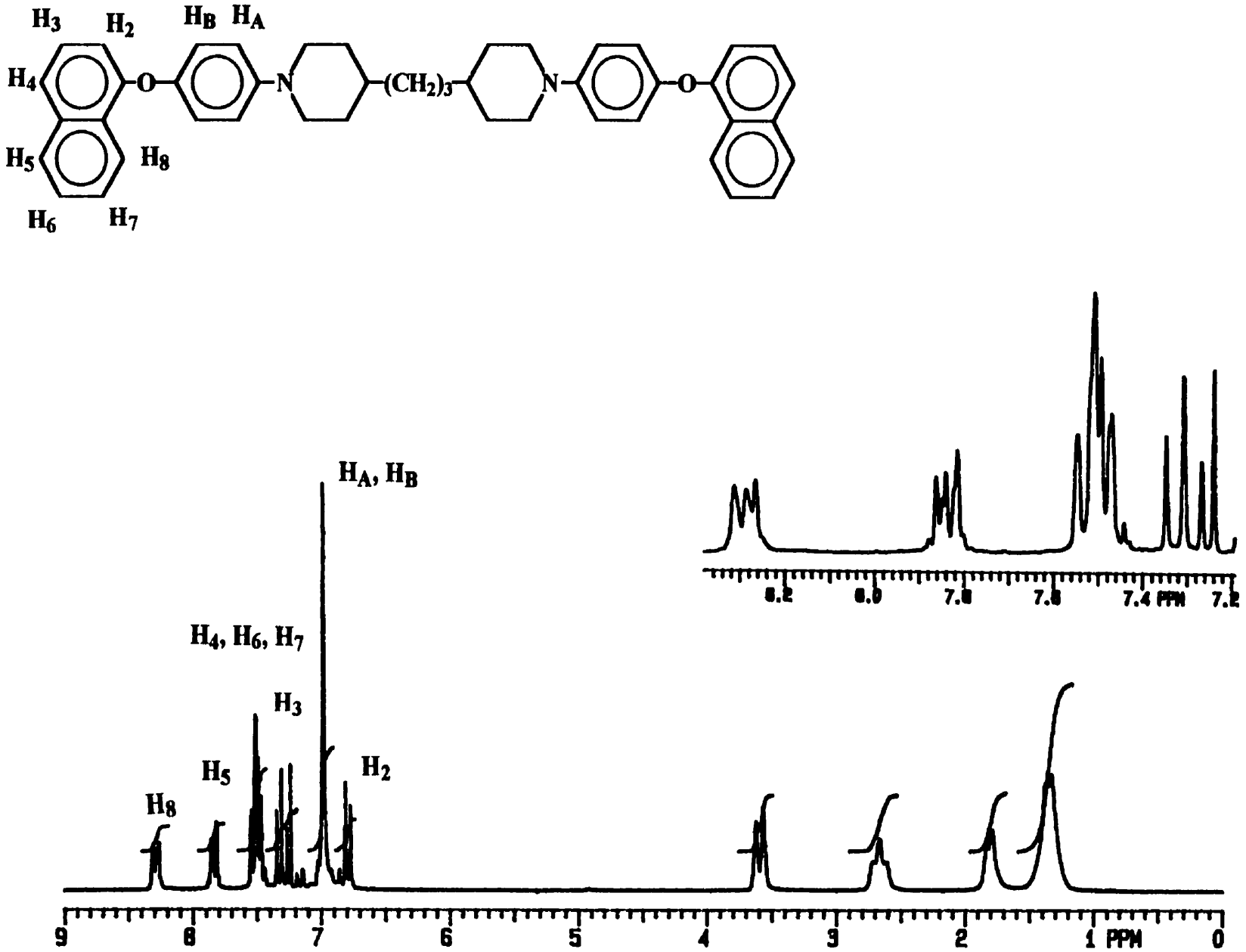

Figure 4.7: ^{1}H NMR spectrum of compound **4.13** in $CDCl_3$.

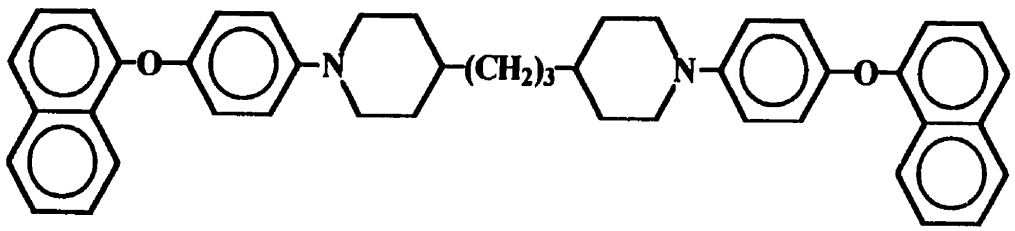

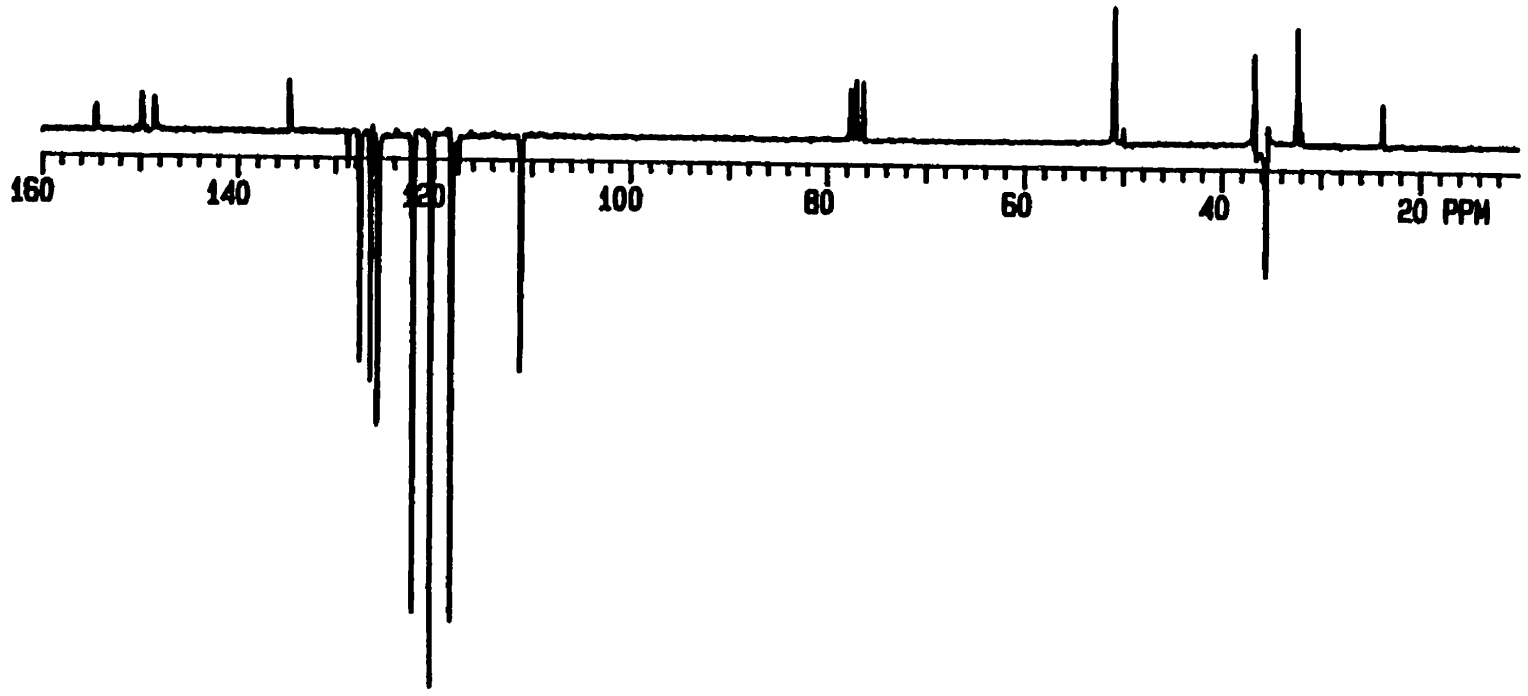

Figure 4.8: ^{13}C NMR spectrum of compound **4.13** in $CDCl_3$.

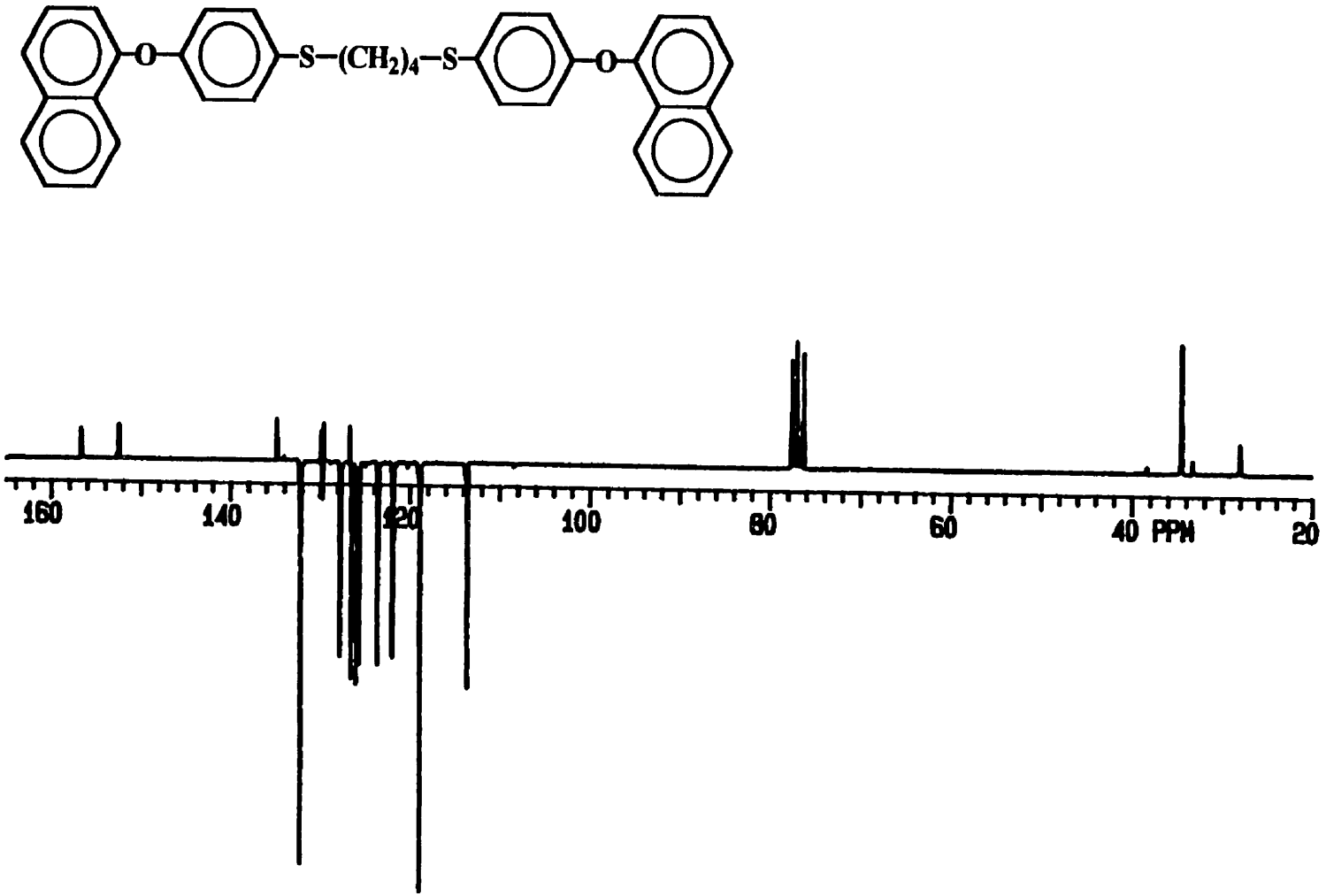

Figure 4.9: ^{13}C NMR spectrum of compound **4.12** in $CDCl_3$.

Table 4.5: ^{1}H NMR and IR Data and Yields of Compounds **4.10-4.14**.

δ ($CDCl_3$), ppm				
Complex	**Yield (%)**	**Aromatic**[a]	**Others**[a]	ν_{max} (cm^{-1})
4.10	85.6	6.74-7.38 (m, 14H) 7.38 (t, 2H, J = 7.8) 7.48-7.54 (m, 4H) 7.61-7.65 (d, 2H, J = 7.2) 7.83-7.87 (m, 6H) 8.16-8.21 (m, 2H)		1105 1258 (SO_2)
4.11	82.5	6.93-7.11 (m, 12H) 7.38 (t, 2H, J = 7.7) 7.48-7.56 (m, 4H) 7.62 (d, 2H, J = 8.2) 7.76-7.91 (m, 8H) 8.19-8.23 (m, 2H)		1655 (CO)
4.12	75.4	6.94 (d, 6H, J = 8.3) 7.20-7.40 (m, 6H) 7.45-7.50 (m, 4H) 7.61 (d, 2H, J = 8.1) 7.84-7.88 (m, 2H) 8.12-8.16 (m, 2H)	1.73 (br.s., 4H, β-CH_2) 2.85 (br.s., 4H, α-CH_2)	
4.13	71.3	6.79 (d, 2H, J = 7.5) 6.98 (s, 8H) 7.31 (t, 2H, J = 7.9) 7.47-7.55 (m, 6H) 7.82 -7.86 (m, 2H) 8.27-8.31 (m, 2H)	1.32-1.37 (br.s, 12H, CH & CH_2) 1.79-1.83 (br.s., 4H, CH_2) 2.66 (t, 4H, J = 9.8, CH_2) 3.59 (d, 4H, J = 11.1, CH_2)	1261 (CN)
4.14	81.1	6.94-7.07 (m, 4H) 7.18-7.49 (m, 8H) 7.51-7.74 (m, 12H) 7.85-7.95 (m, 6H) 8.21-8.25 (m, 2H)		

[a] J values in Hertz.

Table 4.6: ^{13}C NMR and MS Data and Melting Points of Compounds **4.10-4.14**.

δ ($CDCl_3$), ppm				
Complex	**m.p. (°C)**	**Aromatic**	**Others**	**m/z (M^+)**
4.10	107-109	113.34, 117.29, 120.00, 121.86, 123.63, 125.74, 126.06, 126.70, 127.82, 128.71, 134.93*, 135.24*, 150.06*, 152.92*, 154.90*		686 (100)
4.11	88-90	112.91, 116.55, 119.93, 121.49, 121.76, 123.28, 125.61, 125.87, 126.52, 127.64, 131.87*, 132.11, 134.75*, 150.64*, 152.99*, 154.22*, 161.58*	193.97 (CO)	650 (100)
4.12	88.5-91	113.61, 118.87, 121.89, 123.54, 125.67, 125.93, 126.55, 126.68*, 127.71, 129.70*, 132.19, 134.83*, 152.60*, 156.77*	28.02 (β- CH_2) 34.53 (α-CH_2)	558 (12)
4.13	121-124	118.13, 120.26, 122.10, 125.62, 125.73, 126.47, 127.58, 134.76*, 148.56*, 149.87*, 154.53*	23.82 (CH_2) 32.39 (CH_2) 35.54 (CH) 36.74 (CH_2) 50.94 (CH_2)	646 (100)
4.14	118-120	112.66, 112.88, 120.16, 120.27, 120.88, 121.94, 123.18, 125.72, 125.93, 126.63, 126.95, 127.19, 127.74, 128.08, 129.46, 129.92*, 132.79*, 133.51*, 134.88*, 152.07*, 153.42*, 153.66*, 156.20*		---

* Quaternary carbon.

4.2.2 Polymerization via the Scholl Reaction

Until recently, the most common routes for the preparation of thermally stable polyethers and polythioethers focused on the use of nucleophilic and electrophilic techniques. As the field of polymer chemistry has evolved, a variety of innovative synthetic strategies have been developed which have proven instrumental in expanding the repertoire of materials available for a limitless number of applications. One such method which has been of particular interest to Virgil Percec and his coworkers is the Scholl reaction.[148-157] These researchers have demonstrated that a variety of factors including monomer structure and solubility, monomer/catalyst ratio, solution concentration and reaction time may all play significant roles in the polymerization process. In this work, investigation of the Scholl reaction follows a similar strategy while utilizing monomeric species which incorporate either ketone, sulfonyl, thioether or amine bridges as an integral part of their molecular structure.

Scheme 4.4 illustrates the structure of the polymers which result from the Scholl polymerization of monomers **4.10 - 4.14**. It is important to note that according to the mechanism presented in Figure 4.3, carbon-carbon bond formation takes place through the C4 carbon of the naphthyl ring resulting in a linear polymer structure. In all cases, polymerization was carried out following reaction conditions similar to those established previously by Percec and coworkers. Typically, the monomer was dissolved in $PhNO_2$ in a round-bottom flask equipped with a stirbar. In some cases, dissolution of the monomer required the addition of heat. The catalyst solution, prepared in a similar manner in $PhNO_2$, was then added over a 20 minute period via a syringe penetrating a septum and

under a nitrogen atmosphere. Slow addition of the catalyst solution was crucial to control the rate of polymerization. Precipitation of the crude polymer in methanol acidified with 2% HCl followed by filtration allowed for the isolation of the desired polymer. The polymers were then dissolved in a minimal amount of chloroform and re-precipitated in acidified acetone. Purification of the polymeric materials was necessary for the removal of any low molecular weight species which may have formed during the polymerization. This study, therefore, focuses on the investigation of the purified polymers only.

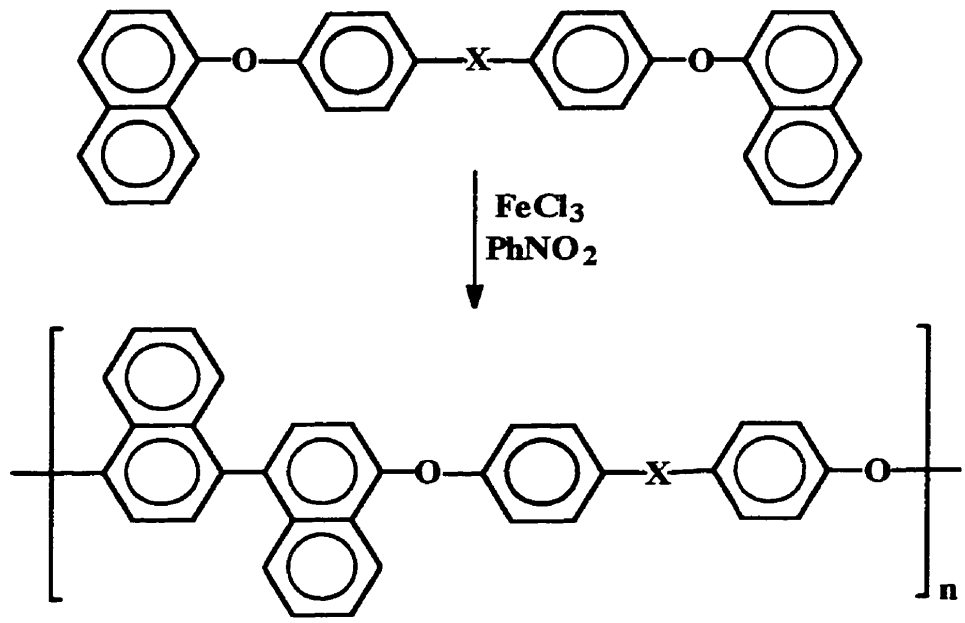

X =

4.15 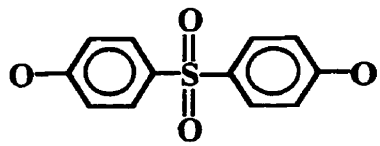

4.16 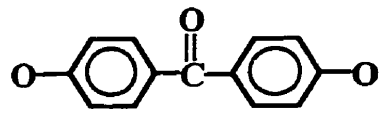

4.17 

4.18 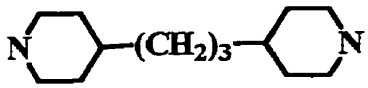

4.19 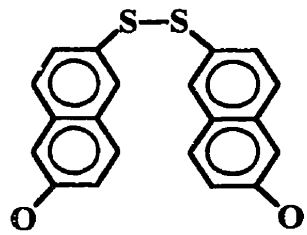

Scheme 4.4

NMR analysis proved to be extremely useful in confirming polymerization. Now, due to the complexity of some of the monomeric units, especially in the aromatic region of the spectra, it is extremely difficult to assign each resonance specifically. However, distinct changes in the NMR spectra have been identified as indicative of polymerization and are traditionally used to determine the success of the reaction. Perhaps the simplest manner in which to discuss the spectral characteristics upon polymerization is by comparison of the ^{1}H and ^{13}C spectra of the polymer with that of the monomer from which it originated. A clear discussion is most easily achieved by the identification of each of the carbon and hydrogen atoms in the naphthyl ring as shown in Figure 4.10

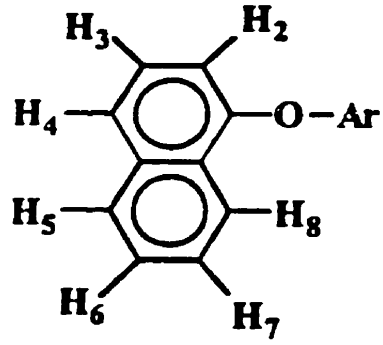

Figure 4.10: Labeling of the naphthyl unit for the Scholl monomers

Several diagnostic spectral changes have been identified as indicative of successful polymerization. For instance, a downfield shift of protons H2 and H8, in the ^{1}H NMR spectrum is typically observed, in addition to an upfield shift of the resonance corresponding to H5 upon polymerization. It is important to note that in a majority of cases it is difficult to measure the chemical shifts of protons H2 and H5 as a result of overlap with other arene resonances. On the other hand, the H8 peak is distinguishable in

the ^{1}H NMR of both the monomer and polymer and is therefore often considered as evidence of polymerization. Typically, the H8 resonance of the monomer is represented by a multiplet. However, following polymerization this peak appears as a doublet at a position further downfield from that in the monomer and remains distinguishable from all other arene resonances. Figures 4.11a and 4.11b show the arene portion of the ^{1}H NMR spectra of monomer **4.10** and its corresponding polymer **4.15**, which illustrates the spectral changes upon polymerization. Perhaps the broadening of the proton resonances following polymerization is one of the most outstanding features of the ^{1}H NMR spectra. This phenomenon has been attributed to the increase in the size of the molecule and consequently the number of protons represented by each resonance. As mentioned previously, the peak corresponding to H8 is generally the most diagnostic resonance in the determination of successful polymerization. The appearance of the doublet at 8.34 ppm in the spectrum associated with the polymer, in comparison with the multiplet located upfield at 8.18-8.21 ppm in the spectrum of the monomer, supports the polymerization of monomer **4.10**. Although the identity of protons H2 and H5 has not been established with any degree of certainty, it is clear that the doublet at 7.62 ppm in the spectrum of the monomer has shifted upfield in the polymer to a position which overlaps with other aromatic resonances and as a result cannot be distinguished. It may be possible to attribute this resonance to H5 since previous research has identified this type of shift to this particular proton in the naphthyl ring. Although the identity of H2 is more difficult to determine, the change of the aromatic region of the spectrum suggests a shift in other proton resonances as well.

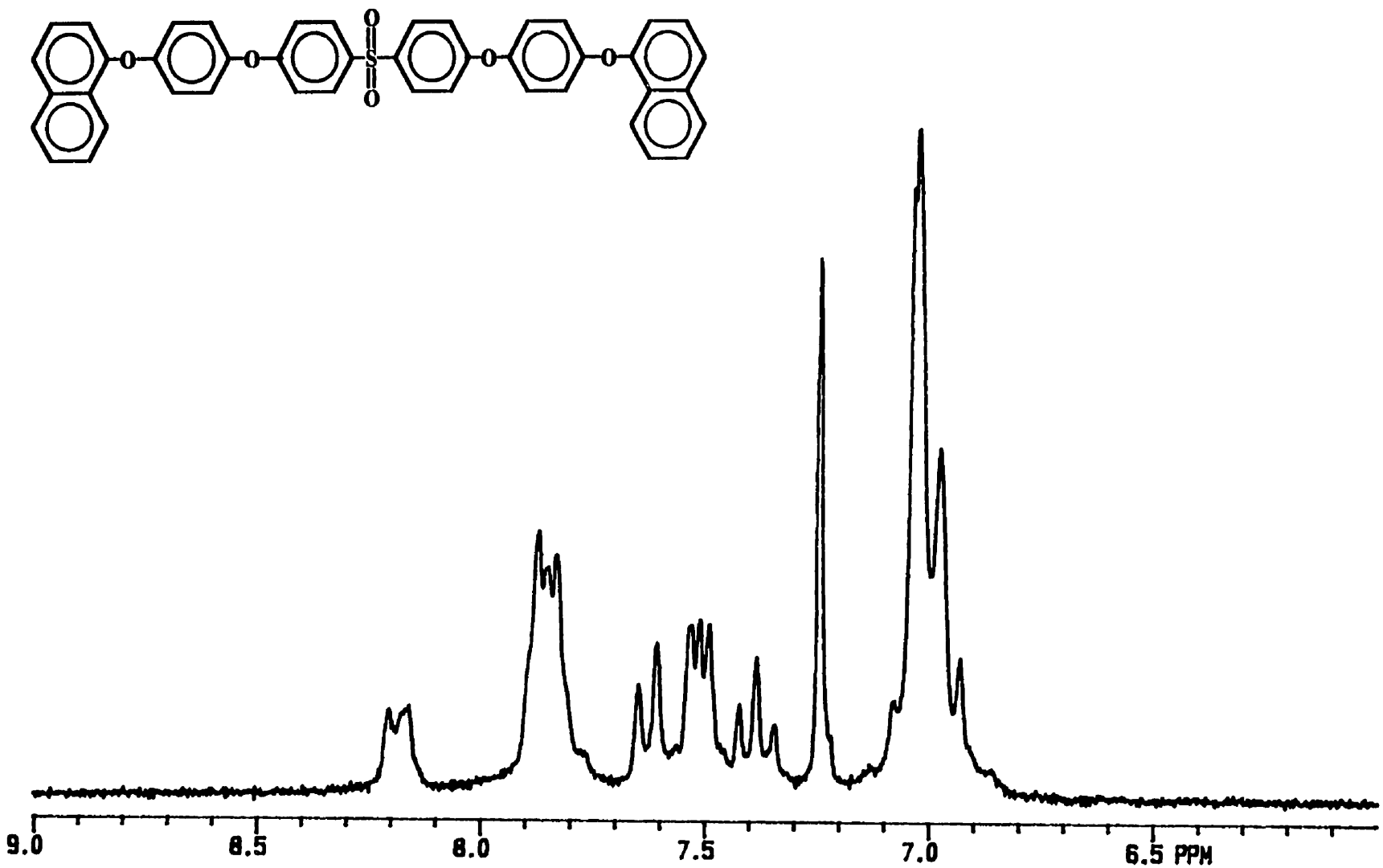

Figure 4.11a: ^{1}H NMR spectrum of monomer **4.10** in $CDCl_3$.

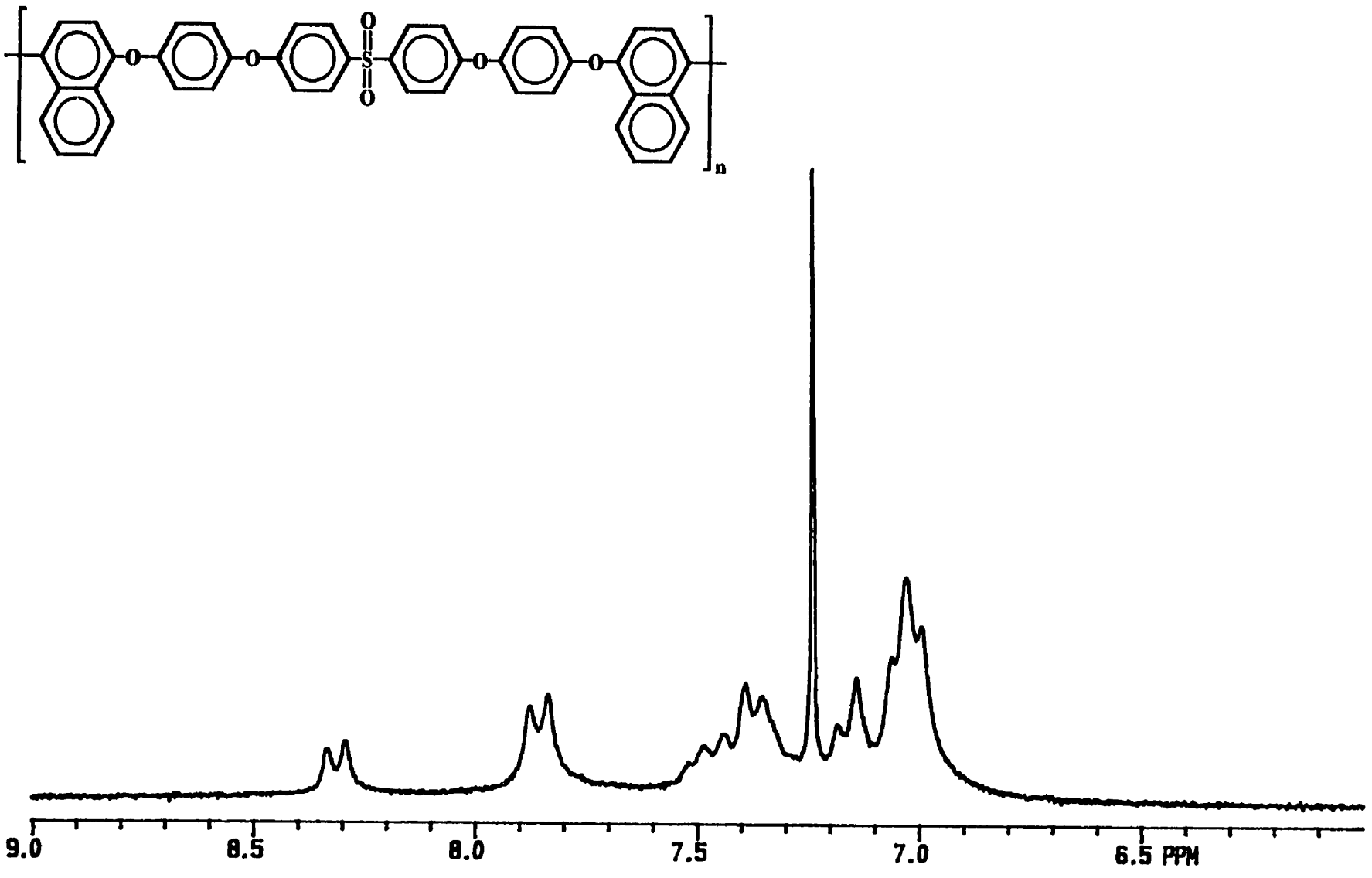

Figure 4.11b: ^{1}H NMR spectrum of polymer **4.15** in $CDCl_3$.

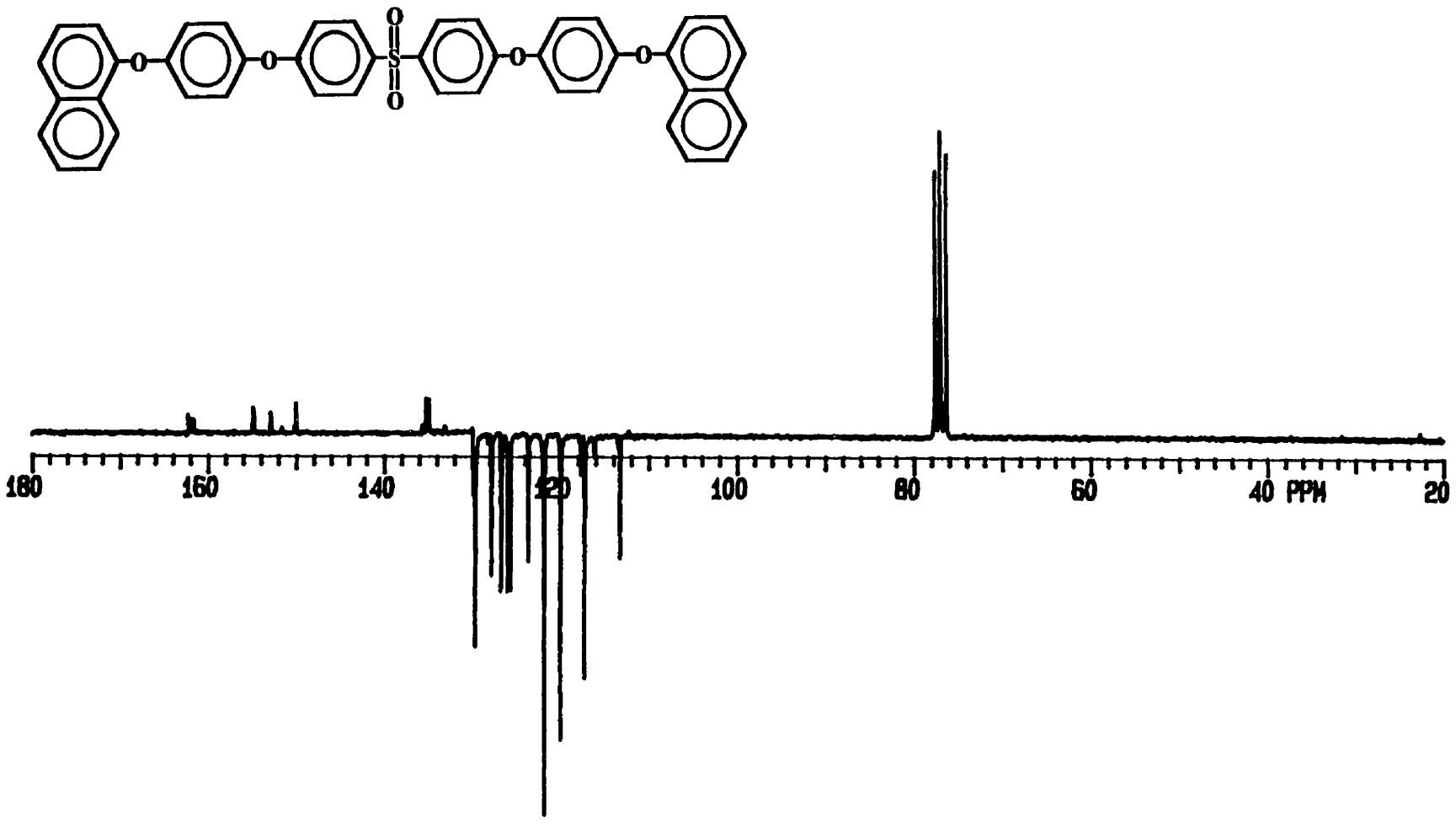

Figure 4.12a: ^{13}C NMR spectrum of monomer **4.10** in $CDCl_3$.

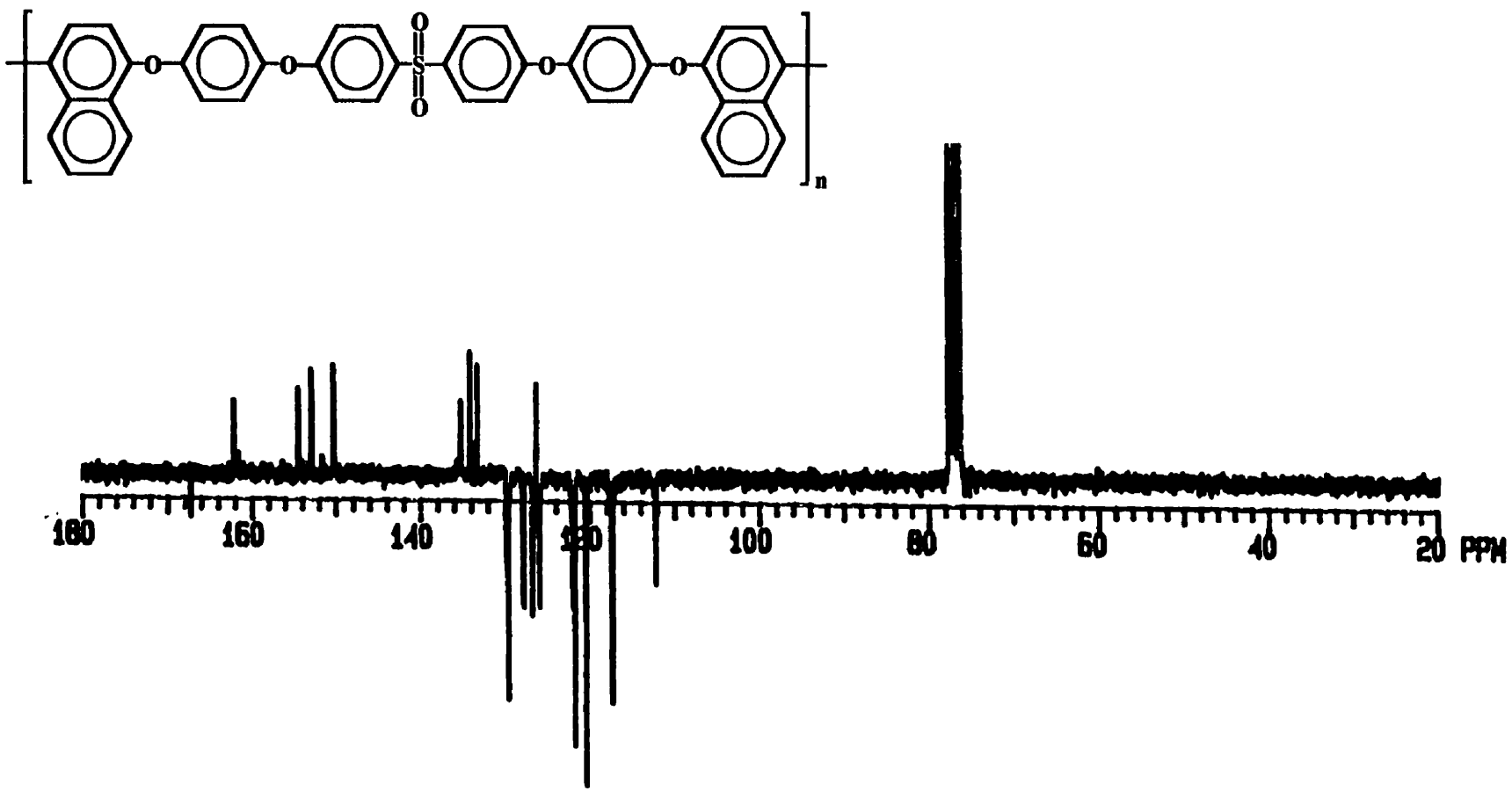

Figure 4.12b: ^{13}C NMR spectrum of polymer **4.15** in $CDCl_3$.

Examination of the ^{13}C NMR spectra of the monomers and their corresponding polymers further supports successful polymerization. Figures 4.12a and 4.12b show the ^{13}C NMR for monomer **4.10** and polymer **4.15**, respectively. Although it is difficult to distinguish the 1-naphthoxy resonances from the other aromatic resonances, it is possible to identify successful polymerization again by comparing the spectrum of the monomer with that of the polymer. One of the most outstanding changes in the spectra upon polymerization is the appearance of the quaternary carbon resonance at 126.50 ppm which may be attributed to the new quaternary carbon that would be expected at C4 in the naphthoxy ring. With the formation of this new quaternary carbon atom, the disappearance of the peak at 123.63 ppm in the spectrum of the monomer may be attributed to C4 in the monomer. These are the most diagnostic changes which were observed upon polymerization in all cases. A more subtle change is the slight shift of the resonance which has been attributed to C2 appearing at 113.34 ppm in the monomer and 112.24 ppm in the polymer.

Following the determination of the solubility of each monomer in $PhNO_2$, the incorporation of various functional groups into the monomeric unit with respect to their polymerization via the Scholl reaction was examined. Monomers **4.10** - **4.14** were investigated under a number of reaction conditions, including various monomer:catalyst ratios, solution concentrations and reaction times, and the molecular weight measurements of the soluble portion of the resulting materials, as determined by gel permeation chromatography (GPC), are summarized in Tables 4.7 - 4.10 (pages 244-247).

A variety of reaction conditions were investigated with respect to monomer **4.10** as outlined in Table 4.7. Entries 1-5 summarize the molecular weight measurements of the

material obtained at a monomer:catalyst ratio of 1:4 at various reaction times. Examination of the weight average molecular weight determinations at all temperatures investigated revealed the preparation of low molecular weight species. Although previous polymerizations of etheric monomers via the Scholl reaction have predicted an increase in molecular weight with an increase in reaction time, the reaction of monomer **4.10** under similar conditions did not exhibit the same trend. As is evident from entries 1-5, reaction times ranging from 0.5 to 24 hours were not observed to affect the degree of polymerization or polydispersity of the resulting material. In an attempt to increase the molecular weight of the polymeric species, the concentration of the reactants was varied and the results included in Table 4.7 as entries 6-9. The studies represented in entries 1-5 indicate that time was not a factor in determining the molecular weight of the polymeric species and consequently a reaction time of 3 hours was selected for these concentration studies. According to previous polymerization studies, it would be expected that a decrease in solution concentration would result in an increased molecular weight of the polymeric material, presuming the growing polymer chain remains soluble in the reaction solvent. Although, entry 6 represents the highest concentration and molecular weight species, a decrease in molecular weight of polymer **4.15** was not observed with a decrease in concentration. Several investigations involving a change in the monomer:catalyst ratio are summarized in entries 2, 10 and 11 in Table 4.7. As is evident from the molecular weight measurements of the species resulting from these studies, an increase in molecular weight was not realized and no trend could be identified. One final attempt was made in increasing the molecular weight of polymer **4.15**. Entry 12 shows that the polymerization was conducted at 65°C in the hope of either increasing the rate of polymerization or the

solubility of the growing polymer chain in solution. However, it was observed that this increase in reaction temperature failed to induce the growth of a higher molecular weight species. However, it is important to note that the increase in temperature did effect an increase in polymer yield.

Monomer **4.11** was studied using reaction conditions similar to those investigated in the polymerization of monomer **4.10**. The effect of time on the polymerization of monomer **4.11** at 22°C and 65°C also allowed for an investigation of temperature on the molecular weight of the corresponding polymers. The molecular weight measurements are summarized in entries 1-8 in Table 4.18. It was observed that neither changes in reaction time nor temperature caused an increase in molecular weight. The effect of concentration and monomer:catalyst ratio was also examined with respect to the potential for increasing the molecular weight of the polymeric species. It is important to note that although these conditions did not increase the degree of polymerization of monomer **4.11**, they did result in an increased yield of the isolated materials. Entries 13 and 14 summarize a variation in reaction conditions which involved the addition of catalyst following a period of time. As outlined in Table 4.8, additional $FeCl_3$ was added to the polymer solution following a 24 hour period and allowed to react further for the following 24 hours. Initially, these experiments were conducted at 22°C resulting in a polymeric material with a molecular weight slightly increased with respect to other reaction conditions. As a result, the same procedure was followed at 65°C. Although this did not allow for the isolation of a higher molecular species, it did cause an increase in the yield.

With the limited success experienced in the polymerization of monomers containing the electron-withdrawing sulfone and carbonyl functionalities, **4.10** and **4.11**, monomer

4.12 was investigated in the preparation of thioether-containing polymers. Based on the results obtained in the polymerizations of monomers **4.10** and **4.11**, monomer **4.12** was initially examined with respect to reaction temperature. The results of the polymerizations at 22°C and 65°C are listed in Table 4.9 as entries 1 and 2. It was observed that reaction temperature had a definite effect on the degree of polymerization of monomer **4.12**, with an increase in molecular weight and decrease in the polydispersity index upon an increased reaction temperature. Due to these results, the effect of reaction time on polymerization for 3 and 24 hours was examined at 65°C. Consideration of entries 2 and 3 indicates that monomer **4.12** exhibits an increase in molecular weight and decrease in polydispersity with increasing reaction time. Although a trend may not be assumed based on these two entries, this observation is in agreement with previous studies conducted by Percec and his coworkers with ether-containing monomers. Entries 4 and 5 in Table 4.9 indicate that variations in monomer:catalyst ratio failed to effect molecular weight changes. However, monomer **4.12** was subjected to polymerization involving reaction conditions similar to those utilized in the study of monomer **4.11**. Monomer **4.12** allowed for the isolation of polymeric materials of increased molecular weight according to the reaction conditions summarized in entries 6 and 7. $FeCl_3$ was added to the polymer solution in 24 hour intervals and allowed for the isolation of polymer **4.17** with molecular weights of 2506 and 3148 $gmol^{-1}$ at 22°C and 65°C, respectively. It is important to note that, although drastic increases in the degree of polymerization as compared to monomers **4.10** and **4.11** were not realized, monomer **4.12** exhibits a decreased polydisperisity.

Table 4.10 summarizes the polymerization attempts of a monomer which incorporates nitrogen into its molecular structure, **4.13**. Regardless of changes in reaction

temperature, time and concentration, GPC measurements of the soluble portion of the isolated material indicated low molecular weight products.

Monomer **4.14** was examined with respect to reaction conditions similar to those applied in the polymerizations of monomers **4.10 - 4.13**. Despite various changes in reaction time and monomer:catalyst ratios, drastic increases in the degree of polymerization were not achieved. The molecular weight measurements corresponding to these reaction conditions are summarized as entries 1-5 in Table 4.11. However, it is important to note that a significant increase in molecular weight was achieved upon a change in temperature. Using a reaction time of 6 hours and a 1:4 monomer:catalyst ratio, monomer **4.14** showed an increase in molecular weight from 1426 to 6350 $gmol^{-1}$ at 22°C and 65°C, respectively. Unfortunately, the polymeric material isolated at the higher reaction temperature also exhibited a higher polydispersity.

The molecular weight measurements by GPC suggest that monomers **4.10-4.14** were not favorable to polymerization using Scholl techniques. However, it is important to note that due to the large degree of insoluble material in most cases, molecular weight determinations were conducted on the soluble portion of the polymer only. As a result, further investigation of the polymeric materials was conducted using thermogravimetric analysis. The examination of weight loss with increasing temperature indicates the thermal stability of the polymeric material of interest. Thermogravimetric analysis of polymers **4.15, 4.16** and **4.19** showed no appreciable weight loss below 500°C. The thermal stability of polymers **4.15, 4.16** and **4.19** is indicated by weight losses of 27%, 35% and 27% at 575°C, 544°C and 533°C, respectively. Polymer **4.17** exhibited a slightly lower thermal stability with 27% weight loss occurring at 385°C. Although GPC indicates the

isolation of only low to moderate molecular weight polymeric species, **4.15-4.19**, consideration of the thermogravimetric data with respect to previous studies of these types of polymers suggests the generation of materials of higher molecular weight.[114,125,141,146,147,150]

Table 4.7: Reaction Conditions and Molecular Weight Measurements for Polymer **4.15**

Trial	Monomer Solution		Catalyst Solution		Time	Temp.	Yield	Mn[a]	Mw[a]	Mw/Mn[a]
	mmol monomer	mL $PhNO_2$	mmol $FeCl_3$	mL $PhNO_2$	(hrs)	(°C)	(%)			
1	0.5	1.0	2.0	2.0	0.5	22	52.5	1469	3990	2.716
2	0.5	1.0	2.0	2.0	3.0	22	55.0	1474	4282	2.904
3	0.5	1.0	2.0	2.0	6.0	22	51.4	835	2295	2.748
4	0.5	1.0	2.0	2.0	18	22	57.7	1516	3998	2.637
5	0.5	1.0	2.0	2.0	24	22	52.9	1811	4613	2.547
6	0.5	0.25	2.0	2.0	3.0	22	51.0	1668	4052	2.429
7	0.5	0.5	2.0	2.0	3.0	22	58.1	1289	2931	2.273
8	0.5	0.75	2.0	2.0	3.0	22	56.7	1076	2838	2.637
9	0.5	1.25	2.0	2.0	3.0	22	51.2	1237	3193	2.390
10	0.5	1.0	1.0	2.0	3.0	22	40.1	1664	3209	1.928
11	0.5	1.0	3.0	2.0	3.0	22	48.9	1127	2323	2.061
12	0.5	1.0	2.0	1.0	6.0	65	84.0	1717	2533	1.475

[a]Soluble portion of polymer was run only.

Table 4.8: Reaction Conditions and Molecular Weight Measurements for Polymer **4.16**

Trial	Monomer Solution		Catalyst Solution		Time	Temp.	Yield	Mn[a]	Mw[a]	Mw/Mn[a]
	mmol monomer	mL $PhNO_2$	mmol $FeCl_3$	mL $PhNO_2$	(hrs)	(°C)	(%)			
1	0.5	0.5	2.0	1.5	3.0	22	33.6	1137	2063	1.815
2	0.5	0.5	2.0	1.5	6.0	22	43.3	1074	2653	2.471
3	0.5	0.5	2.0	1.5	24	22	17.3	850	1601	1.883
4	0.5	0.5	2.0	1.5	48	22	39.6	1318	2677	2.031
5	0.5	0.5	2.0	1.5	3.0	65	31.5	824	1625	1.973
6	0.5	0.5	2.0	1.5	6.0	65	32.4	761	1832	2.405
7	0.5	0.5	2.0	1.5	18	65	23.7	715	1534	2.145
8	0.5	0.5	2.0	1.5	24	65	18.9	1143	3262	1.883
9	0.5	1.0	2.0	1.5	3.0	22	39.8	549	1764	3.214
10	0.5	2.0	2.0	1.5	3.0	22	54.5	547	1660	3.033
11	0.5	1.0	2.0	1.5	3.0	22	48.4	419	1250	2.982
12	0.5	1.0	3.0	1.5	3.0	22	51.7	339	1346	3.967
13	0.5	0.5	1.0 & 1.0	0.5 & 0.5	24 & 24	22	25.1	1532	3636	2.374
14	0.5	0.5	1.0 & 1.0	0.5 & 0.5	24 & 24	65	40.8	963	2213	2.297

[a]Soluble portion of polymer was run only.

Table 4.9: Reaction Conditions and Molecular Weight Measurements for Polymer **4.17**

Trial	Monomer Solution		Catalyst Solution		Time	Temp.	Yield	Mn[a]	Mw[a]	Mw/Mn[a]
	mmol monomer	mL $PhNO_2$	mmol $FeCl_3$	mL $PhNO_2$	(hrs)	(°C)	(%)			
1	0.5	0.5	2.0	1.5	24.0	22	42.5	746	1537	2.059
2	0.5	0.5	2.0	1.5	24.0	65	32.3	1840	3079	1.673
3	0.5	0.5	2.0	1.5	3.0	65	35.3	883	1921	2.175
4	0.5	0.5	1.0	1.0	18.0	22	45.2	1065	1450	1.361
5	0.5	0.5	2.0	1.0	18.0	22	39.9	878	1496	1.702
6	0.5	0.5	1.0 & 1.0	0.5 & 0.5	48	22	43.3	1264	2506	1.982
7	0.5	0.5	1.0 & 1.0	0.5 & 0.5	48	65	30.0	2005	3148	1.570

[a]Soluble portion of polymer was run only.

Table 4.10: Reaction Conditions and Molecular Weight Measurements for Polymer **4.18**

Trial	Monomer Solution		Catalyst Solution		Time	Temp.	Yield	Mn[a]	Mw[a]	Mw/Mn[a]
	mmol monomer	mL $PhNO_2$	mmol $FeCl_3$	mL $PhNO_2$	(hrs)	(°C)	(%)			
1	0.5	0.5	1.0	0.5	1.0	65	21.5	-	-	-
2	0.5	0.5	2.0	1.0	24	22	19.4	327	386	1.179
3	0.5	1.5	2.0	1.0	24	22	18.9	218	320	1.464
4	0.5	0.5	2.0	1.0	3.0	65	24.0	139	280	2.014
5	0.5	0.5	2.0	1.0	24	65	37.0	190	420	2.178

[a]Soluble portion of polymer was run only.

Table 4.11: Reaction Conditions and Molecular Weight Measurements for Polymer **4.19**

Trial	Monomer Solution		Catalyst Solution		Time	Temp.	Yield	Mn[a]	Mw[a]	Mw/Mn[a]
	mmol monomer	mL $PhNO_2$	mmol $FeCl_3$	mL $PhNO_2$	(hrs)	(°C)	(%)			
1	0.5	1.0	1.0	2.0	3.0	22	57.0	761	1477	1.942
2	0.5	1.0	1.0	2.0	18.0	22	63.0	810	1660	2.050
3	0.5	1.0	1.0	1.0	6.0	22	54.1	967	2209	2.283
4	0.5	1.0	2.0	1.0	6.0	22	51.4	582	1426	2.451
5	0.5	1.0	3.0	1.0	6.0	22	85.2	758	1539	2.031
6	0.5	1.0	2.0	1.0	6.0	65	76.4	2119	6350	2.996

[a]Soluble portion of polymer was run only.

5.0 Ring-Opening Metathesis Polymerization of Strained Cyclic Olefins

5.1 Introduction

Ring-opening polymerization has received a great deal of attention in the field of synthetic polymer chemistry and will be the focus of the following discussion. Although several factors have been identified as playing a role in the degree of polymerization as well as the subsequent properties and applications of the polymeric species, the role of the catalyst in ring-opening polymerizations has been of particular interest. The development of catalytic systems has advanced to such a degree that the preparation of polymeric materials with specific structural characteristics has been achieved.

Following the first demonstration of the use of transition metal catalysts for the ring-opening polymerization of cyclic olefins, Truett and coworkers reported the preparation of polynorbornene based on the design of Mo and Ti containing catalysts systems.[261] Figure 5.1 illustrates the lithium aluminum tetraheptyl and titanium tetrachloride catalyst system which resulted in the unexpected ring-opening polymerization of norbornene. It is important to note that this was the first report describing the addition polymerization of a monomer with only one double bond. Furthermore, Truett observed that varying the relative amounts of the two components of his catalyst system had a marked impact on the properties of the

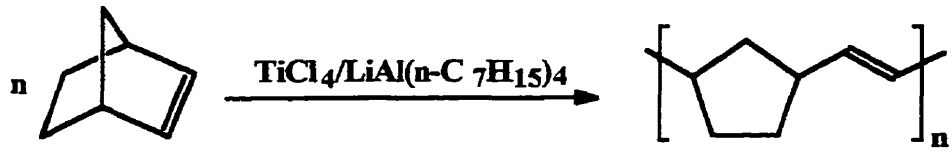

Figure 5.1: Ring-opening polymerization of norbornene using a titanium catalyst system

resulting polymeric material. Since this initial discovery, a number of classical catalysts prepared from a transition metal halide complex and an organometallic or Lewis acid co-catalyst have been found to initiate the ring-opening polymerization of a variety of monocyclic, bicyclic and polycyclic olefins.[262-267] Active catalyst systems based on transition metals including Ti, Zr, Hf, V, Nb, Ta, Cr, Mo, W, Re, Ru, Os, Rh, and Ir reflect the number of systems that have been investigated.[268]

A crucial discovery in the development of catalytic systems for ring-opening polymerization reactions was reported by Calderon and his coworkers who showed that the disproportionation of acyclic olefins and ring-opening polymerization are similar chemical reactions.[269] The final result of this study was the determination that the reaction took place by breaking double bonds and exchanging alkylidene units. Consequently, this type of reaction was labeled olefin metathesis. With this discovery, interest in the mechanistic aspect of the reaction soared. Ultimately, the conflicting opinions of several individual research groups regarding the mechanistic intracacies of the reaction led to the presently accepted mechanism involving the interconversion of metal carbenes and metallacyclobutanes. Herrison and Chauvin proposed the new mechanism involving metal carbenes and metallacyclobutanes to justify the observations

of their studies of cyclic and acyclic olefins (Figure 5.2).[270] Further proof for the metal carbene mechanism was presented by Grubbs and Katz on the basis of isotope labeling studies.[271-272]

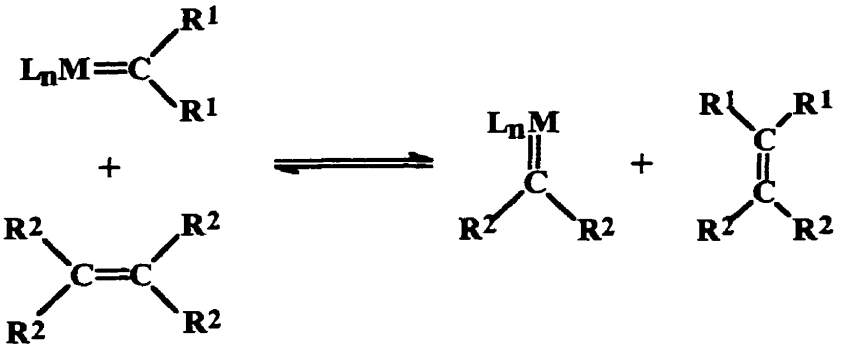

Figure 5.2: Isotope labeling scheme used for proof of the metal carbene mechanism

This mechanism may be applied to cyclic monomers where Figure 5.3 illustrates the formation of the metallacyclobutane intermediate from the corresponding metal carbene.

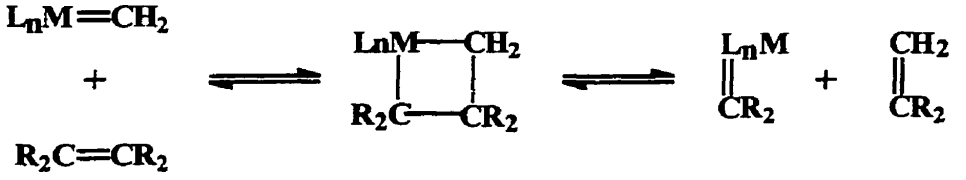

Figure 5.3: Metal carbene-metallocyclobutane mechanism

Another area of ring-opening polymerization methods which has received considerable attention recently is that of living ring-opening metathesis polymerization (ROMP). The interest in living polymerizations stems from the fact that this technique allows for a maximum degree of control over polymer growth and allows for the synthesis of polymers with predictable, and well-defined structures.[273] Although a

general definition of a living polymerization is given as a chain polymerization which takes place in the absence of termination or chain transfer, there are several criteria which have been identified as diagnostic features of living polymerization. The first criterion simply expresses the basis of living polymerization conditions and states that polymer growth must proceed by the continuous addition of the monomeric unit to the propagating species without chain termination or chain transfer reaction interferences. Another differentiating aspect of living polymerizations is that the active center of the polymerization remains intact on the polymer chain even after complete consumption of all the monomer units. The living nature of the process comes into play upon renewed monomer addition which promotes continued polymer growth. Finally, it has been determined that in generating polymeric materials with narrow molecular weight distributions it is essential that the rate of initiation is comparable to or faster than the rate of propagation.[273]

The development of the ideal catalyst system which fulfills each of these requirements and allows for the controlled design of polymeric species with specific properties and applications continues to arouse the curiosity of researchers worldwide. However, it is the work of Richard Schrock and Robert Grubbs and their development of well-defined transition metal compounds which catalyze the ring-opening polymerization of strained cyclic olefins which is often accredited for the strides made in this unique area.[280-303] Most of the catalytic systems investigated by these researchers incorporate transition metal compounds of titanium, tungsten, molybdenum or ruthenium.

5.1.1 Catalyst Systems

5.1.1.1 Organotitanium Catalysts

The development of well-defined transition metal catalysts was initiated in 1986 when Grubbs reported the use of bis(η^5-cyclopentadienyl)-titanacyclobutane, derived from the reaction of the Tebbe reagent with norbornene, in the polymerization of norbornene (Figure 5.4).[274] The large ring strain in norbornene and its derivatives coupled with the relatively low reactivity of titanacyclobutanes presented a method which proceeded without termination or chain transfer resulting in the corresponding polymeric material with a narrow molecular weight distribution.

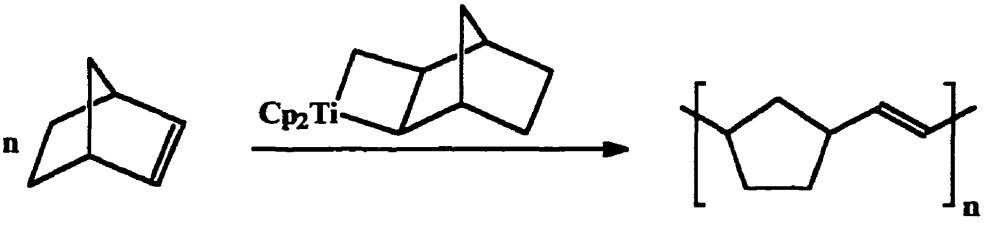

Figure 5.4: Bis(η^5-cyclopentadienyl)titanacyclobutane catalyst for the ring-opening polymerization of norbornene

Kinetic studies suggested a zero-order rate dependence on the monomer based on a constant rate of monomer consumption following an initial induction period. In short, this indicates the ring-opening of the titanacycle as the rate-determining step.

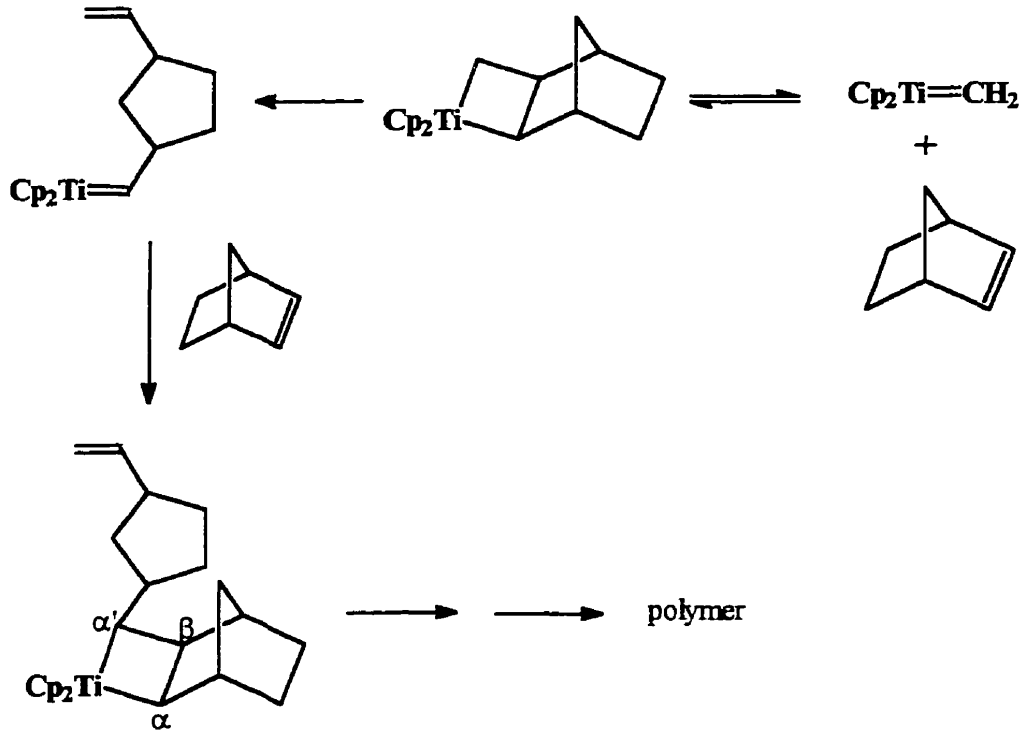

Figure 5.5: Ring-opening polymerization mechanism of norbornene using the bis(η^5-cyclopentadienyl)titanacyclobutane catalyst

These observations in combination with the accepted mechanism of olefin metathesis involving the interconversion of metal carbenes and metallacyclobutanes led to the proposal of the mechanism illustrated in Figure 5.5 for the generation of the growing polymer chain. It was proposed that the metallacycle may cleave to yield a carbene-olefin complex in one of two ways.[274] Cleavage of the titanacycle in a non-productive, but rapidly reversible manner to form norbornene and the titanium methylene complex was suggested as an explanation for the inital induction period. The second option resulted in the formation of an unstable substituted titanacarbene which, when trapped by norbornene, formed the α-β-α'-trisubstituted metallacycle. This substituted titanacycle cleaves exclusively in a productive manner in the generation of the corresponding

substituted carbene which in turn forms the trisubstituted metallacycle in the presence of norbornene. Subsequent cleavage allows for the generation of the growing chain attached to the α' position of the trisubstituted titanacyclobutane.

Further investigation of the titanacyclobutane catalysts identified titanacyclobutane, shown in Figure 5.6, as a better initiator for the polymerization of norbornene than the titanacycle discussed in Figure 5.5 due to the ring-strain in 3,3-dimethylcyclopropene.[274] It was observed that this initiator opened in an exclusively productive fashion at lower reaction temperatures. As a result, no induction period was observed. The polymerization reaction proceeded with initiation being faster than chain propagation allowing for the synthesis of high molecular weight materials with polydispersities lower than 1.1.

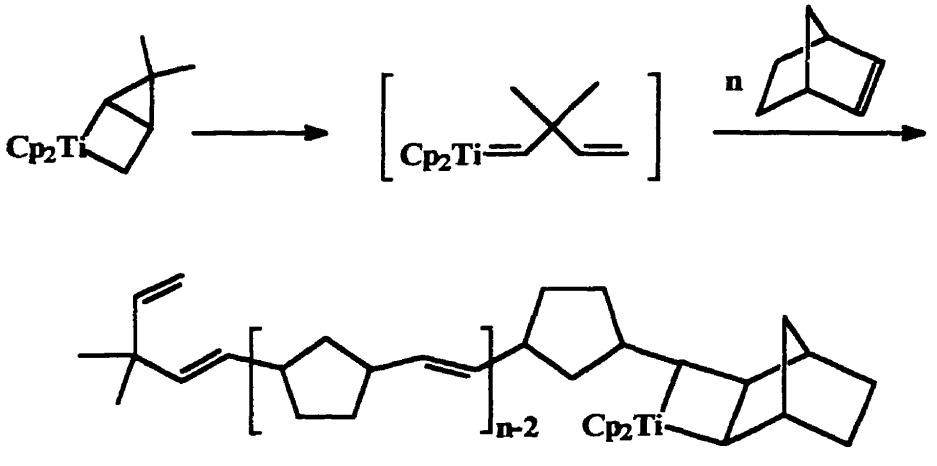

Figure 5.6: Ring-opening polymerization of norbornene using a 3,3-dimethylcyclopropene based titanacyclobutane catalyst

The polymerization reaction itself was found to be sensitive to temperature changes to the degree that the reaction was halted by simply cooling the reaction mixture to room temperature whereas heating it to 65°C renewed chain growth. In addition to the living nature of this catalyst, the linear dependence of molecular weight on monomer consumption allowed for the addition of different cyclic olefins including endo- and exo-dicyclopentadiene, benzonorbornadiene and 6-methylbenzonorbornadiene in the preparation of block copolymers with a well-defined composition, microstructure and molecular weight.[274]

Following complete consumption of the monomeric units, the polymer chain contained one titanacyclobutane end group regardless of the initiator employed. A notable feature of this technique was the capability for storage of the active polymer for long periods of time.[274] Also, it had been shown that the titanium carbenes generated from the ring-opening of the titanacyclobutane reacted with a variety of functionalities such as aldehydes, ketones, esters, amides and imides to give Wittig-type products in excellent yield.[276] The potential advantage of this end-capping technique included the efficient removal of the catalyst, modification of the bulk properties of the ROMP-derived polymer, as well as a facile means of end group analysis. Furthermore, the incorporation of this active group poses a means for further chemical transformations and/or polymerizations. Figures 5.7 and 5.8 illustrate the use of titanacyclobutane terminated polynorbornene in Wittig-type reactions for the production of ABA-triblock and graft copolymers, respectively.

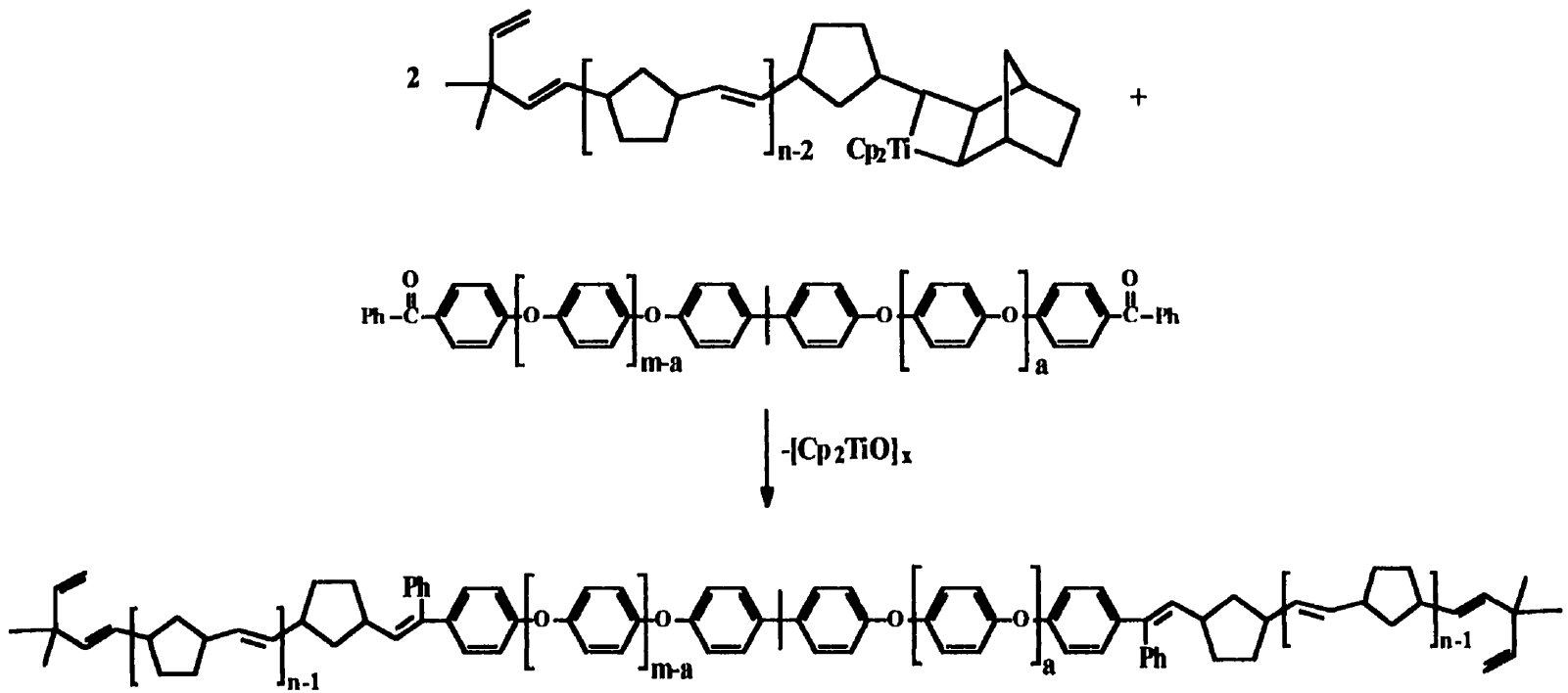

Figure 5.7: Wittig-type end-capping reaction in the preparation of block copolymers

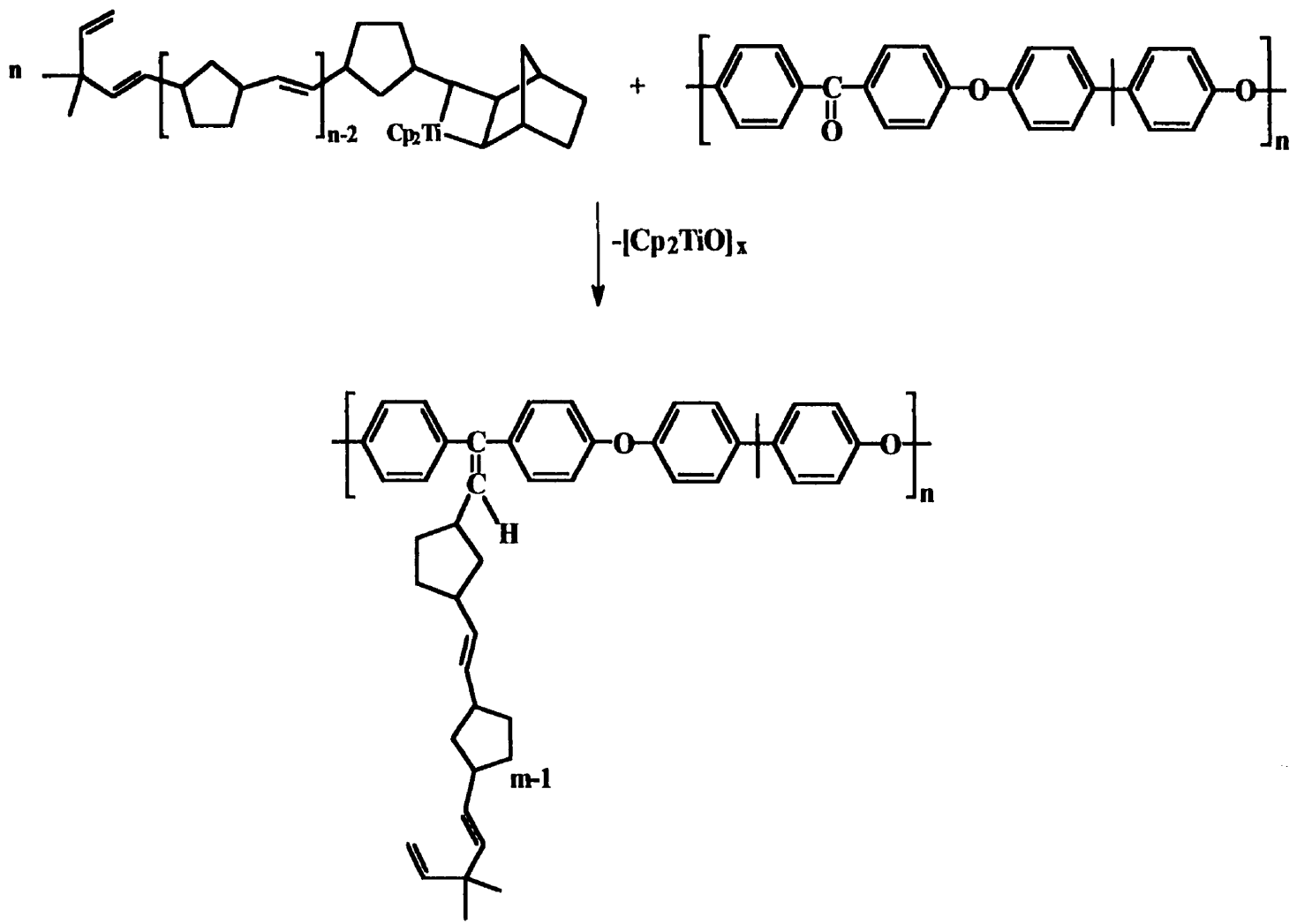

Figure 5.8: Wittig-type end-capping reaction in the preparation of graft copolymers

5.1.1.2 Tungsten Catalysts

The role of metal-carbenes as initiators in olefin metathesis prompted the investigation of various transition metal based catalytic systems. In 1976, Katz introduced (diphenylcarbene)pentacarbonyltungsten, which represented the first metal-carbene prepared without stabilizing heteroatoms attached to the carbene center. Upon reaction in the presence of cis-cycloalkenes, the resultant polymers were isolated as highly stereospecific polymers.[277,278] GPC, IR and ^{13}C NMR were used to verify the preparation of these highly ordered polymers in which 90% or more of the double bonds had the cis configuration. Based on the successful titanacyclobutane and metal carbene ring-opening polymerizations, it became evident that the characteristics of the catalyst played an invaluable role in the control and ultimate design of the polymer microstructure. As a result of these findings, a rapid search into the area of generating novel living polymerization catalysts has been underway.

In 1986, Schrock and coworkers, one of the leading research groups in the development of ROMP initiators, reported the synthesis of a series of alkylidene complexes which demonstrated great promise as living polymerization catalysts.[279] Their investigation began with the preparation of tungsten based catalytic systems due to their higher degree of activity over the previously mentioned titanium complexes as well as for their enhanced tolerance of polar functional groups. Figure 5.9 shows the use of the complex W(CH-t-Bu)(NAr)(O-t-Bu)$_2$ in the polymerization of 50-200 equivalents of norbornene in toluene at 25°C.[280] Analysis of the isolated polymeric material showed a molecular weight proportional to the number of equivalents of the norbornene consumed

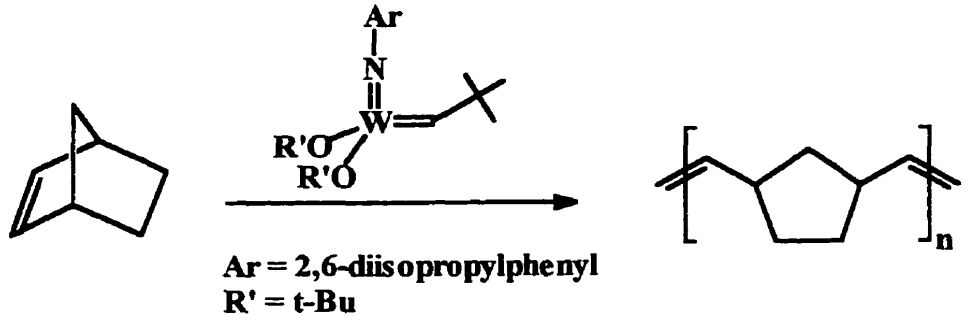

Figure 5.9: Polymerization of norbornene using a tungsten alkylidene complex

and a polydispersity index of 1.05.

More recently, new and unique tungsten alkylidene catalysts, which exhibit the potential to incorporate various ligands, allowed for great flexibility with respect to polymer formation. The preparation of these catalysts follows a three step process by which variation of the metal alkoxide ligand in the final step of the process presented a route for the synthesis of a variety of catalysts where the alkoxide ligand may possess either donating properties (O-t-Bu) or highly electron withdrawing capabilities ($[OC(CF_3)_2(CF_2CF_2CF_3)]$).[279-281] A further modification of the catalyst by the replacement of the alkoxide ligands with fluorinated substituents such as $-OC(CH_3)_2CF_3$ and $-OCCH_3(CF_3)_2$ resulted in the isolation of more active, yet less selective, catalysts.[281-282] The enhanced activity of these catalysts not only allowed for the polymerization of norbornene at temperatures as low as -60°C but were active initiators for acyclic olefin metathesis as well. Yet, the practicality of the fluorinated catalysts as initiators for the polymerization of cyclic olefins was doubtful since the molecular weight of the resulting polymeric materials were determined to be independent both upon the reaction time and the amount of monomer employed. A slow initiation rate relative to the rate of

propagation and secondary metathesis of the double bonds formed along the polymer chain were two factors suggested for the measured molecular weights. Ultimately, it was determined that the reactivity of the $W(CHR')(NAr)(OR)_2$ complex was highly dependent on the electron-withdrawing power and size of the alkoxide ligand.[279-282]

5.1.1.3 Molybdenum Alkylidene Catalysts

The investigation for improved regulation over polymer structure via the design of novel catalytic systems continued with the use of other transition metals in these alkylidene complexes. This was demonstrated by the preparation of various molybdenum based systems with structures similar to those of the tungsten analogues.[283, 284] The synthetic utility of the resulting complexes was evident in the generation of virtually monodisperse polymers, an increased tolerance of functional groups including esters and nitriles, and the production of products of a highly stereoregular nature. The polymerization of endo,endo-5,6-dicarbomethoxynorbornadiene with $Mo(CH\text{-}t\text{-}Bu)(NAr)(O\text{-}t\text{-}Bu)_2$ (Ar = 2,6-diisopropylphenyl) demonstrated the improved characteristics of this catalyst system resulting in the preparation of well-behaved living polymers which were essentially monodisperse with a high degree of stereoregularity (Figure 5.10).[283] The stereoregular nature of the polymeric species was explained on the basis of previous studies which established that this catalyst conforms to a pseudo-tetrahedral orientation in which the major contributor is such that the alkylidene substituent points toward the imido nitrogen atom, the *syn* isomer.[284, 285]

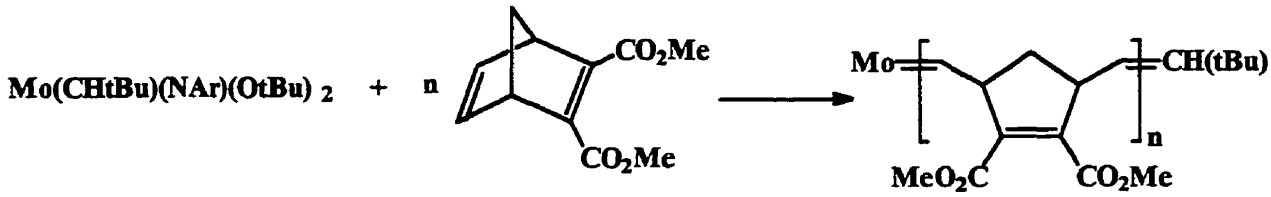

Figure 5.10: ROMP of 5,6-dicarbomethoxynorbornadiene via a molybdenum alkylidene catalyst

The living nature and unique properties of polymers resulting from the ROMP of a variety of 2,3-disubstituted norbornadienes in the presence of Mo(CH-t-Bu)(NAr)(O-t-Bu)$_2$ (Ar = 2,6-diisopropylphenyl) demonstrates its feasibility in polymer preparation. It was reported that 200 equivalents of 2,3-dicarbomethoxynorbornadiene were subjected to ROMP in the presence of Mo(CH-t-Bu)(NAr)(O-t-Bu)$_2$ (Ar = 2,6-diisopropylphenyl) to yield the corresponding ring-opened polymer with molecular weights proportional to the equivalents of monomer used and polydispersities as low as 1.1.[283] Additional features of the molybdenum-based alkylidene catalysts with respect to the ROMP of 2,3-disubstituted norbornadienes were the limited stereochemical arrangements of the monomer units. Figure 5.11 shows the stereochemical conformations of the repeating unit of the polymer based on the symmetrical nature of the monomers. Ring-opening polymerization resulted in the generation of a double bond within the polymeric microstructure with either a cis or trans configuration. Additionally, the chiral allylic carbons of the chain vinylenes were the determining factor on the formation of meso or racemic dyads where the chiral allylic carbons with the same configuration yielded syndiotactic material and those with an

opposite configuration gave an isotactic polymer (Figure 5.11).

The impact of catalyst design on the structural features of the polymeric species was demonstrated in a comparison study which investigated the ROMP of 2,3-bis(trifluoromethyl)norbornadiene in the presence of Mo(CH-t-Bu)(NAr)(O-t-Bu)$_2$ (Ar = 2,6-diisopropylphenyl) and a number of traditional initiators.[284] ^{13}C NMR and Tg were used to verify the enhanced stereoregularity of the ring-opened polymer resulting

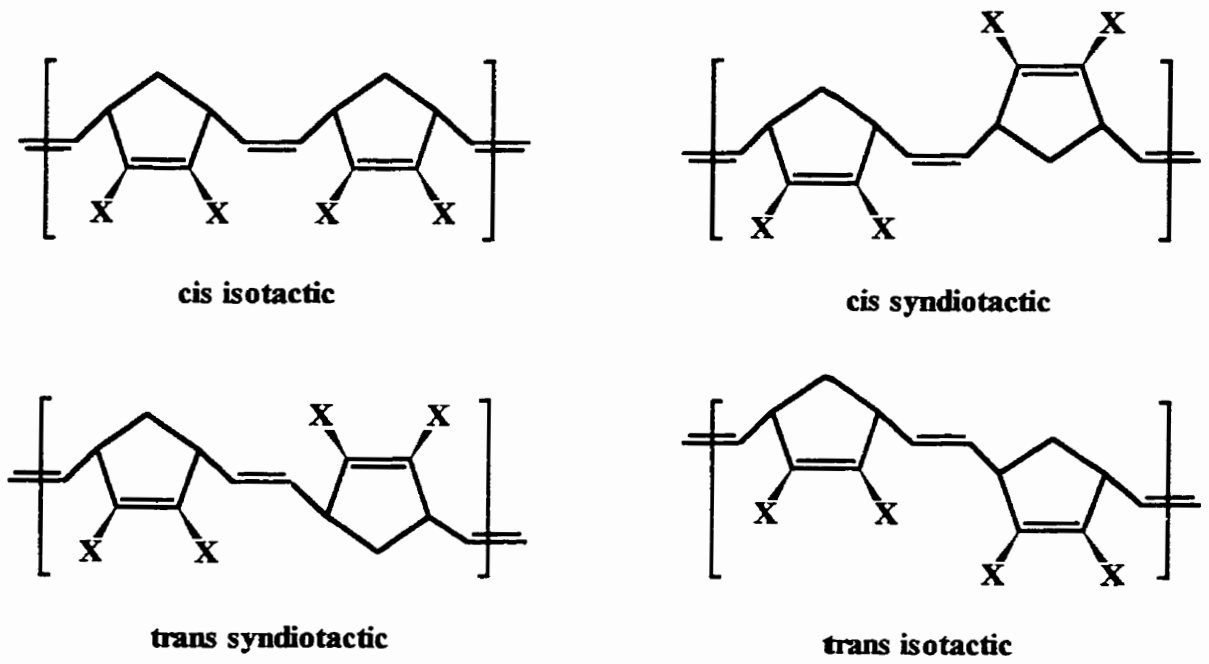

Figure 5.11: Possible stereochemical arrangements of 2,3-disubstituted norbornadienes

from initiation by the molybdenum alkylidene complex as compared to the traditional catalysts listed in Figure 5.12. The resulting trans, syndiotactic microstructure of the isolated polymer was consistent with the nature of this catalyst to form predominantly trans polynorbornene. The tolerance of various functionalities and stereochemical control achieved by the use of molybdenum based catalysts have rendered them exceptionally valuable in the molecular engineering of polymers with novel structures and functionalities. This is exemplified in a report which appeared in 1992 by Schrock and coworkers who demonstrated the utility of the Mo(CH-t-Bu)(NAr)(O-t-Bu)$_2$ (Ar = 2,6-diisopropylphenyl) catalyst in the preparation of Side Chain Liquid Crystalline Polymers (SCLCP's).[286-288]

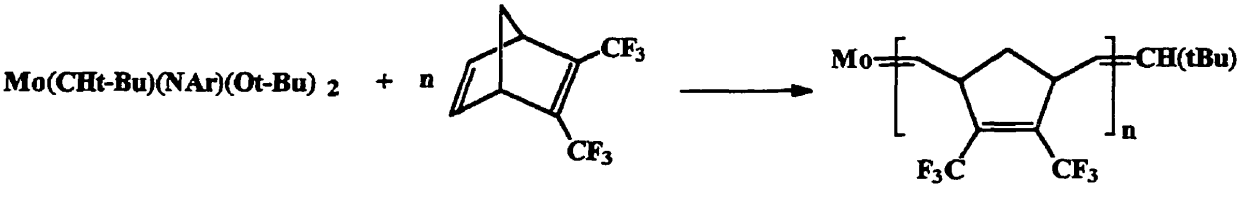

Ar = 2,6-diisopropylphenyl

Initiator	trans %	Tg °C
$WCl_6/SnMe_4$	54	125
$RuCl_3/SnMe_4$	70	117
$MoCl_5/SnMe_4$	87	104
Mo(CHtBu)	98	97

Figure 5.12: Trans stereoregular polymers of 2,3-bis(trifluoromethyl)norbornadiene

5.1.1.4 Ruthenium Coordination Catalysts

An underlying concern in the development of new catalysts, second only to the issues of activity and selectivity, is the stability of an active species to impurities such as air and water.[289] In many of the catalytic systems mentioned thus far, the progression of these catalyst systems from research to full-scale industrial use has often been restricted by the sensitivity of the organometallic complexes to oxygen, water and heteroatomic functionalized substrates. This obstacle was overcome in 1988 by Grubbs and coworkers who described the use of a select group of VIII coordination complexes for the polymerization of 7-oxanorbornene in aqueous solution under an atmosphere of air to yield the desired ROMP polymer in quantitative yield.[290] The aqueous polymerization

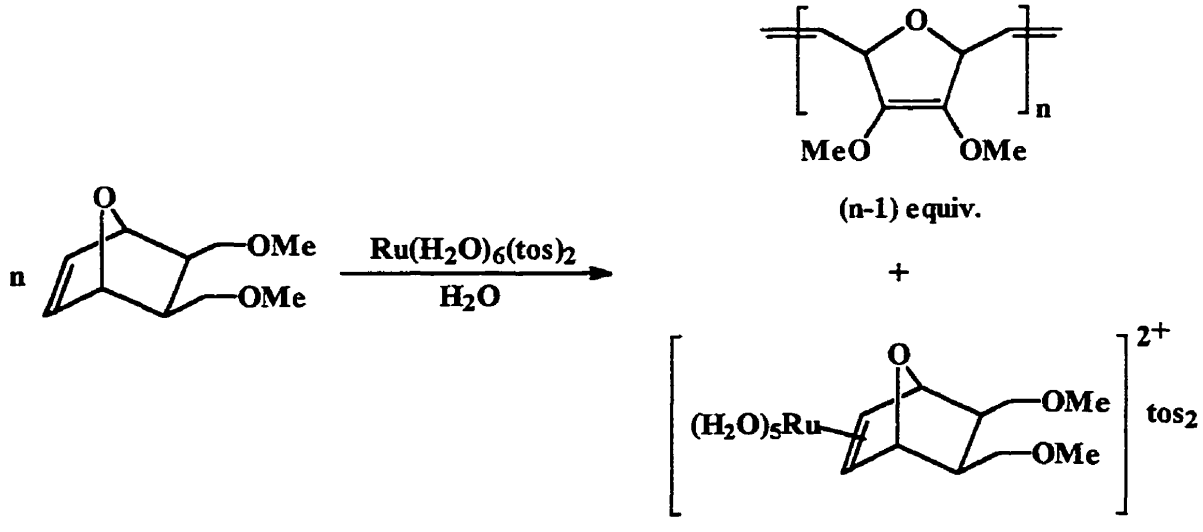

Figure 5.13: The $Ru(H_2O)_6$(p-toluenesulfonate)$_2$ catalyst

of a 7-oxanorbornene derivative via the very active $Ru(H_2O)_6(tos)_2$ (tos = p-toluenesulfonate) salt is illustrated in Figure 5.13. It was discovered that upon polymerization of the 7-oxanorbornene derivative, a Ru^{2+} mono-olefin adduct complex was generated in the process.[291-293] Following polymerization, the metal-olefin coordination catalyst which was formed in situ was found to be recyclable and subsequently found to be more active in later polymerizations. Grubbs reported the use of this Ru^{2+} mono-olefin adduct in the polymerization of less-strained monomers, such as cyclooctene, which were previously unreactive in aqueous media (Figure 5.14).[294]

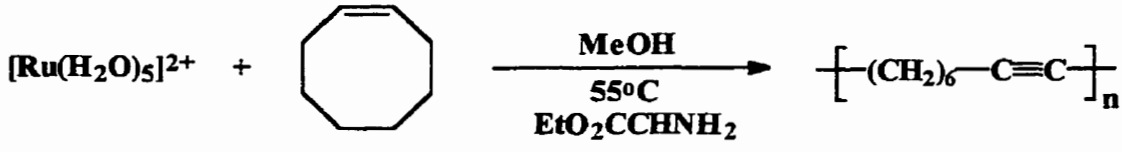

Figure 5.14: Use of a Ru^{2+} mono-olefin adduct complex in the polymerization of less-strained monomers

In 1992, Grubbs and coworkers reported the preparation of the first well-defined ruthenium-based olefin catalyst, $(Ph_3P)_2Cl_2Ru{=}CHCH{=}CPh_2$. The living properties of this catalyst were established by the block copolymerization of 2,3-dideuterionorbornene and norbornene with the generation of a stable active polymer species in which chain termination and chain transfer were extremely slow relative to propagation (Figure 5.15).[295] The features of the ruthenium carbene complex combined unusual stability and

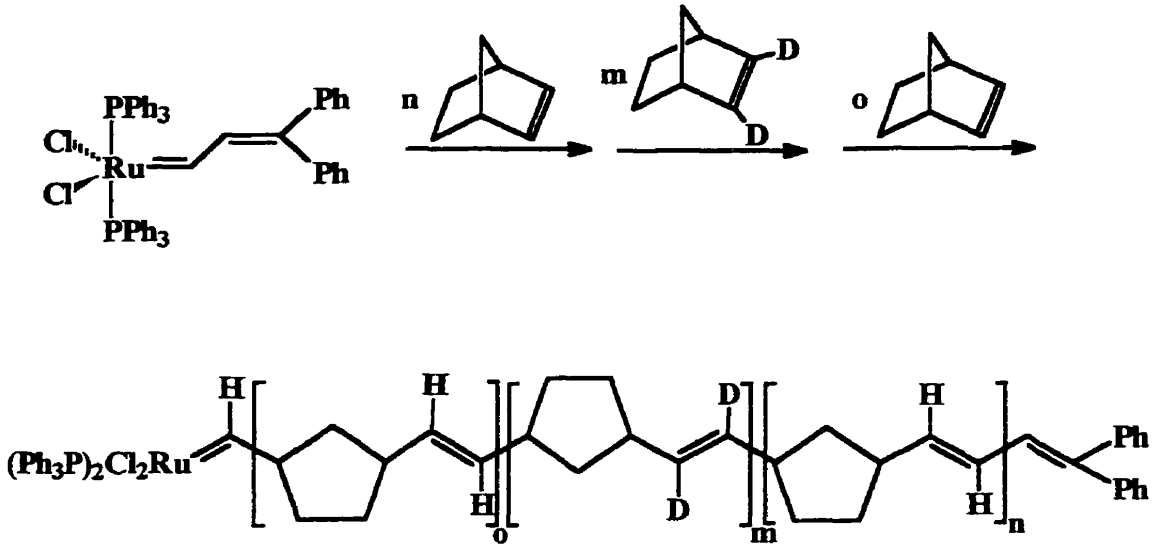

Figure 5.15: Block polymerization using the first well-defined ruthenium catalyst

functional-group tolerance with the ability for polymerization of highly strained cyclic olefins in organic media both in the presence and absence of protic/aqueous solvents. However, the activity of this complex was limited to the metathesis of highly strained cyclic olefins and was inadequate for the polymerization of low-strain cyclic olefins or acyclic olefins.

Subsequent research focused on the potential for fine-tuning the reactivity of this catalyst via ligand modification.[296-302] Figure 5.16 shows the synthesis of new catalysts with high metathesis activity as a result of the substitution of the triphenylphosphine ligands with better σ-donating alkylphosphines. Two isomeric forms of the modified ruthenium catalysts were generated from the reaction of 2 equivalents of PCy_3 or $P(i\text{-}Pr)_3$ with $(Ph_3P)_2Cl_2Ru{=}CHCH{=}CPh_2$ in CH_2Cl_2 where the dominant complex was the

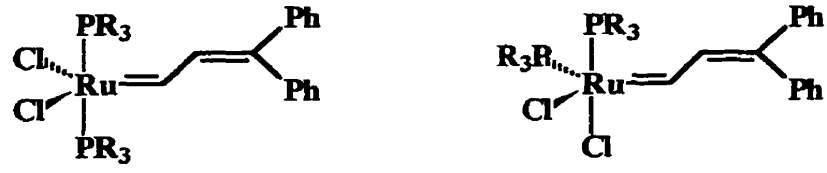

R = Cy, i-Pr

Figure 5.16: Modified single-component ruthenium catalysts

one in which the two phosphine ligands are *trans* to one another.[295]

The promise of these modified catalysts for enhanced activity was exemplified by the polymerization of not only highly strained monomers such as norbornene and its derivatives but also the ROMP of less-strained cyclic monomers including cis-cyclooctene, cyclooctadiene and cyclopentene.[302] Ligand modification affected the activity of the catalysts to such a degree that moderate turnover numbers of unstrained acyclic olefins such as cis-2-pentene were achieved where the robust nature of the catalyst was demonstrated by a rate of metathesis which was unaffected by either a protic or coordinating solvent.[303] Additionally, the use of $(Cy_3P)_2Cl_2Ru{=}CHCH{=}CPh_2$ for the polymerization of cyclooctadiene in the presence of a simple allylic chain transfer agent was found to yield the corresponding difunctional 1,4-polybutadiene.[302]

Thus far, the development of various catalytic systems and their impact on the structural nature of the resulting polymeric material has been the focus of our discussion. However, it is important to keep in mind that polymeric properties depend significantly on the functional substituents along the backbone of the polymer chain. As a result, factors such as monomer structure and reaction conditions must be considered as crucial components in the synthesis and design of polymeric species with specific properties.

In 1989, a paper by Lautens and coworkers described the development of novel monomeric units whose ROMP yielded new polymeric materials which possessed a combination of rigidity and strain.[304-305] This report focused on the effect of various solvent mixtures and monomer/catalyst ratios on the polymerization of deltacyclene in the presence of the ruthenium catalyst, $RuCl_3 \cdot H_2O$ (Figure 5.17). Previous work in the field has emphasized the robust nature of ruthenium catalysts in an oxygen atmosphere and aqueous reaction conditions as one of its greatest features. The initial polymerization of deltacyclene with $RuCl_3 \cdot H_2O$ was carried out using ethanol as the solvent and resulted in the isolation of a low molecular weight material in only moderate yield. Upon the addition of varying amounts of water, however, a dramatic increase in the rate of reaction was realized with a 100-fold increase in the molecular weight of the isolated polymers. It is interesting to note that when water was used exclusively as the solvent of choice, polymerization was achieved despite the insolubility of the monomer albeit with no substantial increase in molecular weight or yield.[304] Additionally, conditions of varying monomer/catalyst ratios were investigated and it was reported that a decrease in catalyst/monomer ratio resulted in an increase in molecular weight. Nonetheless, the efficiency of this catalyst system for the polymerization of deltacyclene, regardless of the ratios employed, was demonstrated by the constant isolation of materials with molecular weights of 10^6. In spite of the fact that ruthenium catalysts have been observed to produce polymers containing *trans* olefins, NMR spectral analysis of these polymers revealed evidence of a low degree of stereoselectivity with signals corresponding to a mixture of *cis*- and *trans* olefinic protons.[304]

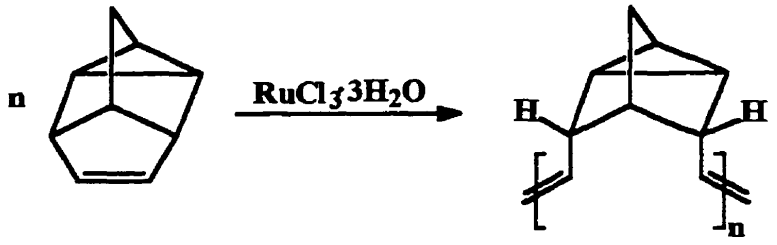

Figure 5.17: The ring-opening metathesis polymerization of deltacyclene

A further modification of the thermal and mechanical properties of the polymer may be achieved by the synthesis of modified monomers. Lautens and coworkers investigated the polymerization of 5-siloxydeltacyclene in the presence of $Mo(=CHCMe_2Ph)(=N\text{-}2,6(i\text{-}Pr)_2Ph)(O\text{-}t\text{-}Bu)_2$, which also possesses a high degree of tolerance for various functional groups.[306-307] In addition to the polymerization of this modified monomer, the ROMP of deltacyclene was once again carried out so as to compare the efficiency of the molybdenum catalyzed reaction with that of the ruthenium catalyzed reaction. It was observed that the species derived from the molybdenum catalyst system possessed an increased molecular weight and decreased polydispersity index in comparison to the $RuCl_3 \cdot H_2O$ catalyst. An extension of the effect of the initiator on ROMP polymerization was conducted with respect to the copolymerization of deltacyclene and 5-siloxydeltacyclene with $RuCl_3 \cdot H_2O$, $ReCl_5$ or $Mo(=CH\text{-}CMe_2Ph)(=N\text{-}2,6(i\text{-}Pr)_2Ph)(O\text{-}t\text{-}Bu)_2$ (Figure 5.18).[307] Several interesting observations were noted with respect to the structural details of the resulting polymeric material. A general increase in molecular weight and decreased polydispersity index of the isolated polymeric material was evident upon the use of the various catalyst systems in the order Mo alkylidene > $ReCl_5$ > $RuCl_3 \cdot H_2O$. Additionally, although the traditional $RuCl_3 \cdot H_2O$

and $ReCl_5$ catalysts resulted in random copolymers, the living nature of the molybdenum alkylidene catalyst allowed for the synthesis of both random and block copolymers. Finally, it has been mentioned previously that the choice of the catalyst may play a crucial role in determining polymer microstructure. Here, it was found that ruthenium and molybdenum catalysts generated polymeric species with *cis* and *trans* olefins whereas as the highly stereoselective nature of the $ReCl_5$ catalyst was demonstrated by the preferential formation of *cis* olefins.

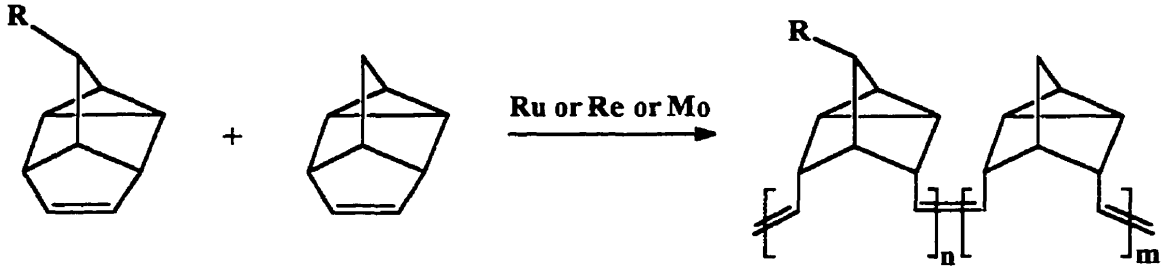

Figure 5.18: The copolymerization of deltacyclene and siloxydeltacyclene using Ru, Re or Mo catalysts systems

5.1.2 Nuclear Magnetic Resonance Spectroscopy

5.1.2.1 Introduction

In the past few decades, such tremendous strides have been made in the development of nuclear magnetic resonance spectroscopy that chemists worldwide recognize it as one of the most powerful and influential tools for the elucidation of both organic and inorganic species.[308] The theoretical basis for nuclear magnetic resonance spectroscopy existed several years prior to the actual development and use of this technique for chemical analysis. It was W. Pauli, in 1924, who first established the theoretical basis of NMR spectroscopy. He suggested the splitting of the energy levels of certain atomic nuclei upon exposure to a magnetic field as a result of the properties of spin and magnetic moment that they should possess. Yet, it was two independent researchers, Bloch and Purcell who have been recognized as the fathers of NMR spectroscopy for their success in demonstrating that nuclei absorb electromagnetic radiation in a strong magnetic field due to the energy level splitting induced by the magnetic field.[308] Subsequent investigation of the absorption properties of atomic nuclei in a magnetic field resulted in the discovery that molecular environment plays a role in this behavior and may be correlated with molecular structure.[309] An NMR spectrum is generated by a plot of the frequencies of the absorption peaks of certain nuclei in the sample versus peak intensities. The appearance of a peak at a particular frequency, the chemical shift, is due to the difference in the magnetic environment of individual nuclei and is instrumental in the elucidation of molecular structure. Coupling constants, which result from the interaction between the nuclear spins of the nuclei in a molecule, are also

an invaluable feature of an NMR spectrum. Since these initial discoveries, the development of NMR spectroscopy has led to its widespread application in the growth of organic, inorganic and biochemical fields.

5.1.2.2 One- and Two-Dimensional Nuclear Magnetic Resonance Spectroscopy

The theoretical basis of NMR spectroscopy stems from the very simple principle that all nuclei carry charge. The spinning of this charge on the nuclear axis in some nuclei results in the generation of a magnetic dipole whose angular momentum may be described in terms of spin numbers, I.[203, 308-310] The values representative of the angular momentum of the spinning charges may have values of either 0, 1/2, 1, 3/2 and so on, where the ^{1}H and ^{13}C nuclei with a spin number of 1/2 are most commonly used. From a quantum mechanical point of view, the spin number is fundamental in determining the number of orientations of a nucleus, given by the formula $2I + 1$, when exposed to an external magnetic field. The ^{1}H and ^{13}C nuclei are of importance in this study and both have a spin number which results in two energy levels. The essence of NMR is the transfer of enough radio frequency (rf) electromagnetic energy to align magnetic nuclei with the magnetic field.[203, 308-310] The quantum of energy required for a transition from one state to another is given by $h\nu$ where h corresponds to Plank's constant and ν is the frequency of the electromagnetic radiation. It is important to note that the frequency, ν, of the electromagnetic radiation is specific for a particular nucleus. Following the promotion of the nuclei to a higher spin state, the nucleus can lose energy to its

environment via several mechanisms or relaxation processes allowing the return to its lower energy state.

Although various techniques have been employed in the excitation of nuclei to higher spin states, the most widely used method results from the development of Fourier Transform techniques involving the simultaneous excitation of a selected set of nuclei with a short powerful rf pulse which provides the required frequency range.[203, 308] The central frequency in the pulse is slightly off-resonance for all of the nuclei resulting in the generation of a free induction decay (FID) sine wave for all the nuclei with each frequency equal to the difference between the applied frequency and the resonance frequency for a particular nucleus. In a compound with more than one ^{1}H or ^{13}C nucleus, the FID display is composed of superimposed sine waves with characteristic frequencies and interference patterns. With computer technology, the automatic digitization of data and its subsequent storage allows for a repetition of pulses and subsequent acquisition of data which results in a build-up of the signal.[203, 308] The available NMR techniques permit control over rf pulse widths and time intervals which may be used between the initial magnetization pulse and the onset of signal acquisition resulting in the generation of either one-dimensional (1-D) or two dimensional (2-D) spectra. Fourier transformation of the time domain FID spectrum converts the data into the conventional frequency domain NMR spectrum. The nature of the information required for structure determination depends on the complexity of the compound of interest and establishes the technique employed.

Conventional 1-D NMR spectra involve the acquisition of the FID as a function of time which is subsequently subjected to Fourier transformation with respect to time,

t_1.[203, 308] The term one-dimensional NMR can be deceiving considering the spectra are generated in two dimensions with the frequency of the resonance plotted with respect to peak intensity. Although they may be rather complex, 2-D experiments consist, in general, of a variable time interval, t_2, in addition to the initial time interval, t_1, followed by the acquisition of the FID as a function of time. The consequence of this procedure is the generation of a series of FID sine waves which are subsequently submitted to Fourier transformation in two dimensions with respect to t_1 and t_2. The results of a 2-D NMR experiment are presented in a spectrum in the form of a contour slice through the peaks which represent intensities perpendicular to the plane of the paper. Figure 5.19 shows a series of FID sine waves generated as a result of variable time intervals which are then subjected to two transformations to yield the corresponding 2-D spectrum (Figure 5.20).[203, 308] The NMR spectrum shown in Figure 5.20 is referred to as a correlated spectroscopy (COSY) spectrum. H-H and C-H COSY or homonuclear correlated spectroscopy and heteronuclear correlated spectroscopy represent two of the most commonly used 2-D NMR techniques today.

Several features of 2-D NMR present valuable information for the elucidation of molecular structure. Figure 5.21 shows a very general representation of an H-H COSY spectrum where the spectrum is generated along the diagonal and off-diagonal resonances. These off-diagonal resonances are commonly referred to as crosspeaks and indicate the relationship between two protons in the compound of interest.[308] As Figure 5.21 illustrates, coupled protons may be identified by drawing vertical and horizontal lines from either one of the crosspeaks to the diagonal. It is important to note

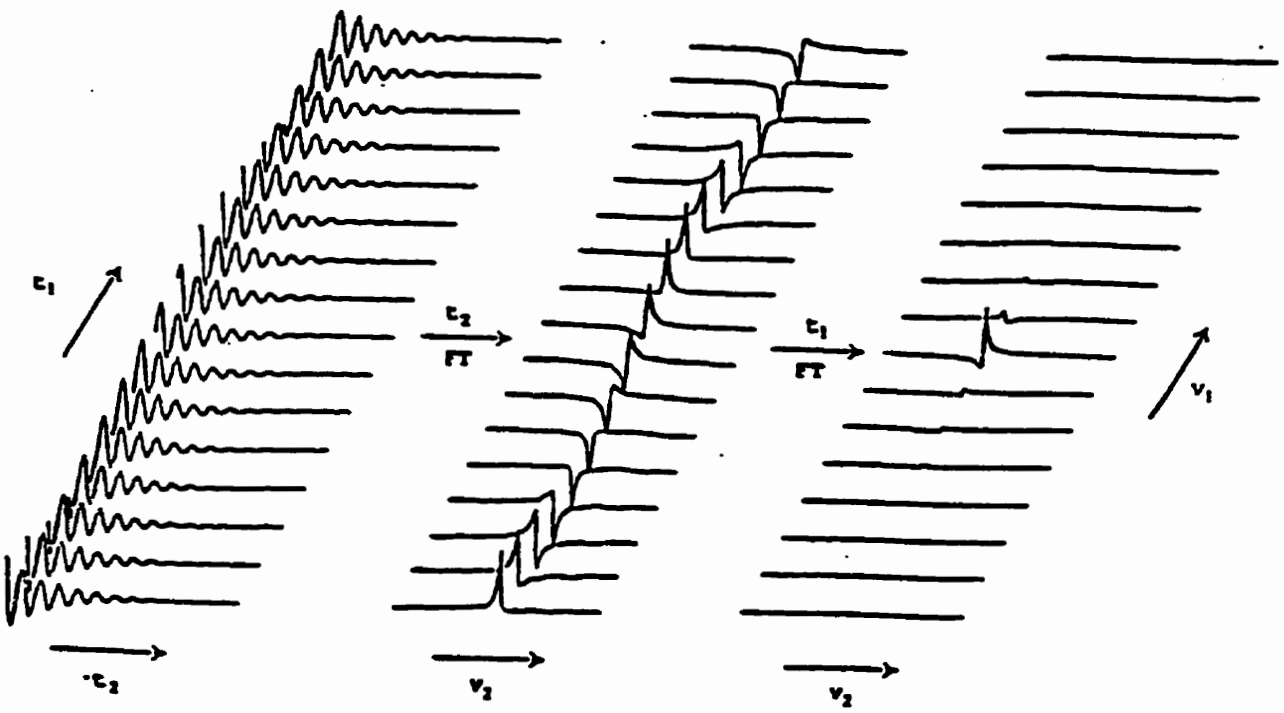

Figure 5.19: Transformation of a series of FID sive waves recorded at variable time intervals.

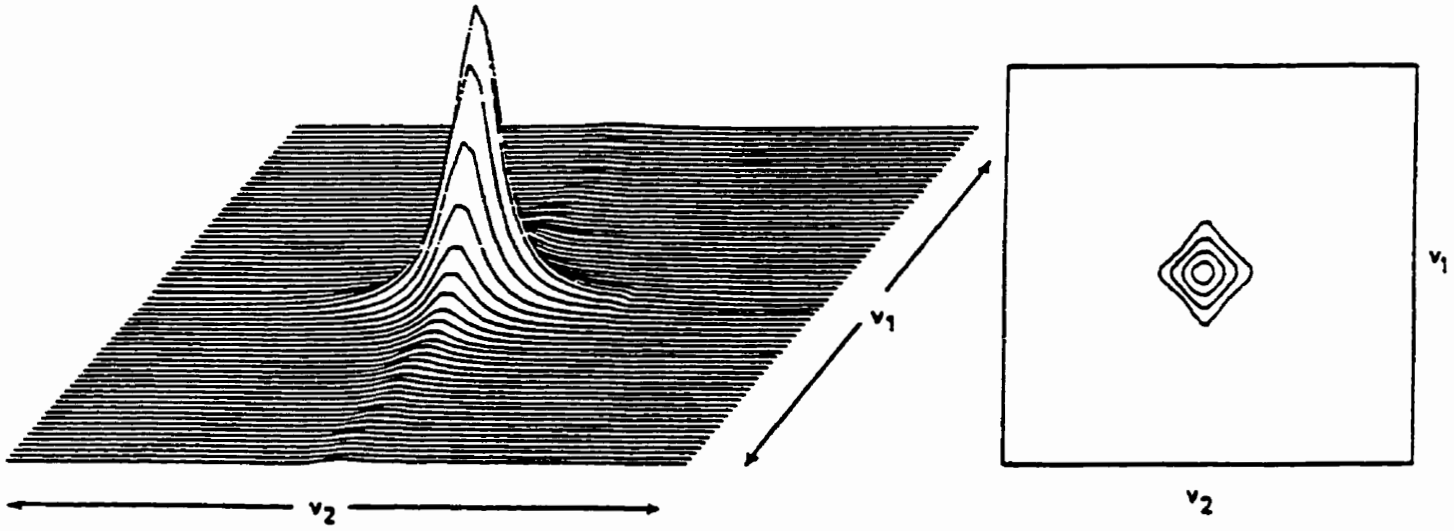

Figure 5.20: 2-D NMR spectrum following transformation of the FID

that although this technique allows for complete identification of the structure of interest CH COSY is more useful for the determination of the connectivities of a proton to a particular carbon atom.[203, 308] The relationship of a proton and carbon atom appears as a crosspeak contour which is intersected by lines drawn from proton and carbon spectra plotted at 90° to one another.

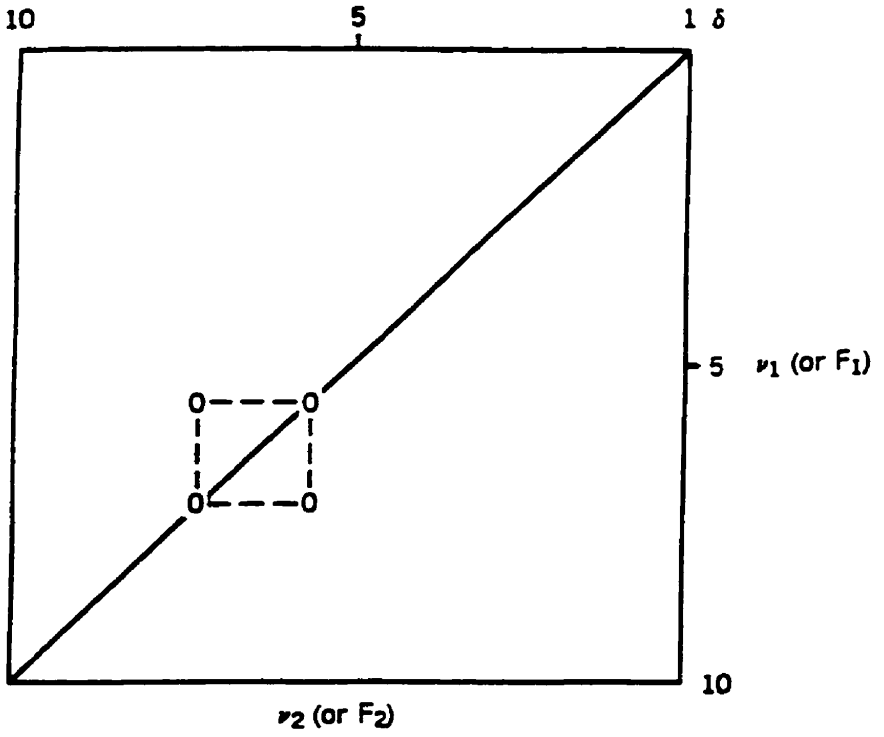

Figure 5.21: H-H COSY spectrum illustrating the identification of coupled protons

5.1.2.3 NMR Studies of Bicyclo[2.2.1]heptenes

Since the development of nuclear magnetic resonance spectroscopy, the use of this technique in the structural identification of compounds of increasing complexity continues to arouse the curiosities of NMR spectroscopists worldwide. Specifically, the generation of two diastereomeric isomers from the Diels-Alder reaction of cyclic dienes and derivatives of ethylene have been found to be of particular interest due to the spectroscopic properties they exhibit.[309, 311-322] For instance, the determination of the chemical shifts and coupling constants of these bicylo[2.2.1]- heptane and heptene ring systems, facilitated by the fixed geometry of these rigid structures, offers enough stereochemical information to distinguish between the *endo* and *exo* isomers. This is by no means meant to suggest that stereochemical assignments in bicyclo[2.2.1]heptane and heptene derivatives are straightforward. In fact, the cage-like structure of these species tends to bring more groups within close enough proximity to one another to complicate identification by significant long-range shielding effects.[309, 319] Nonetheless, due to numerous NMR studies which have been conducted on various bridged ring systems, several spectral consistencies have been identified and aid in the stereochemical determination of the two isomers.[309, 311-322]

Specifically, ^{1}H NMR investigations of bridged ring systems have revealed characteristic relationships between spin-coupling constants of the ring protons and stereochemistry, in addition to long-range spin-coupling and the establishment of substituent configuration by the evaluation of diamagnetic shielding effects of a double bond or a benzene ring.[311-322] A study conducted by Musher and coworkers of various

monohydroxyl derivatives of bicyclo[2.2.1]heptane describes some of the most common spectral features of these compounds.[321] It has been observed that an exceptionally large difference in magnetic shielding exists between an *exo* and *endo* proton with the *exo* proton experiencing larger deshielding. Although the diamagnetic anisotropy of the C-C bonds in the ring have a role in generating this difference, the substantial inequivalency of the magnetic shielding of these two protons may also be attributed to other unidentified factors. Other notable diagnostic characteristics of these species include distinct $J_{exo\text{-}endo}$ and $J_{endo\text{-}endo}$ coupling as well as fairly large long-range coupling.[321] Figure 5.22 summarizes the system which will be used throughout the following discussion to identify the protons and carbon atoms from one another.

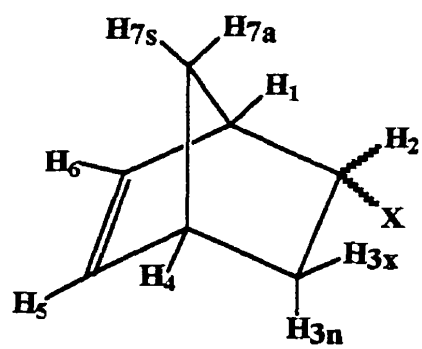

Figure 5.22: Labeling of bicyclo[2.2.1]heptenes

As a result of the numerous NMR studies which have been conducted with respect to bridged ring systems, several spectral regularities have been reported and found to be useful in the stereochemical assignment of these species.[309, 311-322] In particular, much attention has been focused on the *endo-exo* isomerism in both norbornanes and norbornenes as well as the *syn-anti* isomerism at C-7 in norbornenes.[309, 312-314, 316-320, 322] In some instances, it has been established that both vicinal coupling, or coupling across three bonds, and long-range coupling, coupling separated by more than three bonds, may be instrumental in assigning the stereochemical nature of these systems.

One spectral consistency which may be extremely useful in distinguishing between the two isomers of bridged ring systems follows from a generalization regarding the relative chemical shifts of axial and equatorial protons in six-membered rings. In 2-substituted norbornanes and many of their derivatives, it has been established that *endo* protons resonate upfield from their *exo* counterparts.[316, 319, 323] It should be noted, however, that a combination of factors in bicyclic compounds may play a role in the shielding, with particular consideration of other substituents in highly substituted species.[321]

Early studies involving bicyclic systems centered on the establishment of certain chemical shifts and explored the relevance of the Karplus relationship involving vicinal coupling constants and dihedral angles in an attempt to define the species structure and stereochemistry.[313] Experimentally speaking, the accuracy of the theoretical predictions of Karplus, which relate the coupling constants of protons on adjacent carbon atoms with the dihedral angles between the protons using Equations 5.1 and 5.2, have been found to depend on the compound of interest.

$$J = 8.5\cos^2\phi - 0.28,\ 0^\circ \leq \phi \leq 90^\circ \qquad \text{Equation 5.1}$$

$$J = 9.5\cos^2\phi - 0.28,\ 90^\circ \leq \phi \leq 180^\circ \qquad \text{Equation 5.2}$$

It has been suggested that several factors should be considered which may contribute to experimentally determined values which depart from theoretical predictions. Structural aspects including the electronegativities and orientation of substituents, hybridization of carbon atoms as well as bond lengths and bond angles are all possible contributors to variations in theoretically based expectations.[309] In particular, the magnitudes of the vicinal coupling constants and the chemical shifts have been shown to exhibit a linear variation with respect to substituent electronegativities.

As mentioned earlier, *endo*-protons invariably appear upfield from *exo*-protons rendering them an important feature for determining the molecular structure of these species in terms of the assignment of configuration and chemical shifts.[316, 319, 323] It is important to note that although double bond anisotropy is considered an important contributor to this chemical shift difference, it is not the most prominent determinant.[316] Variations in the chemical shifts of the bridge protons with respect to neighboring substituents may also prove beneficial in structural assignment. One study observed the spectral resonances of the bridge protons with respect to an endo-2-chloro-5-norbornene and various dichloro-substituted 5-norbornenes.[319] It was determined that H_{7a} is more sensitive to structural variations than H_{7s} due to the close proximity of H_{7a} to the substituent chlorine atom. Specifically, an upfield resonance representative of H_{7a} in the presence of chlorines in the *endo* position relative to its downfield appearance upon the substitution of even one chlorine in the *exo* position clearly demonstrates the effect

substituent position has on chemical shifts. Another study suggested that chlorine substituents may also play a role in determining the resonances of other protons in the molecule with the effect decreasing with increasing distance of the protons.[320] One report concluded that olefinic protons resonate further downfield in the presence of 2-*endo* substituents as compared to their *exo* counterparts.[319] However, it is important to note that this observation was only evident in this study and has not been verified in other examples in the literature.

Numerous NMR investigations of substituted norbornanes and norbornenes have also led to the establishment of typical spin-spin coupling constants.[309, 311-314, 318-320, 322] The coupling between olefinic protons in norbornene derivatives, $J_{H5\text{-}H6}$, is measured in the range of 5.0-6.0 Hz and is seldom affected by substituents in the 2-position of the ring. The difference of this coupling with that of the vicinal couplings of the olefinic and bridgehead protons, $J_{H1\text{-}H6}$ and $J_{H4\text{-}H5}$, 2.4-3.0 Hz, as well as the magnitude of the $J_{H2\text{-}H3x}$ coupling, 7.5-9.2 Hz, emphasizes the effect of structural variations on the Karplus equations. For each of these coupling constants, although the dihedral angle of the hydrogen nuclei is approximately 0°, the coupling constants vary considerably in magnitude.[319] This difference in coupling constant has been attributed to the hybridization of the carbon to which the proton is attached, as well as the influence of the dihedral angle and the ring size.

In the same way that chemical shifts of *exo* and *endo* protons have been found to be useful diagnostic features in the stereochemical assignment of bridged ring species, *exo-exo*, *endo-endo* and *exo-endo* coupling constants have also proven to be beneficial for this purpose.[313, 319] *Exo-exo* and *exo-endo* coupling constants have been observed to

be highly dependent on substituent electronegativities, yet, generally range from 7.5-9.2 and 2.1-5.8 hertz, respectively. Stereochemical identification may also be verified with respect to the coupling between *endo* and *exo* protons and the adjacent bridgehead protons with the respective coupling constants being 0 and 3.0-5.0 hertz, and unmistakably indicate atomic arrangement. A unique trait of norbornene and norbornadiene derivatives is the inequivalency of the bridge protons.[319] This characteristic is indicated by the difference in the coupling constants of the bridgehead protons with each of the bridge protons. Again, the value of the coupling constants, $J_{H7s\text{-}H4}$ and $J_{H7a\text{-}H4}$, typically in the range of 1.5-2.0 Hz, are different despite identical dihedral angles. An explanation for this anomaly has not yet been established.

An interesting phenomenon which has been explored in a variety of norbornane, norbornene, norbornadiene and 7-oxa derivatives is the magnitude of the long range couplings characteristic of these compounds.[309, 319] This observation has been justified as a direct consequence of the compactness of these species with all of the protons being within five bonds of one another and in a fixed geometrical arrangement. Several long-range interactions which have been established as a result of the investigation of isomeric 7-substituted norbornene derivatives is the coupling between the olefinic and anti-7-protons (Figure 5.23a). Additionally, there is a four bond, long-range coupling between protons H_{7s} and H_{3n} of 2.0-3.1 Hz (Figure 5.23b). A smaller allylic coupling has also been observed in norbornene compounds (Figure 5.23c).

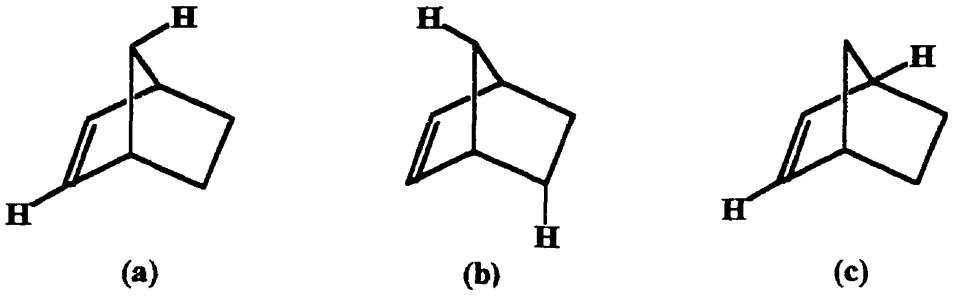

Figure 5.23: Long range coupling in norbornene and its derivatives

An alternative approach to the stereochemical assignment of norbornene and its derivatives involved the hydrogenation of the 5,6-double bond which effected small changes in the chemical shifts of the *endo* and *exo* protons.[316] The study of several norbornene derivatives showed that upon the removal of the unsaturated bond in the molecule, the *exo* and *endo* protons shift to higher and lower fields, respectively. It was suggested that this effect is a result of the appreciable anisotropy of the double bond.

The above may be used as a guideline in the assignment of the chemical shifts of substituted norbornane and norbornene derivatives. Clearly, several spectral features may be used to distinguish the two isomers of bicyclic Diels-Alder adducts. In this work, 5-norbornene-2-methanol has been modified via nucleophilic aromatic substitution and the corresponding isomers identified on the basis of the above mentioned spectral characteristics.

5.2 Results and Discussion

In many ways the design of novel polymeric species is defined by the type of functional groups incorporated into the molecular structure of the macromolecule and its subsequent effect in determining the properties of the corresponding material. Traditionally, functionalization of macromolecular species was attempted following polymerization and often suffered from unforeseen difficulties of the desired chemical transformations on the polymer substrate. With the development of well-defined ROMP catalysts and their increasingly high tolerance for various functional groups, the polymerization of functionalized monomers can be more readily achieved.

5.2.1 Monomer Preparation

5.2.1.1 Preparation of Capped 5-norbornene-2-methanol Monomers

It has been mentioned previously that the presence of terminal chloro groups in (arene)CpFe$^+$ complexes provides an ideal route for further functionality. Additionally, strained cyclic olefins have demonstrated optimal characteristics for polymerization under ring-opening metathesis conditions. In an attempt to prepare polymeric species with unique characteristics, η^6-(chlorobenzene)-η^5-cyclopentadienyliron hexafluorophosphate was reacted with *exo,endo*-5-norbornene-2-methanol in the presence of potassium t-butoxide in a THF/DMF solvent mixture under a nitrogen

atmosphere (Scheme 5.1). Complex **5.1** was isolated as its hexafluorophosphate salt in 85 % yield. The structural features of this novel monomeric unit renders it a potential candidate for ROMP. Due to the structural complexity of norbornene derivatives, 1-D and 2-D NMR analysis was required for its identification and is presented in detail in Section 5.2.2.1 of this work.

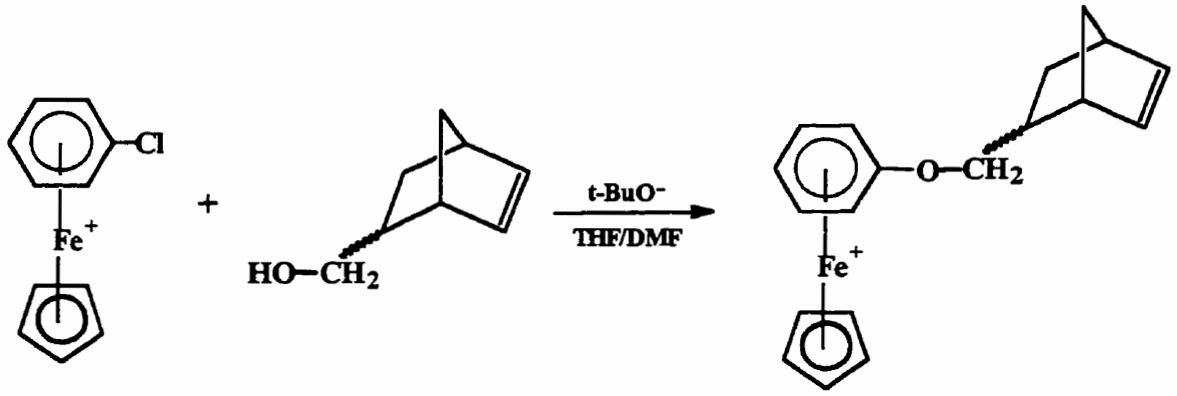

5.1

Scheme 5.1

5.2.1.2 Photolytic Demetallation of Capped 5-norbornene-2-methanol Monomers

Photolytic demetallation has been presented as an efficient and convenient method for the isolation of the modified free arenes. Complex **5.1** was dissolved in a 1:3 v/v acetonitrile-dichloromethane mixture and fitted into a photochemical apparatus equipped with a Xenon lamp and irradiated for 4 hours under a nitrogen atmosphere (Scheme 5.2). Purification of the product via column chromatography allowed for the isolation of the desired organic compound in 83% yield. Mass spectrometry was one of the techniques used for the structural verification of the isolated compound with a m/z of 200.15 for the molecular ion. Additionally, 1-D and 2-D NMR was used for structural identification of compound **5.2** and is presented in detail in Section 5.2.2.2 of this work.

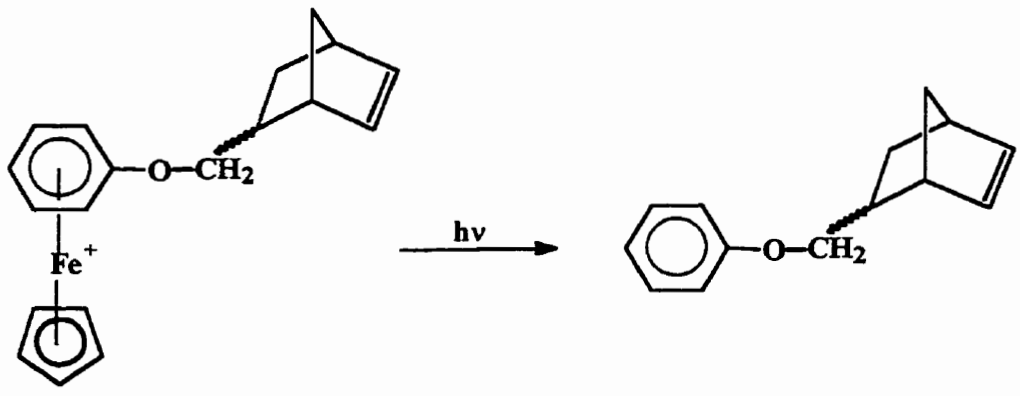

5.1 **5.2**

Scheme 5.2

5.2.2 Structural Identification of the Polyether Capped 5-norbornene-2-methanol Monomer

5.2.2.1 NMR Studies of the Modified 5-norbornene-2-methanol Complex

It was mentioned previously that the preparation of bridged ring species via the Diels-Alder reaction of cyclic dienes and derivatives of ethylene generally results in the generation of two diastereomeric isomers. Section 5.2.1.1 described the S_NAr reaction of a mixture of 5-norbornene-2-methanol with the η^6-(chlorobenzene)-η^5-cyclopentadienyliron complex as the initial step in the preparation of compound **5.2**. The diastereomeric nature of the starting material contributed to the complexity of the NMR spectra of the corresponding products, **5.1** and **5.2**, and prompted the use of both 1-D and 2-D NMR for their identification. Several previously established spectral characteristics inherent to a large majority of bridged bicyclic compounds were crucial in distinguishing the stereochemical nature of the two isomers.[309, 311-322] ^{1}H NMR and 2-D HH COSY allowed for the stereochemical identification of the two isomers by examining the chemical shifts, coupling constants and connectivities of the protons. The assignment of the chemical shifts of the bicyclic ring protons were then used to determine the carbon resonances via CH COSY techniques.

One of the most distinct features of the ^{1}H NMR of all cyclopentadienyliron complexes is the appearance of the strong resonances in the range of 5-6 ppm indicative

of the cyclopentadienyl protons. In this case, the appearance of two strong and closely resonating peaks at 5.13 and 5.15 ppm, which were shifted slightly upfield from the cyclopentadienyl resonance of the η^6-chlorobenzene-η^5-cyclopentadienyliron starting complex, suggested the presence of two isomers and prompted a more thorough examination of the ^{1}H NMR spectrum. Further evidence for the success of the cyclopentadienyliron activated S_NAr reaction with 5-norbornene-2-methanol was the complexity of the spectrum in the range of 0.5 to 4.5 ppm indicative of the bridged ring protons.

Figures 5.24 and 5.25 show the ^{1}H NMR and HH COSY spectra of complex **5.1**. A general analysis of the ^{1}H NMR spectrum of complex **5.1** led to the identification of a series of peaks in the 3.7-4.4 ppm region of the spectrum. The chemical shifts and spectral pattern of the four resonances appearing in this region were indicative of the methylene group attached to the ether linkage of the complexed benzene ring. Two of the four peaks were attributed to the *exo* isomer and the other two resonances to its *endo* counterpart. However, the precise stereochemical identity of the peaks could not be adequately determined using just one-dimensional ^{1}H NMR and as a result two-dimensional HH COSY techniques were incorporated so as to investigate the connectivities and chemical shifts of the bridged ring protons.

The HH COSY is a coupled proton experiment in which each proton resonance is represented by a peak along the diagonal of the generated spectrum.[308] The identity of the peaks in the 1-D ^{1}H NMR spectrum are determined by establishing the connectivities and subsequent chemical shifts and spin-spin coupling relationships of the protons of the

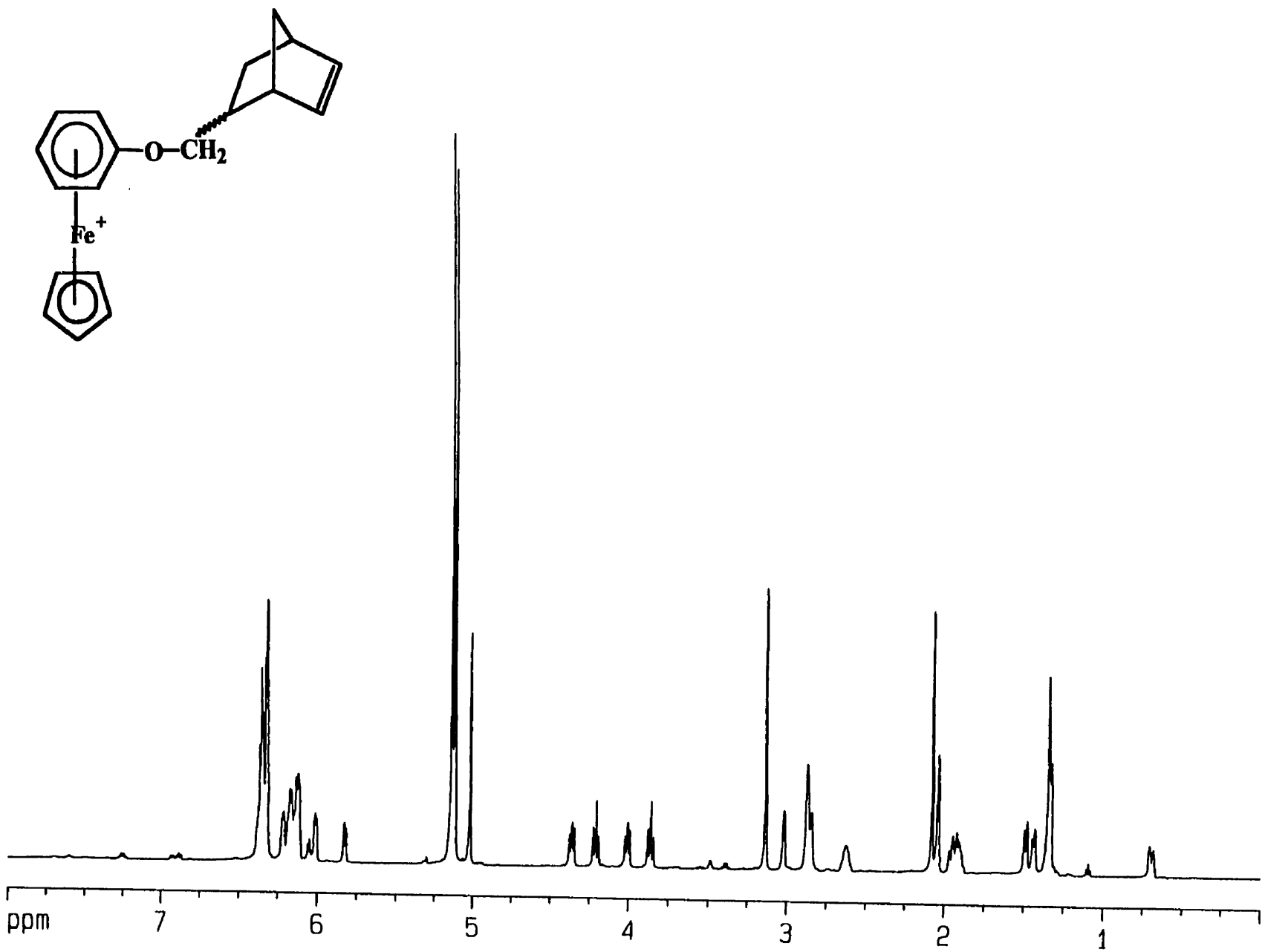

Figure 5.24: ^{1}H NMR spectrum of complex **5.1** in acetone-d_6.

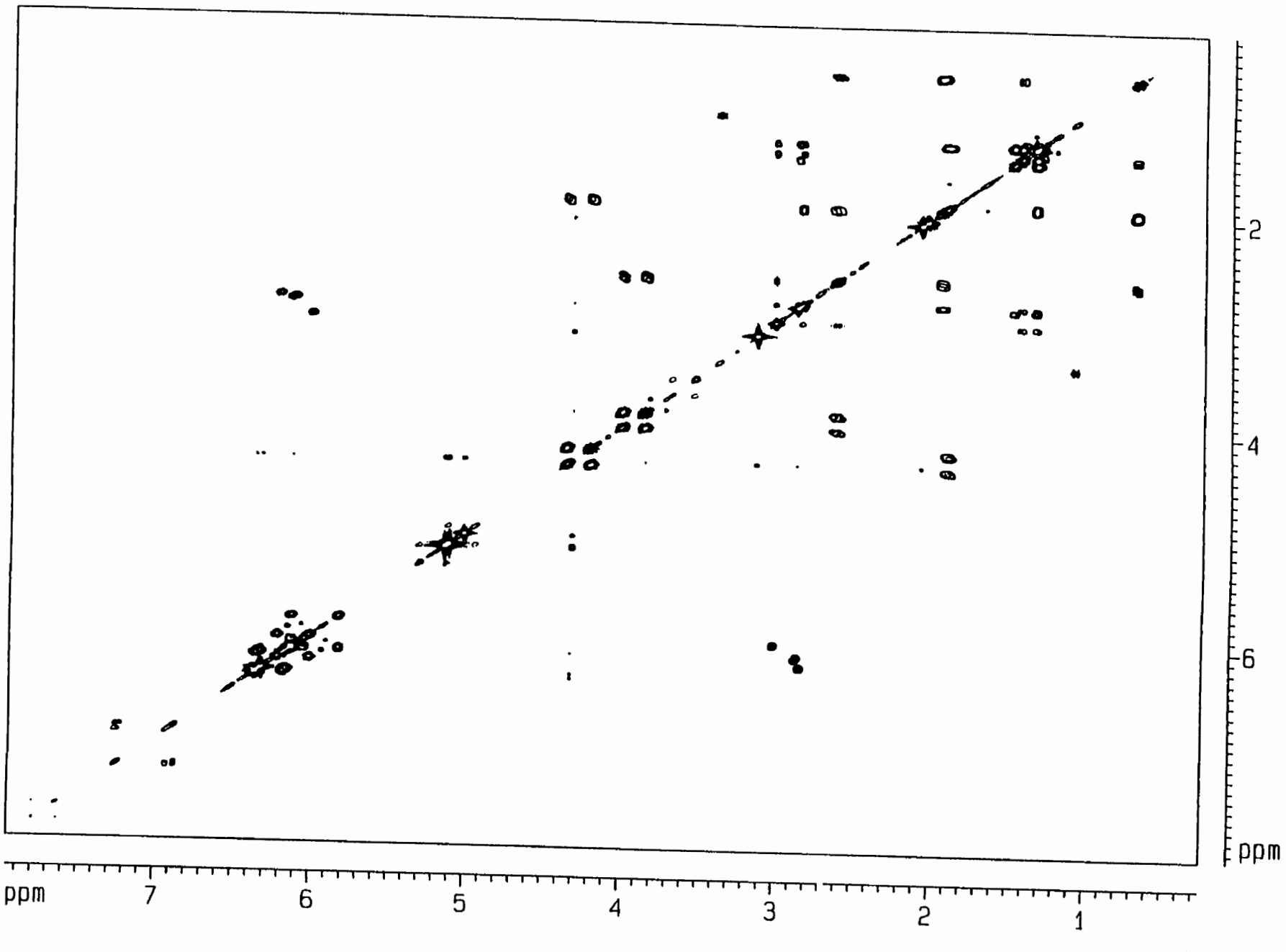

Figure 5.25: HH COSY spectrum of complex **5.1** in acetone-d_6.

bridged ring component of complex **5.1**. In this case, the peaks at 3.87, 4.02, 4.22 and 4.38 ppm corresponding to the methylene protons attached to the ether linkage are a useful starting point for the analysis. To determine the chemical shifts of other protons which are structurally related to these protons, it is necessary to draw vertical and horizontal lines across the entire spectrum corresponding to each of these chemical shifts. These lines also intersect other signals located off the diagonal and are referred to as crosspeaks.[203] It is the intersection of these crosspeaks which indicates the coupling of two points, or protons, along the diagonal. If vertical and horizontal lines are drawn for each peak along the diagonal, the connectivities of all the protons in the structure may be established. The connectivities of other protons in the bridged ring structure will be discussed relative to the peaks of the ether attached methylene protons of one isomer at 3.87 and 4.02 ppm. Horizontal and vertical lines drawn from these chemical shifts indicate that these resonances are strongly coupled with one other proton at 2.62-2.63 ppm. According to the labeling of the bridged ring species as outlined in Figure 5.22, this resonance may be attributed to H_2 since it is the only proton adjacent to the ether attached methylene protons. The identification of H_2 may now be used in the determination of other protons in the structure. For instance, the intensities of the crosspeaks at 1.93-1.98 and 0.70 ppm, which intersect with lines drawn from H_2, suggest strong couplings with the corresponding protons. The literature suggests that the strongest coupling of H_2 with other protons in the structure would be with those protons referred to as H_{3x} and H_{3n} in Figure 5.22.[313, 319-320] It is important to note that the interactions or lack of interactions of H_2, H_{3x} and H_{3n} would be instrumental in determining their stereochemical disposition. It has also been suggested that when H_2 is

in the *exo* position, there is the probability for coupling with H_1.[319-320] One of the trends which has been established as evidence of the stereochemical identity of protons such as H_2 in bridged ring systems is that protons in the *endo* position are not expected to couple at all. Examination of other interactions of H_2 suggest a small coupling to a peak at 3.02 ppm. This peak may be tentatively assigned as H_1. On the basis of the numerous NMR studies for various ring systems, a long-range interaction between H_2 in the *endo* position and one of the bridge protons has been found.[309, 319] Due to the broadness of the resonances, there is no indication of such a coupling for this particular isomer. At this point, it is useful to assume an *exo* position of H_2 for the isomer of interest. H_2 is normally strongly coupled to H_{3x} and H_{3n}, and these two protons are very strongly coupled to one another as would be expected from their structurally defined geminal relationship. In considering the identity of the proton at 1.98 ppm and the interactions which have already been established, vertical and horizontal lines drawn from this chemical shift shows one other crosspeak which corresponds to a proton located at 2.85 ppm. The relative chemical shift of this proton in comparison to the proton which has been assumed as H_1 suggests that this may be the other bridgehead proton, H_4. If this is the case, it may be concluded that the proton at 1.98 ppm must be in the *exo* position and may be referred to as H_{3x}. Verification of H_1 and H_4 as the bridgehead protons is suggested by their relationship with those protons at 6.02 and 6.22 ppm, respectively, whose chemicals shifts identify them as the vinyl protons, H_6 and H_5. The connectivity of H_1 and H_4 with H_2 and H_{3x}, respectively, further acknowledges the *exo* position of H_2 and H_{3x}. The verification of protons H_1 and H_4 as the bridgehead protons allows for the determination of the chemical shifts of the bridge protons. According to the literature,

the bridge and bridgehead protons will without a doubt have some association with one another.[311, 314, 319-320, 322] It is observed that, in accordance with the analytical technique which has been used to determine all of the interactions described up to this point, each of the bridgehead protons are coupled to each of the bridge protons, H_{7s} and H_{7a}. At this point, it is possible to assume that the proton located at 0.70 ppm is in the *endo* position and may be defined as H_{3n}. Its identity is instrumental in distinguishing between the two bridge protons. It has been suggested that due to the compact and rigid nature of bridged ring systems a remarkable number of long-range interactions have been established which may be useful diagnostic features in the structural identification of these molecules.[309, 319] Long-range coupling across four bonds and involving protons such as H_{3n} in the *endo* position and the bridge proton, H_{7s}, has been observed (Figure 5.23b). Coupling of H_{3n} with one of the bridge protons is evident from the interaction at a crosspeak of vertical and horizontal lines drawn from the respective chemical shift positions. This proton is then assumed to be H_{7s}. Verification of its identity is offered by the fact that the vinylic protons have also been observed to participate in long-range interactions with the bridge proton which is anti to it. This would suggest that the vinylic protons would then be coupled to H_{7a} and is spectroscopically evident from the HH COSY of complex **5.1**. The stereochemical nature of the other isomer in this mixture was determined using the same analytical strategy. Table 5.1 summarizes the chemical shifts of both the *endo* and *exo* isomers of the mixture as established by the HH COSY experiment. In comparing the data presented in Table 5.1, our study seems to agree with previous studies of 2-substituted norbornenes and many of their derivatives in which it has been observed that, typically, *endo* protons resonate upfield from their *exo*

counterparts.[316, 319, 323] This is indeed the case when considering the relationship between H_{3x} and H_{3n} in each isomer. Furthermore, our analysis has shown that in considering the two isomers, the H_2 proton in the *endo* position resonates at 1.90-1.92 ppm compared to 2.62-2.63 ppm when in the *exo* position. Following the identification of each proton in the structure as based on their connectivities from the 2-D NMR experiment, this information may be used in conjunction with the 1-D ^1H NMR spectrum in the evaluation of the spin-spin coupling constants of the related protons. Table 5.3 summarizes the spin-spin coupling constants determined from the ^1H NMR spectrum. It is important to note that in many cases the evaluation of the coupling constants was limited by spectral overlap and peak broadening. For instance, as expected on the basis of previous studies of various bridged ring species, the bridgehead protons appear as broad singlets.[320] Clearly, this eliminates the possibility of spin-spin coupling determinations.

Upon assignment of the chemical shifts of the protons of both isomers, the ^{13}C chemical shifts could be determined and used to verify the structures. The presence of two diastereomeric isomers complicated the 1-D ^{13}C NMR spectrum and prompted the use of CH COSY for the carbon atom identification. Figures 5.26 and 5.27 show the 1-D ^{13}C and 2-D CH COSY NMR spectra of complex **5.1**. A CH COSY experiment involves the generation of a spectrum by plotting the ^1H and ^{13}C NMR spectra at a 90° angle to one another resulting in the appearance of a crosspeak contour to indicate the connectivity of a proton and carbon in the molecular structure of interest.[203, 308] The intersection of lines drawn from the ^1H and ^{13}C NMR spectra plotted along the x and y axes, respectively, determines a correlation between a particular proton and the carbon to which it is bonded. It is useful to outline the method used in the identification of the carbon resonances using

one of the isomers as an example. It is also important to keep in mind the structure of the complexes of interest as outlined in Figure 5.22. The 2-endo isomer will be employed in the following explanation. The analysis is initiated by the intersection of the resonances of protons H_{3n} and H_{3x} at 0.70 and 1.93-1.98 ppm, respectively, with the carbon resonance at 28.95 ppm. As suggested by the molecular structure, a horizontal line drawn from this resonance should be intersected by two proton peaks and therefore defines this resonance as C_3. In a similar manner, the line representative of C_7 should intersect two crosspeak contours at the ^1H chemical shifts corresponding to protons, H_{7s} and H_{7a} at 1.45 and 1.35 ppm, respectively. This is verified in the 2-D CH COSY spectrum and observed at 45.02 ppm. The carbon atom corresponding to the methylene group attached to the ether linkage is the other carbon atom whose identity is verified by its relationship to two proton resonances. The intersection of the crosspeak contours representative of these protons established the resonance at 73.54 ppm as the ether linked methylene carbon atom. All the other carbon atoms in the compound are identified by their interaction relative to the chemical shift of only one proton. Table 5.2 summarizes the carbon atom chemical shifts of both diastereomeric isomers.

Table 5.1: ^{1}H NMR Chemical Shifts in ppm of *5*-norbornene-2-methanol Complex, **5.1**

Isomer	H-1	H-2	H-3x	H-3n	H-4	H-5	H-6	H-7s	H-7a	CH_2O	Cp
endo	3.02	2.62-2.63	1.93-1.98	0.70	2.85	6.22	6.02	1.45	1.35	3.87, 4.02	5.13
exo	2.88	1.90-1.92	--	--	2.88	6.15	6.13	1.49	1.35	4.22, 4.38	5.15

Sample run in acetone-d_6 (ppm from solvent peak at 2.04 ppm)
Complexed aromatic protons in the 6-7 ppm region
Severe overlap rendered H_{3x} and H_{3n} of exo- isomer unobservable

Table 5.2: ^{13}C NMR Chemical Shifts in ppm of 5-norbornene-2-methanol Complex, **5.1**

Isomer	C-1	C-2	C-3	C-4	C-5	C-6	C-7	CH_2O	Cp
endo	44.03	38.24	28.95	42.04	138.19	132.26	45.02	73.54	76.74
exo	43.85	--	--	41.92	136.44	137.35	49.45	74.06	76.74

Sample run in acetone-d_6 (ppm from solvent peak at 29.8 ppm)
Complexed aromatic carbons in the 70-90 ppm region
Severe overlap rendered H_{3x} and H_{3n} of exo- isomer unobservable

Table 5.3: Determined Coupling Constants (Hz) for 5-norbornene-2-methanol Complex, **5.1**

	endo	*exo*
J(1,6)	2.6	-
J(2,CH)	7.1	6.5
J(3x,3n)	11.6	-
J(3x,4)	3.8	-
J(3n,7s)	2.6	-
J(4,5)	3.0	-
J(5,6)	5.3	-
J(7a,7s)	7.8	-
J(CH_2)	9.1	9.2

*Where values are not included, they are not measurable due to overlap/broadness of lines.

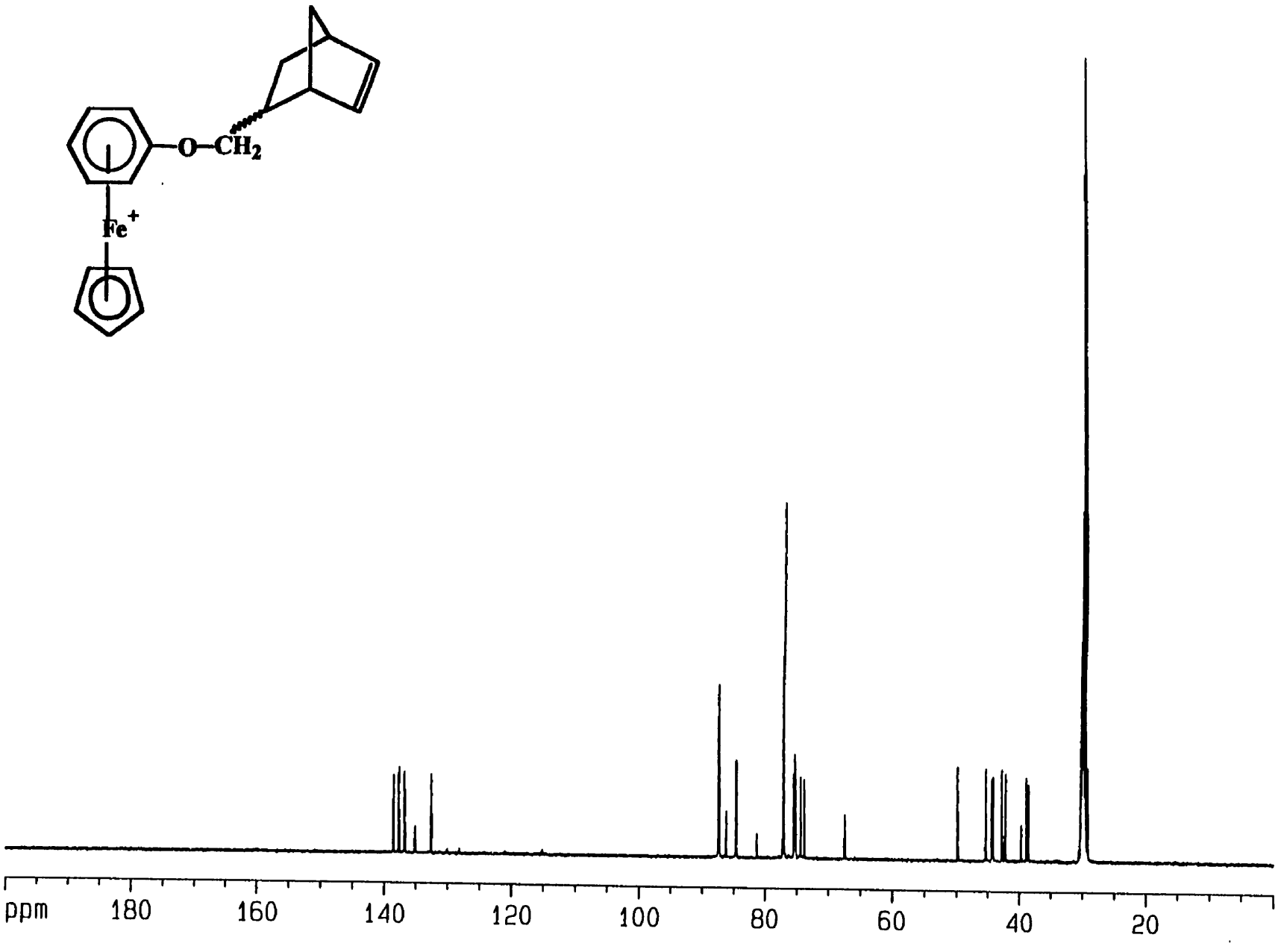

Figure 5.26: ^{13}C NMR spectrum of complex **5.1** in acetone-d_6.

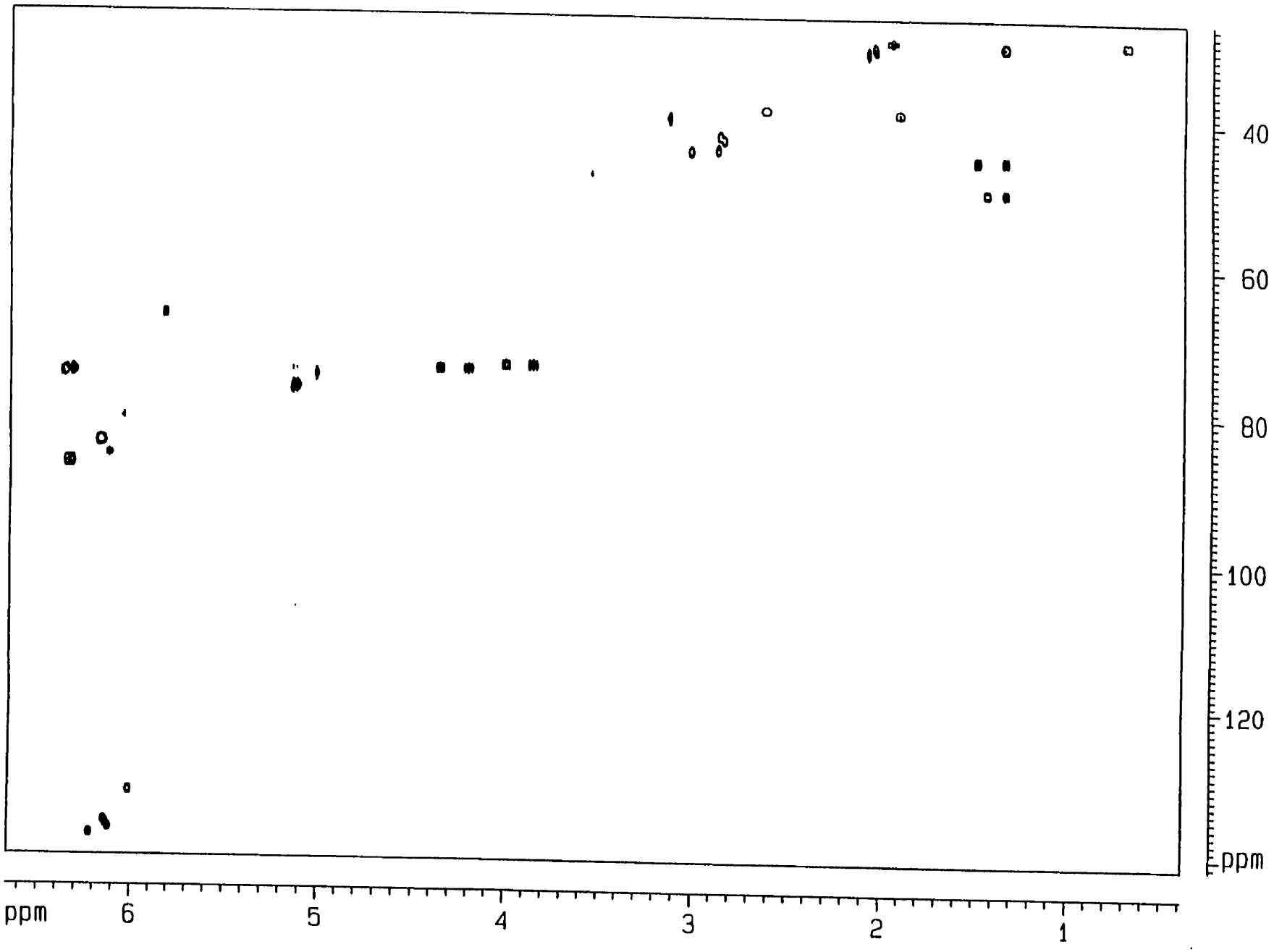

Figure 5.27: CH COSY spectrum of complex **5.1** in acetone-d_6.

5.2.2.2 NMR Studies of the Modified 5-norbornene-2-methanol Compound

It has been mentioned previously that photolytic demetallation has been shown as an extremely effective method for the liberation of the modified ligand from its organometallic counterpart. Upon the photolysis of the diastereomers of the complex, two isomers were evident in the organic species as well. Again, a combination of 1-D ^1H NMR and HH COSY techniques were used to determine the proton chemical shifts corresponding to the two isomers of compound **5.2** (Figures 5.28 and 5.29) . In the same way that the analysis of the complex was initiated by the identification of the methylene protons attached to the ether linkage, this was a good starting point for the structural analysis of the isomers of the compound as well. Following the connectivities of the peaks resonating at 3.57 and 3.73 ppm, allowed for the determination of the stereochemical nature of one of the isomers. Vertical and horizontal lines drawn from these chemical shifts led to the identification of the adjacent proton, H_2, at 2.56-2.62 ppm. Recall, that it is the relationship of this proton with other protons in the structure which is crucial in establishing the *exo* and *endo* arrangement of this proton. It has been stated that H_2 should exhibit a strong relationship with protons H_{3x} and H_{3n}.[313, 319-320] Indeed, two large intensity crosspeaks were identified and allowed the protons at 0.66 and 1.91-1.97 ppm to be associated to H_{3x} and H_{3n}. Furthermore, a less intense connectivity to a proton at 3.07 ppm was evident and tentatively assigned as H_1 since a small coupling is expected between the bridgehead proton and H_2 in the *exo* position. With this suggestion in mind, the stereochemical nature of H_2 may be verified by the identification and

connectivities of all the other bridged ring protons. Referring back to H_{3x} and H_{3n}, it is clear that these two protons are very strongly coupled as would be expected from their geminal arrangement to one another (J = 9-12 Hz). In order to determine the exact identity of each of these protons, their relationships to other protons in the spectrum must be examined. It is observed that the proton at 1.91-1.97 ppm is associated with the proton at 2.87 ppm. It is suggested that this proton corresponds to the bridgehead proton, H_4, since a proton in the 3-position of the ring would demonstrate a small coupling to the bridgehead proton if it were in the *exo* position. The identity of H_1 and H_4 is further verified by their coupling with the vinylic protons at 5.98 and 6.19 ppm allowing for the identification of these resonances as H_6 and H_5, respectively. The identity of the bridgehead protons leads to the determination of the bridge protons appearing at 1.33 and 1.51 ppm. A distinction between these two protons can be made by examining the connectivities of the proton at 0.66 ppm which is suggested to represent H_{3n}. Other than the relationship of this proton to H_2 and H_{3x}, it is evident that there is also a connection of this proton to the proton at 1.51 ppm or, in other words, to one of the bridge protons. Based on long-range coupling which has been observed in other bridged ring systems, the coupling of H_{3n} with the bridge proton at 1.51 ppm defines it as the proton anti to H_{3n} and therefore identifies it as H_{7s}.[309, 319] Additionally, the identity of the proton at 1.33 ppm as H_{7a} is established on the basis of its connection with the vinyl protons, H_5 and H_6, since it has been determined that these protons will couple to the bridge proton anti to them. The connectivities of the protons as described here identifies this isomer as the one in which H_2 is in the *exo* position. A similar strategy was used for the identification of the other isomer where H_2 is in the *endo* position. Table 5.4 summarizes the chemical

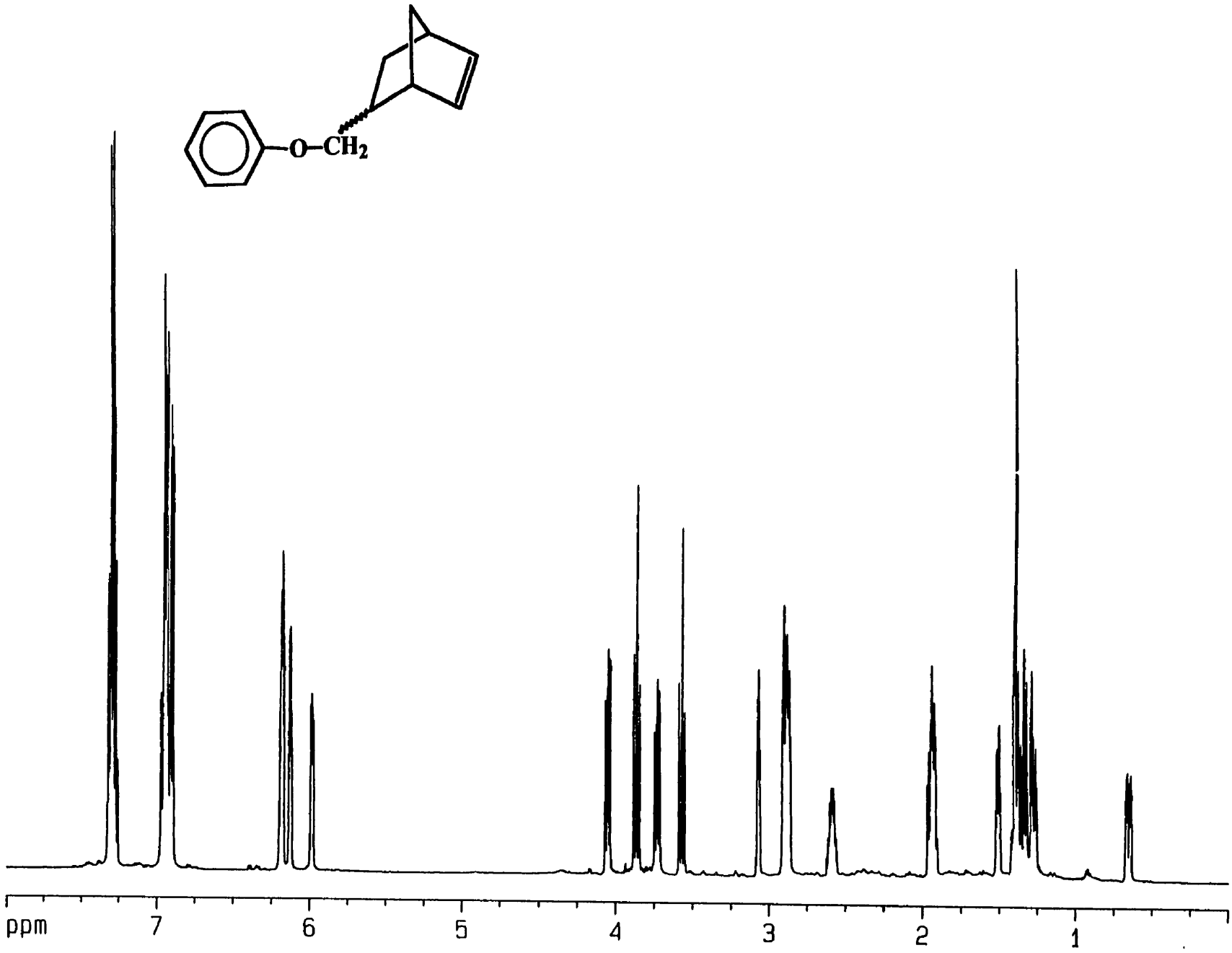

Figure 5.28: ^{1}H NMR spectrum of compound **5.2** in $CDCl_3$.

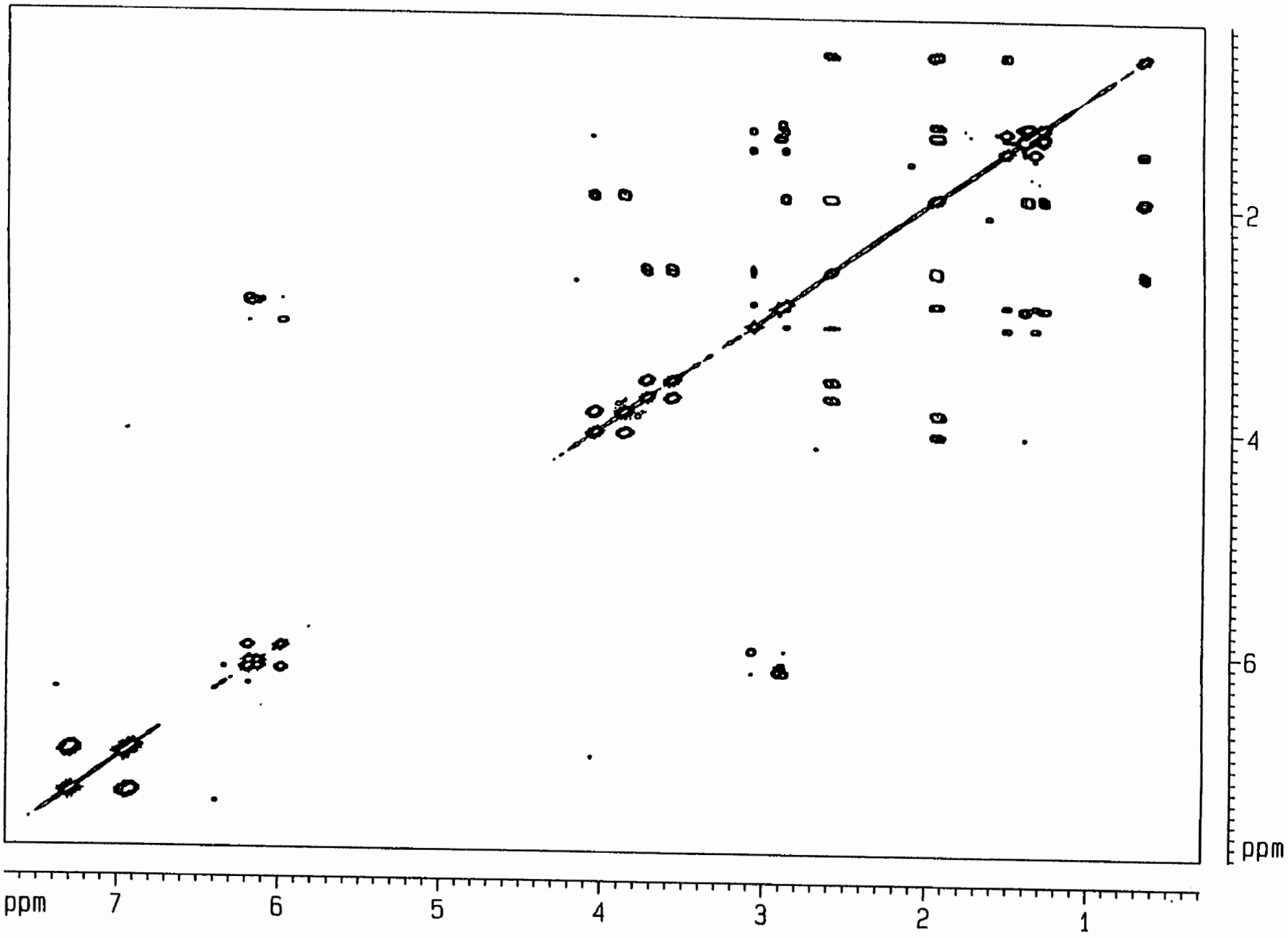

Figure 5.29: HH COSY spectrum of compound **5.2** in $CDCl_3$.

shifts of the two isomers according to the above described analysis. Keep in mind that a comparison of certain resonances of the two isomers helps to confirm the stereochemical assignment of the two isomers. In particular, the upfield position of the H_2 proton at 1.92 ppm when in the *endo* position compared to its appearance at 2.56-2.62 ppm when in the exo position is an established trend in various bridged ring systems.[316, 319, 323] Upon the determination of the chemical shifts of the protons in each isomer, ^{1}H NMR may be used to evaluate the coupling constants of the connected protons. As was mentioned previously, some difficulty was experienced in determining certain coupling constants due to peak overlap or broadened resonances. However, as shown in Table 5.6, many spin-spin coupling constants were determined for the diastereomeric compounds. It is important to note that the coupling constants coincide with the literature values thereby verifying the stereochemical assignment of the isomers as described above and summarized in Table 5.6.[309, 311-322]

It was mentioned previously that ^{13}C NMR was another technique used to verify the identity of complex **5.1**. The same techniques as described above in the determination of the chemical shifts of the carbon atoms of the complexed species were used for the verification of the structure of the corresponding compound. The CH COSY spectrum of the isomers of compound, **5.2**, allowed for the determination of the proton and carbon connectivities and the identification of the carbon resonances. The ^{13}C NMR and CH COSY spectra shown in Figures 5.30 and 5.31, respectively, and the results of the analysis corresponding to both isomers are presented in Table 5.5. It is important to note that in the cases in which two protons are associated with one carbon atom, the horizontal line representative of the carbon resonance will intersect two crosspeak

contours corresponding to the chemical shifts of the two protons.

Table 5.4: ^{1}H NMR Chemical Shifts in ppm of 5-norbornene-2-methanol, **5.2**

Isomer	H-1	H-2	H-3x	H-3n	H-4	H-5	H-6	H-7s	H-7a	CH_2O
endo	3.07	2.56-2.62	1.91-1.97	0.66	2.87	6.19	5.98	1.51	1.33	3.57, 3.73
exo	2.87	~1.92	~2.55	~0.63	2.90	6.18	6.13	1.50	~1.29	3.87, 4.05

Sample run in $CDCl_3$ (ppm from solvent peak at 7.24 ppm)
Uncomplexed aromatic protons in the 6.7-7.5 ppm region

Table 5.5: ^{13}C NMR Chemical Shifts in ppm of 5-norbornene-2-methanol, **5.2**

Isomer	C-1	C-2	C-3	C-4	C-5	C-6	C-7	CH_2O
endo	43.96	38.42	29.06	42.23	137.45	132.37	49.41	71.38
exo	42.29	38.65	29.72	43.78	136.47	136.78	49.41	72.24

Sample run in $CDCl_3$ (ppm from solvent peak at 77.0 ppm)
Uncomplexed aromatic protons in the 110-160 ppm region
Where values are not included, they are not measurable due to overlap of lines

Table 5.6: Determined Coupling Constants (Hz) for 5-norbornene-2-methanol

Compound, **5.2**

	endo	*exo*
J(1,6)	2.9	2.9
J(2,3x)	9.4	-
J(2,3n)	4.3	-
J(2,CH)	6.5	6.2
J(3x,3n)	11.6	-
J(3x,4)	3.8	-
J(3n,7s)	2.6	-
J(4,5)	3.0	-
J(5,6)	5.6	5.6
J(7a,7s)	8.1	-
J(CH_2)	9.3	9.1

*Where values are not included, they are not measurable due to overlap/broadness of lines.

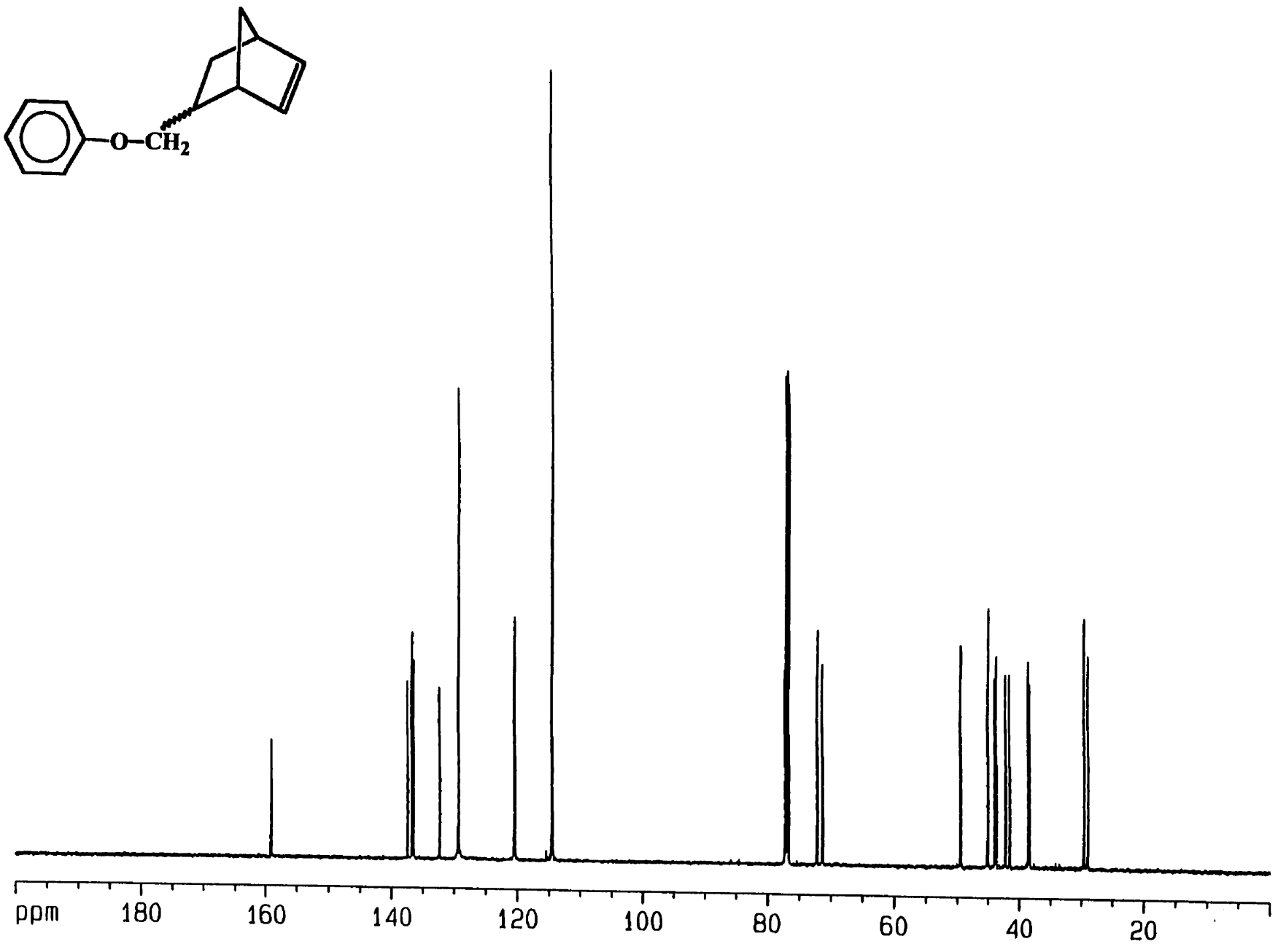

Figure 5.30: ^{13}C NMR spectrum of compound **5.2** in $CDCl_3$.

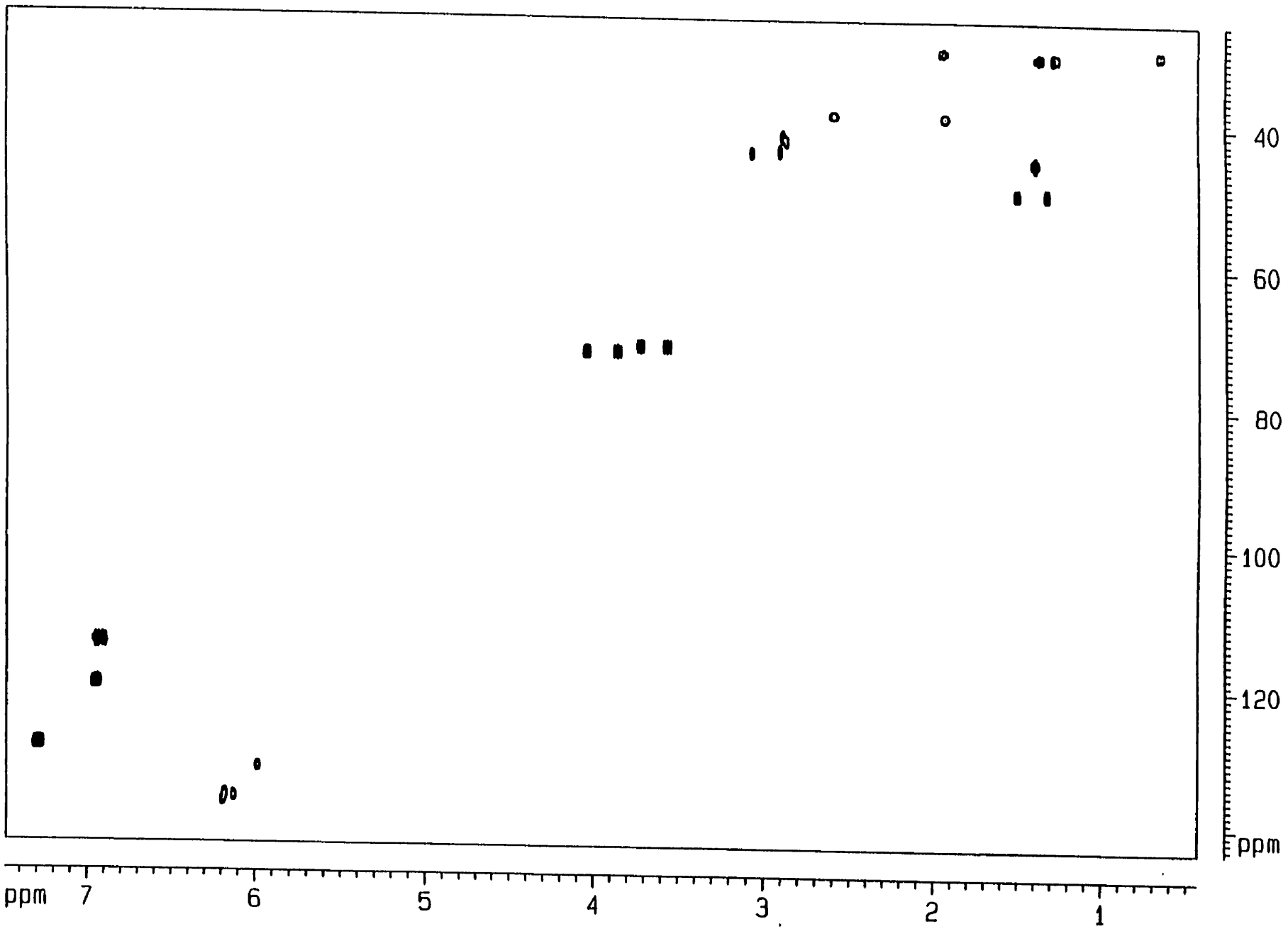

Figure 5.31: CH COSY spectrum of compound **5.2** in $CDCl_3$.

5.3 Ring-Opening Metathesis Polymerization of Polyether Substituted Norbornene

Studies of the ring-opening metathesis polymerization of strained cyclic olefins have reported that a number of factors including the nature of the catalyst, monomer composition and solvent conditions may play an important role in the structural features and molecular weight of the resulting polymeric materials. Initially, the degree of polymerization of **5.2** was investigated with the treatment by 1 mol % $RuCl_3 \cdot H_2O$ in anhydrous ethanol at 60°C.[324] The resulting polymeric material with a weight average molecular weight of 298 000 g mol^{-1} was isolated as a creamy fibrous solid by precipitation in methanol. Scheme 5.3 illustrates the methodology employed in the polymerization of compound **5.2** using $RuCl_3 \cdot H_2O$ as the catalyst.

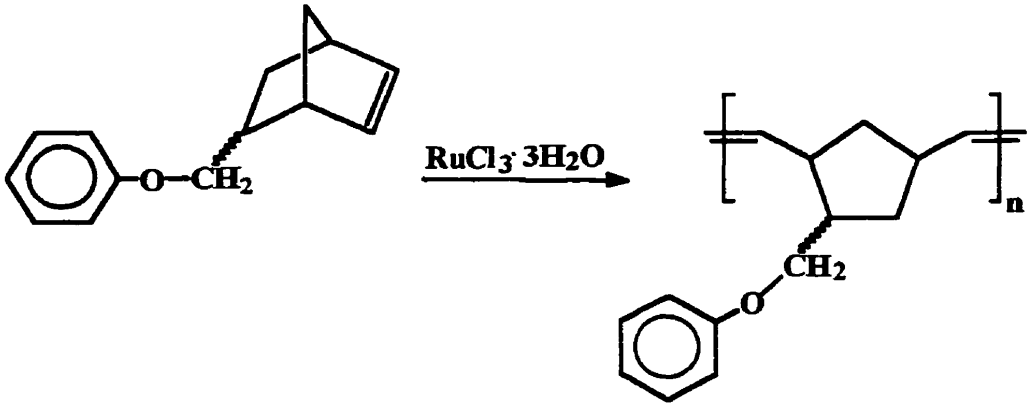

Scheme 5.3

Grubbs and coworkers have reported that in ROMP studies involving ruthenium catalysts, an increase in polymeric molecular weight has been noted with increasing amounts of water in the reaction solvent.[290] In keeping with these observations and in an attempt to increase the molecular weight of the polymeric species, ROMP of compound **5.2** was carried out using $RuCl_3 \cdot H_2O$ as a catalyst with varying amounts of water/ethanol. gel permeation chromatographic analysis versus polystyrene standards was employed for the molecular weight determination of the isolated polymers and the results are summarized in Table 5.7. It is important to note that in keeping with previous studies, molecular weights in the 10^6 range were consistently obtained.[304] It was observed that an increasing ratio of water in the ethanol/water solvent mixture resulted in polymeric materials with higher molecular weights. Furthermore, a significant decrease in the polydispersity index was evident. It is important to note that even though polymerization was attained when the solvent was pure water, this solvent system did not result in the highest molecular weight material and produced species with low polydispersity indices. This observation may be attributed to the lack of solubility of the monomer in this solvent. As dictated by the solubility of the monomer, an ethanol/THF solvent mixture was investigated in an attempt to increase the molecular weight of the polymeric material. Unfortunately, polymerization under these conditions did not prove favorable and resulted in a drastic decrease in molecular weight.

Table 5.7: Effect of Increasing Water on the Molecular Weight of the ROMP of Compound **5.2**

Entry	Starting Material/ Catalyst Ratio	Solvent Ratio (mL)	Mw	Mn	Mw/ Mn	Yield (%)
1	100/1	1.0 EtOH	298 000	87 000	3.4	32
2	100/1	0.97 EtOH/0.03 H_2O	328 000	12 500	2.6	45
3	100/1	0.5 EtOH/0.5 H_2O	535 000	248 000	2.2	73
4	100/1	1.0 H_2O	397 000	177 000	2.2	82
5	100/1	0.5 EtOH/0.5 THF	1530	900	1.7	45

In addition to the determination of high molecular weight species using molecular weight determination, verification of the polymerization was also confirmed using NMR techniques. Perhaps the most outstanding feature of the ^{1}H NMR spectrum indicative of successful polymerization is the broadness of the resonances as compared to the fine structure evident in the ^{1}H NMR spectra of the corresponding monomeric unit. This would be attributed to the increased number of protons represented by each resonance upon polymerization. Further analysis of the ^{1}H NMR spectra showed the disappearance of the resonances attributed to the double bond of the bridged ring species at 5.98 and 6.19 ppm and at 6.13 and 6.18 ppm, for the 2-*endo* and 2-*exo*- isomers of compound **5.2**, respectively. However, upon polymerization a broad resonance at 5.26-5.38 ppm appeared which was assigned to the olefinic protons with a *trans* stereochemical arrangement on the basis of previous studies.[304] This agrees with earlier reports which have stated that ruthenium catalysts commonly yield polymers containing trans-olefins.[325] Due to the limited solubility of the polymeric species, analysis via ^{13}C NMR was inconclusive.

6.0 Synthesis of Cyclic and Acyclic Cyclopentadienyliron Complexes with Ether, Thioether or Amine Bridges

6.1 Polyaromatic Ethers and Thioethers

Polyaromatic ethers and thioethers are representative of a class of polymeric materials referred to as engineering thermoplastics.[111, 113, 121-123] Characteristics such as thermal stability, chemical and flame resistance, high mechanical strength, and the potential for electrical properties have provoked increased attention from industry.[111-119] As a result of these attributes, these materials have been found to be useful in a variety of applications including moldings, coatings and adhesives thereby making the commercial development of these "high performance plastics" highly profitable.[111, 113, 121-123] The industrial importance of this type of polymer prompts the continued synthetic exploration of novel routes for their preparation. Section 1.4 of this work outlines some of the traditional as well as more recently developed synthetic techniques used in this field.

Several approaches have been explored towards the synthesis of polyaromatic ethers and thioethers in an attempt to alter their properties for specific applications. In addition to utilizing different reaction conditions in an attempt to control the molecular weight and molecular weight distribution of the resulting polymeric materials, monomer structure variations have been investigated. Changing the nature of the material by the incorporation of rigid or flexible linkages or various functional groups or side chains have been explored in the preparation of these materials.[116-117, 120, 123-124] In the past few decades, organometallic polymers with metallic moieties within, or pendent to the

backbone of the polymer chain have proven to be of importance due to their thermal, optical and magnetic properties.[111, 113, 121-123]

Although the incorporation of metallic moieties into etheric and thioetheric polymer structures has been investigated previously, a recent resurgence of interest in this area of study has arisen with respect to $CpRu^+$, Cp^*Ru^+ and $CpFe^+$ metallic moieties pendent to the polymer chain.[17, 19, 70, 86, 109-110] Segal and his coworkers used metal activated nucleophilic aromatic substitution of an aryl halide in the preparation of poly(ether-ether-ketone) with pendent $CpRu^+$ moieties.[17] Not only was Segal able to prepare the organometallic polymer, but the subsequent subjection of this material to photolytic or thermolytic demetallation allowed for the isolation of the purely organic counterpart.

More recently, Cp^*Ru^+ has been used, upon its complexion to 1,4-dichlorobenzene, in reactions with several hydroxy- and thioxy- aromatic dinucleophiles to yield the corresponding polyethers and polythioethers.[19, 110] However, Dembek's attempts to isolate the organic derivatives resulted in only partial demetallation. The solubility of the organometallic polymers in acetonitrile, DMF and DMSO demonstrates that the π-coordination of polymers with an aromatic backbone to metallic species enhances their solubility. Despite the success experienced with ruthenium systems for polymer preparation, drawbacks such as difficulties involved in the synthesis of the starting ruthenium complexes, high cost and consequent small scale investigations as well as the inefficiency of the demetallation process limits the practicality of this methodology.

The success in utilizing transition metal moieties in the activation of aryl halides towards nucleophilic aromatic substitution reactions in the presence of dinucleophiles for the synthesis of polymers generated an investigation of $CpFe^+$ as a potential activator. The attraction of this metallic moiety is prompted by the ease of complexation and decomplexation of the iron moieties, the use of commercially available starting materials, mild reaction conditions and large scale reaction quantities. It has been demonstrated that (1,4-dichlorobenzene)$CpFe^+$ hexafluorophosphate reacted in a stepwise manner with hydroquinone allowed for the preparation of soluble oligomeric aromatic ethers containing up to 35 metals.[70] The subsequent dissolution of these oligomeric species in an CH_3CN/CH_2Cl_2 solvent mixture followed by irradiation using a xenon lamp allowed for their complete demetallation and the isolation of the purely organic analogues of controlled molecular weights. Although this methodology offers a great deal of molecular weight control over the resulting polymeric material, a major obstacle for its application on an industrial scale is the numerous reaction steps necessary for the preparation of high molecular weight species.

6.2 Nitrogen-containing Macrocyles

6.2.1 Introduction

C. J. Pederson is often referred to as the father of supramolecular chemistry due to his milestone discovery in 1967 that described a systematic approach to the synthesis of oxygen-containing macrocyclic ligands.[326] This initial report aroused a great deal of interest in this field of chemistry and subsequent research continues regarding the fundamental chemical nature and potential applications of this class of compounds. It is important, however, to acknowledge that this was not the beginning of the era of macrocycles. Eight decades earlier Baeyer had prepared tetraazaquaterene (Figure 6.1a), a nitrogen-based macrocycle.[327] Several variations of nitrogen-containing macrocycles were reported by Alphen in 1937, and Krässig and Greber in 1953 and 1956, and are illustrated in Figures 6.1b and 6.1c, respectively.

The complex nomenclature associated with the cyclic compounds prepared by Pederson prompted him to develop a more convenient naming system for their identification.[326] The basis of his identification system stems from the appearance of these molecules to crown the cations with which they interacted. The first cyclic polyether synthesized was referred to as a "crown" and the group of compounds came to be known as "crown" compounds.

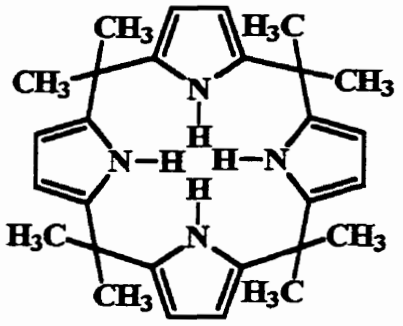

6.1a

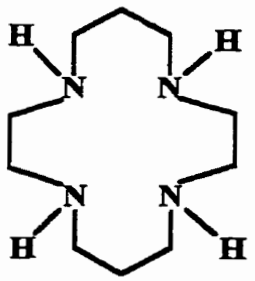

6.1b

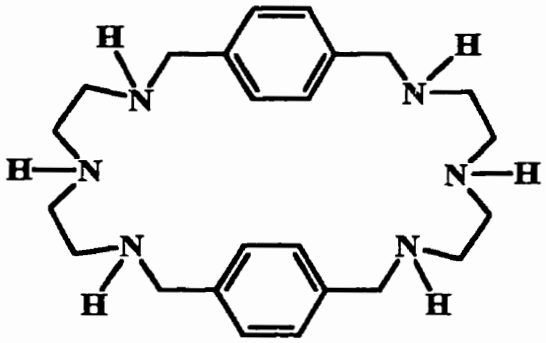

6.1c

Figure 6.1: The first nitrogen-based macrocyclic ligands

Several rules were outlined to ensure that the compounds were named systematically.[326] His nomenclature consisted of (1) the number and kind of hydrocarbon rings, (2) the total number of ring members, (3) the class name, crown, and (4) the number of heteroatoms in the cyclic ring. This nomenclature has been extended to the identification of macrocyclic ligands containing heteroatoms other than oxygen, where the position of nitrogen heteroatoms are indicated by a number.

6.2.2 Factors Determining Complexation

Metal-ion recognition plays important roles in both chemistry and biochemistry. Specifically, macrocyclic ligands have demonstrated the potential to act as metal-ion selective reagents.[328] Current synthetic efforts focus on the design of macrocycles which are able to discriminate among different cations. Several factors including macrocycle cavity dimensions, shape and topology, substituent effects, conformational flexibility/rigidity and donor atom type, number and arrangement have been identified as influences on the selectivity of the macrocyclic species for specific cations.[329-332]

The ability of oxygen and nitrogen containing macrocycles to form complexes with cations, anions and neutral organic molecules has been reviewed.[329-331] Although bi- and trinuclear complexes in which two or three metal ions form a complex with one macrocycle exist, nitrogen crown macrocycles mainly form 1:1 complexes with metal ions in which the ion is located in the central cavity of the macrocycle.

A crucial factor in determining the maximum stability in complex formation is the identification of a macrocyclic ligand for which the cavity size best matches the radius of the ion.[328] However, it is important to keep in mind that in many cases this lock-key relationship is overcome by other influences. The number, kind and arrangement of donor atoms also play an important role in macrocycle selectivities. Past investigations have shown that oxygen donor atoms have the greatest affinity for alkali, alkaline-earth and lanthanide cations.[333] When affinity values of an alkali metal ion such as K^+ in the presence of oxygen and nitrogen containing macrocyclic ligands are considered, this complexation trend is apparent. Generally, it was observed that log K values decrease in

the order of decreasing electronegativity of the heteroatom, with O > N (containing an alkyl substituent) > N (containing a proton).[334] Conversely, replacing oxygen donor atoms with nitrogen results in increased affinities for transition-metal cations. Figure 6.2 illustrates this observation by comparing the log K values in water of 12- and 18 membered macrocycles for Pb^{2+} interactions.[335]

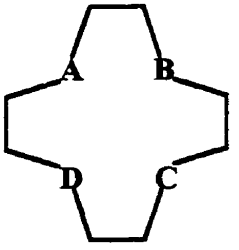

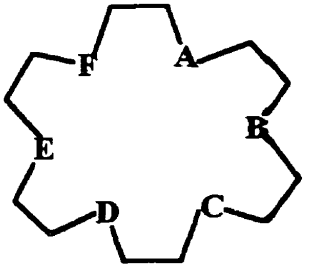

	log K		log K
a.) A-D = O	2.0	f.) A-F = O	4.4
b.) A = NH; B-D = O	4.1	g.) A, D = NH; B, C, E, F = O	6.9
c.) A, C = NH; B, D = O	6.3	h.) A, D = O; B, C, E, F = NH	9.0
d.) A-C = NH; D = O	10.5	i.) A-F = NH	14.1
e.) A- D = NH	15.9		

Figure 6.2: Affinity values of 12- and 18-membered macrocycles for Pb^{2+}

The details gathered in relation to the changing macrocycle-metal relationship based on variations in the macrocycle cavity size, donor atom type and substituents justifies the great interest in these compounds. Research of this type has allowed for great strides in the design and synthesis of macrocycles possessing selectivity for a desired cation or group of cations.

6.2.3 Applications of Macrocyclic Ligands

Achieving selective complexation of macrocyclic ligands with various cations, anions and neutral organic molecules has resulted in the use of these interactions in a remarkable number of applications.[330-331, 336–340] An area of chemistry in which metal ion-ligand interactions are particularly prominent is in biological processes.[339-350] It has been discovered that certain metal ion-ligand interactions are of particular importance in the prevention of undesirable biological processes.

Specifically, several macrocyclic ligands have been investigated for their potential antitumor activity. For instance, the nitrogen-containing macrocycle shown in Figure 6.3 when complexed to copper, gold and silver has been tested for their antitumor activity.[341] The localization and treatment of tumors using a ligand-radioisotope complex attached to an antibody represents some of the more recent investigations in metal ion-ligand applications.[342-348] With the knowledge that radioactive metal ions can damage liver and bone marrow, it is necessary that ligands which form very strong complexes with the appropriate cations are identified. It has been determined that several cyclic nitrogen-containing ligands are ideal for this purpose because they may be attached to the antibody and form strong complexes with the suitable radioactive metal ions.[342-348] The value of these cyclic nitrogen-containing ligands is their ability to form complexes with radioactive metal ions which do not dissociate in the presence of either the pH of body fluids or react with common metal ions in body fluids.

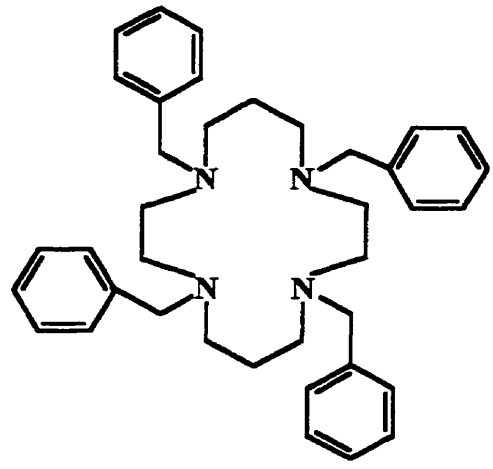

Figure 6.3: Nitrogen-based macrocycle which exhibits antitumor activity when complexed to copper, gold and silver

Recently, macrocyclic ligands have also demonstrated their potential as chelating agents in the immobilization of toxic metals.[349-350] For instance, Figure 6.4 illustrates an oxygen and nitrogen based macrocycle that enhances the urinary excretion of nickel, whose presence can be lethal, and corrects the levels of other necessary trace metal ions including Cu^{2+}, Zn^{2+} and Fe^{3+}.[350]

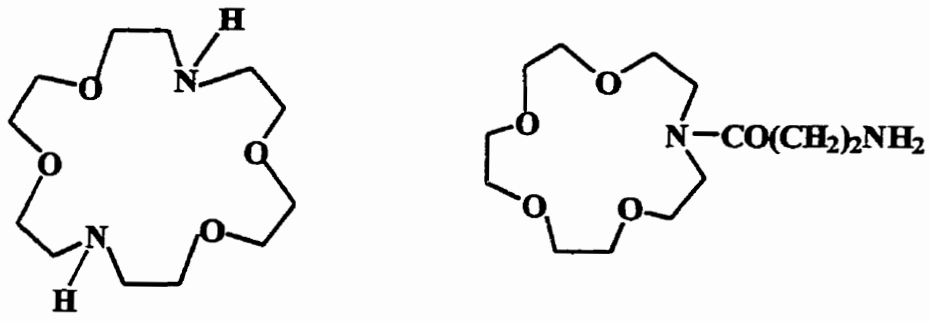

Figure 6.4: Macroheterocyclic ligand which enhances the excretion of toxic metal ions from the body

In addition to their biologically significant applications, certain nitrogen-containing macrocycles have been used as catalysts in nucleophilic substitution and oxidation reactions as well as in the chromatographic separation of metal cations.[327] Strides in chemical analysis have also benefited from nitrogen-containing macrocycle-metal ion interactions. Several of these complexes have been discovered as effective proton relaxation enhancement agents in aqueous solution in which the degree of enhancement is valuable in the development of clinical nuclear magnetic resonance (NMR) imagers.[326, 351]

6.2.4 Synthetic Methods in Macrocyclic Chemistry

6.2.4.1 Cyclization Versus Polymerization

Since Pederson's ground-breaking report presenting a systematic strategy to the synthesis of oxygen-based macrocyclic ligands, a vast array of macrocycles with mixed donor atom sets have been prepared.[326] The procedures which have been developed for their preparation are as numerous and varied as the compounds themselves, and a comprehensive review of all the techniques is beyond the scope of this presentation.[327, 359] Consequently, the following discussion will focus on the most promising and successful methodologies which have been employed in the preparation of nitrogen-based macrocyclic compounds.

In many cases, the reactants for both cyclization and polymerization are similar, and as a result one of the greatest challenges encountered in the synthesis of macrocycles is the production of macrocyclic products over their linear counterparts.[326, 352-357] It is therefore important that the strategies designed for the synthesis of macrocyclic ligands favor the cyclization process and inhibit the competing linear reaction. It has been determined that one of the most important factors influencing the formation of macrocyclic compounds over polymeric materials is reactant concentration.[327] Typically, relatively low concentrations of the reactants favor the cyclization process. Other factors that must be considered in the formation of cyclic products over acyclic products include reaction time and temperature, type of solvent and rate of stirring. Another important contributor to macrocyclic formation is the number of macroring members. It has

generally been determined that smaller sized rings incorporating 11 to 13 members are more difficult to prepare than larger sized rings.[358]

Generally, the most successful methodologies which have been applied in the preparation of macrocyclic ligands may be classified as variations of two principle techniques: (1) production of the cyclic product in the presence of a metal "template" ion and (2) production of the cyclic product via high dilution techniques without a metal "template".[359]

The influence of a metal ion on the generation of cyclic products has been recognized for a long time. The fundamental concept of this method of synthesis is that the coordination sphere of the metal ion ultimately orients the reactive groups of the starting materials in such a way to promote the cyclization reaction.[327] That is to say, that the metal ion acts as a "template". Macrocyclic formation in the presence of a metal ion has been determined to be highly dependent on the geometry of the ligand relative to the metal ion used, and in many cases the stability of the macrocycle itself depends on its coordination with the metal ion.

The second most commonly used route to the synthesis of macrocyclic ligands is the use of high-dilution techniques. The principle on which this technique is based is that the functional groups of the two reactants will initially react together to form a linear chain. The remaining reactants will be present in such low concentrations that the two unreacted functional groups on either end of this initial linear chain are more likely to react together to form the cyclic product over the acyclic product.[327] It is often assumed that in applying high-dilution techniques that large amounts of solvent are required. However, the volume of solvent used may be decreased upon the precise addition of the two

reactants relative to one another. By using syringe pumps, for example, the ideal concentration of the reactants may be maintained in the solvent in order to favor the cyclization process.[327] In addition to careful control over reactant concentration, high-dilution strategies are normally performed at room temperature or lower with very vigorous stirring. It has been determined that cyclization reactions are usually slow in comparison to polymer formation and that each of these factors may influence the likelihood of cyclization. Although a variety of methodologies outlining the synthesis of macrocyclic ligands have been reported, two routes in particular have been identified as common approaches applied in the preparation of these compounds with mixed donor atom sets.[327, 359]

A common method of preparation for macrocyclic products utilizes a basic condensation reaction. These condensation reactions may occur between two different substrates (Figure 6.5) or between two equivalents of the same reactant (Figure 6.6).[327] Figure 6.5 illustrates a [1:1] condensation in which two reactants each containing two terminal functional groups, which differ from each other, combine to yield the desired product. The [1:1] condensation reaction shown in Figure 6.6 demonstrates a reaction which occurs between two identical reactants, with two different terminal functional groups.

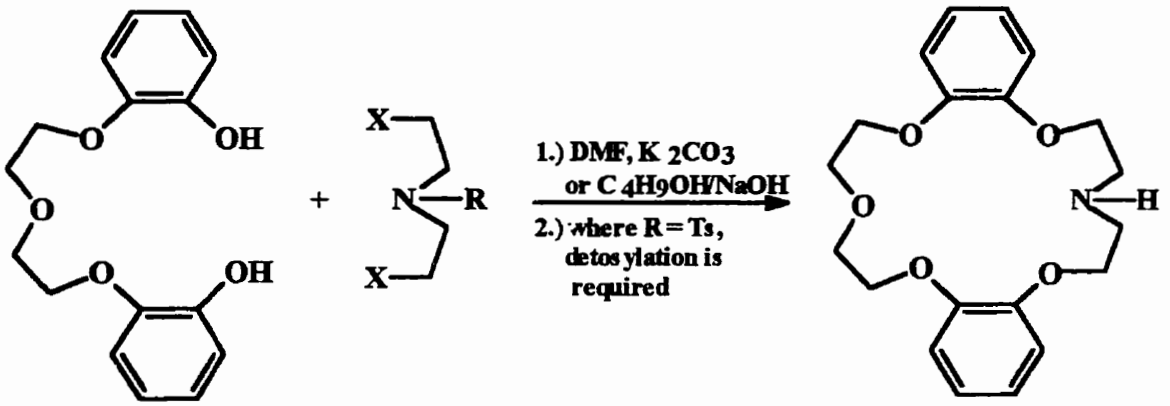

X = Cl, Br, OTs

Figure 6.5: Macrocyclic formation by the [1:1] condensation reaction of two different substrates

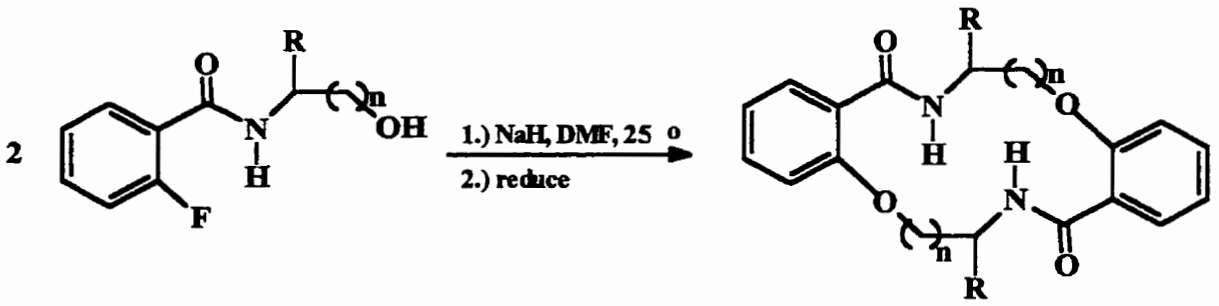

Figure 6.6: Macrocyclic formation by the [1:1] condensation of a substrate with two different terminal functional groups

Another approach used in the preparation of nitrogen-based monocyclic products is the reaction of two substrate molecules with two other substrate molecules commonly referred to as a [2:2] cyclization process.[327, 359] In order to influence the generation of the [2:2] products over the [1:1] products, higher reactant concentrations are usually required. However, although increased reactant concentrations favor the [2:2] cyclization process, the likelihood for the formation of the corresponding polymeric species also increases. Figure 6.7 presents an example of the [2:2] cyclization process in the preparation of a nitrogen-based macrocyclic ligand.

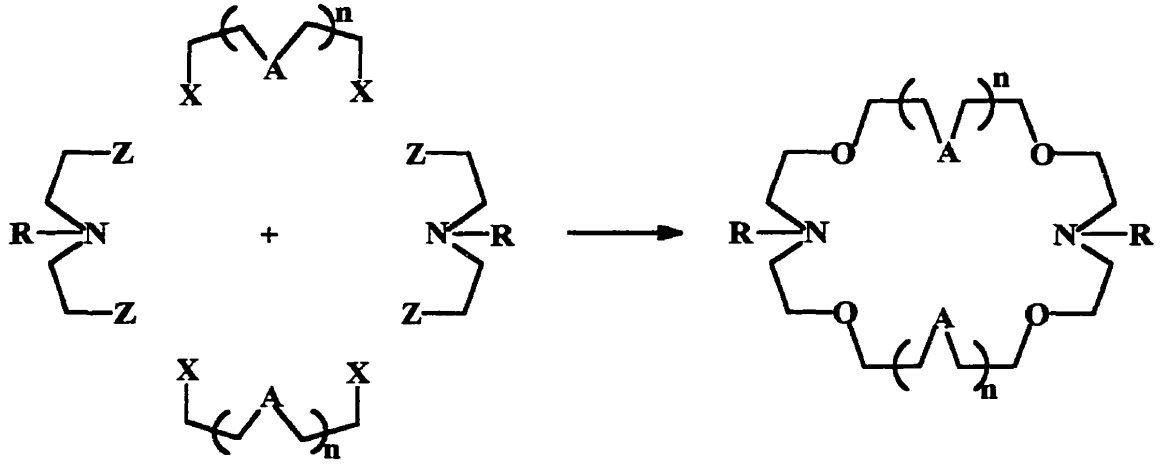

Figure 6.7: Use of the [2:2] cyclization process in the preparation of the corresponding macrocyclic ligand.

The field of macrocyclic chemistry has developed extensively since the initial discovery of macrocyclic compounds. An extensive number of crown compounds have been synthesized and found to be useful in a broad variety of applications. The design of new and inexpensive routes for the preparation of macrocyclic compounds is continually being investigated due to the extreme expense of those that are presently commercially available and the promising applications for which they have been shown to be useful.

6.3 Results and Discussion

6.3.1 Preparation of Polyaromatic Ethers and Thioethers

As a result of the initial success experienced in the stepwise preparation of dimeric and oligomeric complexes with $CpFe^+$ moieties, it was of interest to examine similar techniques in the direct synthesis of polyethers and polythioethers. Using the same types of starting materials employed in the preparation of dimeric and oligomeric ether and thioether $CpFe^+$ complexes, the one step synthesis of the corresponding soluble polymers with pendent cationic cyclopentadienyliron moieties has been achieved.

6.3.1.1 Soluble Polyaromatic Ethers and Thioethers with Pendent Cationic Cyclopentadienyliron Moieties

The preparation of polyaromatic ethers and thioethers via the reaction of 1,4-dichlorobenzene $CpFe^+$ complexes with oxygen and sulfur dinucleophiles are presented in Schemes 6.1 and 6.2. Scheme 6.1 outlines the reaction of η^6-(1,4-dichlorobenzene)-η^5-(cyclopentadienyliron) hexafluorophosphate, **2.6**, with bisphenol-A, **6.1**, in the presence of excess K_2CO_3 in DMF resulting in the preparation of the corresponding polyether with pendent metallic moieties. Isolation of a beige solid,

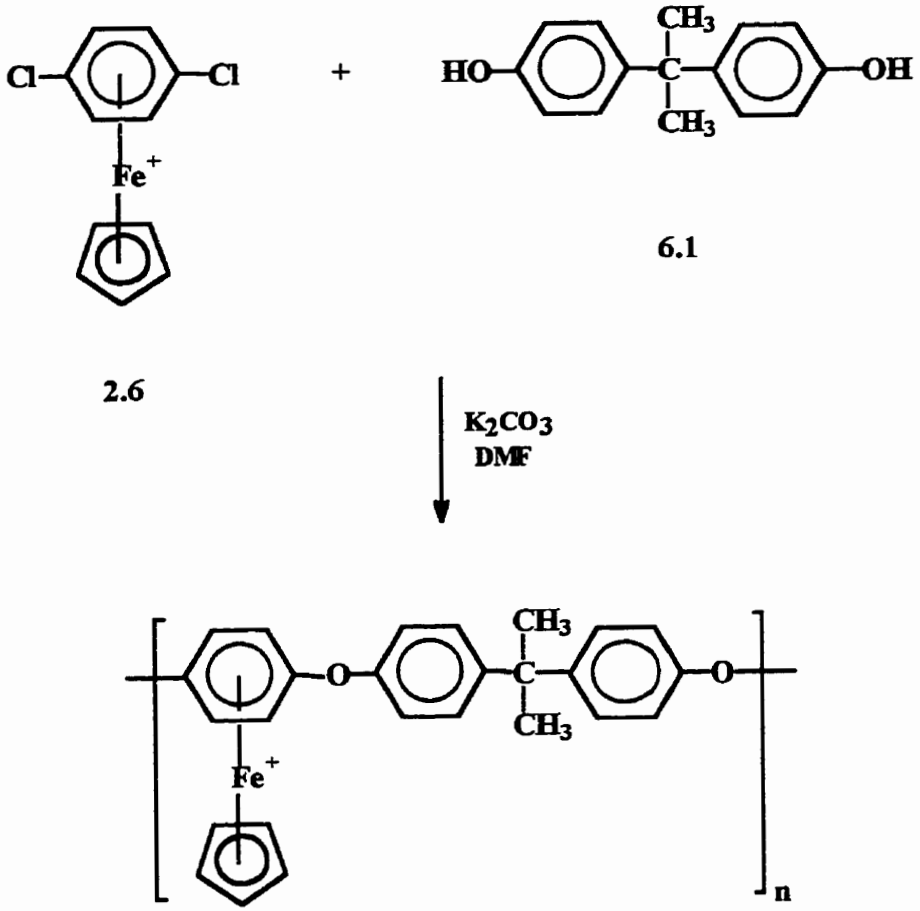

Scheme 6.1

6.2, in 83% yield was achieved by precipitation in 10% HCl. Identification of the polymer was verified using ^{1}H and ^{13}C NMR data shown in Tables 6.1 and 6.2, respectively.

An extension of this methodology involves the synthesis of a series of polyaromatic thioethers with aliphatic linkages. Reaction of the 1,4-dichlorobenzene complex, **2.6**, with 1,2-, 1,4-, 1,6- and 1,8- terminated aliphatic dithiols, **2.9-2.12**, allowed for the isolation of the corresponding organometallic polythioethers, **6.3-6.5**, as shown in Scheme 6.2. The efficiency of this methodology is demonstrated by the preparation of the desired polymers in yields ranging from 51-92%. It is important to note that although 1,2-ethanedithiol was explored as a potential bridge in the polymeric chain, **6.3**, these attempts resulted in the isolation of oligomeric chains in moderate yield rather than the desired polymeric species. ^{1}H and ^{13}C NMR were used to determine the identity of the polymeric materials and the data are summarized, along with their respective yields, in Tables 6.1 and 6.2. The ease and cost-efficient preparative nature of η^{6}-(1,4-dichlorobenzene)-η^{5}-(cyclopentadienyliron) hexafluorophosphate in large quantities and the commercial availability of the dinucleophiles renders this novel synthetic strategy conducive to further investigation.

Comparison of the ^{1}H NMR of the starting dichlorobenzene complex and the organometallic polymer indicates that the desired compounds were formed. The ^{1}H NMR spectrum of the starting arene complex shows a distinctive resonance representative of the cyclopentadienyl ring protons at 5.47 ppm with the four complexed aromatic protons

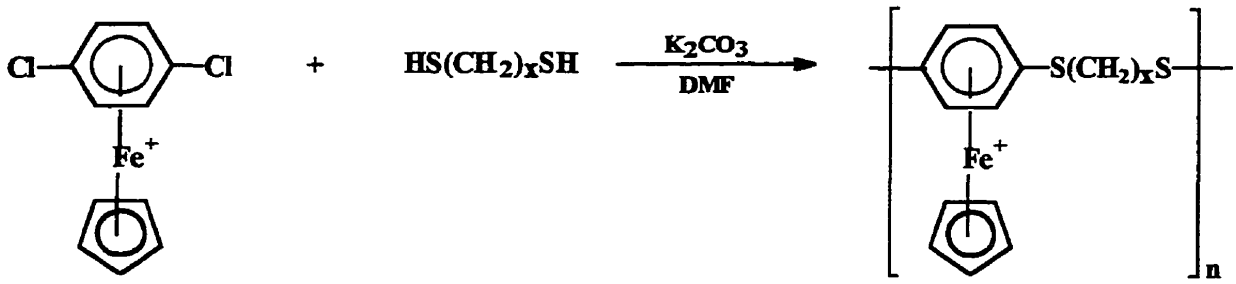

2.6

2.9 x = 2
2.10 x = 4
2.11 x = 6
2.12 x = 8

6.3 x = 2
6.3 x = 4
6.4 x = 6
6.5 x = 8

Scheme 6.2

appearing as a strong singlet at 7.00 ppm. The ^{1}H NMR spectrum of the metallated polymeric material with a 1,8-octanedithiol bridge is represented in Figures 6.8 and is useful in representing several of the spectral features which were typically observed upon the successful formation of the metallated polymeric species. The polymerization of the η^6-(1,4-dichlorobenzene)-η^5-cyclopentadienyliron complex with 1,8-octanedithiol was found to effect an upfield shift of both the cyclopentadienyl and complexed aromatic protons to 5.01 ppm and 6.44 ppm, respectively. The presence of several peaks between 1.28 and 3.14 ppm, representative of the aliphatic bridging ligand, provided additional evidence for the success of the reaction. With the knowledge that the same reactants have been used in the preparation of the corresponding bimetallic species, **2.31**, comparison of these spectra with that of the corresponding polymer is useful to verify the generation of a material with a greater number of repeat units. Although the broad nature of the peaks in the ^{1}H NMR spectra suggest polymer formation, a more indicative characteristic is the

appearance of the complexed aromatic protons as a singlet in the polymer as compared to the doublet observed in the spectra of the bimetallic species.

Comparison of the ^{13}C NMR spectra of the polymeric materials with that of the starting 1,4-dichlorobenzene complex and the corresponding bimetallic complex is also useful in determining the success of the polymerization reaction. The ^{13}C NMR spectrum of the metallated polymer, **6.6**, is shown in Figure 6.9. Several spectral changes which indicate the success of the reaction include a shift of the cyclopentadienyl and complexed aromatic carbons from 89.13 and 82.02 ppm in the starting complex to 79.06 and 83.19 ppm in the polymeric species. Four resonances between 27.9 and 38.7 ppm representative of the 1,8-octanedithiol bridge are further evidence for the preparation of the polymer. Differences in the ^{13}C NMR spectrum of the bimetallic complex as compared to the polymeric species further supports polymer formation. The most distinctive features of the ^{13}C NMR spectrum of the bimetallic complex are the presence of two complexed aromatic resonances at 84.64 and 88.44 ppm and two quaternary carbon peaks at 105.97 and 108.60 ppm. Conversely, polymer formation is represented by one complexed aromatic and one quaternary carbon resonance at 83.19 and 106.75 ppm, respectively. Similar spectral changes were noted as evidence for the formation of polymers **6.2, 6.4** and **6.5**.

Table 6.1: ^{1}H NMR Data of Complexed Polymers **6.2, 6.4-6.6.**

δ (DMSO-d_6), ppm				
Complex	**Cp (s, 5H)**	**Complexed Aromatic[a]**	**Uncomplexed Aromatic[a]**	**Others[a]**
6.2	5.02	6.25 (s, 4H)	7.22 (d, 4H, J = 8.2) 7.40 (d, 4H, J = 8.4)	
6.4	5.01	6.45 (br.s., 4H)		1.87 (br.s, 4H, β-CH_2) 3.44-3.45 (br.s., 4H, α-CH_2)
6.5	5.01	6.41 (s, 4H)		1.42 (br.s., 4H, γ-CH_2) 1.71 (br.s., 4H, β-CH_2) 3.26 (br.s., 4H, α-CH_2)
6.6	5.02	6.44 (s, 4H)		1.28 (m, 4H, δ-CH_2) 1.59 (m, 4H, γ-CH_2) 2.66 (m, 4H, β-CH_2) 3.14 (br.t., 4H, α-CH_2)

[a] J values in Hertz.

Table 6.2: ^{13}C NMR Data of Complexed Polymers **6.2, 6.4-6.6.**

δ (DMSO-d_6), ppm					
Complex	**Yield (%)**	**Cp (s, 10C)**	**Complexed Aromatic**	**Uncomplexed Aromatic**	**Others**
6.2	83	77.93	75.00, 130.19*	120.01, 128.83, 147.80*, 151.45*	30.62 (CH_3)
6.4[a]	62				
6.5	78	76.56	83.14, 107.08*		28.01 (γ-CH_2) 29.32 (β-CH_2) 31.06 (α-CH_2)
6.6	92	79.06	83.19, 106.75*		27.96 (δ-CH_2) 28.29 (γ-CH_2) 28.36 (β-CH_2) 31.15 (α-CH_2)

* Quaternary carbon. [a]Observance of many peaks due to the formation of oligomers.

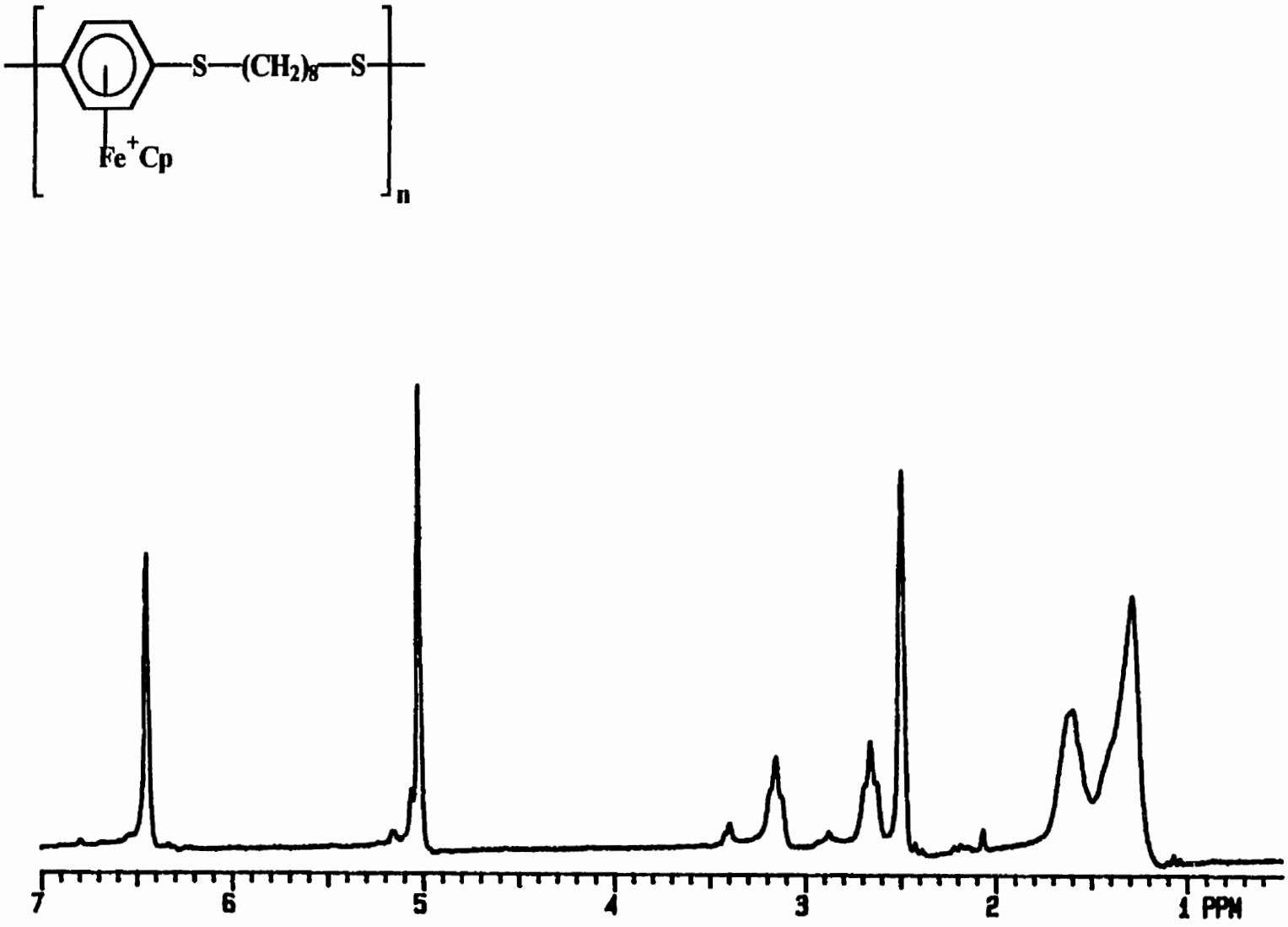

Figure 6.8: ^{1}H NMR spectrum of complex **6.6** in DMSO-d_6.

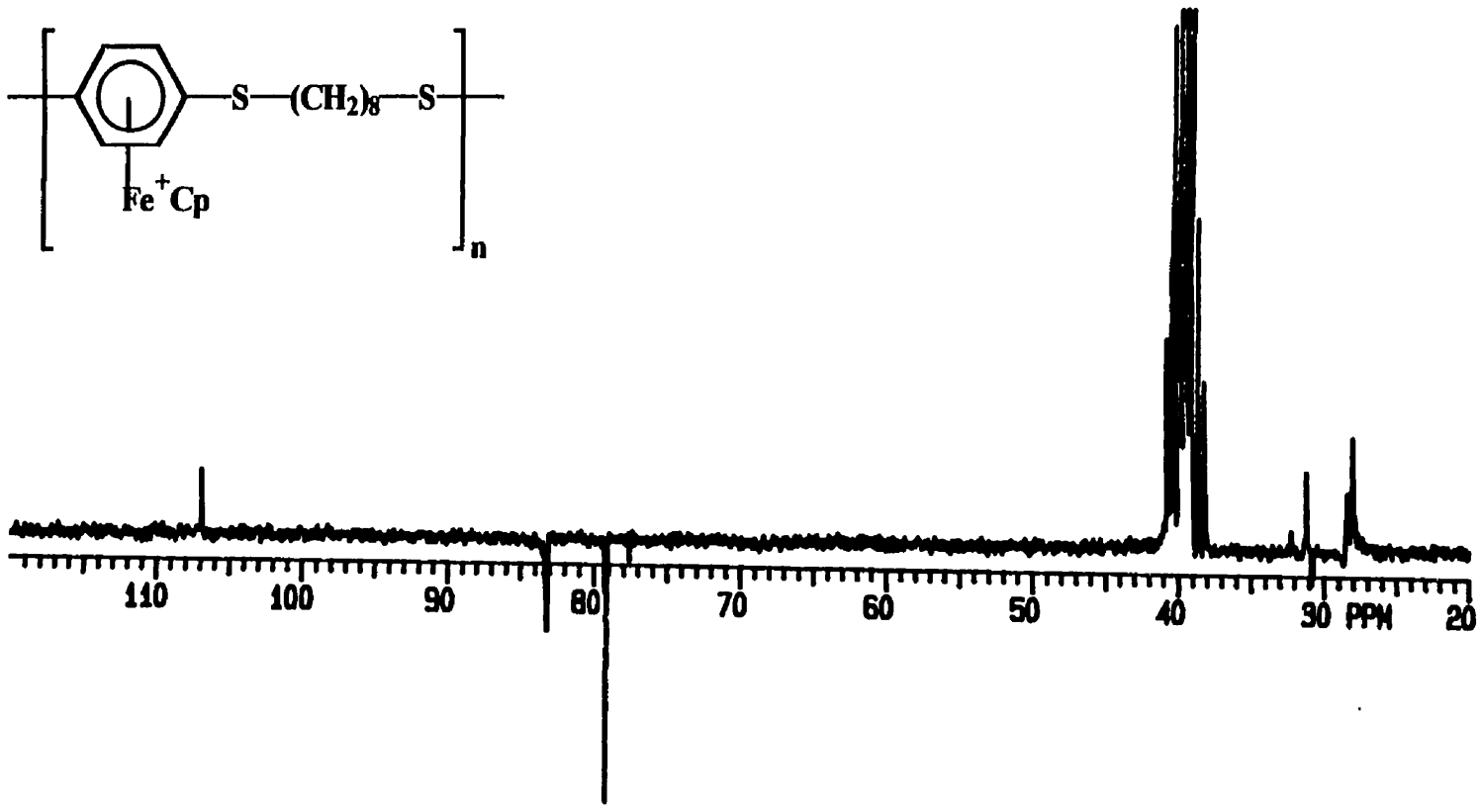

Figure 6.9: ^{13}C NMR spectrum of complex **6.6** in DMSO-d_6.

6.3.1.2 Isolation of Organic Polymers by Photolytic Demetallation

Segal and Dembek have shown that the determination of the degree of polymerization of this class of organometallic polymers using Gel Permeation Chromatography (GPC) is difficult due to the tendency of the cationic metallic moieties pendent to the polymeric chains to interact with the GPC column.[19, 110] In light of this observation, successful cleavage of the iron moieties from the backbone of these materials enabled the determination of the degree of polymerization.

The metallated polymeric materials, **6.2, 6.4-6.6**, were stirred in DMF for several hours and upon their complete dissolution were irradiated under a xenon lamp for 6 hours with stirring. Following the appropriate work-up procedure, as outlined in Section 8.6.3, the corresponding organic polymers, **6.7-6.10**, were isolated in 42-85 % yield (Schemes 6.3 and 6.4). It is important to note that upon demetallation, the resulting purely organic polymers were found to be much less soluble in comparison to their corresponding metallated materials.

^{1}H and ^{13}C NMR were used to verify the isolation of the organic polymers from the corresponding metallated species (Tables 6.3 and 6.4). Figures 6.10 and 6.11 show the ^{1}H and ^{13}C NMR spectra of polymer **6.10** and illustrate the typical spectral changes observed upon liberation of the modified organic ligand from its metallic counterpart. The most outstanding spectral change noted upon demetallation is the disappearance of the cyclopentadienyl resonances at 5.02 ppm and 79.01 ppm in the ^{1}H and ^{13}C NMR spectra, respectively. Additionally, a singlet at 6.44 ppm in the ^{1}H NMR spectrum representative of the

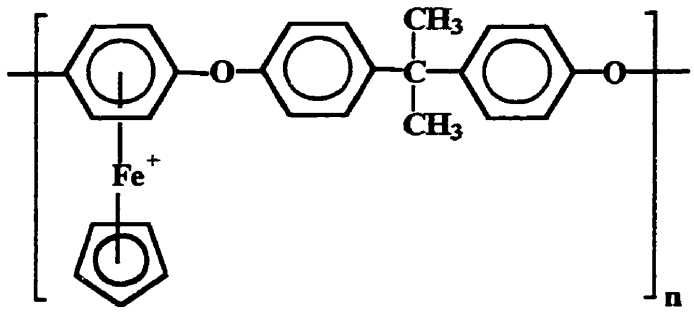

6.2

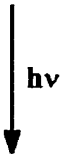

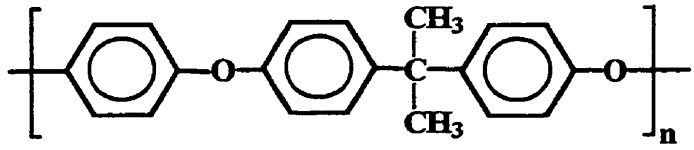

6.7

Scheme 6.3

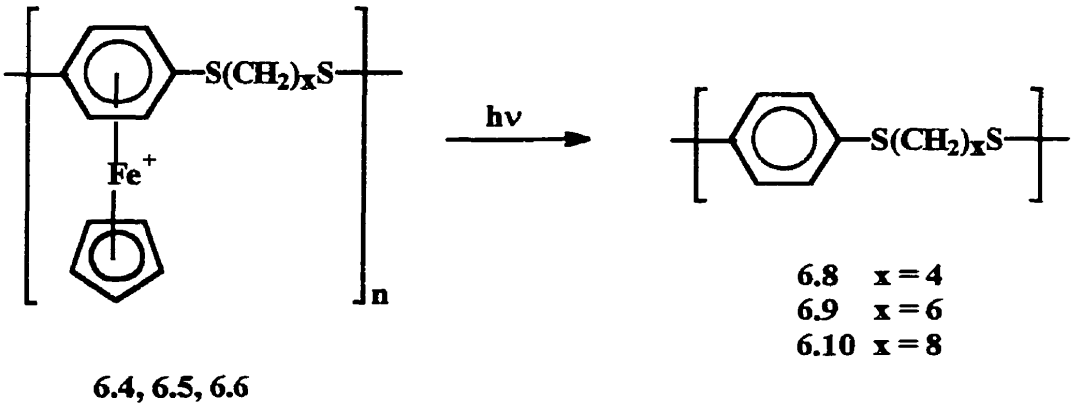

6.4, 6.5, 6.6

6.8 x = 4
6.9 x = 6
6.10 x = 8

Scheme 6.4

complexed aromatic protons shifted downfield to 7.22 ppm in the organic spectrum. A downfield shift of the resonances representative of the complexed aromatic carbon atoms from 83.19 to 129.57 ppm and quaternary carbon resonance from 106.75 to 134.31 ppm, respectively, in the ^{13}C NMR spectrum of polymer **6.10** further supports the successful isolation of the purely organic polymer.

Table 6.3: ^{1}H NMR Data of Polymers **6.7-6.10**

δ ($CDCl_3$), ppm		
Complex	**Uncomplexed Aromatic**[a]	**Others**[a]
6.7	6.97 (s, 4H) 6.93 (d, 4H, J = 8.1) 7.17 (d, 4H, J = 8.3)	1.66 (s, 6H, CH_3)
6.8[a]	---	---
6.9	7.20 (s, 4H)	1.40 (br.s., 4H, γ-CH_2) 2.66 (br.s., 4H, β-CH_2) 2.88 (br.s., 4H, α-CH_2)
6.10	7.21 (s, 4H)	1.30 (m, 4H, δ-CH_2) 1.65 (m, 4H, γ-CH_2) 2.63 (m, 4H, β-CH_2) 2.89 (m, 4H, α-CH_2)

[a] J values in Hertz. [a]Observance of many peaks due to the formation of oligomers.

Table 6.4: ^{13}C NMR Data and Yield of Polymers **6.7-6.10**

δ ($CDCl_3$), ppm			
Complex	**Yield (%)**	**Uncomplexed Aromatic**	**Others**
6.7	73	118.14, 128.49, 145.77*, 153.18*, 156.09	31.52 (CH_3) 42.55*
6.8[a]	42	---	---
6.9	61	129.67, 134.31*	28.95 (γ-CH_2) 33.83 (β-CH_2) 38.92 (α-CH_2)
6.10	85	129.56, 134.31*	28.94 (δ-CH_2) 29.03 (γ-CH_2) 33.87 (β-CH_2) 39.05 (α-CH_2)

* Quaternary carbon. [a]Observance of many peaks due to the formation of oligomers.

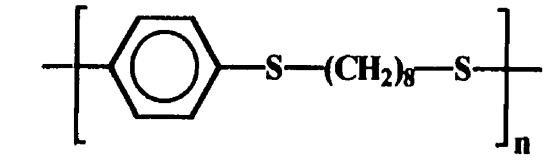

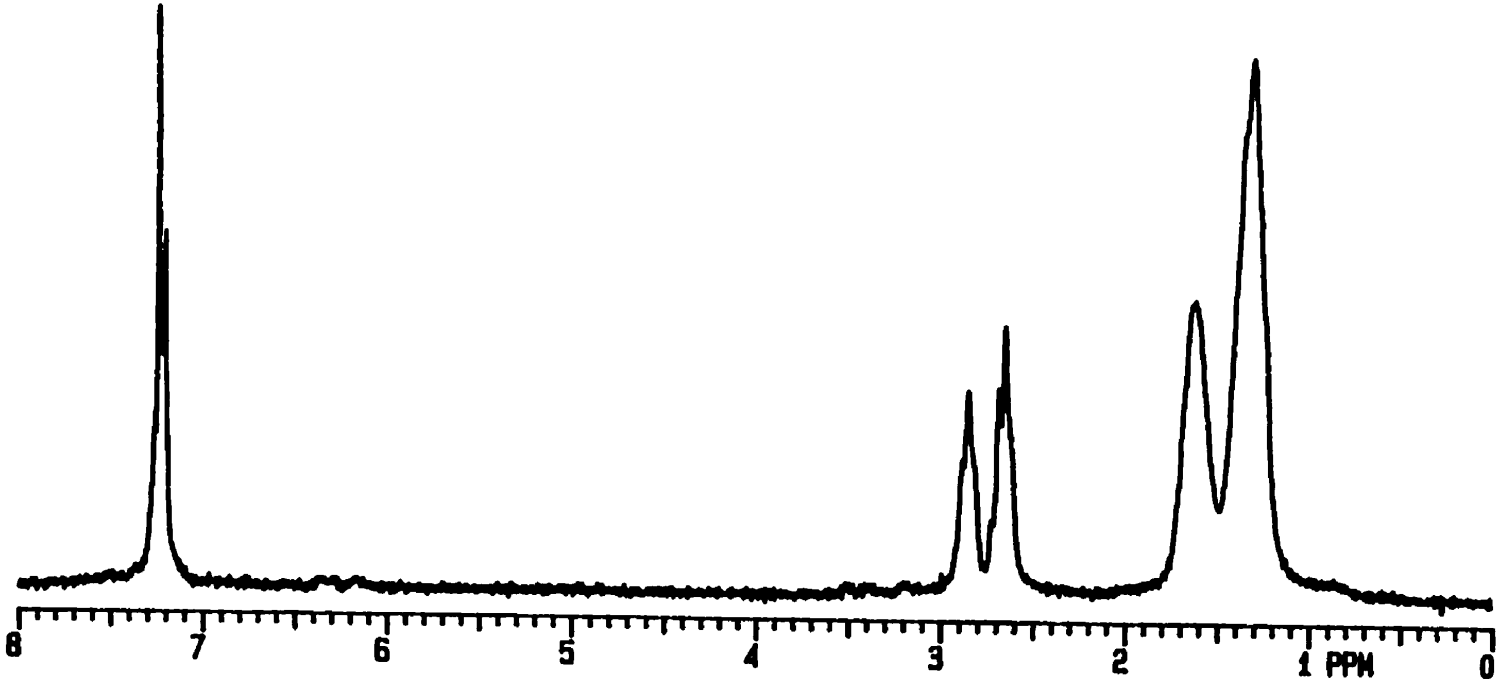

Figure 6.10: ^{1}H NMR spectrum of compound **6.10** in $CDCl_3$.

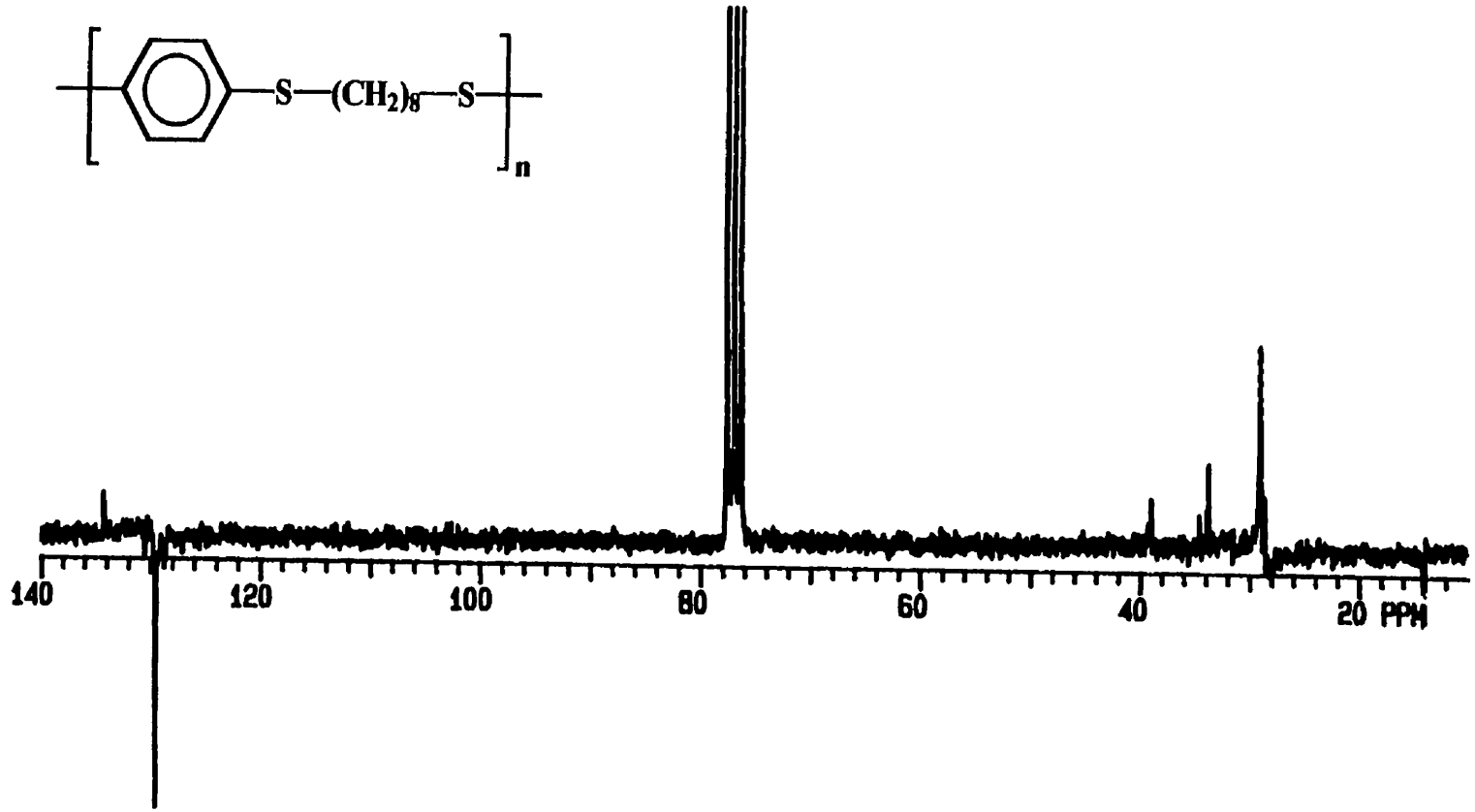

Figure 6.11: ^{13}C NMR spectrum of compound **6.10** in $CDCl_3$.

6.3.1.3 Molecular Weight Determination of Polymeric Species 6.2-6.5 and 6.7-6.10

Gel Permeation Chromatography was used for the determination of the weight average molecular weights (Mw) and number average molecular weights (Mn) of demetallated polymers, **6.7-6.10**, and allowed for the prediction of the molecular weights of the organometallic polymers, **6.2** and **6.4-6.6**, using the ratio of the molecular weight of the repeat unit of the organometallic polymer to that of its organic counterpart. In the investigation of the molecular weights of polymers **6.8-6.10**, an increase in molecular weight was observed with increasing aliphatic chain length. In the case of the organic counterpart of species **6.3**, a Mw of 800 and Mn of 700 indicates the formation of oligomers rather than the polymeric material. However, polymers **6.8, 6.9** and **6.10** were measured as having Mw's of 2 100, 13 500 and 21 400 $gmol^{-1}$, respectively, and Mn's equal to 700, 5 900 and 6 300 $gmol^{-1}$ thereby verifying polymer formation and clearly demonstrating an increase in molecular weight with increasing aliphatic chain length. By relating the molecular weight of the repeat unit of the organic polymer with that of its organometallic counterpart, it was possible to estimate the molecular weight of the polymeric materials with pendent $CpFe^{+}$ moieties. These data are listed is Table 6.5.

This is the first example detailing the one-step synthesis of polyaromatic ethers and thioethers with pendent cyclopentadienyliron moieties. The introduction of the metallic species into the backbone of these polymers allows for the increase in their solubility. The ease of decomplexation of the iron moieties and the use of commercially available starting materials makes this method quite desirable.

Table 6.5: GPC of Polymers **6.7-6.10** in $CHCl_3$

$CHCl_3$				
Polymer	**Mw***	**Mn***	**Mw/Mn**	**Mw#**
6.7	11 000	5 500	2.0	20 500
6.8	2 100	700	3.0	3 500
6.9	13 500	5 900	2.3	29 500
6.10	21 400	6 300	3.4	44 500

*Molecular weight determinations of the soluble portion of the polymer using GPC.
#Calculated molecular weight of the corresponding metallated polymer.

6.3.2 Synthesis of Nitrogen-based Macrocycles via Cyclopentadienyliron Activated S_NAr Reactions

It has been mentioned that several synthetic methods have been developed for the preparation of macrocyclic ligands.[2, 33] However, it is important to note that in many cases, poor yields and harsh reaction conditions limit the practicality of these techniques. As a result, the search continues for more efficient and general routes to the preparation of these compounds.

Several metallic moieties including $CpRu^+$ and $Cr(CO)_3$ have been investigated and have exhibited their potential as an alternative strategy to the preparation of macrocyclic ligands.[360-361] The successful use of η^6-(dichloroarene)-η^5-cyclopentadienyliron hexafluorophosphate complexes in the design of bimetallic and polymetallic species prompted the investigation of $CpFe^+$ activated macrocyclic preparation. A similar stepwise strategy using η^6-(1,3-dichlorobenzene)-η^5-cyclopentadienyliron complexes allowed for the design of bimetallic complexes with structural compositions that allowed for ring closure in the presence of various nucleophiles. The subsequent removal of the pendent $CpFe^+$ metallic moieties via photolytic demetallation allowed for the isolation of the corresponding organic macrocycles.

6.3.2.1 Reactions of η^6-(1,3-dichlorobenzene)-η^5-(cyclopentadienyliron) Complexes with Dinucleophiles

The number, nature and positional organization of donor atoms in addition to cavity size have been mentioned as crucial factors in determining the resulting composition of metal ion-ligand complexes. The stepwise strategy presented in this work emphasizes the importance of designing structural units with compositions conducive to ring closure. These units must also contain spacers with the desired donor atoms and allow for the generation of cavities appropriate for metal ion interactions.

The initial framework of the desired macrocycle is established by the preparation of bimetallic complexes with terminal chlorine groups. It has been thoroughly established that the reaction of chloro- and nitro- (arene)$CpFe^+$ complexes in the presence of various dinucleophiles in a 2:1 molar ratio using K_2CO_3 as a base and a THF/DMF solvent mixture generated the corresponding bimetallic complexes in high yield. In a similar manner, η^6-(1,3-dichlorobenzene)-η^5-(cyclopentadienyliron) hexafluorophosphate, **6.11**, was reacted with diol and diamine nucleophiles resulting in the corresponding diiron complexes as outlined in Schemes 6.5 and 6.6. The analytical data corresponding to complexes **6.12-6.14** are summarized in Tables 6.6 - 6.7.

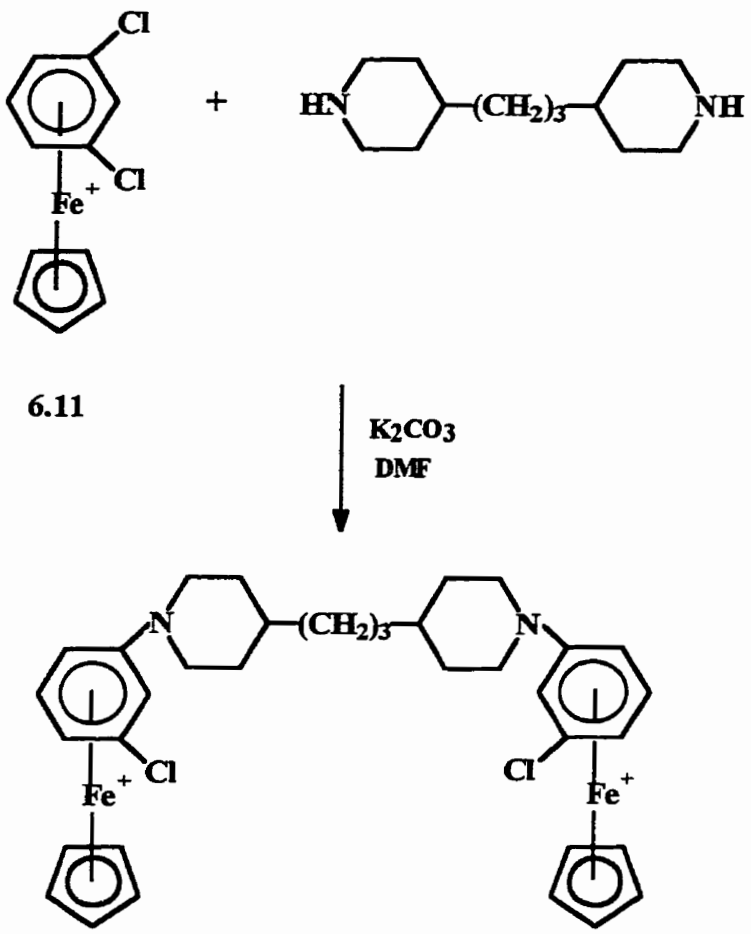

6.12

Scheme 6.5

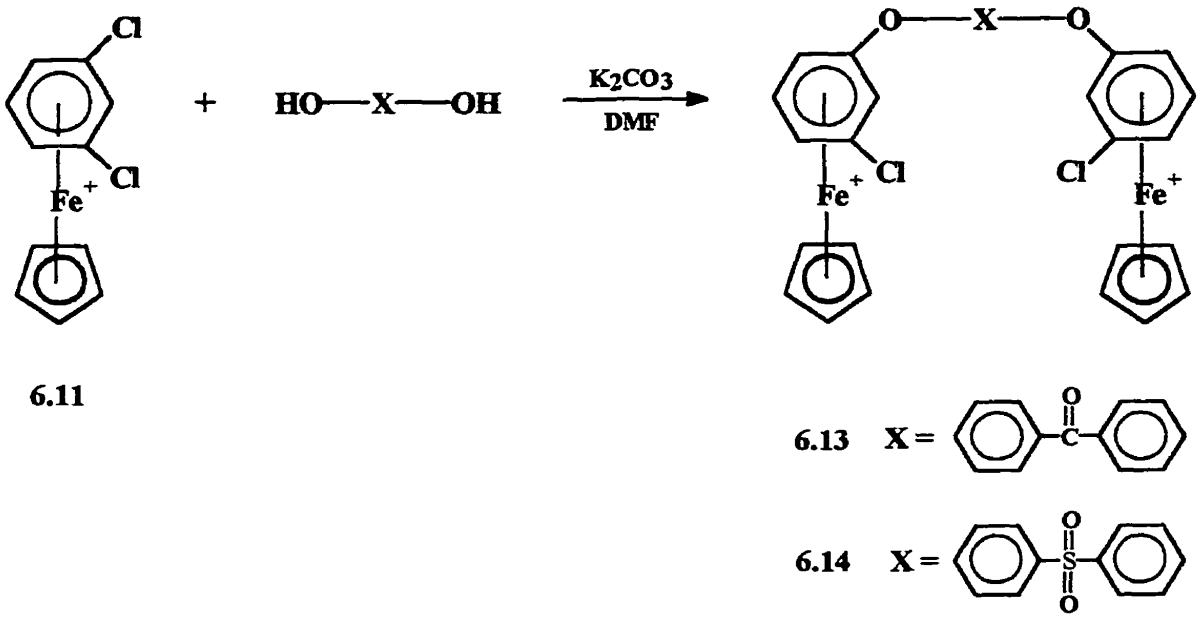

6.11

6.13 X =

6.14 X =

Scheme 6.6

Figures 6.12 and 6.13 show the ^{1}H and ^{13}C NMR spectra corresponding to complex **6.12**. The distinguishing features of the ^{1}H NMR spectrum are similar to those mentioned for the bimetallic complexes featured in Section 2.2 of this work and reflect the symmetrical nature of these complexes. A strong singlet at 5.13 ppm appears as expected and represents the cyclopentadienyliron protons of the pendent metallic moiety. A series of two doublets, a triplet and a singlet appear in the range of 5.97-6.52 ppm and reflects the pattern expected for a 1,3-disubstituted aromatic ring. However, the appearance of the resonances representative of the nitrogen based spacer is the most distinctive feature indicative of a successful reaction. These peaks are located upfield with respect to the cyclopentadienyl resonance and appear in the range of 1.29-4.15 ppm.

Verification of complex **6.12** is found in examining the ^{13}C NMR spectrum. A strong peak representative of the cyclopentadienyl carbons appears below the baseline at 77.21 ppm while the complexed aromatics appear as four peaks in the region between 65.91 - 85.04 ppm and reflects the substitution pattern expected for complex **6.12**. Five peaks appear between 23.44 - 46.98 ppm representing the aliphatic portion of the nitrogen linkage with four of the peaks of the CH_2 groups appearing above the baseline and the CH resonance appearing below the baseline. The analysis of complex **6.12** is completed by the appearance of two quaternary carbon resonances at 106.58 and127.35 ppm with the peak corresponding to the carbon attached to the chlorine atom identified as the peak furthest upfield. The ^{1}H and ^{13}C NMR spectra of complexes **6.13** and **6.14** would be similar with respect to the complexed atoms to that described for complex **6.12**. It can be generally stated that, for complexes **6.13** and **6.14**, the uncomplexed aromatic protons are distinguishable from their complexed counterparts in that they resonate significantly downfield.

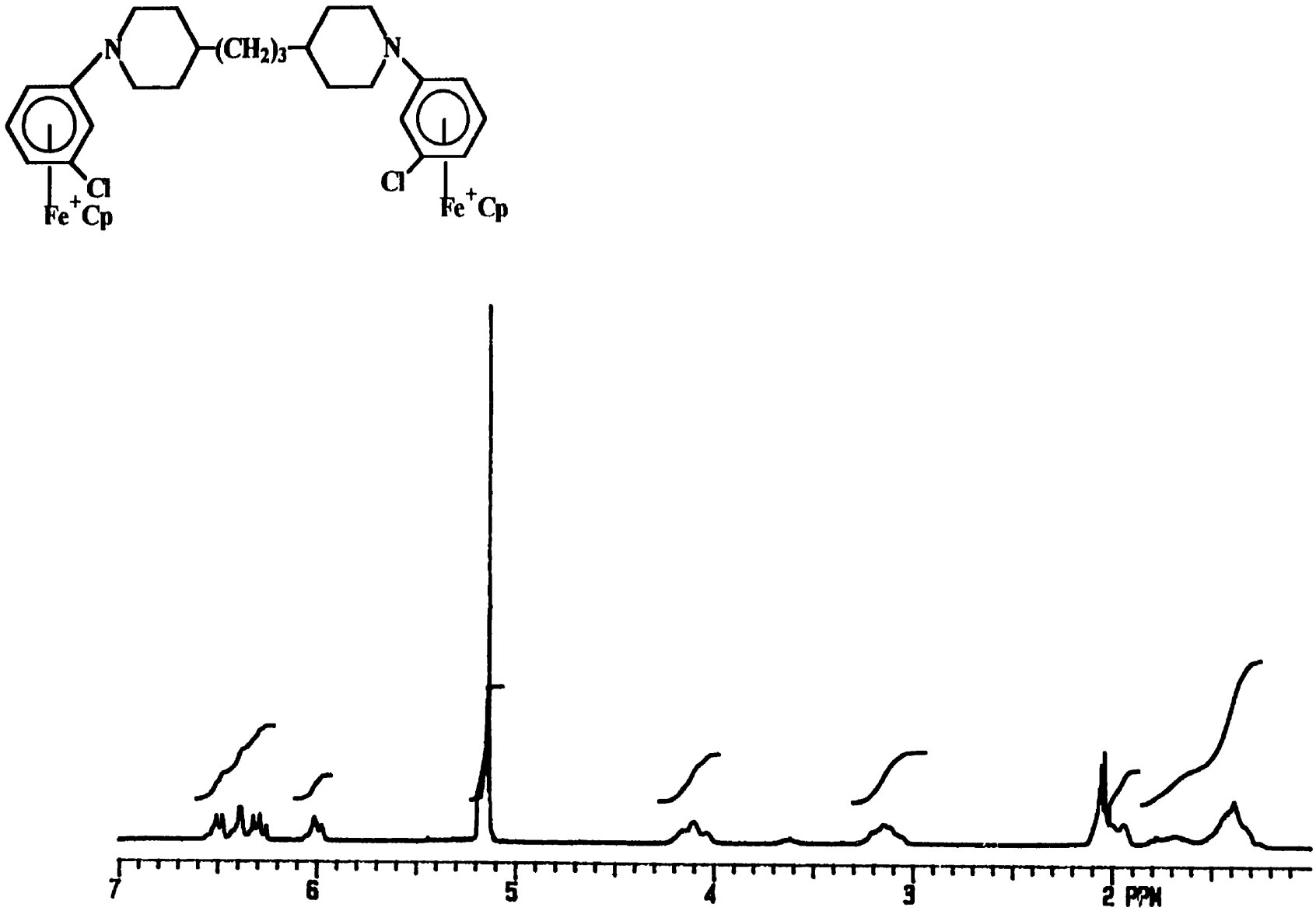

Figure 6.12: ^{1}H NMR spectrum of complex **6.12** in acetone-d_6.

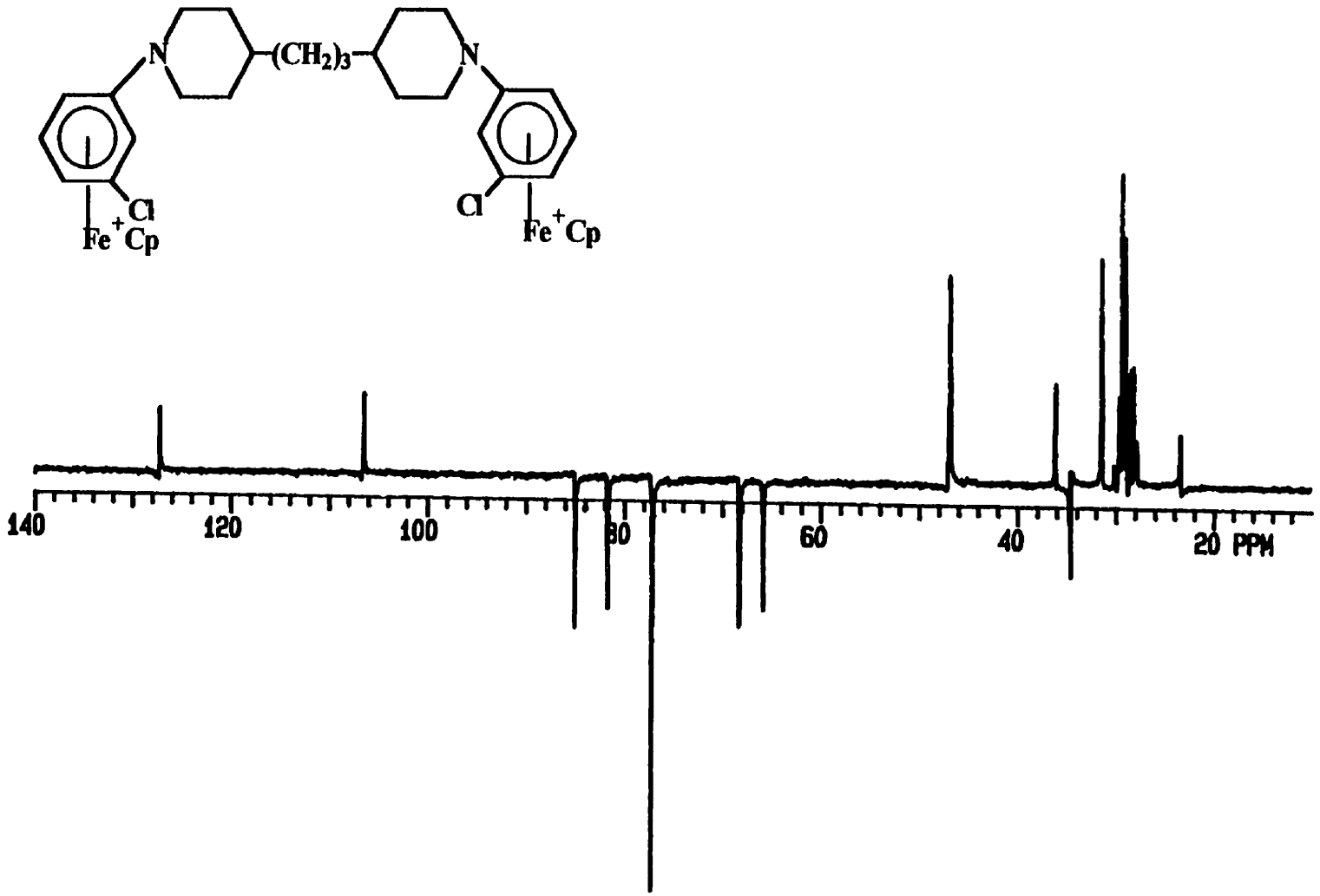

Figure 6.13: ^{13}C NMR spectrum of complex **6.12** in acetone-d_6.

Table 6.6: ^{1}H NMR Data of Diiron Complexes **6.12-6.14**

δ (acetone-d_6), ppm				
Complex	**Cp (s, 10H)**	**Complexed Aromatic[a]**	**Uncomplexed Aromatic[a]**	**Others[a]**
6.12	5.13	5.97-6.00 (d, 2H, J = 6.9) 6.25-6.31 (t, 2H, J = 6.9) 6.37 (s, 2H) 6.47-6.52 (d, 2H, J = 6.2)		1.29-1.38 (m, 10H, CH_2) 1.63-1.76 (m, 2H, CH) 1.94-2.00 (m, 4H, CH_2) 3.05-3.20 (m, 4H, CH_2) 4.02-4.15 (m, 4H, CH_2)
6.13	5.41	6.53-6.75 (m, 6H) 7.03 (s, 2H)	7.57 (d, 4H, J = 8.8) 8.02 (d, 4H, J = 8.8)	
6.14	5.40	6.56 (d, 2H, J = 5.8) 6.64 (t, 2H, J = 6.1) 6.73 (d, 2H, J = 5.9) 7.06 (s, 2H)	7.53-7.62 (m, 4H) 8.10-8.18 (m, 4H)	

[a] J values in Hertz.

Table 6.7: ^{13}C NMR and IR Data and Yields of Diiron Complexes **6.12-6.14**

δ (acetone-d_6), ppm						
Complex	**Yield (%)**	**Cp (s, 10H)**	**Complexed Aromatic**	**Uncomplexed Aromatic**	**Others**	**ν_{max} (cm^{-1})**
6.12	82.6	77.21	65.91, 68.29, 81.71, 85.04, 106.58*, 127.35*		23.44 (CH_2) 31.42 (CH_2) 34.69 (CH) 36.17 (CH_2) 46.98 (CH_2)	1266 (CN)
6.13	79.4	79.43	76.98, 78.08, 78.98, 85.78, 105.65*, 130.95*	120.05, 132.35, 134.31*, 156.62*	193.29 (CO)	1655 (CO)
6.14	83.6	79.51	77.80, 79.76, 86.03, 105.65*, 130.00*	120.59, 130.33, 137.66*, 157.76*		1106, 1267 (SO_2)

* Quaternary carbon.

6.3.2.2 Cyclization Reactions

An initial communication has appeared describing the use of $CpFe^+$ activated nucleophilic aromatic substitution in the synthesis of macrocyclic aryl ethers.[362] This report emphasized the design of an initial unit such that the terminal chlorine substituents were oriented in such a way as to allow for facile ring closure. Schemes 6.7 and 6.8 illustrate the use of a similar strategy in the preparation of nitrogen-containing macrocyclic ligands. Although the strategies applied in Schemes 6.7 and 6.8 are conceptually identical, the versatility of the technique is demonstrated by the fact that the formation of the ring may be achieved using various dinucleophiles. In one case, ring closure resulted from the reaction of the nitrogen-based bimetallic complex, **6.12**, with 4,4'-biphenol in the presence of K_2CO_3 and DMF. Although similarly structured macrocycles are generated by the route employed in Scheme 6.7, cyclization was achieved by the reaction of bimetallic complexes **6.13** and **6.14** with the nitrogen dinucleophile, 4,4'-trimethylenedipiperidine. ^1H and ^{13}C NMR were used for the identification of the complexed macrocycles, **6.15-6.17**, and the data summarized in Tables 6.8. and 6.9.

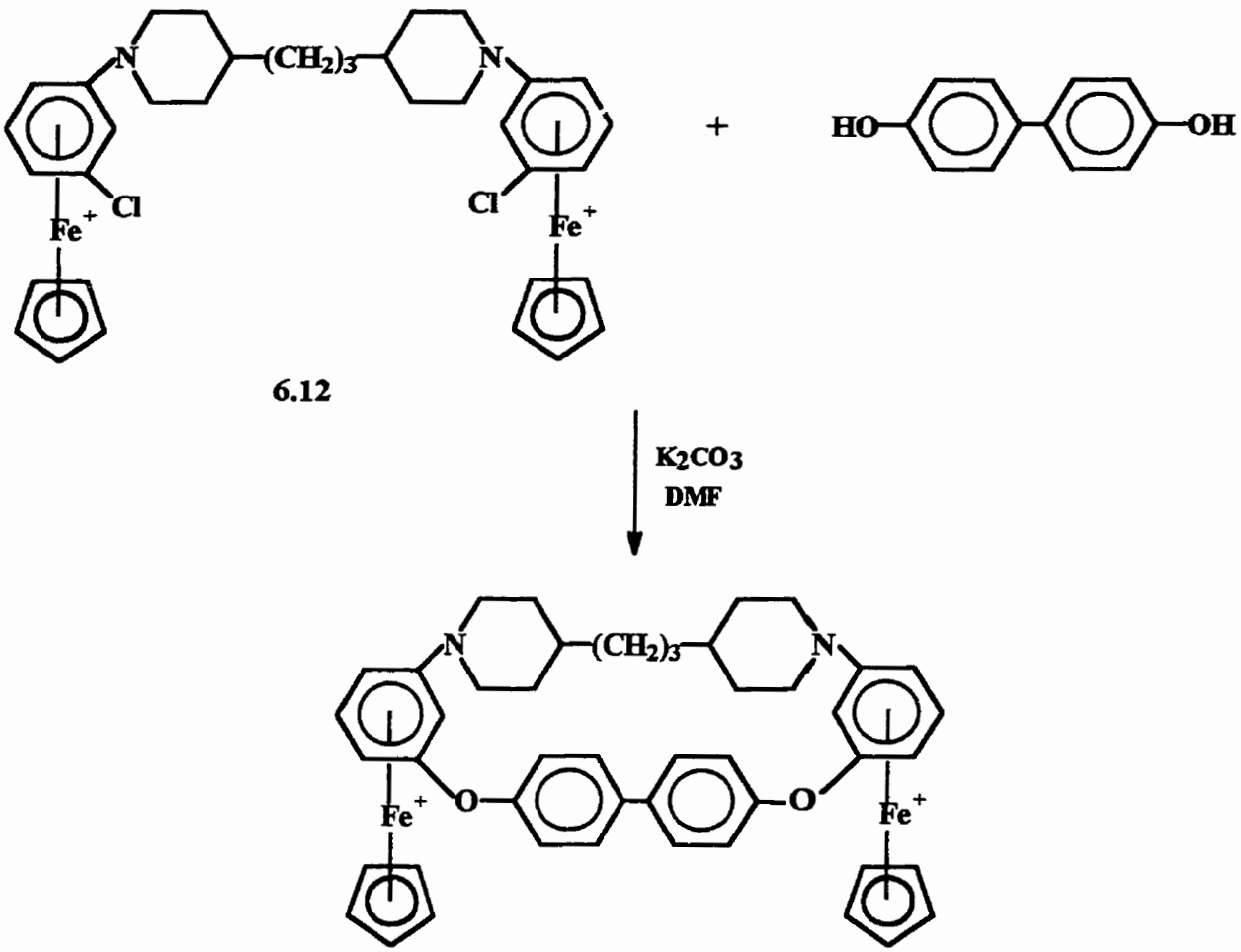

6.12

6.15

Scheme 6.7

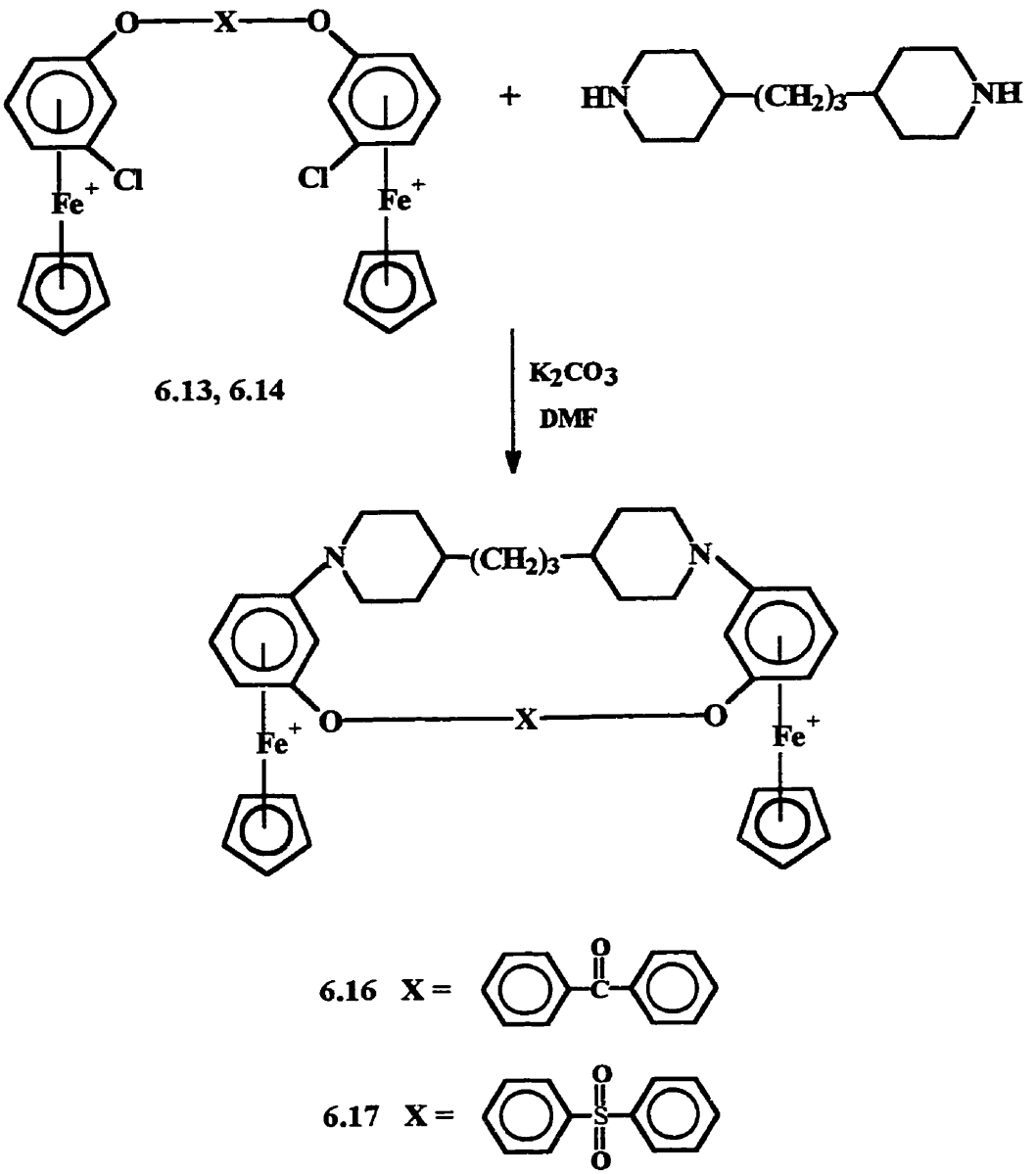
O
X
O
Cl
Cl
Fe+
Fe+
+
HN
(CH2)3
NH
6.13, 6.14
K2CO3
DMF
N
(CH2)3
N
O
X
O
Fe+
Fe+
6.16 X =
O
C
6.17 X =
O
S
O

Scheme 6.8

Spectral features typical of the macrocycles represented in Schemes 6.7 and 6.8 may be identified by examining the ^{1}H NMR spectrum of macrocycle, **6.15** (Figure 6.14). The most characteristic spectral feature of $CpFe^+$ complexes is the strong singlet between 5 and 6 ppm representative of the cyclopentadienyl protons. In this case, the appearance of a strong singlet does not necessarily confirm the formation of a macrocycle since the same structural feature would also appear as a result of the presence of the bimetallic starting complex. However, a shift in the cyclopentadienyl resonance does suggest complex formation. In the case of complex **6.15**, the Cp peak appears at 5.12 ppm which is shifted slightly upfield from its position of 5.13 ppm in the starting bimetallic complex, **6.12**. In comparing the ^{1}H NMR spectra of macrocycle **6.15** and the bimetallic complex, **6.12**, changes in the region corresponding to the complexed aromatic protons can indicate ring closure. The spectral pattern of the complexed aromatic protons of the starting bimetallic complex, **6.12**, appear distinctly as a singlet, two doublets and a triplet in the region between 5.97-6.52 ppm whereas the complexed aromatic region corresponding to complex **6.15** appear in the range of 5.91-6.23 ppm as a doublet and a multiplet. The appearance of two doublets at 7.40 and 7.85 ppm are perhaps the most striking characteristics of the ^{1}H NMR spectrum of complex **6.15**, indicative of ring closure. These resonances correspond to the uncomplexed aromatic protons of the 4,4'-biphenol unit and are evidence of its incorporation into the macrocyclic structure. In considering the formation of macrocycles **6.16** and **6.17**, successful ring closure would be suggested by the appearance of those resonances corresponding to the 4,4'-trimethylenedipiperidine unit.

The ^{13}C NMR also verifies the formation of complexes **6.15-6.17**. The ^{13}C NMR of complex **6.15** is shown in Figure 6.15 and demonstrates some characteristic features of the complexed macrocycles. In comparing the spectrum of complexed macrocycle, **6.15**, and that of the corresponding starting bimetallic complex, **6.12**, several distinguishing features indicate ring closure. The appearance of the peaks at 121.88, 130.88, 134.48 and 155.55 ppm represent the aromatic carbons of the 4,4'-biphenol unit and indicate its incorporation into the macrocyclic structure. Additionally, the nucleophilic displacement of chlorine by the oxygen dinucleophile results in a significant chemical shift of the adjacent complexed quaternary carbon atom from 106.59 ppm in the starting bimetallic complex, **6.12**, to 133.56 ppm in the macrocyclic ligand, **6.15**. For complexes **6.16** and **6.17**, the presence of several peaks in the range of 24.92 - 48.79 ppm representing the methylene and methine carbons of the 4,4'-trimethylenedipiperidine nucleophile are evidence of ring closure.

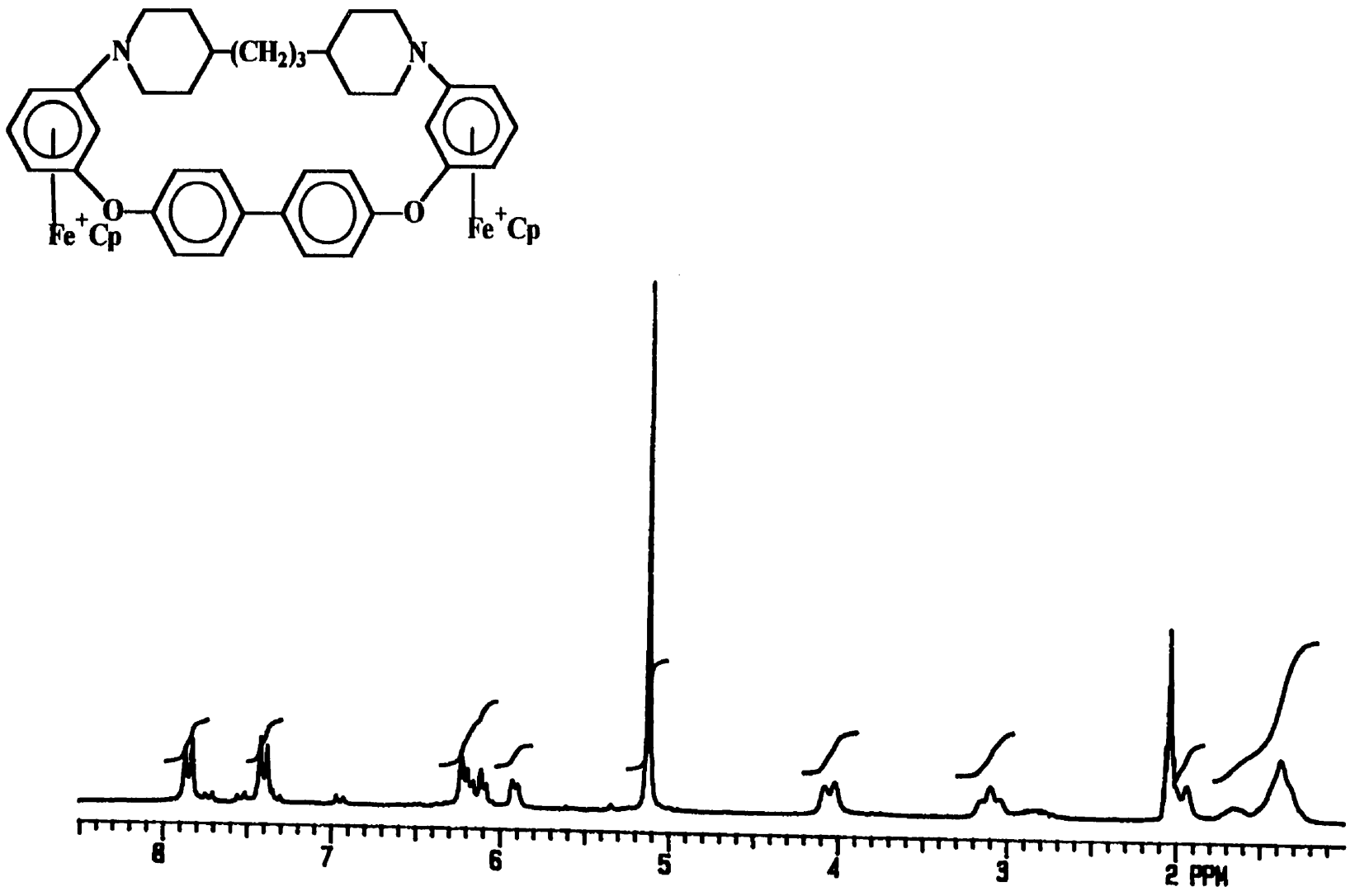

Figure 6.14: ^{1}H NMR spectrum of complex **6.15** in acetone-d_6.

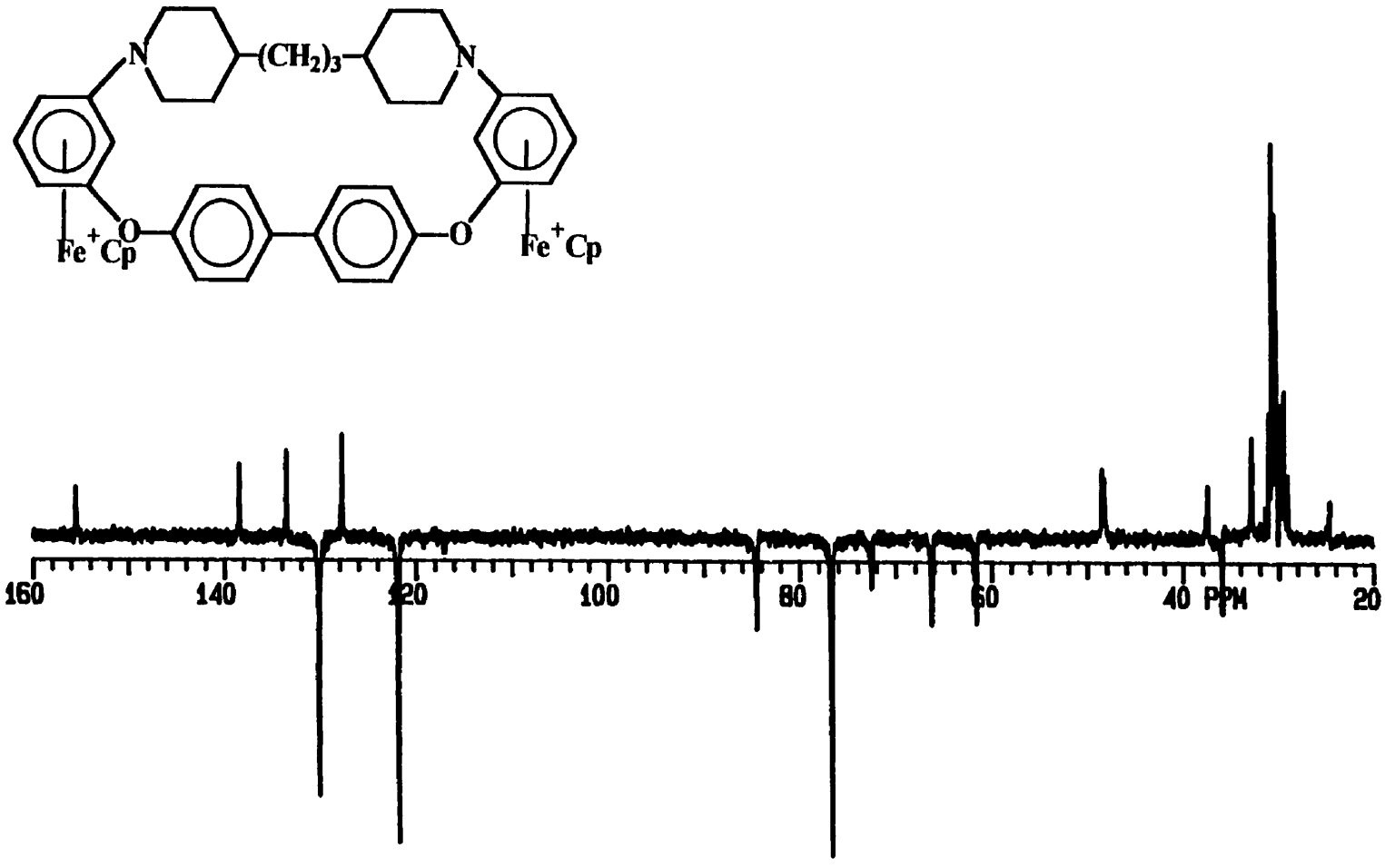

Figure 6.15: ^{13}C NMR spectrum of complex **6.15** in acetone-d_6.

Table 6.8: ^{1}H NMR Data of Complexed Macrocycles **6.15-6.17**

δ (acetone-d_6), ppm				
Complex	**Cp (s, 10H)**	**Complexed Aromatic[a]**	**Uncomplexed Aromatic[a]**	**Others[a]**
6.15	5.12	5.91 (d, 2H, J = 6.3) 6.08-6.23 (m, 6H)	7.40 (d, 4H, J = 8.4) 7.85 (d, 4H, J = 8.3)	1.27-1.38 (m, 10H) 1.51-1.67 (br.s., 2H) 1.94-2.00 (m, 4H) 3.10 (t, 4H, J = 9.3) 4.05 (d, 4H, J = 9.2)
6.16	5.14	5.91-5.95 (br.s., 2H) 6.19-6.23 (m, 6H)	7.15-7.19 (m, 2H) 7.35-7.48 (m, 4H) 7.81-7.98 (m, 2H)	1.36-1.59 (m, 10H) 1.61-1.80 (br.s., 2H) 1.92-1.97 (br.s., 4H) 3.09-3.16 (m, 4H) 4.11 (t, 4H, J = 12.8)
6.17	5.12	5.91-6.19 (br.s., 2H) 6.24-6.27 (m, 6H)	7.02 (d, 2H, J = 8.4) 7.34-7.38 (m, 2H) 7.84 (d, 2H, J = 8.6) 7.97-8.02 (m, 2H)	1.35-1.36 (m, 10H) 1.59-1.65 (br.s., 2H) 1.84-1.91 (br.s., 4H) 2.98-3.18 (m, 4H) 3.96-4.01 (t, 4H, J = 12.8)

[a] J values in Hertz.

Table 6.9: ^{13}C NMR and IR Data and Yields of Complexed Macrocycles **6.15-6.17**

δ (acetone-d_6), ppm						
Complex	**Yield (%)**	**Cp (s, 10H)**	**Complexed Aromatic**	**Uncomplexed Aromatic**	**Others**	**ν_{max} (cm^{-1})**
6.15	78.7	76.77	61.67, 66.35, 72.56, 84.58, 127.75*, 133.56*	121.88, 130.16, 138.48*, 155.55*	24.89 (CH_2) 32.78 (CH_2) 35.97 (CH) 37.48 (CH_2) 48.32 (CH_2)	1212 (CN)
6.16	78.9	76.66	61.95, 66.20, 73.74, 84.34, 127.44*, 131.82*	115.95, 118.77, 119.79, 119.87, 132.74, 133.04, 133.13, 133.24, 136.09*, 162.48*	24.22 (CH_2) 32.27 (CH_2) 35.44 (CH) 36.97 (CH_2) 47.85 (CH_2) 194.00 (CO)	1252 (CN) 1549 (CO)
6.17	82.2	77.73	63.34, 67.19, 75.08, 85.29, 126.42*, 133.58*	117.54, 120.25, 131.31, 131.49, 140.27*, 163.24*	24.92 (CH_2) 33.33 (CH_2) 36.02 (CH) 37.61 (CH_2) 48.79 (CH_2)	1223 (CN) 1106, 1292 (SO_2)

* Quaternary carbon.

6.3.2.3 Photolytic Liberation of the Organic Macrocyclic Ligand

Photolytic demetallation is the most commonly employed method for the isolation of purely organic ligands from their $CpFe^+$ complexed counterparts. The macrocyclic complexes, **6.15-6.17**, were dissolved in a solvent mixture of $MeCN/CH_2Cl_2$ and irradiated under a xenon lamp for 5 hours. Scheme 6.9 summarizes the photolytic methodology applied in the isolation of organic macrocycles **6.18-6.20**. Analysis of the organic macrocyclic systems using ^1H and ^{13}C NMR, IR and MS verified their identity. The data along with the yields are recorded in Tables 6.10 and 6.11.

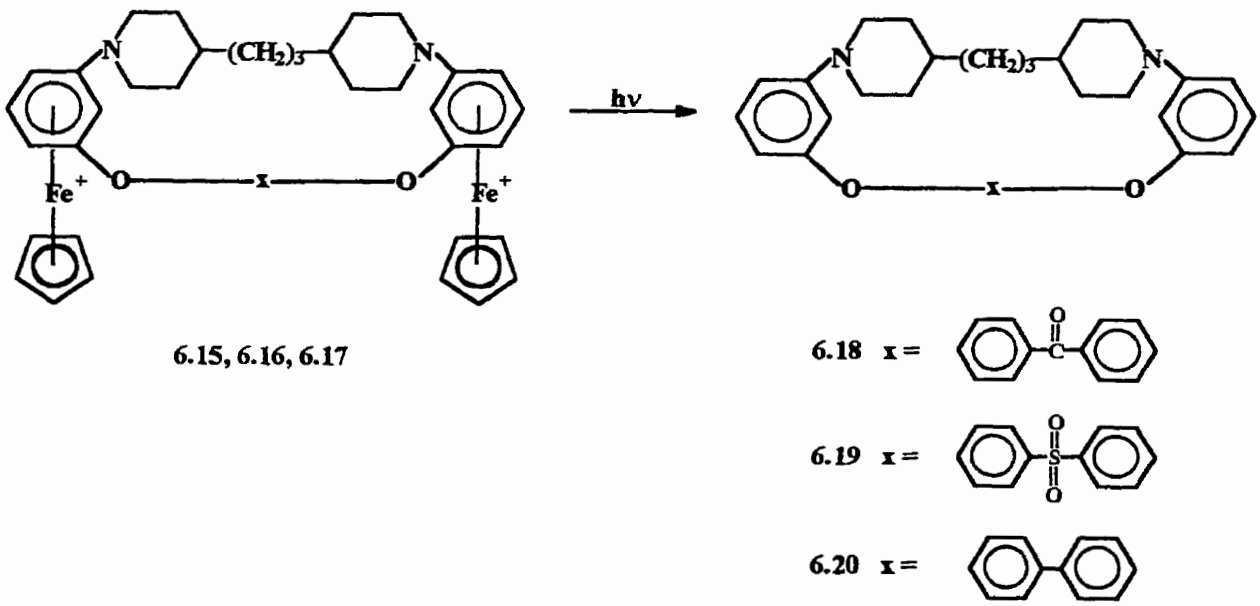

Scheme 6.9

The ^{1}H and ^{13}C NMR spectra of the macrocyclic ligand, **6.18**, are shown in Figures 6.16 and 6.17, respectively, and are useful in demonstrating the spectral changes noted upon demetallation of **6.16** and subsequent isolation of the organic macrocycles. The most distinct change in the ^{1}H and ^{13}C NMR spectra are the disappearances of the resonances representative of the cyclopentadienyl protons and carbons, respectively. In the case of macrocycle **6.18**, the disappearance of the strong singlet at 5.14 ppm in the ^{1}H NMR spectrum and of the peak at 76.66 ppm in the ^{13}C NMR spectrum are evidence for the success of the demetallation reaction. Furthermore, the shift in the complexed aromatic resonances to positions further downfield are noted in both the ^{1}H and ^{13}C NMR spectra upon decomplexation. Comparison of the ^{1}H NMR spectrum of the macrocyclic complex **6.16** in which the complexed aromatic protons appear at 5.91-5.95 and 6.19-6.23 ppm with its organic analogue, **6.18**, whose aromatic protons all resonate in the region between 6.48-7.78 ppm demonstrate the expected spectral changes upon the isolation of the purely organic ligand. Additional evidence for successful demetallation is obtained from the ^{13}C NMR spectrum which shows a similar downfield shift of the complexed aromatic carbons upon cleavage of the metal moiety from 61.95-84.34 ppm to 107.95-132.63 ppm.

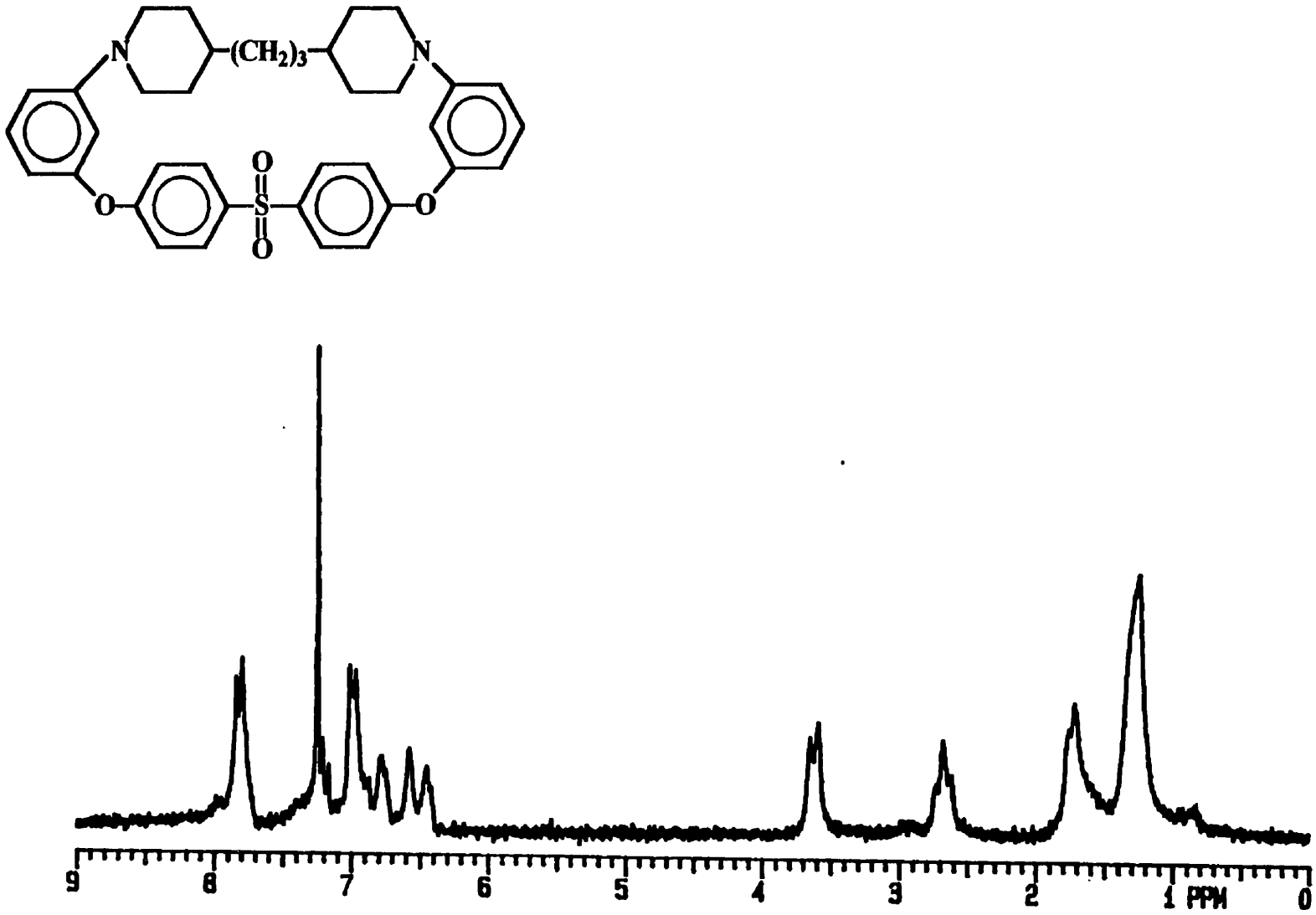

Figure 6.16: ^{1}H NMR spectrum of compound **6.18** in $CDCl_3$.

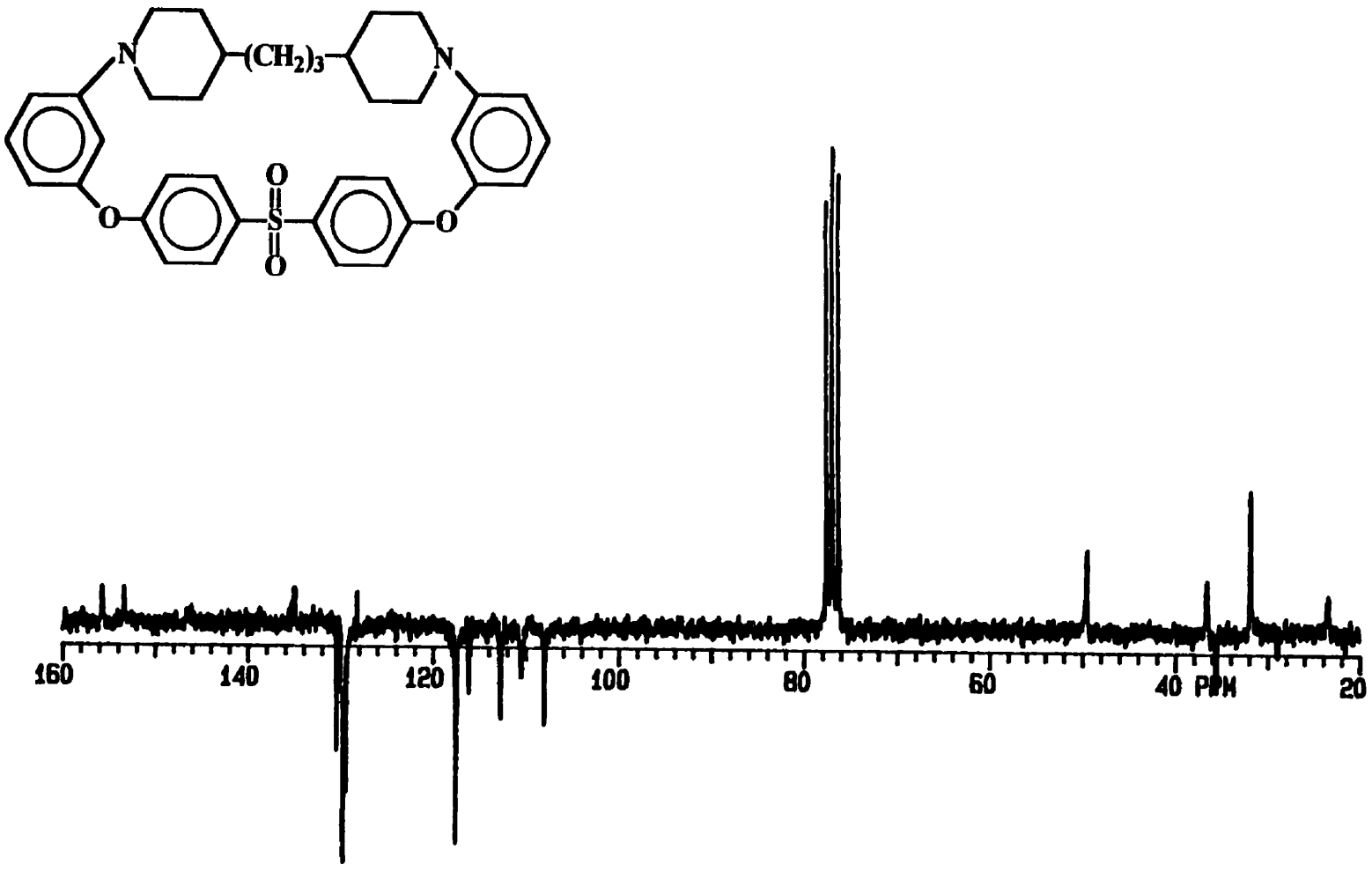

Figure 6.17: ^{13}C NMR spectrum of compound **6.18** in $CDCl_3$.

Table 6.10: ^{1}H NMR and MS Data and Yields of Macrocycles **6.18-6.20**

δ ($CDCl_3$), ppm				
Complex	**Yield (%)**	**Uncomplexed Aromatic[a]**	**Others[a]**	**m/z (M^+, %)**
6.18	40.5	6.5 (d, 2H, J = 7.3) 6.64 (s, 2H) 6.76 (d, 2H, J = 7.2) 6.90-6.91 (m, 2H) 7.0 (d, 2H, J = 8.7) 7.18-7.22 (m, 2H) 7.74 (t, 4H, J = 8.4)	1.16-1.27 (br.s, 12H) 1.69-1.77 (br.s., 4H) 2.63-2.69 (m, 4H) 3.59-3.67 (m, 4H)	572 (10)
6.19	20.4	6.45-6.46 (m, 2H) 6.58 (s, 2H) 6.75-6.79 (m, 2H) 6.99 (d, 4H, J = 8.4) 7.17-7.23 (m, 2H) 7.77-7.84 (m, 4H)	1.16-1.40 (br.s, 12H) 1.64-1.77 (br.s., 4H) 2.62-2.68 (m, 4H) 3.60-3.66 (m, 4H)	608 (11)
6.20	53.6	6.46 (d, 2H, J = 8.4) 6.64-6.71 (m, 4H) 7.03 (d, 4H, J = 8.3) 7.18 (t, 2H, J = 7.7) 7.17-7.23 (d, 4H, J = 8.4)	1.22-1.41 (m, 12H) 1.70-1.78 (m, 4H) 2.68 (t, 4H, J = 10.6) 3.60-3.66 (d, 4H, J = 9.2)	545 (9)

[a] J values in Hertz.

Table 6.11: ^{13}C NMR and IR Data of Macrocycles **6.18- 6.20**

δ ($CDCl_3$), ppm			
Complex	**Uncomplexed Aromatic**	**Others**	**ν_{max} (cm^{-1})**
6.18	107.95, 110.43, 112.34, 115.23, 117.00, 130.23, 131.90*, 132.21, 132.63, 153.37*, 156.35*, 161.71*	23.65(CH_2), 31.99 (CH_2) 35.61 (CH), 36.62 (CH_2) 49.66 (CH_2), 195.85 (CO)	1226 (CN) 1595 (CO)
6.19	108.00, 112.69, 116.11, 117.53, 128.35*, 129.44, 129.62, 129.79, 130.37, 135.00*, 153.38*, 155.76*	23.66 (CH_2), 31.96 (CH_2) 35.58 (CH), 36.63 (CH_2), 49.56 (CH_2)	1151 (CN) 1106, 1216 (SO_2)
6.20	107.23, 109.55, 111.44, 114.29, 115.68, 118.83, 128.00, 133.15*, 135.31*, 153.25*, 153.29*, 155.10*, 157.88*	23.71 (CH_2), 32.04 (CH_2) 35.63 (CH), 36.65 (CH_2), 49.81 (CH_2)	1218 (CN)

* Quaternary carbon.

7.0 Conclusions

The use of cyclopentadienyliron mediated nucleophilic aromatic substitution has been used in the preparation of a variety of bimetallic, polymetallic and macrocyclic species.

The versatility of $CpFe^{+}$ mediated aromatic nucleophilic substitution in the preparation of various bimetallic complexes has been demonstrated by the incorporation of oxygen, sulfur and nitrogen containing linkages. Both aliphatic and aromatic dithiols were reacted with cyclopentadienyliron complexes of chloroarenes to yield the corresponding bis(cyclopentadienyliron) arene dications. Diiron complexes with mixed ether/thioether bridges were prepared using the same methodology. A slight variation of this synthetic strategy involving the reaction of starting nitroarene complexes with aliphatic or aromatic diamines allowed for the incorporation of nitrogen into these bimetallic systems. The enhanced reactivity of the nitroarene complexes resulted in shorter reaction times, minimizing the decomposition process and allowing for the isolation of the desired diiron complexes in good yield. Functionalization of the thioether complexes was achieved in the presence of H_2O_2 and CF_3COOH giving the corresponding sulfone bridged species. The efficient liberation of the metallic moieties via photolytic demetallation allowed for the isolation of the organic compounds under very mild conditions. This methodology provides one of the most general and least expensive routes to a variety of complexes and compounds which may be of great importance in material science.

Selected mono- and bimetallic complexes were investigated with respect to their electrochemical behavior. It was found that although the oxygen bridged species, $\mathbf{[3.3]^{2+}}$,

exhibited isolated redox centers whereas isomeric thioether analogues, $[\mathbf{3.4}]^{2+}$ and $[\mathbf{3.6}]^{2+}$, demonstrated a small degree of electronic interaction between the two metal centers. This interaction was established on the basis of the measured difference in formal potentials of the 36 $e^-/37e^-$ and 37 $e^-/38e^-$ reduction steps. Furthermore, the rate of reaction of the 19 e^- and 38 e^- reduction species of the monomeric and bimetallic complexes, respectively, with the solvent was determined to not only increase with increasing temperature but to take place more readily in the presence of the oxygen-based species. The use of controlled potential coulometry of complex $[\mathbf{3.2}]^{2+}$ provided evidence for the transfer of two electrons in the initial reduction step. A large $\Delta E°$ of 200 mV between the two reduction waves of complex $[\mathbf{3.3}]^{2+}$ leading to the 38 e^- further supports the transfer of two electrons. The investigation of the rate of reaction of the 38 e^- species with the solvent of a series of aliphatic sulfur bridged complexes, $[\mathbf{3.9}]^{2+}$-$[\mathbf{3.12}]^{2+}$, at various temperatures was extended to the determination of several activation parameters using the activated complex theory. It was observed that the activation energy corresponding to the 38 e^- species with the solvent decreased with increasing chain length.

A three-step process involving the synthesis of a bimetallic species with terminal chlorine substituents, reaction of this species with an excess of 1-naphthol and its subsequent photolytic demetallation allowed for the isolation of monomers with structural features which make them suitable for Scholl polymerization. Several monomeric units incorporating sulfone, ketone, sulfur or nitrogen bridges were subjected to Scholl polymerization under a variety of reaction conditions. Reactions of these monomers with respect to time, temperature, concentration and monomer:catalyst ratio showed no concrete trends in their polymerization. ^1H and ^{13}C NMR and GPC were used in the

characterization of the isolated materials where verification of polymerization was indicated by distinct spectral changes. It is suggested that due to the low solubility of the polymeric materials obtained, the molecular weight determinations using GPC are not indicative of the actual molecular weights of these species. Thermogravimetric studies suggested the isolation of polymeric materials with molecular weights greater than that calculated using GPC.

Reaction of the (η^6-chloroarene)CpFe$^+$ complex with 5-norbornene-2-methanol followed by photolytic demetallation also allowed for the generation of a monomer, **5.2**, suitable for ROMP polymerization. A detailed NMR investigation using a variety of 1- and 2-dimensional experiments was necessary for the positive identification of the complexed and organic monomeric units. Polymerization of compound **5.2** in the presence of $RuCl_3 \cdot H_2O$ allowed for the isolation of the corresponding high molecular weight material as measured by GPC. An increase in molecular weight and reaction yield was observed with increasing amounts of water in the reaction solvent. Furthermore, despite a limited degree of solubility in water, polymerization was successful when water was used as the only solvent. However, no substantial increase in the molecular weight of the isolated polymeric material was observed.

The final polymerization technique allowed for the generation of metallated polyethers and polythioethers in a one-pot reaction. The combination of (1,4-dichlorobenzene)CpFe$^+$ with various diols and dithiols yielded the corresponding metallated polymers. Identification of the polymeric materials was indicated by comparison of their ^{1}H and ^{13}C NMR spectra with those of the starting material and bimetallic analogues. Furthermore, removal of the metallic moiety via photolytic

demetallation allowed for the molecular weight determination of the organic species using GPC which was then used to calculate the molecular weight of the organometallic materials.

The synthetic utility of cyclopentadienyliron activated aromatic nucleophilic substitution is further demonstrated by the preparation of macrocyclic compounds. The preparation of bimetallic species with terminal chlorine substituents in the meta position allowed a second nucleophilic aromatic substitution step to be used in the formation of the desired cyclic structure. Comparison of the ^{1}H and ^{13}C NMR spectra of the complexed macrocycles with those of their corresponding starting materials indicated successful ring closure. Photolytic demetallation was an efficient means for the isolation of the organic macrocycles whose structures were verified using ^{1}H and ^{13}C NMR and MS.

8.0 Experimental

8.1 General Methods

^{1}H and ^{13}C NMR spectra were recorded at 200MHz and 50 MHz (Gemini 200), respectively, while HH COSY and CH COSY were recorded on a Bruker 500 NMR spectrometer (Mr. T. Wolowiec, technician), with chemical shifts measured from the solvent signals. Coupling constants are reported in Hz. IR spectra were measured on a Perkin-Elmer Model 781 or FT-IR Bomen MB102 Spectrophotometers. Positive ion EI (electron impact) spectra were obtained on a Hewlett-Pakard 5970 Series Mass Selective Detector, by use of a direct insertion probe (70eV). Signals are given in m/z units. GPC measurements were performed using a BL-gel mixed column (Phenomenex) equipped with a CH-30 column heater (Eppendorf), a PL-DCU (Polymer Laboratories) and a Gilson Model 302 pump and Gilson Model 131 refractive index detector. All polymer molecular weights were estimated versus polystyrene standards at 35°C with $CHCl_3$ as the eluent at a flow rate of 0.7 ml min^{-1}. An EG&G Princeton Applied Research Model 263A potentiostat, interfaced with a microcomputer was used in all experiments. CV simulations were run using the Digisim simulation program, version 2.0, from Bioanalytical Systems Incorporated. All coulometry and voltammetry associated with bulk-electrolysis experiments (conducted at the Chemistry Department, University of North Dakota with the aid of Dr. D. Pierce) was performed with a three-electrode cell that was controlled by an EG&G Princeton Applied Research model 273 potentiostat. Thermogravimetric analysis were carried out using a Mettler Toledo TGA/SDTA851^{e}

instrument and the data collected via the use of Mettler Toledo STAR^e system software, STAR^e SW V1.5x. Elemental analyses were performed at the University of Saskatchewan and Guelph Chemical Laboratories Ltd.

8.2 Chemicals

Anhydrous aluminum chloride, aluminum powder, ferrocene, ammonium hexafluorophosphate, 3-chloroperbenzoic acid, chloroarenes, anilines, hydrogen peroxide, trifluoroacetic acid, and all oxygen, sulfur and nitrogen-containing nucleophiles, tetra-N-butylammonium perchlorate and tetra-N-butylammonium hexafluorophosphate are commercially available and were used without further purification. THF was purified by distillation over sodium metal under nitrogen. High quality N,N'-dimethylformamide (DMF, Aldrich; Burdick and Jackson Brand, Baxter Scientific), used for all electrochemical investigations, was purged with purified dinitrogen and stored over Linde molecular sieves 4A (Strem Chemicals). All other solvents (reagent grade) were used without purification.

8.3 Ligand Exchange Reactions

8.3.1 Synthesis of Chloroarene Cyclopentadienyliron Complexes

A typical reaction is the combination of 27.9 g (150 mmol) ferrocene, 40.0 g (330 mmol) aluminum trichloride, 4.2 g (150 mmol) aluminum powder, and a 4-fold excess of the appropriate arene in a 500 mL 3-necked round bottom flask. The reaction mixture is then heated at 135-140°C for 5 h under a nitrogen atmosphere. Upon cooling the green-black mixture to approximately 50°C, it is slowly poured into 200 mL of an ice-water slurry. It is crucial that this step is performed very carefully since this is an extremely exothermic reaction. The resulting aqueous mixture is filtered through rough sand and the filtrate extracted with petroleum ether (3 x 50 mL) and diethyl ether (1 x 50 mL) to remove any unreacted materials. Adding 13.9 g (75 mmol) of NH_4PF_6 to the aqueous layer results in the generation of a yellow-green precipitate. This material is dissolved in a dichloromethane/acetone mixture (4:1) and the water layer extracted with dichloromethane until it is virtually colorless. The resulting dichloromethane/acetone solution is dried over $MgSO_4$, filtered, and concentrated by rotary evaporation to approximately 25 mL. Diethyl ether is then added to precipitate the desired product as a yellow-green solid which is collected by suction filtration, rinsed with diethyl ether, and dried prior to analysis.

8.3.2 Synthesis of Aniline Cyclopentadienyliron Complexes

A similar reaction procedure to that described for the preparation of the chloroarene cyclopentadienyliron complexes was employed. That is, 27.9 g (150 mmol) ferrocene, 40.0 g (330 mmol) aluminum trichloride, 4.2 g (150 mmol) aluminum powder, and a 4-fold excess of the appropriate arene were placed in a 500 mL 3-necked round bottom flask. In the case of the preparation of the aniline cyclopentadienyliron complexes, the reaction mixture was stirred at 145-160°C for 5 h under a nitrogen atmosphere. The aniline complexes were isolated as brownish-yellow solids following the same workup procedure as described for the isolation of the chloroarene cyclopentadienyliron complexes.

8.4 Oxidation Reactions

8.4.1 Preparation of the Nitroarene Cyclopentadienyliron Complexes

Typically, 5.0 mmol of the aniline cyclopentadienyliron complex was dissolved in 50 mL of a 1:1 mixture of 30% H_2O_2 and CF_3COOH and heated at 60°C for 20 minutes. The mixture was then cooled to room temperature and extracted with a 4:1 dichloromethane/nitromethane solvent mixture. This organic solvent mixture was then dried over $MgSO_4$, filtered and concentrated by rotary evaporation to approximately 25 mL. The addition of a concentrated aqueous solution of NH_4PF_6 resulted in the

precipitation of a yellow-brown solid. This solid was rinsed with diethyl ether and dried prior to analysis.

8.4.2 Preparation of Bis(cyclopentadienyliron) Arene Sulfone Complexes

Complexes **2.86-2.105** were prepared by the dissolution of the corresponding disulfide complex (1 mmol) in 2 mL of DMF in a 50 mL round-bottom flask equipped with a stir bar. To this solution, a ten-fold ratio of m-chloroperbenzoic (m-CPBA) acid (10 mmol, 1.73 g) dissolved in 1 mL of DMF was added. Finally, CH_2Cl_2 was added until the complex just began to precipitate out of solution. This reaction mixture was then refluxed at 60°C for 8 hours. The resulting yellow solution was allowed to cool to room temperature, at which time the CH_2Cl_2 was removed under reduced pressure at 25°C using rotary evaporation. Diethyl ether was added resulting in a thick yellow oil. A 2:3 chloroform/diethyl ether mixture (5 x 10 mL) was prepared and used to rinse the resulting oil to remove excess m-CPBA. Finally, the oil was dissolved in a minimal amount of acetone and upon the addition of diethyl ether yellow-brown oils or yellow solids were obtained and dried under vacuum prior to analysis.

8.5 Nucleophilic Substitution Reactions

8.5.1 Preparation of Bis(cyclopentadienyliron) Arene Sulfur Complexes

Typically, complexes **2.13-2.33, 2.37-2.47** and **2.49-2.54** were prepared by the combination of 1.0 mmol of the appropriate (η^6-chloroarene)(η^5-cyclopentadienyl)iron hexafluorophosphate complex with 0.5 mmol of the dinucleophile in a 50 mL round-bottom flask containing 2.5 mmol (0.345 g) of K_2CO_3 and 10 ml of a 4:1 THF/DMF mixture. The resulting green-gold solution was stirred under a nitrogen atmosphere for 16 h at room temperature, while its color changed to a yellow-brown. A standard workup procedure was followed, in which the reaction mixture was filtered through a sintered glass crucible into a 10% (v/v) HCl solution, causing the formation of a granular precipitate. Acetone washings were added to the filtrate, causing the dissolution of the product. This solution was then concentrated by evaporation of the acetone under reduced pressure, and the desired diiron complex precipitated as a yellow granular solid upon the addition of a concentrated aqueous solution of NH_4PF_6. At this point, the product was recovered by filtration and washed with several portions of cold distilled water. After drying for several hours under vacuum, the product was washed with small amounts of diethyl ether and further dried. The resulting products (fine yellow powders) did not require additional purification in most cases.

8.5.2 Preparation of Bis(cyclopentadienyliron) Arene Nitrogen Complexes 2.123 - 2.124

Complexes **2.123** and **2.124** were prepared by the combination of 1 mmol of the appropriate (η^6-chloroarene)(η^5-cyclopentadienyl)iron hexafluorophosphate complex with 0.5 mmol of 1,6-hexanediamine in a 50 mL round-bottom flask containing 30 mL of THF. The reaction mixture was refluxed for 12 h under a nitrogen atmosphere. The solution was then allowed to cool and the solvent concentrated to approximately 5 mL under reduced pressure. The resulting orange residue was redissolved in dichloromethane, and to this solution was added 1.0 mmol of NH_4PF_6 in 20 mL of distilled water. The product was washed once with distilled water and dried over anhydrous magnesium sulfate, and the solvent was removed under reduced pressure to yield an orange solid. This solid was collected by suction filtration, washed with diethyl ether, and then dried under vacuum for several hours.

8.5.3 Preparation of Cyclopentadienyliron Arene Nitrogen Complex 2.125

One millimole (0.413 g) of (η^6-dichlorobenzene)(η^5-cyclopentadienyl)iron hexafluorophosphate was combined with a large excess (1.39 g, 12 mmol) of 1,6-hexanediamine in a 50 mL round-bottom flask containing 10 mL of a 1:1 mixture of THF/DMF and 4 mL of glacial acetic acid. The reaction mixture was then refluxed for

12 h under a nitrogen atmosphere. The resulting disubstituted monoiron complex was isolated by extracting the product with dichloromethane and adding a concentrated aqueous solution of NH_4PF_6. The product was washed several times with distilled water to remove the reaction solvents and worked up in the same manner as complexes **2.123** and **2.124**.

8.5.4 Preparation of Bis(cyclopentadienyliron) Arene Nitrogen Complexes 2.134 - 2.147

Complexes **2.134 - 2.147** were prepared by the combination of 1 mmol of the appropriate (η^6-nitroarene)(η^5-cyclopentadienyl)iron hexafluorophosphate complex with 0.5 mmol of an aliphatic diamine in a 50 mL round-bottom flask containing 2.5 mmol (0.345 g) of K_2CO_3 and 10 mL of a 1:1 THF/DMF mixture. The resulting solution was then heated at 60°C under a nitrogen atmosphere for 5h. The reaction mixture was allowed to cool and was filtered into 10 mL of 10% (v/v) HCl; the reaction flask was washed with dichloromethane, and the washings were filtered. To this was added a concentrated aqueous solution of NH_4PF_6. The product was then extracted with dichloromethane, and the extract was washed several times with distilled water. After drying over anhydrous magnesium sulfate, the solvent was removed under reduced pressure to yield a brownish-orange oil. The oil was rinsed with diethyl ether and allowed to dry under vacuum for several hours.

8.4.5 Preparation of Bis(cyclopentadienyliron) Arene Nitrogen Complexes 2.150 - 2.154

Complexes **2.150- 2.154** were prepared by the combination of 1.0 mmol of the appropriate (η^6-nitroarene)(η^5-cyclopentadienyl)iron hexafluorophosphate complex with 0.5 mmol of an aromatic diamine, and the mixture was added to a 50 mL round-bottom flask containing 2.5 mmol (0.345 g) of K_2CO_3 and 10 mL of DMF. The resulting solution was then heated at 60°C under a nitrogen atmosphere for 3 h. The final diiron complexes were isolated as oils in the same manner used for complexes **2.134 - 2.147**.

8.4.6 Preparation of Bis(cyclopentadienyliron) Arene Complexes 4.1, 4.2, 4.4, 6.13 and 6.14

A typical reaction involved the combination of 2.0 mmol of η^5-(1,3-dichlorobenzene)- or η^5-(1,4-dichlorobenzene)-η^6-cyclopentadienyliron hexafluoro-phosphate with 1.0 mmol of the dinucleophile in a 50 mL round-bottom flask containing 2.5 mmol (0.245 g) of K_2CO_3 and 10 mL of DMF. The resulting red-yellow solutions were stirred under a nitrogen atmosphere for 16 h at room temperature. A standard workup procedure as outlined for the isolation of the bis(cyclopentadienyliron) arene sulfur complexes in section 8.5.1. The resulting products were isolated as yellow powders and did not require further purification.

8.4.7 Preparation of Bis(cyclopentadienyliron) Nitrogen Complexes 4.3 and 6.12

Complexes **4.3** and **6.12** were prepared by the reaction of 2.0 mmol of η^5-(1,3-dichlorobenzene)- or η^5-(1,4-dichlorobenzene)-η^6-cyclopentadienyliron hexafluorophosphate with 1.0 mmol of the 4,4'-trimethylenedipiperidine in a 50 mL round-bottom flask containing 2.5 mmol (0.245 g) of K_2CO_3 and 10 ml of a 1:1 THF/DMF mixture. The resulting orange-red solution was stirred at 65°C for 6 hours under a nitrogen atmosphere. A standard workup procedure as outlined in section 8.5.1 for the isolation of the bis(cyclopentadienyliron) arene sulfur complexes allowed for the desired products as orange solids.

8.4.8 Preparation of Capped 1-Naphthol Complexes 4.5-4.7 and 4.9

The generation of complexes **4.5-4.7** and **4.9** involved the reaction of complexes **2.29, 4.1-4.2** and **4.4** (1.0 mmol) with 2.5 mmol (0.260 g) of 1-naphthol in the presence of 2.5 mmol (0.245 g) of K_2CO_3 and 10 mL of DMF. Dark red-orange solutions resulted which were stirred for 8 hours at room temperature under a nitrogen atmosphere. The desired complexes were then isolated according to the typical procedure as outlined in section 8.5.1.

8.4.9 Preparation of Capped 1-Naphthol Complex, 4.8

Complex **4.8** was prepared by the combination of 1.0 mmol of complex **4.3** with 2.5 mmol (0.260 g) of 1-naphthol, 2.5 mmol (0.245 g) of K_2CO_3 and 10 mL of DMF in a 10 mL round-bottom flask equipped with a stirbar. These substrates were stirred at 65°C for 7 hours under a nitrogen atmosphere and isolated as a dull yellow solid following the workup procedure described in section 8.5.1.

8.4.10 Synthesis of Complexed Macrocycles

The complexed macrocycles **6.15-6.17** were prepared by the reaction of 0.3 mmol of the appropriate bimetallic complex with 0.3 mmol of a suitable nucleophile in the presence of an excess of K_2CO_3 and 5 mL of DMF. These reagents were stirred for 24 h at 65°C under a nitrogen atmosphere. The red-yellow solutions were filtered through a sintered glass crucible into a 10% (v/v) HCl solution resulting in the formation of a yellow precipitate. The reaction flask and crucible were rinsed with acetone which allowed for the dissolution of the precipitate. Upon the concentration of this solution by rotary evaporation, a concentrated aqueous solution of NH_4PF_6 was added causing the precipitation of the desired product. The yellow solid was isolation by filtration and washed with several portions of distilled water. The precipitate was allowed in dry under vacuum for several hours and rinsed with diethyl ether and further dried.

8.4.11 Synthesis of the modified 5-norbonene-2-methanol complex, 5.1

2.1 mmol (0.25 mL) of 5-norbornene-2-methanol, 2.5 mmol (0.2806 g) of potassium tert-butoxide and 3 mL of freshly distilled THF were placed in a 50 mL round-bottom flask and stirred at room temperature for 1 h under a nitrogen atmosphere. To the resulting pale yellow solution was added 3 mL of DMF and 1 mL of freshly distilled THF and this solution stirred at room temperature under a nitrogen atmosphere for an addition 20 minutes. At this point, 1.0 mmol (0.378 g) of η^6-(chlorobenzene)-η^5-(cyclopentadienyliron) hexafluorophospate was added and the solution mixture stirred for 16 h at room temperature under a nitrogen atmosphere. The resulting orange solution was then filtered through a sintered glass crucible into a 10% (v/v) HCl solution resulting in the generation of a yellow solution. The reaction flask and crucible were rinsed with a small amount of CH_2Cl_2 and a concentrated aqueous solution of NH_4PF_6 added. This solution was then transferred to a separatory funnel and extracted with CH_2Cl_2 (4 x 50 mL). The organic layer was then washed with distilled water (3 x 50 mL) and dried over $MgSO_4$, filtered and the solvent removed by rotary evaporation. An orange oil resulted which was rinsed with several portions of diethyl ether and dried under vacuum.

8.5 Photolytic Demetallation Reactions

8.5.1 Isolation of Sulfur, Nitrogen and Sulfone Compounds

Compounds **2.55-2.85, 2.106-2.121, 5.2, 6.18-6.20** were prepared by the dissolution of the corresponding diiron or macrocyclic complex in a CH_2Cl_2/CH_3CN (30 mL/10 mL) solvent mixture in a Pyrex tube. The solution was then deoxygenated by bubbling nitrogen through it, fitted into a photochemical chamber and irradiated for 5 hours, using a wide wavelength range of visible light supplied by a Xenon lamp. The solvent was then concentrated to a volume of 1-2 mL using rotary evaporation. The residue was applied to a silica gel column and washed with hexane and eluted with chloroform. It is important to note that in the case of the sulfone compounds, the products were eluted using ethyl acetate. Removal of the solvent yielded the expected liberated arenes.

8.5.2 Isolation of Capped 1-Nathphyl Compounds, 4.10-4.14

0.5 mmol of complexes **4.10-4.14** were dissolved in a CH_2Cl_2/CH_3CN (30 mL/10 mL) solvent mixture in a Pyrex tube, the resulting solution deoxygenated with nitrogen for 30 minutes and subjected to irradiation in the presence of a Xenon lamp for 5 h. This dark colored solution was then evaporated to dryness by rotary evaporation and the resulting residue dissolved in chloroform. The solution was transfer to a separatory

funnel and washed with distilled water (3 x 20 mL). The chloroform was dried over $MgSO_4$, filtered and concentrated under reduced pressure. This concentrated solution was then added dropwise with swirling to cold hexane resulting in the isolation of the desired compounds as white or cream colored solids.

8.5.2 Isolation of Polyethers and Polythioethers

0.5 mmol of complexes **6.2, 6.4-6.6** were dissolved in a DMF (50mL) in a Pyrex tube, the solution deoxygenated with nitrogen for 30 minutes and subjected to irradiation in the presence of a Xenon lamp for 5 h. This dark colored solution was then evaporated to dryness under vacuum and the resulting residue dissolved in a chloroform/nitromethane solvent mixture. The solution was transfer to a separatory funnel and washed with distilled water (3 x 20 mL). The chloroform/nitromethane solvent mixture was dried over $MgSO_4$, filtered and concentrated under reduced pressure resulting in the isolation of the desired compounds as white or cream colored solids.

8.6 Polymerization Reactions

8.6.1 ROMP of monomer 5.2

Generally, a 1 mol % solution of $RuCl_3 \cdot H_2O$ was prepared in the solvent of choice and the mixture stirred for 2-3 h. The monomer was then added via syringe and the mixture heated at 60°C for a 24 h period which resulted in a dark brown viscous solution or solid mass. Regardless of the state of the product, it was dissolved in chloroform and then precipitated by the slow addition of methanol with vigorous stirring. A fibrous, cream colored solid was obtained following this purification process.

8.6.2 Scholl Polymerizations

Each Scholl polymerization involved the initial preparation of the monomer solution separate from that of the catalyst solution. The monomer solution was generally generated by dissolving 0.5 mmol of a suitable monomer in $PhNO_2$ in a 10 mL round bottom flask under a nitrogen atmosphere. Next, a solution of FeCl3 is prepared by its dissolution in $PhNO_2$ and subsequently added dropwise to the monomer solution over 20 minutes via a syringe penetrating the rubber septum. This reaction misture was stirred either at room temperature or 65°C for the desired period of time. Isolation of the solid crude polymeric material was achieved by pouring the viscous dark brown-black solution into methanol (150 mL) acidified with 2% HCl. Finally, the polymeric material was

collected using suction filtration, rinsed with methanol and dried under vacuum. Prior to purification of this material, its identity was verified using ^{1}H and ^{13}C NMR and GPC. Purification of the polymer involved its dissolution in a minimal amount of $CHCl_3$ (5-10 mL) followed by the slow addition of this solution into acetone (150 mL) acidified with 2% HCl. Finally, the polymeric material was isolated by suction filtration, rinsed with acetone and dried under vacuum in preparation for its analysis.

8.6.3 Polymerization by $CpFe^{+}$ activated Aromatic Nucleophilic Substitution

Polymers **6.2-6.6** were prepared by the combination of 0.5 mmol of η^6-(1,4-dichlorobenzene)-η^5-cyclopentadienyliron hexafluorophosphate with 0.5 mmol of the desired oxygen or sulfur-containing dinucleophile in a 25 mL round-bottom flask containing 2.5 mmol (0.245 g) K2CO3 and 0.5 mL of DMF. The resulting solution was stirred under a nitrogen atmosphere for 16 h at 65°C. The reaction mixture was then added to a 10% (v/v) HCl solution resulting in the formation of a granular precipitate or gummy solid. The flask was then rinsed with acetone and added to the HCl solution. Further precipitation of the product was achieved upon the addition of a concentrated aqueous solution of NH_4PF_6. At this point the product was recovered by filtration and wahed with several portions of cold distilled water. After drying for several hours under vaccuum, the product was washed with small amounts of diethyl ether and further dried.

8.7 Instrumental Methods

8.7.1 Cyclic Voltammetric Studies

All cyclic voltammograms were obtained using an EG&G Princeton Applied Research Model 263A potentiostat, interfaced with a microcomputer. Cyclic voltammetric experiments were performed using a conventional three- electrode cell. The working electrode was either a platinum disk electrode (ca. 2 mm diam.) or a glassy carbon disk electrode (ca. 3 mm diam.). A quasi-reference electrode (Ag/AgCl) was utilized. However, ferrocene was added at the end of each experiment and served as the reference redox couple. The auxiliary electrode in these studies was a Pt wire. The cyclic voltammetric behavior of selected complexes was investigated at various scan rates of 0.2-1.0 V/s. Temperatures ranging from 293 to 233 K were obtained by means of a dry ice-acetone slush bath in a Dewar flask. The concentration of the complex was 2.0 mM, while that of the supporting electrode was 0.1 M. Before measurements, solutions were deaerated by passing high-purity nitrogen through them and the experiment was run under a blanket of purified nitrogen.

8.7.2 Digital Simulations

CV simulations were run using the Digisim simulation program, version 2.0, from Bioanalytical Systems Incorporated. Simulations were performed to fit experimentally determined cyclic voltammograms of a 2.0 mM solution in DMF using a 0.1 mM of TBAP as the supporting electrolyte. The simulations were performed over a potential range of –0.3 - -1.9 V at 233 K assuming a cylindrical electrode geometry with a 1 cm^2 area. Scan rates of 0.2 – 2.0 V/s were used in the simulation and E_{pc} and E_{pa} varied to fit the experimental data. The difference in the formal potentials of the two 1-electron transfer steps was taken as an average value of ΔE° determined from these applied scan rates.

8.7.3 Controlled Potential Coulometry

All coulometry and voltammetry associated with bulk-electrolysis experiments were performed with the aid of Dr. D. Pierce at the chemistry department, University of North Dakota using a three-electrode cell that was controlled by an EG&G Princeton Applied Research model 273 potentiostat. Electrolysis currents were recorded for a user-specified applied potential and were acquired over more then 300 s with a time interval of less then 0.5 s. The current-time set for each electrolysis was digitally integrated to yield

total charge passed to within less than ±1.0% of comparable, electronically integrated currents. Stirred solution voltammograms were recorded before and after electrolysis to analyze for solution composition and were performed with a potential sweep rate of 0.02 V/s.

Bulk-scale electrolysis experiments were performed with the analyte at 3 mM concentration in 50 mL of DMF/0.1M $TBAPF_6$. Solutions were contained within a sealed electrochemical cell that was constantly purged with purified nitrogen and was cooled by partial immersion in a dry ice-acetone slush bath. Rapid stirring during electrolysis and voltammetry immediately before and after electrolysis was performed with a magnetic stir bar that was rotated at a constant rate at the cell bottom. The working electrodes used for controlled-potential coulometry were high surface area cylinders and were composed of either platinum mesh or reticulated vitreous carbon. A small platinum disk electrode 9ca.2 mm diam.) or a larger glassy carbon disk electrode (ca.3 mm diam.) was used as the working electrode for all voltammetry. The counter electrode in all cases was a platinum-mesh cylinder that was contained within a large, separate compartment containing DMF/0.1 $TBAPF_6$ in ionic contact with the analyte solution through a medium porosity glass frit. A silver wire coated with solver chloride acted as a quasi-reference electrode in DMF/0.1 $TBAPF_6$ and was separated from solution within a smaller fritted compartment. At the conclusion of each experiment, the quasi-reference potential was correlated to the potential of the ferrocene/ferrocinium couple (Fc/Fc^+) by addition of ferrocene to the solution.

8.7.4 Gel Permeation Chromatography

GPC measurements were performed using a BL-gel mixed column (Phenomenex) equipped with a CH-30 column heater (Eppendorf), a PL-DCU (Polymer Laboratories) and a Gilson Model 302 pump and Gilson Model 131 refractive index detector. All polymer molecular weights were determined versus polystyrene standards, using the method of narrow standards, at 35°C with $CHCl_3$ as the eluent at a flow rate of 0.7 ml min^{-1}.

8.7.5 Thermogravimetric Analysis

. Thermogravimetric analysis were performed using a Mettler Toledo TGA/SDTA851^e instrument at a heating rate of 30°C/min. in a nitrogen atmosphere. Typically, samples ranging from 5-8 mg were subjected to analysis in a 70 μL alumina crucible and the data collected via the use of Mettler Toledo STAR^e system software, STAR^e SW V1.5x.

9.0 References

1. Pauson, P.L., *Pure & Appl. Chem.*, **1977**, 49, 839.
2. Kealy, T.J. and Pauson, P.L., *Nature (London)*, **1951**, 168, 1039.
3. Janiak, C. and Schumann, H., *Adv. Organomet. Chem.*, **1991**, 33, 291.
4. Fessenden, R.J. and Fessenden, J.S., Organic Chemistry, 4th ed., Brooks/Cole Publishing Company, CA, 1990.
5. Fox, M.A. and Whiteshell, J.K., Organic Chemistry, Jones and Bartlett Publishers, Boston, MA, 1994.
6. Knipe, A.C., McGuinness, S. J. and Watts, W.E., *J. Chem. Soc. Perkin Trans. II*, **1981**, 193.
7. Knipe, A.C., McGuinness, S.J. and Watts, W.E., *J. Chem. Soc., Chem. Commun.*, **1979**, 842.
8. Astruc, D., *Topics Curr. Chem.*, **1991**, 160, 47.
9. Pearson, A.J., Bruhn, P.R. and Hsu, S.-Y., *J. Org. Chem.*, **1986**, 51, 2137.
10. Pearson, A.J., Park, J.G. and Zhu, P.Y., *J. Org. Chem.*, **1992**, 57, 3583.
11. Pearson, A.J. and Bruhn, P.R., *J. Org. Chem.*, **1991**, 56, 7092.
12. Bunnett, J.F. and Herman, H., *J. Org. Chem.*, **1971**, 36, 4081.
13. Semmelhack, M.F., Clark, G.R., Garcia, J.L., Harrison, J.J., Thebtaranonth, Y., Wulff, W. and Yamashita, A., *Tetrahedron*, **1981**, 37, 3957.
14. Wright, M.E., Macromolecules, 1989, 22, 3256.
15. Baldoli, C., Del Buttero, P. Licandro, E. and Maiorana, S., *Gazzetta Chimica Italiano*, **1988**, 118, 409.

16. Percec, V. and Okita, S., *J. Polym. Sci., Part A: Polym. Chem.*, **1993**, 31, 923.

17. Segal, J.A., *J. Chem. Soc., Chem. Commun.*, **1985**, 1338.

18. Dembek, A.A. and Fagan, P.J., *Organometallics*, **1995**, 14, 3741.

19. Dembek, A.A., Fagan, P.J. and Marsi, M., *Macromolecules*, **1993**, 26, 2992.

20. Coffield, T.H., Sandel, V. and Closson, R.D., *J. Am. Chem. Soc.*, **1957**, 79, 5826.

21. Nesmeyanov, A.N., Vol'kenau, N.A. and Bolesova, I.N., *Dokl. Akad. Nauk. SSSR*, **1963**, 149, 615.

22. Nesmeyanov, A.N., Vol'kenau, N.A. and Bolesova, I.N., *Tetrahedron Lett.*, **1963**, 25, 1725.

23. Sirotkina, E.I., Nesmeyanov, A.N. and Vol'kenau, N.A., *Dokl. Akad. Nauk. SSSR*, **1969**, 155, 615.

24. Nesmeyanov, A.N., Vol'kenau, N.A. and Petrakova, V.A., *J. Organomet. Chem.*, **1977**, 136, 363.

25. Sutherland, R.G., Iqbal, M. and Piorko, A.J., *Organomet. Chem.*, **1986**, 302, 307.

26. Khand, I.U., Pauson, P.L. and Watts, W.E., *J. Chem. Soc. C*, **1968**, 2257.

27. Khand, I.U., Pauson, P.L. and Watts, W.E., *J. Chem. Soc. C*, **1968**, 2261.

28. Khand, I.U., Pauson, P.L. and Watts, W.E., *J. Chem. Soc. C*, **1969**, 116.

29. Helling, J.F. and Hendrickson, W.A., *J. Organomet. Chem.*, **1977**, 141, 99.

30. Lee, C.C., Piorko, A. and Sutherland, R.G., *J. Organomet. Chem.*, **1983**, 248, 357.

31. Lee. C.C., Chowdhury, R.L., Piorko, A. and Sutherland, R.G., *J. Organomet. Chem.*, **1986**, 310, 391.

32. Lacoste, M., Rabaa, H., Astruc, D., Le Beuze, A., Saillard, J.-Y., Precigoux, G., Courseille, C., Ardon, N. and Bowyer, W., *Organometallics*, **1989**, 8, 2233.

33. Morrison, Jr., W.H., Ho, E.Y. and Hendrickson, D.N., *J. Am. Chem. Soc.*, **1974**, 96, 3606.

34. Lee, C.C., Demchuk, K.J. and Sutherland, R.G., *Synth. React. Inorg. Met.-Org. Chem.*, **1978**, 8, 361.

35. Astruc, D., *Tetrahedron*, **1983**, 39, 4027.

36. Abd-El-Aziz, A.S., Lee, C.C., Piorko, A. and Sutherland, R.G., *Synth. Commun.*, **1988**, 18, 291.

37. Astruc, D. and Dabard, R., *J. Organomet. Chem.*, **1975**, 96, 283.

38. Astruc, D. and Dabard, R., *J. Organomet. Chem.*, **1976**, 111, 339.

39. Sutherland, R.G., *J. Organomet. Chem. Library*, **1977**, 3, 311.

40. Dabirmanesh, Q. and Roberts, R.M.G., *J. Organomet. Chem.*, **1993**, 460, C28.

41. Lee, C.C., Demchuk, K.J. and Pannekock, W.J., *J. Organomet. Chem.*, **1978**, 162, 253.

42. Lee, C.C., Sutherland, R.G. and Thomson, B.J., *J. Chem. Soc., Chem. Commun.*, **1972**, 907.

43. Morrison, Jr., W.H., Ho, E.Y. and Hendrickson, D.N., *Inorg. Chem.*, **1975**, 14, 500.

44. Van Rooyen, P.H., Schindehutte, M. and Lotz, S., *Organometallics*, **1992**, 11, 1104.

45. Sutherland, R.G., Pannekoek, W.J. and Lee, C.C., *Can. J. Chem.*, **1978**, 56, 1782.

46. Astruc, D., *Top. Curr. Chem.*, **1991**, 160, 47.

47. Astruc, D., *New. J. Chem.*, **1992**, 16, 305.

48. Nesmeyanov, A.N., Vol'kenau, N.A. and Bolesova, I.N., *Dokl. Akad. Nauk. SSSR*, **1967**, 175, 606.

49. Nesmeyanov, I.N., Vol'kenau, N.A., Isaeva, L.S. and Bolesova, I.N., *Dokl. Akad. Nauk. SSSR*, **1968**, 183, 834.

50. Moriarty, R.M., Gill, U.S. and Ku, Y.Y., *Polyhedron*, **1988**, 7, 2685.

51. Gill, U.S. and Moriarty, R.M., *Synth. React. Inorg. Met.-Org. Chem.*, **1986**, 16, 1103.

52. Gill, U.S. and Moriarty, R.M., *Synth. React. Inorg. Met.-Org. Chem.*, **1986**, 16, 485.

53. Abd-El-Aziz, A.S., de. Denus, C.R. and Hutton, H.M., *Can. J. Chem.*, **1995**, 73, 289.

54. Abd-El-Aziz, A.S., Tesfalidet, S., de Denus, C.R. and Lezynska, K., *Synth. Commun.*, **1993**, 23, 1415.

55. Abd-El-Aziz, A.S. and de Denus, C.R., *Synth. Commun.*, **1992**, 22, 581.

56. Abd-El-Aziz, A.S., de Denus, C.R. and Lezynska, K., *Proc. Indian Acad. Sci., (Chem. Sci.)*, **1993**, 105, 575.

57. Abd-El-Aziz, A.S., Lee, C.C., Piorko, A. and Sutherland, R.G., *J. Organomet. Chem.*, **1988**, 348, 95.

58. Lee, C.C., Zhang, C.H., Abd-El-Aziz, A.S., Piorko, A. and Sutherland, R.G., *J. Organomet. Chem.*, **1989**, 364, 217.

59. Helling, J.F. and Hendrickson, W.A., *J. Organomet. Chem.*, **1979**, 168, 87.

60. Pauson, P.L. and Segal, J.A., *J. Chem. Soc., Dalton Trans.*, **1975**, 1677.

61. Pearson, A.J., Park, J.G, Yang, S.H. and Chuang, Y.-H., *J. Chem. Soc., Chem. Commun.*, **1989**, 1363.

62. Lee, C.C., Abd-El-Aziz, A.S., Chowdhury, R.L., Gill, U.S., Piorko, A. and Sutherland, R.G., *J. Organomet. Chem.*, **1986**, 315, 79.

63. Cambie, R.C., Janssen, S.J., Rutledge, P.S. and Woodgate, P.D., *J. Organomet. Chem.*, **1992**, 434, 97.

64. Sutherland, R.G., Piorko, A., Lee, C.C., Simonsen, S.H. and Lynch, V.M., *J. Heterocyclic Chem.*, **1988**, 25, 1911.

65. Sutherland, R.G., Piorko, A., Gill, U.S. and Lee, C.C., *J. Heterocyclic Chem.*, **1982**, 19, 801.

66. Sutherland, R.G., Abd-El-Aziz, A.S., Piorko, A., Gill, U.S. and Lee, C.C., *J. Heterocyclic Chem.*, **1988**, 25, 1107.

67. Abd-El-Aziz, A.S., Schriemer, D.C. and de Denus, C.R., *Organometallics*, **1994**, **1**, 374.

68. Abd-El-Aziz, A.S. and Schriemer, D.C., *Inorg. Chim. Acta.*, **1992**, 202, 123.

69. Abd-El-Aziz, A.S., Lei, Y. and de Denus, C.R., *Polyhedron*, **1995**, 17, 1585.

70. Abd-El-Aziz, A.S., de Denus. C.R., *J. Chem. Soc. Dalton Trans.*,**1995**, 3375.

71. Davies, S.G., Organotransition Metal Chemistry: Applications to Organic Synthesis, Pergamon Press, Oxford, U.K., 1982.

72. Collman, J.B., Hegedus, L.S., Norton, J.R., Finke, R.J., Principles and Application of Organotransition Metal Chemistry, University Science Books, C.A., 1987.

73. McQuillin, F.J., Parker, D.G., Stephenson, G.R., Transition Metal Organometallics for Organic Synthesis, Cambridge University Press, U.K., 1991.

74. Jevnaker, N., Benneche, T. and Undheim, K., *Acta. Chem. Scand.*, **1993**, 47, 406.

75. Darchen, A., *J. Chem. Soc., Chem. Commun.*, **1983**, 768.

76. Hamon, J.-R., Saillard, J.-Y., LeBeuze, A., McGlinchey, M.J. and Astruc, D., *J. Am. Chem. Soc.*, **1982**, 104, 7549.

77. Abd-El-Aziz, A.S. and de Denus, C.R., *J. Chem. Soc., Perkin Trans. I*, **1993**, 293.

78. Nesmeyanov, A.N., Vol'kenau, N.A. and Shilovtseva, L.S., *Dokl. Akad. Naul. SSSR*, **1970**, 190, 354.

79. Nesmeyanov, A.N., Vol'kenau, N.A. and Shilovtseva, L.S., *Dokl. Akad. Naul. SSSR*, **1970**, 190, 857.

80. Gill, T.P. and Mann, K.R., *Inorg. Chem.*, **1980**, 19, 3007.

81. Gill, T.P. and Mann, K.R., *Inorg. Chem.*, **1981**, 20, 65.

82. Schrenk, J.L., Palazzotto, M.C. and Mann, K.R., *Inorg. Chem.*, **1983**, 22, 4047.

83. Nesmeyanov, A.N., Leschova, I.F., Ustynyuk, Y.A, Sirotkina, Y.I., Bolesova, I.N., Isayeva, L.S. and Vol'kenau, N.A., *J. Organomet. Chem.*, **1970**, 689.

84. Steele, B.R., Sutherland, R.G. and Lee, C.C., *J. Chem. Soc., Dalton Trans*, **1981**, 529.

85. Wisian-Neilson, P, Allcock, H.R. and Wynne, K.J., Inorganic and Organometallic Polymer II - Advanced Materials and Intermediates, American Chemical Society, Washington, D.C., 1994.

86. Carraher, Jr., C.E., *J. Chem. Educ.*, **1981**, 58, 921.

87. Carraher, Jr., C.E., Sheats, J.E. and Pittman, Jr., C.U., Organometallic Polymers, Academic Press, New York, 1978.

88. Mark, H.F., Bikales, N.M., Overberger, C.G., Menges, G., Kroschwitz, J.I., (Eds.), Encyclopedia of Polymer Science and Engineering, Volume 10, John Wiley & Sons, New York, N.Y., 1987.

89. Sheats, J.E., Carraher, Jr., C.E. and Pittman, Jr., C.U., Metal-Containing Polymeric Systems, Plenum Press, New York, N.Y., 1985.

90. Pittman, Jr., C.U., Carraher, Jr., C.E., Zeldin, M., Sheats, J.E. and Culbertson, B.M., Metal-Containing Polymeric Materials, Plenum Press, New York, N.Y., 1996.

91. Knobloch, F.W. and Rauscher, W.H., *J. Poly. Sci.*, **1961**, 54, 651.

92. Pittman, Jr., C.U., *J. Polym. Sci., Part A-1*, **1968**, 6, 1687.

93. Patterson, W.J., McManus, S.P. and Pittman, Jr., C.U., *J. Polymer Sci.: Polym. Chem. Educ.*, **1974**, 12, 837.

94. Gonsalves, K., Zhan-ru, L. and Rausch, M.D., *J. Am. Chem. Soc.*, **1984**, 106, 3862.

95. Gonsalves, K.E., Lewis, R.W. and Rausch, M.D., *Appl. Organomet. Chem.*, **1987**, 81.

96. Finckh, W., Tang, B.-Z., Foucher, D.A., Zamble, D.B., Ziembinski, R., Lough, A. and Manners, I., *Organometallics*, **1993**, 12, 823.

97. Foucher, D.A., Tang, B.-Z. and Manners, I., *J. Am. Chem. Soc.*, **1992**, 114, 6246.

98. Foucher, D.A., Peterson, R., Tang, B.-Z., Ziembinski, R., Coombs, N., Macdonald, P.M., Sodhi, R.N.S., Massey, J., Vansco, G.J. and Manners, I., *Polym. Prepr., Am. Chem. Soc., Civ. Polym. Chem.*, **1993**, 34, 328.

99. Manners, I., *Adv. Materials*, **1994**, 6, 68.

100. Foucher, D.A., *Rapid Commun.*, **1993**, 14, 63.

101. Honeyman, C., Foucher, D.A., Mourad, O., Rulkens, R. and Manners, I., *Polym. Prepr., Am. Chem. Soc., Div. Polym. Chem.*, **1993**, 34, 330.

102. Nelson, J.M., Rengal, H. and Manners, I., *J. Am. Chem. Soc.*, **1993**, 115, 7035.

103. Foucher, D.A., Honeyman, C.H., Nelson, J.M., Tang, B.-Z. and Manners, I., *Angew. Chem. Int. Ed. Engl.*, **1993**, 32, 1709.

104. Rulkens, R., Lough, A.J. and Manners, I., *J. Am. Chem. Soc.*, **1994**, 116, 797.

105. Rulkens, R., Ni, Y. and Manners, I., *J. Am. Chem. Soc.*, **1994**, 116, 12121.

106. Ni, Y., Rulkens, R. and Manners, I., *J. Am. Chem. Soc.*, **1996**, 118, 4102.

107. Rulkens, R., Lough, A.J., Manners, I., Lovelace, S.R., Grant, C. and Geiger, W.E., *J. Am. Chem. Soc.*, **1996**, 118, 12683.

108. Faulkner, C.W., Ingham, S.L., Khan, M.S., Lewis, J., Long, N.J. and Raithby, P.R., *J. Organomet. Chem.*, **1994**, 482, 139.

109. Pittman, C.U., Ayers, O.E. and McManus, S.P., *Macromolecules*, **1974**, 1, 737.

110. Dembek, A.A., Burch, R.R. and Feiring, A.E., *J. Am. Chem. Soc.*, **1993**, 115, 2087.

111. Blackwell, J.P., Brady, D.G. and Hill, Jr., H.W., *J. Coatings Technology*, **1978**, 50, 62.

112. Brady, D.G. and Hill, H.W., *Modern Plastics*, **1974**, 51,60.

113. Hill, Jr., H.W. and Brady, D.G., *J. Coatings, Technology*, **1977**, 49, 33.

114. Hill, Jr., H.W., *ACS Symposium Series*, **1979**, 95, 183.

115. Mehmet-Alkan, A.A., Biddlestone, F. and Hay, J.N., *Thermochimics Acta.*, **1995**, 256, 123.

116. Robeson, L.M., Farnham, A.G. and McGrath, J.E., *Applied Polymer Symposium*, **1975**, 26, 373.

117. Rose, J.B., *Plastics and Rubber International*, **1984**, 10, 11.

118. Attwood, T.E., Dawson, P.C., Freeman, J.L., Hoy, L.R.J., Rose, J.B. and Staniland, P.A., *Polymer*, **1981**, 22, 1096.

119. Belbin, G.B., *Proc. Instn. Mech. Engrs.*, **1984**, 198B, 71.

120. Attwood, T.E., King, T., Leslie, V.J. and Rose, J.B., *Polymer*, **1977**, 18, 369.

121. Smith, C.P., *Swiss Plastics*, **1981**, 3, 37.

122. Leslie, V.J., *Chemtech*, **1975**, 426.

123. Seymour, R.B. and Kirshenbaum, G.S., High Performance Polymers: Their Origin and Development, Elsevier Science Publishing Co., Inc., New York, N.Y., 1986.

124. Cotter, R.J., Engineering Plastics - A handbook of Polyarylethers, Gordon and Breach Publishers, Postfach, Switzerland, 1995.

125. Smith, H.A., Encyclo. *Polym. Sci. Technol.*, **1969**, 10, 653.

126. Cleary, J.W., *ACS Polymer Div. Preprints*, **1984**, 25, 36.

127. Vogel, H.A., *J. Polym. Sci., Part A-1*, **1970**, 8, 2035.

128. Cudby, M.E.A., Feasey, R.G., Jennings, B.E., Jones, M.E.B. and Jones, J.B., *Polymer*, **1965**, 589.

129. Jennings, B.E., Jones, M.E.B. and Rose, J.B., *J. Polym. Sci., Part C*, **1967**, 715.

130. Cudby, M.E.A., Feasey, R.G., Gaskin, S., Kendall, V. and Rose, J.B., *Polymer*, **1968**, 9, 265.

131. Cudby, M.E.A., Feasey, R.G., Gaskin, S., Jones, M.E.B. and Rose, J.B., *J. Polym. Sci., Part C*, **1969**, 747.

132. Maiti, S. and Mandal, B.K., *Prog. Polym. Sci.*, **1986**, 12, 111.

133. Pearson and Robinson, *J. Chem. Soc.*, **1931**, 413, 1473.

134. Short, J.N. and Hill, Jr., H.W., *Chemtech*, **1972**, 2, 481.

135. Macallum, A.D., *J. Org. Chem.*, **1948**, 13, 154.

136. Lenz, R.W. and Carrington, W.K., *J. Polym. Sci.*, **1959**, 41, 333.

137. Lenz, R.W. and Handlovits, C.E., *J. Polym. Sci.*, **1960**, 43, 167.

138. Lenz, R.W., Handlovits, C.E. and Smith, H.A., *J. Polym. Sci..*, **1962**, 58, 351.

139. Johnson, R.N., Farnham, A.G., Clendinning, R.A., Hale, W.F. and Merriam, C.N., *J. Polym. Sci., Part A-1*, **1967**, 5, 2375.

140. Newton, A.B. and Rose, J.B., *Polymer*, **1972**, 13, 465.

141. Hale, W.F., Farnham, A.G., Johnson, R.N. and Clendinning, R.A., *J. Polym. Sci., Part A-1*, **1967**, 5, 2399.

142. Johnson, R.N. and Farnham, A.G., *J. Polym. Sci., Part A-1*, **1967**, 5, 2415.

143. Hergenrother, P.M., Jensen, B.J. and Havens, *Polymer*, ???

144. Viswanathan, R., Johnson, B.C. and McGrath, J.E., *Polymer*, **1984**, 25, 1827.

145. Keitoku, F., Kakimoto, M.-A. and Imai, Y., *J. Polym. Sci., Part A, Polym. Chem.*, **1994**, 32, 317.

146. Babu, J.R., Brink, A.E., Konas, M. and Riffe, J.S., *Polymer*, **1994**, 23, 4949.

147. Dutta, P.K. and Maiti, S., Die Angew. *Makromol. Chemie*, **1993**, 211, 79.

148. Percec, V. and Nava, H., *J. Polym. Sci., Part A, Polym. Chem.*, **1988**, 26, 783.

149. Percec, V., Wang, J.H. and Oishi, Y., *J. Polym. Sci., Part A, Polym. Chem.*, **1991**, 29, 949.

150. Percec, V., Wang, J.H., Oishi, Y. and Feiring, A.E., *J. Polym. Sci., Part A, Polym. Chem.*, **1991**, 29, 965.

151. Percec, V., Wang, J.H. and Okita, S., *J. Polym. Sci., Part A, Polym. Chem.*, **1991**, 29, 1789.

152. Percec, V., Okita, S. and Wang, J.H., *Macromolecules*, **1992**, 25, 64.

153. Percec, V., Wang, J.H. and Okita, S., *J. Polym. Sci., Part A, Polym. Chem.*, **1992**, 30, 429.

154. Percec, V., Wang, J.H. and Oishi, Y., *J. Polym. Sci., Part A, Polym. Chem.*, **1992**, 30, 439.

155. Percec, V. and Wang, J.H., *J. Mater. Chem.*, **1991**, 1, 1051.

156. Percec, V., Wang, J.H. and Yu, L., *Polym. Bull.*, **1992**, 27, 503.

157. Matyjaszewski, K., Cationic Polymerizations - Mechanisms, Synthesis, and Applications, Marcel Dekker, Inc., New York, N.Y., 1996.

158. Robeson, L.M., Farnham, A.G. and McGrath, J.E., *Appl. Polym. Symp. No. 26*, **1975**, 373.

159. Williams, A.L., Kinney, R.E. and Bridger, R.F.,

160. van Dort, H.M., Hoefs, C.A.M., Magre, E.P., Schopf, A.J. and Yntema, K., Eur. *Polym. J.*, **1968**, 4, 275.

161. Bacon, R.G.R. and Stewart, O.J., *J. Chem. Soc.*, **1965**, 4953.

162. Bunnett, J.F. and Zahler, R.E., *Chem. Rev.*, **1951**, 49, 394.

163. Bacon, R.G.R. and Hill, H.A.O., *Proc. Chem. Soc.*, **1962**, 113.

164. Weingarten, H., *J. Org. Chem.*, **1964**, 29, 977.

165. Weingarten, H., *J. Org. Chem.*, **1964**, 29, 3624.

166. van Heyningen, E., *J. Org. Chem.*, **1961**, 26, 3850.

167. Farnham, A.G. and Johnson, R.N., U.S. Pat. 3332909, 1967. Union Carbide Corp.

168. Colon, I. and Kelsey, D.R., J. Org. Chem., 1986, 51, 2627.

169. Colon, I. and Kwiatkowski, G.J., *J. Polym. Sci., Part A, Polym. Chem.*, **1990**, 23, 367.

170. Ueda, M. and Ito, T., *Polymer J.*, **1991**, 23, 297.

171. Kwiatkowski, G.T. and Colon, I, *Polym. Preprints*, **1991**, 32, 342.

172. Bochmann, M., Kelly, K., Lu, J., *J. Polym. Sci., Part A, Polym. Chem.*, **1992**, 30, 2511.

173. Deeter, G.A. and Moore, J.S., *Macromolecules*, **1993**, 26, 2535.

174. Rehahn, M., Schluter, A. and Wegner, G., *Makromol.Chem., Rapid Commun.*, **1990**, 11, 535.

175. Baldoli, C., Del Buttero, P., Maiorana, S. and Papagni, A., *J. Chem. Soc. Chem. Commun.*, **1985**, 1181.

176. Pearson, A.J. and Gelormini, A.M., *J. Org. Chem.*, **1994**, 59, 4561.

177. Pearson, A.J. and Gelormini, A.M., *Macromolecules*, **1994**, 27, 3675.

178. Pearson, A.J. and Gelormini, A.M., *J. Org. Chem.*, **1995**, 60, 281.

179. Frye, L.L., Sulllivan, E.L., Cusack, K.P. and Funaro, J.M., *J. Org. Chem.*, **1992**, 57, 697.

180. Cozan, V., Butuc, E. and Stoleru, A., *Pure Appl. Chem.*, **1993**, A30(12), 889.

181. Itsuno, S., Shimizu, K., Kamahori, K. and Ito, K., *Tetrahedron Letters*, **1992**, 33, 6339.

182. Takeuchi, H., Oya, H., Yanase, T., Itou, K., Adachi, T., Sugiura, H. and Hayashi, N., *Chem. Soc. Perkin Trans. 2*, **1994**, 827.

183. Marcus, P.D., *Tetrahedron*, **1977**, 33, 2019.

184. Campbell, J.R., *J. Org. Chem.*, **1962**, 27, 2207.

185. Campbell, J.R., *J. Org. Chem.*, **1964**, 29, 1831.

186. Bunnett, J.F. and Creary, X., *J. Org. Chem.*, **1974**, 39, 3611.

187. Bunnett, J.F. and Creary, X., *J. Org. Chem.*, **1974**, 39, 3173.

188. Field, L., *Synthesis*, **1978**, 713.

189. Trost, B.M., *Bull. Chem. Soc. Jpn.*, **1988**, 61, 107.

190. Downie, I.M., Heaney, H. and Kemp, G., *Tetrahedron*, **1988**, 44, 2619.

191. Guindon, Y., Frenette, R., Fortin, R. and Rokach, J., *J. Org. Chem.*, **1983**, 48, 1357.

192. Walker, K.A.M., *Tetrahedron Letters*, **1977**, 51, 4475.

193. Brown, H.C. and Midland, M.M., *J. Am. Chem. Soc.*, **1971**, 93, 3291.

194. Brois, S.J., Pilot, J.F. and Barnum, H.W., *J. Am. Chem. Soc.*, **1970**, 92, 7629.

195. Cabiddu, S., Fattuoni, C., Floris, C., Gelli, G., Melis, S. and Sotgiu, F., *Tetrahedron*, **1990**, 46, 861.

196. Harpp, D.N., Gleason, J.G. and Snyder, J.P., *J. Am. Chem. Soc.*, **1968**, 90, 4181.

197. Field, I. and Ravichandran, *J. Org. Chem.*, **1979**, 44, 2624.

198. Griesbaum, K., *Angew. Chem. Internat. Edit.*, **1970**, 9, 273.

199. March, J., Advanced Organic Chemistry - Reactions, Mechanisms, and Structure, 4th Ed., John-Wiley & Sons, New York, 1992.

200. Herriott, A. and Picker, D.,

201. Landini, D., Maotanario, F., and Rolla, F.,

202. Olah, Husain, Singh and Mehrotra, *J. Org. Chem.*, **1983**, 48, 3667.

203. Silverstein, R.M., Bassler, G.C. and Morrill, T.C., Spectroscopic Identification of Organic Compounds, 5th Ed., John Wiley & Sons, New York, 1991.

204. Aberkane, O., Mieloszynski, J.L., Robert, D., Born, M. and Paquer, D., *Phosphorus, Sulfur and Silicon*, **1993**, 79, 245.

205. Wardell, J.L., The Chemistry of Thiol Group, Part I, S. Patai, Ed., Wiley-Interscience, New York, 1974.

206. Madesclaire, M., *Tetrahedron*, **1986**, 42, 5459.

207. Baarschers, W.H., *Can, J. Chem.*, **1976**, 54, 3056.

208. Rosen, S., Bareket, Y., *J. Org. Chem.*, **1997**, 62, 1457.

209. Dutta, P.K. and Sukumar, M., *Die Angew. Makro. Chem.*, **1993**, 211, 79.

210. Joseph, K.A. and Srinivasan, M., *J. Poly. Sci.: Poly A: Polymer Chem.*, **1993**, 31, 3485.

211. Tsuchida, E., Yamamoto, K. and Shouji, E., *Macromolecules*, **1993**, 26, 7389.

212. Keitoku, F., Kakimoto, M. and Imai, Y., *J. Poly. Sci.: Part A: Polymer Chem.*, **1994**, 32, 317.

213. Lee, C.C., Gill, U.S., Iqbal, M., Azogu, C.L. and Sutherland, R.G., *J. Organomet. Chem.*, **1982**, 231, 151.

214. Abd-El-Aziz, A.S., Piorko, A., Lee, C.C. and Sutherland, R.G., *Can. J. Chem.*, **1989**, 67, 1618.

215. Abd-El-Aziz, A.S. and Epp, K.M., *Polyhedron*, **1995**, 14, 957.

216. Abboud, K.A., Simonsen, S.H., Piorko, A. and Sutherland, R.G., *Acta, Cryst.*, **1991**, C47, 860.

217. Heinze, J., *Top, Curr. Chem.*, **1990**, 152, 1.

218. Moulton, R., Weidman, T.W., Vollhardt, K.P.C and Bard, A.J., *Inorg. Chem.*, **1986**, 25, 1846.

219. Hunter, A.D. and Szigety, A.B., *Organometallics*, **1989**, 8, 2670.

220. Brandt, P.F. and Rauchfuss, T.B., *J. Am. Chem. Soc.*, **1992**, 114, 1926.

221. Astruc, D., Electron Transfer and Radical Processes in Transition-Metal Chemistry, VCH, New York, 1995.

222. Lacoste, M., Varret, F., Toupet, L. and Astruc, D., *J. Am. Chem. Soc.*, **1987**, 109, 6504.

223. Desbois, M.-H. and Astruc, D., *New. J. Chem.*, **1989**, 13, 595.

224. Moinet, C., Roman, E. and Astruc, D., *J. Electroanal. Chem.*, **1981**, 121, 241.

225. Astruc, D., *Angew. Chem. Int. Ed. Engl.*, **1988**, 27, 643.

226. Geiger, W.E., *Prog. Inorg. Chem.*, **1985**, 33, 275.

227. Geiger, W.E. and Connelly, N.G., *Adv. Organomet. Chem.*, **1984**, 23, 1.

228. Debois, M.-H. and Astruc, D., *Organometallics*, **1989**, 8, 1841.

229. Obendorf, D., Schottenberger, H. and Reiker, C., *Organometallics*, **1991**, 10, 1293.

230. Guerchais, V. and Astruc, D., *J. Organomet. Chem.*, **1986**, 316, 335.

231. Richter-Addo, G.B. and Hunter, A.D., *Inorg. Chem.*, **1989**, 28, 4063.

232. Bligh, R.Q., Moulton, R., Bard, A.J., Piorko, A. and Sutherland, R.G., *Inorg, Chem.*, **1989**, 28, 2652.

233. Abd-El-Aziz, A.S., Winkler, K. and Baranski, A.S., *Inorg. Chim. Acta.*, **1992**, 194, 207.

234. Abd-El-Aziz, A.S., Baranski, A.S., Piorko, A. and Sutherland, R.G., *Inorg. Chim. Acta.*, **1988**, 147, 77.

235. Pierce, D.T. and Geiger, W.E., *J. Am. Chem. Soc.*, **1992**, 114, 6063.

236. Neilson, R.M. and Weaver, M.J., *Organometallics*, **1989**, 8, 1636.

237. Bowyer, W.J. and Geiger, W.E., *J. Am. Chem. Soc.*, **1985**, 107, 5657.

238. Holloway, J.D.L. and Geiger, W.E., *J. Am. Chem. Soc.*, **1979**, 101, 2038.

239. Sutherland, R.G., *J. Organomet. Chem. Lib.*, **1977**, 3, 311.

240. Nesmeyanov, A.N., Vol'kenau, N.A., Shilovtseva, L.S. and Petrokova, V.A., *J. Organomet. Chem.*, **1973**, 61, 329.

241. El Murr, N., *J. Chem. Soc., Chem. Commun.*, **1981**, 251.

242. Nesmeyanov, A.N., Denisovich, L.I., Gubin, S.P., Vol'kenau, N.A., Sirotkina, E.I. and Bolesova, I.N., *J. Organomet. Chem.*, **1969**, 20, 169.

243. Dessy, R.E., Stary, F.E., King, R.B. and Waldrop, M., *J. Am. Chem. Soc.*, **1966**, 88, 471.

244. Astruc, D. and Dabard, R., *Bull. Soc. Chim. Fr.*, **1976**, 228.

245. Nesmeyanov, A.N., Vol'kenau, N.A., Petrovskii, P.V., Kotova, L.S., Petrakova, V.A. and Denisovich, L.T., *J. Organomet. Chem.*, **1981**, 210, 103.

246. Hamon, J.R., Astruc, D., and Michaud, P., *J. Am. Chem. Soc.*, **1981**, 103, 758.

247. Darchen, A., *J. Organomet. Chem.*, **1986**, 302, 389.

248. Solodovnikov, S.P., Vol'kenau, N.A. and Shilovtesa, L.C., *Izv. Akad. Nauk, SSSR, Ser Khim*, **1985**, 8, 1733.

249. Fillaut, J.-L. and Astruc, D., *New. J. Chem.*, **1996**, 20, 945.

250. Richardson, D.E. and Taube, H., *Inorg, Chem.*, **1981**, 20, 1278.

251. Flanagan, J.B., Margel, S., Bard, A.J. and Anson, F.C., *J. Am. Chem. Soc.*, **1978**, 100, 4248.

252. Mevs, J.M., Gennett, T. and Geiger, W.E., *Organometallics*, **1991**, 10, 1229.

253. Bard, A.J. and Faulkner, L.R., Electrochemical Methods: Fundamentals and Applications, John Wiley and Sons, New York, 1980.

254. Sawyer, D.T. and Roberts, J.L., Experimental Electrochemistry for Chemists, John Wiley and Sons, New York, 1974.

255. Atkins, P.W., Physical Chemistry, W.H. Freeman and Company, New York, 1994.

256. Berry, R.S., Rice, S.A. and Ross, J., Physical Chemistry, John Wiley & Sons, New York, 1980.

257. Noggle, J.H., Physical Chemistry, 2nd Ed., Scott, Foresman and Company, Glenview, Ill. 1989.

258. Rieker, R.D., Tucker, I., Milligan, S.N., Wright, D.R., Willeford, B.R., Radonovich, L.J. and Erying, M.W., *Organometallics*, **1982**, 1, 938.

259. Van Order, Jr., N., Gieger, W.E., Bitterwolf, T.E. and Rheingold, A.L., *J. Am. Chem. Soc.*, **1987**, 109, 5680.

260. Nicholson, R.S. and Shain, I., *Anal. Chem.*, **1964**, 36, 706.

261. Truett, W.L., Johnson, D.R., Robinson, I.M. and Montagur, B.A., *J. Am. Chem. Soc.*, **1960**, 82, 2337.

262. Calderon, N., Chen, H.Y. and Scott, K.W., *Tetrahedron Letters*, **1967**, 34, 3327.

263. Uchida, Y., Hihai, M. and Tatsumi, T., *Bull. Chem. Soc. Jpn.*, **1972**, 45, 1158.

264. Grubbs, R.H. and Swetnick, S.J., J. *Mol. Catal.*, **1980,** 8, 25.

265. Mol, J.C. and Moulijn, J.A., *Adv. Catal.*, **1975**, 24, 131.

266. Bamks, R.L. and Bailey, G.C., *Ind. Eng. Chem., Prod. Res. Dev.*, **1964**, 3, 170.

267. Hughes, W.B., *Organomet. Chem. Synth.*, **1972**, 1, 341.

268. Ivin, K.J., Olefin Metathesis, Academic, London, 1983.

269. Calderon, N., Ofstead, E.A., Ward, J.P., Judy, A. and Scott, K.W., *J. Am. Chem. Soc.*, **1968**, 90, 4133.

270. Herrison, J.L. and Chauvin, Y., *Makromol. Chem.*, **1971**, 141, 161.

271. Grubbs, R.H., Burk, P.L. and Carr, D.D., *J. Am. Chem. Soc.*, **1975**, 97, 3265.

272. Katz, T.J. and Rothchild, R., *J. Am. Chem. Soc.*, **1976**, 98, 2519.

273. Quirk, R.P. and Lee, B., *Polym. Int.*, **1992**, 27, 359.

274. Gilliom, L.R. and Grubbs, R.H., *J. Am. Chem. Soc.*, **1986**, 108, 733.

275. Cannizzo, L.F. and Grubbs, R.H., *Macromolecules*, **1988**, 21, 1961.

276. Cannizzo, L.F. and Grubbs, R.H., *Macromolecules*, **1987**, 20, 1488.

277. Katz, T.J. and Acton, N., *Tetrahedron Lett.*, **1976**, 4251.

278. Katz, T.J., Lee, S.J. and Acton, N., *Tetrahedron Lett.*, **1976**, 4247.

279. Schrock, R.R., *J. Am. Chem. Soc.*, **1986**, 108, 2771.

280. Schrock, R.R., Feldman, J., Cannizzo, L.F. and Grubbs, R.H., *Macromolecules*, **1987**, 26, 1169.

281. Schrock, R.R., Depue, R.T., Feldman, J., Schaverien, C.J., Dewan, J.C. and Liu, A.H., *J. Am. Chem. Soc.*, **1988**, 110, 1423.

282. Schaverien, C.J., Dewan, J.C. and Schrock, R.R., *J. Am. Chem. Soc.*, **1986**, 108, 2771.

283. Schrock, R.R., *Acc. Chem. Res.*, **1990**, 23, 158.

284. Bazan, G.C., Khosravi, E., Schrock, R.R., Feast, W.J., Gibson, V.C. and O'Regan, M.B., Thomas, J.K. and Davis, W.M., *J. Am. Chem. Soc.*, **1990**, 112, 8378.

285. Bazan, G.C., Schrock, R.R., Khosravi, E., Feast, W.J. and Gibson, V.C., *Polym. Commun.*, **1989**, 30, 258.

286. Komiya, Z., Pugh, C. and Schrock, R.R., *Macromolecules*, **1992**, 25, 3609.

287. Komiya, Z., Pugh, C. and Schrock, R.R., *Macromolecules*, **1992**, 25, 6586.

288. Pugh, C. and Schrock, R.R., *Macromolecules*, **1992**, 25, 6593.

289. Novak, B.M., Risse, W. and Grubbs, R.H., *Adv. Polym., Sci.*, **1992**, 102, 47.

290. Novak, B.M. and Grubbs, R.H., *J. Am. Chem. Soc.*, **1988**, 100, 7542.

291. Hillmyer, M.A., Lepitit, C., McGrath, D.V., Novak, B.M. and Grubbs, R.H., *Macromolecules*, **1992**, 92, 3345.

292. France, M.B., Grubbs, R.H. and McGrath, D.V., *Macromolecules*, **1993**, 26, 4742.

293. McGrath, D.V. and Grubbs, R.H., *Organometallics*, **1994**, 13, 224.

294. France, M.B., Paciello, R.A. and Grubbs, R.H., *Macromolecules*, **1993**, 26, 4739.

295. Nguyen, S.T., Johnson, L.K., Grubbs, R.H. and Ziller, J.W., *J. Am. Chem. Soc.*, **1992**, 114, 3974.

296. Nguyen, S.T. and Grubbs, R.H., *J. Am. Chem. Soc.*, **1993**, 115, 9858.

297. Fraser, C. and Grubbs, R.H., *Macromolecules*, **1995**, 28, 7248.

298. Schwab, P., France, M.B., Ziller, J.W. and Grubbs, R.H., *Angew. Chem. Int. Ed. Engl.*, **1995**, 34, 2039.

299. Kanaoko, S. and Grubbs, R.H., *Macromolecules*, **1995**, 28, 4707.

300. Schwab, P., Grubbs, R.H. and Ziller, J.W., *J. Am. Chem. Soc.*, **1996**, 118, 100.

301. Lynn, D.M., Kanaoko, S. and Grubbs, R.H., J. Am. Chem. Soc., 1996, 118, 784.

302. Hillmyer, M.A., Nguyen, S.T. and Grubbs, R.H., *Macromolecules*, **1997**, 30, 718.

303. Fu, G.C., Nguyen, S.T. and Grubbs, R.H., *J. Am. Chem. Soc.*, **1993**, 115, 9856.

304. Lautens, M., Abd-El-Aziz, A.S. and Reibel, J., *Macromolecules*, **1989**, 22, 4132.

305. Lautens, M., Abd-El-Aziz, A.S. and Schmidt, G., *Macromolecules*, **1990**, 23, 2819.

306. Lautens, M., Crudden, C.M., Abd-El-Aziz, A.S. and Wada, T., *Macromolecules*, **1991**, 24, 1425.

307. Lautens, M., Abd-El-Aziz, A.S. and Crudden, C.M., *J. Polym. Sci., Part A, Polym. Chem.*, **1993**, 31, 569.

308. Skoog, D.A. and Leary, J.J., Principles of Instrumental Analysis, 4th Ed., Saunders College Publishing, Orlando, Florida, 1992.

309. Jackman, L.M. and Sternhell, S., Applications of Nuclear Magnetic Resonance Spectroscopy in Organic Chemistry, 2nd Ed., Pergamon Press Ltd., New York, 1969.

310. Jackman, L.M., Applications of Nuclear Magnetic Resonance Spectroscopy in Organic Chemistry, Pergamon Press Ltd., New York, N.Y., 1959.

311. Tori, K., Muneyuki, R. and Tanida, H., *Can. J. Chem.*, **1963**, 41, 3142.

312. Neale, R.S. and Whipple, E.B., *J. Am. Chem. Soc.*, **1964**, 86, 3130.

313. Williamson, K.L., *J. Am. Chem. Soc.*, **1963**, 85, 516.

314. Synder, E.I. and Franzus, B., *J. Am. Chem. Soc.*, **1964**, 86, 1166.

315. Kuivila, H.G. and Warner, C.R., *J. Org. Chem.*, **1964**, 29, 2845.

316. Fraser, R.R., *Can. J. Chem.*, **1962**, 40, 78.

317. Tori, K., Hata, Y., Muneyuki, R., Takano, Y., Tsuji, T. and Tanada, H., *Can. J. Chem.*, **1964**, 42, 926.

318. Wong, E.W.C. and Lee, C.C., *Can. J. Chem.*, **1964**, 42, 1245.

319. Laszlo, P. and von Rague Schleyer, P., *J. Am. Chem. Soc.*, **1964**, 86, 1171.

320. Laszlo, P. and von Rague Schleyer, P., *J. Am. Chem. Soc.*, **1963**, 85, 2709.

321. Musher, J.I., *Mol. Phys.*, **1963**, 6, 93.

322. Fisher, J. and Gradwell, M.J., *Magn. Res. Chem.*, **1991**, 29, 1068.

323. Flautt, T.J. and Erman, W.F., *J. Am. Chem. Soc.*, **1963**, 85, 3212.

324. Michelotti, F.W. and Keaveney, W.P., *J. Polym. Sci., Part A*, **1965**, 3, 895.

325. Hamilton, J.G., Ivin, K.J. and Rooney, J.J., *J. Mol. Catal.*, **1985**, 28, 255.

326. Pederson, C.J., *J. Am. Chem. Soc.*, **1967**, 89, 7017.

327. Bradshaw, J.S., Krakowiak, K.E. and Izatt, R.M., Aza-Crown Macrocycles, John Wiley & Sons Inc., New York, 1993.

328. Adam, K.R., Dancey, K.P., Leong, A.J., Lindoy, L.F., McCool, B.J., McPartlin, M. and Tasker, P.A., *J. Am. Chem. Soc.*, **1988**, 110, 8471.

329. Bianchi, A., Micheloni, M. and Paoletti, P., *Coord. Chem. Rev.*, **1991**, 110, 17.

330. Izatt, R.M., Bradshaw, J.S., Nielson, S.A., Lamb, J.D., Christensen, J.J. and Sen, D., *Chem. Rev.*, **1985**, 85, 271.

331. Izatt, R.M., Pawlak, K. Bradshaw, J.S. and Bruening, R.L., *Chem. Rev.*, **1991**, 91, 1721..

332. Lindoy, L.F., *Pure Appl. Chem.*, **1989**, 61, 1575.

333. Vogtle, F. and Weber, E., Crown Ethers and Analogs, Patai, S. and Rappoports, Eds., Wiley-Interscience, New York, 1989.

334. Frensdorff, H.K., *J. Am. Chem. Soc.*, **1971**, 93, 600.

335. Hancock, R.D. and Matell, A.E., *Chem. Rev.*, **1989**, 89, 1875.

336. Lindoy, L.F. and Baldwin, D.S., Pure Appl. Chem., **1989**, 61, 909.

337. Kimura, E., *J. Coord. Chem.*, **1986**, 15, 1.

338. Sutherland, I.O., *Chem. Soc. Rev.*, **1986**, 15, 63.

339. Lehn, J.M., *Science*, **1985**, 227, 849.

340. Yohannes, P.G., Mertes, M.P. and Bowman-Mertes, K., *J. Am. Chem. Soc.*, **1985**, 107, 8288.

341. Haiduc, I. and Silvestru, C., Organometallics in Cancer Chemotherapy, CRC Press, Boca Raton, FL, 1989.

342. Cox, J.P.L., Jankowshi, K.J., Kataky, R., Parker, D., Beeley, N.R.A., Boyce, B.A., Eaton, M.A.W., Millar, K., Millican, A.T., Harrison, A. and Walker, C., *J. Chem. Soc., Chem. Commun.*, **1989**, 797.

343. Craig, A.S., Helps, I.M., Jankowski, K.J., Parker, D., Beely, N.R.A., Boyse, B.A., Eaton, M.A.W., Millican, A.T., Millar, K. Phipps, A., Rhind, S.K., Harrison, A. and Walker, C., *J. Chem. Soc., Chem. Commun.*, **1989**, 794.

344. Moi, M.K., Yanuck, M., Deshpande, V., Hope, H., DeNardo, S.J. and Meares, C.F., *Inorg. Chem.*, **1987**, 26, 3458.

345. Moi, M.K., Meares, C.F. and DeNardo, S.J., *J. Am. Chem. Soc.*, **1988**, 110, 6266.

346. Morphy, J.R., Parker, D., Alexander, R., Bains, A., Carne, A.F., Eaton, M.A.W., Harrison, A., Millican, A., Phipps, A., Rhind, S.K., Titmas, R. and Weatherby, D., *J. Chem. Soc., Chem. Commun.*, **1988**, 156.

347. Morphy, J.R., Parker, D., Kataky, R., Harrison, A., Eaton, A.W., Millican, A., Phipps, A. and Walker, C., *J. Chem. Soc., Chem. Commun.*, **1989**, 792.

348. Riesen, A., Kaden. T.A., Ritter, W. and Macke, H.R., *J. Chem. Soc., Chem. Commun.*, **1989**, 460.

349. Jones, M.M., *J. Coord. Chem.*, **1991**, 23, 187.

350. Misra, M., Athar, M., Hasau, S.K. and Srivastava, R.C., *Fund. Appl. Toxicol.*, **1988**, 11, 285.

351. Lauffer, R.B., *Chem. Rev.*, **1987**, 87, 901.

352. Feti, S., Maravigna, P. and Montaudo, G., *Macromolecules*, **1982**, 15, 883.

353. Goethals, E.J., *Adv. Polym. Sci.*, **1977**, 23, 103.

354. Semlyen, J.A., *Adv. Polym. Sci.*, **1976**, 21, 41.

355. Zahn, H. and Gleitsman, G.B., *Angew. Chem. Internat., Ed. Engl.*, **1963**, 2, 410.

356. Ballistreri, A., Foti, S., Matavigna, P., Montaudom G. and Scamporrino, E., J. *Polym. Chem. Ed.*, **1980**, 18, 1923.

357. Foti, S., Maravigna, P. and Montaudo, G., *J. Polym. Sci., Polym. Chem. Ed.*, **1981**, 19, 1679.

358. Mandolini, L. and Vontor, T., *Synth. Commun.*, **1979**, 9, 857.

359. Pietraszkiewicz, M., *J. Coord. Chem.*, **1992**, 27, 151.

360. Baldoli, C., Buttero, P.D., Maiorana S. and Papagni, A., *J. Chem. Soc., Chem. Commun.*, **1985**, 1181.

361. Janetka, J.W. and Rich, D.H., *J. Am. Chem. Soc.*, **1995**, 117, 10585.

362. Abd-El-Aziz, A.S., De Denus, C.R., Zaworotko, M.J., Sharma, C.V.K, *J. Chem. Soc., Chem. Commun.*, **1998**, 265.